

## Index

### Bers, DM

#### Sarcoplasmic reticulum Ca release in intact ventricular myocytes.

Front Biosci. 2002 Jul 1;7:d1697-711. Review.

Cheng H, Wang SQ

Calcium signaling between sarcolemmal calcium channels and ryanodine receptors in heart cells.

Front Biosci. 2002 Sep 1;7:d1867-78. Review.

Dirksen RT

Bi-directional coupling between dihydropyridine receptors and ryanodine receptors.

Front Biosci. 2002 Mar 1;7:d659-70. Review.

Trafford AW, Diaz ME, O'Neill SC, Eisner DA

Integrative analysis of calcium signalling in cardiac muscle.

Front Biosci. 2002 Apr 1;7:d843-52. Review.

### Fill M

#### Mechanisms that turn-off intracellular calcium release channels.

Front Biosci. 2003 Jan 1;8:D46-54.

Benitah JP, Kerfant BG, Vassort G, Richard S, Gomez AM

Altered communication between L-type calcium channels and ryanodine receptors in heart failure.

Front Biosci. 2002 May 1;7:e263-75. Review.

Guerrero-Hernandez A, Gomez-Viquez L, Guerrero-Serna G, Rueda A

Ryanodine receptors in smooth muscle.

Front Biosci. 2002 Jul 1;7:d1676-88. Review.

Gyorke S, Gyorke I, Lukyanenko V, Terentyev D, Viatchenko-Karpinski S, Wiesner TF

Regulation of sarcoplasmic reticulum calcium release by luminal calcium in cardiac muscle.

Front Biosci. 2002 Jun 1;7:d1454-63. Review.

Tang W, Sencer S, Hamilton SL

Calmodulin modulation of proteins involved in excitation-contraction coupling.

Front Biosci. 2002 Jun 1;7:d1583-9. Review.

Ikemoto N, Yamamoto T

Regulation of calcium release by interdomain interaction within ryanodine receptors.

Front Biosci. 2002 Mar 1;7:d671-83. Review.

Lamb GD

Voltage-sensor control of Ca<sup>2+</sup> release in skeletal muscle: insights from skinned fibers.

Front Biosci. 2002 Apr 1;7:d834-42. Review.

Ma J, Pan Z

Junctional membrane structure and store operated calcium entry in muscle cells.

Front Biosci. 2003 Jan 1;8:D242-55. Review

Marks AR

Ryanodine receptors, FKBP12, and heart failure.

Front Biosci. 2002 Apr 1;7:d970-7. Review.

Meissner G  
Regulation of mammalian ryanodine receptors.  
Front Biosci. 2002 Nov 1;7:d2072-80. Review.

Niggli E, Egger M  
Calcium quarks.  
Front Biosci. 2002 May 1;7:d1288-97. Review.

Ogawa Y, Murayama T, Kurebayashi N  
Ryanodine receptor isoforms of non-Mammalian skeletal muscle.  
Front Biosci. 2002 May 1;7:d1184-94. Review.

Pessah IN, Kim KH, Feng W  
Redox sensing properties of the ryanodine receptor complex.  
Front Biosci. 2002 May 1;7:a72-9.

Protasi F  
Structural interaction between RYRs and DHPRs in calcium release units of cardiac and skeletal muscle cells.  
Front Biosci. 2002 Mar 1;7:d650-8. Review.

Rios E, Brum G  
Ca<sup>2+</sup> release flux underlying Ca<sup>2+</sup> transients and Ca<sup>2+</sup> sparks in skeletal muscle.  
Front Biosci. 2002 May 1;7:d1195-211. Review.

Schneider MF, Ward CW  
Initiation and termination of calcium sparks in skeletal muscle.  
Front Biosci. 2002 May 1;7:d1212-22. Review.

Sorrentino V  
Ryanodine receptor type 3: why another ryanodine receptor isoform?  
Front Biosci. 2003 Jan 1;8:D176-82.

Takeshima H  
Intracellular Ca<sup>2+</sup> store in embryonic cardiac myocytes.  
Front Biosci. 2002 Jul 1;7:d1642-52. Review.

Wagenknecht T, Samsó M  
Three-dimensional reconstruction of ryanodine receptors.  
Front Biosci. 2002 Jun 1;7:d1464-74. Review.

Welch W  
Quantitative relationships between ryanoids, receptor affinity and channel conductance.  
Front Biosci. 2002 Aug 1;7:d1727-42. Review.

Williams AJ  
Ion conduction and selectivity in the ryanodine receptor channel.  
Front Biosci. 2002 May 1;7:d1223-30. Review.

# Sarcoplasmic Reticulum Ca release in Intact Ventricular Myocytes

Donald M. Bers

Department of Physiology, Loyola University Chicago, Stritch School of Medicine, Maywood, IL 60153.

Email: [dbers@lumc.edu](mailto:dbers@lumc.edu)

**ABSTRACT** Sarcoplasmic reticulum (SR) Ca release in intact ventricular myocytes is the major source of Ca which activates cardiac contraction (although Ca influx makes a non-negligible contribution in most species). The fundamental events of SR Ca release are known as Ca sparks. The twitch Ca transient is composed of ~10,000 Ca sparks occurring in a given cell, and they are synchronized by the action potential and Ca current. Many factors influence SR Ca release amplitude and kinetics, and the focus here is on understanding how these factors work in the intact cellular environment. The intracellular [Ca] ( $[Ca]_i$ ) and intra-SR [Ca] ( $[Ca]_{SR}$ ) are two of the most important dynamic modulators of SR Ca release. Indeed, while  $[Ca]_i$  (and Ca current which initiates systolic SR Ca release) is widely acknowledged to be important, it is increasingly clear that  $[Ca]_{SR}$  changes dynamically under physiological conditions and that this has very important regulatory effects on the SR Ca release process. While elevation of  $[Ca]_{SR}$  obviously increases the driving force and amount of SR Ca available for release, it also increases the fractional release and can be responsible for spontaneous diastolic SR Ca release. These issues are discussed in both normal physiological and pathophysiological contexts.

## INTRODUCTION

During cardiac excitation-contraction (E-C) coupling Ca enters the cell via L-type Ca channels as Ca current ( $I_{Ca}$ ), while a smaller amount of Ca enters the cell via Na/Ca exchange (NCX) working in the outward NCX current ( $I_{Na/Ca}$ ) mode (Fig 1 ; ref 1,2). Ca influx via  $I_{Ca}$  triggers Ca release from the sarcoplasmic reticulum (SR) via the ryanodine receptor (RyR). While Ca entry via NCX can modulate or in extreme cases contribute to direct triggering of SR Ca release, this and other potential trigger mechanisms will be discussed below. The combination of Ca influx and SR Ca release raises free cytosolic [Ca] ( $[Ca]_i$ ) which drives Ca binding to troponin C that switches on the contractile machinery. The rise in  $[Ca]_i$  during a twitch is typically from ~100 nM to 1  $\mu$ M. However, because  $[Ca]_i$  is buffered (e.g. by 70  $\mu$ M troponin C and 50  $\mu$ M SR Ca-ATPase) the total amount of Ca added to the cytosol to achieve this  $[Ca]_i$  is about 50-100  $\mu$ mol/l cytosol.

For relaxation to occur,  $[Ca]_i$  must decline and this requires Ca transport out of the cytosol. Four transport systems can contribute to this  $[Ca]_i$  decline: 1) the SR Ca-ATPase, 2) NCX in the Ca extrusion mode, 3) sarcolemmal Ca-ATPase and 4) mitochondrial Ca uniporter. The SR Ca-ATPase and NCX are the dominant mechanisms by far, but their relative contributions vary. In most mammalian ventricular myocytes (including rabbit, guinea-pig, ferret, dog, cat and human), the SR Ca-ATPase is responsible for about 60-75% of Ca extrusion with 25-40% attributable to NCX. In rat and mouse ventricular myocytes the SR Ca-ATPase is more dominant, taking up more than 90% of the Ca involved in E-C coupling. This balance can differ in different conditions. For example, at higher frequency and/or with sympathetic stimulation the SR

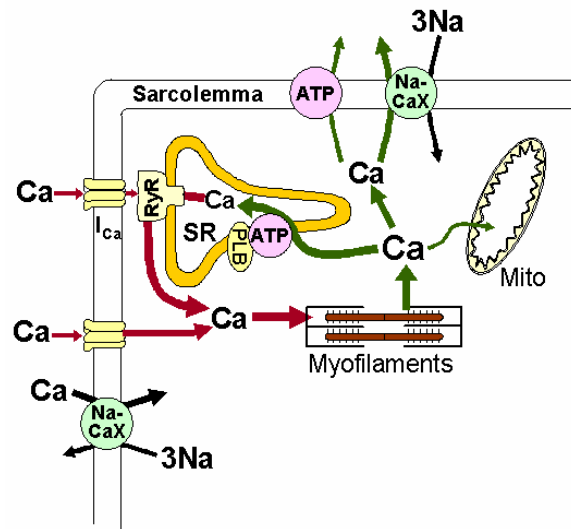


Figure 1. Ca movements in cardiac myocytes. Ca enters via Ca current ( $I_{Ca}$ ) and a smaller amount via Na/Ca exchange (NaCaX), triggering SR Ca release via RyR at the cleft. Ca is transported out of the cytosol (allowing Ca dissociation from the myofibrils) via the SR Ca-ATPase (regulated by phospholamban, PLB), NaCaX, sarcolemmal Ca-ATPase and mitochondrial (mito) Ca uniporter (ATP indicates the two ATPases).

becomes more dominant, while during heart failure the transsarcolemmal Ca fluxes are even more important (see section 6). In general this means that, unlike in skeletal muscle, Ca influx and extrusion plays an important quantitative role in E-C coupling in heart.

Much work has been done at the subcellular and molecular level as to how the key molecular

players ( $I_{Ca}$ , RyR, SERCA2, phospholamban, NCX) function and are regulated. Indeed, this has provided a very rich array of important fundamental mechanistic information. However, it is crucial that the characteristics of these transporters be understood in the real cellular environment. While this inevitably entails sacrificing some degree of control over intracellular conditions, the advantages of understanding how the system works in the natural cellular environment make this a scientific imperative. Thus, the focus of this article will be to extend basic properties of Ca transport systems to the integrated cellular environment. In line with the focus of this volume, I will deal primarily with the SR Ca release in intact ventricular myocytes.

### **Ca SPARKS AND TWITCH Ca TRANSIENTS**

The fundamental unit of SR Ca release in cardiac muscle is the Ca spark (3). Ca sparks are local SR Ca release events that likely represent the concerted opening of 6-20 individual RyR channels in a fairly stereotypical process (4-8). Once one RyR in a junctional cluster opens, it raises local  $[Ca]_i$  causing an entire cluster to fire. Several RyRs may also be mechanically coupled (9), thereby assuring the local regenerative nature of Ca-induced Ca-release (CICR) within a junction (a cylinder  $\sim 100$  nm in diameter and 15 nm high). However, in the space between individual junctions (300-2,000 nm) local  $[Ca]_i$  declines, thus limiting propagation of SR Ca release from one junction to another under normal conditions. When cellular Ca loads are very high, the RyR sensitivity is increased and CICR can propagate as a Ca wave along the entire length of a cell at  $\sim 100$   $\mu\text{m/s}$ .

Ca sparks occur with a low stochastically probability in the resting myocyte ( $P_o \sim 10^{-4}$ ), but are spatially and temporally synchronized during E-C coupling, when almost every junctional coupling region contributes to SR Ca release (10-13). When Ca influx via  $I_{Ca}$  raises local  $[Ca]_i$  in the junctional cleft to 5-10  $\mu\text{M}$  (within 2-5 ms of depolarization), this abruptly and dramatically increases RyR open probability, at all junctions in the cell. Because of spatial and temporal overlap during E-C coupling, Ca sparks cannot normally be well visualized, unless most  $I_{Ca}$  is blocked to diminish overlap (11,13) or high Ca buffer concentrations are used to trap released Ca more locally (14). Thus, the normal myocyte Ca transient is the summation of some 10,000 synchronized Ca sparks (1 per junction) and each Ca spark releases  $2-3 \times 10^{-19}$  mol Ca, or 12-18,000 Ca ions.

Because Ca sparks and twitch Ca transients have a similar basis, we can expect that things that alter diastolic Ca sparks may have qualitatively similar effects on RyR during E-C coupling. Other chapter herein will address some of the details summarized above in more detail. Here the focus is extrapolation and integration up to the cellular level, while keeping characterizations at more fundamental levels in mind.

### **FACTORS AFFECTING SR Ca RELEASE**

Numerous factors alter the frequency and amplitude of diastolic Ca sparks and the sensitivity of the RyR to activation by local intracellular Ca, which is generally considered to be the primary physiological activator of SR Ca release. How  $[Ca]_i$  and several modulators of RyR gating may affect SR Ca release in intact myocytes is described below.

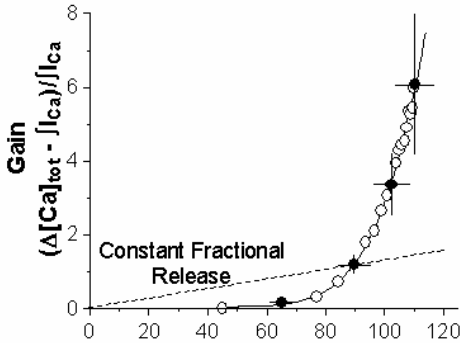
#### **Intracellular Free [Ca]**

Since Fabiato described CICR in permeabilized cardiac myocytes (15) it has become increasingly clear that the amount of Ca entry can regulate SR Ca release. This is also completely consistent with the cytosolic  $[Ca]$ -dependence of RyR open probability measured in lipid bilayers studies (16). Indeed, when cellular SR Ca load in intact cells is held constant, altering  $I_{Ca}$  amplitude by changing extracellular  $[Ca]$  ( $[Ca]_o$ ) or test membrane potential ( $E_m$ ) produces gradation of SR Ca release (17,18). However, since individual junctions fire largely in a stereotypical all-or-none fashion, the gradation may come mostly from the fraction of junctions which contribute to a Ca spark. On the other hand, there is also some evidence that the amplitude of the local SR Ca release can also be modulated by  $I_{Ca}$  trigger size (19). Intact cell voltage clamp experiments have also suggested that opening of a single L-type Ca channel is sufficient to activate a Ca spark and that  $\sim 2$  Ca ions have to bind to an RyR. Single channel bilayers experiments suggest that up to 4 Ca ions may be required and that the apparent  $K_d$  for Ca is in the range of several  $\mu\text{M}$  (20). This is consistent with models of diffusion around the inner mouth of a Ca channel, where  $[Ca]_i$  within a radius of  $\sim 15$  nm is expected to rise to 10-20  $\mu\text{M}$  within 1 ms of L-type Ca channel opening (21,22). The above bilayer studies suggested that there is also very little temporal delay ( $< 1$  ms) between the rise in local  $[Ca]_i$  and RyR opening. This agrees with our measurements in intact cells where the peak of SR Ca release measured locally (as the effect on  $I_{Ca}$  inactivation) occurred within 2-5 ms of the rise of the action potential, which is similar to the time to peak  $I_{Ca}$ .

While it is important to understand these local events which are critical determinants of E-C coupling, it is also important to keep in mind that it is the global cellular Ca and binding of Ca to troponin C which produces the end effect of E-C coupling. The peak of the global Ca transient and Ca release flux sensed by global Ca indicators is slower and smaller than that in the junctional cleft. Indeed, global  $[Ca]_i$  only reaches  $\sim 1$   $\mu\text{M}$  during a twitch. This has important implications with respect to the local control of CICR indicated above. That is, activation of SR Ca release may normally require a rapid rise in local  $[Ca]_i$  to  $> 10$   $\mu\text{M}$ . As Ca diffuses away from the junction  $[Ca]_i$  decreases due to dilution into the cytosolic volume, strong buffering and Ca removal fluxes. This means that at the neighboring junctions ( $> 0.3$   $\mu\text{m}$  in the transverse and  $\sim 2$   $\mu\text{m}$  in the longitudinal direction)  $[Ca]_i$  will be well below the threshold to trigger that neighboring SR Ca release unit. This normally prevents propagated SR Ca release in

ventricular myocytes, which could cause asynchrony in the ventricle and contribute to arrhythmogenesis. As we will see, increasing SR Ca content (and other factors) may shift this apparent threshold for local  $[Ca]_i$  to trigger neighboring junctions.

### A. Gain of E-C Coupling



### B. Fractional SR Ca Release

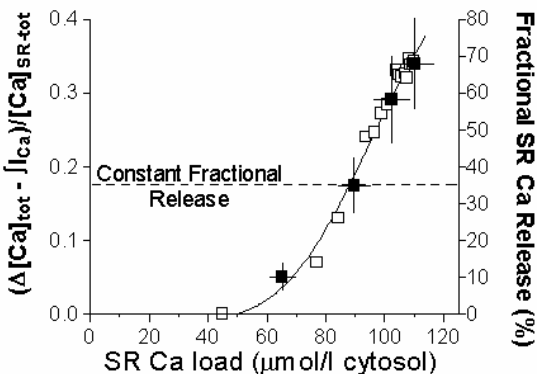


**Figure 2.** Fractional SR Ca release and gain of E-C coupling. Data from Shannon *et al.* (25) as regraphed, showing the SR Ca load-dependence of E-C coupling gain (A) or fractional release (B). Gain is defined as the total Ca transient amplitude ( $\Delta[Ca]_i$  translated to total Ca  $[Ca]_{tot}$ ) minus integrated  $I_{Ca}$ , divided by the integrated  $I_{Ca}$ . Fractional SR Ca release is the same  $\Delta[Ca]_{tot}$  minus integrated  $I_{Ca}$ , but divided by the SR Ca load at the time of the twitch. Since some Ca can be taken up and released again, the right axis may reflect the total fractional release.

### Intra-SR Free $[Ca]$

Clearly, one expects the amount of SR Ca release to depend on the amount of SR Ca available for release. Indeed, the release rate should be related to the free intra-SR  $[Ca]$  ( $[Ca]_{SR}$ ) in a relatively direct way. If this were the only effect, we would expect the "gain" of E-C coupling (Ca release/ $I_{Ca}$ ) to rise roughly linearly as a function of  $[Ca]_{SR}$  and the fraction of SR Ca released to be relatively constant as a function of  $[Ca]_{SR}$ . Cellular data clearly indicate that this simple expectation is incorrect. That is, at SR Ca content below about 40% of normal ( $\sim 40 \mu\text{mol/l}$  cytosol) a normal  $I_{Ca}$  trigger causes almost no SR Ca release, but as SR Ca rises there is an increasingly steep relationship between either gain or fractional SR Ca release and SR Ca

content or  $[Ca]_{SR}$  (18,23-26). Figure 2 shows the dependence of gain and fractional release on SR Ca content. It is also clear that increasing intra-SR Ca content greatly increases the frequency (as well as amplitude) of resting Ca sparks, even when diastolic  $[Ca]_i$  is unchanged (3,27-29).

This effect is completely consistent with isolated RyR measurements in bilayers, where higher luminal  $[Ca]$  greatly increases RyR2 open probability (30-35). Indeed, higher  $[Ca]_{SR}$  greatly shifts the  $[Ca]_i$ -dependence of RyR gating. The same  $[Ca]_i$  that caused half-maximal activation of RyR  $P_o$  at  $[Ca]_{SR} = 5\text{mM}$  produced no RyR opening when  $[Ca]_{SR}$  was low ( $20 \mu\text{M}$ ). Some investigators claim that the luminal Ca effect is due to more Ca passing through the channel and acting at the cytoplasmic activating site (33,34). However, Györke & Györke (35) showed that this activating effect of  $[Ca]_{SR}$  on RyR gating was due to Ca binding on the luminal side, because the  $[Ca]_{SR}$  effect was independent of driving voltage direction. In any event, at the cellular level  $[Ca]_{SR}$  has a profound role in regulating the RyR. At low  $[Ca]_{SR}$  the SR can fail to release Ca, while at high  $[Ca]_{SR}$  the luminal  $[Ca]$  may be the important trigger for what is normally called spontaneous SR Ca release associated with cellular Ca overload and arrhythmogenic delayed afterdepolarizations (DADs). Since SR Ca content affects both the amount of Ca available for release and the gating of the RyR, it is an extremely powerful modulator of SR Ca release. Thus, I will address determinants of SR Ca load separately below (section 5).

### Turn -off of SR Ca release

Since CICR is inherently a positive feedback mechanism, it is important to consider what turns off release. Moreover, there is good evidence indicating that only about half of the SR Ca content is actually released during a twitch. In addition, SR Ca release must turn off to allow diastolic refilling of the heart. Three possibilities contributors are: 1) local  $[Ca]_{SR}$  depletion, 2) RyR inactivation (or adaptation) and 3) stochastic attrition (36-38). Stochastic attrition means that as channels gate stochastically, there is a finite probability that all of the L-type Ca channels and RyRs in a junction close simultaneously, in which case local  $[Ca]_i$  would fall very rapidly and interrupt regenerative release. This could work for a small number of Ca channels, but with more realistic numbers of channels, it is far too unlikely that all would close at once. However, if RyRs gate as a synchronized or coupled group (9) stochastic attrition could contribute to the shut off of SR Ca release. However, it is not yet clear whether most RyRs in a spark site really worked that way.

The local depletion of SR Ca cannot completely explain the turn-off of release, because very long lasting Ca sparks can be seen (e.g. with ryanodine or caffeine) that do not decline with time ( $>200 \text{ms}$ ; ref 3,27). Diffusion from other regions of the SR might limit local SR Ca depletion, but during the global Ca transient, the entire  $[Ca]_{SR}$  declines. Since  $[Ca]_{SR}$  strongly modulates RyR gating, the decline in local  $[Ca]_{SR}$  may contribute dynamically to

the turn-off of global SR Ca release during a twitch. As stated above though, this cannot explain fully why either Ca sparks or global SR Ca release turn off.

Cardiac RyRs can also undergo inactivation or adaptation (both of which may depend on  $[Ca]_i$ ). Classically, inactivation is absorbing (as in Na channels) such that the RyR would be unavailable for re-activation until it recovers (37,39-41). Adaptation refers to a reduction in RyR open probability from a peak upon rapid activation, but from which point the RyR can still be reactivated by a higher  $[Ca]_i$  (39,42). Whether the decline in RyR open probability observed is solely inactivation, adaptation or some combination is controversial, and few cellular studies have addressed this in any unequivocal manner. Nevertheless, there is clearly some refractoriness in cellular and local SR Ca release events (27,37,43,44).

In summary, RyR inactivation and partial luminal SR Ca depletion (by reducing RyR opening) probably both contribute to the turn-off of release during a twitch Ca transient. Coupled gating of RyRs (so many RyRs gate as one) may also mean that a variant of stochastic attrition might contribute as well.

### Restitution

After a twitch or spontaneous Ca spark RyR availability recovers with two time constants, a fast one (100-300 ms; ref 44) and a very slow one (several seconds; ref 27,45). RyR inactivation may be important in minimizing inappropriate SR Ca release events between heartbeats. It may also play a central role in the force-frequency relationship that is recorded in myocytes, muscles and the intact heart. In particular, if the SR Ca content does not increase, then increased pacing frequency results in decreased contractile force which cannot be attributed to altered SR Ca availability,  $I_{Ca}$ , action potential or myofilament properties. Thus, there is a refractoriness in the E-C coupling mechanism that has physiological impact. Based on Fabiato's early work on CICR, this sort of refractoriness is expected and ought to be sensitive to the level of  $[Ca]_i$ , in a manner analogous to the  $E_m$ -dependence of Ca or Na channel recovery from inactivation. That is, lower  $[Ca]_i$  ought to favor more rapid restitution of RyR function. This has not been well tested, but elevations in diastolic  $[Ca]_i$  in pathophysiological conditions could also compromise RyR availability. On the other hand, when  $[Ca]_{SR}$  and  $[Ca]_i$  are both elevated, Ca sparks occur immediately after a twitch (27). The high  $[Ca]_{SR}$  may hasten recovery of RyR even when  $[Ca]_i$  is relatively high.

### Mg, ATP and pH

Many factors can modulate the RyR open probability, but for practical reasons most bilayer experiments have been done with relatively non-physiological solutions. Intracellular free  $[Mg]$  is normally 0.5-1 mM in cardiac myocytes, and mM Mg inhibits RyR gating. When the cardiac RyR is activated by Ca (without ATP), Mg inhibits  $P_o$  half-maximally at 2.3 mM (46). However, at physiological  $[ATP]$  (5 mM) the inhibitory effect of free  $[Mg]$  is modest at 2 mM, and half-inhibition occurs at 5 mM free  $[Mg]$ . The precise  $[Ca]_i$  vs.  $P_o$  relationship in vivo

is not known, but ATP shifts activation to lower  $[Ca]$ , while Mg shifts it to the higher  $[Ca]$ . Mejia-Alvarez *et al.* (47) also made great efforts to study cardiac RyR single channel current under solution conditions which approach physiological. A unitary current of  $\sim 0.30$  pA can be inferred at 2 mM  $[Ca]_{SR}$  and 0.15 pA at 1 mM  $[Ca]_{SR}$  (150 mM  $[K]$ , and 1 mM  $[Mg]$ ).

Since  $[ATP]$  and  $[Mg]$  do not change rapidly during E-C coupling these levels may set the physiological Ca-sensitivity of the RyR. For example, Valdivia *et al.* (42) found that mM Mg inhibits steady state cardiac RyR open probability ( $P_o$ ) at a given free  $[Ca]$ , but also accelerates the decline in  $P_o$  induced by a rapid increase in local  $[Ca]$ . During ischemia free intracellular  $[Mg]$  increases several-fold as  $[ATP]$  falls, presumably because ATP is a major Mg buffer (48). These changes would reduce RyR sensitivity to Ca. Ischemia is also accompanied by acidosis and cardiac RyR  $P_o$  is reduced by  $>50\%$  upon reduction of pH from 7.3 to 6.5 (46,49,50). Thus, ischemia may greatly depress the responsiveness of the RyR to a given local activating Ca.

### Na/Ca exchange

Ca entry via NCX has been implicated as a potential trigger of SR Ca release in two different ways. First, the rapid Na current associated with the action potential upstroke may raise local submembrane  $[Na]$  ( $[Na]_{sm}$ ), causing Ca entry via outward  $I_{Na/Ca}$  to trigger SR Ca release (51-53). This interpretation has, however, been challenged (54-56). Data also suggests that Na channels are excluded from the junctional cleft and from regions where NCX is localized (57), making this mechanism less likely. Second, outward  $I_{Na/Ca}$  is activated directly by depolarization, and can trigger SR Ca release and contraction, especially at very positive  $E_m$  and when  $I_{Ca,L}$  is blocked (58,59). However, a given Ca influx via  $I_{Na/Ca}$  is much less effective and slower than  $I_{Ca,L}$  in triggering SR Ca release (60). Thus, when both  $I_{Ca}$  and  $I_{Na/Ca}$  triggers coexist, CICR is controlled almost entirely by  $I_{Ca}$ . Na/Ca exchanger molecules may also be excluded from the junctional cleft, making this less physically feasible (57). Thus, outward  $I_{Na/Ca}$  can trigger SR Ca release, but its physiological role may be modest. It might gradually trigger SR Ca release if there is no nearby Ca channel activated, or it may raise local submembrane  $[Ca]_i$  to allow a given  $I_{Ca}$  trigger to be more efficacious in causing SR Ca release.

### Dihydropyridine receptor, Bay K 8644 and FK-506

In skeletal muscle there is fairly clear evidence that the skeletal L-type Ca channel (DHPR) physically interacts with the skeletal RyR, especially in the region of the loop between the second and third domain of the DHPR (II-III loop; reviewed in ref. 1). In heart, the situation is less clear, despite highly homologous RyR and DHPR proteins. The emerging cardiac picture is of a much less robust DHPR-RyR interaction than in skeletal muscle. This is consistent with the lack of voltage-dependent Ca release (VDCR, see below), a less ordered physical array of DHPR

over RyR in junctions (61) and the 4-10-fold excess of RyR over DHPR (62). This excess of RyR implies that at most 10-25% of RyR could possibly interact with a DHPR. Nevertheless, cardiac DHPRs are concentrated at sarcolemmal-SR junctions, albeit not as tetrads (61). The carboxy half of a cardiac DHPR II-III loop peptide (Ac-10C, KERKKLARTA) was found to activate skeletal RyR1 and enhance SR Ca release in skinned skeletal muscle (63,64). We found that Ac-10C can inhibit cardiac Ca spark frequency by 63% in voltage clamped ventricular myocytes, for the same SR Ca load and diastolic  $[Ca]_i$  (65). A peptide from the carboxy region common to both cardiac and skeletal DHPR also inhibits ryanodine binding to cardiac RyR (66). Thus, the analogous cardiac DHPR and RyR domains may interact, but clarifying work is needed.

The dihydropyridine L-type Ca-channel agonist, Bay K 8644 has also provided data suggestive of molecular communication between cardiac DHPR and RyR. Bay K 8644 (100 nM) accelerates resting loss of SR Ca in ventricular myocytes in a manner that is completely independent of Ca influx, and which is competitively inhibited by DHP antagonists (67-71). Bay K 8644, even at 100 times higher concentration, had no direct effect on cardiac RyR channel gating in bilayer experiments. Another Ca channel agonist (FPL-64176) which does not compete at the same DHPR site did not alter Ca sparks, but enhanced  $I_{Ca}$  in a manner similar to Bay K 8644. Bay K 8644 also increased ryanodine binding in intact cells, but not after mechanical disruption. We proposed that Bay K 8644 binds to the DHPR and transmits a Ca-independent signal to the RyR, altering its resting open probability. This effect of Bay K 8644 via the DHPR differs from effects on  $I_{Ca}$  that occur more slowly and in a depolarization-dependent manner (71). We concluded that after binding to the DHPR the pathways diverge for the  $I_{Ca}$  gating effect and the intramolecular effect on the RyR, manifest as increased resting Ca sparks.

Ca sparks occur in the complete absence of extracellular Ca, even without Bay K 8644. This emphasizes that Ca sparks do not require Ca entry. Moreover, even at this microscopic level action potentials produce no SR Ca release or change in resting Ca sparks in the absence of  $[Ca]_o$  (with or without Bay K 8644). Thus, while these Bay K 8644 effects may imply a weak intramolecular link between cardiac DHPR and RyR, they do not support  $E_m$ -dependent SR Ca release in heart. With respect to E-C coupling, it is notable that Bay K 8644 depresses E-C coupling (lower Ca release for a given  $I_{Ca}$  and SR Ca load; 72,73). This effect can be explained by the long open times induced by Bay K 8644 modified Ca channels, without invoking the modulation above. That is, a given whole cell  $I_{Ca}$  in the presence of Bay K 8644 requires fewer channels (because openings are longer). Since only the first couple of ms of  $I_{Ca}$  are needed to trigger SR Ca release, much of the Ca influx will be wasted with respect to triggering SR Ca release (i.e. lower Ca release for a given  $I_{Ca}$ ). In conclusion, there may only be a weak DHPR-RyR link in heart.

### CaMKII, Protein Kinase A

Phosphorylation of the cardiac RyR by cAMP-dependent protein kinase (PKA) alters RyR gating in bilayers. Valdivia *et al.* (42) found that PKA decreased basal  $P_o$  at 100 nM  $[Ca]$ , but greatly increased peak  $P_o$  (to nearly 1.0) during a rapid photolytic increase of  $[Ca]$ . PKA also accelerated the subsequent decline in  $P_o$  attributed to adaptation. In contrast, Marx *et al.* (74) found that PKA-dependent phosphorylation at Ser-2809 enhanced steady state open probability of single RyRs in bilayers, and attributed this to displacement of FKBP-12.6 from the RyR. However, in more intact cellular systems, we could not detect any effect of PKA-dependent RyR phosphorylation on resting Ca sparks in the absence of phospholamban (with unchanged SR Ca load; 29). RyR phosphorylation might also alter the intrinsic responsiveness of SR Ca release to an  $I_{Ca}$  trigger signal, but results are mixed, showing increase, decrease and lack of change (19,75,76). Thus, whether PKA-dependent phosphorylation alters RyR behavior during rest or E-C coupling remains controversial. This is particularly challenging to measure in intact cells, because increases in  $I_{Ca}$  and SR Ca uptake make isolation of intrinsic RyR effects difficult.

Ca-Calmodulin dependent protein kinase (CaMKII) also phosphorylates the cardiac RyR at Ser-2809 (77). In bilayer recordings with cardiac RyR, CaMKII was reported to either increase or decrease channel  $P_o$  (77-79). This discrepancy may be partly explained by dynamic changes of RyR gating, as discussed above for PKA (but similar data are not available for CaMKII). In voltage clamped myocytes, we found that inhibition of CaMKII prevented a  $[Ca]_i$ -dependent increase in the fraction of SR Ca released for the same  $I_{Ca}$  and SR Ca content (80). Introduction of phosphatases (PP1 & PP2A) into myocytes also depresses E-C coupling gain (81). Thus, in the intact cardiac cell repeated Ca transients may activate CaMKII, phosphorylate RyR2 and enhance the efficacy of E-C coupling.

Calmodulin (CaM) has independent effects on the RyR, which complicates CaMKII effects. Fruen *et al.* (82) reported that 4 CaM molecules bind per skeletal muscle RyR (RyR1) tetramer at both low and high  $[Ca]$ . They found the same thing for the cardiac RyR2 at 200  $\mu$ M  $[Ca]$ , but when  $[Ca]$  was 100 nM RyR2 bound only 1 CaM per RyR tetramer (with lower CaM affinity at low  $[Ca]$ ). Balshaw *et al.* (83) showed 4 CaM molecules bind per RyR1 tetramer at both low and high  $[Ca]$ , and the same was true for the RyR2 in the absence of Ca. However, CaM binding increased to 7.5 CaM molecules per RyR2 tetramer at 100  $\mu$ M  $[Ca]$ . Thus, there is agreement that high  $[Ca]$  increases the CaM:RyR2 stoichiometry. CaM also regulates RyR gating.

CaM inhibits Ca release from both cardiac and skeletal SR at  $[Ca]_i > 100$  nM (82-88). For skeletal RyR1 at low  $[Ca]$  ( $< 100$  nM) CaM activates RyR1 opening, but at higher  $[Ca]$  ( $> 1$   $\mu$ M) CaM inhibits RyR1 channel opening. Using a mutant CaM which is unable to bind Ca, Rodney *et al.* (89) showed

enhanced RyR1 Ca affinity and single-channel activity at high [Ca], consistent with Ca bound CaM inhibiting RyR1. For cardiac RyR2 CaM inhibits RyR2 opening at both low and high [Ca], and shifts the Ca-dependence of RyR2 activation to higher [Ca] (83). In contrast, Fruen *et al.* (82) found no effect of CaM on RyR2 flux or ryanodine binding at 100 nM [Ca] (in the presence or absence of Mg). In conclusion, under physiological conditions we might expect CaM bound to RyR2 to exhibit either no effect or an inhibitory effect on the Ca-dependent activation of the RyR.

FK-506-binding proteins (FKBPs) bind to and co-purify with the RyR (90-93), but the intrinsic peptidyl-prolyl isomerase activity is not essential for RyR effects (94). FKBP-12 (MW 12,000) binds tightly to skeletal RyR, while heart expresses both FKBP-12 and -12.6, and the latter associates with the cardiac RyR2, due to a 600-fold higher affinity (93). FK-506 and rapamycin cause dissociation of FKBP from the RyR and modify RyR gating in bilayer studies (95-99). FKBP removal from skeletal RyR causes the appearance of subconductance states. Kaftan *et al.* (98) found analogous results with the cardiac RyR, which increased overall  $P_o$  (despite the lower conductance states). Indeed, when exogenous recombinant FKBP was added to recombinant RyR in bilayers the normal channel gating properties with FKBP were restored. On the other hand, Barg *et al.* (99) found no functional effect of FKBP on cardiac RyR. FK-506 also inhibits cardiac RyR adaptation (100) and increases Ca-sensitivity of RyR gating. Complementary measurements in intact cells show that FK-506 increases resting Ca spark frequency and causes resting SR Ca content to decline (100,101). Twitch Ca transients are also higher in ventricular myocyte where FKBP is either removed by FK-506 or genetically ablated (100-102). This confirms that the overall enhanced  $P_o$  of RyR in bilayers after FKBP removal extends functionally to resting Ca leak in intact ventricular myocytes and to E-C coupling effects as well.

A current working model is that FKBP physically stabilizes the coordinated gating of the 4 RyRs in one homotetramer so that openings go from the fully closed to the fully open state, but with reduced overall  $P_o$  for a given [Ca] (e.g. shifting the  $P_o$  vs. [Ca] relationship to higher [Ca]). Marx *et al.* (103) showed that FKBP may also be involved in physical coupling between RyR tetramers, allowing more than one tetramer to gate simultaneously.

Sorcin, a ubiquitous 22 kDa Ca binding protein ( $K_{m(Ca)}=1 \mu M$ ) associates with both cardiac RyR and DHPR (104,105). Sorcin could reduce RyR open probability and ryanodine binding ( $IC_{50}=480-700$  nM), but this inhibitory effect was relieved by PKA-dependent phosphorylation of sorcin (106). Thus, sorcin and FKBP might serve as endogenous inhibitors of SR Ca release, that can be relieved by PKA-dependent phosphorylation (107).

Eisner *et al.* (108) suggested that altered systolic RyR gating properties alone in intact cells exert only transitory effects on Ca transient amplitude, invoking a sort of autoregulation. That is, abrupt increases in RyR opening or fractional SR Ca

release cause greater Ca extrusion via Na/Ca exchange at the first beat, thereby decreasing SR Ca available for the next beat. In the steady state this lower SR Ca content offsets the increased fractional SR Ca release such that Ca transients are almost unchanged. This may limit the overall impact of RyR modulation in the intact cellular environment. On the other hand, there must also be some limit for this autoregulation, such that if the RyR is too leaky (especially through diastole), the SR Ca content could be reduced to the point that SR Ca release fails (as discussed above with respect to the effect of  $[Ca]_{SR}$  on fractional release). Thus, the process of SR Ca release must be interpreted in the complex cellular environment of the myocyte. SR Ca load serves as an important subcellular preload that could be considered analogous with end diastolic volume. As such factors regulating SR Ca load deserve a bit more detailed discussion.

## SR Ca CONTENT

### Thermodynamics and Leak vs. Pump-mediated Backflux

In principle, the maximal SR Ca content in the intact cell would occur in the absence of leak, when the SR Ca-ATPase reaches its thermodynamic limit. That is, for a stoichiometry of 2Ca ions transported per ATP consumed the free energy required from ATP is  $\Delta G_{SR-CaP} = 2RT \cdot \ln([Ca]_{SR}/[Ca]_i)$ . We measured a maximal SR [Ca] gradient of 7,000, consistent with  $\Delta G_{SR-CaP} = 44$  kJ/mol (109), which is 74% of the energy available from ATP (for  $\Delta G_{ATP}=59$  kJ/mol, ref 110). Thus, for  $[Ca]_i = 150$  nM,  $[Ca]_{SR}$  would be 1 mM, in agreement with estimates of  $[Ca]_{SR}$  in the beating heart (111), and energetic efficiencies of other P-type ATPases.

The SR Ca-pump is reversible and Ca can move out of the SR and even make ATP in doing so (112,113). Of course net reverse Ca-pump flux is not expected physiologically, because  $[Ca]_{SR}/[Ca]_i$  would have to exceed the  $\Delta G$  which built the gradient in the first place. However, it is important to appreciate that at thermodynamic equilibrium (with leak of Ca via other pathways at zero) both forward and reverse flux through the SR Ca-pump occur, but are equal and opposite. This can be appreciated by the following equation (114) :

$$\frac{V_{mFor}}{J_{Pump}} = \frac{([Ca]_i/K_{mRev})^2 - V_{mRev}([Ca]_{SR}/K_{mRev})^2}{1 + ([Ca]_i/K_{mFor})^2 + ([Ca]_{SR}/K_{mRev})^2} \quad (1)$$

where  $V_{mFor}$  and  $V_{mRev}$  are the forward and reverse maximum rates, and  $K_{mFor}$  and  $K_{mRev}$  are the forward and reverse dissociation constants. It can be seen that if  $[Ca]_{SR} = 0$ , the last term in both numerator and denominator drop out and this reduces to the standard Hill equation ( $V_{max}/(1+\{K_m/[Ca]_i\}^n)$ ). Thus, at equilibrium (with zero leak) the net SR Ca-ATPase flux ( $J_{Pump}$ ) is 0. At this point the numerator in Eq 1 is zero so the two terms are equal. For the reasonable assumption (based on data) that  $V_{mFor} = V_{mRev}$  this relationship implies that the limiting [Ca]

gradient above  $[Ca]_{SR}/[Ca]_i = K_{mRev}/K_{mFor}$  which is the well known Haldane relationship. It also means that the affinity of the Ca-pump for cytosolic Ca is 7000 times higher than that for intra-SR Ca (e.g.  $K_{mFor} = 300$  nM,  $K_{mRev} = 2$  mM). That is why Ca dissociates from the pump readily after it is transported into the SR. Thus, without any leak the SR Ca-pump should approach asymptotically a  $[Ca]_{SR}/[Ca]_i$  gradient of 7000. However, leak of Ca from the SR (e.g. as Ca sparks) is not normally zero, so the net SR Ca flux ( $J_{SR}$ ) is the sum of  $J_{pump}$  (as in Eq 1) plus  $J_{Leak}$ . In this more realistic steady state scenario the forward pump rate ( $J_{pumpF}$ ) must equal the sum of the pump backflux ( $J_{pumpR}$ ) plus  $J_{Leak}$ .

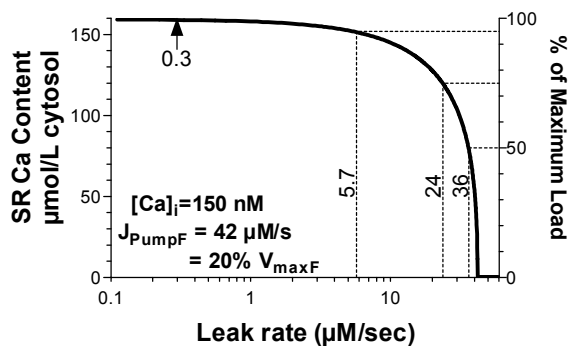


Figure 3. Dependence of SR Ca content on SR Ca leak rate. Curves are based on Eq 1 in the steady state ( $J_{pumpF} - J_{pumpR} = J_{Leak}$ ), where  $[Ca]_{SR}$  is a function of  $J_{Leak}$  and  $[Ca]_i$ :  $[Ca]_{SR} = 7000 \{ ([Ca]_i^2 (V_{max}/J_{Leak} - 1) - (K_{mFor})^2) / (V_{max}/J_{Leak} + 1) \}^{1/2}$  and SR Ca content,  $([Ca]_{SRtot} = [Ca]_{SR} + (B_{maxSR}/(1 + \{K_{dSR}/[Ca]_{SR}\}))$ , where  $B_{maxSR}$  (3 mmol/l cytosol) is the intra-SR binding capacity and  $K_{dSR}$  (0.6 mM) is the dissociation constant. Thus  $[Ca]_{SR}$  and  $[Ca]_{SRtot}$  are functions of  $[Ca]_i$  (150 nM),  $V_{max}$  (210  $\mu$ mol/l cytosol/s),  $K_{mFor}$  (300 nM) and  $J_{Leak}$ .

Figure 3 shows how the SR Ca content is affected by  $J_{Leak}$  at  $[Ca]_i$  of 150 nM (including consideration of intra-SR Ca buffering). When  $J_{Leak}$  is zero  $[Ca]_{SR}$  is  $\sim 1$  mM and the SR Ca content is 160  $\mu$ mol/l cytosol. As  $J_{Leak}$  increases the SR Ca content declines. In intact ventricular myocytes from rat and rabbit we measured  $J_{Leak}$  to be  $\sim 0.3$   $\mu$ mol/l cytosol/s and found this to be consistent with resting Ca spark frequency (115). This would suggest that leak is not very important in limiting the SR Ca load. That was consistent with our follow up study in voltage clamped rabbit ventricular myocytes, where stimulation or inhibition of the SR Ca-ATPase failed to significantly change the SR Ca load achieved at steady state (116). Of course achieving that  $[Ca]_{SR}/[Ca]_i$  gradient took longer when the pump was partially inhibited. However, if leak were predominant the final load should have been significantly lower as well (Fig 3). At odds with these observations, blocking RyR-mediated leak with tetracaine can dramatically increase SR Ca content (117-119). This effect would not be expected if leak were very small and might imply a  $J_{Leak}$  closer to  $\sim 5$ -10  $\mu$ mol/l cytosol/s (119). We have recently re-evaluated this issue with a novel experimental approach that allows us to measure SR

Ca leak at different SR Ca loads (120). We find the same sort of steep SR Ca load-dependence of leak as we reported for either E-C coupling gain or fractional release (in Fig 2) and for Ca spark frequency (27). The result was that  $J_{Leak}$  varies over a broad range and might be closer to 5  $\mu$ mol/l cytosol/s at relatively physiological SR Ca load and  $[Ca]_i$ . Considering that  $J_{Leak}$  increases steeply with  $[Ca]_{SR}$  and that increasing  $J_{Leak}$  limits SR Ca load (Fig 3), it is easy to appreciate that this creates an intrinsic limit to SR Ca load. That is, if SR Ca is high, it increases leak, thereby limiting SR Ca content.

It is also worthwhile to consider the energetic consequences of  $J_{Leak}$ . If  $J_{Leak}$  were zero then the SR Ca content during diastole could be maintained with no net ATP consumption (since  $J_{pumpF}$  would equal  $J_{pumpR}$ ). Of course, any intrinsic slippage or inefficiency in the pump mechanism would make some net energetic ATP cost to maintain  $[Ca]_{SR}$ . However, if  $J_{Leak}$  is 6  $\mu$ mol/l cytosol/s this must be compensated by an equivalent net  $J_{pumpF}$ , requiring 3  $\mu$ M ATP consumption per second. This constitutes an additional energetic demand for the heart. Figure 3 also shows that as  $J_{Leak}$  approaches 10-15% of the forward  $V_{max}$  of the pump the SR Ca load drops precipitously as a function of leak (because  $J_{pumpF}$  is  $\sim 15\%$  of  $V_{max}$  at diastolic  $[Ca]_i$ ). Thus if the physiological leak rate is very close to this steep region of the curve, small changes in SR Ca leak (as might occur in heart failure) could have a disproportionately large effect on SR Ca content.

During a normal cellular Ca transient  $[Ca]_{SR}$  declines during SR Ca release and consequently reverse Ca-pump flux is decreased, while forward Ca-pump flux is stimulated by high  $[Ca]_i$ . Thus there is an increase in net SR Ca uptake by the pump. As  $[Ca]_i$  declines and  $[Ca]_{SR}$  rises the forward Ca-pump rate falls and reverse Ca-pump rate increases, until the net pump flux comes into balance with the SR Ca leak flux. At that point the SR Ca content has returned to the steady state level for the next beat. During the cardiac cycle the amount of Ca which entered via  $I_{Ca}$  will also have to have been extruded by Na/Ca exchange. Of note in the non-steady state, either increased Ca extrusion by Na/Ca exchange or reduction of SR Ca-pump activity would result in less net Ca uptake by the SR and a lower steady state SR Ca content (and more extrusion of Ca from the cell). These perturbations may contribute to reduced SR Ca load and contractile dysfunction in heart failure (see Section 6).

An important functional consequence of this thermodynamic consideration is that SR Ca uptake (especially during late relaxation and diastole) will be sensitive to energetic limitations that may occur under pathophysiological conditions. For example, if  $[ATP]$  declines or  $[ADP]$  or  $[PO_4]$  rise, the  $\Delta G_{ATP}$  available to the Ca-pump will be reduced. While this may not alter  $V_{max}$  or initial rates of  $[Ca]_i$  decline, it will reduce the  $[Ca]$  gradient that the SR Ca-pump can generate. This will have preferential effects on the latter phase of  $[Ca]_i$  decline and on diastolic  $[Ca]_i$  as the pump approaches a different thermodynamic equilibrium (at lower  $[Ca]_{SR}$  and higher  $[Ca]_i$ ). The

lower SR Ca content would also disproportionately depress Ca transients by reducing both the amount of SR Ca available and also the fraction released.

### Measurement of SR Ca content

SR Ca content has been measured in a variety of ways, including radiotracer  $^{45}\text{Ca}$  fluxes, electron x-ray microprobe analysis, extracellular  $[\text{Ca}]_o$  depletions and rapid cooling contractures (see ref 1 for details and references). However, a convenient and widely used approach these days is the caffeine-induced Ca transient, as illustrated in Figure 4. This method has the advantage that it can be applied acutely to an isolated myocytes at any time (e.g. under different experimental conditions). Rapid application of 10-20 mM caffeine releases all SR Ca and prevents net reuptake because of open SR Ca release channels. Then quantitative measures of SR Ca load can be obtained from either the amplitude of the resultant contraction or Ca transient, or by integrating  $I_{\text{Na}/\text{Ca}}$  (since most of the SR Ca is removed from the cell this way; see Fig 4A). Caffeine must be very rapidly applied in order to achieve a rapid and relatively uniform rise in  $[\text{Ca}]_i$  throughout the cell. This is especially important when using either the contraction or Ca transient amplitude as an index of SR Ca content (less so when  $I_{\text{Na}/\text{Ca}}$  is integrated).

If one measures caffeine-induced  $\Delta[\text{Ca}]_i$  there are two important interpretational caveats. First, if there is significant Ca extrusion between the time that caffeine is applied and the peak  $[\text{Ca}]_i$  is observed (e.g. due to NCX) the peak  $[\text{Ca}]_i$  may be underestimated. Thus, caffeine-induced Ca transient are sometimes measured in conditions which inhibit NCX (e.g.  $0\text{Na}$ ,  $0\text{Ca}$  solution; 116,121). Of course this can limit the ability to simultaneously integrate  $I_{\text{Na}/\text{Ca}}$  (but see also ref 116). This issue makes it impractical to use caffeine-induced contractures or Ca transients in multicellular preparations, because  $[\text{Ca}]_i$  may already decline in surface cells prior to SR Ca release in cells at the center of the preparation. Caffeine-induced contractures and  $\Delta[\text{Ca}]_i$  can be useful from a comparative standpoint, but the second caveat is that to convert  $\Delta[\text{Ca}]_i$  to SR Ca content one must account for the buffering of Ca in the cytosol. This can be done using measured values of cytosolic Ca buffering (e.g. measured during  $I_{\text{Na}/\text{Ca}}$  as in Fig 4; refs 1,122,123).

Integration of  $I_{\text{Na}/\text{Ca}}$  during caffeine application can also provide a rather direct measure of the SR Ca content. This works because almost all of the Ca released by caffeine is extruded via  $I_{\text{Na}/\text{Ca}}$ . This same  $I_{\text{Na}/\text{Ca}}$  data (where  $[\text{Ca}]_i$  is also measured) can be used to measure cytosolic Ca buffering as illustrated in Fig 4B. This is like a simple reverse titration where integrated  $I_{\text{Na}/\text{Ca}}$  counts the total number of Ca ions removed for a measured change in  $[\text{Ca}]_i$ . There are also three main caveats in using the  $I_{\text{Na}/\text{Ca}}$  integral to measure SR Ca content. First, not all of the  $[\text{Ca}]_i$  decline during a caffeine-induced Ca transient is due to  $I_{\text{Na}/\text{Ca}}$ , but can also include contributions from the sarcolemmal Ca-ATPase and mitochondrial Ca uniporter (1,121). While these are relatively minor, one can account for this by dividing

the integrated  $I_{\text{Na}/\text{Ca}}$  by the fraction of  $[\text{Ca}]_i$  decline

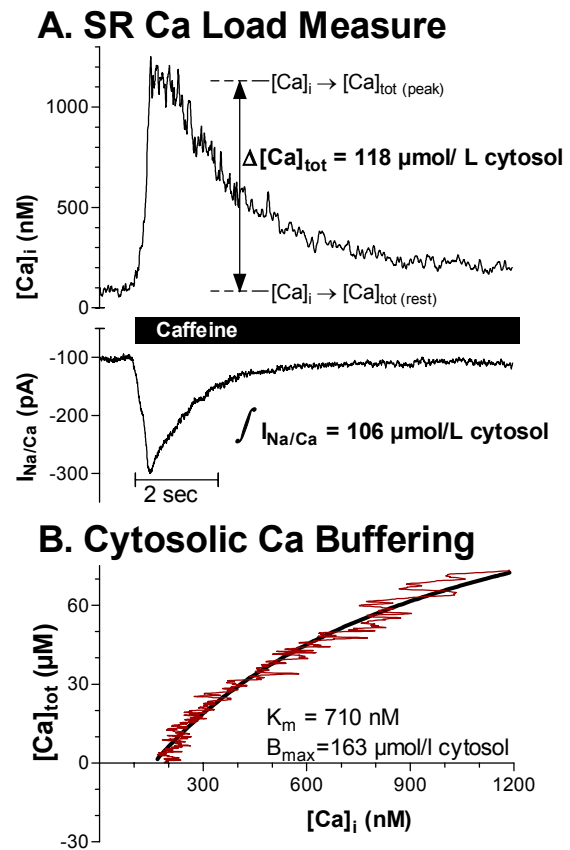


Figure 4. Measurement of SR Ca content and cytosolic Ca buffering during a caffeine-induced Ca transient in a rabbit ventricular myocyte under voltage clamp. A. Caffeine (10 mM) was applied rapidly and  $[\text{Ca}]_i$  is converted to total cytosolic  $[\text{Ca}]$  ( $[\text{Ca}]_{\text{tot}}$  in  $\mu\text{mol/l}$  cytosol) using previously measured Ca buffering ( $272/\{1+(673 \text{ nM}/[\text{Ca}]_i)\}$  as in ref 1). This yields SR Ca content of 118  $\mu\text{mol/l}$  cytosol. SR Ca content is also obtained by integrating  $I_{\text{Na}/\text{Ca}}$  (multiplying by 6.44 pF/pL cytosol, and dividing by 96,490 C/mol and 0.93 to account for non- $I_{\text{Na}/\text{Ca}}$  mediated Ca transport). B. To measure Ca buffering  $I_{\text{Na}/\text{Ca}}$  is integrated from the end backward as  $[\text{Ca}]_{\text{tot}}$  and fit as a function of  $[\text{Ca}]_i$  ( $[\text{Ca}]_{\text{tot}} = \{B_{\text{max}}/(1+K_m/[\text{Ca}]_i)\} + B_{\text{min}}$ , ref 120). Data recorded by K.S. Ginsburg and modified from ref. 1).

due to NCX ( $\sim 0.75$ - $0.93$  depending on species). A second conversion required is to transform the surface Ca flux (usually in A/F) into "volume flux" (in  $\mu\text{mol/l}$  cytosol). We have measured the surface to volume ratio for ventricular myocytes in several species allowing this conversion (6.4-13 pF/pL cytosol; ref 124). A third potential issue is the possibility that NCX stoichiometry might not be 3Na:1Ca under all experimental conditions (125,126). It is less clear how to deal with this potential caveat and most investigators still assume that the NCX stoichiometry is fixed at 3Na:1Ca. Given the different assumptions and limitations between  $\Delta[\text{Ca}]_i$  and integrated  $I_{\text{Na}/\text{Ca}}$  methods, it is especially advantageous if one can measure SR Ca load in both complementary ways simultaneously, especially when the results are in good agreement, as in Fig 4. This

also helps to reinforce the reasonable nature of the assumptions required. Maximal SR Ca content under relatively physiological conditions is about 90-130  $\mu\text{mol/L}$  cytosol, or about twice the amount of Ca required to activate a twitch (116,127,128).

### **PATHOPHYSIOLOGICAL ALTERATIONS IN HEART FAILURE**

Under pathophysiological conditions there may be a reduction in the amount of Ca released from the SR and this can be a significant contributing factor in contractile dysfunction (1). An important pathophysiological case in point (and major health problem) is heart failure, where contractile dysfunction has been shown to be caused in large part by altered myocyte Ca regulation (129-136). Most, but not all results have indicated that Ca current and myofilament Ca sensitivity are not significantly changed in heart failure (1). While alterations in these systems cannot be unequivocally excluded for participating in the heart failure phenotype, the focus here is on SR Ca release (and there is much experimental support for reduced SR Ca release in heart failure). There are three main mechanisms which have been implicated in the reduced SR Ca release in heart failure. Two of these are associated with reduced SR Ca content, which has been documented in human, canine and rabbit heart failure (74,134,136-138). The third is associated with unaltered SR Ca content, but reduced E-C coupling gain or fractional SR Ca release in rat or mouse heart failure (139-141).

#### **Reduced SERCA2 and Enhanced Na/Ca Exchange**

Many heart failure studies have demonstrated that the expression of SR Ca-ATPase is reduced, NCX is increased or both (130-135). Considering the fate of Ca during relaxation and  $[\text{Ca}]_i$  decline, it is easy to understand how either reduced SR Ca-ATPase, or enhanced NCX (or both) will tend to reduce SR Ca content by shifting more Ca back out of the cell vs. the SR. On the other hand, if both of these changes occur, they can be offsetting with respect to the rate of  $[\text{Ca}]_i$  decline during a twitch. That is, a large increase in NCX can compensate for a small reduction in SR Ca-ATPase function in terms of the rate of  $[\text{Ca}]_i$  decline, but both changes would cause reduction in SR Ca load. The most compelling data for this mechanism is in heart failure in humans (ischemic and non-ischemic), rapid pacing-induced failure in the dog and non-ischemic pressure/volume overload in rabbit. In these cases, measurements of SR Ca-pump and NCX expression and function have been well documented and the reduction in SR Ca content has been measured via caffeine-induced Ca transients (134,136,137). It is of interest to note that either SERCA reduction alone or NCX increase alone can largely cause the reduced SR Ca content by shifting the competition between these systems away from the SR and toward extrusion via NCX during relaxation and  $[\text{Ca}]_i$  decline (as demonstrated by experiments where SR Ca-ATPase is inhibited or NCX is overexpressed in normal cells, 142,143). Obviously, when both changes occur the results can

be additive. The reduction in SR Ca content in heart failure reduces the amount of SR Ca available for release for a given  $I_{\text{Ca}}$  trigger, but this depressant effect is likely compounded by the inhibitory effect of low luminal  $[\text{Ca}]_{\text{SR}}$  on the gating of the RyR during E-C coupling (as in Fig 2). Thus, reduced SR Ca content may be a crucial proximal cause of contractile dysfunction in heart failure.

#### **Enhanced SR Ca Leak**

Another mechanism that could reduce SR Ca content in heart failure is an enhanced diastolic leak of Ca from the SR (74,138). This would allow NCX another opportunity to compete with the SR Ca-pump for the Ca which had already been taken up by the SR during twitch  $[\text{Ca}]_i$  decline. The strongest evidence for this possibility comes from studies by Marx *et al.* (74). They found that in heart failure RyRs are hyperphosphorylated by PKA (nearly 1 phosphate group per RyR monomer), and suggested that this was caused by a reduction in the amount of phosphatase associated specifically with the RyR. They showed also that this degree of RyR phosphorylation caused FKBP-12.6 to dissociate from the RyR and that this caused an increase in Ca-sensitivity of RyR channel opening in lipid bilayer recordings. This might increase the diastolic leak of Ca from the SR, which according to the curve in Fig 3 would reduce SR Ca content. This agrees with observations that Ca spark frequency is enhanced by FK-506 which displaces FKBP-12.6 from the cardiac RyR (100,101). Although we could not detect any effect on Ca spark frequency when we directly phosphorylated the RyR by PKA in a cellular environment (29), this possibility remains intriguing and merits further study. Enhanced diastolic Ca leak could work synergistically with the changes in functional expression of the SR Ca-ATPase and NCX in reducing SR Ca load, and contribute to reduced SR Ca release during E-C coupling along the same lines just described.

#### **Altered E-C coupling**

In certain rat and mouse heart failure models E-C coupling is depressed without a reduction of  $I_{\text{Ca}}$ , SR Ca content or isolated RyR function. This includes spontaneous hypertensive heart failure (SHHF) rats, post-myocardial infarct rats and MLP knockout mice (139-141). In these cases a given  $I_{\text{Ca}}$  results in reduced SR Ca release (in some cases where SR Ca load was determined to be unchanged). It did not seem to be due to alteration in either the number or Ca-sensitivity of individual RyRs. This led these investigators to propose that there might be either a spatial change in the juxtaposition of Ca channels at the junction, or some other reduction in RyR Ca sensitivity that depends on the intact cellular environment. It is interesting that this mechanism has been most frequently reported in rats. While this might reflect a species-dependent difference in heart failure phenotype, this will require further study. This sort of intrinsic reduction in E-C coupling could also coexist with reduced SR Ca content as discussed above. Indeed, reduced SR Ca-ATPase expression

and function has also been reported by several groups in rat models of hypertrophy and heart failure, especially at the transition from compensated to overt heart failure (130,144). Thus, while there are likely to be multiple contributing factors to heart failure, reduced SR Ca release probably plays a major role in the contractile dysfunction.

## CONCLUSIONS

Release of Ca from the SR in the intact cardiac myocytes is influenced by numerous factors. We have learned much from studies in isolated systems (RyRs in bilayers and vesicles), but these results must be translated to the intact cellular environment. In some cases this can be approached with relatively direct cellular experiments, but this is not always the case. We do know that two of the most important physiological regulators of SR Ca release during diastole as well as systole are local  $[Ca]_i$  and  $[Ca]_{SR}$ . Other factors may modulate this relationship (e.g. ATP, Mg, pH, calmodulin, FKBP-12.6, phosphorylation, redox state, nitric oxide), but Ca is probably the main dynamic regulator.  $I_{Ca}$  is the primary trigger for SR Ca release during E-C coupling. While Ca influx via other pathways (e.g. NCX) can make some contribution under certain circumstances, these effects are likely to be primarily modulatory. Intra-SR Ca is crucial in regulating SR Ca release in two ways. First, it determines the amount of SR Ca available for release. However, the effect of luminal  $[Ca]_{SR}$  in regulating the gating of the RyR in the intact cell is also extremely important. This may increase the sensitivity of the RyR to cytosolic  $[Ca]_i$ . When SR Ca load is elevated, it may be the rise in  $[Ca]_{SR}$  which triggers the so-called spontaneous SR Ca release during Ca overload that can be directly arrhythmogenic. Low SR Ca content may be a central cause of contractile dysfunction in heart failure, where it can be caused by reduced SR Ca-ATPase functional expression, increased NCX expression, increased diastolic SR Ca leak or even energetic limitations which affect  $\Delta G_{ATP}$ . As a result, it is important to understand the functional cellular environment (and microenvironment) where the RyR exists in order to appreciate fully how it is functioning under any particular situation.

## ACKNOWLEDGEMENTS

The author acknowledges research support from the NIH (HL30077, HL64098 and HL64724).

## References

1. Bers, D.M.: Excitation-Contraction Coupling and Cardiac Contractile Force. 2<sup>nd</sup> ed. Dordrecht, Netherlands, Kluwer Academic Publishers (2001)
2. Bers, D.M.: Cardiac excitation-contraction coupling. *Nature* 415, 198-205 (2002)
3. Cheng, H., W.J. Lederer, & M.B. Cannell: Calcium sparks: Elementary events underlying excitation-contraction coupling in heart muscle. *Science* 262, 740-744 (1993)
4. Parker, I., W.J. Zang, & W.G. Wier:  $Ca^{2+}$  sparks involving multiple  $Ca^{2+}$  release sites along Z-lines in rat heart cells. *J Physiol* 497, 31-38 (1996)
5. Lipp, P. & E. Niggli: Submicroscopic calcium signals as fundamental events of excitation-contraction coupling in guinea-pig cardiac myocytes. *J Physiol* 492, 31-38 (1996)

6. Blatter, L.A., J. Hüser, & E. Ríos: Sarcoplasmic reticulum  $Ca^{2+}$  release flux underlying  $Ca^{2+}$  sparks in cardiac muscle. *Proc Natl Acad Sci USA* 94, 4176-4181 (1997)
7. Bridge, J.H.B., P.R. Ershler, & M.B. Cannell: Properties of  $Ca^{2+}$  sparks evoked by action potentials in mouse ventricular myocytes. *J Physiol* 518, 469-478 (1999)
8. Lukyanenko, V., I. Györke, S. Subramanian, A. Smirnov, T.F. Wiesner, & S. Györke: Inhibition of  $Ca^{2+}$  sparks by ruthenium red in permeabilized rat ventricular myocytes. *Biophys J* 79, 1273-1284 (2000)
9. Marx, S.O., J. Gaburjakova, M. Gaburjakova, C. Henrikson, K. Ondrias, & A.R. Marks: Coupled gating between cardiac calcium release channels (ryanodine receptors). *Circ Res* 88, 1151-1158 (2001)
10. Cannell, M.B., H. Cheng, & W.J. Lederer: Spatial non-uniformities in  $[Ca^{2+}]_i$  during excitation-contraction coupling in cardiac myocytes. *Biophys J* 67, 1942-1956 (1994)
11. Cannell, M.B., H. Cheng, & W.J. Lederer: The control of calcium release in heart muscle. *Science* 268, 1045-1049 (1995)
12. López-López, J.R., P.S. Shacklock, C.W. Balke, & W.G. Wier: Local, stochastic release of  $Ca^{2+}$  in voltage-clamped rat heart cells: Visualization with confocal microscopy. *J Physiol* 480, 21-29 (1994)
13. López-López, J.R., P.S. Shacklock, C.W. Balke, & W.G. Wier: Local calcium transients triggered by single L-type calcium channel currents in cardiac cells. *Science* 268, 1042-1045 (1995)
14. Song, L.S., J.S. Sham, M.D. Stern, E.G. Lakatta, & H.P. Cheng: Direct measurement of SR release flux by tracking ' $Ca^{2+}$  spikes' in rat cardiac myocytes. *J Physiol* 512, 677-691 (1998)
15. Fabiato, A. & F. Fabiato: Contractions induced by a calcium-triggered release of calcium from the sarcoplasmic reticulum of single skinned cardiac cells. *J Physiol* 249, 469-495 (1975)
16. Rousseau, E. & G. Meissner: Single cardiac sarcoplasmic reticulum  $Ca^{2+}$ -release channel: Activation by caffeine. *Am J Physiol* 256, H328-H333 (1989)
17. Beuckelmann, D.J. & W.G. Wier: Mechanism of release of calcium from sarcoplasmic reticulum of guinea-pig cardiac cells. *J Physiol* 405, 233-255 (1988)
18. Bassani, J.W.M., W. Yuan, & D.M. Bers: Fractional SR Ca release is regulated by trigger Ca and SR Ca content in cardiac myocytes. *Am J Physiol* 268, C1313-C1319 (1995)
19. Song, L.S., S.Q. Wang, R.P. Xiao, H. Spurgeon, E.G. Lakatta, & H. Cheng: Beta-adrenergic stimulation synchronizes intracellular  $Ca^{2+}$  release during excitation-contraction coupling in cardiac myocytes. *Circ Res* 88, 794-801 (2001)
20. Zahradníková, A., I. Zahradník, I. Györke, & S. Györke: Rapid activation of the cardiac ryanodine receptor by submillisecond calcium stimuli. *J Gen Physiol* 114, 787-798 (1999a)
21. Bers, D.M. & A. Peskoff: Diffusion around a cardiac calcium channel and the role of surface bound calcium. *Biophys J* 59, 703-721 (1991)
22. Soeller, C. & M.B. Cannell: Numerical simulation of local calcium movements during L-type calcium channel gating in the cardiac diad. *Biophys J* 73, 97-111 (1997)
23. Han, S., A. Schiefer, & G. Isenberg:  $Ca^{2+}$  load of guinea-pig ventricular myocytes determines efficacy of brief  $Ca^{2+}$  currents as trigger for  $Ca^{2+}$  release. *J Physiol* 480, 411-421 (1994b)
24. Spencer, C.I. & J.R. Berlin: Control of sarcoplasmic reticulum calcium release during calcium loading in isolated rat ventricular myocytes. *J Physiol* 488, 267-279 (1995)
25. Shannon, T.R., K.S. Ginsburg, & D.M. Bers: Potentiation of fractional SR Ca release by total and free intra-SR Ca concentration. *Biophys J* 78, 334-343 (2000b)
26. Trafford, A.W., M.E. Díaz, G.C. Sibbring, & D.A. Eisner: Modulation of CICR has no maintained effect on systolic  $Ca^{2+}$ : Simultaneous measurements of sarcoplasmic

- reticulum and sarcolemmal  $\text{Ca}^{2+}$  fluxes in rat ventricular myocytes. *J Physiol* 522, 259-270 (2000)
27. Satoh, H., L.A. Blatter, & D.M. Bers: Effects of  $[\text{Ca}^{2+}]_i$ , SR  $\text{Ca}^{2+}$  load, and rest on  $\text{Ca}^{2+}$  spark frequency in ventricular myocytes. *Am J Physiol* 272, H657-H668 (1997)
  28. Lukyanenko, V. & S. Györke:  $\text{Ca}^{2+}$  sparks and  $\text{Ca}^{2+}$  waves in saponin-permeabilized rat ventricular myocytes. *J Physiol* 521, 575-585 (1999)
  29. Li, Y., E.G. Kranias, G.A. Mignery & D.M. Bers: Protein kinase A phosphorylation of the ryanodine receptor does not affect Ca sparks in permeabilized mouse ventricular myocytes. *Circ Res* 90, 309-316 (2002)
  30. Sitsapesan, R. & A.J. Williams: Regulation of the gating of the sheep cardiac sarcoplasmic reticulum  $\text{Ca}^{2+}$ -release channel by luminal  $\text{Ca}^{2+}$ . *J Membr Biol* 137, 215-226 (1994)
  31. Sitsapesan, R. & A.J. Williams: Regulation of current flow through ryanodine receptors by luminal  $\text{Ca}^{2+}$ . *J Membr Biol* 159, 179-185 (1997)
  32. Lukyanenko, V., I. Györke, & S. Györke: Regulation of calcium release by calcium inside the sarcoplasmic reticulum in ventricular myocytes. *Pflügers Arch* 432, 1047-1054 (1996)
  33. Tripathy, A. & G. Meissner: Sarcoplasmic reticulum luminal  $\text{Ca}^{2+}$  has access to cytosolic activation and inactivation sites of skeletal muscle  $\text{Ca}^{2+}$  release channel. *Biophys J* 70, 2600-2615 (1996)
  34. Xu, L. & G. Meissner: Regulation of cardiac muscle  $\text{Ca}^{2+}$  release channel by sarcoplasmic reticulum luminal  $\text{Ca}^{2+}$ . *Biophys J* 75, 2302-2312 (1998)
  35. Györke, I. & S. Györke: Regulation of the cardiac ryanodine receptor channel by luminal  $\text{Ca}^{2+}$  involves luminal  $\text{Ca}^{2+}$  sensing sites. *Biophys J* 75, 2801-2810 (1998)
  36. Stern, M.D.: Theory of excitation-contraction coupling in cardiac muscle. *Biophys J* 63, 497-517 (1992)
  37. Sham, J.S.K., L.S. Song, Y. Chen, L.H. Deng, M.D. Stern, E.G. Lakatta, & H.P. Cheng: Termination of  $\text{Ca}^{2+}$  release by a local inactivation of ryanodine receptors in cardiac myocytes. *Proc Natl Acad Sci USA* 95, 15096-15101 (1998)
  38. Lukyanenko, V., T.F. Wiesner, & S. Györke: Termination of  $\text{Ca}^{2+}$  release during  $\text{Ca}^{2+}$  sparks in rat ventricular myocytes. *J Physiol* 507, 667-677 (1998)
  39. Györke, S. & M. Fill: Ryanodine receptor adaptation: Control mechanism of  $\text{Ca}^{2+}$ -induced  $\text{Ca}^{2+}$  release in heart. *Science* 260, 807-809 (1993)
  40. Sitsapesan, R., R.A.P. Montgomery, & A.J. Williams: New insights into the gating mechanisms of cardiac ryanodine receptors re-vealed by rapid changes in ligand concentration. *Circ Res* 77, 765-772 (1995)
  41. Schiefer, A., G. Meissner, & G. Isenberg:  $\text{Ca}^{2+}$  activation and  $\text{Ca}^{2+}$  inactivation of canine reconstituted cardiac sarcoplasmic re-ticulum  $\text{Ca}^{2+}$ -release channels. *J Physiol* 489, 337-348 (1995)
  42. Valdivia, H.H., J.H. Kaplan, G.C.R. Ellis-Davies, & W.J. Lederer: Rapid adaptation of cardiac ryanodine receptors: Modulation by  $\text{Mg}^{2+}$  and phosphorylation. *Science* 267, 1997-2000 (1995)
  43. Fabiato, A.: Time and calcium dependence of activation and inactivation of calcium-induced release of calcium from the sarcoplasmic reticulum of a skinned canine cardiac Purkinje cell. *J Gen Physiol* 85, 247-290 (1985)
  44. Cheng, H., M.R. Lederer, W.J. Lederer, & M.B. Cannell: Calcium sparks and  $[\text{Ca}^{2+}]_i$  waves in cardiac myocytes. *Am J Physiol* 270, C148-C159 (1996)
  45. Bers, D.M., R.A. Bassani, J.W.M. Bassani, S. Baudet, & L.V. Hryshko: Paradoxical twitch potentiation after rest in cardiac muscle: Increased fractional release of SR calcium. *J Mol Cell Cardiol* 25, 1047-1057 (1993)
  46. Xu, L., G. Mann, & G. Meissner: Regulation of cardiac  $\text{Ca}^{2+}$  release channel (ryanodine receptor) by  $\text{Ca}^{2+}$ ,  $\text{H}^+$ ,  $\text{Mg}^{2+}$ , and adenine nucleotides under normal and simulated ischemic conditions. *Circ Res* 79, 1100-1109 (1996)
  47. Mejia-Alvarez, R., C. Kettlun, E. Ríos, M. Stern, & M. Fill: Unitary  $\text{Ca}^{2+}$  current through cardiac ryanodine receptor channels under quasi-physiological ionic conditions. *J Gen Physiol* 113, 177-186 (1999)
  48. Murphy, E., C. Steenbergen, L.A. Levy, B. Raju, & R.E. London: Cyto-solic free magnesium levels in ischemic rat heart. *J Biol Chem* 264, 5622-5627 (1989)
  49. Ma, J., M. Fill, C.M. Knudson, K.P. Campbell, & R. Coronado: Ryanodine receptor of skeletal muscle is a gap junction-type channel. *Science* 242, 99-102 (1988)
  50. Rousseau, E. & J. Pinkos: pH modulates conducting and gating behavior of single calcium release channels. *Pflügers Arch* 415, 645-647 (1990)
  51. Leblanc, N. & J.R. Hume: Sodium current-induced release of calcium from cardiac sarcoplasmic reticulum. *Science* 248, 372-376 (1990)
  52. Levesque, P.C., N. Leblanc, & J.R. Hume: Release of calcium from guinea pig cardiac sarcoplasmic reticulum induced by sodium-calcium exchange. *Cardiovasc Res* 28, 370-378 (1994)
  53. Lipp, P. & E. Niggli: Sodium current-induced calcium signals in isolated guinea-pig ventricular myocytes. *J Physiol* 474, 439-446 (1994)
  54. Sham, J.S.K., L. Cleemann, & M. Morad: Gating of the cardiac  $\text{Ca}^{2+}$  release channel: the role of  $\text{Na}^+$  current and  $\text{Na}^+$ - $\text{Ca}^{2+}$  exchange. *Science* 255, 850-853 (1992)
  55. Bouchard, R.A., R.B. Clark, & W.R. Giles: Role of sodium-calcium exchange in activation of contraction in rat ventricle. *J Physiol* 472, 391-413 (1993)
  56. Sipido, K.R., E. Carmeliet, & A. Pappano:  $\text{Na}^+$  current and  $\text{Ca}^{2+}$  release from the sarcoplasmic reticulum during action potentials in guinea-pig ventricular myocytes. *J Physiol* 489, 1-17 (1995)
  57. Scriven, D.R.L., P. Dan, & E.D.W. Moore: Distribution of proteins implicated in excitation-contraction coupling in rat ventricular myocytes. *Biophys J* 79, 2682-2691 (2000)
  58. Levi, A.J., K.W. Spitzer, O. Kohmoto, & J.H.B. Bridge: Depolarization-induced Ca entry via Na-Ca exchange triggers SR release in guinea pig cardiac myocytes. *Am J Physiol* 266, H1422-H1433 (1994)
  59. Litwin, S.E., J. Li, & J.H.B. Bridge: Na-Ca exchange and the trigger for sarcoplasmic reticulum Ca release: Studies in adult rabbit ventricular myocytes. *Biophys J* 75, 359-371 (1998)
  60. Sipido, K.R., M. Maes & F. van de Werf: Low efficiency of  $\text{Ca}^{2+}$  entry through the  $\text{Na}^+$ - $\text{Ca}^{2+}$  exchanger as trigger for  $\text{Ca}^{2+}$  release from the sarcoplasmic reticulum - A comparison between L-type  $\text{Ca}^{2+}$  current and reverse-mode  $\text{Na}^+$ - $\text{Ca}^{2+}$  exchange. *Circ Res* 81, 1034-1044 (1997)
  61. Franzini-Armstrong, C. & F. Protasi: Ryanodine receptors of striated muscles: A complex channel capable of multiple interactions. *Physiol Rev* 77, 699-729 (1997)
  62. Bers, D.M. & V.M. Stiffel: Ratio of ryanodine to dihydropyridine receptors in cardiac and skeletal muscle and implications for E-C coupling. *Am J Physiol* 264, C1587-C1593 (1993)
  63. el-Hayek, R. & N. Ikemoto: Identification of the minimum essential region in the II-III loop of the dihydropyridine receptor  $\alpha_1$  subunit required for activation of skeletal muscle-type excitation-contraction coupling. *Biochemistry* 37, 7015-7020 (1998)
  64. Lamb, G.D., R. el-Hayek, N. Ikemoto, & D.G. Stephenson: Effects of dihydropyridine receptor II-III loop peptides on  $\text{Ca}^{2+}$  release in skinned skeletal muscle fibers. *Am J Physiol* 279, C891-C905 (2000)
  65. Li, Y. & D.M. Bers: A cardiac dihydropyridine receptor II-III loop peptide inhibits resting ryanodine receptor opening in ferret ventricular myocytes. *J Physiol* 537, 17-26 (2001)
  66. Slavik, K.J., J.P. Wang, B. Aghdasi, J.Z. Zhang, F. Mandel, N. Malouf, & S.L. Hamilton: A carboxy-terminal peptide of the  $\alpha_1$ -subunit of the dihydropyridine receptor inhibits  $\text{Ca}^{2+}$ -release channels. *Am J Physiol* 272, C1475-C1481 (1997)
  67. Hryshko, L.V., R. Bouchard, T. Chau, & D. Bose: Inhibition of rest potentiation in canine ventricular muscle by BAY K 8644: Comparison with caffeine. *Am J Physiol* 257, H399-H406 (1989a)

68. Hryshko, L.V., T. Kobayashi, & D. Bose: Possible inhibition of canine ventricular sarcoplasmic reticulum by BAY K 8644. *Am J Physiol* 257, H407-H414 (1989b)
69. McCall, E., L.V. Hryshko, V.M. Stiffel, D.M. Christensen, & D.M. Bers: Possible functional linkage between the cardiac dihydropyridine and ryanodine receptor: Acceleration of rest decay by Bay K 8644. *J Mol Cell Cardiol* 28, 79-93 (1996)
70. Satoh, H., H. Katoh, P. Velez, M. Fill, & D.M. Bers: Bay K 8644 increases resting  $Ca^{2+}$  spark frequency in ferret ventricular myocytes independent of Ca influx: contrast with caffeine and ryanodine effects. *Circ Res* 83, 1192-1204 (1998)
71. Katoh, H., K. Schlotthauer, & D.M. Bers: Transmission of information from cardiac dihydropyridine receptor to ryanodine receptor: Evidence from BayK 8644 effects on resting  $Ca^{2+}$  sparks. *Circ Res* 87, 106-111 (2000)
72. McCall, E. & D.M. Bers: BAY K 8644 depresses excitation-contraction coupling in cardiac muscle. *Am J Physiol* 270, C878-C884 (1996)
73. Adachi-Akahane, S., L. Cleemann & M. Morad: BAY K 8644 modifies  $Ca^{2+}$  cross signaling between DHP and ryanodine receptors in rat ventricular myocytes. *Am J Physiol* 276, H1178-H1189 (1999)
74. Marx, S.O., S. Reiken, Y. Hisamatsu, T. Jayaraman, D. Burkhoff, N. Rosemblyt, & A.R. Marks: PKA phosphorylation dissociates FKBP12.6 from the calcium release channel (ryanodine receptor): Defective regulation in failing hearts. *Cell* 101, 365-376 (2000)
75. Viatchenko-Karpinski, S. & S. Gyorko: Modulation of the  $Ca^{2+}$ -induced  $Ca^{2+}$  release cascade by beta-adrenergic stimulation in rat ventricular myocytes. *J Physiol* 533, 837-848 (2001)
76. Ginsburg, K.S. & D.M. Bers: Isoproterenol does not increase the intrinsic gain of cardiac E-C coupling (ECC). *Biophys J* 80, 590a (2001)
77. Witcher, D.R., R.J. Kovacs, H. Schulman, D.C. Cefali, & L.R. Jones: Unique phosphorylation site on the cardiac ryanodine receptor regulates calcium channel activity. *J Biol Chem* 266, 11144-11152 (1991)
78. Hain, J., H. Onoue, M. Mayreleitner, S. Fleischer, & H. Schindler: Phosphorylation modulates the function of the calcium release channel of sarcoplasmic reticulum from cardiac muscle. *J Biol Chem* 270, 2074-2081 (1995)
79. Lokuta, A.J., T.B. Rogers, W.J. Lederer, & H.H. Valdivia: Modulation of cardiac ryanodine receptors of swine and rabbit by a phosphorylation-dephosphorylation mechanism. *J Physiol* 487, 609-622 (1995)
80. Li, L., H. Satoh, K.S. Ginsburg, & D.M. Bers: The effect of  $Ca^{2+}$ -calmodulin-dependent protein kinase II on cardiac excitation-contraction coupling in ferret ventricular myocytes. *J Physiol* 501, 17-31 (1997)
81. duBell, W.H., W.J. Lederer & T.B. Rogers: Dynamic modulation of excitation-contraction coupling by protein phosphatases in rat ventricular myocytes. *J Physiol* 493, 793-800 (1996)
82. Fruen, B.R., J.M. Bardy, T.M. Byrem, G.M. Strasburg & C.F. Louis: Differential  $Ca^{2+}$  sensitivity of skeletal and cardiac muscle ryanodine receptors in the presence of calmodulin. *Am J Physiol* 279, C724-C733 (2000)
83. Balshaw, D.M., L. Xu, N. Yamaguchi, D.A. Pasek, & G. Meissner: Calmodulin binding and inhibition of cardiac muscle calcium release channel (ryanodine receptor). *J Biol Chem* 276, 20144-20153 (2001)
84. Tripathy A., L. Xu, G. Mann, & G. Meissner. Calmodulin activation and inhibition of skeletal muscle Ca release channel (ryanodine receptor). *Biophys J* 69: 106-119 (1995)
85. Meissner G. Evidence of a role for calmodulin in the regulation of calcium release from skeletal muscle sarcoplasmic reticulum. *Biochemistry* 25: 244-251 (1986)
86. Meissner G & J.S. Henderson. Rapid calcium release from cardiac sarcoplasmic reticulum vesicles is dependent on Ca and is modulated by Mg, adenine nucleotide, and calmodulin. *J Biol Chem* 262: 3065-3073 (1987)
87. Plank B, W. Wyskovsky, M. Hohenegger, G. Hellmann & J. Suko. Inhibition of calcium release from skeletal muscle sarcoplasmic reticulum by calmodulin. *Biochim Biophys Acta* 938: 79-88 (1988)
88. Fuentes O, C. Valdivia, D. Vaughan, R. Coronado & H.H. Valdivia. Calcium-dependent block of ryanodine receptor channel of swine skeletal muscle by direct binding of calmodulin. *Cell Calcium* 15: 305-316 (1994)
89. Rodney, G.G., B.Y. Williams, G.M. Strasburg, K. Beckingham, & S.L. Hamilton: Regulation of RYR1 activity by  $Ca^{2+}$  and calmodulin. *Biochemistry* 39, 7807-7812 (2000)
90. Jayaraman, T., A.M. Brillantes, A.P. Timerman, S. Fleischer, H. Erdjument-Bromage, P. Tempst & A.R. Marks: FK506 binding protein associated with the calcium release channel (ryanodine receptor). *J Biol Chem* 267, 9474-9477 (1992)
91. Timerman, A.P., E. Ogunbumni, E. Freund, G. Wiederrecht, A.R. Marks, & S. Fleischer: The calcium release channel of sarcoplasmic reticulum is modulated by FK-506-binding protein. Dissociation and reconstitution of FKBP-12 to the calcium release channel of skeletal muscle sarcoplasmic reticulum. *J Biol Chem* 268, 22992-22999 (1993)
92. Timerman, A.P., T. Jayaraman, G. Wiederrecht, H. Onoue, A.R. Marks & S. Fleischer: The ryanodine receptor from canine heart sarcoplasmic reticulum is associated with a novel FK-506 binding protein. *Biochem Biophys Res Commun* 198, 701-706 (1994)
93. Timerman, A.P., H. Onoue, H.B. Xin, S. Barg, J. Copello, G. Wiederrecht, & S. Fleischer S: Selective binding of FKBP12.6 by the cardiac ryanodine receptor. *J Biol Chem* 271, 20385-20391 (1996)
94. Marks, A.R.: Cardiac intracellular calcium release channels - Role in heart failure. *Circ Res* 87, 8-11 (2000)
95. Brillantes, A.M., K. Ondrias, A. Scott, E. Kobrinsky, E. Ondriasová, M.C. Moschella, T. Jayaraman, M. Landers, B.E. Ehrlich, & A.R. Marks: Stabilization of calcium release channel (ryanodine receptor) function by FK506-binding protein. *Cell* 77, 513-523 (1994)
96. Ahern, G.P., P.R. Junankar, & A.F. Dulhunty: Single channel activity of the ryanodine receptor calcium release channel is modulated by FK-506. *FEBS Lett* 352, 369-374 (1994)
97. Chen, S.R.W., L. Zhang, & D.H. MacLennan: Asymmetrical blockade of the  $Ca^{2+}$  release channel (ryanodine receptor) by 12-kDa FK506 binding protein. *Proc Natl Acad Sci USA* 91, 11953-11957 (1994)
98. Kaftan, E., A.R. Marks, & B.E. Ehrlich: Effects of rapamycin on ryanodine receptor  $Ca^{2+}$ -release channels from cardiac muscle. *Circ Res* 78, 990-997 (1996)
99. Barg, S., J.A. Copello, & S. Fleischer: Different interactions of cardiac and skeletal muscle ryanodine receptors with FK-506 binding protein isoforms. *Am J Physiol* 272, C1726-C1733 (1997)
100. Xiao, R.P., H.H. Valdivia, K. Bogdanov, C. Valdivia, E.G. Lakatta, & H.P. Cheng HP: The immunophilin FK506-binding protein modulates  $Ca^{2+}$  release channel closure in rat heart. *J Physiol* 500, 343-354 (1997)
101. McCall, E., L. Li, H. Satoh, T.R. Shannon, L.A. Blatter, & D.M. Bers: Effects of FK-506 on contraction and  $Ca^{2+}$  transients in rat cardiac myocytes. *Circ Res* 79, 1110-1121 (1996a)
102. Xin, H.B., T. Senbonmatsu, D.S. Cheng, Y.X. Wang, J.A. Copello, G.J. Ji, M.L. Collier, Deng KY, L.H. Jeyakumar, A.A. Magnuson, T. Inagami, M.I. Kotlikoff, & S. Fleischer: Oestrogen protects FKBP12.6 null mice from cardiac hypertrophy. *Nature* 416, 334-338 (2002)
103. Marx, S.O., K. Ondrias, & A.R. Marks: Coupled gating between individual skeletal muscle  $Ca^{2+}$  release channels (ryanodine receptors). *Science* 281, 818-821 (1998a)
104. Meyers, M.B., V.M. Pickel, S.S. Sheu, V.K. Sharma, K.W. Scotto, & G.I. Fishman: Association of sorcin with the cardiac ryanodine receptor. *J Biol Chem* 270, 26411-26418 (1995)
105. Meyers, M.B., T.S. Puri, A.J. Chien, T.Y. Gao, P.H. Hsu, M.M. Hosey, & G.I. Fishman: Sorcin associates with the pore-forming subunit of voltage-dependent L-type  $Ca^{2+}$  channels. *J Biol Chem* 273, 18930-18935 (1998)

106. Lokuta, A.J., M.B. Meyers, P.R. Sander, G.I. Fishman & H.H. Valdivia: Modulation of cardiac ryanodine receptors by sorcin. *J Biol Chem* 272, 25333-25338 (1997)
107. Valdivia, H.H.: Modulation of intracellular  $\text{Ca}^{2+}$  levels in the heart by sorcin and FKBP12, two accessory proteins of ryanodine receptors. *Trends Pharmacol Sci* 19, 479-482 (1998)
108. Eisner, D.A., H.S. Choi, M.E. Díaz, S.C. O'Neill, & A.W. Trafford AW: Integrative analysis of calcium cycling in cardiac muscle. *Circ Res* 87, 1087-1094 (2000)
109. Shannon, T.R. & D.M. Bers: Assessment of intra-SR free [Ca] and buffering in rat heart. *Biophys J* 73, 1524-1531 (1997)
110. Allen, D.G., P.G. Morris, C.H. Orchard, & J.S. Pirolo: A nuclear magnetic resonance study of metabolism in the ferret heart during hypoxia and inhibition of glycolysis. *J Physiol* 361, 185-204 (1985)
111. Chen, W., C. Steenbergen, L.A. Levy, J. Vance, R.E. London, & E. Murphy: Measurement of free  $\text{Ca}^{2+}$  in sarcoplasmic reticulum in perfused rabbit heart loaded with 1,2-bis(2-amino-5,6-difluorophenoxy)ethane- $\text{N,N,N',N'}$ -tetraacetic acid by  $^{19}\text{F}$  NMR. *J Biol Chem* 271, 7398-7403 (1996b)
112. Feher, J.J. & F.N. Briggs: Unidirectional calcium and nucleotide fluxes in cardiac sarcoplasmic reticulum. II. Experimental results. *Biophys J* 45, 1135-1144 (1984)
113. Takenaka, H., P.N. Adler, & A.M. Katz: Calcium fluxes across the membrane of sarcoplasmic reticulum vesicles. *J Biol Chem* 257, 12649-12656 (1982)
114. Shannon, T.R., K.S. Ginsburg, & D.M. Bers: Reverse mode of the SR Ca-pump and load-dependent cytosolic Ca decline in voltage clamped cardiac ventricular myocytes. *Biophys J* 78, 322-333 (2000)
115. Bassani, R.A. & D.M. Bers: Rate of diastolic Ca release from the sarcoplasmic reticulum of intact rabbit and rat ventricular myocytes. *Biophys J* 68, 2015-2022 (1995)
116. Ginsburg, K.S., C.R. Weber, & D.M. Bers: Control of maximum sarcoplasmic reticulum Ca load in intact ferret ventricular myocytes. Effects of thapsigargin and isoproterenol. *J Gen Physiol* 111, 491-504 (1998)
117. Györke, S., V. Lukyanenko & I. Györke: Dual effects of tetracaine on spontaneous calcium release in rat ventricular myocytes. *J Physiol* 500, 297-309 (1997)
118. Overend, C.L., S.C. O'Neill, & D.A. Eisner: The effect of tetracaine on stimulated contractions, sarcoplasmic reticulum  $\text{Ca}^{2+}$  content and membrane current in isolated rat ventricular myocytes. *J Physiol* 507, 759-769 (1998)
119. Lukyanenko, V., S. Viatchenko-Karpinski, A. Smirnov, T.F. Wiesner, & S. Györke: Dynamic regulation of sarcoplasmic reticulum Ca content and release by luminal Ca<sup>-</sup>sensitive leak in rat ventricular myocytes. *Biophys J* 81, 785-798 (2001)
120. Shannon, T.R., K.S. Ginsburg & D.M. Bers: Measurement of load-sensitive sarcoplasmic reticulum (SR) Ca leak in intact isolated ventricular myocytes. *Biophys J* 82, 597a (2002)
121. Bassani, J.W.M., R.A. Bassani, & D.M. Bers: Relaxation in rabbit and rat cardiac cells: Species-dependent differences in cellular mechanisms. *J Physiol* 476, 279-293 (1994)
122. Hove-Madsen, L. & D.M. Bers: Passive Ca buffering and SR Ca uptake in permeabilized rabbit ventricular myocytes. *Am J Physiol* 264, C677-C686 (1993)
123. Trafford, A.W., M.E. Díaz & D.A. Eisner: A novel, rapid and reversible method to measure Ca buffering and time-course of total sarcoplasmic reticulum Ca content in cardiac ventricular myocytes. *Pflügers Arch* 437, 501-503 (1999)
124. Satoh, H., L.M. Delbridge, L.A. Blatter, & D.M. Bers: Surface volume relationship in cardiac myocytes studied with confocal microscopy and membrane capacitance measurements: species-dependence and developmental effects. *Biophys J* 70, 1494-1504 (1996)
125. Fujioka, Y., M. Komeda, & S. Matsuoka: Stoichiometry of  $\text{Na}^+$ - $\text{Ca}^{2+}$  exchange in inside-out patches excised from guinea-pig ventricular myocytes. *J Physiol* 523, 339-351 (2000)
126. Egger, M., & E. Niggli: Paradoxical block of the  $\text{Na}^+$ - $\text{Ca}^{2+}$  exchanger by extracellular protons in guinea-pig ventricular myocytes. *J Physiol* 523, 353-366 (2000)
127. Delbridge, L.M., J.W.M. Bassani, & D.M. Bers: Steady-state twitch  $\text{Ca}^{2+}$  fluxes and cytosolic  $\text{Ca}^{2+}$  buffering in rabbit ventricular myocytes. *Am J Physiol* 270, C192-C199 (1996)
128. Negretti, N., S.C. O'Neill, & D.A. Eisner: The relative contributions of different intracellular and sarcolemmal systems to relaxation in rat ventricular myocytes. *Cardiovasc Res* 27, 1826-1830 (1993)
129. Beuckelmann, D.J. & E. Erdmann:  $\text{Ca}^{2+}$ -currents and intracellular [ $\text{Ca}^{2+}$ ]-transients in single ventricular myocytes isolated from terminally failing human myocardium. *Basic Res Cardiol* 87, 1235-1243 (1992)
130. Hasenfuss, G.: Alterations of calcium-regulatory proteins in heart failure. *Cardiovasc Res* 37, 279-289 (1998)
131. Hasenfuss, G., W. Schillinger, S.E. Lehnart, M. Preuss, B. Pieske, L.S. Maier, J. Prestle, K. Minami, & H. Just: Relationship between  $\text{Na}^+$ - $\text{Ca}^{2+}$ -exchanger protein levels and diastolic function of failing human myocardium. *Circulation* 99, 641-648 (1999)
132. Pieske, B., L.S. Maier, D.M. Bers, & G. Hasenfuss:  $\text{Ca}^{2+}$  handling and sarcoplasmic reticulum  $\text{Ca}^{2+}$  content in isolated failing and nonfailing human myocardium. *Circ Res* 85, 38-46 (1999)
133. Pogwizd, S.M., M. Qi, W. Yuan, A.M. Samarel, & D.M. Bers: Upregulation of  $\text{Na}^+$ / $\text{Ca}^{2+}$  exchanger expression and function in an arrhythmogenic rabbit model of heart failure. *Circ Res* 85, 1009-1019 (1999)
134. Pogwizd, S.M., K. Schlotthauer, L. Li, W. Yuan, & D.M. Bers: Arrhythmogenesis and contractile dysfunction in heart failure: Roles of sodium-calcium exchange, inward rectifier potassium current and residual  $\square$ -adrenergic responsiveness. *Circ Res* 88, 1159-1167 (2001)
135. O'Rourke, B., D.A. Kass, G.F. Tomaselli, S. Käbb, R. Tunin, & E. Marbán: Mechanisms of altered excitation-contraction coupling in canine tachycardia-induced heart failure, I - Experimental studies. *Circ Res* 84, 562-570 (1999)
136. Hobai, I.A., & B. O'Rourke: Decreased sarcoplasmic reticulum calcium content is responsible for defective excitation-contraction coupling in canine heart failure. *Circulation* 103, 1577-1584 (2001)
137. Lindner, M., E. Erdmann, & D.J. Beuckelmann: Calcium content of the sarcoplasmic reticulum in isolated ventricular myocytes from patients with terminal heart failure. *J Mol Cell Cardiol* 30, 743-749 (1998)
138. Yano, M., K. Ono, T. Ohkusa, M. Suetsugu, M. Kohno, T. Hisaoka, S. Kobayashi, Y. Hisamatsu, T. Yamamoto, M. Kohno, N. Noguchi, S. Takasawa, H. Okamoto & M. Matsuzaki: Altered stoichiometry of FKBP12.6 versus ryanodine receptor as a cause of abnormal  $\text{Ca}^{2+}$  leak through ryanodine receptor in heart failure. *Circulation* 102, 2131-2136 (2000)
139. Gómez, A.M., H.H. Valdivia, H. Cheng, M.R. Lederer, L.F. Santana, M.B. Cannell, S.A. McCune, R.A. Altschuld, & W.J. Lederer: Defective excitation-contraction coupling in experimental cardiac hypertrophy and heart failure. *Science* 276, 800-806 (1997)
140. Esposito, G., L.F. Santana, K. Dilly, J.D. Cruz, L. Mao, W.J. Lederer, & H.A. Rockman: Cellular and functional defects in a mouse model of heart failure. *Am J Physiol Heart Circ Physiol* 279, H3101-1012 (2000)
141. Gómez, A.M., S. Guatimosim, K.W. Dilly, G. Vassort & W.J. Lederer: Heart failure after myocardial infarction: altered excitation-contraction coupling. *Circulation* 104, 688-693 (2001)
142. Schillinger, W., P.M.L. Janssen, S. Emami, S.A. Henderson, R.S. Ross, N. Teucher, O. Zeitz, K.D. Philipson, J. Prestle, & G. Hasenfuss: Impaired contractile performance of cultured rabbit ventricular myocytes after adenoviral gene transfer of  $\text{Na}^+$ - $\text{Ca}^{2+}$  exchanger. *Circ Res* 87, 581-587 (2000)
143. Ranu, H.K., C.M.N. Terracciano, K. Davia, E. Bernobich, B. Chaudhri, S.E. Robinson, Z.B. Kang, R.J. Hajjar, K.T. MacLeod, & S.E. Harding: Effects of  $\text{Na}^+$ / $\text{Ca}^{2+}$ -exchanger

overexpression on excitation-contraction coupling in adult rabbit ventricular myocytes. *J Mol Cell Cardiol* In Press (2002)

144. Ito, K., X. Yan, M. Tajima, Z. Su, W.H. Barry & B.H. Lorell: Contractile reserve and intracellular calcium regulation in mouse myocytes from normal and hypertrophied failing hearts. *Circ Res* 87, 588-595 (2000)

# Calcium Signaling Between Sarcolemmal Calcium Channels and Ryanodine Receptors in Heart Cells.

Heping Cheng, Shi-Qiang Wang

Laboratory of Cardiovascular Sciences, National Institute on Aging, National Institutes of Health Baltimore, Maryland 21224, USA Email: [chengp@grc.nia.nih.gov](mailto:chengp@grc.nia.nih.gov)

**ABSTRACT** Cardiac excitation- $\text{Ca}^{2+}$  release coupling is, in essence, a tale of two molecules, sarcolemmal voltage-gated L-type  $\text{Ca}^{2+}$  channels (LCCs) and intracellular ryanodine receptors (RyRs), communicating via the  $\text{Ca}^{2+}$ -induced  $\text{Ca}^{2+}$  release mechanism. Recent advances have provided a microscopic view of the intermolecular  $\text{Ca}^{2+}$  signaling between LCCs and RyRs. In a dyadic junction or a "couplon", LCCs open and close stochastically upon depolarization, delivering a train of high local  $\text{Ca}^{2+}$  pulses (" $\text{Ca}^{2+}$  sparklets") to the RyRs in the abutting SR terminal cisternae. Stochastic activation of RyRs discharges " $\text{Ca}^{2+}$  sparks" from different couplons, which summate into global  $\text{Ca}^{2+}$  transients. Hence, ignition of  $\text{Ca}^{2+}$  sparks by  $\text{Ca}^{2+}$  sparklets constitute elementary events of EC coupling. While the sparklet-spark coupling is of low fidelity (at 0 mV, about one out of 50 sparklets triggers a spark under physiological conditions), the *high-gain amplification* of CICR ( $\sim 15$  at 0 mV) is achieved because of the greater single-channel flux and open time of RyRs and multi-RyR origin of  $\text{Ca}^{2+}$  spark. The *global stability* of CICR is safeguarded by many factors acting in synergy, including physical separation of RyR clusters, sheer  $\text{Ca}^{2+}$  gradients around the channel pores, low intrinsic  $\text{Ca}^{2+}$  sensitivity of RyRs *in vivo*, and high cooperativity for the  $\text{Ca}^{2+}$ -dependence spark activation. The *local stability* of CICR is insured because of strong, use-dependent inactivation of RyRs, that terminates  $\text{Ca}^{2+}$  sparks and confers persistent local SR refractoriness.

## Introduction

In heart muscle cells, excitation-contraction (EC) coupling is a cascade of  $\text{Ca}^{2+}$ -mediated intracellular signal transduction that links membrane depolarization to activation of cell contraction. Its pivotal first step involves crosstalk between two types of  $\text{Ca}^{2+}$  channels, the voltage-operated L-type  $\text{Ca}^{2+}$  channels (LCCs) (1) in the sarcolemma and the  $\text{Ca}^{2+}$  release channels/type 2 ryanodine receptors (RyRs) (2,3) in the sarcoplasmic reticulum (SR). The LCC-to-RyR communication relies on the incoming  $\text{Ca}^{2+}$  as the second messenger to activate the RyRs via the  $\text{Ca}^{2+}$ -induced  $\text{Ca}^{2+}$  release (CICR) mechanism (4,5). Simultaneously simple and enigmatic, CICR has attracted much attention over the last decade, calling for elucidation of its reliability, controllability, and stability. Many advances, including the conception of local control of CICR (6,7), the discovery of tale-telling microscopic  $\text{Ca}^{2+}$  events, namely " $\text{Ca}^{2+}$  sparks" (8), " $\text{Ca}^{2+}$  sparklets" (9) and " $\text{Ca}^{2+}$  spikes" (10), as well as the ongoing quest for the mechanism that terminates CICR (11-14), have greatly deepened our understanding of this core  $\text{Ca}^{2+}$  signaling mechanism at the molecular level. This brief review focuses on mechanistic aspects of intermolecular signaling between LCCs and RyRs, to provide a microscopic view of EC coupling. Comprehensive overview of related topics can be found elsewhere (15-18) and in companion articles in this issue of *Frontiers in Bioscience*.

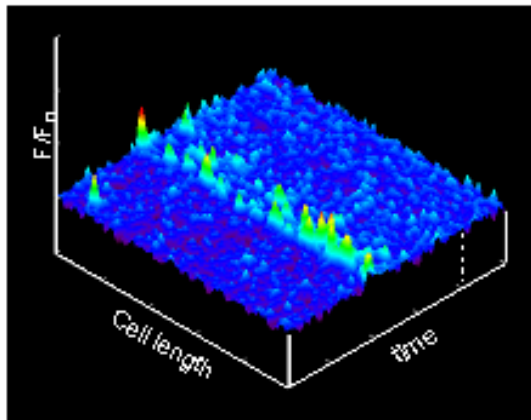
## Local Control of CICR

The phenomenon of CICR was initially demonstrated in skinned skeletal muscle fibers (19,20) and cardiac Purkinje cells (4,5) by abruptly increasing the bathing  $\text{Ca}^{2+}$  concentration, where the trigger  $\text{Ca}^{2+}$  comes from the bulk solution surrounding the exposed SR. In his classic and elegant experiments, Fabiato demonstrated that cardiac CICR is graded both by the magnitude and the rate of change ( $d[\text{Ca}]/dt$ ) of the trigger  $\text{Ca}^{2+}$ , and that supra-optimal trigger  $\text{Ca}^{2+}$  negatively regulates CICR, resulting in attenuated SR  $\text{Ca}^{2+}$  release (5). These observations have been interpreted by a model in which fast, low affinity  $\text{Ca}^{2+}$ -dependent activation occurs concurrently with a slow, high-affinity  $\text{Ca}^{2+}$ -dependent inactivation (5).

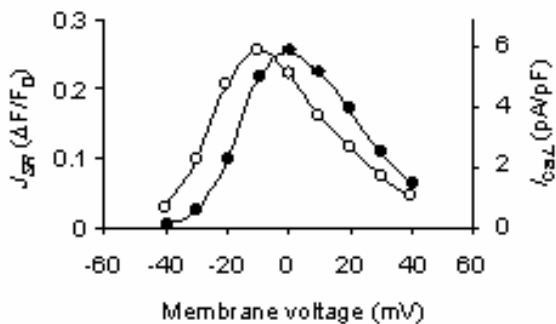
A contemporary version of the Fabiato experiment has been performed in intact cardiac myocytes, where flash photorelease of caged  $\text{Ca}^{2+}$  produces a homogenous step increase of cytosolic  $\text{Ca}^{2+}$ . The photolytic  $\text{Ca}^{2+}$  suffices to activate the SR  $\text{Ca}^{2+}$  release, in a similarly graded fashion (7,21). During normal EC coupling, however, LCC current ( $I_{\text{Ca,L}}$ ) serves as the physiological trigger of CICR. Several salient features of the  $I_{\text{Ca,L}}$ -elicited SR  $\text{Ca}^{2+}$  release have been identified by independent laboratories. These include a bell-shaped voltage dependence that reminisces that for  $I_{\text{Ca,L}}$  (22-27), a high-gain amplification ( $\sim 10-20$  at 0 mV) (26,27), a voltage-dependent reduction of the "gain" function (26,27) (Fig. 1), and a variable endurance of the release that is controlled by the duration of  $I_{\text{Ca,L}}$  (22).

To explain properties of the  $I_{\text{Ca,L}}$ -elicited CICR, a parsimonious model implies that  $\text{Ca}^{2+}$  entry as  $I_{\text{Ca,L}}$  raises uniformly the cytosolic  $\text{Ca}^{2+}$  and

**A**



**B**



**C**

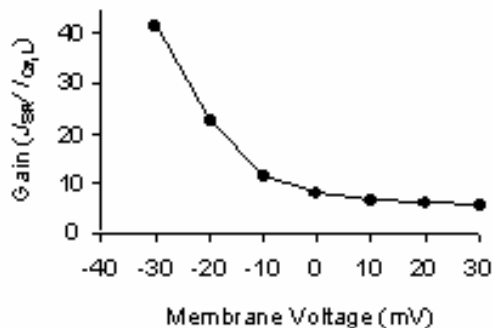


Figure 1.  $\text{Ca}^{2+}$  spikes and the gain function of EC coupling. Whole-cell patch-clamp was established with the cell dialyzed with 1 mM Oregon Green BAPTA 5N and 4 mM EGTA. A.  $\text{Ca}^{2+}$  spikes elicited by a 300-ms depolarization to  $-30$  mV. Vertical dash lines mark the beginning and end of the voltage pulse, and data are shown as surface plot. B. Bell-shaped voltage-dependence for SR  $\text{Ca}^{2+}$  release flux ( $J_{\text{SR}}$ , measured by spatially averaged  $\text{Ca}^{2+}$  spikes) (open symbols) and  $I_{\text{Ca,L}}$  (solid symbols). Note that the  $J_{\text{SR}}$  curve is shifted leftward by about 10 mV. C. Voltage-dependence of the gain function  $J_{\text{SR}}/I_{\text{Ca,L}}$ . (A: unpublished data; B&C: data from reference 27).

thereby affects all RyRs equally. However, Stern proved mathematically that such a “common pool” model in the high-gain zone is inherently unstable, resulting in nearly all-or-nothing behavior (6). Indeed, Niggli and Lederer found that it is rather

inefficient for photoreleased  $\text{Ca}^{2+}$  (i.e. common pool  $\text{Ca}^{2+}$ ) to trigger SR  $\text{Ca}^{2+}$  release as compared to the  $I_{\text{Ca,L}}$  (7). These experimental and theoretical reasoning have led to the proposal that RyRs are instead under tight *local control* by LCCs (6,7). Specifically, co-localization of RyRs and LCCs (28) allows the high local  $\text{Ca}^{2+}$  in the close proximity of open LCCs preferential access to RyRs, which are presumably insensitive to low levels of  $\text{Ca}^{2+}$ . Stern further envisaged that a single LCC controls either a single RyR (“kiss” model) or a group of RyRs (“cluster bomb” model) (6), and individual units operate independently, by virtue of spatial separation and of sheer  $\text{Ca}^{2+}$  gradients from a point source (29). As a result, a high-gain amplification (reliability) can be achieved without jeopardizing the stability and controllability of CICR. This model also explains why an early interruption of  $I_{\text{Ca,L}}$  abbreviates the SR  $\text{Ca}^{2+}$  release (22).

To evaluate the competing CICR models, Wier et al (26) examined the efficiency of  $I_{\text{Ca,L}}$  to activate SR  $\text{Ca}^{2+}$  release at different voltages. In the “local control” model, properties of unitary LCC currents ( $i_{\text{Ca}}$ ) is an important determinant, so the SR  $\text{Ca}^{2+}$  release is not necessarily a unique function of the whole-cell  $I_{\text{Ca,L}}$ . To the contrary, the common pool model predicts that SR release depends solely on the  $I_{\text{Ca,L}}$ . The experimental results revealed that the efficiency of  $I_{\text{Ca,L}}$  as the trigger is progressively decreased with increasing voltage, as is the  $i_{\text{Ca}}$ : comparable  $I_{\text{Ca,L}}$  triggers greater  $\text{Ca}^{2+}$  release at more negative voltages, when  $i_{\text{Ca}}$  and hence local  $\text{Ca}^{2+}$  pulses are bigger. This provides strong indirect evidence in favor of the local control theory.

An independent line of evidence for the local control theory came from investigation of the efficacy of  $\text{Ca}^{2+}$  influx via routes other than the LCCs. The prediction is that CICR would be less effective if these alternative routes are not as well aligned to RyRs. To this end,  $\text{Ca}^{2+}$  entry via the reverse mode  $\text{Na}^+/\text{Ca}^{2+}$  exchange ( $I_{\text{Ca, NCX}}$ ) is 20-160 times less effective (30), while T-type  $\text{Ca}^{2+}$  channel current ( $I_{\text{Ca,T}}$ ) is also very inefficient in triggering CICR (31). Early evidence for localized CICR also includes the observation that local activation of  $\text{Ca}^{2+}$  transient from one end of a rat cardiac myocyte does not propagate into the remote end of the cell (32).

### **$\text{Ca}^{2+}$ Sparks: Elementary Events of SR $\text{Ca}^{2+}$ Release**

“ $\text{Ca}^{2+}$  sparks” are local, brief and small increases of intracellular  $\text{Ca}^{2+}$  visualized by confocal microscopy in conjunction with the new generation of fast and high-contrast  $\text{Ca}^{2+}$  indicators (8,33) (Fig. 2). Originated from RyRs in the SR, they occur spontaneously in resting myocytes, while identical  $\text{Ca}^{2+}$  sparks can also be evoked by  $I_{\text{Ca,L}}$  (34-38). These spontaneous  $\text{Ca}^{2+}$  sparks are independent of LCC  $\text{Ca}^{2+}$  entry (8,33,39,40), are sensitized by low doses of caffeine and ryanodine, and are inhibited by high doses of caffeine or ryanodine as well as  $\text{Mg}^{2+}$  and tetracaine (8,39). During EC coupling, spatial and temporal summation of up to  $10^4$   $\text{Ca}^{2+}$  sparks gives rise to the cell-wide global  $\text{Ca}^{2+}$  transients (34-

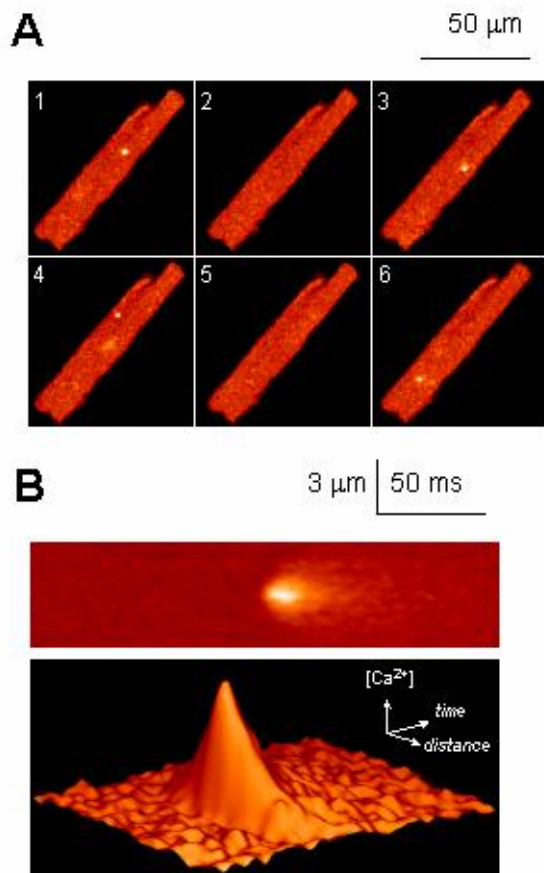


Figure 2.  $\text{Ca}^{2+}$  sparks in cardiac myocytes. A. Six consecutive confocal raster-scan images (1 s apart) of a quiescent ventricular myocyte loaded with the  $\text{Ca}^{2+}$  indicator, fluo-3.  $\text{Ca}^{2+}$  sparks are discernible as bright spots occurring randomly inside the cell. B. Linescan confocal image of a typical  $\text{Ca}^{2+}$  spark (top) and its surface plot (bottom), showing the temporal (horizontal) and spatial (vertical) characteristics of the spark. (Unpublished data)

38). Hence,  $\text{Ca}^{2+}$  sparks constitute elementary events of cardiac EC coupling. When CICR is somehow tipped to the verge of instability, however, solitary  $\text{Ca}^{2+}$  sparks no longer remain confined (41-43); recruitment of discrete  $\text{Ca}^{2+}$  sparks often evolves into saltatory propagating waves of  $\text{Ca}^{2+}$  excitation (41), indicating that  $\text{Ca}^{2+}$  sparks are also elemental to initiation and propagation of  $\text{Ca}^{2+}$  waves.

The existence of  $\text{Ca}^{2+}$  sparks immediately told us something that we had not appreciated before. First, SR  $\text{Ca}^{2+}$  release occurs in a stochastic and discrete manner. Mapping the origin of  $\text{Ca}^{2+}$  sparks revealed that spark-generating sites, coincident with T-tubules, are separated by  $\sim 1.8$  in the longitudinal direction and  $0.5\text{-}1.5$   $\mu\text{m}$  in the transverse direction (6,41,42,44). Genesis of  $\text{Ca}^{2+}$  spark at T-SR junctions during small depolarization has been shown to be governed by Poisson statistics (35). The finding that CICR is discrete and random is not trivial, because not all properties of a stochastic and discrete system can

be described by a deterministic and continual model. From an engineering's standpoint, the discreteness provides a straightforward, yet ingenious, solution to the stability and controllability of CICR: gradedness of CICR can be achieved simply by varying the number of sparks recruited. Izu et al (45) has recently noted another intriguing difference between the two classes of models with respect to  $\text{Ca}^{2+}$  wave initiation and propagation.

Second, the rate of occurrence of spontaneous sparks suggests that RyRs *in situ* are surprisingly *insensitive* to  $\text{Ca}^{2+}$ , validating an important premise of the local control theory. Out of  $\sim 10^6$  RyRs exposed to  $\sim 100$  nM resting  $\text{Ca}^{2+}$  in a typical myocyte, approximately 100  $\text{Ca}^{2+}$  sparks ignite every second (8). This translates into an open frequency of  $0.0001$   $\text{s}^{-1}$  or a mean close time of 10,000 s for RyRs in cells, differing by orders of magnitude from those in the planar lipid bilayer (46,47). The low excitability of RyRs in milieu of intact cells should help to confine CICR both in space and time.

Once activated,  $\text{Ca}^{2+}$  sparks evolve autonomously and reach the peak in  $\sim 10$  ms, regardless of the mechanism that turns-off trigger  $\text{Ca}^{2+}$  (35). The brevity of  $\text{Ca}^{2+}$  sparks is unexpected, and indicates that regenerative CICR within a spark-generating unit must be somehow terminated promptly (see below). Together, the spontaneous termination, the spatial confinement of  $\text{Ca}^{2+}$  sparks, and the low  $\text{Ca}^{2+}$  sensitivity of RyRs provide important bases for the local control theory.

Because of their intracellular location, RyRs in intact cells have thus far defied direct electrophysiological measurement. Confocal imaging of  $\text{Ca}^{2+}$  sparks has provided a novel and powerful means by which RyR activity *in situ* can be observed non-invasively, on the smallest physiological scale. To date,  $\text{Ca}^{2+}$  sparks are shown to be present in all types of muscles (8,48-50).  $\text{Ca}^{2+}$  sparks of both RyR and  $\text{IP}_3$  receptor ( $\text{IP}_3\text{R}$ ) origin are present in non-excitable cells such as glial cells (51) and endothelial cells (52). Analogous  $\text{IP}_3\text{R}$   $\text{Ca}^{2+}$  sparks, named " $\text{Ca}^{2+}$  puffs", have also been extensively characterized in xenopus oocytes (53).  $\text{Ca}^{2+}$  sparks as the universal building blocks of  $\text{Ca}^{2+}$  signaling fulfill distinctly different physiological roles in these cells.

While  $\text{Ca}^{2+}$  sparks appear to constitute the totality of SR  $\text{Ca}^{2+}$  release in  $I_{\text{Ca,L}}$ -elicited  $\text{Ca}^{2+}$  transients, Niggli and Lipp have demonstrated non-spark, spatially uniform  $\text{Ca}^{2+}$  release when the SR is activated by photolytic  $\text{Ca}^{2+}$  (54,55) or reverse mode  $\text{Na}^+/\text{Ca}^{2+}$  exchange (56). They proposed that this type of release is mediated by sub-spark events, termed " $\text{Ca}^{2+}$  quarks" (54), that are perhaps from single RyRs and are not readily discernible (17,54-56). However, if quarks and sparks differ only in the number of RyRs involved, it is difficult to reconcile why  $\text{Ca}^{2+}$  entry other than  $I_{\text{Ca,L}}$  activates only the subtler events, whereas resting  $\text{Ca}^{2+}$  activates SR release in the form of spontaneous  $\text{Ca}^{2+}$  sparks. The condition, extent and physiological relevance of non-spark SR  $\text{Ca}^{2+}$  release merits further investigation.

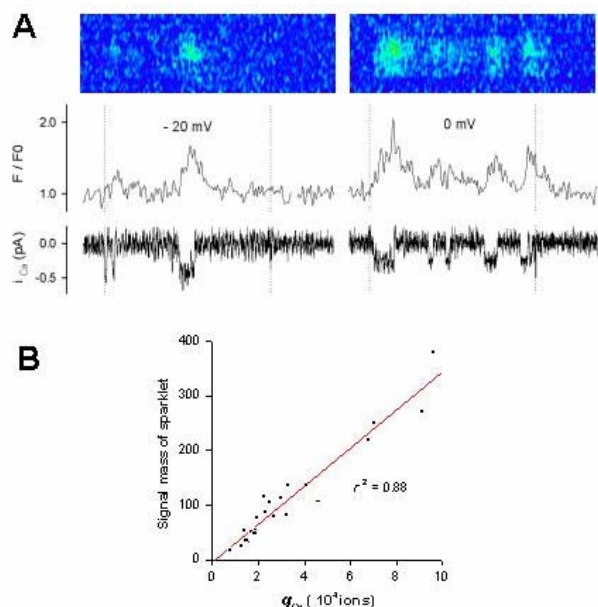


Figure 3.  $\text{Ca}^{2+}$  sparklets due to single LCC openings. G $\Omega$ -seal patch clamp was established on an intact cardiac myocyte whose SR was paralyzed by 10 mM caffeine and 10  $\mu\text{M}$  thapsigargin. The patch pipette (3-5 M $\Omega$ ) contained 10  $\mu\text{M}$  FPL64176 and 20 mM  $\text{Ca}^{2+}$ . Confocal linescan was focused right beneath the patch membrane. A.  $\text{Ca}^{2+}$  sparklets during 400-ms depolarization at -20 and 0 mV (top), their line plots (middle), and the simultaneously recorded unitary  $\text{Ca}^{2+}$  current,  $i_{\text{Ca}}$  (bottom). B. Linear correlation between sparklet signal mass ( $\Pi\Delta F/F_0 dxdt$ ) (in arbitrary unit) and the integral of the corresponding  $i_{\text{Ca}}$ ,  $Q_{\text{Ca}}$  (number of  $\text{Ca}^{2+}$  ions). (Data from reference 9)

### Trigger $\text{Ca}^{2+}$ Entry: Visualization of $\text{Ca}^{2+}$ Sparklets from Single LCCs

In a microscopic perspective,  $\text{Ca}^{2+}$  entry gated by single LCC openings ought to be discontinuous and stochastic as well. A typical  $i_{\text{Ca}}$  at 0 mV amounts to  $\sim 0.12$  pA (2 mM  $\text{Ca}^{2+}$  as the charge carrier) (57) and lasts  $\sim 0.3$  ms (58), carrying a packet of  $\text{Ca}^{2+}$  of  $\sim 110$  ions. This tiny amount of  $\text{Ca}^{2+}$  is still beyond the detection limit of current generation of confocal fluorescent microscopy. Nevertheless, when  $i_{\text{Ca}}$  is prolonged and enlarged by the LCC agonist FPL64176 and 10-20 mM external  $\text{Ca}^{2+}$ , we were able to visualize  $\text{Ca}^{2+}$  entry from single LCCs, dubbed " $\text{Ca}^{2+}$  sparklets", in cells whose SR  $\text{Ca}^{2+}$  release was paralyzed (9) (Fig. 3). The onset and offset of a  $\text{Ca}^{2+}$  sparklet follow closely the open and closure of the channel; the fluorescent "signal mass" of  $\text{Ca}^{2+}$  sparklets linearly correlates with the integral of the corresponding  $i_{\text{Ca}}$  (8,000 to 100,000  $\text{Ca}^{2+}$  ions) (Fig. 3). Thus, in addition to  $\text{Ca}^{2+}$  sparks,  $\text{Ca}^{2+}$  sparklets afford another tool for investigation of microscopic properties of LCC-to-RyR coupling. In circumstances when it is impossible to record  $i_{\text{Ca}}$  electrophysiologically,  $\text{Ca}^{2+}$  sparklets as an optical readout of  $i_{\text{Ca}}$  can be exploited to monitor gating of single LCCs (9). Moreover,  $\text{Ca}^{2+}$  sparklets produced by a known size of  $i_{\text{Ca}}$  may serve as an optical standard to calibrate  $\text{Ca}^{2+}$  release flux underlying a spark (9). This calibration is basically model- and parameter-independent, because sparklets and sparks

share the common microenvironments with respect to  $\text{Ca}^{2+}$  buffering and diffusion.

### Triggering $\text{Ca}^{2+}$ Sparks by Single LCC Excitation

The ultimate test for the local control theory would be the demonstration that single LCC excitation triggers discrete SR  $\text{Ca}^{2+}$  release events, or  $\text{Ca}^{2+}$  sparks. Two independent groups provided the first supporting evidence. Cannell et al (35) noticed that the voltage-dependence of  $\text{Ca}^{2+}$  spark activation ( $P_s$ ) is proportional to LCC activation ( $P_{o,L}$ ) at near-threshold voltages (from -60 to -40mV), displaying an e-fold increment per  $\sim 7$  mV depolarization. Under conditions when most LCCs are inhibited (for resolution of solitary sparks), López-López et al (36) demonstrated kinetic similarities between the residual  $i_{\text{Ca},L}$  and the latency distribution of spark activation over a wide range of voltages. Both lines of evidence indicate that spark activation does not require cooperative interaction among LCCs, because, otherwise,  $P_s$  would be expected to be a power function of  $P_{o,L}$ , or  $P_s \propto P_{o,L}^x$ , with  $x > 1$ .

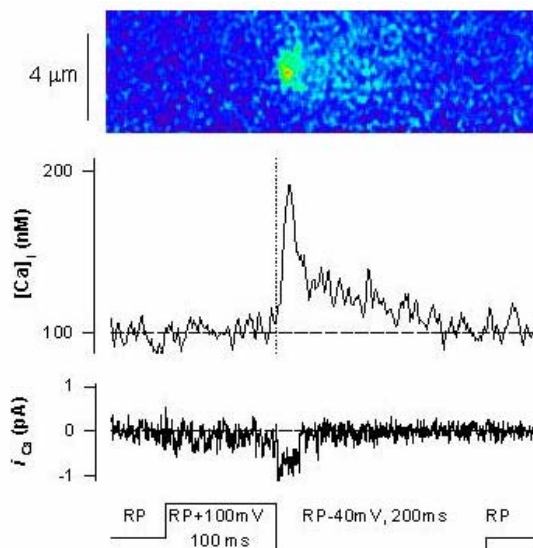


Figure 4. Triggering  $\text{Ca}^{2+}$  spark by single LCC excitation. The experimental conditions were the same as in Figure 2, except that the cell was bathed in normal physiological saline. A  $\text{Ca}^{2+}$  spark is evoked by tail  $i_{\text{Ca}}$  upon hyperpolarization. RP: resting potential,  $\sim -70$  mV in rat ventricular myocytes. (From reference 9)

To directly demonstrate that a single opening of an LCC triggers a  $\text{Ca}^{2+}$  spark, it is crucial to record  $i_{\text{Ca}}$  and its triggered spark simultaneously. Ever since the first recording of evoked  $\text{Ca}^{2+}$  sparks, this has been a formidable task attempted by many laboratories (9,59). With the development of a novel method to combine G $\Omega$ -seal single-channel patch clamp and confocal spark detection in our laboratory, we visualized  $\text{Ca}^{2+}$  sparks activated beneath the patch membrane by single LCC openings (9) (Fig. 4). Further, to avoid the " $\Omega$ "-shaped membrane deformation associated with G $\Omega$ -seal patch clamping, which disrupts the delicate LCC-to-RyR coupling on

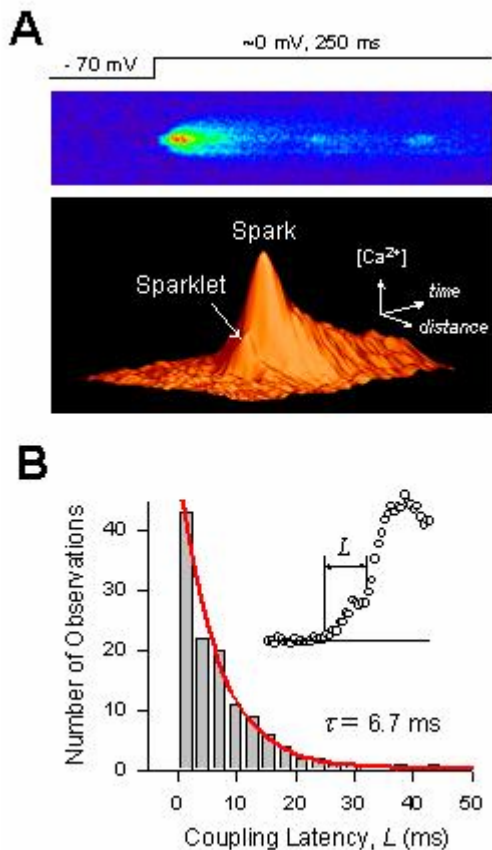


Figure 5. Sparklet-spark coupling under loose-seal patch clamp conditions. The patch pipette (3-5 M $\Omega$ ) was gently pressed against the cell membrane to form low-resistance seal (30~50 M $\Omega$ ) without suction. Other experimental conditions were the same as in Fig. 4. A. Representative example showing that a Ca<sup>2+</sup> sparklet of LCC origin directly triggers a Ca<sup>2+</sup> spark. Note that two additional Ca<sup>2+</sup> sparklets in the wake of the spark fail to trigger further SR Ca<sup>2+</sup> release, suggestive of local refractoriness. B. Histogram distribution of the sparklet-spark coupling latency ( $L$ , insert). Monoexponential fitting yields a time constant  $\tau = 6.7$  ms. (Data from reference 9).

most occasions (9), we adopted the so-called loose-seal patch-clamp technique (9) (Fig. 5). In the presence of FPL64176, both high- and low-amplitude local Ca<sup>2+</sup> events are evoked in loose patches responding to depolarization to  $\sim 0$  mV. The low-amplitude events are ryanodine-resistant, representing Ca<sup>2+</sup> sparklets, whereas the high-amplitude events represent Ca<sup>2+</sup> sparks. Fig 5 shows a Ca<sup>2+</sup> spark rising from the shoulder of an ongoing Ca<sup>2+</sup> sparklet. These results not only validate a prescient prediction by Stern (6), but also provide the first real-time recording of Ca<sup>2+</sup> signal transduction at the single-molecule resolution.

### Fidelity, Kinetics and Stoichiometry of LCC-to-RyR Coupling

With the advances in ultrastructural and functional studies, a microscopic view of cardiac EC coupling emerges. Dozens of LCCs, up to a few hundreds of RyRs, along with their accessory and regulatory proteins, co-localize to dyadic junctions

where the surface membrane and transverse tubules come within 15 nm of the SR membrane (28,60). The two membrane systems, the junctional cleft, and the molecules wherein form a structural, functional and regulatory unit, or a "couplon" (61). LCCs open and close stochastically upon depolarization, delivering a train of trigger Ca<sup>2+</sup> pulses or Ca<sup>2+</sup> sparklets, to the RyRs in the abutting SR terminal cisternae. Stochastic activation of RyRs discharges Ca<sup>2+</sup> sparks from different couplons, which summate into global Ca<sup>2+</sup> transients. Hence, from a reductionism's perspective, to understand the EC coupling and its physiological regulation is, in essence, to unravel the secrets concealed within the nanoscale couplon.

The ability to observe Ca<sup>2+</sup> sparklets directly igniting Ca<sup>2+</sup> sparks (Fig. 5) permitted us to determine the kinetics of LCC-to-RyR communication. By measuring the temporal length from the onset of a sparklet to the onset of its triggered spark, we obtained the latency of LCC-to-RyR coupling in intact cells at  $\sim 0$  mV in the presence of FPL64176 and high external Ca<sup>2+</sup>. Its histogram distribution is well described by a single-exponential function, with a time constant of 6.7 ms (9) (Fig. 5). Because of stochastic variations of both LCC open time and spark activation, not every LCC opening is expected to trigger a Ca<sup>2+</sup> spark. The LCC-to-RyR coupling fidelity ( $\delta$ ), i.e., the fraction of LCC openings that successfully trigger sparks, was determined to be  $\delta \approx 0.7$  under our experimental conditions (9).

For EC coupling under normal conditions, a  $\delta$  value of 0.02 has been estimated based on macroscopic gain function and microscopic properties of  $i_{Ca}$  (62). In other words, on average, one out of  $\sim 50$  LCC openings at 0 mV triggers a Ca<sup>2+</sup> spark under normal conditions. This is in general agreement with the results of single RyRs reconstituted in planar lipid bilayers, where photoreleased Ca<sup>2+</sup> of 9  $\mu$ M and 0.1-0.4 ms activates the channel with  $\delta \approx 0.06$  (63). Despite the low coupling fidelity, a high-gain amplification is realized because of the large single-channel flux and long open time of RyRs, and likely, multi-RyR activation in a spark (see below).

### Nonlinear Ca<sup>2+</sup>-Dependence of Ca<sup>2+</sup> Spark Activation

The efficacy of  $I_{Ca,L}$  as the trigger of SR Ca<sup>2+</sup> release or the "gain" function is a tale-telling quantity of EC coupling, and has been measured in different experimental settings. Under whole-cell voltage-clamp conditions, the "gain" is usually defined as the ratio between peak SR Ca<sup>2+</sup> release flux ( $J_{SR}$ ) and peak  $I_{Ca,L}$ , where the  $J_{SR}$  is derived from global Ca<sup>2+</sup> transients with the aid of mathematical modeling (26,64), or directly measured using a combination of a fast, low-affinity Ca<sup>2+</sup> indicator (such as Oregon green BAPTA 5N) and a slow, high-affinity nonfluorescent Ca<sup>2+</sup> chelator (such as EGTA) (10,27). When solitary, evoked Ca<sup>2+</sup> sparks can be counted (e.g., in the presence of LCC antagonist), the gain function can also be defined as the ratio between  $P_s$  and  $I_{Ca,L}$  (65). All measurements indicate that the gain function decays with increasing voltage.

Importantly, Santana et al (65) noticed that the voltage-dependence of gain function essentially overlaps the voltage-dependence of  $i_{Ca}$  predicted from the Nernst-Planck relationship. This result has been interpreted to reflect that spark activation depends on the square of intra-couplon  $Ca^{2+}$  concentration (which should be proportional to  $i_{Ca}$  (66)), or  $P_s \propto i_{Ca}^2 \propto [Ca^{2+}]^2$  (65). Highly cooperative  $Ca^{2+}$ -dependent activation has also been observed *in vitro* for RyRs in response to  $Ca^{2+}$  steps (46,47) or  $Ca^{2+}$  pulses (63), indicating that it is an intrinsic property of the RyR.

The high cooperativity for  $Ca^{2+}$ -dependent activation appears to be one of the most important features of cardiac EC coupling. Owing to the steep power relationship, RyRs, which are essentially insensitive to resting  $Ca^{2+}$  (0.1  $\mu$ M), can robustly respond to  $i_{Ca}$ -produced local  $Ca^{2+}$  pulses (several tens  $\mu$ M) (66). It also confers the ability for RyRs to discriminate local trigger  $Ca^{2+}$  against spatially averaged  $Ca^{2+}$  ( $\mu$ M) during an ongoing  $Ca^{2+}$  transient.

### How Many RyRs Activated in a Spark?

The exact nature of  $Ca^{2+}$  sparks remains elusive. Initial evidence was ambivalent as to single- or multi-channel origin of  $Ca^{2+}$  sparks (8). Evidence in favor of single-channel origin of sparks has been twofold. First, low concentration of ryanodine (8) or FK506 (13,14) favor the appearance of long-lasting sparks with halved amplitude, akin to subconductance states of RyR in planar lipid bilayer in the presence of the channel ligand. This interpretation is now known to be flawed because plateau amplitude at 50% height implies a  $Ca^{2+}$  flux several times smaller than that generating the peak (67). Second, the estimated  $Ca^{2+}$  flux underlying a spark ( $i_{spark}$ , 2~4 pA) (8,68) was close to unitary  $Ca^{2+}$  current of the RyR measured with 10 mM  $Ca^{2+}$  at 0 mV (69,70). However, more recent *in vitro* measurement under quasi-physiological ionic conditions (inclusion of 1 mM  $Mg^{2+}$ ) has revised it downward to ~0.35-0.6 pA (71). Based on the new estimate of unitary RyR current and sparklet-calibrated  $i_{spark}$  (2.1 pA) (9), we suggested that a  $Ca^{2+}$  spark consists of ~4-6 RyRs in (9), similar to what was proposed for  $Ca^{2+}$  sparks in skeletal fibers (67, see also 72)

While virtually all numerical models using 1-3 pA  $i_{spark}$  can reproduce amplitude and temporal characteristics of sparks, the predicted width (1- $\mu$ m) is only about half of the value observed experimentally (2- $\mu$ m) (73-75). On one extreme, Izu et al (76) proposed that 10-20-pA  $i_{spark}$  is required to resolve the "spark-width paradox" (74). This large  $i_{spark}$  would place the number of RyRs in a spark in the neighborhood of 20-40. Unfortunately, this prediction is somewhat compromised by the fact that detailed properties of  $Ca^{2+}$  buffering and diffusion in the cytosol are not well known.

Much work has focused on spark amplitude as an index of RyR open time and of total  $Ca^{2+}$  discharged in a spark. Theory (77,78) and numerical analysis (73,74) predicted that *apparent*  $Ca^{2+}$  spark amplitudes recorded by confocal microscopy should always display a monotonic decaying distribution, regardless of their *true* amplitude distribution.

Experimental measurements with the aid of an automated detection algorithm (77) have confirmed it. However,  $Ca^{2+}$  sparks evoked at fixed positions (79) or occurring spontaneously at hyperactive sites (80) demonstrated rather stereotyped amplitude. Most recently, we have shown that  $Ca^{2+}$  sparks evoked beneath the patch membrane, free of out-of-focus blurring, exhibit a broad modal amplitude distribution (9). The modality of the spark amplitude distribution was initially interpreted to reflect a multi-RyR origin of sparks, for single channels are expected to have exponentially-distributed open time, and so are the amplitudes of sparks of single-RyR origin (79). Alternatively, the modality could be a manifestation of irreversible gating of a single RyR (78,81) (see below).

Taken together, increasing evidence strongly suggests that sparks originate from multiple, instead of single, RyRs; but no study is conclusive as to the exact number of RyRs involved. Interestingly, even for the wildest estimate, RyRs in a spark encompass only a minor fraction of total RyRs in a couplon (100-200 in rat and mouse) (28). So, an outstanding question is why the opening of a few RyRs in a couplon does not fire all RyRs therein? This observation perhaps calls for new, nanoscopic "local control" models to address the molecule-to-molecule crosstalk in a couplon.

### Thermodynamically Irreversible Gating of RyRs in vivo

For a single or a group of Markov channels gating reversibly, distributions of open and closed times should be the sum of positively weighted decaying exponentials. Violation of this microscopic reversibility has been demonstrated previously on a number of occasions at the single channel level (82-84), and has been attributed to possible channel coupling to external sources of free energy. Like the vast majority of ionic channels, single RyRs *in vitro* have been described by Markovian models (68,70,85-87) in which transition between discrete conformational states is determined solely by the present state of the channel, independent of history (only beyond 10-20 transitions (85)). When such a channel is unperturbed, i.e., uncoupled from an external source of energy, thermodynamic laws require microscopic reversibility of the channel reaction. This means that, at equilibrium, a cyclic reaction must take place at the same rate in forward and backward directions; the stochastic properties of the channel must show time reversibility; and distributions of statistical quantities, such as open time, closed time, and burst time, must each equal a sum of positively weighted, decaying exponential terms (88). The same conclusions hold true for a cluster of inter-linked channels that are uncoupled to an external energy source, because such cluster as a whole can be treated as a Markovian entity.

The dual role of  $Ca^{2+}$  as both a permeating ion and a regulator of RyR channel (89,90) creates the intriguing possibility that RyR gating might be coupled to the free energy in  $Ca^{2+}$  electrochemical gradients across the SR. If this were the case, RyRs

in intact cells (or in bilayers under asymmetric  $\text{Ca}^{2+}$  electrochemical potentials) might be expected to gate irreversibly. By measuring release duration of  $\text{Ca}^{2+}$  sparks (as duration of spontaneous  $\text{Ca}^{2+}$  spikes), we found that distribution of the release duration exhibits a prominent mode at around 8 ms (80). Analysis of the cycle time for repetitive sparks at hyperactive sites revealed a lack of intervals briefer than  $\sim 35$  ms and a mode at around 90 ms (80). These results provide the first clue that  $\text{Ca}^{2+}$  sparks are generated by thermodynamically *irreversible* stochastic processes. In a sense, a single RyR or, more exactly, a couplon can be considered as the tiniest molecular "clock" that displays somewhat ordered temporal behavior in spite of thermodynamic fluctuations.

Because data from cardiac and skeletal RyRs in planar lipid bilayers with asymmetric *cis* and *trans*  $\text{Ca}^{2+}$  were consistent with *reversible* gating at the single channel level (80,89,90), the irreversibility for  $\text{Ca}^{2+}$  spark genesis may reside at a supra-molecular level. For instance, CICR and  $\text{Ca}^{2+}$ -induced inactivation among adjacent RyRs may couple the free energy in the SR transmembrane  $\text{Ca}^{2+}$  gradients to RyR gating *in situ*, shaping up the unique temporal characteristics of  $\text{Ca}^{2+}$  sparks. The stereotyped  $\text{Ca}^{2+}$  spark duration also illustrates how collective RyR gating *in vivo* differs qualitatively from single RyR gating *in vitro*.

### Termination of Local $\text{Ca}^{2+}$ Release

As discussed above, the *global stability* of CICR is safeguarded by many factors acting in synergy, including physical separation of RyR clusters, rapid decay of  $\text{Ca}^{2+}$  gradients from a point source in the heavily buffered cytoplasm, low intrinsic  $\text{Ca}^{2+}$  sensitivity of RyRs *in vivo*, and non-linear  $\text{Ca}^{2+}$ -dependence of spark activation. However, gradedness of CICR requires also *local stability* of CICR, i.e., the turn off of release in a single couplon. If the inherent positive feedback were not counteracted, CICR within the release units should result in everlasting  $\text{Ca}^{2+}$  sparks. Several mechanisms have been proposed for the termination of SR  $\text{Ca}^{2+}$  release. (i)  *$\text{Ca}^{2+}$ -dependent inactivation* (5). Binding of released  $\text{Ca}^{2+}$  to a high affinity site of RyRs inactivates the channels and shuts off  $\text{Ca}^{2+}$  release. (ii) *Adaptation of RyRs* (46,47,86). The open probability of RyR channels in lipid-bilayers declines spontaneously after activation by a step increase in  $[\text{Ca}^{2+}]$ . The "adapted" state differs from the inactivated state as it retains the responsiveness to subsequent higher  $[\text{Ca}^{2+}]$  steps. (iii) *Stochastic attrition* (6). Simultaneous stochastic closing of RyRs in an active couplon results in rapid dissipation of local  $[\text{Ca}^{2+}]$  and thereby interruption of the positive feedback. In addition, *local SR  $\text{Ca}^{2+}$  depletion* may also extinguish  $\text{Ca}^{2+}$  release due to the lack of releasable  $\text{Ca}^{2+}$  or reduction in the gain of CICR (39,91,92, see also 93).

Test of  $\text{Ca}^{2+}$ -dependent inactivation in intact cardiac myocytes was first attempted by Nabauer and Morad (21). They showed that a mild to moderate photolytic elevation of cytoplasmic  $\text{Ca}^{2+}$  does not prevent the SR from subsequent activation by  $I_{\text{Ca,L}}$

though the magnitude of release is apparently attenuated. This has been interpreted as evidence against  $\text{Ca}^{2+}$ -dependent inactivation of RyRs *in situ* (21). Yasui et al (94) demonstrated that depolarization to +30 mV in the presence of FPL64176 elicits a transient  $\text{Ca}^{2+}$  release that terminates despite continued  $I_{\text{Ca,L}}$ . Yet, additional  $\text{Ca}^{2+}$  release can be triggered by tail  $I_{\text{Ca,L}}$  upon repolarization. This has been interpreted as evidence for RyR adaptation (94). By direct measurement of local SR  $\text{Ca}^{2+}$  release fluxes (" $\text{Ca}^{2+}$  spikes") at individual T-SR junctions, we found that that the tail  $I_{\text{Ca,L}}$ -elicited  $\text{Ca}^{2+}$  spikes are most likely originated from RyRs unfired during depolarization, rather than from those in the adapted state (11). Furthermore, increasing the open duration and promoting the reopening of LCCs with FPL64176 does not prolong or trigger secondary  $\text{Ca}^{2+}$  spikes. At 50 ms after a maximal release, a multi-fold increase in  $i_{\text{Ca}}$  (by hyperpolarization to -120 mV) fails to evoke any additional release, indicating absolute refractoriness of RyRs (11). These results support the notion that  $\text{Ca}^{2+}$  release is terminated primarily by a strong, local, and use-dependent inactivation of RyRs, and argues against the stochastic closing and adaptation of RyRs as major termination mechanisms of SR  $\text{Ca}^{2+}$  release in intact cardiac myocytes.

### Local Refractoriness of SR $\text{Ca}^{2+}$ Release

Recently, DelPrincipe et al (12) reported that, unlike global SR  $\text{Ca}^{2+}$  release in response to homogenous flash, focal photolytic  $\text{Ca}^{2+}$  pulses at 300-ms intervals activate local SR  $\text{Ca}^{2+}$  releases that do not undergo refractoriness whatsoever. They argued that global refractoriness might be due to SR  $\text{Ca}^{2+}$  depletion, whereas the lack of local SR refractoriness is due to rapid replenishment during local excitation. However, the apparent lack of RyR inactivation in these experiments can be explained by several other possibilities, e.g., recruitment of different RyRs in consecutive pulses, recovery of inactivated RyRs (absolute refractoriness in the  $\text{Ca}^{2+}$  spike experiment was detected within 50 ms (11)), and overload of local SR with the exogenous photolytic  $\text{Ca}^{2+}$ .

Using the loose-seal patch clamping and confocal imaging technique, we have revisited the issue of local SR refractoriness by activating single couplons with single LCC excitation (9). We found that repetitive  $\text{Ca}^{2+}$  sparklets can trigger more than one  $\text{Ca}^{2+}$  spark during a single voltage step. However, the sparklet-spark coupling fidelity,  $\delta$ , decreases from 0.7 to 0.3 once a spark has being fired. This observation provides direct evidence that RyRs display use-dependent inactivation at the single couplon level. The robust termination of  $\text{Ca}^{2+}$  sparks and persistent refractoriness add to the repertoire of safekeeping mechanisms that insure the stability and controllability of CICR.

### Perspective

From the conception of local control of CICR, to the first recording of  $\text{Ca}^{2+}$  sparks, to the demonstration of ignition of  $\text{Ca}^{2+}$  sparks by single

LCCs, and to the search for possible termination mechanisms, our understanding of the physiological processes of EC coupling has been greatly advanced since the discovery of CICR. The emergence of a microscopic picture of LCC-to-RyR communication, along with the advent of novel methods and investigative tools, allows one to define normal, altered and dysfunctional EC coupling with unprecedented accuracy. As the frontier expands, many challenging questions remain open. The following presents our perspective of the six most enigmatic issues in this field.

### **Role of SR luminal $\text{Ca}^{2+}$ in regulation of CICR.**

It is generally accepted that increasing the SR  $\text{Ca}^{2+}$  content beyond a critical level greatly enhances RyR sensitivity to induce unstable CICR (95). The converse effect, i.e. whether decreasing SR  $\text{Ca}^{2+}$  negatively regulates RyR gating and thereby terminates the SR  $\text{Ca}^{2+}$  release, remains controversial. On one hand, we observed that up to 60% depletion of SR  $\text{Ca}^{2+}$  has no significant effect on the rate of occurrence of spontaneous  $\text{Ca}^{2+}$  sparks, when the low-amplitude missing events are accounted for (93). On the other hand, in chemically skinned cardiac myocytes whose SR  $\text{Ca}^{2+}$  is primed to a supra-normal level, altering the SR  $\text{Ca}^{2+}$  load does change  $\text{Ca}^{2+}$  spark frequency after correction (39). At the cellular level, while it has been reported that reduction of SR  $\text{Ca}^{2+}$  content reduces proportionally the  $I_{\text{Ca,L}}$ -elicited  $\text{Ca}^{2+}$  release (96), Shannon et al (91) showed that ~50% depletion of SR  $\text{Ca}^{2+}$  completely abolishes the RyR response to the trigger  $I_{\text{Ca,L}}$ . *In vitro* experiments also yielded contradicting results. Gyorke and Gyorke (92) have shown that a 250-fold reduction of luminal  $\text{Ca}^{2+}$  (from 5 mM to 20  $\mu\text{M}$ ) shifts the  $\text{Ca}^{2+}$ -dependent activation of RyR rightward (0.57 logarithmic unit) and downward (by 60%); however, Meissner and colleagues have shown that permeating  $\text{Ca}^{2+}$  acting at cytosolic RyR sites may pose as luminal  $\text{Ca}^{2+}$ -mediated regulation (89,90). Future experiments are warranted to determine the condition, extent and physiological relevance of allosteric modulation of the RyR by SR luminal  $\text{Ca}^{2+}$ .

### **Nature of SR Refractoriness.**

While use-dependent inactivation of RyRs has been established at the cellular (11, 12,41), T-SR junctional (11), and single-couplon (9) levels, it is unclear whether it is a manifestation of  $\text{Ca}^{2+}$ -dependent negative feedback control mechanism, or a fateful consequence of channel activation *per se*. Moreover, luminal  $\text{Ca}^{2+}$  might play a role if a partial depletion affects RyR sensitivity to cytosolic  $\text{Ca}^{2+}$ .

### **Intermolecular communication in a couplon.**

This utterly important yet utterly difficult issue is yet to be determined. How many RyRs crosstalk to a given LCC, and how many LCCs to a given RyR? Do a single LCC communicate privately to its nearest neighbors, or promiscuously to all RyRs in a couplon? Do RyRs communicate via CICR, or are coupled mechanically by FK506 binding proteins (FKBP) (97), or both? If a mechanical coupling is

involved, is it rigid or dynamic in nature? At any rate, it is imperative to explain what prevents the entire couplon encompassing ~150 RyRs from firing all at once in a spark.

### **Gating scheme for RyRs in vivo.**

For various gating schemes derived from *in vitro* experiments, none could reproduce essential features of cardiac EC coupling when implanted into a stochastic couplon model of EC coupling (61). Future research should aim also at elucidating the physiologically relevant gating scheme of the channel. At present, we have only a glimpse of some key features involved: a rapid, highly cooperative  $\text{Ca}^{2+}$ -dependent activation; a fast, profound, and enduring inactivation; and a mechanism that produces preferred active time of the couplon. It should also be emphasized that the collective behavior of a group of RyRs may differ quantitatively and qualitatively from a RyR acting *solo* (61,80).

### **Regulatory role of signaling molecules complexed with RyRs.**

Gating of RyRs in intact cells could be even more complex than we thought, for the native channel protein is associated with numerous other proteins, such as calmodulin (98), protein kinases (protein kinase A, calmodulin kinase II) and phosphatases (PP1 and PP2a) (99) to form a macromolecular signaling complex. In addition, accessory proteins including FKBP and sorcin may also play functional roles (13,14,100, 101). Critical examination of the involvement of these possible regulatory mechanisms in activation, termination and refractoriness of  $\text{Ca}^{2+}$  sparks calls for future studies.

### **Molecular definition of altered or dysfunctional EC coupling.**

Recent advances have provided an array of novel concepts and microscopic readouts of EC coupling. For apparently similar phenotypes at the cellular level ( $I_{\text{Ca,L}}$ ,  $J_{\text{SR}}$ , global  $\text{Ca}^{2+}$  transients, SR  $\text{Ca}^{2+}$  load, and "gain" function), the underlying microscopic mechanisms may vary ( $i_{\text{Ca}}$  and sparklets; amplitude, duration and width of  $\text{Ca}^{2+}$  sparks; temporal synchrony of  $\text{Ca}^{2+}$  spikes; fidelity and latency of sparklet-to-spark coupling). The mechanistic understanding of normal EC empowers one to better define altered or dysfunctional states of EC coupling, as in diseased hearts, in the physiological process of cardiac senescence, or in genetically engineered hearts. Insights gained from these studies will certainly enhance our understanding how the heart works in health and in disease.

### **Acknowledgements**

We thank Drs. Edward G. Lakatta, Michael D. Stern, Jon Lederer, Mark Cannell, Eduardo Rios, Martin Schneider, James Sham, Héctor H. Valdivia, Rui-Ping Xiao and many colleagues for invaluable discussions that directly or indirectly contribute to the thoughts presented in this review. This work was supported by NIH intramural research program.

## References

1. T. F. McDonald, S. Pelzer, W. Trautwein & D. J. Pelzer: Regulation and modulation of calcium channels in cardiac, skeletal & smooth muscle cells. *Physiol Rev* 74(2), 365-507 (1994)
2. G. Meissner: Ryanodine receptor/ $\text{Ca}^{2+}$  release channels and their regulation by endogenous effectors. *Ann Rev Physiol* 56, 485-508 (1994)
3. C. Franzini-Armstrong & F. Protasi: Ryanodine receptors of striated muscles, a complex channel capable of multiple interactions. *Physiol Rev* 77(3), 699-729 (1997)
4. A. Fabiato & F. Fabiato: Contractions induced by a calcium-triggered release of calcium from the sarcoplasmic reticulum of single skinned cardiac cells. *J Physiol* 249(3), 469-495 (1975)
5. A. Fabiato: Time and calcium dependence of activation and inactivation of calcium-induced release of calcium from the sarcoplasmic reticulum of a skinned canine cardiac Purkinje cell. *J Gen Physiol* 85, 247-289 (1985)
6. M. D. Stern. Theory of excitation-contraction coupling in cardiac muscle. *Biophys J* 63(2), 497-517 (1992)
7. E. Niggli & W. J. Lederer: Voltage-independent calcium release in heart muscle. *Science* 250(4980), 565-568 (1990)
8. H. Cheng, W. J. Lederer & M. B. Cannell: Calcium sparks: The elementary events underlying excitation-contraction coupling in heart muscle, *Science* 262, 740-744 (1993)
9. S.Q. Wang, L.-S. Song, E. G. Lakatta & H. Cheng:  $\text{Ca}^{2+}$  Signaling between single L-type  $\text{Ca}^{2+}$  channels and ryanodine receptors in heart cells. *Nature* 410, 592-596 (2001)
10. L.-S. Song, J. S. Sham, E. G. Lakatta & H. Cheng: Direct measurement of SR  $\text{Ca}^{2+}$  release by tracking " $\text{Ca}^{2+}$  spikes" in rat cardiac myocytes. *J Physiol* 512, 677-691 (1998)
11. J. S. K. Sham, Song, L.-S., L. H. Deng, Y. Chen-Izu, E. G. Lakatta, M. D. Stern & H. Cheng: Termination of  $\text{Ca}^{2+}$  release by local inactivation of ryanodine receptors in cardiac myocytes. *Proc Natl Acad Sci U S A*, 95, 15096-15101 (1998)
12. F. DelPrincipe, M. Egger & E. Niggli: Calcium signalling in cardiac muscle: refractoriness revealed by coherent activation. *Nat Cell Biol* 1(6), 323-329 (1999)
13. R.-P. Xiao, H. H. Valdivia, K. Bogdanov, C. Valdivia, E. G. Lakatta & H. Cheng: The immunophilin FK506 binding protein (FKBP) modulates  $\text{Ca}^{2+}$  release channel closure in rat heart cells. *J Physiol* 500, 343-354 (1997)
14. V. Lukyanenko, T. F. Wiesner & S. Gyorke: Termination of  $\text{Ca}^{2+}$  release during  $\text{Ca}^{2+}$  sparks in rat ventricular myocytes. *J Physiol* 507 ( Pt 3), 667-677 (1998)
15. W. G. Wier & C. W. Balke:  $\text{Ca}^{2+}$  release mechanisms,  $\text{Ca}^{2+}$  sparks & local control of excitation-contraction coupling in normal heart muscle. *Circ Res* 85(9), 770-776 (1999)
16. H. Cheng, M. R. Lederer, R.-P. Xiao, A. M. Gomez, Y.-Y. Zhou, B. Ziman, H. Spurgeon, E.G. Lakatta & W. J. Lederer: Excitation-contraction coupling in heart: New insights from  $\text{Ca}^{2+}$  sparks. *Cell Calcium* 20, 129-140 (1996)
17. E. Niggli: Localized intracellular calcium signaling in muscle: calcium sparks and calcium quarks. *Annu Rev Physiol* 61, 311-335 (1999)
18. D. Bers: *Excitation-contraction coupling and cardiac contractile force*. 2nd edition. Kluwer Academic Publishers Dordrecht/Boston/London (2001)
19. M. Endo, M. Tanaka & Y. Ogawa: Calcium induced release of calcium from the sarcoplasmic reticulum of skinned skeletal muscle fibres. *Nature* 228, 34-36 (1970)
20. L. E. Ford & R. J. Podolsky: Regenerative calcium release within muscle cells. *Science* 167(914), 58-59 (1970)
21. M. Nabauer & M. Morad:  $\text{Ca}^{2+}$ -induced  $\text{Ca}^{2+}$  release as examined by photolysis of caged  $\text{Ca}^{2+}$  in single ventricular myocytes. *Am J Physiol* 258(1 Pt 1), C189-193 (1990)
22. M. B. Cannell, J. R. Berlin & W. J. Lederer: Effect of membrane potential changes on the calcium transient in single rat cardiac muscle cells. *Science* 238(4832), 1419-1423 (1987)
23. G. Callewaert, L. Cleemann & M. Morad: Epinephrine enhances  $\text{Ca}^{2+}$  current-regulated  $\text{Ca}^{2+}$  release and  $\text{Ca}^{2+}$  reuptake in rat ventricular myocytes. *Proc Natl Acad Sci U S A* 85(6), 2009-2013 (1988)
24. D. J. Beuckelmann & W. G. Wier: Mechanism of release of calcium from sarcoplasmic reticulum of guinea-pig cardiac cells. *J Physiol* 405, 233-255 (1988)
25. W. H. duBell & S. R. Houser: Voltage and beat dependence of  $\text{Ca}^{2+}$  transient in feline ventricular myocytes. *Am J Physiol* 257(3 Pt 2), H746-759 (1989)
26. W. G. Wier, T. M. Egan, J.R. Lopez-Lopez & C. W. Balke: Local control of excitation-contraction coupling in rat heart cells. *J Physiol* 474(3), 463-471 (1994)
27. L.-S. Song, S. Q. Wang, R.-P. Xiao, H. Spurgeon, E. G. Lakatta & H. Cheng:  $\beta$ -adrenergic stimulation synchronizes intracellular  $\text{Ca}^{2+}$  release during excitation-contraction coupling in cardiac myocytes. *Circ Res* 88, 794-801 (2001)
28. C. Franzini-Armstrong, F. Protasi & V. Ramesh: Shape, size & distribution of  $\text{Ca}^{2+}$  release units and couplons in skeletal and cardiac muscles. *Biophys J* 77(3), 1528-1539 (1999)
29. M. D. Stern: Buffering of calcium in the vicinity of a channel pore. *Cell Calcium* 13(3), 183-192 (1992)
30. J. S. Sham, L. Cleemann & M. Morad: Functional coupling of  $\text{Ca}^{2+}$  channels and ryanodine receptors in cardiac myocytes. *Proc Natl Acad Sci U S A* 92(1), 121-125 (1995)
31. K. R. Sipido, E. Carmeliet, F. & Van de Werf: T-type  $\text{Ca}^{2+}$  current as a trigger for  $\text{Ca}^{2+}$  release from the sarcoplasmic reticulum in guinea-pig ventricular myocytes. *J Physiol* 508 ( Pt 2), 439-451 (1998)
32. S. C. O'Neill, J. G. Mill & D. A. Eisner: Local activation of contraction in isolated rat ventricular myocytes. *Am J Physiol* 258(6 Pt 1), C1165-1168 (1990)
33. P. Lipp & E. Niggli: Modulation of  $\text{Ca}^{2+}$  release in cultured neonatal rat cardiac myocytes. Insight from subcellular release patterns revealed by confocal microscopy. *Circ Res* 74(5), 979-990 (1994)
34. M. B. Cannell, H. Cheng & W. J. Lederer: Spatial non-uniformities in  $[\text{Ca}^{2+}]_i$  during E-C coupling in cardiac myocytes. *Biophys J* 67, 1942-1956 (1994)
35. M. B. Cannell, H. Cheng & W. J. Lederer: The control of calcium release in heart muscle, *Science* 268, 1045-1050 (1995)
36. J. R. Lopez-Lopez, P. S. Shacklock, C. W. Balke & W. G. Wier: Local calcium transients triggered by single L-type calcium channel currents in cardiac cells. *Science* 268(5213), 1042-1045 (1995)
37. J. R. Lopez-Lopez, P. S. Shacklock, C. W. Balke & W. G. Wier: Local, stochastic release of  $\text{Ca}^{2+}$  in voltage-clamped rat heart cells: visualization with confocal microscopy. *J Physiol* 480 ( Pt 1), 21-29 (1994)
38. H. Cheng, W. J. Lederer & M. B. Cannell: Partial inhibition of calcium current by D600 reveals spatial non-uniformities in  $[\text{Ca}^{2+}]_i$  during excitation-contraction coupling in cardiac myocytes. *Circ Res* 76, 236-241 (1995)
39. V. Lukyanenko, S. Viatchenko-Karpinski, A. Smirnov, T. F. Wiesner & S. Gyorke: Dynamic regulation of sarcoplasmic reticulum  $\text{Ca}^{2+}$  content and release by luminal  $\text{Ca}^{2+}$ -sensitive leak in rat ventricular myocytes. *Biophys J* 81(2), 785-798 (2001)
40. H. Satoh, L. A. Blatter & D. M. Bers: Effects of  $[\text{Ca}^{2+}]_i$ , SR  $\text{Ca}^{2+}$  load & rest on  $\text{Ca}^{2+}$  spark frequency in ventricular myocytes. *Am J Physiol* 272(2 Pt 2), H657-668 (1997)

41. H. Cheng, M. R. Lederer, M. B. Cannell & W. J. Lederer: Calcium sparks and  $[Ca^{2+}]_i$  waves in cardiac myocytes, *Am J Physiol* 270, C148-C159 (1996)
42. I. Parker, W. J. Zang & W. G. Wier.  $Ca^{2+}$  sparks involving multiple  $Ca^{2+}$  release sites along Z-lines in rat heart cells. *J Physiol* 497 ( Pt 1), 31-38 (1996)
43. W. G. Wier, ter Keurs HE, Marban E, Gao WD & C. W. Balke:  $Ca^{2+}$  'sparks' and waves in intact ventricular muscle resolved by confocal imaging. *Circ Res* 81(4), 462-469 (1997)
44. L. Cleemann, W. Wang & M. Morad: Two-dimensional confocal images of organization, density & gating of focal  $Ca^{2+}$  release sites in rat cardiac myocytes. *Proc Natl Acad Sci U S A* 95(18), 10984-10989 (1998)
45. L. T. Izu, W. G. Wier & C. W. Balke: Evolution of cardiac calcium waves from stochastic calcium sparks. *Biophys J* 80(1), 103-120 (2001)
46. S. Gyorke & M. Fill: Ryanodine receptor adaptation: control mechanism of  $Ca^{2+}$ -induced  $Ca^{2+}$  release in heart. *Science* 260(5109), 807-809 (1993)
47. H. H. Valdivia, J. H. Kaplan, G. C. Ellis-Davies & W. J. Lederer: Rapid adaptation of cardiac ryanodine receptors: modulation by  $Mg^{2+}$  and phosphorylation. *Science* 267(5206), 1997-2000 (1995)
48. A. Tsugorka, E. Rios & L. A. Blatter: Imaging elementary events of calcium release in skeletal muscle cells. *Science* 269(5231), 1723-1726 (1995)
49. M. G. Klein, H. Cheng, L. F. Santana, W. J. Lederer & M. F. Schneider: Discrete sarcomeric calcium release events activated by dual mechanisms in skeletal muscle. *Nature* 379, 455-458 (1996)
50. M. T. Nelson, H. Cheng, M. Rubart, L. F. Santana, A. Bonev, H. Knot & W. J. Lederer: Relaxation of arterial smooth muscle by calcium sparks, *Science* 270, 633-637 (1995)
51. L. Haak, L.-S. Song, T. F. Molinski, I. Pessah, H. Cheng & J. T. Russell: Oligodendrocyte progenitor Sparks and puffs: Crosstalk between ryanodine receptors and IP3 receptors. *J Neurosci* 21, 3860-3870. (2001)
52. J. Huser, L. & A. Blatter: Elementary events of agonist-induced  $Ca^{2+}$  release in vascular endothelial cells. *Am J Physiol* 273(5 Pt 1), C1775-1782 (1997)
53. Y. Yao, J. Choi & I. Parker: Quantal puffs of intracellular  $Ca^{2+}$  evoked by inositol trisphosphate in *Xenopus* oocytes. *J Physiol* 482 ( Pt 3), 533-553 (1995)
54. P. Lipp & E. Niggli: Submicroscopic calcium signals as fundamental events of excitation--contraction coupling in guinea-pig cardiac myocytes. *J Physiol* 492 ( Pt 1), 31-38 (1996)
55. P. Lipp & E. Niggli: Fundamental calcium release events revealed by two-photon excitation photolysis of caged calcium in Guinea-pig cardiac myocytes. *J Physiol* 508 ( Pt 3), 801-809 (1998)
56. P. Lipp, M. Egger & E. Niggli: Spatial characteristics of SR  $Ca^{2+}$  release events triggered by  $I_{Ca,L}$  and  $I_{Na}$  in guinea-pig cardiac myocytes. *J Physiol*, in press (2002)
57. A. Guia, M. D. Stern, E. G. Lakatta & I. R. Josephson: Ion concentration-dependence of rat cardiac unitary L-type calcium channel conductance. *Biophys J* 80(6), 2742-2750 (2001)
58. W. C. Rose, C. W. Balke, W. G. Wier & E. Marban: Macroscopic and unitary properties of physiological ion flux through L-type  $Ca^{2+}$  channels in guinea-pig heart cells. *J Physiol* 456, 267-284 (1992)
59. S. R. Shorofsky, L. Izu, W. G. Wier & C. W. Balke:  $Ca^{2+}$  sparks triggered by patch depolarization in rat heart cells. *Circ Res* 82(4), 424-429 (1998)
60. X. H. Sun, F. Protasi, M. Takahashi, H. Takeshima, D. G. Ferguson, C. Franzini-Armstrong: Molecular architecture of membranes involved in excitation-contraction coupling of cardiac muscle. *J Cell Biol* 129(3), 659-671 (1995)
61. M. D. Stern, L.-S. Song, H. Cheng, J. S. K. Sham, H. T. Yang, K. R. Boheler & E. Rios: Local Control Models of Cardiac Excitation-Contraction Coupling: A Possible Role for Allosteric Interactions Between Ryanodine Receptors. *J Gen Physiol* 113, 469-489 (1999)
62. Y.-Y. Zhou, L.-S. Song, E. G. Lakatta, R.-P. Xiao & H. Cheng: Constitutive  $\beta_2$ -Adrenergic Signaling Enhances SR  $Ca^{2+}$  Cycling to Augment Contraction in Mouse Heart. *J Physiol* 521, 351-361 (1999)
63. A. Zahradnikova, I. Zahradnik, I. Gyorke & S. Gyorke: Rapid activation of the cardiac ryanodine receptor by submillisecond calcium stimuli. *J Gen Physiol* 114(6), 787-798 (1999)
64. K. R. Sipido & W. G. Wier: Flux of  $Ca^{2+}$  across the sarcoplasmic reticulum of guinea-pig cardiac cells during excitation-contraction coupling. *J Physiol* 435, 605-630 (1991)
65. L. F. Santana, H. Cheng, A.M. Gomez, M. B. Cannell & W. J. Lederer: Relationship between the sarcolemmal calcium current and calcium sparks and local control of cardiac excitation-contraction coupling. *Circ Res* 78, 166-171 (1996)
66. C. Soeller, M. B. Cannell: Numerical simulation of local calcium movements during L-type calcium channel gating in the cardiac diad. *Biophys J* 73(1), 97-111 (1997)
67. A. Gonzalez, W. G. Kirsch, N. Shirokova, G. Pizarro, M. D. Stern, H. Cheng & E. Rios: Involvement of Multiple Intracellular Release Channels in Calcium Sparks of Muscle. *Proc. Natl. Acad. Sci. USA*, 97, 4380-4385 (2000)
68. L. A. Blatter, J. Huser & E. Rios: Sarcoplasmic reticulum  $Ca^{2+}$  release flux underlying  $Ca^{2+}$  sparks in cardiac muscle. *Proc Natl Acad Sci U S A* 94(8), 4176-4181 (1997)
69. E. Rousseau & G. Meissner: Single cardiac sarcoplasmic reticulum  $Ca^{2+}$ -release channel: activation by caffeine. *Am J Physiol* 256(2 Pt 2), H328-333 (1989)
70. A. Tinker, AR. Lindsay & A. J. Williams: A model for ionic conduction in the ryanodine receptor channel of sheep cardiac muscle sarcoplasmic reticulum. *J Gen Physiol*, 100(3), 495-517 (1992)
71. R. Mejia-Alvarez, C. Kettlun, E. Rios, M. D. Stern & M. Fill: Unitary  $Ca^{2+}$  current through cardiac ryanodine receptor channels under quasi-physiological ionic conditions. *J Gen Physiol* 113(2), 177-186 (1999)
72. M. F. Schneider:  $Ca^{2+}$  sparks in frog skeletal muscle: generation by one, some, or many SR  $Ca^{2+}$  release channels? *J Gen Physiol* 113(3), 365-372 (1999)
73. V. R. Pratusевич & C. W. Balke: Factors shaping the confocal image of the calcium spark in cardiac muscle cells. *Biophys J* 71(6), 2942-2957 (1996)
74. G. Smith, J. Kiezer, M. D. Stern, W. J. Lederer & H. Cheng: A simple numerical model of calcium spark formation and detection in cardiac myocytes. *Biophys J* 75, 15-32 (1998)
75. Y. H. Jiang, M. G. Klein & M. F. Schneider: Numerical simulation of  $Ca^{2+}$  "Sparks" in skeletal muscle *Biophys J* 77(5), 2333-2357 (1999)
76. L. T. Izu, J. R. Mauban, C. W. Balke & W. G. Wier: Large currents generate cardiac  $Ca^{2+}$  sparks. *Biophys J* 80(1), 88-102 (2001)
77. H. Cheng, S. L. Song, N. Shirokova, A. Gonzalez, E. G. Lakatta, E. Rios & M. D. Stern: Amplitude distribution of calcium sparks in confocal images: theory and studies with an automatic detection method. *Biophys J* 76(2), 606-617 (1999)
78. E. Rios, N. Shirokova, W. G. Kirsch, G. Pizarro, M. D. Stern, H. Cheng & A. Gonzalez: A preferred amplitude of calcium sparks in skeletal muscle. *Biophys J* 80(1), 169-183 (2001)
79. J. H. Bridge, P. R. Ershler & M. B. Cannell: Properties of  $Ca^{2+}$  sparks evoked by action potentials in mouse ventricular myocytes. *J Physiol* 518 ( Pt 2), 469-478 (1999)
80. Wang, S.Q., L. S. Song, L. Xu, G. Messiner, E. Rios, M. D. Stern & H. Cheng, Thermodynamically irreversible gating of ryanodine receptors *in situ* revealed by

- stereotyped duration of release in Ca<sup>2+</sup> sparks. *Biophysical J*, in press (2002)
81. N. Shirokova, A. Gonzalez, W.G. Kirsch, E. Rios, G. Pizarro, M. D. Stern & H. Cheng: Calcium sparks: release packets of uncertain origin and fundamental role. *J Gen Physiol* 113, 377-384 (1999)
  82. K. A. Gration, J. J. Lambert, R. L. Ramsey, R. P. Rand & P. N. Usherwood: Closure of membrane channels gated by glutamate receptors may be a two-step process. *Nature* 295, 599-603 (1982)
  83. T. Chen & C. Miller.: Nonequilibrium gating and voltage dependence of the CIC-0 Cl channel. *J Gen Physiol* 108, 237-250 (1996)
  84. R. Schneggenburger & P. Ascher: Coupling of permeation and gating in an NMDA-channel pore mutant. *Neuron* 18, 167-177 (1997)
  85. R. H. Ashley & A. J. Williams: Divalent cation activation and inhibition of single calcium release channels from sheep cardiac sarcoplasmic reticulum. *J Gen Physiol* 95, 981-1005 (1990)
  86. H. Cheng, M. Fill, H. Valdivia & W.J. Lederer: Models of Ca<sup>2+</sup> release channel adaptation. *Science* 267, 2009-2010. (1995)
  87. A. Zahradnikova & I. Zahradnik: A minimal gating model for the cardiac calcium release channel. *Biophys J* 71, 2996-3012. (1996)
  88. D. Colquhoun & A. G. Hawkes: The principles of the stochastic interpretation of ion-channel mechanisms. In *Single Channel Recording*, chapter 18, second edition. B. Sakmann & E. Neher, editors. Plenum Press, New York. 397-482 (1995)
  89. A. Tripathy & G. Meissner: Sarcoplasmic reticulum luminal Ca<sup>2+</sup> has access to cytosolic activation and inactivation sites of skeletal muscle Ca<sup>2+</sup> release channel. *Biophys J* 70, 2600-2615 (1996)
  90. L. Xu & G. Meissner: Regulation of cardiac muscle Ca<sup>2+</sup> release channel by sarcoplasmic reticulum luminal Ca<sup>2+</sup>. *Biophys J* 75, 2302-2312. (1998)
  91. T. R. Shannon, K. S. Ginsburg & D. M. Bers: Potentiation of fractional sarcoplasmic reticulum calcium release by total and free intra-sarcoplasmic reticulum calcium concentration. *Biophys J* 78(1), 334-343 (2000)
  92. I. Gyorke & S. Gyorke: Regulation of the cardiac ryanodine receptor channel by luminal Ca<sup>2+</sup> involves luminal Ca<sup>2+</sup> sensing sites. *Biophys J* 75(6), 2801-2810 (1998)
  93. L.-S. Song, M. D. Stern, Lakatta, E.G. & H. Cheng, Partial depletion of sarcoplasmic reticulum calcium does not prevent calcium sparks in rat ventricular myocytes. *J Physiol* 505, 655-675 (1997)
  94. K. Yasui, P. Palade & S. Gyorke: Negative control mechanism with features of adaptation controls Ca<sup>2+</sup> release in cardiac myocytes. *Biophys J* 67(1), 457-460 (1994)
  95. M. E. Diaz, S. J. Cook, J. P. Chamunorwa, A. W. Trafford, M. K. Lancaster, S. C. O'Neill & D. A. Eisner: Variability of spontaneous Ca<sup>2+</sup> release between different rat ventricular myocytes is correlated with Na<sup>+</sup>-Ca<sup>2+</sup> exchange and [Na<sup>+</sup>]<sub>i</sub>. *Circ Res* 78, 857-862 (1996)
  96. A. M. Janczewski & E. G. Lakatta: Thapsigargin inhibits Ca<sup>2+</sup> uptake & Ca<sup>2+</sup> depletes sarcoplasmic reticulum in intact cardiac myocytes. *Am J Physiol* 265(2 Pt 2), H517-522 (1993)
  97. S. O. Marx, K. Ondrias & A. R. Marks: Coupled gating between individual skeletal muscle Ca<sup>2+</sup> release channels (ryanodine receptors). *Science* 281, 818-821 (1998)
  98. S. L. Hamilton, I. Serysheva & G. M. Strasburg: Calmodulin and Excitation-Contraction Coupling. *News Physiol Sci* 15, 281-284 (2000)
  99. S. O. Marx, S. Reiken, Y. Hisamatsu, T. Jayaraman, D. Burkhoff, N. Roseblit & A. R. Marks: PKA phosphorylation dissociates FKBP12.6 from the calcium release channel (ryanodine receptor): defective regulation in failing hearts. *Cell* 101, 365-376 (2000)
  100. A. J. Lokuta, M. B. Meyers, P. R. Sander, G. L. Fishman & H. H. Valdivia: Modulation of cardiac ryanodine receptors by sorcin. *J Biol Chem* 272(40), 25333-25338 (1997)
  101. H. H. Valdivia: Modulation of intracellular Ca<sup>2+</sup> levels in the heart by sorcin and FKBP12, two accessory proteins of ryanodine receptors. *Trends Pharmacol Sci* 19(12), 479-482 (1998)

**Address Correspondence to**

Heping Cheng, Ph.D.  
 Laboratory of Cardiovascular Sciences  
 National Institute on Aging  
 National Institutes of Health  
 5600 Nathan Shock Drive  
 Baltimore, Maryland 21224  
 Tel: 410-558-8634  
 Fax: 410-558-8150  
 Email: chengp@grc.nia.nih.gov

# Bi-Directional Coupling Between Dihydropyridine Receptors and Ryanodine Receptors

Robert T. Dirksen

University of Rochester School of Medicine and Dentistry, Rochester, NY, 14534, USA.

Email: [Robert\\_Dirksen@URMC.Rochester.edu](mailto:Robert_Dirksen@URMC.Rochester.edu)

**ABSTRACT** The control of calcium signaling between plasma membrane dihydropyridine receptors (DHPRs or L-type calcium channels) and ryanodine receptors (RyRs or calcium release channels) located in the endoplasmic/sarcoplasmic reticulum (ER/SR) underlies a broad array of functions including skeletal muscle contraction, cardiac performance, arteriole tone, neurosecretion, synaptic plasticity, and gene regulation. It has long been appreciated that DHPR activation of RyRs and subsequent calcium release from intracellular stores represents a key event in the control of these processes. In excitable cells, DHPRs trigger the release of intracellular calcium by promoting the opening of nearby RyRs (termed *orthograde coupling*). Interestingly, the signaling interaction between DHPRs and RyRs is often bi-directional such that the calcium-conducting activity of DHPR channels is also regulated by its interaction with the RyR (termed *retrograde coupling*). Recent data indicate that skeletal, cardiac, and neuronal cells utilize fundamentally distinct DHPR/RyR bi-directional coupling mechanisms (chemical and mechanical) in order to control the efficiency, fidelity, and activity of each of these two essential calcium channels. This review will focus on evaluating the nature and molecular determinants of these coupling mechanisms, as well as the extent to which excitable cell function is influenced by bi-directional DHPR/RyR calcium signaling.

## INTRODUCTION

In muscle cells, the process whereby depolarization of the muscle plasma membrane (i.e. an action potential) leads to an increase in intracellular  $Ca^{2+}$ , ultimately resulting in muscle contraction is referred to as excitation-contraction (EC) coupling. In both cardiac and skeletal muscle, dihydropyridine receptors (DHPRs) (also known as L-type calcium channels or L-channels) link sarcolemmal depolarization to the rapid release of calcium ions through calcium release channels (also termed ryanodine receptors or RyRs) located in the terminal cisternae of the sarcoplasmic reticulum (SR). Over the past quarter century, considerable effort has focused on the nature of the signal transmission by which cardiac and skeletal muscle DHPRs trigger the opening of SR calcium release channels (DHPR-to-RyR signaling or orthograde coupling). In cardiac muscle, the prolonged ventricular action potential duration results in significant calcium influx through cardiac L-type calcium channels (1-3). This calcium influx subsequently activates nearby SR calcium release channels via a calcium-induced-calcium-release (CICR) mechanism (1,2,4). Thus, the mechanism of signal transmission in cardiac muscle is believed to predominantly involve a chemical signal (i.e. calcium). On the other hand, calcium influx through L-type calcium channels is not required for skeletal muscle contraction (5) and muscle contraction persists even in the complete absence of extracellular calcium (6). Rather, skeletal muscle DHPRs function as voltage sensors for EC coupling by providing a physical, possibly direct, link between sarcolemmal depolarization and the release of calcium from the sarcoplasmic reticulum (7). Thus, the triggering mechanism of skeletal muscle EC coupling is thought to be primarily mechanical in nature (8,9).

In the process of investigating the molecular mechanisms of orthograde coupling, recent results

have revealed that signaling between DHPR and RyR proteins is bi-directional in cardiac muscle, skeletal muscle, and neurons. Accordingly, the calcium conducting activity attributable to the DHPR is strongly influenced by a functional association with its respective RyR. The ability of the presence/activity of the RyR to alter DHPR channel behavior (RyR-to-DHPR signaling) is referred to as retrograde coupling (10). The balance of this review will focus on recent advances made in understanding the molecular and mechanistic nature of bi-directional coupling between DHPRs and RyRs in cardiac muscle, skeletal muscle, and neurons. Wherever possible, the following sections will discuss the current state of knowledge with regard to three central questions: 1) What is the nature of the bi-directional signal (chemical and/or mechanical)? 2) What regions of the DHPR and RyR proteins are required for bi-directional coupling? 3) What role does retrograde coupling play in regulating excitable cell function?

## CHEMICAL CROSS-TALK

### Bi-directional calcium signaling in cardiac muscle

#### Orthograde coupling in cardiac muscle

It has now been more than 15 years since the classic work by Fabiato (1,4,11) demonstrated that a rapid rise in intracellular free calcium is able to trigger a concentration-dependent release of calcium from the SR and that this release could be blocked by ryanodine. As a result of these experiments, Fabiato surmised that rapid and local calcium influx through voltage-gated L-type calcium channels triggers a larger release of calcium from the SR via a calcium-induced-calcium release (CICR) mechanism. Since the pioneering work of Fabiato, numerous other groups have confirmed that CICR represents the primary mechanism of orthograde coupling in cardiac muscle. Measurements of

spontaneous and localized calcium release events (calcium sparks), first recorded by Cheng and colleagues (1993), demonstrated that CICR in cardiac myocytes occurs within discrete calcium microdomains (12). More recently, elegant experiments conducted by Wang et al. (2001) demonstrated that calcium influx through a single L-channel opening is sufficient to trigger the opening of ~4-6 ryanodine receptors, and thereby, lead to the generation of a localized calcium spark (13). Thus, orthograde coupling in cardiac muscle is widely believed (but see section 6 below) to involve a chemical signal (i.e. calcium ions) transmitted from sarcolemmal DHPRs to cardiac isoform of the RyR (RyR2) that occurs within a limited structural and functional calcium microdomain (Fig. 1, Fig1.avi).

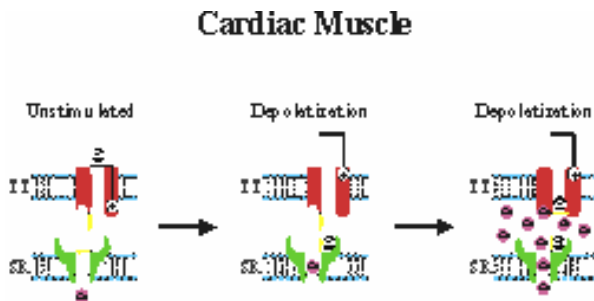


Figure 1: Bi-directional DHPR/RyR2 signaling in cardiac muscle. (Left) In unstimulated cardiac ventricular myocytes, L-type calcium channels (DHPR, red) and SR calcium release channels (RyR2, green) are in a closed state. For clarity, calcium ions originating from extracellular (black) and intracellular release sites (magenta) in Figs. 1-3 are depicted using different colors. (Middle) Sarcolemmal depolarization during the ventricular action potential causes conformational changes in the DHPR that result in L-channel opening and the rapid influx of extracellular calcium. Influx of extracellular calcium triggers the opening of nearby SR calcium release via calcium-induced-calcium-release (orthograde coupling). Calcium released from the SR promotes both activation of the myofilaments, calcium-induced L-channel inactivation, and a subsequent reduction in further calcium influx and CICR (negative retrograde coupling).

Although calcium activation of RyR2 is thought to result from the binding of calcium to a specific site(s) within the RyR homotetramere (14), the precise molecular determinants of the high affinity calcium activation site(s) has yet to be determined. Recent site-directed mutagenesis studies indicate that a highly conserved glutamate residue within the putative transmembrane segment M2 (according to the topological model of 15) of the neuronal (RyR3) (16) and cardiac (RyR2) RyR isoforms (17) contributes to a well-conserved high affinity calcium sensor. Accordingly, substitution of an alanine residue for the conserved glutamate residue at this location in rabbit RyR3 (E3885A) reduces the sensitivity for calcium activation of the release channel by ~10,000-fold (16). Alanine substitution for the conserved glutamate residue in mouse RyR2 (E3987A) caused >1,000-fold reduction in release channel sensitivity to activation by calcium (17). Although alanine substitution of the corresponding glutamate residue in the skeletal muscle isoform of the RyR (RyR1) also reduces release channel sensitivity to activation by calcium (18), this effect may arise from alterations in the proper folding of the RyR transmembrane assembly

in a manner that results in a global insensitivity of the release channel to activation by various agonists, including calcium (19,20). Clearly, further work will be required to more completely characterize the structural determinants for calcium activation of the RyR and to what degree the mechanism for calcium activation is conserved across the three different RyR isoforms.

#### Retrograde coupling in cardiac muscle

Since the early work of Brehm and Eckert (1977) (21), it has become widely appreciated that L-type calcium channels, particularly those in cardiac muscle (22-24), exhibit prominent calcium dependent inactivation. Since a localized calcium microdomain between DHPR and RyR proteins mediates orthograde coupling (DHPR-to-RyR coupling) in cardiac muscle (12), it follows that this same calcium microdomain may in turn regulate calcium dependent inactivation of the cardiac L-channel during EC coupling. According to this idea, calcium released from the sarcoplasmic reticulum would act as a negative feedback mechanism for cardiac EC coupling by promoting L-channel inactivation, and thereby, reducing subsequent calcium influx and release (25) (Fig. 1, Fig1.avi). Support for such a "negative retrograde feedback mechanism" in cardiac EC coupling was first provided by experiments conducted by Morad and colleagues (26-28). These experiments revealed that calcium released from the SR promotes L-channel inactivation even when global calcium transients were eliminated by introduction of high concentrations of high affinity calcium buffers. Under these conditions, the majority of calcium ions would be bound before having diffused ~50 nm away from the site of release (27). Consequently, L-channel inactivation that occurs as a result of SR calcium release must arise from local, rather than global, calcium signaling.

Recent results clearly indicate that calmodulin acts as a  $Ca^{2+}$  sensor for calcium-dependent inactivation and facilitation of cardiac L-channels (29-31). The molecular determinants for  $Ca^{2+}$ -dependent inactivation and facilitation of cardiac L-channels involve the proximal region of the cytoplasmic C-terminus of  $\alpha_{1C}$ , which contains a putative  $Ca^{2+}$  binding EF hand motif, an IQ-like domain, and a CaM-binding (CB) domain (29-32). In addition to effects on inactivation and facilitation, the C-terminal region of  $\alpha_{1C}$  also regulates cardiac L-channel targeting (33-36), conductance, and open probability (35). Although calcium flux through one L-channel can facilitate the inactivation of an adjacent L-channel (37), ~70% of L-channel inactivation that occurs during EC coupling in rat ventricular myocytes arises from calcium released from the SR (27). The somewhat surprising preference of L-channel inactivation for calcium released from the SR rather than calcium flux through the L-channel itself presumably arises from the higher abundance and larger single channel conductance of RyRs compared to DHPRs (27). As a consequence, calcium ions entering the cell through cardiac L-channels activate ryanodine receptors to release an even greater amount of calcium from the SR such that the released calcium serves a more important role in inactivating sarcolemmal L-

channels than calcium flux through the L-channels themselves. Alternatively, it is conceivable that the calmodulin-binding region of the  $\alpha_{1C}$  C-terminus resides closer to RyR2 pore than the pore of the L-channel. In either case, retrograde calcium signaling in cardiac muscle serves to fine-tune the gain of EC coupling. Consequently, the close physical association between DHPRs and RyRs in cardiac muscle creates a bi-directional calcium signaling microdomain such that calcium flux through either channel modifies the functional behavior of the other channel (Fig. 1, Fig1.avi).

The functional components of the calcium signaling microdomain in cardiac muscle may extend beyond the reciprocal interaction between sarcolemmal DHPRs and RyRs of the SR. Electron microscopic studies of rat ventricular muscle indicate that junctions between t-tubules and individual SR calcium release channels are located in close proximity (from 37 to 270 nm) to mitochondria (38). These morphological observations suggest that temporal dynamics of the DHPR-RyR calcium microdomain may be influenced by nearby mitochondrial calcium transport mechanisms. Support for this hypothesis comes from the observation that blockade of mitochondrial calcium uptake mechanisms significantly delays the recovery from frequency-dependent inactivation of cardiac L-type calcium channels that occurs during EC coupling (39), particularly at high stimulation frequencies. These observations suggest that mitochondrial clearance of calcium from the DHPR-RyR microdomain limits the accumulation of L-channel inactivation during EC coupling (39), and therefore influences the degree of retrograde negative feedback (RyR-to-DHPR signaling) in cardiac muscle. It will be important for future work to determine whether bi-directional coupling between cardiac DHPRs and RyRs are altered in response to regulatory factors (e.g. PKA) and under various pathophysiological conditions (e.g. hypertrophy and heart failure).

#### **Bi-directional calcium signaling in skeletal muscle**

It has long been appreciated that influx of extracellular calcium through voltage-gated L-type calcium channels is not required for SR calcium release in skeletal muscle (5,6,40). Rather, depolarization of the skeletal muscle sarcolemma induces voltage-driven conformational changes in the DHPR that are recorded as intramembrane charge movement that precede L-channel opening (41,42). These voltage-driven charge movements presumably gate the opening of skeletal muscle RyRs (RyR1s) in the SR via a mechanical, possibly direct, link between the two proteins (7). Thus, under normal circumstances, bi-directional chemical signaling between DHPRs and RyRs does not occur in mammalian skeletal muscle. However, components of bi-directional chemical signaling in skeletal muscle may occur under some conditions. For example, calcium influx through DHP-sensitive L-channels may contribute to the force of contraction during tetanic stimulation (43), the regulation of gene expression (44,45), or metabolic stabilization of skeletal muscle acetylcholine receptors (46). In frog skeletal muscle, intramembrane charge movements

attributable to the activation of sarcolemmal DHPRs exhibit two distinct kinetic components: 1) an early component ( $Q_{\beta}$ ) that decays exponentially and 2) a late component ( $Q_{\square}$ ) that appears as a “hump” at the base of  $Q_{\beta}$  (see ref. 8,47 for reviews). Rios and colleagues have suggested that  $Q_{\beta}$  reflects gating current of the voltage sensor induced by depolarization of the sarcolemma and  $Q_{\square}$  arises at least in part from an increase in sarcolemmal surface potential introduced by local changes in intracellular calcium that occur during SR calcium release (8). In this way, calcium release could promote further activation of the voltage sensor (positive feedback) and result in additional SR calcium release (48). However, while calcium released during EC coupling clearly influences voltage sensor activity (via a retrograde chemical signal) in amphibian muscle, similar effects are not observed in mammalian skeletal muscle.

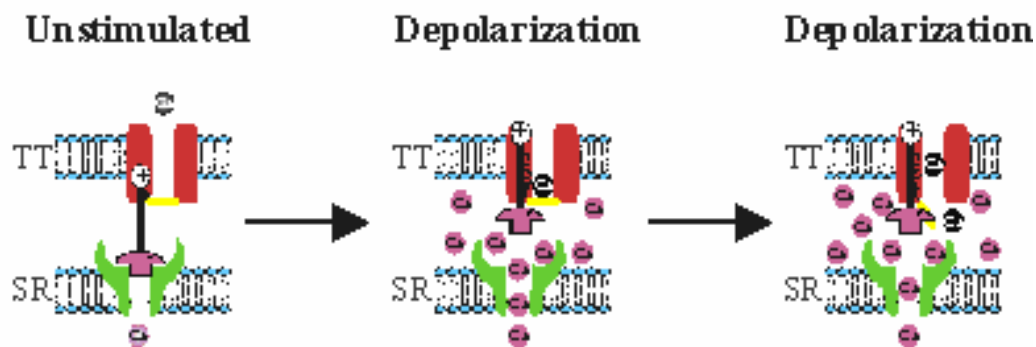
#### **MECHANICAL CROSS-TALK**

##### **Mechanism of bi-directional coupling in skeletal muscle**

Over the years, several different mechanisms have been proposed to account for how changes in t-tubule membrane potential trigger calcium release from the SR in skeletal muscle (see 8,47 for excellent reviews). These mechanisms have included (among others) calcium influx dependent activation of RyR1, activation of calcium release by inositol trisphosphate, and mechanical coupling between the DHPR and RyR1. It is beyond the scope of this review to present a comprehensive evaluation of each of these hypotheses. However, the demonstration of a clear fixed stoichiometry and ordered alignment of sarcolemmal DHPR and RyR proteins of the SR in elegant morphological studies (49) and strong correlations between the presence and properties of charge movements and SR calcium release in skeletal muscle in physiological experiments (41,42) provides compelling support for the mechanical coupling hypothesis (Fig. 2a, Fig2.avi).

The recent observation that the calcium conducting activity of skeletal muscle DHPRs is strongly dependent upon the presence of RyR1 provides additional support for a direct interaction between these two proteins (10,50). This finding was originally based on the observation that skeletal myotubes derived from mice homozygous for a disrupted RyR1 gene (RyR1 knockout or dyspedic mice) lack both voltage-gated SR calcium release (DHPR-to-RyR1 or orthograde coupling) and robust voltage-gated L-type calcium currents (RyR1-to-DHPR or retrograde coupling) (10) (Fig. 2b, Fig2.avi). The low level of L-current in dyspedic myotubes does not arise from an absence of DHPR expression since dyspedic myotubes exhibit both significant DHP binding (51,52) and voltage-driven intramembrane charge movements (53). Moreover, freeze fracture studies reveal that surface membranes of dyspedic myotubes exhibit clusters of unordered (i.e. non-tetradic) DHPRs within sarcolemmal/SR junctions (54). Finally, expression of RyR1 proteins in dyspedic myotubes is sufficient to restore both voltage-gated SR calcium release and high density L-type calcium current (55) in the

## A. Normal Skeletal Muscle



## B. Dyspedic Skeletal Muscle

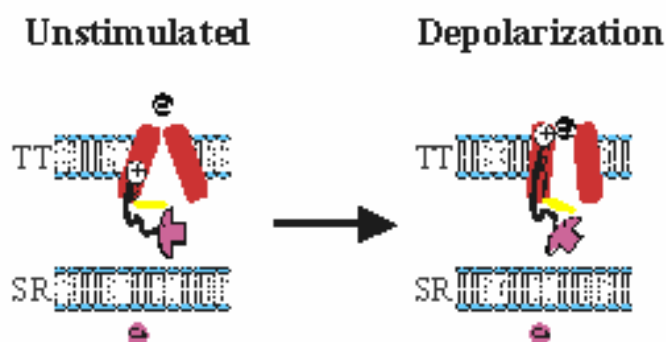


Figure 2: Bi-directional DHPR/RyR1 signaling in skeletal muscle. (A) (Left) At resting membrane potentials, skeletal L-type calcium channels (DHPR, red) are in a closed state. A putative physical interaction between the II-III loop of the skeletal muscle DHPR is shown to inhibit release channel opening via a the “plunger model” proposed by Chandler et al. (1976) (7). (Middle) Sarcolemmal depolarization causes conformational changes in the DHPR that result in rapid DHPR gating charge movements and a mechanical activation of RyR1 that is independent of the influx of extracellular calcium (orthograde coupling) (5,6). (Right) The activation or opening of the skeletal L-channel and influx of extracellular calcium occurs very slowly (shown here to be mediated by a sluggish, spring-loaded activation gate), only after SR calcium release has already been maximally activated. (B) RyR1 promotes the calcium-conducting activity of the skeletal muscle DHPR (positive retrograde coupling). In dyspedic myotubes, which lack RyR1 proteins, the absence of an interaction between the DHPR II-III loop and RyR1 causes global conformational changes in the L-channel complex (shown as a tilting in the transmembrane segments) (57) (left). L-channels in dyspedic myotubes continue to undergo voltage-driven conformational changes that produce charge movements following depolarization, but are unable to activate SR calcium release and exhibit significant alterations in the functional properties of L-channel (conductance, kinetics, divalent permeation, and modulation by DHPs) (50,55).

absence of a change in the magnitude of intramembrane charge movement (but see ref. 53). As a result, RyR1 expression increases the ratio between maximal L-channel conductance and charge movement ( $G_{max}/Q_{max}$ ), indicating that uncoupled DHPRs function poorly as calcium-permeable L-channels. Thus, RyR1 functions not only as an effector that is activated by the DHPR, but also as a transducer that delivers a retrograde signal that enhances L-channel activity (Fig. 2, Fig2.avi).

The precise mechanism (chemical or mechanical) for the retrograde signal from RyR1 to the DHPR in skeletal muscle is still unclear. Feldmeyer et al. (1993) found that calcium release from the SR augments L-type calcium channel activity in frog skeletal muscle (56). However, the lack of SR calcium release in dyspedic myotubes is unlikely to account for the observed reduction in L-current magnitude since: 1) robust L-currents persist even under recording conditions (40 mM BAPTA and no ATP) in which voltage-gated calcium transients are abolished (57), 2) L-currents are augmented by

agents that inhibit SR calcium release and attenuated by agents that activate calcium release (58) in murine skeletal myotubes, and 3) retrograde coupling is restored following expression of RyR1 mutants that lack depolarization-induced SR calcium release (e.g. I4897T [59] or C4958S [K. G. Beam, personal communication]). Thus, in contrast to cardiac muscle, retrograde coupling in skeletal muscle involves a positive feedback signal that is not conveyed by calcium released from the SR. Rather, the mechanism of retrograde coupling in skeletal muscle is likely to involve an allosteric modulation of L-channel activity that results from the DHPR/RyR1 mechanical interaction that underlies orthograde coupling (50,55,57) (Fig. 2b, Fig2.avi).

There is considerable precedence for bi-directional coupling mediated by a mechanical interaction between two signaling partners. One needs only look at well-established paradigms for receptor/G-protein signaling for analogies with regard to how direct interactions between signaling partners result in bi-directional control of the

efficiency, fidelity, and functional activity of each molecule. For example, the binding of  $G\alpha_q$  to PLC- $\beta_1$  following agonist stimulation leads to both activation of PLC- $\beta_1$  and an increase in the intrinsic GTPase activity of  $G\alpha_q$  (60). Consequently, the catalytic activities of both PLC- $\beta_1$  and  $G\alpha_q$  are reciprocally controlled by a direct interaction between these two signaling proteins. In an analogous manner, the "catalytic activity" of skeletal muscle DHPRs and RyR1s (i.e. their ability to promote the movement of calcium ions from one compartment to another) may similarly be promoted by a physical interaction between the two proteins. One way in which such a mechanical interaction could promote DHPR calcium conductance is if RyR1 acts analogous to that of a conventional calcium channel accessory subunit that stabilizes global conformations of the L-channel that result in increased channel activity upon activation (50). For example,  $\beta$ -subunits augment calcium influx through activated L-channels by increasing L-channel surface expression (61,62), enhancing channel open probability (63,64), promoting the coupling between charge movements and channel opening (63), and by accelerating channel gating kinetics (62). The recent observations that RyR1 not only influences L-channel current magnitude (50,55), but also DHPR expression (50,53), activation kinetics, modulation by DHP agonists, and divalent conductance (50) supports the notion that RyR1 is an important allosteric modulator of the skeletal L-channel.

Although a direct DHPR/RyR1 physical interaction represents a parsimonious mechanism for both orthograde and retrograde coupling in skeletal muscle, other mechanisms for retrograde coupling in skeletal muscle have yet to be excluded. For example, mechanical DHPR/RyR1 coupling may depend on or be facilitated by an intermediary protein(s). Alternatively, the presence of RyR1 in the junction may produce a messenger other than calcium or alter the local chemical environment (e.g. redox state) in a manner that influences DHPR function. Finally, the expression of RyR1 proteins in the SR could conceivably promote  $\alpha_1$  association with accessory subunits (e.g.  $\beta_{1a}$ ), which serves to enhance L-channel open probability (55). Clearly, more work will be required before more definitive conclusions can be made with regard to the molecular mechanism of retrograde coupling in skeletal muscle.

### **Structural determinants of orthograde coupling in skeletal muscle**

Following a series of classic experiments conducted almost thirty years ago, Chandler and colleagues (7,65,66) proposed that charge movements associated with the t-tubule voltage sensor directly control calcium release from the SR via a mechanical linkage. Ever since this pioneering work, numerous laboratories have attempted to characterize the molecular determinants of this linkage. The identification of specific regions within the DHPR and RyR1 proteins that mediate orthograde and retrograde coupling is essential because such information would provide: 1) compelling confirmation for the mechanical coupling hypothesis, 2) insight into possible mechanisms of mechanical coupling between other surface

membrane and intracellular ion channels (e.g. store-operated  $Ca^{2+}$  channels and  $IP_3$  receptors), and 3) critical insight into how mutations within specific regions of the DHPR and RyR1 proteins results in altered EC coupling efficiency and muscle dysfunction (e.g. malignant hyperthermia and central core disease).

A major breakthrough in identifying the structural determinants of bi-directional coupling came 15 years ago with the cloning of the  $\alpha_1$ -subunit of the skeletal muscle DHPR by Tanabe et al. (1987) (67) and the observation by Beam et al. (1986) (68) that myotubes derived from dysgenic mice lack slowly-activating L-type calcium currents. Subsequent collaborations between these two groups lead to the demonstration that: 1) introduction of the skeletal muscle DHPR  $\alpha_1$ -subunit into dysgenic myotubes restores skeletal-type (calcium influx independent) EC coupling, slowly-activating L-currents (69), and intramembrane charge movements (41) 2) introduction of the cardiac muscle DHPR  $\alpha_1$ -subunit into dysgenic myotubes reconstitutes both cardiac-type (calcium influx-dependent) EC coupling and cardiac-like, rapidly-activating L-currents (70), and 3) a chimeric DHPR of cardiac origin except for skeletal sequence for the intracellular loop connecting the second and third transmembrane repeats (II-III loop) exhibits skeletal-type EC coupling and rapidly-activating L-currents (71). These results demonstrated that the intracellular II-III loop plays an obligatory role in orthograde coupling between the skeletal muscle DHPR to RyR1 and that difference in skeletal and cardiac L-channel activation kinetics is determined by the identity of the DHPR transmembrane repeats (72).

Subsequent work focused on narrowing down regions within the II-III loop of the skeletal muscle DHPR that are responsible for orthograde coupling. Chimeric dissection of the II-III loop and expression in dysgenic myotubes identified a minimal region in the middle of the II-III loop (CSk48; skeletal residues 725-742) that supported weak skeletal type EC coupling (i.e. calcium influx-independent calcium release was observed in some cases) (73). A slightly larger region of skeletal identity (CSk53; skeletal residues 720-765) produced strong skeletal type EC coupling (i.e. calcium influx-independent calcium release was observed in all cases) (73).

Investigations of the effects of synthetic peptides derived from regions of the DHPR II-III loop on RyR1 activity assessed using various *in vitro* approaches (e.g. [ $^3H$ ] ryanodine binding,  $^{45}Ca^{2+}$  flux measurements, open probability of RyR1 channels incorporated into planar lipid bilayers) have identified a different region of the II-III loop that activates RyR1. The series of studies conducted by Lu et al. (74,75) found that the N-terminal half of the skeletal muscle DHPR II-III loop specifically activates RyR1 activity. In a similar manner, the work of Ikemoto and colleagues identified an N-terminal portion of the skeletal muscle DHPR II-III loop (671-690, termed peptide A), but not the cardiac II-III loop, that strongly activates RyR1 as deduced from [ $^3H$ ] ryanodine binding and  $^{45}Ca^{2+}$  efflux assays in triad-enriched microsomes (76,77). Moreover, peptide A also activates single RyR1 channels incorporated into

planar lipid bilayers (78-80). Finally, the skeletal II-III loop strongly interacts with a 37 amino acid segment of RyR1, and this interaction is disrupted following replacement of K677 and K682 in peptide A with the corresponding residues found in the cardiac II-III loop (81).

Interestingly, a different II-III loop peptide (peptide C, residues 724-760), that roughly corresponds to the region of the II-III loop that supports strong skeletal-type EC coupling identified by Nakai et al. (1998), failed to activate RyR1 and antagonized peptide A activation of RyR1 (76,82). These observations led to the proposal that peptide C binds to and inhibits RyR1 activity at rest. According to this hypothesis, voltage-driven alterations in the voltage sensor might modify the conformation of the II-III loop in a manner that relieves peptide C inhibition of RyR1 and permits access of peptide A to its activation site on RyR1 (79,82,83). However, recent work conducted by several groups seriously calls into question the validity of this hypothesis. For example, according to this hypothesis the observation that expression of CSk53 (skeletal DHPR sequence only for residues 720-765) in dysgenic myotubes restores strong skeletal-type EC coupling could only be explained by cardiac sequence within the peptide A region being as efficient in activating RyR1 as skeletal sequence for peptide A; a result that was not observed in the *in vitro* experiments of El Hayek et al., (1998). Secondly, the magnitude and voltage dependence of skeletal EC coupling is unaltered following expression of DHPR constructs in which the peptide A sequence was either scrambled (84), deleted (85), or replaced by highly divergent II-III loop sequence obtained from the DHPR of the housefly, *Musca domestica* (86). In addition, Stange et al. (2001) demonstrated that a 46 amino acid peptide identical to that of the region of the II-III loop that supports strong orthograde coupling (720-765) and completely overlaps with the peptide C region, activates submaximally calcium-activated RyR1 channels, even under pseudo-physiological recording conditions (150 mM symmetrical KCl, 0 mV holding potential, and 10 mM luminal calcium as charge carrier) (80). Together, these results indicate that peptide A is not required for RyR1 activation in intact cells and suggest that under appropriate conditions the subregion of the II-III loop identified by Nakai et al. (1998) is sufficient to activate RyR1 during EC coupling.

The combined strengths of studies conducted on purified DHPR peptides in isolated systems and the expression of chimeric DHPRs in intact dysgenic myotubes clearly indicate that the intracellular II-III loop of the skeletal muscle DHPR plays an essential role in mediating orthograde coupling in skeletal muscle. Other regions of the skeletal muscle DHPR also influence the function and/or targeting of junctional DHPR and RyR1 proteins. For example, a series of reports from Coronado and colleagues have demonstrated that binding of the DHPR  $\beta_{1a}$ -subunit to the I-II intracellular loop of the  $\alpha_{15}$ -subunit is required for the proper targeting of the  $\alpha_{15}$ -subunit to the membrane (87,88) and that a 35-amino acid region of the C-terminus of  $\beta_{1a}$  facilitates voltage-gated SR calcium release either by promoting the interaction

between DHPR and RyR1 or by contributing to the orthograde signal that activates the release channel during depolarization (89). In addition, a region of the C-terminus of the  $\alpha_{15}$ -subunit (including amino acids 1607-1610) that is proximal to a putative truncation site mediates triad targeting of the skeletal muscle DHPR (36,90). Interestingly, this triad targeting domain resides immediately downstream of a region of the  $\alpha_{15}$ -subunit C-terminus that has been shown to interact strongly with a calmodulin binding domain in RyR1 (3609-3643) (91). However, a functional role for the interaction between the C-terminus of the  $\alpha_{15}$ -subunit and RyR1 has yet to be determined. Similarly, Leong and MacLennan (1998) reported that the III-IV linker of the  $\alpha_{15}$ -subunit of the DHPR interacts with a specific region of RyR1 (954-1112) (92), though the functional implications of this putative interaction remain unknown.

Much less information is available with regard to the regions of the RyR that mediate orthograde coupling. Functional expression of the cardiac isoform of the RyR (RyR2) in dysgenic myotubes restores neither orthograde nor retrograde coupling (93). Thus, specific regions within both the DHPR and RyR1 proteins encode bi-directional DHPR/RyR coupling in skeletal muscle. Expression of RyR1/RyR2 chimeras in dysgenic myotubes identified a region within RyR1 (R10; 1635-2636) that supports both orthograde (calcium influx-independent calcium release) and retrograde (robust slowly-activating calcium currents) coupling, while an adjacent region (R9; 2659-3720) of RyR1 supported only retrograde coupling (94). However, in a preliminary report, Protasi et al (2001) found that chimeras containing either the R9 region or a smaller region with R10 (R16; 1837-2154) were sufficient to restore weak skeletal-type EC coupling and DHPR tetrads following expression in 1B5 myotubes (a myogenic cell line that lacks RyR proteins) (95). These studies indicate that functional domains within RyRs may be comprised of residues derived from very different regions of the primary sequence that are brought together by appropriate protein folding of the tetramere (94,95). As a consequence, interpretations of data obtained using the chimeric approach applied to RyRs may not be as straightforward as has historically proven to be the case for DHPRs. Such limitations will provide exciting challenges for future work designed to more precisely determine essential structural domains within different RyR isoforms.

### **Structural determinants of retrograde coupling in skeletal muscle**

The identification of multiple regions within the skeletal muscle DHPR that potentially interact with RyR1 raises the question of whether or not the critical region within the DHPR II-III loop that is essential for transmitting an orthograde signal during EC coupling is also responsible for receiving a retrograde signal from RyR1. Grabner et al. (1999) addressed this question by expressing in dysgenic myotubes chimeric GFP-tagged DHPR constructs containing the entire (or portions of) the cardiac II-III loop in an otherwise skeletal DHPR background (57). Dysgenic myotubes expressing a skeletal DHPR with the entire cardiac II-III loop (SkLC)

exhibited large DHPR-mediated intramembrane charge movements but lacked voltage-gated SR calcium release and large slowly-activating L-currents. Thus, SkLC-expressing dysgenic myotubes were similar to dyspedic myotubes in that both orthograde and retrograde coupling were absent under both conditions. Substitution of the 46 amino acid segment of the skeletal muscle DHPR II-III loop shown by Nakai et al. (1998) to support strong orthograde coupling into SkLC (SkLCS<sub>46</sub>) was sufficient to restore both robust voltage-gated SR calcium release and slowly-activating L-current in the absence of a change in the magnitude of intramembrane charge movement ( $G_{max}/Q_{max}$  was 15 nS/pC and 39 nS/pC for the SkLC and SkLCS<sub>46</sub>, respectively; ref. 57). Interestingly, retrograde coupling was not restored by insertion of the smaller region of the II-III loop (725-742) identified by Nakai et al. (1998) to support weak orthograde coupling, suggesting the possibility that orthograde and retrograde coupling may not be strictly encoded a single motif within the II-III loop. Nevertheless, the critical role of the skeletal DHPR II-III loop in receiving the retrograde signal from RyR1 is reinforced by the observation that L-currents of cardiac DHPRs expressed in dysgenic myotubes are also enhanced by replacement of the II-III loop with sequence from the skeletal muscle DHPR ( $G_{max}/Q_{max}$  was 55 nS/pC and 157 nS/pC for the wild-type cardiac DHPR and CSk3, respectively; ref. 41). Although these results demonstrate that skeletal muscle II-III loop sequence is required for both orthograde and retrograde coupling with RyR1, contributions of other regions of the DHPR to retrograde coupling, particularly those that may be conserved between cardiac and skeletal muscle DHPRs, cannot be excluded.

As is the case with orthograde coupling, much less is known with regard to the regions of RyR1 that are critical for transmitting the retrograde signal to the DHPR. As discussed in Section 4.2, expression of RyR2 into dyspedic myotubes restores neither orthograde (calcium influx-independent calcium release) nor retrograde (enhanced skeletal muscle L-channel activity) coupling (93). In addition, experiments in which RyR1/RyR2 chimeras were expressed in dyspedic myotubes indicates that two separate regions within RyR1 (R10; 1635 – 2636 and R9; 2659 – 3720) are sufficient to support retrograde coupling (94) and a 318 amino acid subregion within R10 (R16; 1837 – 2154) is also sufficient to restore weak DHPR/RyR coupling (95). Since the R9, R10, and R16 regions of RyR1 are each capable of at least partially restoring DHPR channel activity, no single region within RyR1 is obligatorily required for retrograde coupling. Rather, the results to date suggest that two or more regions from different parts of the RyR1 primary sequence may come together in the folded protein to form an interaction domain for the critical region of the DHPR II-III loop (94,95).

#### BI-DIRECTIONAL CROSS-TALK IN NEURONS

The current state of knowledge regarding the functional role of bi-directional coupling between dihydropyridine receptors and ryanodine receptors in neuronal tissue is still in its infancy. However, many types of neurons express different isoforms of both

L-type calcium channels and ryanodine receptors. Calcium influx through neuronal L-channels is known to promote activity-dependent gene expression through recruitment of specific calcium-dependent transcription factors, such as CREB (96,97) and NF-Atc4 (98). Knockout mice that lack the gene for the ubiquitously expressed isoform of the ryanodine receptor (RyR3) exhibit enhanced long-term potentiation and spatial learning suggesting that neuronal ryanodine receptors may inhibit synaptic plasticity (99). Considering these observations, recent evidence demonstrating bi-directional chemical and mechanical coupling between DHPRs and RyRs in neurons (100-102) suggests that orthograde and retrograde DHPR/RyR signaling may regulate neuronal gene expression and/or synaptic plasticity.

### NG108-15 cells

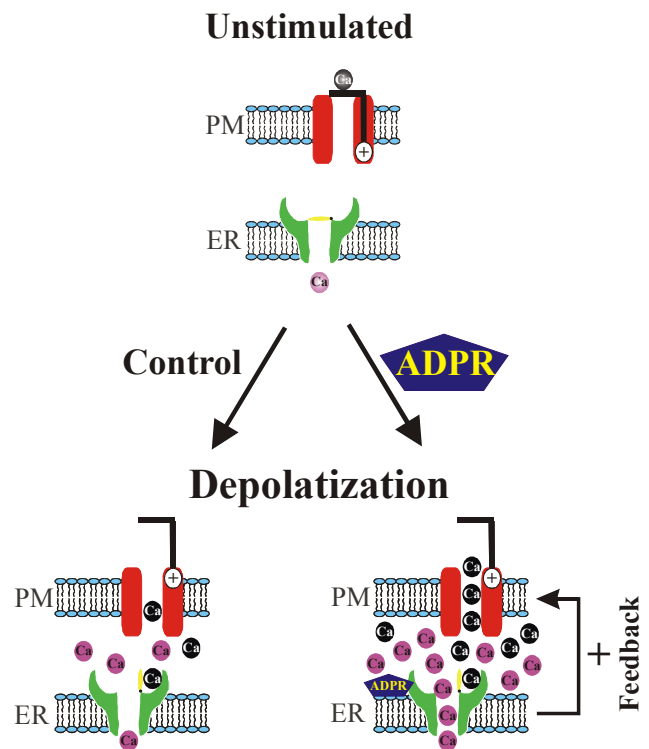


Figure 3: Bi-directional DHPR/RyR signaling in neuronal NG108-15 neuroblastoma x glioma hybrid cells. (Top) L-type calcium channel (red) and RyR (green) co-localization within NG108-15 cells results in the formation of a bi-directional calcium signaling microdomain that is modulated by cADPR. In unstimulated cells, significant calcium influx and calcium release from intracellular calcium stores does not occur. (Bottom Left) Depolarization that occurs in the absence of cADPR results in calcium influx through voltage-gated L-type calcium channels and minimal RyR-mediated calcium release (orthograde coupling). (Bottom Right) The presence of cADPR hypersensitizes RyR release channels such that depolarization-induced activation of the DHPR results in both calcium influx and a large increase in RyR-mediated calcium release (enhanced orthograde coupling). Enhanced calcium release through sensitized RyR channels induces greater calcium entry through voltage-gated L-type calcium channels (positive retrograde coupling) and additional CICR. The precise mechanistic nature (chemical and/or mechanical) of the bi-directional DHPR/RyR signaling interaction in NG108-15 cells is unclear, but does not appear to involve activation of a conventional capacitative calcium-entry pathway (101).

Hashii et al. (2001) reported that intracellular cyclic ADP-ribose (cADPR) amplifies bi-directional calcium signaling between RyRs and DHP-sensitive calcium channels in NG108-15 cells neuroblastoma x glioma hybrid cells (101). In this study, depolarization-induced calcium release through RyRs (DHPR-to-RyR or orthograde signaling) was larger in cADPR-dialyzed cells. This potentiation was mimicked by  $\beta$ -NAD<sup>+</sup> (a cADPR precursor), blocked by 8-bromo cADPR (a cADPR competitive antagonist), and antagonized by ryanodine and FK-506. In addition, Mn<sup>2+</sup> quench assays indicated that calcium influx through DHP-sensitive calcium channels were augmented in cADPR- and  $\beta$ -NAD<sup>+</sup>-dialyzed cells (positive RyR-to-DHPR or retrograde signaling). The increase in DHP-sensitive Mn<sup>2+</sup> influx was attributed to an effect of cADPR on RyRs rather than L-type calcium channels because the cADPR-induced enhancement in Mn<sup>2+</sup> influx was inhibited by pretreatment with either ryanodine or the immunosuppressant FK506. The authors concluded that cADPR modulates neuronal calcium signaling by amplifying the degree of bi-directional coupling between DHPRs and RyRs (101,102) (Fig. 3). It will be important for future work to confirm this hypothesis by more directly assessing the impact of cADPR on the magnitude, voltage-dependence, and kinetics of macroscopic L-type calcium currents (rather than Mn<sup>2+</sup> quench) in the presence and absence releasable calcium stores in patch clamped NG108-15 cells.

Although the results obtained from NG108-15 cells are provocative, several essential questions remain to be resolved. For example, while cADPR may sensitize neuronal RyRs to activation by calcium, it is unclear whether cADPR modifies RyR activity by directly binding to the RyR, binding to a RyR-associated accessory protein, or altering the content of intracellular calcium stores (102,103). In addition, the nature (chemical and/or mechanical) of the bi-directional signaling interaction controlled by cADPR has yet to be rigorously evaluated. While the orthograde signal in NG108-15 cells is likely to involve calcium influx through voltage-gated L-channels, the role of mechanical DHPR/RyR coupling cannot be ruled out since similar experiments conducted in the absence of extracellular calcium have yet to be reported. The retrograde (RyR-to-DHPR) signal could be mediated by calcium released through RyRs, a depletion-operated mechanism, or a direct (or indirect) mechanical interaction between the DHPR and RyR proteins (102). Interestingly, a tight functional, and ryanodine-sensitive signaling from RyRs-to-DHPRs (positive retrograde coupling), possibly arising from a direct physical interaction, has also been demonstrated in cerebellar granule cells (100). However, the relationship between bi-directional DHPR/RyR coupling in NG108-15 and cerebellar granule cells is unclear since dialysis with cADPR was not required for retrograde coupling in cerebellar granule cells.

## PERSPECTIVES

DHPRs or voltage-gated L-type calcium channels play pivotal roles in transducing extracellular stimuli into a variety of distinct cellular responses including muscle contraction, synaptic

plasticity, neurosecretion, and gene regulation. This review has focused on the subset of these processes that are orchestrated by bi-directional coupling between DHPRs and RyRs that occurs within unique signaling microdomains present in cardiac muscle, skeletal muscle, and neurons. These signaling microdomains involve regions of close apposition between cell surface membranes and specialized portions of the ER/SR. The mechanisms and molecular components that coordinate the specialized arrangement of DHPR/RyR signaling microdomains, and how they are differentially regulated in cardiac muscle, skeletal muscle, and neurons is still not understood (104). Continued work in identifying the constituents of these microdomains and the processes that underlie their formation may lead to approaches that enable the assembly of artificial bi-directional DHPR/RyR1 signaling microdomains within heterologous expression systems. Such a breakthrough would enable the development of more straightforward and systematic dissections of both the molecular determinants of bi-directional DHPR/RyR coupling and the mechanisms that underlie the assembly of specialized DHPR/RyR microdomains found in different types of excitable cells.

The degree to which a mechanism of bi-directional DHPR/RyR coupling originally defined within one system also applies to another system will likely represent another focus of future research. For example, an increase in cADPR levels and subsequent sensitization of RyR2 to activation by calcium following stimulation of cardiac  $\beta$ -adrenergic receptors has been suggested to contribute to enhanced SR calcium release during sympathetic stimulation (102). However, the putative role of cADPR in the modulation of RyR function in skeletal and cardiac muscle is controversial (105). Clearly, much work will be required in order to determine whether or not cADPR influences bi-directional chemical signaling between DHPRs and RyRs in cardiac muscle. Although CICR represents the dominant mechanism of SR calcium release in cardiac muscle, recent reports have suggested that a voltage-sensitive release mechanism may operate under certain conditions (cAMP, physiologic temperatures, negative membrane holding potentials) in cardiac muscle (106-108). Unlike CICR, the voltage-sensitive release mechanism is characterized by calcium release that is graded by membrane voltage rather than the magnitude of L-type calcium current (see for 109 review). Although certain properties of the voltage-sensitive release mechanism in cardiac muscle are similar to those observed in skeletal muscle, the molecular details that underlie the voltage-gated SR Ca<sup>2+</sup> release (e.g. a mechanical link between DHPRs and RyRs) are still unknown. Given the complex requirements for its activation and inherent technical difficulties in separating the voltage-sensitive release from CICR (110), the putative role of the voltage-sensitive release mechanism in regulating cardiac muscle contraction is still a very contentious and controversial topic. Nevertheless, if a voltage-sensitive release mechanism does operate under some conditions in cardiac muscle, it will be important to determine if bi-directional DHPR/RyR mechanical coupling regulates calcium conductance

through cardiac L-channels as has been documented in skeletal muscle.

Several key questions with regard to bi-directional DHPR/RyR coupling in skeletal muscle also remain unresolved. For example, is mechanical cross-talk in skeletal muscle mediated by a single, direct interaction between the DHPR and RyR1 or are other regions/proteins involved? What single channel properties (e.g. open probability, conductance behavior) of the skeletal L-channel are allosterically modulated by RyR1? How does a single critical domain in the DHPR II-III loop mediate both orthograde and retrograde coupling via distinct regions of the RyR1 primary sequence? Given that calcium influx through L-channels is not required for skeletal-type EC coupling (5,6), what is the functional role of retrograde coupling in skeletal muscle? These and other questions are likely to provide substantial motivation for future work in defining the determinants and physiological roles of bi-directional coupling between DHPRs and RyRs in excitable cells.

#### ACKNOWLEDGEMENTS

I would like to thank Dr. Kurt G. Beam for his insightful comments and suggestions on this review, our many provocative discussions regarding bi-directional coupling over the years, as well as his continued support. I also thank Ms. K.M.S. O'Connell and Dr. G. Avila for helpful discussions and comments on this review. This work was supported by grants to Robert Dirksen from the National Institutes of Health (AR 44657), a Neuromuscular Disease Research Grant from the Muscular Dystrophy Association, and a Grant-In-Aid from the American Heart Association, New York State Affiliate (00550884T).

#### References

1. Fabiato A: Simulated calcium current can both cause calcium loading in and trigger calcium release from the sarcoplasmic reticulum of a skinned canine cardiac Purkinje cell. *J. Gen. Physiol.* 85, 291-320, (1985)
2. Nabauer M, G. Callewaert, L. Cleemann & M. Morad: Regulation of calcium release is gated by calcium current, not gating charge, in cardiac myocytes. *Science* 244, 800-803, (1989)
3. Beuckelmann D J & W.G. Wier: Mechanism of release of calcium from sarcoplasmic reticulum of guinea-pig cardiac cells. *J. Physiol.* 405, 233-255, (1988)
4. Fabiato A: Rapid ionic modifications during the aequorin-detected calcium transient in a skinned canine cardiac Purkinje cell. *J. Gen. Physiol.* 85, 189-246, (1985)
5. Dirksen R T & K.G. Beam: Role of calcium permeation in dihydropyridine receptor function. Insights into channel gating and excitation-contraction coupling. *J. Gen. Physiol.* 114, 393-403, (1999)
6. Armstrong C M, F.M. Bezanilla & P. Horowicz: Twitches in the presence of ethylene glycol bis(2-aminoethyl ether)-N,N'-tetracetic acid. *Biochimica et Biophysica Acta* 267, 605-608, (1972)
7. Chandler W K, R.F. Rakowski & M.F. Schneider: Effects of glycerol treatment and maintained depolarization on charge movement in skeletal muscle. *J. Physiol.* 254, 285-316, (1976)
8. Rios E & G. Pizarro: Voltage sensor of excitation-contraction coupling in skeletal muscle. *Physiological Reviews* 71, 849-908, (1991)
9. Melzer W, A. Herrmann-Frank & H.C. Luttgau: The role of Ca<sup>2+</sup> ions in excitation-contraction coupling of skeletal muscle fibres. *Biochimica et Biophysica Acta* 1241, 59-116, (1995)
10. Nakai J, R.T. Dirksen, H.T. Nguyen, I.N. Pessah, K.G. Beam & P.D. Allen: Enhanced dihydropyridine receptor channel activity in the presence of ryanodine receptor. *Nature* 380, 72-75, (1996)
11. Fabiato A: Time and calcium dependence of activation and inactivation of calcium-induced release of calcium from the sarcoplasmic reticulum of a skinned canine cardiac Purkinje cell. *J. Gen. Physiol.* 85, 247-289, (1985)
12. Cheng H, W.J. Lederer & M.B. Cannell: Calcium sparks: elementary events underlying excitation-contraction coupling in heart muscle. *Science* 262, 740-744, (1993)
13. Wang S Q, L.S. Song, E.G. Lakatta & H. Cheng: Ca<sup>2+</sup> signalling between single L-type Ca<sup>2+</sup> channels and ryanodine receptors in heart cells. *Nature* 410, 592-596, (2001)
14. Meissner G, E. Darling & J. Eveleth: Kinetics of rapid Ca<sup>2+</sup> release by sarcoplasmic reticulum. Effects of Ca<sup>2+</sup>, Mg<sup>2+</sup>, and adenine nucleotides. *Biochemistry* 25, 236-244, (1986)
15. Zorzato F, J. Fujii, K. Otsu, M. Phillips, N.M. Green, F.A. Lai, G. Meissner & D.H. MacLennan: Molecular cloning of cDNA encoding human and rabbit forms of the Ca<sup>2+</sup> release channel (ryanodine receptor) of skeletal muscle sarcoplasmic reticulum. *J. Biol. Chem.* 265, 2244-2256, (1990)
16. Chen S R, K. Ebisawa, X. Li & L. Zhang: Molecular identification of the ryanodine receptor Ca<sup>2+</sup> sensor. *J. Biol. Chem.* 273, 14675-14678, (1998)
17. Li P & S.R. Chen: Molecular basis of Ca(2+) activation of the mouse cardiac Ca(2+) release channel (ryanodine receptor). *J. Gen. Physiol.* 118, 33-44, (2001)
18. O'Brien J J, P.D. Allen, K.G. Beam & S.R. Chen: Effects of mutation E4032A on the function of RyR1 expressed in HEK293 cells and in dyspedic myotubes. *Biophys. J.* 76, A302, (1999)
19. Du G G & D.H. MacLennan: Functional consequences of mutations of conserved, polar amino acids in transmembrane sequences of the Ca<sup>2+</sup> release channel (ryanodine receptor) of rabbit skeletal muscle sarcoplasmic reticulum. *J. Biol. Chem.* 273, 31867-31872, (1998)
20. Fessenden J D, L. Chen, Y. Wang, C. Paolini, C. Franzini-Armstrong, P.D. Allen & I.N. Pessah: Ryanodine receptor point mutant E4032A reveals an allosteric interaction with ryanodine. *Proc. Natl. Acad. Sci. USA* 98, 2865-2870, (2001)
21. Brehm P & R. Eckert: Calcium entry leads to inactivation of calcium channel in *Paramecium*. *Science* 202, 1203-1206, (1978)
22. Kass R S & M.C. Sanguinetti: Inactivation of calcium channel current in the calf cardiac Purkinje fiber. Evidence for voltage- and calcium-mediated mechanisms. *J. Gen. Physiol.* 84, 705-726, (1984)
23. Lee K S, E. Marban & R.W. Tsien: Inactivation of calcium channels in mammalian heart cells: joint dependence on membrane potential and intracellular calcium. *J. Physiol.* 364, 395-411, (1985)
24. Chad J E & R. Eckert: An enzymatic mechanism for calcium current inactivation in dialysed *Helix* neurones. *J. Physiol.* 378, 31-51, (1986)
25. Sham J S, L. Cleemann & M. Morad: Functional coupling of Ca<sup>2+</sup> channels and ryanodine receptors in cardiac myocytes. *Proc. Natl. Acad. Sci. USA* 92, 121-125, (1995)
26. Adachi-Akahane S, L. Cleemann & M. Morad: Calcium cross-signaling between DHP and ryanodine receptors in cardiomyocytes. *Heart and Vessels* 9, 163-166, (1995)
27. Adachi-Akahane S, L. Cleemann & M. Morad: Cross-signaling between L-type Ca<sup>2+</sup> channels and ryanodine receptors in rat ventricular myocytes. *J. Gen. Physiol.* 108, 435-454, (1996)
28. Sham J S, L. Cleemann & M. Morad: Functional coupling of Ca<sup>2+</sup> channels and ryanodine receptors in cardiac myocytes. *Proc. Natl. Acad. Sci. USA* 92, 121-125, (1995)
29. Peterson B Z, C.D. DeMaria, J.P. Adelman & D.T. Yue: Calmodulin is the Ca<sup>2+</sup> sensor for Ca<sup>2+</sup>-dependent inactivation of L-type calcium channels. *Neuron* 22, 549-558, (1999)
30. Zuhlke R D, G.S. Pitt, K. Deisseroth, R.W. Tsien & H. Reuter: Calmodulin supports both inactivation and

- facilitation of L-type calcium channels. *Nature* 399, 159-162, (1999)
31. Zuhlke R D, G.S. Pitt , R.W. Tsien & H. Reuter: Ca<sup>2+</sup>-sensitive inactivation and facilitation of L-type Ca<sup>2+</sup> channels both depend on specific amino acid residues in a consensus calmodulin-binding motif in the(α)1C subunit. *J. Biol. Chem.* 275, 21121-21129, (2000)
  32. Pate P, J. Buneca-Morales, Y. Wu, J.Z. Zhang, G.G. Rodney, I.I. Serysheva, B.Y. Williams, M.E. Anderson & S.L. Hamilton: Determinants for calmodulin binding on voltage-dependent Ca<sup>2+</sup> channels. *J. Biol. Chem.* 275, 39786-39792, (2000)
  33. Flucher B E, N. Kasielke, U. Gerster, B. Neuhuber & M. Grabner: Insertion of the full-length calcium channel α(1S) subunit into triads of skeletal muscle in vitro. *FEBS Lett.* 474, 93-98, (2000)
  34. Gao T, M. Bunemann, B.L. Gerhardstein, H. Ma & M.M. Hosey: Role of the C terminus of the α 1C (CaV1.2) subunit in membrane targeting of cardiac L-type calcium channels. *J. Biol. Chem.*275, 25436-25444, (2000)
  35. Kepplinger K J, H. Kahr, G. Forstner, M. Sonnleitner, H. Schindler, T. Schmidt, K. Groschner, N.M. Soldatov & C. Romanin: A sequence in the carboxy-terminus of the α(1C) subunit important for targeting, conductance and open probability of L-type Ca(2+) channels. *FEBS Lett.*477, 161-169, (2000)
  36. Proenza C, C. Wilkens , N.M. Lorenzon & K.G. Beam: A carboxyl-terminal region important for the expression and targeting of the skeletal muscle dihydropyridine receptor. *J. Biol. Chem.*275, 23169-23174, (2000)
  37. Imredy J P & D.T. Yue: Mechanism of Ca(2+)-sensitive inactivation of L-type Ca<sup>2+</sup> channels. *Neuron* 12, 1301-1318, (1994)
  38. Sharma V K, V. Ramesh , C. Franzini-Armstrong & S.-S. Sheu: Transport of Ca<sup>2+</sup> from Sarcoplasmic Reticulum to Mitochondria in Rat Ventricular Myocytes. *J. Bioenergetics and Biomembranes* 32, 97-104, (2000)
  39. Sanchez J A, M.C. Garcia, V.K. Sharma, K.C. Young, M.A. Matlib & S.S. Sheu: Mitochondria regulate inactivation of L-type Ca(2+) channels in rat heart. *J. Physiol.*536, 387-396, (2001)
  40. Garcia J & K.G. Beam: Measurement of calcium transients and slow calcium current in myotubes. *J. Gen. Physiol.* 103, 107-123, (1994)
  41. Adams B A, T. Tanabe, A. Mikami, S. Numa & K.G. Beam: Intramembrane charge movement restored in dysgenic skeletal muscle by injection of dihydropyridine receptor cDNAs. *Nature* 346, 569-572, (1990)
  42. Garcia J, T. Tanabe & K.G. Beam: Relationship of calcium transients to calcium currents and charge movements in myotubes expressing skeletal and cardiac dihydropyridine receptors. *J. Gen. Physiol.* 103, 125-147, (1994)
  43. Sculptoreanu A, T. Scheuer & W.A. Catterall: Voltage-dependent potentiation of L-type Ca<sup>2+</sup> channels due to phosphorylation by cAMP-dependent protein kinase. *Nature* 364, 240-243, (1993)
  44. Shainberg A, S.A. Cohen & P.G. Nelson: Induction of acetylcholine receptors in muscle cultures. *Pflugers Archiv* 361, 255-261, (1976)
  45. Klarsfeld A & J.P. Changeux: Activity regulates the levels of acetylcholine receptor alpha-subunit mRNA in cultured chicken myotubes. *Proc. Natl. Acad. Sci. USA* 82, 4558-4562, (1985)
  46. Rotzler S, H. Schramek & H.R. Brenner: Metabolic stabilization of endplate acetylcholine receptors regulated by Ca<sup>2+</sup> influx associated with muscle activity. *Nature* 349, 337-339, (1991)
  47. Melzer W, A. Herrmann-Frank & H.C. Luttgau: The role of Ca<sup>2+</sup> ions in excitation-contraction coupling of skeletal muscle fibres. *Biochimica et Biophysica Acta* 1241, 59-116, (1995)
  48. Pizarro G, L. Csernoch, I. Uribe, M. Rodriguez & E. Rios: The relationship between Q gamma and Ca release from the sarcoplasmic reticulum in skeletal muscle. *J. Gen. Physiol.* 97, 913-947, (1991)
  49. Block B A, T. Imagawa , K.P. Campbell & C. Franzini-Armstrong: Structural evidence for direct interaction between the molecular components of the transverse tubule/sarcoplasmic reticulum junction in skeletal muscle. *J. Cell Biol.* 107, 2587-2600, (1988)
  50. Avila G & R.T. Dirksen: Functional impact of the ryanodine receptor on the skeletal muscle L-type Ca(2+) channel. *J. Gen. Physiol.*115, 467-480, (2000)
  51. Buck E D, H.T. Nguyen , I.N. Pessah & P.D. Allen: Dyspedic mouse skeletal muscle expresses major elements of the triadic junction but lacks detectable ryanodine receptor protein and function. *J. Biol. Chem.* 272, 7360-7367, (1997)
  52. Fleig A, H. Takeshima & R. Penner: Absence of Ca<sup>2+</sup> current facilitation in skeletal muscle of transgenic mice lacking the type 1 ryanodine receptor. *J.Physiol.* 496, 339-345, (1996)
  53. Avila G, K.M. O'Connell, L.A. Groom & R.T. Dirksen: Ca<sup>2+</sup> release through ryanodine receptors regulates skeletal muscle L-type Ca<sup>2+</sup> channel expression. *J. Biol. Chem.*276, 17732-17738, (2001)
  54. Takekura H, M. Nishi, T. Noda, H. Takeshima & C. Franzini-Armstrong: Abnormal junctions between surface membrane and sarcoplasmic reticulum in skeletal muscle with a mutation targeted to the ryanodine receptor. *Proc. Natl. Acad. Sci. USA* 92, 3381-3385, (1995)
  55. Nakai J, R.T. Dirksen , H.T. Nguyen, I.N. Pessah, K.G. Beam & P.D. Allen: Enhanced dihydropyridine receptor channel activity in the presence of ryanodine receptor. *Nature* 380, 72-75, (1996)
  56. Feldmeyer D, W. Melzer, B. Pohl & P. Zollner: A possible role of sarcoplasmic Ca<sup>2+</sup> release in modulating the slow Ca<sup>2+</sup> current of skeletal muscle. *Pflugers Archiv* 425, 54-61, (1993)
  57. Grabner M, R.T. Dirksen, N. Suda & K.G. Beam: The II-III loop of the skeletal muscle dihydropyridine receptor is responsible for the Bi-directional coupling with the ryanodine receptor. *J. Biol. Chem.* 274, 21913-21919, (1999)
  58. Balog E M & E.M. Gallant: Modulation of the sarcolemmal L-type current by alteration in SR Ca<sup>2+</sup> release. *Am. J.Physiol.* 276, C128-C135(1999)
  59. Avila G, J.J. O'Brien & R.T. Dirksen: Excitation-contraction uncoupling by a human central core disease mutation in the ryanodine receptor. *Proc. Natl. Acad. Sci. U S A* 98, 4215-4220, (2001)
  60. Berstein G, J.L. Blank, D.Y. Jhon, J.H. Exton, S.G. Rhee & E.M. Ross: Phospholipase C-beta 1 is a GTPase-activating protein for Gq/11, its physiologic regulator. *Cell* 70, 411-418, (1992)
  61. Lacerda A E, H.S. Kim , P. Ruth, E. Perez-Reyes, V. Flockerzi, F. Hofmann, L. Birnbaumer & A.M. Brown: Normalization of current kinetics by interaction between the alpha 1 and beta subunits of the skeletal muscle dihydropyridine-sensitive Ca<sup>2+</sup> channel. *Nature* 352, 527-530, (1991)
  62. Singer D, M. Biel, I. Lotan, V. Flockerzi, F. Hofmann & N. Dascal: The roles of the subunits in the function of the calcium channel. *Science* 253, 1553-1557, (1991)
  63. Neely A, X. Wei, R. Olcese, L. Birnbaumer & E. Stefani: Potentiation by the beta subunit of the ratio of the ionic current to the charge movement in the cardiac calcium channel. *Science* 262, 575-578, (1993)
  64. Shistik E, T. Ivanina , T. Puri, M. Hosey & N. Dascal: Ca<sup>2+</sup> current enhancement by alpha 2/delta and beta subunits in Xenopus oocytes: contribution of changes in channel gating and alpha 1 protein level. *J. Physiol.* 489, 55-62, (1995)
  65. Chandler W K, R.F. Rakowski & M.F. Schneider: A non-linear voltage dependent charge movement in frog skeletal muscle. *J. Physiol.* 254, 245-283, (1976)
  66. Schneider M F & W.K. Chandler: Voltage dependent charge movement of skeletal muscle: a possible step in excitation-contraction coupling. *Nature* 242, 244-246, (1973)
  67. Tanabe T, H. Takeshima, A. Mikami, V. Flockerzi, H. Takahashi, K. Kangawa, M. Kojima, H. Matsuo, T. Hirose & S. Numa: Primary structure of the receptor for calcium channel blockers from skeletal muscle. *Nature* 328, 313-318, (1987)
  68. Beam K G, C.M. Knudson & J.A. Powell: A lethal mutation in mice eliminates the slow calcium current in skeletal muscle cells. *Nature* 320, 168-170, (1986)

69. Tanabe T, K.G. Beam, J.A. Powell & S. Numa: Restoration of excitation-contraction coupling and slow calcium current in dysgenic muscle by dihydropyridine receptor complementary DNA. *Nature* 336, 134-139, (1988)
70. Tanabe T, A. Mikami, S. Numa & K.G. Beam: Cardiac-type excitation-contraction coupling in dysgenic skeletal muscle injected with cardiac dihydropyridine receptor cDNA. *Nature* 344, 451-453, (1990)
71. Tanabe T, K.G. Beam, B.A. Adams, T. Niidome & S. Numa: Regions of the skeletal muscle dihydropyridine receptor critical for excitation-contraction coupling. *Nature* 346, 567-569, (1990)
72. Tanabe T, B.A. Adams, S. Numa & K.G. Beam: Repeat I of the dihydropyridine receptor is critical in determining calcium channel activation kinetics. *Nature* 352, 800-803, (1991)
73. Nakai J, T. Tanabe, T. Konno, B. Adams & K.G. Beam: Localization in the II-III loop of the dihydropyridine receptor of a sequence critical for excitation-contraction coupling. *J. Biol.Chem.*273, 24983-24986, (1998)
74. Lu X, L. Xu & G. Meissner: Activation of the skeletal muscle calcium release channel by a cytoplasmic loop of the dihydropyridine receptor. *J. Biol. Chem.* 269, 6511-6516, (1994)
75. Lu X, L. Xu & G. Meissner: Phosphorylation of dihydropyridine receptor II-III loop peptide regulates skeletal muscle calcium release channel function. Evidence for an essential role of the beta-OH group of Ser687. *J. Biol. Chem.* 270, 18459-18464, (1995)
76. el-Hayek R, B. Antoniu, J. Wang, S.L. Hamilton & N. Ikemoto: Identification of calcium release-triggering and blocking regions of the II-III loop of the skeletal muscle dihydropyridine receptor. *J. Biol. Chem.* 270, 22116-22118, (1995)
77. el-Hayek R & N. Ikemoto: Identification of the minimum essential region in the II-III loop of the dihydropyridine receptor alpha 1 subunit required for activation of skeletal muscle-type excitation-contraction coupling. *Biochemistry* 37, 7015-7020, (1998)
78. Dulhunty A F, D.R. Laver, E.M. Gallant, M.G. Casarotto, S.M. Pace & S. Curtis: Activation and inhibition of skeletal RyR channels by a part of the skeletal DHPR II-III loop: effects of DHPR Ser687 and FKBP12. *Biophys. J.* 77, 189-203, (1999)
79. Gurrola G B, C. Arevalo, R. Sreekumar, A.J. Lokuta, J.W. Walker & H.H. Valdivia: Activation of ryanodine receptors by imperatoxin A and a peptide segment of the II-III loop of the dihydropyridine receptor. *J.Biol. Chem.*274, 7879-7886, (1999)
80. Stange M, A. Tripathy & G. Meissner: Two domains in dihydropyridine receptor activate the skeletal muscle Ca<sup>2+</sup> release channel. *Biophys. J.*81, 1419-1429, (2001)
81. Leong P & D.H. MacLennan: A 37-amino acid sequence in the skeletal muscle ryanodine receptor interacts with the cytoplasmic loop between domains II and III in the skeletal muscle dihydropyridine receptor. *J. Biol.Chem.*273, 7791-7794, (1998)
82. Saiki Y, R. el-Hayek & N. Ikemoto: Involvement of the Glu724-Pro760 region of the dihydropyridine receptor II-III loop in skeletal muscle-type excitation-contraction coupling. *J. Biol. Chem.* 274, 7825-7832, (1999)
83. Ikemoto N & R. el-Hayek: Signal transmission and transduction in excitation-contraction coupling. *Advances in Experimental Medicine & Biology* 453, 199-207, (1998)
84. Proenza C, C.M. Wilkens & K.G. Beam: Excitation-contraction coupling is not affected by scrambled sequence in residues 681-690 of the dihydropyridine receptor II-III loop. *J. Biol. Chem.* 275, 29935-29937, (2000)
85. Ahern C A, J. Arikath, P. Vallejo, C.A. Gurnett , P.A. Powers, K.P. Campbell & R. Coronado: Intramembrane charge movements and excitation-contraction coupling expressed by two-domain fragments of the Ca<sup>2+</sup> channel. *Proc. Natl. Acad. Sci.USA* 98, 6935-6940, (2001)
86. Wilkens C M, N. Kasielke, B.E. Flucher, K.G. Beam & M. Grabner: Excitation-contraction coupling is unaffected by drastic alteration of the sequence surrounding residues L720-L764 of the alpha 1S II-III loop. *Proc. Natl. Acad. Sci.USA*98, 5892-5897, (2001)
87. Strube C, M. Beurg, P.A. Powers, R.G. Gregg & R. Coronado: Reduced Ca<sup>2+</sup> current, charge movement, and absence of Ca<sup>2+</sup> transients in skeletal muscle deficient in dihydropyridine receptor beta 1 subunit. *Biophys. J.* 71, 2531-2543, (1996)
88. Strube C, M. Beurg, M. Sukhareva, C.A. Ahern, J.A. Powell, P.A. Powers, R.G. Gregg & R. Coronado: Molecular origin of the L-type Ca<sup>2+</sup> current of skeletal muscle myotubes selectively deficient in dihydropyridine receptor beta1a subunit. *Biophys. J.* 75, 207-217, (1998)
89. Beurg M, C.A. Ahern, P. Vallejo, M.W. Conklin, P.A. Powers, R.G. Gregg & R. Coronado: Involvement of the carboxy-terminus region of the dihydropyridine receptor beta1a subunit in excitation-contraction coupling of skeletal muscle. *Biophys. J.* 77, 2953-2967, (1999)
90. Flucher B E, N. Kasielke & M. Grabner: The triad targeting signal of the skeletal muscle calcium channel is localized in the COOH terminus of the alpha(1S) subunit. *J. Cell Biol.*151, 467-478, (2000)
91. Sencer S, R.V. Papineni, D.B. Halling, P. Pate, J. Krol, J.Z. Zhang & S.L. Hamilton: Coupling of RYR1 and L-type Calcium Channels via Calmodulin Binding Domains. *J. Biol Chem.*276, 38237-38241, (2001)
92. Leong P & D.H. MacLennan: The cytoplasmic loops between domains II and III and domains III and IV in the skeletal muscle dihydropyridine receptor bind to a contiguous site in the skeletal muscle ryanodine receptor. *J.Biol.Chem.* 273, 29958-29964, (1998)
93. Nakai J, T. Ogura, F. Protasi, C. Franzini-Armstrong, P.D. Allen & K.G. Beam: Functional nonequality of the cardiac and skeletal ryanodine receptors. *Proc. Natl. Acad. Sci. USA* 94, 1019-1022, (1997)
94. Nakai J, N. Sekiguchi , T.A. Rando, P.D. Allen & K.G. Beam: Two regions of the ryanodine receptor involved in coupling with L-type Ca<sup>2+</sup> channels. *J.Biol.Chem.*273, 13403-13406, (1998)
95. Protasi F, J. Nakai, K.G.Beam, H. Takekura, C. Franzini-Armstrong, & P.D. Allen: Two independent regions of RyR1 (1837-2154 and 2659-3720) restore skeletal type E-C coupling and DHPR junctional tetrads. *Biophys. J.* 80, 330a (2001)
96. Deisseroth K, E.K. Heist & R.W. Tsien: Translocation of calmodulin to the nucleus supports CREB phosphorylation in hippocampal neurons. *Nature* 392, 198-202, (1998)
97. Mermelstein P G, H. Bito, K. Deisseroth & R.W. Tsien: Critical dependence of cAMP response element-binding protein phosphorylation on L-type calcium channels supports a selective response to EPSPs in preference to action potentials. *J. Neurosci.*20, 266-273, (2000)
98. Graef I A, P.G. Mermelstein, K. Stankunas, J.R. Neilson, K. Deisseroth, R.W. Tsien & G.R. Crabtree: L-type calcium channels and GSK-3 regulate the activity of NF-ATc4 in hippocampal neurons. *Nature* 401, 703-708, (1999)
99. Futatsugi A, K. Kato, H. Ogura, S.T. Li, E. Nagata, G. Kuwajima, K. Tanaka, S. Itohara & K. Mikoshiba: Facilitation of NMDAR-independent LTP and spatial learning in mutant mice lacking ryanodine receptor type 3. *Neuron* 24, 701-713, (1999)
100. Chavis P, L. Fagni, J.B. Lansman & J. Bockaert: Functional coupling between ryanodine receptors and L-type calcium channels in neurons. *Nature* 382, 719-722, (1996)
101. Hashii M, Y. Minabe & H. Higashida: cADP-ribose potentiates cytosolic Ca<sup>2+</sup> elevation and Ca<sup>2+</sup> entry via L-type voltage-activated Ca<sup>2+</sup> channels in NG108-15 neuronal cells. *Biochem. J.*207-215, (2000)
102. Higashida H, M. Hashii, S. Yokoyama, N. Hoshi, X. Chen, A. Egorova, M. Noda & J. Zhang: Cyclic ADP-ribose as a second messenger revisited from a new aspect of signal transduction from receptors to ADP-ribosyl cyclase. *Pharmacol. Ther.* 90, 283-296, (2001)
103. Lukyanenko V, I. Gyorke, T.F. Wiesner & S. Gyorke: Potentiation of Ca(2+) release by cADP-ribose in the heart is mediated by enhanced SR Ca(2+) uptake into

- the sarcoplasmic reticulum. *Circ. Res.* 89, 614-622, (2001)
104. Flucher B E & C. Franzini-Armstrong: Formation of junctions involved in excitation-contraction coupling in skeletal and cardiac muscle. *Proc. Natl. Acad. Sci. USA* 93, 8101-8106, (1996)
  105. Copello J A, Y. Qi, L.H. Jeyakumar, E. Ogunbunmi & S. Fleischer: Lack of effect of cADP-ribose and NAADP on the activity of skeletal muscle and heart ryanodine receptors. *Cell Calcium* 30, 269-284, (2001)
  106. Ferrier G R & S.E. Howlett: Contractions in guinea-pig ventricular myocytes triggered by a calcium-release mechanism separate from Na<sup>+</sup> and L-currents. *J. Physiol.* 484, 107-122, (1995)
  107. Hobai I A, F.C. Howarth, V.K. Pabbathi, G.R. Dalton, J.C. Hancox, J.Q. Zhu, S.E. Howlett, G.R. Ferrier & A.J. Levi: "Voltage-activated Ca release" in rabbit, rat and guinea-pig cardiac myocytes, and modulation by internal cAMP. *Pflugers Archiv* 435, 164-173, (1997)
  108. Howlett S E, J.Q. Zhu & G.R. Ferrier: Contribution of a voltage-sensitive calcium release mechanism to contraction in cardiac ventricular myocytes. *Am. J. Physiol.* 274, H155-H170 (1998)
  109. Ferrier G R & S.E. Howlett: Cardiac excitation-contraction coupling: role of membrane potential in regulation of contraction. *Am. J. Physiol.* 280, H1928-H1944(2001)
  110. Piacentino V, K. Diplà, J.P. Gaughan & S.R. Houser: Voltage-dependent Ca<sup>2+</sup> release from the SR of feline ventricular myocytes is explained by Ca<sup>2+</sup>-induced Ca<sup>2+</sup> release. *J. Physiol.* 523, 533-548, (2000)

# Integrative Analysis of Calcium Signalling in Cardiac Muscle

A.W. Trafford, M.E. Díaz, S.C. O'Neill & D.A. Eisner.

Unit of Cardiac Physiology, The University of Manchester, 1.524 Stopford Building, Oxford Rd, Manchester M13 9PT, U.K. Email address: [eisner@man.ac.uk](mailto:eisner@man.ac.uk)

**ABSTRACT** This review discusses the control of the amplitude of the cardiac systolic Ca transient. The Ca transient arises largely from release from the sarcoplasmic reticulum (SR). Release is triggered by calcium-induced calcium release (CICR) whereby the entry of a small amount of Ca on the L-type Ca current, "the trigger", results in the release of much more Ca from the SR. There are three potential control points: (1) the Ca content of the SR; (2) the properties of the SR Ca release channel or ryanodine receptor (RyR); (3) the amplitude of the L-type Ca current. The data reviewed show that the Ca content of the SR has pronounced effects on systolic  $[Ca^{2+}]_i$  and, reciprocally, the amount of Ca released from the SR affects sarcolemmal Ca fluxes thereby "autoregulating" SR content. Modulation of the ryanodine receptor has no steady-state effect due to compensating changes of SR Ca content. An increase of the L-type Ca current results in an abrupt increase of systolic  $[Ca^{2+}]_i$  with little change of SR content. This is because of a coordinated increase of both the trigger and loading function of the Ca current. These results emphasise the importance of considering all aspects of Ca handling in the context of SR Ca release and thus the regulation of the systolic Ca transient and contraction in cardiac muscle.

## Overview of excitation contraction coupling

The other contributions in this volume deal largely with specific aspects of the Ca release process from the sarcoplasmic reticulum (SR). It is, however, important to note that the Ca release process is but one of many steps involved in Ca handling in cardiac cells. The function of this article is to integrate all these steps and show that, when considering the consequences of altering any one step (such as SR Ca release via the ryanodine receptor) effects of the other steps must also be considered.

The consensus scheme of excitation-contraction coupling (illustrated in Fig. 1A) is that of calcium-induced calcium release (CICR) in which the entry of Ca ions through the surface L-type Ca channel produces a small "trigger" increase of calcium concentration ( $[Ca^{2+}]_i$ ). This increase of  $[Ca^{2+}]_i$  increases the probability that the sarcoplasmic reticulum (SR) Ca release channels or ryanodine receptors (RyR) are open. The increased opening of the RyRs results in efflux of Ca from the SR. Thus a small trigger entry of  $Ca^{2+}$  through the L-type channel is amplified by a larger release of  $Ca^{2+}$  from the SR. The "gain" of this amplification can be up to a factor of 10 [1,2]

It should be obvious that if the heart is to work effectively as a pump then this systolic rise of  $[Ca^{2+}]_i$  must be returned to control levels on each beat. There are two major routes to do this. (1) Calcium can be pumped back out of the cell largely via the Na-Ca exchange (for reviews see [3])[4] with a smaller contribution from the plasma membrane Ca-ATPase (PMCA) [5-7]. (2) Calcium can be taken back into the SR via the SR Ca-ATPase (SERCA). The coordination of all these processes is required to produce the normal Ca transient and contraction shown in Fig. 1B.

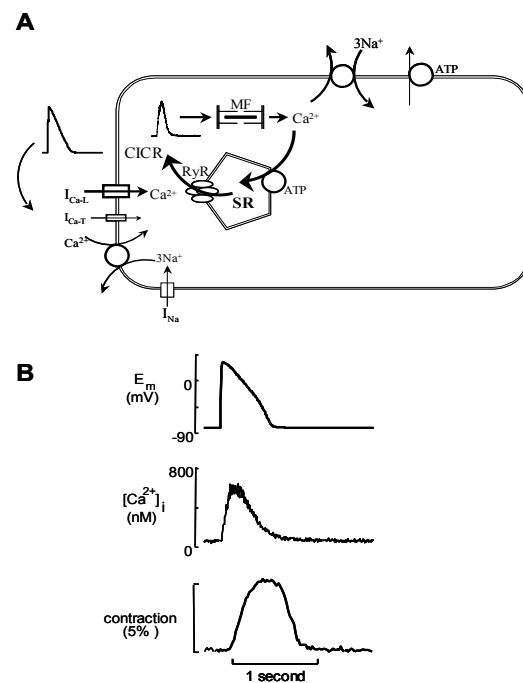


Fig. 1. **A.** Schematic diagram of the processes involved in excitation-contraction coupling. The action potential activates Ca entry via the L-type Ca current. The resulting "trigger" increase of  $[Ca^{2+}]_i$  then opens the SR Ca release channels (RyR). This released Ca activated the myofibrils (MF) resulting in contraction. For relaxation to occur Ca is removed from the cytoplasm. This occurs mainly via the SR Ca-ATPase (SERCA) and also by the sarcolemmal Na-Ca exchange with a small contribution from the sarcolemmal Ca-ATPase. **B.** Cellular measurements obtained from a single cardiac myocyte showing the relationship between the action potential (top), the systolic Ca transient (middle) and contraction (bottom).

## Control Points

On this scheme for CICR, there are at least three potential points at which the amplitude of the systolic Ca transient can be regulated. (1). The amount of Ca entering the cell via the L-type Ca current; (2) the properties of the RyR; (3) the Ca content of the SR. In the remainder of this review we will show that, contrary to what has often been suggested, the RyR (2) is not a site for controlling the amplitude of the systolic Ca transient. Rather, coordinated control of 1 and 3 seem to be used by the cell.

## Steady state Ca flux balance

As discussed above, there are two sources and sinks for calcium: the extracellular fluid and the SR. One would therefore expect that, in the steady state, on each beat exactly that amount of Ca which enters the cell from the extracellular fluid will be pumped back out of the cell and that amount which is released from the SR will be resequenced by the SR. If this condition did not hold then, inevitably, there would be a net gain or loss of Ca from the SR. An experimental demonstration of this steady state condition is shown in Fig. 2. The top trace shows the Ca transient produced by a voltage clamp depolarisation. The middle trace shows the accompanying membrane current.

On depolarisation, Ca enters via the L-type Ca current. The bottom trace shows the integral of this current demonstrating that about 4  $\mu\text{mol}$  of Ca enter per l cell. On repolarization there is an inward Na-Ca exchange current that is more evident in the amplified record. Again this can be integrated and, assuming that the Na-Ca exchange transports 3  $\text{Na}^+$  per  $\text{Ca}^{2+}$  then the amount of Ca transported by the exchange can be calculated. Another correction must be made for the fact that the electroneutral sarcolemmal Ca-ATPase also transports Ca. With these corrections, the Ca efflux from the cell can be calculated [8]. As shown by the integral, the Ca efflux exactly balances Ca entry. This therefore provides experimental evidence for the maintenance of Ca flux balance. As will be shown later in this article, the need for the cell to maintain Ca flux balance has profound implications for our understanding of cellular Ca handling.

## CONTROL OF SR CA CONTENT AND IMPLICATIONS FOR THE REGULATION OF E-C COUPLING

SERCA is stimulated by an increase of cytoplasmic Ca and inhibited by an increase of luminal Ca [9]. In addition to this regulation by Ca concentration, there is a powerful effect of the inhibitory accessory protein phospholamban. Phosphorylation of phospholamban removes this inhibition and stimulates SERCA activity [10,11]. This is partly responsible for the acceleration of the decay of the Ca transient on beta stimulation [12,13]. Similarly, mice which have no phospholamban ("knock out" animals) have faster decaying Ca transients than controls and a smaller response to catecholamines

[14,15]. Importantly they also have greater SR Ca contents than control [16].

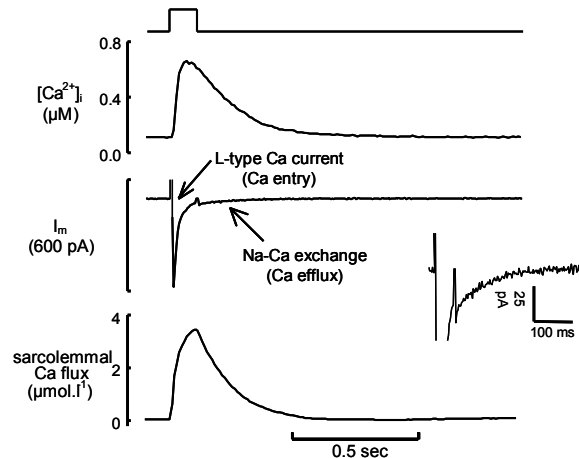


Fig. 2. Equality of Ca influx and efflux in the steady state. A rat ventricular myocyte was stimulated with a 100 ms duration depolarizing pulse from  $-40$  to  $0$  mV. The top trace shows  $[\text{Ca}^{2+}]_i$ ; the middle membrane current and the bottom the integrated Ca fluxes. The inset shows an expanded version of the current on repolarization making it easier to see the Na-Ca exchange current.

## Autoregulation of sarcolemmal Ca fluxes and SR content

As mentioned above, SERCA activity is controlled, in part, by  $[\text{Ca}^{2+}]_i$ . This will include the levels of  $[\text{Ca}^{2+}]_i$  throughout the entire cardiac cycle. A further complexity is provided by the fact that sarcolemmal Ca fluxes are affected by Ca release from the SR and thence by SR Ca content. This arises because an increase of systolic  $[\text{Ca}^{2+}]_i$  increases Ca efflux on Na-Ca exchange [17] and decreases Ca entry on the L-type Ca current [18-20].

The interactions between these phenomena are shown in Fig. 3 [8]. Before the record began the SR had been emptied of Ca by the application of 10 mM caffeine. Stimulation initially resulted in very small Ca transients (Fig. 3A) because the SR was depleted. However, with time the Ca transient increased in amplitude. Specimen membrane currents are shown in Fig. 3B. In the steady state (trace *b*) the integrated current records show that Ca influx and efflux are equal. However a very different result is seen for the first transient (trace *a*). On this pulse, the Ca current inactivates more slowly than in the steady state (see Fig. 3C, left) resulting in a greater calculated Ca entry. In contrast the Ca efflux (see Fig. 3C, right) is less than in control. The second panel of Fig. 3A shows the calculated Ca entry and efflux on each pulse. It is clear that entry is initially greater than efflux but, with time, entry decreases and exit increases until the two are in balance. This change in the balance between influx and efflux is emphasised in the third panel of Fig. 3A. Finally the bottom panel shows the cumulative calculated Ca gain. In this particular experiment, the cell (and presumably therefore the SR), gains 80  $\mu\text{mol}$  Ca per litre cell.

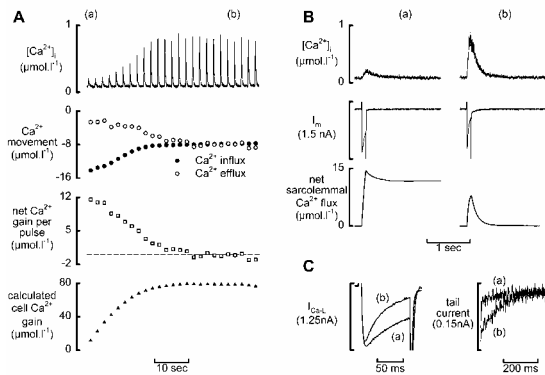


Fig. 3. Interactions between SR Ca content and sarcolemmal Ca fluxes. A. Changes associated with refilling the SR. Before the record began the SR had been emptied by exposure to 10 mM caffeine. Following caffeine removal, the cell was stimulated with 100 ms duration pulses from  $-40$  to  $0$  mV. Panels show (top to bottom):  $[Ca^{2+}]_i$ , calculated sarcolemmal fluxes – influx is from the L-type Ca current and efflux from Na-Ca exchange (note that larger fluxes are downward); net Ca gain per pulse calculated as influx – efflux; cumulative Ca gain. B. Specimen records obtained from the pulses (a & b) indicated on A. Traces show (top to bottom):  $[Ca^{2+}]_i$ ; current; calculated fluxes. C Expanded records of (left) Ca current, (right) Na-Ca exchange tail current. Data modified from [8]

The effects of SR Ca release on sarcolemmal fluxes are important in controlling SR Ca content. Consider what happens if SR Ca content increases. This will result in an increase of Ca release from the SR, leading to an increase of Ca efflux from the cell and decrease of Ca influx, thereby decreasing SR Ca content. The steeper the dependence of sarcolemmal Ca fluxes on SR content, the more tightly controlled will be SR Ca content. It should, however, be noted that, as is the case for other feedback systems, excessive gain can result in instability. Thus, if the dependence of sarcolemmal fluxes on SR Ca is very steep, an increase of SR content may result in such a large effect on sarcolemmal fluxes that content decreases to a very low level at which the resulting small Ca transient results in a net cellular gain of Ca and thence an increased SR content. If this persists, alternation in the amplitude of the Ca transient and SR content would be expected [21].

### The effect of SR Ca content on Ca release

Experiments such as that described in Fig. 3 also provide information about the dependence of SR Ca release on content. As shown in Fig. 4, the relationship is very steep [22,23].

At least 4 factors may contribute to this steepness. (1) The greater the SR Ca concentration, the larger the driving force for Ca efflux. If the intra-SR buffers tend to saturate then a given increase of total SR content will result in a larger fractional change of free SR Ca. (2) Increased Ca efflux will result in increased activation of adjacent RyRs [23,24]. (3) An increase of  $[Ca^{2+}]_i$  on the

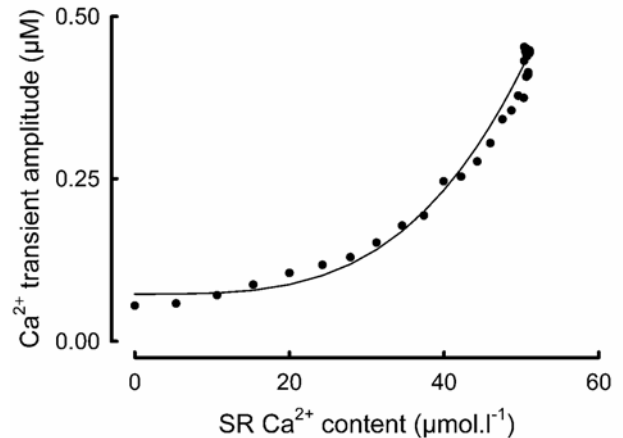


Fig. 4. The relationship between the amplitude of the systolic Ca transient and the SR Ca content. Data were obtained from an experiment similar to that of Fig. 3. The points are the original data, the curve a best fit to:  $Ca \text{ transient} = a \cdot (SR \text{ Ca})^n$  where  $n = 3.4$ .

luminal face of the SR increases the open probability of the RyR [25-27]. In this context, increased SR content results in increased frequency of Ca sparks [28-30]. (4) Finally, a tendency towards saturation of *cytoplasmic* Ca buffers would mean that, as  $[Ca^{2+}]_i$  increases, a given further increase of total Ca will produce a larger fractional change of  $[Ca^{2+}]_i$ .

### SR Ca content and contraction – an overview

The work described above shows that an intrinsic “autoregulation” mechanism allows the SR Ca content to modify sarcolemmal Ca fluxes and thereby control the SR content. This mechanism can be compared with the phenomenon of capacitative control of Ca entry which occurs in many other cell types. On this mechanism, a decrease of endoplasmic reticulum Ca content increases Ca influx into the cell through store operated Ca channels (for reviews see [31,32]). The control by SR Ca release of Na-Ca exchange and the L-type Ca current serves a similar function in the heart.

The previous discussion might make it seem that the SR Ca content could be a major site for modifying cardiac contraction. Indeed, over a certain range, experimental manoeuvres that increase SR Ca content do increase contraction [33-36]. However, there are few measurements of SR content under physiologically relevant conditions. Furthermore, there is a limit to the extent to which SR Ca content can be increased. If the cell is overloaded with Ca then spontaneous release of this Ca occurs in the form of propagating waves of Ca release [37-39]. The tendency for such Ca release to occur limits the usefulness of SR Ca as a regulator of contractility. It is therefore important to consider now the effects of other control points.

## MODULATION OF THE RYR

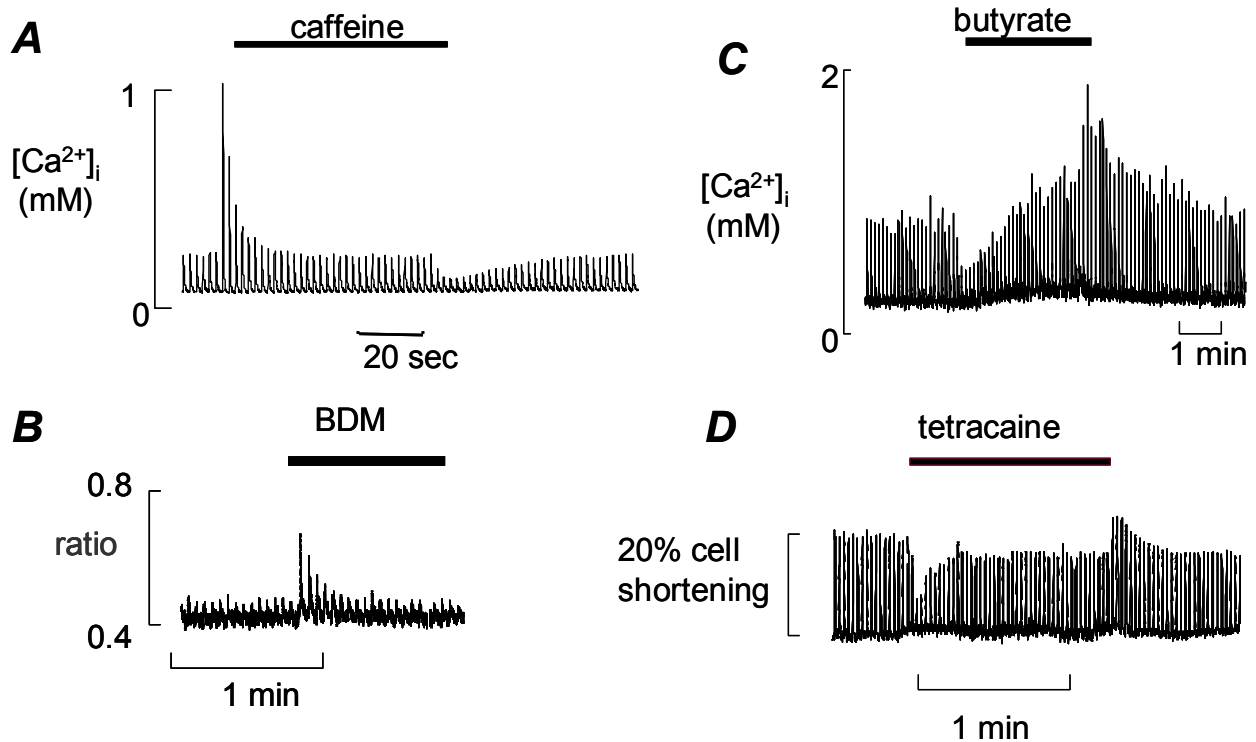


Fig. 5. The effects of modifiers of RyR function on systolic  $[Ca^{2+}]_i$ . The panels show the effects of: A. caffeine (0.5 mM); B. BDM (butanedione monoxime), 5 mM; C. butyrate (30 mM at constant external pH); D. tetracaine (100  $\mu$ M).

In this section we will consider the effects of modifying either the numbers or the properties of the RyRs. We do this in the context of suggestions that changes in these parameters may contribute to the depressed Ca transient seen in heart failure [40-43]. In addition decreased coupling between the L-type Ca current and the RyR has also been suggested to contribute to failure [44-46]. It has also been reported that cyclic ADP Ribose may be a natural regulator of contractility via its effects on regulating the RyR [47-50]

Many substances affect the properties of the RyR and these effects can be most simply studied by measuring the currents through isolated RyRs (for reviews see [51,52]). We have investigated the effects of four such substances on systolic Ca. These are caffeine and 2,3-butanedione monoxime (BDM) which increase the open probability of the isolated RyR [53,54] and tetracaine and intracellular acidification which decrease it [55-57]. The effects of applying these agents are shown in Fig. 5. It can be seen that although both caffeine (A) and BDM (B) produce an increase of the systolic Ca transient, this increase is only transient with the amplitude of the transient declining towards control in a few beats [58-60]. Likewise acid (C) and tetracaine (D) decrease the amplitude of the transient in a purely transient manner [61,62].

An explanation of these transient effects is presented in Fig. 6. Fig 6Aa shows that caffeine produces a transient increase of systolic  $[Ca^{2+}]_i$ . In the steady state in caffeine the amplitude of the systolic transient is identical to that in control [59]. Specimen  $[Ca^{2+}]_i$  and current records from (i) control and (ii) the first response in caffeine are presented in Fig. 6B. As shown in Fig. 2, in control Ca influx is equal to Ca efflux. In contrast the Na-Ca exchange current is larger for transient (ii) than in the control. This effect, which is presumably due to greater activation by the elevated systolic  $[Ca^{2+}]_i$  means that the Ca efflux is now greater than the influx (6Bc). Fig. 6Ab shows the net sarcolemmal Ca flux as a function of time. In control there is no net Ca flux. When caffeine is applied, the larger Ca transient results in net Ca efflux and this changes to no net Ca flux as the amplitude of the Ca transient declines. On removal of caffeine there is a calculated net Ca influx as the smaller Ca transient results in less Ca efflux. Fig. 6Ac shows the calculated SR Ca content. The upper envelope of this record gives the SR Ca content before Ca release. It is clear that this is predicted to decrease during caffeine application. The lower envelope was calculated by calculating the amount of Ca released from the SR (see [59,63]).

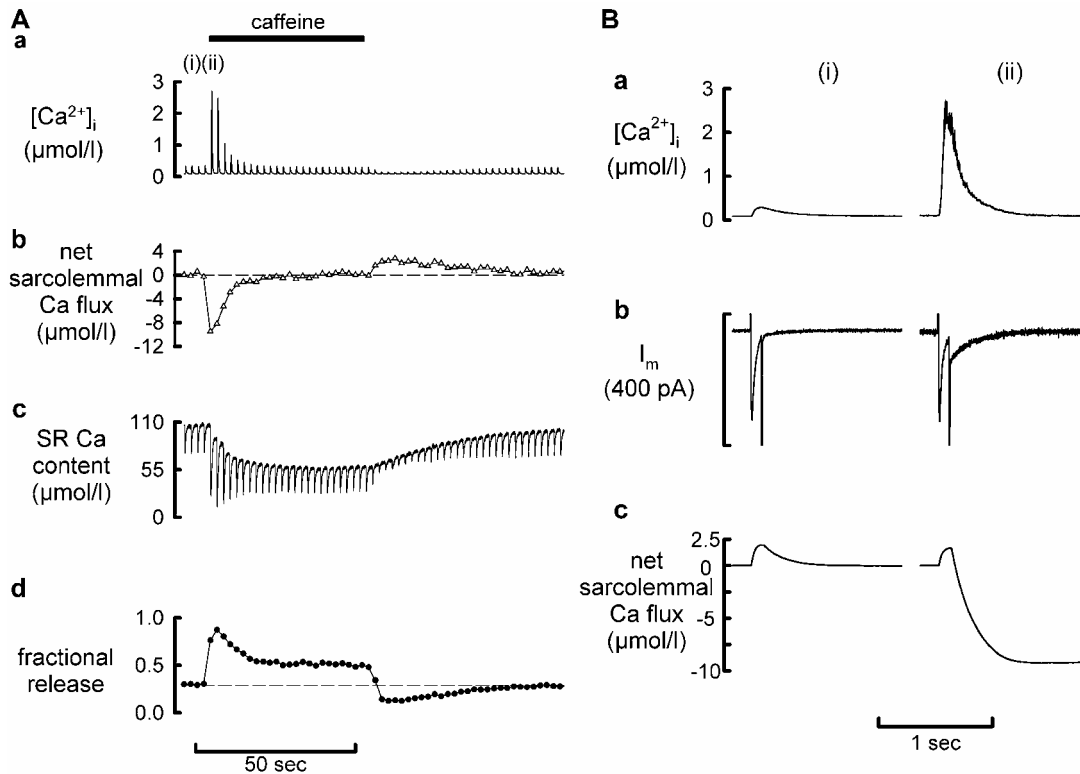


Fig. 6. Measurements of sarcolemmal fluxes and SR  $Ca^{2+}$  release during potentiation of CICR by low concentrations of caffeine. A. Time course. traces show (from top to bottom): a,  $[Ca^{2+}]_i$ ; b, net sarcolemmal flux (influx - efflux); c, time course of changes of SR Ca content; d, fraction of SR Ca released per pulse. The cell was held at  $-40$  mV and 100 ms duration depolarizing pulses applied to 0 mV. B. Specimen records from the control transient (i) and the first in caffeine (ii). Traces show (from top to bottom):  $[Ca^{2+}]_i$ ; membrane current; net sarcolemmal flux.

These data demonstrate, therefore, that the secondary fall of systolic  $[Ca^{2+}]_i$  in caffeine is due to a decrease of SR Ca content. In caffeine, a potentiated RyR in combination with a decreased SR Ca content results in a transient of the same amplitude as the control. The fact that the amplitude of the transient in the steady state in caffeine is identical to that in control can be understood as follows. In the steady state Ca influx must equal efflux. So long as the manoeuvre being considered does not affect Ca influx then this condition requires that the Ca efflux in the steady state in caffeine be the same as in control. If we assume that the properties of Na-Ca exchange are not affected then the requirement for a constant Ca efflux means that the amplitude of the Ca transient must be constant. It can therefore be seen that manoeuvres which affect only the RyR will have no effect on the amplitude of the systolic Ca transient, rather they will affect the SR content. It should, however, be noted that the above analysis will not hold if the efflux of Ca from the SR during diastole is affected. For example high concentrations of caffeine make the SR release Ca even in the absence of stimulation thereby depleting it of Ca and greatly decreasing the amplitude of the transient [64,65]. This circumstance may also occur in heart failure where it has been reported that the RyR is

hyperphosphorylated and therefore leaky to  $[Ca^{2+}]_i$ ; thereby resulting in a depleted SR [66].

The above argument is difficult to reconcile with the fact that some agents which affect the RyR (e.g. phosphorylation) have maintained effects on the amplitude of the systolic Ca transient. This dichotomy can be resolved if the agent has other cellular targets as well as the RyR. For example the ability of cyclic ADP Ribose to increase the amplitude of the Ca transient has recently been suggested to result from stimulation of SERCA resulting in increased SR Ca content [67].

#### REGULATION OF THE CA TRANSIENT BY CA ENTRY INTO THE CELL

One of the earliest studies of cardiac contraction showed that external Ca was required for the heart to contract [68]. Since then, much work has found that an increase of the L-type Ca current increases the systolic Ca transient and contraction [69-71]. There are three possible explanations for this. (1) Increased Ca influx directly activates the contractile machinery. Although this may make a small contribution, the fact that most of the Ca which activates contraction comes from the SR argues against this being the major factor.

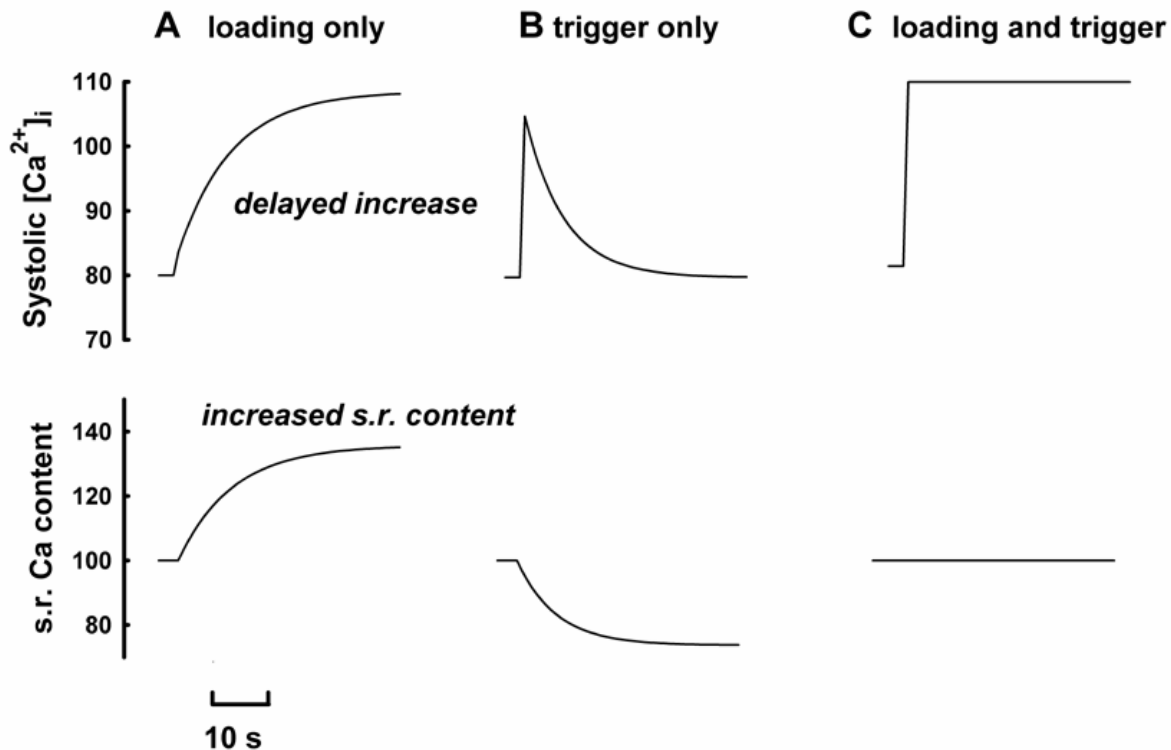


Fig. 7. Simulation of the effects of increasing either or both of the loading or the trigger function of the L-type Ca current. The top shows the amplitude of the calculated systolic Ca transient and the bottom trace the SR content. A. The effects of increasing the loading function of the Ca current. B. The effects of increasing the trigger function; C. The effects of increasing trigger and loading. Reproduced from [73]

(2) An increase of Ca influx will increase the trigger releasing Ca from the SR and (3) the increase of Ca influx will increase the Ca content of the SR and thence the amount released. These latter two roles of the Ca current ("trigger" and "load") in excitation-contraction coupling have been identified previously [72]. Our recent work has examined which of the two dominates in the inotropic response to increased sarcolemmal Ca current.

Figure 7 is a simple computer model of the effects of increasing Ca entry into the cell [74]. Fig. 7A shows the effects of only considering the loading property of the Ca current to be increased. In this case there is a gradual increase of the calculated SR Ca content because the Ca entry is greater than the Ca efflux. This results in an increase of the Ca transient as a result of which there is an increase in Ca efflux until a new steady state is reached where Ca entry and efflux are in balance, again, at a higher level. Therefore an increase of the Ca loading function, alone, would result in a positive inotropic effect. However this would be delayed in onset and would occur in conjunction with an increased SR Ca content. Fig. 7B shows the effect of considering only the trigger function of the Ca current. This produces

an immediate increase of the Ca transient. However, as the Ca efflux is now greater than the entry, this will result in a decrease of SR Ca and the amplitude of the Ca transient will decrease to basal levels. In other words the predicted response of increasing only the trigger function is identical to that of low concentrations of caffeine and is not expected to produce a maintained inotropic response. In the real case presumably both the loading and the trigger functions are increased and the expected response will be a combination of those seen in A and B. In Fig. 7C the parameters were adjusted such that there is no change of SR Ca content. This can be seen to be accompanied by an abrupt and maintained increase of the Ca transient.

#### **Coordinated trigger and load effects of increased L-type Ca current**

The above model indicates the variety of responses predicted to accompany an increase in the L-type Ca current. Figure 8 presents an experimental test to identify which, if any, of these actually occur. In this experiment the amplitude of the L-type

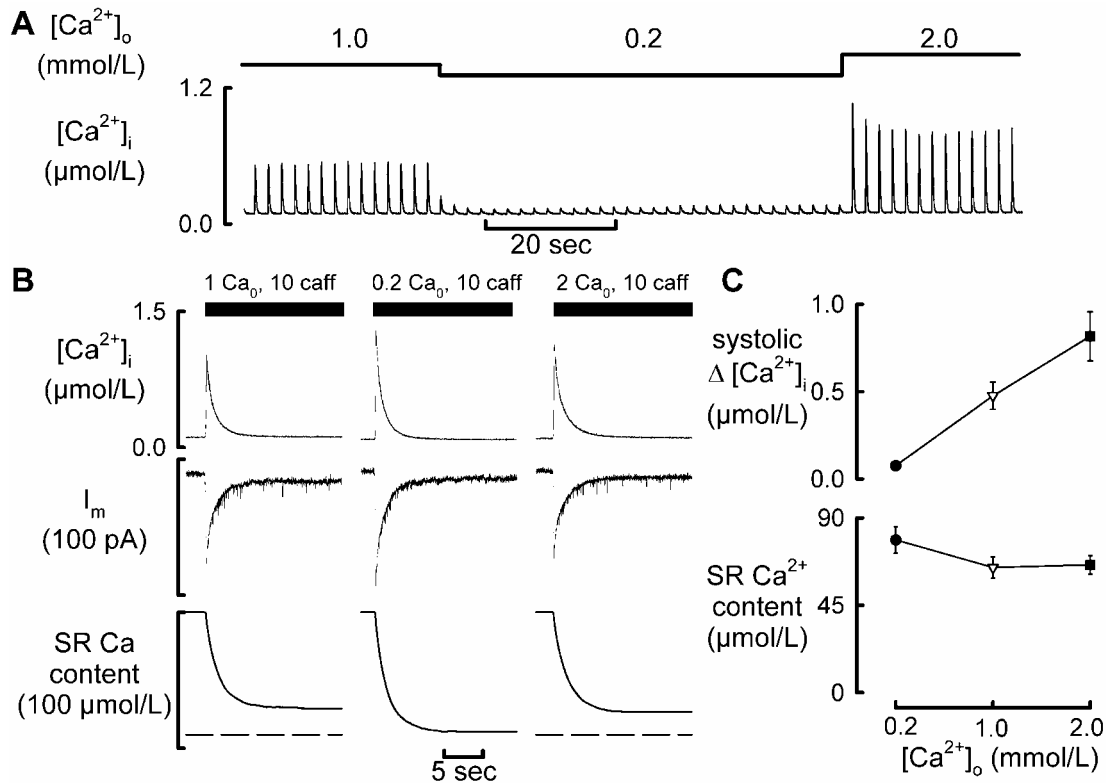


Fig. 8 Changing Ca entry has a large effect on systolic  $[Ca^{2+}]_i$  but little on SR content. A. Timecourse of change of systolic  $[Ca^{2+}]_i$  in response to the indicated changes of external Ca concentration. B. SR Ca content following exposure to the indicated external Ca. In each panel 10 mM caffeine was applied to activate SR Ca release and the resulting electrogenic Na-Ca exchange used as an index of SR content. C. Mean data showing the dependence of: top, SR Ca content; bottom, systolic  $[Ca^{2+}]_i$  on external Ca concentration. Taken from [75].

Ca current was altered by changing external Ca concentration ( $[Ca^{2+}]_o$ ). Fig. 8A confirms that lowering  $[Ca^{2+}]_o$  from 1 to 0.2 mM decreases the systolic Ca transient whereas an increase to 2 mM increases  $[Ca^{2+}]_i$ . The records of Fig. 8B show corresponding measurements of SR Ca content. The SR content is the same in 1 and 2 mM  $[Ca^{2+}]_o$  but is slightly *increased* in 0.2 mM. The mean data of Fig 8C reveal that the amplitude of the systolic Ca transient is a linear function of  $[Ca^{2+}]_o$ . In contrast there is a much smaller change of SR content and, indeed, SR content increases at the lowest  $[Ca^{2+}]_o$ . To a first approximation, SR content is independent of  $[Ca^{2+}]_o$ . In other words the real cell behaves rather like the simulation of Fig. 7C where an increase of Ca entry results in balanced effects on Ca entry and loading. This means that both the trigger and the loading functions of the Ca current increase by the same relative amount as  $[Ca^{2+}]_o$  is increased. This behaviour is required if the observed rapid and more or less maintained increase of the amplitude of the Ca transient is to be produced.

The importance of the coordinated changes of trigger and load is shown in Fig. 9. This compares two inotropic manoeuvres. (1) The recovery from

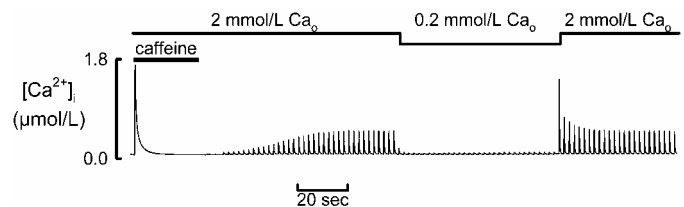


Fig. 9. Comparison of the timecourse of the inotropic effects resulting from store refilling with those due to increased Ca current. In the record caffeine (10 mM) was initially applied to empty the SR. On removal of caffeine, the resulting recovery of the amplitude of the systolic Ca transient is much slower than that due to increased Ca current produced by raising external Ca concentration. Modified from [75]

an emptied SR. At the start of the record caffeine was applied to empty the SR. After removal of caffeine the empty SR results in a very small Ca transient. It then takes several beats for the control Ca transient to be reached; the slowness of the response being determined by sarcolemmal fluxes. (2) The second manoeuvre is the recovery from a reduction of  $[Ca^{2+}]_o$ . This is almost instantaneous and the speed of this response is due to the fact that there is no change of SR content.

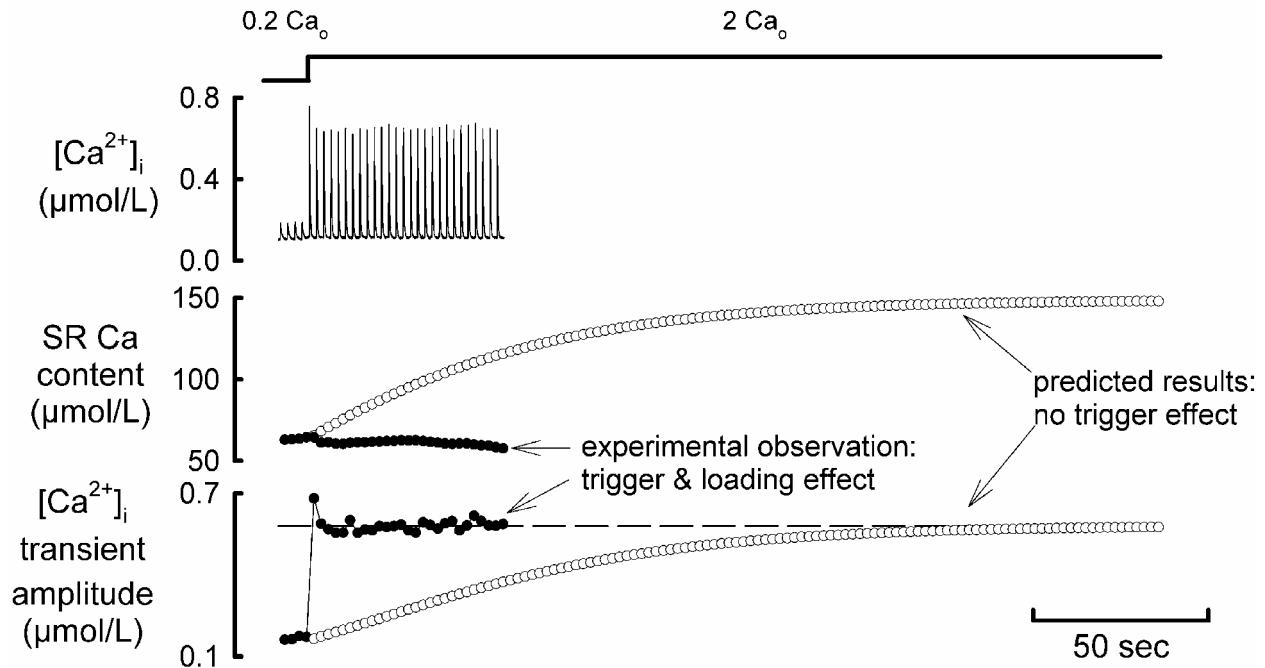


Fig. 10. Comparison of the effects of increasing external Ca concentration with the effects expected if only the loading effect was present. External Ca concentration was increased from 0.2 to 2 mM for the period shown. The top trace shows the experimental record of  $[Ca^{2+}]_i$ . The solid symbols show the measured amplitude of systolic  $[Ca^{2+}]_i$  and the calculated SR content. The open circles show the calculated results if there was no trigger effect. Modified from [75]

Fig. 10 considers what would happen if there was no change of loading. The experimental records show the timecourse of Ca transient (top) on increasing  $[Ca^{2+}]_o$ . Again, a rapid response is observed. The open circles show a simulation of what would happen if raising external Ca only increased the loading function of the Ca current. This would increase the SR Ca content and thence the Ca transient. The observed amplitude of the Ca transient could only be achieved with more than a doubling of SR content and after a considerable delay. The importance of the coordination of trigger and loading is clear from these data.

Close inspection of the data shows that the response of systolic Ca to an increase of  $[Ca^{2+}]_o$  has a slight overshoot. There is also a small decrease of SR content (Fig. 8). This presumably means that changing  $[Ca^{2+}]_o$  over the range 0.2 to 1 mM has a slightly greater effect on the trigger than on the loading function. Nevertheless, to a first approximation, the overshoot and decrease of SR content are small and do not detract from the above conclusions.

Finally, it is worth noting that the design of Ca induced Ca release means that one process, the L-type Ca current, provides not only the trigger for Ca release but also the load which maintains the SR content. As we have seen above, this dual role for one channel is important in controlling the SR Ca content and thence contraction.

## CONCLUSIONS

Work considered in the review emphasises the need to consider interactions between various Ca handling mechanisms. This should inform, not only consideration of normal excitation-contraction coupling but also those brought about by various inotropic manoeuvres or disease states e.g. in heart failure.

## ACKNOWLEDGEMENTS

Work from the authors laboratory was supported by grants from the British Heart Foundation and the Wellcome Trust

## References

1. Wier WG, TM Egan, JR López-López, CW Balke. Local control of excitation-contraction coupling in rat heart cells. *J Physiol (Lond)*. 474,463-471 (1994)
2. Sipido KR, WG Wier. Flux of  $Ca^{2+}$  across the sarcoplasmic reticulum of guinea-pig cardiac cells during excitation-contraction coupling. *J Physiol (Lond)*. 435,605-630 (1991)
3. Blaustein MP, WJ Lederer. Sodium/calcium exchange: its physiological implications. *Physiol Rev*. 79,763-854 (1999)
4. Philipson KD, DA Nicoll. Sodium-calcium exchange: a molecular perspective. *Ann Rev Physiol*. 62,111-133 (2000)
5. Negretti N, SC O'Neill, DA Eisner. The relative contributions of different intracellular and sarcolemmal systems to relaxation in rat ventricular myocytes. *Cardiovasc Res*. 27,1826-1830 (1993)
6. Bassani JWM, RA Bassani, DM Bers. Relaxation in rabbit and rat cardiac cells: species-dependant differences in cellular mechanisms. *J Physiol (Lond)*. 476,279-293 (1994)
7. Choi HS, DA Eisner. The role of the sarcolemmal Ca-ATPase in the regulation of resting calcium concentration

- in rat ventricular myocytes. *J Physiol (Lond)*. 515,109-118 (1999)
8. Trafford AW, ME Díaz, N Negretti, DA Eisner. Enhanced calcium current and decreased calcium efflux restore sarcoplasmic reticulum Ca content following depletion. *Circ Res*. 81,477-484 (1997)
  9. Inesi G, L De Meis. Regulation of steady state filling in sarcoplasmic reticulum. Roles of back-inhibition, leakage and slippage of the calcium pump. *J Biol Chem*. 264,5929-5936 (1989)
  10. Hicks MJ, M Shigekawa, AM Katz. Mechanism by which cyclic adenosine 3':5'-monophosphate-dependent protein kinase stimulates calcium transport in cardiac sarcoplasmic reticulum. *Circ Res*. 44,384-391 (1979)
  11. Tada M, MA Kirchberger, DI Repke, AM Katz. The stimulation of calcium transport in cardiac sarcoplasmic reticulum by adenosine 3':5'-monophosphate-dependent protein kinase. *J Biol Chem*. 249,6174-6180 (1974)
  12. McIvor ME, CH Orchard, EG Lakatta. Dissociation of changes in apparent myofibrillar Ca<sup>2+</sup> sensitivity and twitch relaxation induced by adrenergic and cholinergic stimulation in isolated ferret cardiac muscle. *J Gen Physiol*. 92,509-529 (1988)
  13. Endoh M, JR Blinks. Actions of sympathomimetic amines on the Ca<sup>2+</sup> transient and contraction of rabbit myocardium: Reciprocal changes in myofibrillar responsiveness to Ca<sup>2+</sup> mediated through  $\alpha$ - and  $\beta$ -adrenoceptors. *Circ Res*. 62,247-265 (1988)
  14. Wolska BM, MO Stojanovic, W Luo, EG Kranias, RJ Solaro. Effect of ablation of phospholamban on dynamics of cardiac myocyte contraction and intracellular Ca<sup>2+</sup>. *Am J Physiol*. 271,C391-C397 (1996)
  15. Li L, J Desantiago, G Chu, EG Kranias, DM Bers. Phosphorylation of phospholamban and troponin I in  $\beta$ -adrenergic-induced acceleration of cardiac relaxation. *Am J Physiol*. 278,H769-H779 (2000)
  16. Li L, G Chu, EG Kranias, DM Bers. Cardiac myocyte calcium transport in phospholamban knockout mouse: relaxation and endogenous CaMKII effects. *Am J Physiol*. 274,H1335-H1347 (1998)
  17. Barcenas-Ruiz L, DJ Beuckelmann, WG Wier. Sodium-calcium exchange in heart: Membrane currents and changes in [Ca<sup>2+</sup>]<sub>i</sub>. *Science*. 238,1720-1722 (1987)
  18. Adachi-Akahane S, L Cleemann, M Morad. Cross-signaling between L-type Ca<sup>2+</sup> channels and ryanodine receptors in rat ventricular myocytes. *J Gen Physiol*. 108,435-454 (1996)
  19. Sipido KR, G Callewaert, E Carmeliet. Inhibition and rapid recovery of Ca<sup>2+</sup> current during Ca<sup>2+</sup> release from sarcoplasmic reticulum in guinea pig ventricular myocytes. *Circ Res*. 76,102-109 (1995)
  20. Grantham CJ, MB Cannell. Ca<sup>2+</sup> influx during the cardiac action potential in guinea pig ventricular myocytes. *Circ Res*. 79,194-200 (1996)
  21. Eisner DA, HS Choi, ME Díaz, SC O'Neill, AW Trafford. Integrative analysis of calcium cycling in cardiac muscle. *Circ Res*. 87,1087-1094 (2000)
  22. Bassani JWM, W Yuan, DM Bers. Fractional SR Ca release is regulated by trigger Ca and SR Ca content in cardiac myocytes. *Am J Physiol*. 268,C1313-C1329 (1995)
  23. Spencer CI, JR Berlin. Control of sarcoplasmic reticulum calcium release during calcium loading in isolated rat ventricular myocytes. *J Physiol (Lond)*. 488,267-279 (1995)
  24. Spencer CI, JR Berlin. Calcium-induced release of strontium from the sarcoplasmic reticulum of rat cardiac ventricular myocytes. *J Physiol (Lond)*. 504,565-578 (1997)
  25. Sitsapesan R, AJ Williams. Regulation of the gating of the sheep cardiac sarcoplasmic reticulum Ca<sup>2+</sup> release channel by luminal Ca<sup>2+</sup>. *J Memb Biol*. 137,215-226 (1994)
  26. Sitsapesan R, AJ Williams. Regulation of current flow through ryanodine receptors by luminal Ca<sup>2+</sup>. *J Memb Biol*. 159,179-185 (1997)
  27. Lukyanenko V, S Subramanian, I Györke, TF Wiesner, S Györke. The role of luminal Ca in the generation of Ca waves in rat ventricular myocytes. *J Physiol (Lond)*. 518,173-186 (1999)
  28. Lukyanenko V, I Györke, S Györke. Regulation of calcium release by calcium inside the sarcoplasmic reticulum in ventricular myocytes. *Pflügers Archiv*. 432,1047-1054 (1996)
  29. Satoh H, LA Blatter, DM Bers. Effects of [Ca<sup>2+</sup>]<sub>i</sub>, SR Ca<sup>2+</sup> load, and rest on Ca<sup>2+</sup> spark frequency in ventricular myocytes. *Am J Physiol*. 272,H657-H668 (1997)
  30. Lukyanenko V, S Viatchenko-Karpinski, A Smirnov, TF Wiesner, S Györke. Dynamic Regulation of Sarcoplasmic Reticulum Ca<sup>2+</sup> Content and Release by Luminal Ca<sup>2+</sup>-Sensitive Leak in Rat Ventricular Myocytes. *Biophys J*. 81,785-798 (2001)
  31. Barritt GJ. Receptor-activated Ca<sup>2+</sup> inflow in animal cells: a variety of pathways tailored to meet different intracellular Ca<sup>2+</sup> signalling requirements. *Biochem J*. 337,153-169 (1999)
  32. Elliott AC. Recent developments in non-excitabile cell calcium entry. *Cell Calcium*. 30,73-93 (2001)
  33. Smith GL, M Valdeolmillos, DA Eisner, DG Allen. Effects of rapid application of caffeine on intracellular calcium concentration in ferret papillary muscles. *J Gen Physiol*. 92,351-368 (1988)
  34. Bers DM. Mechanisms contributing to the cardiac inotropic effect of Na pump inhibition and reduction of extracellular Na. *J Gen Physiol*. 90,479-504 (1987)
  35. Bennett DL, SC O'Neill, DA Eisner. Strophantidin-induced gain of Ca<sup>2+</sup> occurs during diastole and not systole in guinea-pig ventricular myocytes. *Pflügers Archiv*. 437,731-736 (1999)
  36. Meme W, SC O'Neill, DA Eisner. Low sodium inotropy is accompanied by diastolic Ca<sup>2+</sup> gain and systolic loss in isolated guinea-pig ventricular myocytes. *J Physiol (Lond)*. 530,487-495 (2001)
  37. Orchard CH, DA Eisner, DG Allen. Oscillations of intracellular Ca<sup>2+</sup> in mammalian cardiac muscle. *Nature*. 304,735-738 (1983)
  38. Wier WG, AA Kort, MD Stern, EG Lakatta, E Marban. Cellular calcium fluctuations in mammalian heart: direct evidence from noise analysis of aequorin signals in Purkinje fibers. *Proc Natl Acad Sci, USA*. 80,7367-7371 (1983)
  39. Wier WG, MB Cannell, JR Berlin, E Marban, WJ Lederer. Cellular and subcellular heterogeneity of [Ca<sup>2+</sup>]<sub>i</sub> in single heart cells revealed by fura-2. *Science*. 235,325-328 (1987)
  40. Vatner DE, N Sato, K Kiuchi, RP Shannon, SF Vatner. Decrease in myocardial ryanodine receptors and altered excitation-contraction coupling early in the development of heart failure. *Circulation*. 90,1423-1430 (1994)
  41. Hittinger L, B Ghaleh, J Chen, JG Edwards, RK Kudej, M Iwase, S-J Kim, SF Vatner, DE Vatner. Reduced subendocardial ryanodine receptors and consequent effects on cardiac function in conscious dogs with left ventricular hypertrophy. *Circ Res*. 84,999-1006 (1999)
  42. Yamamoto T, M Yano, M Kohno, T Hisaoka, K Ono, T Tanigawa, Y Saiki, Y Hisamatsu, T Ohkusa, M Matsuzaki. Abnormal Ca<sup>2+</sup> release from cardiac sarcoplasmic reticulum in tachycardia-induced heart failure. *Cardiovasc Res*. 44,146-155 (1999)
  43. Teshima Y, N Takahashi, T Saikawa, M Hara, S Yasunaga, S Hidaka, T Sakata. Diminished expression of sarcoplasmic reticulum Ca<sup>2+</sup>-ATPase and ryanodine sensitive Ca<sup>2+</sup> channel mRNA in streptozotocin-induced diabetic rat heart. *J Mol Cell Cardiol*. 32,655-664 (2000)
  44. Gómez AM, HH Valdivia, H Cheng, MR Lederer, LF Santana, MB Cannell, SA McCune, RA Altschuld, WJ Lederer. Defective excitation-contraction coupling in experimental cardiac hypertrophy and heart failure. *Science*. 276,800-806 (1997)
  45. Wessely R, K Klingel, LF Santana, N Dalton, M Hongo, WJ Lederer, R Kandolf, KU Knowlton. Transgenic expression of replication-restricted enteroviral genomes in heart muscle induces defective excitation-contraction

- coupling and dilated cardiomyopathy. *J Clin Invest.* 102,1444-1453 (1998)
46. Gomez AM, S Guatimosim, KW Dilly, G Vassort, WJ Lederer. Heart Failure After Myocardial Infarction: Altered Excitation-Contraction Coupling. *Circulation.* 104,688-693 (2001)
  47. Rakovic S, A Galione, GA Ashamu, BVL Potter, DA Terrar. A specific cyclic ADP-ribose antagonist inhibits cardiac excitation-contraction coupling. *Current Biology.* 6,989-996 (1996)
  48. Iino S, Y Cui, A Galione, DA Terrar. Actions of cADP-Ribose and its antagonists on contraction in guinea pig isolated ventricular myocytes: Influence of temperature. *Circ Res.* 81,879-884 (1997)
  49. Cui Y, A Galione, DA Terrar. Effects of photoreleased cADP-ribose on calcium transients and calcium sparks in myocytes isolated from guinea-pig and rat ventricle. *Biochem J.* 342,269-273 (1999)
  50. Rakovic S, Y Cui, S Iino, A Galione, GA Ashamu, BVL Potter, DA Terrar. An antagonist of cADP-ribose inhibits arrhythmic oscillations of intracellular Ca<sup>2+</sup> in heart cells. *J Biol Chem.* 274,17820-17827 (1999)
  51. Zucchi R, S Ronca-Testoni. The sarcoplasmic reticulum Ca<sup>2+</sup> channel/ryanodine receptor: modulation by endogenous effectors, drugs and disease states. *Pharmacol Rev.* 49,1-51 (1997)
  52. Meissner G. Ryanodine receptor/Ca<sup>2+</sup> release channels and their regulation by endogenous effectors. *Ann Rev Physiol.* 56,485-508 (1994)
  53. Rousseau E, G Meissner. Single cardiac sarcoplasmic reticulum Ca<sup>2+</sup>-release channel: activation by caffeine. *Am J Physiol.* 256,H328-H333 (1989)
  54. Tripathy A, L Xu, DA Pasek, G Meissner. Effects of 2,3-butanedione 2-monoxime on Ca<sup>2+</sup> release channels (ryanodine receptors) of cardiac and skeletal muscle. *J Memb Biol.* 169,189-198 (1999)
  55. Tinker A, AJ Williams. Charged local anesthetics block ionic conduction in the sheep cardiac sarcoplasmic reticulum calcium release channel. *Biophys J.* 65,852-864 (1993)
  56. Györke S, V Lukyanenko, I Györke. Dual effects of tetracaine on spontaneous calcium release in rat ventricular myocytes. *J Physiol (Lond).* 500,297-309 (1997)
  57. Xu L, G Mann, G Meissner. Regulation of cardiac Ca<sup>2+</sup> release channel (Ryanodine receptor) by Ca<sup>2+</sup>, H<sup>+</sup>, Mg<sup>2+</sup>, and adenine nucleotides under normal and simulated ischemic conditions. *Circ Res.* 79,1100-1109 (1996)
  58. O'Neill SC, DA Eisner. A mechanism for the effects of caffeine on Ca<sup>2+</sup> release during diastole and systole in isolated rat ventricular myocytes. *J Physiol (Lond).* 430,519-536 (1990)
  59. Trafford AW, ME Díaz, GC Sibbring, DA Eisner. Modulation of CICR has no maintained effect on systolic Ca<sup>2+</sup>: simultaneous measurements of sarcoplasmic reticulum and sarcolemmal Ca<sup>2+</sup> fluxes in rat ventricular myocytes. *J Physiol (Lond).* 522,259-270 (2000)
  60. Adams WA, AW Trafford, DA Eisner. 2,3-butanedione monoxime (BDM) decreases sarcoplasmic reticulum Ca content by stimulating Ca release in isolated rat ventricular myocytes. *Pflügers Archiv.* 436,776-781 (1998)
  61. Overend CL, SC O'Neill, DA Eisner. The effect of tetracaine on stimulated contractions, sarcoplasmic reticulum Ca<sup>2+</sup> content and membrane current in isolated rat ventricular myocytes. *J Physiol (Lond).* 507,759-769 (1998)
  62. Choi HS, AW Trafford, CH Orchard, DA Eisner. The effect of acidosis on systolic Ca and sarcoplasmic reticulum Ca content in isolated rat ventricular myocytes. *J Physiol (Lond).* 529,661-668 (2000)
  63. Trafford AW, ME Díaz, DA Eisner. A novel, rapid and reversible method to measure Ca buffering and timecourse of total sarcoplasmic reticulum Ca content in cardiac ventricular myocytes. *Pflügers Archiv.* 437,501-503 (1999)
  64. Hess P, WG Wier. Excitation-contraction coupling in cardiac Purkinje fibers. Effects of caffeine on the intracellular [Ca<sup>2+</sup>] transient, membrane currents, and contraction. *J Gen Physiol.* 83,417-433 (1984)
  65. Negretti N, SC O'Neill, DA Eisner. The effects of inhibitors of sarcoplasmic reticulum function on the systolic Ca<sup>2+</sup> transient in rat ventricular myocytes. *J Physiol (Lond).* 468,35-52 (1993)
  66. Marx SO, S Reiken, Y Hisamatsu, T Jayaraman, D Burkhoff, N Roseblit, AR Marks. PKA phosphorylation dissociates FKBP12.6 from the calcium release channel (ryanodine receptor): defective regulation in failing hearts. *Cell.* 101,365-376 (2000)
  67. Lukyanenko V, I Gyorke, TF Wiesner, S Gyorke. Potentiation of Ca<sup>2+</sup> Release by cADP-Ribose in the Heart Is Mediated by Enhanced SR Ca<sup>2+</sup> Uptake Into the Sarcoplasmic Reticulum. *Circ Res.* 89,614-622 (2001)
  68. Ringer S. A further contribution regarding the influence of the different constituents of the blood on the contraction of the heart. *J Physiol (Lond).* 4,29-42 (1883)
  69. Beeler GWJr, H Reuter. The relation between membrane potential, membrane currents and activation of contraction in ventricular myocardial fibres. *J Physiol (Lond).* 207,211-229 (1970)
  70. Barceñas-Ruiz L, WG Wier. Voltage dependence of intracellular (Ca<sup>2+</sup>)<sub>i</sub> transients in guinea pig ventricular myocytes. *Circ Res.* 61,148-154 (1987)
  71. Cannell MB, JR Berlin, WJ Lederer. Effect of membrane potential changes on the calcium transient in single rat cardiac muscle cells. *Science.* 238,1419-1423 (1987)
  72. Fabiato A. Simulated calcium current can both cause calcium loading in and trigger calcium release from the sarcoplasmic reticulum of a skinned canine cardiac purkinje cell. *J Gen Physiol.* 85,291-320 (1985)
  73. Eisner DA, AW Trafford. No role for the ryanodine receptor in regulating cardiac contraction? *News in Physiological Sciences.* 15,275-279 (2000)
  74. Eisner DA, AW Trafford, ME Díaz, CL Overend, SC O'Neill. The control of Ca release from the cardiac sarcoplasmic reticulum: regulation versus autoregulation. *Cardiovasc Res.* 38,589-604 (1998)
  75. Trafford AW, ME Díaz, DA Eisner. Coordinated control of cell Ca<sup>2+</sup> loading and triggered release from the sarcoplasmic reticulum underlies the rapid inotropic response to increased L-type Ca<sup>2+</sup> current. *Circ Res.* 88,195-201 (2001)

# Mechanisms that Turn-Off Intracellular Calcium Release Channels

Michael Fill

Loyola University Chicago, Department of Physiology

**ABSTRACT** Calcium release from intracellular stores is a common phenomenon in cells. Calcium release is mediated by two classes of  $\text{Ca}^{2+}$  release channels, the ryanodine receptors (RyRs) and the inositol trisphosphate receptors ( $\text{IP}_3\text{Rs}$ ). There are three types of RyR and three types of  $\text{IP}_3\text{Rs}$ . Different cells have different complements of RyR and  $\text{IP}_3\text{Rs}$ . In most cases, it is clear what turns-on these channels. It is often unclear what turns them off. It appears that a composite of factors/processes may act in synergy to regulate these channels and terminate local intracellular Ca release events. This review details some of the potential negative control mechanisms that may govern individual RyR and  $\text{IP}_3\text{R}$  channel activity.

## INTRODUCTION

Intracellular  $\text{Ca}^{2+}$  signaling is associated with a diverse array of cellular phenomena. The intracellular  $\text{Ca}^{2+}$  signals are generated by  $\text{Ca}^{2+}$  entry through the surface membrane and/or  $\text{Ca}^{2+}$  release from intracellular  $\text{Ca}^{2+}$  stores. The endoplasmic and/or sarcoplasmic reticulum (ER or SR, respectively) are the primary intracellular  $\text{Ca}^{2+}$  storage/release repositories. Specialized  $\text{Ca}^{2+}$  release channels are present in the ER/SR membranes. There are two classes of  $\text{Ca}^{2+}$  release channels, ryanodine receptors (RyRs) and inositol trisphosphate receptors ( $\text{IP}_3\text{Rs}$ ). The RyR channels bind the plant alkaloid ryanodine with nanomolar affinity and are the primary  $\text{Ca}^{2+}$  release effectors in the excitation-contraction coupling process in striated muscles. The  $\text{IP}_3\text{R}$  channels are activated by the ubiquitous second messenger inositol 1,4,5-trisphosphate and are involved in other intracellular  $\text{Ca}^{2+}$  signaling events. The RyR and  $\text{IP}_3\text{R}$  channels are both large oligomeric structures formed by either four RyR or  $\text{IP}_3\text{R}$  subunits, respectively. The RyRs and  $\text{IP}_3\text{R}$  proteins share significant homology but have little homology with the more widely studied voltage-dependent  $\text{Ca}^{2+}$  channels found in the surface membrane (Mignery et al., 1989; Takeshima, 1993). The function of single RyR and  $\text{IP}_3\text{R}$  channels in striated muscle will be the focus of this review. The concepts and principles, however, can be applied more generally.

## LOCAL INTRACELLULAR $\text{Ca}^{2+}$ RELEASE

In heart cells, intracellular  $\text{Ca}^{2+}$  release events are controlled by local events (e.g. local  $\text{Ca}^{2+}$  trigger signal, local positive/negative feedback, etc.). This concept has been substantiated by the identification of small-localized RyR-mediated  $\text{Ca}^{2+}$  release events in heart cells called " $\text{Ca}^{2+}$  sparks" (Cheng et al., 1993). Analogous  $\text{IP}_3\text{R}$ -mediated  $\text{Ca}^{2+}$  release events have been identified in other types of cells (Yao et al., 1995) as well as in heart (Lipp et al., 2000). Many studies of local  $\text{Ca}^{2+}$  release event have focused on RyR-mediated  $\text{Ca}^{2+}$  sparks in heart (e.g. Bridge et al., 1999). Global  $\text{Ca}^{2+}$  release phenomena are thought to arise from the spatio-temporal summation of local  $\text{Ca}^{2+}$  release events.

The stereotypic RyR-mediated  $\text{Ca}^{2+}$  spark is thought to arise from the opening of multiple RyR channels arranged in discrete clusters of channels. The current estimates of the number of RyR channels involved in generating a  $\text{Ca}^{2+}$  spark range from 10 to 30 (Mejia-Alvarez et al., 1999, Bridge et al., 1999; Lukyanenko et al., 2000). Thus, the time course of the  $\text{Ca}^{2+}$  spark is thought to depend on the interplay of positive and negative control mechanism(s) that govern individual RyR channel in a stochastic cluster of multiple channels. The same may be true for local  $\text{IP}_3\text{R}$ -mediated  $\text{Ca}^{2+}$  release events as well. However, it is likely that control of RyR and  $\text{IP}_3\text{R}$  channels in heart likely depends on both the properties of the individual channels and the "group dynamics" between channels. We will focus here on single channel properties.

## RYR-MEDIATED $\text{Ca}^{2+}$ RELEASE

Surface membrane depolarization of mammalian working cardiac myocytes is spread axially into the cell down surface membrane invaginations called transverse tubules (T-tubules). These T-tubules come into close association with the sarcoplasmic reticulum (SR). Depolarization of the T-tubule membrane activates voltage-dependent  $\text{Ca}^{2+}$  channels resulting in a small-localized  $\text{Ca}^{2+}$  influx ( $I_{\text{Ca}}$ ). This small local  $\text{Ca}^{2+}$  influx is the second messenger signal that activates the RyR channel in the SR. Open RyR channels are responsible for the large SR  $\text{Ca}^{2+}$  release signal that initiates muscle contraction. This process is called Ca-induced  $\text{Ca}^{2+}$  release (CICR).

The CICR process is inherently self-regenerating. The  $\text{Ca}^{2+}$  released by one RyR channel should intuitively feedback on itself and promote further  $\text{Ca}^{2+}$  release. Interestingly, the CICR process is finely graded by the amplitude of the initial  $\text{Ca}^{2+}$  trigger signal. Small triggers produce small  $\text{Ca}^{2+}$  release events. Large triggers produce large  $\text{Ca}^{2+}$  release event. How can CICR be so stable and precisely controlled? This is the classical paradox of CICR in heart.

Many investigators using a variety of different methodologies have studied the control of intracellular  $\text{Ca}^{2+}$  release in heart. Intuitively, there must be some

## The Ryanodine Receptors

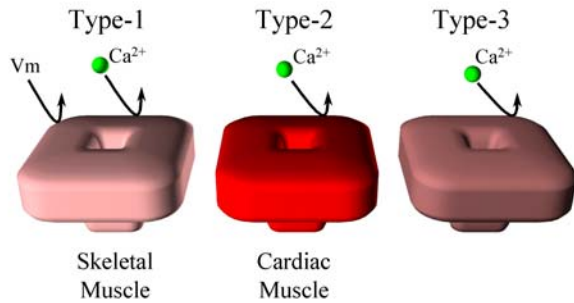


Figure 1: Cartoon illustrating the 3 isoforms of the RyR channel. Most cells contain multiple types of RyR. Expression levels of any one particular isoform varies dramatically tissue to tissue. Tissues listed correspond to primary source from which a particular channel isoform can be isolated for study. The type-1 RyR (from skeletal muscle) is primarily activated by transverse tubule membrane potential changes ( $V_m$ ). All channels can be activated by calcium.

sort of RyR-based negative control mechanism(s) to counter the inherent positive feedback of the CICR process. The nature of the mechanism(s) that turns-off RyR-mediated  $Ca^{2+}$  release in heart remains unresolved. Various candidate RyR negative control mechanisms have been proposed. Some intriguing possibilities include Ca-dependent inactivation, stochastic attrition, luminal  $Ca^{2+}$  actions and/or coupled gating of neighboring channels.

The negative control mechanism(s) that control single RyR channels in heart may also be very different than those that control the much better defined voltage- and ligand-dependent ion channels found in the surface membrane. This would not be surprising considering the entirely different roles these different channels play. The conventional wisdom gleaned from other systems and other channels may not be directly applicable to the RyR channel. For example, it appears that incremental stimuli (e.g.  $I_{Ca}$ , caffeine or depolarization in skeletal muscle) induce transient and multiple SR  $Ca^{2+}$  release events (Yasui et al., 1994; Dettbarn et al., 1994; Pizzaro et al., 1997). This phenomenon has been referred to as quantal or adaptive behavior. This type of phenomena may suggest other potential underlying RyR control mechanisms, namely quantal "all-or-none" release from functionally heterogeneous  $Ca^{2+}$  stores or adaptive behavior of individual release channels.

### IP<sub>3</sub>-MEDIATED $Ca^{2+}$ RELEASE

Activation of G-protein linked receptors generates inositol 1,4,5-trisphosphate (IP<sub>3</sub>), a ubiquitous soluble second messenger. The IP<sub>3</sub> is produced at the surface membrane by phospholipase hydrolysis of a phospholipid (i.e. phosphatidylinositol). The IP<sub>3</sub> diffuses through the cytosol and binds to the IP<sub>3</sub>R channel (Berridge,

1993). Binding of IP<sub>3</sub> activates (opens) the channels generating a rise in cytosolic  $Ca^{2+}$  levels (Mignery and Sudhof, 1993). Such IP<sub>3</sub> mediated  $Ca^{2+}$  signals regulate several cellular phenomena including secretion, synaptic transmission, fertilization, nuclear pore regulation and transcription (Berridge, 1987; Berridge and Irvine, 1984). It would not be an overstatement to say that IP<sub>3</sub>-dependent intracellular  $Ca^{2+}$  signaling is an essential element in mammalian cell physiology, including the heart.

In heart, however, a small  $Ca^{2+}$  influx across the surface membrane activates the large RyR-mediated cytosolic  $Ca^{2+}$  elevations that govern contraction (see above). Like other mammalian cells, heart muscle cells contain IP<sub>3</sub>R channels and IP<sub>3</sub>-dependent  $Ca^{2+}$  signaling cascades. Like the RyR channels, the IP<sub>3</sub>R channels, are activated by cytosolic  $Ca^{2+}$  elevations (Erhlich, 1994). Thus, there is potential cross talk between the RyR- and IP<sub>3</sub>R-mediated  $Ca^{2+}$  signaling in heart. The extent and nature of RyR-IP<sub>3</sub>R cross talk will depend on the functional attributes of the IP<sub>3</sub>R channels involved. Whether or not the IP<sub>3</sub>R channels are governed by negative control mechanisms similar to those that may regulate RyR channels remains an open question. We will focus here on single channel properties.

### RYR: SINGLE CHANNEL PROPERTIES

There are 3 different isoforms of the RyR protein (figure 1). The 3 RyR isoforms are encoded by 3 different genes (RyR1, RyR2 & RyR3) on different chromosomes (Takeshima et al., 1993; Zorzoto et al., 1990). At the amino acid level, the three RyR isoforms share about 70% identity. Thus, the RyRs form a relatively small but well-conserved family of proteins. The different RyR isoforms are found in a variety of tissues. The RyR1 isoform is the most prominent type in skeletal muscle. The RyR2 isoform is the most abundant in cardiac muscle. The RyR3 isoform is found in a variety of smooth muscle, diaphragm, as well as many other tissues (including neurons). Typically, a particular tissue will contain more than one type of RyR protein. For example, aortic smooth muscle contains both the RyR1 and RyR3 forms (Marks et al., 1989). Cerebellum contains both RyR1 and RyR2 (Furuichi et al., 1994). The importance of having multiple RyR isoforms in the same cell is not known. One might speculate, however, that this apparent morphological heterogeneity reflects functional heterogeneity, different RyR channels doing different  $Ca^{2+}$  signaling tasks. Recall that every cell must carry out a myriad of  $Ca^{2+}$  signaling tasks to survive. Just because skeletal muscle is specialized for contraction does not mean that it mediates only the  $Ca^{2+}$  signaling required for the cell to contract. The RyR channels are modulated by  $Ca^{2+}$ , ATP,  $Mg^{2+}$ , phosphorylation, calmodulin, and several other ligands. Calcium and ATP are both potent activators of the RyR channel while  $Mg^{2+}$  is a potent inhibitor (particularly the RyR1 isoform). A classic property of the RyR channels is their bell-shaped steady-state  $Ca^{2+}$  dependence. The RyR channels are activated by micromolar  $Ca^{2+}$  and inhibited by high  $Ca^{2+}$  concentrations. Inhibition at

high  $\text{Ca}^{2+}$  is isoform specific. The RyR1 channel is almost entirely inhibited by 1 mM  $\text{Ca}^{2+}$  (Chu et al., 1993; Rousseau et al., 1989). The RyR2 channel is inhibited at  $\text{Ca}^{2+}$  concentrations in excess of 10 mM (Laver et al., 1995). It is not clear that such high cytoplasmic  $\text{Ca}^{2+}$  concentrations are ever reached in the cells. Thus, the physiological role of high  $\text{Ca}^{2+}$  inhibition of RyR2 channels is not yet clear.

The  $\text{Mg}^{2+}$  inhibition of the RyR channel is also somewhat isoform specific. The RyR1 channel is more sensitive to  $\text{Mg}^{2+}$  than the RyR2 channel. It has also been suggested that phosphorylation of the RyR channel modulates its  $\text{Mg}^{2+}$  sensitivity (Hain et al., 1995). It appears that dephosphorylated channels are inhibited by physiological  $\text{Mg}^{2+}$  concentrations while phosphorylated channels are not. However, this idea needs further experimental verification. The action of ATP on the RyR is also isoform specific. The RyR2 channel is much less sensitive to ATP than the RyR1 channel. Most potential RyR regulatory agents act on the cytoplasmic side of the channel. This is not surprising considering that about 90% of the RyR's mass is on the cytoplasm side of the SR membrane. Although only a small portion of the RyR is in the lumen of the SR, the possibility that this part of the RyR contains ligand regulatory sites has also been explored (Sitsapesan et al., 1995; Tripathy and Meissner, 1996).

The RyR channel may also be modulated by several closely associated regulatory proteins (e.g. dihydropyridine receptor, triadin, junctin, calsequestrin, FK-506 binding protein, sorcin, etc.). The dihydropyridine receptor (DHPR) protein is a voltage-dependent L-type  $\text{Ca}^{2+}$  channel found in the transverse tubules (T-tubules) of striated muscles. The DHPR is also found in surface membrane of many other types of cells. In skeletal muscle, the DHPR is intimately involved in RyR regulation. It has been suggested that an integral SR protein called triadin may also be somehow involved in DHPR-RyR communication (Kim et al., 1990). The FK-506 binding protein (FKBP) is tightly bound to the RyR channel complex (Marks, 1996). The impact of FKBP on RyR function is not yet clearly understood. Another potentially important protein that is closely associated with the RyR channel is calsequestrin. Calsequestrin is a low affinity, high capacity  $\text{Ca}^{2+}$  buffer that appears to be attached to the luminal surface of the RyR channel protein (Franzini-Armstrong et al., 1987). The position of calsequestrin implies that it plays an important role in buffering  $\text{Ca}^{2+}$  near the mouth of the RyR channel.

In striated muscles, the RyR1 and RyR2 channels interact with the DHPR channels in the T-tubule membrane. Depolarization of the T-tubule membrane (i.e. excitation) induces conformational changes in DHPR that lead to RyR channel activation. Activation of RyR channels leads to  $\text{Ca}^{2+}$  released from the SR and this  $\text{Ca}^{2+}$  triggers contraction of the cell. The process of DHPR-RyR communication is commonly referred to as excitation-contraction (E-C) coupling. Its role in striated muscle E-C coupling is probably the RyR channel's most notable claim to

fame. Defining RyR channel regulation during E-C coupling promises to generate important insights into how RyR channels are regulated in other cells.

#### **RYR: EXCITATION-CONTRACTION COUPLING**

The E-C coupling process is different in skeletal and cardiac muscle. In skeletal muscle, the DHPR communicates with the RyR1 channel through some sort of physical protein-protein link. Voltage-induced changes in DHPR conformation directly induce conformational changes in the RyR1 channel that trigger it to open. The voltage-induced conformational changes in the DHPR generate measurable non-linear capacitive currents called charge movements (Schneider et al., 1976). Expressing mutant DHPRs in mouse myotubes that lacked endogenous DHPR provided evidence for physical DHPR-RyR1 communication (Adams et al., 1990). These studies revealed that a particular intracellular loop of the DHPR is involved in DHPR-RyR1 signaling. Signal transmission between the DHPR and RyR1 channel must be quite fast because skeletal E-C coupling must occur during the very brief ( $\sim 2$  ms) skeletal muscle action potential. This action potential is long enough for the DHPR voltage sensor to move and induce RyR opening but not long enough to allow significant  $\text{Ca}^{2+}$  entry through the DHPR  $\text{Ca}^{2+}$  channel itself. This explains why skeletal muscle E-C coupling is independent of extracellular  $\text{Ca}^{2+}$  levels (Armstrong et al., 1972). It appears that the skeletal muscle "need for speed" has converted the DHPR from  $\text{Ca}^{2+}$  channel to a specialized voltage-sensor.

The physiological role of the DHPR in cardiac muscle is quite different. During the long cardiac action potential ( $\sim 100$  ms), the DHPR  $\text{Ca}^{2+}$  channel has ample time to open and a significant  $\text{Ca}^{2+}$  influx occurs. This  $\text{Ca}^{2+}$  influx is the signal that triggers RyR2 channel activity. Specifically,  $\text{Ca}^{2+}$  acts as a diffusible second messenger that binds to and activates the RyR2 channel. This process is called  $\text{Ca}^{2+}$ -induced  $\text{Ca}^{2+}$  release (Fabiato, 1985; CICR). Intuitively, the CICR process should be self-regenerating because the  $\text{Ca}^{2+}$  released from the SR should feedback and activate further SR  $\text{Ca}^{2+}$  release. However, the CICR process is not self-regenerating in the cell suggesting that some sort of negative feedback must exist to counter the inherent positive feedback of CICR. Defining the nature of this negative feedback is a target of current investigation. The involvement of a diffusible second messenger (i.e.  $\text{Ca}^{2+}$ ) makes DHPR-RyR2 signaling much slower than the DHPR-RYR1 signaling described above. However, this lack of "speed" provides greater opportunity for regulating the  $\text{Ca}^{2+}$  release process. Such regulation is fundamental to normal cardiac function (Bers, 1990).

#### **RYR: NEGATIVE CONTROL MECHANISMS**

The negative feedback that counters the inherent positive feedback of CICR may arise from a single mechanism. Alternatively, a composite of factors/processes acting in synergy may terminate the  $\text{Ca}^{2+}$  release process. I believe the latter possibility is more likely because no individual mechanism seems

sufficient by itself. Potential negative control mechanisms are summarized in figure 2 and discussed in some detail below.

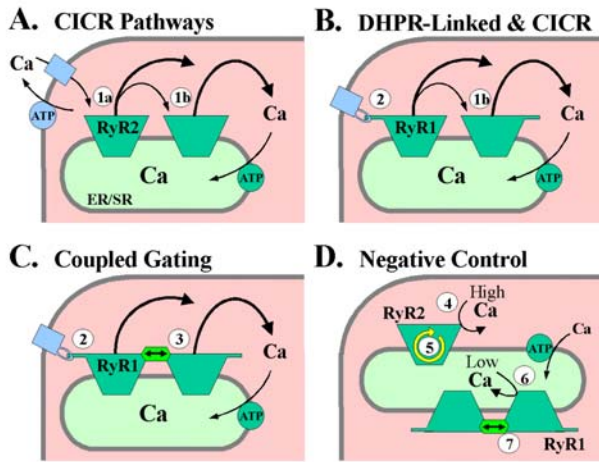


Figure 2: Mechanisms that Turn-On and Turn-Off RyR Channels. A. Summary of cardiac muscle E-C coupling. The Ca-induced Ca<sup>2+</sup> release (CICR) process turns-on the RyR2 channel. The trigger Ca<sup>2+</sup> may arise from Ca<sup>2+</sup> entry through sarcolemmal DHPR Ca<sup>2+</sup> channels (1a) or neighboring RyR2 channels (1b). B. Summary of skeletal muscle E-C coupling. Some RyR1 channels are turned-on by a physically coupling to voltage-sensing sarcolemmal DHPRs (2). Neighboring RyR1 channels may be activated by CICR (1b). C. Summary of coupled RyR1 channel gating. Here, adjacent RyR1 channels are physically linked together. A RyR1 channel turned-on via the DHPR-RyR linkage (2) drives the opening of its neighbor (3). D. Summary of potential RyR negative control mechanisms. There is evidence that RyR1 and RyR2 channels may be turned-off by Ca<sup>2+</sup> inactivation at high cytosolic Ca<sup>2+</sup> levels (4), some sort of programmed "fateful" inactivation (5) and/or low intra-SR Ca<sup>2+</sup> levels (6). Coupled gating could also drive RyR1 channel closure (7).

### Stochastic Attrition

Stochastic attrition of single RyR channel activity may be responsible for terminating a local Ca<sup>2+</sup> release event. Stern (1992) demonstrated using mathematical modeling that a SR Ca<sup>2+</sup> release unit composed of one or relatively small number of channels will "turn-off" spontaneously as a result of reduced local Ca<sup>2+</sup> levels generated by the stochastic closures of single RyR channels. Stochastic attrition, however, is very sensitive to the number of channels and the positive feedback gain of CICR in the RyR channel cluster. Stochastic attrition is sufficient to terminate local Ca<sup>2+</sup> release only if there are less than 10 RyR channels per release unit. If release units are composed of 10-30 single RyRs (Bridge et al., 1999; Lukyanenko et al., 2000), then it becomes less likely that termination of local Ca<sup>2+</sup> release is due solely to stochastic attrition. Experimentally, Lukyanenko et al. (1998) showed that rate of termination of local Ca<sup>2+</sup> release events is proportional to the magnitude of the release event (i.e. large events terminate faster than small events). Sham et al. (1998) demonstrated that local Ca<sup>2+</sup> events terminate rapidly despite the presence of a sustained trigger Ca<sup>2+</sup> signal (i.e., sustained Ca<sup>2+</sup> influx through L-type channels in presence of the agonist FPL64176). These

experimental results are inconsistent with the possibility that stochastic attrition plays a primary role in termination of local Ca<sup>2+</sup> release events. Nevertheless, stochastic attrition could still contribute to local Ca<sup>2+</sup> release termination if it acts in combination with other negative control mechanisms. Lastly, the action of stochastic attrition in any scenario would be expected to be highly non-linear because once the number of active channels falls below some critical level the remaining channels would be increasingly vulnerable to stochastic attrition.

### Calcium Dependent Inactivation

Calcium dependent inactivation was originally proposed by Fabiato (1985) as the negative feedback mechanism that counters the intrinsic positive feedback of CICR. He proposed that inactivation of the intracellular Ca<sup>2+</sup> release is due to slow binding of Ca<sup>2+</sup> to a high affinity inactivation site on the SR Ca<sup>2+</sup> release channel. He presented evidence collected in a skinned cardiac cell preparation that the SR Ca<sup>2+</sup> release mechanism is substantially inactivated at steady-state Ca<sup>2+</sup> concentrations as low as 60 nM. Subsequent studies on intact cells presented contradictory results concerning the existence of Ca<sup>2+</sup> dependent inactivation (Nabauer and Morad, 1990). In a more recent example, Lukyanenko et al. (1999) imaged permeabilized ventricular myocytes using a confocal microscope and showed that elevation of resting Ca<sup>2+</sup> levels resulted in an increase in Ca<sup>2+</sup> spark activity (not a decrease as would be expected if release sites or RyR channels inactivate). Single RyR (i.e., RyR2) channel studies have also shown that there is no evidence of Ca<sup>2+</sup> dependent inactivation at low Ca<sup>2+</sup> concentrations (Coronado et al., 1994). Thus, there is experimental evidence that rules out the possibility that the SR Ca<sup>2+</sup> release process is regulated by a high affinity Ca<sup>2+</sup> dependent inactivation mechanism.

There is, however, the possibility of low affinity Ca<sup>2+</sup> dependent inactivation. In single RyR2 channel studies, spontaneous RyR channel activity is reduced at relatively high steady state Ca<sup>2+</sup> concentrations (Laver et al., 1995; Copello et al., 1997; Gyorke and Gyorke, 1996). This is consistent with observations of SR Ca<sup>2+</sup> release inactivation in studies in SR vesicle preparations (Coronado et al., 1994). In these cases, Ca<sup>2+</sup> dependent inactivation was evident at Ca<sup>2+</sup> levels higher than ~100 μM. It has been estimated that local Ca<sup>2+</sup> levels in the RyR microenvironment during a local Ca<sup>2+</sup> release event may reach the 0.6-1 mM range (Langer and Peskoff, 1996). Thus, low affinity Ca<sup>2+</sup> dependent inactivation is a potential negative control mechanism that could account for (or contribute to) the termination of local Ca<sup>2+</sup> release events.

### Adaptation

Until 1993, single RyR channels studies focused on defining RyR behavior under steady state conditions. Using laser flash photolysis of caged Ca, Gyorke and Fill (1993) were the first to apply fast trigger Ca<sup>2+</sup> signals to single RyR channels in artificial

planar bilayers. They found that single RyR2 channels activated with a time constant of  $\sim 1$  ms and reached an open probability that was well above that predicted from steady state studies. Channel activity peaked and then spontaneously decayed with a time constant of  $\sim 1$  second. Application of second fast trigger  $\text{Ca}^{2+}$  signal reactivated the apparently "inactivated" channels. These experimental data suggested that the spontaneous decay was not due to a conventional (i.e. Fabiato-like)  $\text{Ca}^{2+}$  inactivation mechanism. Gyorke and Fill (1993) proposed that the spontaneous decay was mediated by a different process they called adaptation. It is now clear that the spontaneous decay (i.e. adaptation) was very likely due to a Ca- and time-dependent, transient shift in the modal gating behavior of the RyR2 channel (Zahradnikova et al., 1999).

The RyR adaptation phenomenon has been controversial. It is observed when the channel is activated by a free  $\text{Ca}^{2+}$  waveform generated by flash photolysis of DM-Nitrophen which generates a very fast ( $< 1$  ms)  $\text{Ca}^{2+}$  overshoot at the leading edge of the applied  $\text{Ca}^{2+}$  stimulus (Zucker et al., 1993; Escobar et al., 1995; Ellis-Davies et al., 1996). Lamb et al. (1994) suggested that the presence of the fast  $\text{Ca}^{2+}$  overshoot may complicate data interpretation. They speculate that single RyR channel  $\text{Ca}^{2+}$  deactivation is very slow following the  $\text{Ca}^{2+}$  overshoot. However, the existence of such slow RyR  $\text{Ca}^{2+}$  deactivation is not supported by the literature. There is no published experimental evidence showing slow RyR  $\text{Ca}^{2+}$  deactivation at the single channel or whole cell levels. Further, single RyR channel  $\text{Ca}^{2+}$  deactivation upon a rapid  $\text{Ca}^{2+}$  reduction has been measured by several labs and is quite fast (Schiefer et al., 1995; Velez et al., 1997; Zahradniková et al., 1999). Single RyR channel  $\text{Ca}^{2+}$  deactivation occurs within 10 ms over a wide range of  $\text{Ca}^{2+}$  concentrations (0.5  $\mu\text{M}$ -3 mM). Additionally, the rate of adaptation correlates well with the "steady state"  $\text{Ca}^{2+}$  changes rather than the estimated amplitude/kinetics of the fast  $\text{Ca}^{2+}$  overshoot (Gyorke and Fill, 1993; Valdivia et al., 1995; Zahradnikova et al., 1999). Thus, it is not likely that the adaptation phenomenon is due to slow RyR  $\text{Ca}^{2+}$  deactivation following a fast  $\text{Ca}^{2+}$  overshoot.

Another point of controversy has been that RyR adaptation has not been reported by all investigators. When a very fast  $\text{Ca}^{2+}$  stimulus is applied by flash photolysis, adaptive behavior is clearly and consistently observed (Gyorke and Fill, 1993; Gyorke et al., 1994; Valdivia et al., 1995). When  $\text{Ca}^{2+}$  stimuli were applied using a mechanical solution change method (Sitsapeasan et al., 1995; Schiefer et al., 1995; Laver and Curtis, 1996; Laver and Lamb, 1998), RyR2 channel activity usually peaks and then spontaneously decays. The decay has been typically interpreted as conventional inactivation, not adaptation. In some cases, this is appropriate. For example, the inactivation reported by Schiefer et al. (1995) occurs at  $\text{Ca}^{2+}$  concentrations that are known to inhibit RyR channel activity under steady state conditions. However, the rate/extent and nature of inactivation reported in other studies varies dramatically and is difficult to reconcile with the well-

defined steady state behavior of the channel. This variability in data likely reflects the vastly different kinetics of the  $\text{Ca}^{2+}$  stimuli applied (Fabiato, 1985; Gyorke and Fill, 1993; Sitsapeasan et al., 1995; Schiefer et al., 1995).

Overall, the data reported in the flash photolysis and mechanical solution change studies are consistent. The main disagreements between the studies appear to lie in the realm of interpretation. For example, the apparent  $\text{Ca}^{2+}$  inactivation reported by Laver and Lamb (1998, figure 10) does not appear to be consistent with the well-defined  $\text{Ca}^{2+}$  sensitivity of the channel. We believe this type of interpretive confusion stems from two factors, 1) the modal gating of the RyR channel and, 2) the forced application of conventional theory to describe RyR behavior. A spontaneous shift to a low or zero activity RyR gating mode could be mistaken for inactivation (see below). The point is that describing RyR channel behavior and particularly its  $\text{Ca}^{2+}$  regulation is difficult. Ironically, this realization is what compelled Gyorke and Fill (1993) to propose the existence of a novel non-conventional RyR regulatory mechanism (i.e. adaptation) in the first place.

#### **Activation Dependent or "Fateful" Inactivation**

Pizarro et al. (1997) found that the global  $\text{Ca}^{2+}$  release transient in frog skeletal muscle triggered by a maximally depolarizing stimulus was inhibited in proportion to the fraction of  $\text{Ca}^{2+}$  release activated during a prepulse. Thus, RyR channels that have been activated during the prepulse are not available in the maximal test pulse implying that pre-activated RyRs are inactivated or refractory. These authors proposed that RyR inactivation is strictly and "fatefully" linked to their activation (i.e. use-dependent). Interestingly, certain single RyR channel studies are quite consistent with this notion. The modal gating behavior of single RyR channels has been reported by several different investigators (Zahradniková and Zahradník, 1995; Armisen et al., 1996; Zahradniková et al., 1999). It has been proposed (Zahradniková et al., 1999) that a modal gating shift (high to low) in single RyR channel activity may be the single channel manifestation of the "fateful" inactivation.

#### **Depletion/Luminal $\text{Ca}^{2+}$ Effects**

Single RyRs are regulated by low affinity  $\text{Ca}^{2+}$  binding sites residing on the luminal side of the channel or associated luminal protein (Gyorke and Gyorke, 1996). These sites may sense changes in intra-SR  $\text{Ca}^{2+}$  level in the physiologically relevant range (0.2-20 mM). Thus, SR  $\text{Ca}^{2+}$  depletion may directly impact single RyR channel activity. In this scenario, single RyR channel activity would be under continuous control of luminal  $\text{Ca}^{2+}$  concentration. A decrease in luminal  $\text{Ca}^{2+}$  would lead to a decrease in channel activity and thus representing a highly nonlinear negative control mechanism. It appears that there is no significant depletion of SR  $\text{Ca}^{2+}$  during repeated  $\text{Ca}^{2+}$  sparks at the same release site (Parker et al, 1996). This observation, however, does not rule out the possibility that very localized brief decreases in luminal  $\text{Ca}^{2+}$  levels contribute to termination of

release. If changes in luminal  $\text{Ca}^{2+}$  are indeed important, then the impact of luminal  $\text{Ca}^{2+}$  would be expected to be larger for global  $\text{Ca}^{2+}$  release events where changes in luminal  $[\text{Ca}]$  would be much larger.

### Allosteric or Coupled RyR Gating

Recently, Stern et al. (1999) evaluated several published single RyR gating schemes and found that all generated unacceptable instability when applied in a local control model. One reason the instability arose was because of a lack of a strong negative feedback to minimize local regenerative release in clusters of RyR channels. Another reason the instability arose was because of a relatively low level of cooperativity in the RyR  $\text{Ca}^{2+}$  activation process. The low cooperativity simply does not allow the RyR to adequately discriminate between trigger and background  $\text{Ca}^{2+}$  signals. Interestingly, Stern et al. (1999) has shown that introducing RyR-RyR allosteric interactions can theoretically overcome the problems introduced by weak inactivation and low cooperativity. Bilayer studies demonstrate that RyR channels can inactivate strongly but at relatively high  $\text{Ca}^{2+}$  concentrations (Laver et al., 1995; Copello et al., 1997; Gyorke and Gyorke, 1996). In addition, kinetic studies examining RyR channel response to fast  $\text{Ca}^{2+}$  applications reveals that activation of single RyR channels may require binding of multiple ( $n \geq 4$ )  $\text{Ca}^{2+}$  ions (Zahradníková et al., 1999). This suggests that RyR  $\text{Ca}^{2+}$  activation may be highly cooperative.

Recently, it has been suggested that neighboring RyR channels may be physically coupled by FK-506 binding protein 12 (FKBP-12) and gate synchronously (Marx et al., 1998). Is this coupled RyR gating the needed allosteric interaction? The answer to this question is not clear. Coupled RyR channel gating has not yet been reported by other investigators. The thermodynamic considerations associated with microsecond synchrony of multiple large macromolecules (e.g. RyR channels) may also be a problem (Bers and Fill, 1998; Stern et al., 1999). Interestingly, the removal of FKBP12 did not abolish  $\text{Ca}^{2+}$  sparks but actually increased their frequency and duration (McCall et al., 1996). Thus, FKBP12 and coupled gating may not be as important as previously argued. Nevertheless, coupled RyR gating is an interesting and provocative hypothesis. Its existence and nature still requires further verification.

### RYR: MODAL GATING, A $\text{Ca}^{2+}$ REGULATORY SCHEME

Modal gating of single RyR channels in planar lipid bilayers has been defined under steady state conditions (Zahradníková et al., 1995; Armisen et al., 1996; Villalba-Galea et al., 1998). The RyR channel opens in distinct bursts of high or low open probability ( $P_o$ ). These bursts do not occur randomly. Instead the bursts are temporally clustered into modes (high and low- $P_o$  modes). The channel also has a quiescent "inactivated" mode (at high  $\text{Ca}^{2+}$  levels). At any particular  $\text{Ca}^{2+}$  concentration, there will be dynamic equilibrium between the different modes. Sudden changes in  $\text{Ca}^{2+}$  concentration will force the system to re-equilibrate. It will take time to reach the new

equilibrium between modes. During this time, the activity of the RyR channel will vary. This type of  $\text{Ca}^{2+}$  dependent modal gating scheme is not unique to the RyR channel. An analogous proposal has been forwarded to describe the  $\text{Ca}^{2+}$  dependent gating of dihydropyridine receptor (DHPR)  $\text{Ca}^{2+}$  channels (Imredy and Yue, 1994).

The modal gating of single RyR channels is an important observation because it can account for all the known kinetics of RyR channel  $\text{Ca}^{2+}$  regulation. The first modal RyR gating model was presented by Zahradníková and Zahradník (1996). Theoretical simulations illustrate that this modal gating model can reproduce many of the known steady-state and kinetic features of single RyR channel behavior. It can account for the RyR channel's classical steady-state  $\text{Ca}^{2+}$  dependency as well as adaptation and low affinity  $\text{Ca}^{2+}$  inactivation. In this context, these phenomena (i.e. steady-state  $\text{Ca}^{2+}$  dependence, adaptation and inactivation) may actually represent three different manifestations of the same underlying  $\text{Ca}^{2+}$  dependent mechanism (i.e. modal RyR gating).

### The Inositol Trisphosphate Receptors

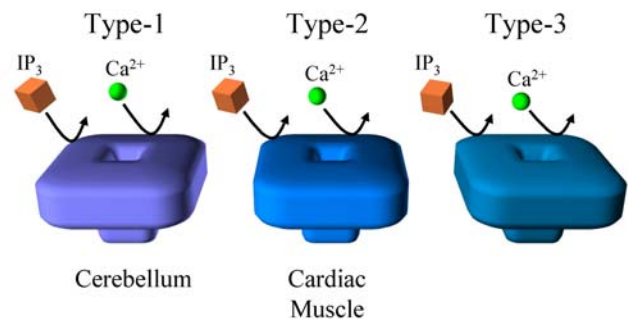


Figure 3: Cartoon illustrating the 3 isoforms of the  $\text{IP}_3\text{R}$  channel. Most cells contain multiple types of  $\text{IP}_3\text{R}$ . Expression levels of any one particular isoform varies dramatically tissue to tissue. The type-1 receptor is found in high density in the cerebellum. This tissue has served as a primary source from which a particular channel isoform has been isolated for study. The  $\text{IP}_3\text{R}$  channels are all activated by  $\text{IP}_3$  and calcium.

### $\text{IP}_3\text{R}$ : SINGLE CHANNEL PROPERTIES

There are three homologous  $\text{IP}_3\text{R}$  proteins (sharing 60-70% homology) that are encoded by three different genes (figure 3). These large proteins are highly conserved among species but are differentially expressed in various tissues in any one species (Berridge, 1987; Berridge and Irvine, 1984). They tetramerize to form  $\text{Ca}^{2+}$  release channels that are activated by  $\text{IP}_3$  and blocked by heparin. Each  $\text{IP}_3\text{R}$  individual protein is composed of three domains: a N-terminal  $\text{IP}_3$  binding domain, a C-terminal channel domain, and a large interceding regulatory domain. The regulatory domain contains consensus phosphorylation, ATP-binding and  $\text{Ca}$ -binding sites (Mignery et al., 1989). The proteins also have potential sites that may interact with certain accessory proteins (e.g. calmodulin & FKBP). The type-1  $\text{IP}_3\text{R}$  is found in high density in the mammalian

cerebellum (Berridge, 1993). The type-1 IP<sub>3</sub>R is found in high density in mammalian spinal cord, glial cells and cardiomyocytes (Ramos-Franco et al., 1998). The type-3 IP<sub>3</sub>R is found in the kidney, diaphragm, gastrointestinal tract and pancreatic islets (Berridge, 1993).

The IP<sub>3</sub>R channels are regulated by cytoplasmic IP<sub>3</sub>, Ca<sup>2+</sup> and nucleotides (Berridge, 1993). The cytoplasmic Ca<sup>2+</sup> sensitivity of the IP<sub>3</sub>R channel is isoform-specific (Thrower et al., 2001). The Ca<sup>2+</sup> sensitivity of the type-2 and type-3 receptors is broader than that of the type-1 receptor. Type-1 IP<sub>3</sub>R channel activity occurs over a relatively narrow range (~0.1 to ~1 μM) of free Ca<sup>2+</sup> concentrations. Type-2 and type-3 IP<sub>3</sub>R channels can be active at much higher Ca<sup>2+</sup> levels. The Ca<sup>2+</sup> sensitivity of the IP<sub>3</sub>R channels is modulated by cytoplasmic IP<sub>3</sub> levels (Thrower et al., 2001). The 3 IP<sub>3</sub>R proteins bind IP<sub>3</sub> but with different affinities (Berridge, 1993; Mignery et al., 1989). The type-2 receptor has the highest affinity and the type-1 receptor has the lowest. The IP<sub>3</sub> binding affinities of the IP<sub>3</sub>R proteins are reflected in the EC<sub>50</sub>'s of IP<sub>3</sub>R channel function (Ramos-Franco et al., 1998). The activity of the IP<sub>3</sub>R channels is also governed by certain nucleotides (e.g. ATP, GTP, AMP). However, it appears that ATP has the highest efficacy. Low nucleotide concentrations activate the channel while high nucleotide levels inhibit it (Thrower et al., 2001; Berridge, 1993). Nucleotide action is dependent on cytoplasmic IP<sub>3</sub> levels. The inhibitory action of ATP may involve the competition between ATP and IP<sub>3</sub> at the same site. In contrast, ATP binding to a unique site on the receptor may generate the activating action of ATP. However, the details of IP<sub>3</sub>R channel nucleotide regulation are still being debated.

The permeation properties of the 3 different IP<sub>3</sub>R channel isoforms are similar (Ramos-Franco et al., 1998). They are all poorly selective Ca<sup>2+</sup> channels (P<sub>Ca</sub>/P<sub>K</sub> ratio ~5) that have a unit Ca<sup>2+</sup> conductance many times larger than that of the voltage-dependent Ca<sup>2+</sup> channels found in the surface membrane. These permeation properties are shared with the RyR channels and permit both these channels to achieve their physiological role (i.e. mediate large local Ca<sup>2+</sup> release events).

### **IP<sub>3</sub>R: NEGATIVE CONTROL MECHANISMS**

Like the RyR channels, the IP<sub>3</sub>R channels are Ca<sup>2+</sup> activated Ca<sup>2+</sup> release channels. Intuitively, IP<sub>3</sub>R mediated Ca<sup>2+</sup> released should be regenerative. The Ca<sup>2+</sup> released by a IP<sub>3</sub> bound channel should feedback and activate the channel further. In cells, IP<sub>3</sub> mediated Ca<sup>2+</sup> signaling is well controlled. This implies that there must be negative feedback mechanisms that counter the inherent positive feedback discussed above. Many of the negative feedback mechanisms discussed in detail for the RyR channel above may also apply to the IP<sub>3</sub>R channel. Unlike the RyR function, IP<sub>3</sub> generation and degradation ultimately govern IP<sub>3</sub>R channel function. The IP<sub>3</sub>R channels turn-on when local IP<sub>3</sub> levels rise and turn-off when they fall. The situation, however, is not so simple. The activity of an IP<sub>3</sub>R channel depends on the concerted actions of several ligands (e.g. IP<sub>3</sub>, Ca<sup>2+</sup>, ATP,

calmodulin etc.). The interaction of IP<sub>3</sub>R regulators is currently a focus of intense investigation. Certain specific regulatory interactions are discussed below.

### **Calmodulin-IP<sub>3</sub>R Association**

The type-1 IP<sub>3</sub>R channel has a bell-shaped Ca<sup>2+</sup> sensitivity. Low Ca<sup>2+</sup> levels activate while high Ca<sup>2+</sup> concentrations (e.g. 1 μM) inhibit. The implication is that Ca<sup>2+</sup> release mediated by this channel may be self-limiting (released Ca<sup>2+</sup> will feedback and turn-off the channel). This is a form of Ca<sup>2+</sup> dependent inactivation analogous to that proposed for single RyR channels (see above). Calcium dependent inactivation of the type-2 and type-3 IP<sub>3</sub>R channel occurs at substantially higher Ca<sup>2+</sup> concentrations. The nature of this IP<sub>3</sub>R channel Ca<sup>2+</sup> inactivation is controversial. Some IP<sub>3</sub>R channel studies argue that Ca<sup>2+</sup> inactivation is absent when the channels are "purified" biochemically. It has been proposed that "purification" removes calmodulin which acts as a critical cofactor in the Ca<sup>2+</sup> inactivation. The implication is that Ca<sup>2+</sup> inactivation may not be the result of Ca<sup>2+</sup> binding directly to the IP<sub>3</sub>R protein. It may be mediated via a Ca<sup>2+</sup> dependent calmodulin-IP<sub>3</sub>R interaction. In other studies (Ramos-Franco et al., 1989), the bell-shaped Ca<sup>2+</sup> sensitivity is present in both purified and non-purified receptor IP<sub>3</sub>R channel studies. The role of calmodulin in IP<sub>3</sub>R regulation is still poorly understood and requires more detailed analysis.

### **Ca<sup>2+</sup>-IP<sub>3</sub> Interaction**

The interaction of cytosolic Ca<sup>2+</sup> and IP<sub>3</sub> in the regulation of single IP<sub>3</sub>R channels is controversial. There is agreement that the type-1 receptor has a bell-shaped Ca<sup>2+</sup> sensitivity at low IP<sub>3</sub> concentrations and that this bell-shape is lost at high IP<sub>3</sub> concentrations. There is some disagreement as to how much IP<sub>3</sub> is required to abolish the bell-shaped Ca<sup>2+</sup> sensitivity of the channel (Kaftan et al., 1997; Mak et al., 1998). There is also certain disagreement concerning the nature of the Ca-IP<sub>3</sub> interaction. One group argues that two IP<sub>3</sub> binding sites with different affinities regulate the channel (Kaftan et al., 1997). Occupancy of the low affinity site alters the Ca<sup>2+</sup> sensitivity of the channel. The other group argues that a single high affinity IP<sub>3</sub> binding site regulates the channel (Mak et al., 1998). Occupancy of the low affinity "tunes" the Ca<sup>2+</sup> sensitivity of the channel. Low occupancy results in a bell-shaped Ca<sup>2+</sup> sensitivity. High occupancy abolishes the bell-shaped Ca<sup>2+</sup> sensitivity. In either case, it is clear that Ca<sup>2+</sup> and IP<sub>3</sub> interact in interesting ways to regulate these channels.

### **RYR-IP<sub>3</sub>R CHANNEL CROSS TALK**

Most cells contain both RyR and IP<sub>3</sub>R channels. In fact, most cells contain multiple types of each. The mechanisms that regulate these channels impart a substantial degree of functional heterogeneity. The existence of multiple functionally heterogeneous Ca<sup>2+</sup> release channels suggests that they may mediate different physiological processes in the cell. Interestingly, all these channels are activated

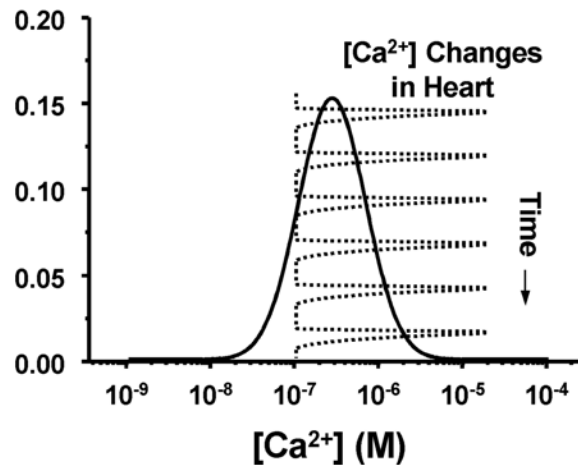


Figure 4: The  $\text{Ca}^{2+}$  sensitivity of single type-1  $\text{IP}_3\text{R}$  channels in planar lipid bilayers are represented as solid lines. These plots are based on the work of Bezprozvanny et al. (1991). Dotted line represents the theoretical free  $\text{Ca}^{2+}$  changes that occur during the cardiac cycle.

by cytosolic calcium presenting the possibility of inter-channel  $\text{Ca}^{2+}$  cross talk.

The situation in cardiac muscle is a case in point (figure 4). Moschella and Marks (1993) suggested that the type-1  $\text{IP}_3\text{R}$  was the predominant  $\text{IP}_3\text{R}$  in heart muscle cells. The single channel behavior of the type-1  $\text{IP}_3\text{R}$  isolated from cerebellum was well defined in planar lipid bilayer studies (Figure 4, solid line). Channel activity is a bell-shaped function of cytosolic  $\text{Ca}^{2+}$  concentration at a constant activating  $\text{IP}_3$  level. The channel is open at 200 nM  $\text{Ca}^{2+}$  and closed at cytosolic  $\text{Ca}^{2+}$  greater than 2.5  $\mu\text{M}$ . In heart muscle, the cytosolic  $\text{Ca}^{2+}$  concentration changes dramatically through out the cross-section of the cell during the normal cardiac cycle. During diastole (rest), the cytosolic  $\text{Ca}^{2+}$  concentration is near 100 nM. During systole (active), cytosolic  $\text{Ca}^{2+}$  may rise to very high levels ( $\sim 100 \mu\text{M}$ ) in certain regions of the cell. In the presence of a constant  $\text{IP}_3$  signal in these regions, the type-1  $\text{IP}_3\text{R}$  would be turning on and off (as a consequence of the RyR-mediate  $\text{Ca}^{2+}$  release during the normal cardiac cycle). There would be substantial cross talk between the RyR-mediated and  $\text{IP}_3\text{R}$   $\text{Ca}^{2+}$  signaling pathways undercutting the fidelity of each. How can a cell avoid this obstacle? In most cases, cross talk may be avoided by specific discrete sub-cellular localization (i.e. sub-compartmentalization of  $\text{Ca}^{2+}$  signaling phenomena). In other cases (e.g. cardiac muscle), cross talk may be avoided by expression of specific release channel isoforms. The predominant  $\text{IP}_3\text{R}$  in ventricular myocytes is not the type-1 form as previously thought. We now know that the type-2  $\text{IP}_3\text{R}$  is the predominant isoform present. The type-2 channel lacks the sharp bell-shaped  $\text{Ca}^{2+}$  sensitivity characteristic of the type-1 channel. The type-2 receptor will more directly follow local  $\text{IP}_3$  levels and be much less impacted by the local  $\text{Ca}^{2+}$

concentrations changes that occur during the cardiac cycle.

It is clear that there is potential for substantial  $\text{Ca}^{2+}$  signaling cross talk in cells. How cells avoid (or take advantage) of this situation is an interesting and developing field of study.

## PERSPECTIVE

Over the last decade, the roles of the RyR and  $\text{IP}_3\text{R}$   $\text{Ca}^{2+}$  release channels in intracellular  $\text{Ca}^{2+}$  signaling has started to be defined. Many basic properties of the different RyR and  $\text{IP}_3\text{R}$   $\text{Ca}^{2+}$  release channels have been described. Further, small local elementary  $\text{Ca}^{2+}$  release events that are generated by these channels were identified and the hierarchical nature of  $\text{Ca}^{2+}$  signaling revealed. The  $\text{Ca}^{2+}$  mobilized by individual channels generates local elemental  $\text{Ca}^{2+}$  release events. These local  $\text{Ca}^{2+}$  release events combine to produce the global  $\text{Ca}^{2+}$  release signals that drive a host of cellular phenomena. The specific sub-cellular localization of particular types of intracellular  $\text{Ca}^{2+}$  release channels is an important factor in the complex spatiotemporal nature of intracellular  $\text{Ca}^{2+}$  signaling. Although certain key elements and general concepts that govern intracellular  $\text{Ca}^{2+}$  release are known, it is clear that there are several others that are either poorly understood or entirely unknown.

Over the next decade, I believe it will become increasingly apparent that individual intracellular  $\text{Ca}^{2+}$  release channels are just one component in complex multi-protein  $\text{Ca}^{2+}$  signaling assemblies. I also believe that these assemblies will have all the components (i.e. surface receptors, enzymes, regulatory proteins, release channels, structural elements, etc.) that allow them to carry out specific and local  $\text{Ca}^{2+}$  signaling tasks. Research emphasis will gradually shift away from defining the function of the individual  $\text{Ca}^{2+}$  signaling elements to defining how a collection of elements operate in concert to control a local signaling process. In this context, defining mechanism will likely become increasingly important and challenging.

## References

1. Adams B.A., Tanabe T., Mikami A., Numa S., Beam KG. 1990. Intramembrane charge movement restored in dysgenic skeletal muscle by injection of dihydropyridine receptor cDNAs. *Nature*. 346(6284):569-72.
2. Armisen R., Sierralta J., Véllez P., Naranjo D., Suarez-Isla B.A. 1996. Modal gating in neuronal and skeletal muscle ryanodine-sensitive  $\text{Ca}^{2+}$  release channels. *Am.J.Physiol.* 271(1 Pt 1):C144-53.
3. Armstrong C.M., Bezaniilla F.M., Horowicz P. 1972. Twitches in the presence of ethylene glycol bis(-aminoethyl ether)-N,N'-tetracetic acid. *Biochimica et Biophysica Acta*. 267(3):605-8.
4. Berridge M.J. 1987. Inositol Trisphosphate and Diacylglycerol: Two Interacting second messengers, *Ann. Review Biochem.* 56:159-193.
5. Berridge M.J. and R.F. Irvine. 1984. Inositol Trisphosphate: A Novel Second Messenger in Cellular Signal Transduction, *Nature* 312:315-321.
6. Berridge, M.J., 1993. Inositol Trisphosphate and Calcium Signaling, *Nature* 361:567-570.
7. Bers, D.M. Excitation-contraction coupling and cardiac contractile force. *Kluwer Academic Pub (London)*, 1990.

8. Bers D.M., Fill M. 1998. Coordinated feet and the dance of ryanodine receptors. *Science*. 281:790-791.
9. Bezprozvanny I. et al. 1991. Bell-shaped Calcium-response Curves of Ins(1,4,5)P<sub>3</sub>- and Calcium-gated Channels from Endoplasmic Reticulum of Cerebellum, *Nature* 351:751-754.
10. Bridge JH, Ershler PR, Cannell MB. 1999. Properties of Ca<sup>2+</sup> sparks evoked by action potentials in mouse ventricular myocytes. *J Physiol* 518:469-478.
11. Cheng H., Lederer w.j., Cannell m.b. 1993. Calcium sparks: Elementary events underlying excitation-contraction coupling in heart muscle. *Science* 262:740-8.
12. Chu A., Fill M., Stefani E., Entman M.L. 1993. Cytoplasmic Ca<sup>2+</sup> does not inhibit the cardiac muscle sarcoplasmic reticulum ryanodine receptor Ca<sup>2+</sup> channel, although Ca<sup>2+</sup>-induced Ca<sup>2+</sup> inactivation of Ca<sup>2+</sup> release is observed in native vesicles. *J.Memb.Biol.* 135(1):49-59.
13. Copello J.A., Barg S., Onoue H., Fleischer S. 1997. Heterogeneity of Ca gating of skeletal muscle and cardiac ryanodine receptors. *Biophys.J.* 73(1):141-56.
14. Coronado R., Morrisette J., Sukhareva M., Vaughan D.M. 1994. Structure and function of ryanodine receptors. *Am.J.Physiol.* 266 (Cell Physiol. 35):C1485-C1504.
15. Dettbarn C, Gyorke S, Palade P. 1994. Many agonists induce "quantal" Ca<sup>2+</sup> release or adaptive behavior in muscle ryanodine receptors. *Mol Pharmacol.* 46:502-507.
16. Ehrlich B.E. et al. 1994. The Pharmacology of Intracellular Ca<sup>2+</sup>-release Channels, *TIPS* 15:145-149.
17. Ellies-Davies G.C.R., Kaplan j.h., Barsotti R.J. 1996. Laser photolysis of caged calcium: rates of calcium release by nitrophenyl-EGTA and DM-nitrophen. *Biophys.J.* 70:1006-1016.
18. Escobar A.L., Cifuentes F., Vergara J.L. 1995. Detection of Ca<sup>2+</sup>-transients elicited by flash photolysis of DM-nitrophen with a fast calcium indicator. *FEBS Letter* 364:335-338.
19. Fabiato A. 1985. Time and calcium dependence of activation and inactivation of calcium-induced release of calcium from the sarcoplasmic reticulum of a skinned cardiac Purkinje cell. *J.Gen.Physiol.* 85:247-289.
20. Franzini-Armstrong C., Kenney I.J., Varriano-Marson E. 1987. The structure of calsequestrin in triads of vertebrate skeletal muscle: a deep-etch study. *J. Cell Biol.* 105:49-56.
21. Furuichi T., Furutama D., Hakamata Y., Nakai J., Takeshima H., Mikoshiba K. 1994. Multiple types of ryanodine receptor/Ca<sup>2+</sup> release channels are differentially expressed in rabbit brain. *Journal of Neuroscience.* 14(8):4794-805.
22. Györke S., Fill m. 1993. Ryanodine receptor adaptation: control mechanism of Ca<sup>2+</sup>-induced Ca<sup>2+</sup> release in heart. *Science* 1993; 260:807-809.
23. Györke S., Vélez P., Suárez-Isla B.A., Fill M. 1994. Activation of single cardiac and skeletal ryanodine receptor channels by flash photolysis of caged Ca<sup>2+</sup>. *Biophys. J.* 66:1879-1886.
24. Györke I., Györke S. 1996. Adaptive control of intracellular Ca<sup>2+</sup> release in C2C12 mouse myotubes. *Pflügers Arch.* 431(6):838-843.
25. Hain J., Onoue h., Mayrleitner m., Fleischer s., Schindler h. 1995. Phosphorylation modulates the function of the calcium release channel of sarcoplasmic reticulum from cardiac muscle. *J.Biol.Chem.* 270:2074-2081.
26. Imredy JP, Yue DT. 1994. Mechanism of Ca(2+)-sensitive inactivation of L-type Ca<sup>2+</sup> channels. *Neuron.* 12:1301-1318.
27. Kaftan, E.J, B.E. Ehrlich and J. Watras. 1997. Inositol 1,4, 5-trisphosphate (InsP<sub>3</sub>) and calcium interact to increase the dynamic range of InsP<sub>3</sub> receptor-dependent calcium signaling. *J.Gen.Physiol.* 110:529-538.
28. Kim K.C., Caswell A.H., Talvenheim J.A., Brandt N.R. 1990. Isolation of a terminal cisterna protein which may link the dihydropyridine receptor to the junctional foot protein in skeletal muscle. *Biochemistry.* 29(39):9281-9.
29. Lamb G.D., Stephenson D.G. 1994. Activation of ryanodine receptors by flash photolysis of caged Ca<sup>2+</sup>. *Biophys. J.* 68:946-948.
30. Langer GA, Peskoff A. 1996. Calcium concentration and movement in the diadic cleft space of the cardiac ventricular cell. *Biophys.J.* 70:1169-1182.
31. Laver D.R., Roden I.d., Ahern g.p., Eager k.r., Junankar p.a., Dulhunty a.f. 1995. Cytoplasmic Ca<sup>2+</sup> inhibits the ryanodine receptor from cardiac muscle. *J. Memb. Biol.* 147:7-22.
32. Laver D.R., Curtis B.A. 1996. Response of ryanodine receptor channels to Ca<sup>2+</sup> steps produced by rapid solution exchange. *Biophys. J.* 71:732-741
33. Laver D.R, Lamb G.D. 1998. Inactivation of Ca<sup>2+</sup> release channels (ryanodine receptors RyR1 and RyR2) with rapid steps in [Ca<sup>2+</sup>] and voltage. *Biophys J.* 74:2352-2364.
34. Lipp P., Laine M., Tovey S.C., Burrell K.M., Berridge M.J., Li W. and Bootman MD. 2000. Functional InsP<sub>3</sub> receptors that may modulate excitation-contraction coupling in the heart. *Curr. Biol.* 2000 Jul 27-Aug 10;10(15):939-42
35. Lukyanenko V, Wiesner TF, Györke S. 1998. Termination of Ca<sup>2+</sup> release during Ca<sup>2+</sup> sparks in rat ventricular myocytes. *J.Physiol.* 507:667-677.
36. Lukyanenko V, Györke S. 1999. Ca<sup>2+</sup> sparks and Ca<sup>2+</sup> waves in saponin-permeabilized rat ventricular myocytes. *J.Physiol.* 521:575-585.
37. Lukyanenko V, Gyorke I, Subramanian S, Smirnov A, Wiesner TF, Gyorke S. 2000. Inhibition of Ca<sup>2+</sup> Sparks by Ruthenium Red in Permeabilized Rat Ventricular Myocytes. *Biophys. J.* 79(3).
38. Mak, D.-O. D., S. McBride and J.K. Foskett. 1998. Inositol-1,4,5-trisphosphate activation of inositol trisphosphate receptor Ca<sup>2+</sup> channel by ligand tuning of Ca<sup>2+</sup> inhibition. *Proc. Natl. Acad. Sci. USA* 95:15821-15825.
39. Marks A.R., Tempst p., Hwang k.s., Taubman m.b., Inui c., Chadwick c.c., Fleischer s., Nadal-Ginard b. 1989. Molecular cloning and characterization of the ryanodine receptor/junctional channel complex cDNA from skeletal muscle sarcoplasmic reticulum. *Proc. Natl. Acad. Sci. USA* 86:8683-8687.
40. Marks AR. 1996. Cellular functions of immunophilins. *Physiological Reviews.* 76(3):631-49.
41. Marx O.S., Ondrias K., Marks A.R. 1998 Coupled gating between individual skeletal muscle calcium release channels. *Science.* 281:818-820.
42. McCall E, Li L, Satoh H, Shannon TR, Blatter LA, Bers DM. 1996. Effects of FK-506 on contraction and Ca<sup>2+</sup> transients in rat cardiac myocytes. *Circ. Res. Dec;79(6):1110-21*
43. Mejia-Alvarez R, Kettlun C, Rios E, Stern M, Fill M. 1999. Unitary Ca<sup>2+</sup> current through cardiac ryanodine receptor channels under quasi-physiological ionic conditions. *J Gen Physiol.* 113:177-186.
44. Mignery G.A., Sudhof T.C., Takei K., Camilli P. 1989. Putative receptor for inositol 1,4,5-trisphosphate similar to ryanodine receptor. *Nature.* 342(6246):192-5.
45. Mignery G.A. and T.C. Sudhof. 1993. Molecular Analysis of Inositol 1,4,5-Trisphosphate Receptors, *Methods Neurosci.* 18: 247-265.
46. Moschella, M.C. and A.R Marks. 1993. Inositol 1,4,5-Trisphosphate Receptor Expression in Cardiac Myocytes, *J. Cell Biol.* 120:1137-1146.
47. Näbauer M., Morad m. 1990. Ca<sup>2+</sup>-induced Ca<sup>2+</sup> release as examined by photolysis of caged Ca<sup>2+</sup> in single ventricular myocytes. *Am. J. Physiol.* 285:C189-93.
48. Parker I., Zang w.j., Wier w.g. 1996. Ca<sup>2+</sup> sparks involving multiple Ca<sup>2+</sup> release sites along Z-lines in rat heart cells. *J. Physiol.* 497(Pt 1): 31-38.

49. Pizarro G., Shirokova N., Tsugorka A., Rios E. 1997. 'Quantal' calcium release operated by membrane voltage in frog skeletal muscle. *J. Physiol.* 501:289-303.
50. Ramos-Franco J. et al. 1998. Isoform-specific Function of Single Inositol 1,4,5-Trisphosphate Receptor Channels, *Biophys. J.* 75:834-839.
51. Rousseau E., Meissner G. 1989. Single cardiac sarcoplasmic reticulum Ca-release channel: activation by caffeine. *Am. J. Physiol.* 256(2 Pt 2):H328-33.
52. Schiefer A., Meissner G., Isenberg G. 1995. Ca<sup>2+</sup> activation and Ca<sup>2+</sup> inactivation of canine reconstituted cardiac sarcoplasmic reticulum Ca<sup>2+</sup>-release channels. *J. Physiol.* 489:337-348.
53. Schneider M.F., Chandler W.K. 1976. Effects of membrane potential on the capacitance of skeletal muscle fibers. *Journal of General Physiology.* 67(2):125-63.
54. SHAM J.S., Song L.S., Chen Y., Deng L.H. Stern M.D., Lakatta E.G., Cheng H. 1998. Termination of Ca<sup>2+</sup> release by a local inactivation of ryanodine receptors in cardiac myocytes. *Proc.Natl.Acad.Sci.USA.* 95:15096-15101.
55. Sitsapesan R., Williams a.j. 1995. The gating of the sheep skeletal sarcoplasmic reticulum Ca<sup>2+</sup> release channel is regulated by luminal Ca<sup>2+</sup>. *J. Memb.. Biol.* 146:133-144.
56. Stern M.D. 1992. Theory of excitation-contraction coupling in cardiac muscle. *Biophys J;* 63(2):497-517.
57. Stern M.D., Song L.S., Cheng H, Sham J.S., Yang H.T., Boheler K.R., Rios E. 1999. Local control models of cardiac excitation-contraction coupling. A possible role for allosteric interactions between ryanodine receptors. *J.Gen.Physiol.* 113:469-489.
58. Takeshima H. 1993. Primary structure and expression from cDNAs of the ryanodine receptor. *Ann. NY Acad. Sci. USA* 707:165-177.
59. Thrower EC, Hagar RE, Ehrlich BE. 2001. Regulation of Ins(1,4,5)P3 receptor isoforms by endogenous modulators. *Trends Pharmacol Sci,* 22(11):580-6
60. Tripathy A., Meissner G. 1996. Sarcoplasmic reticulum lumenal Ca<sup>2+</sup> has access to cytosolic activation and inactivation sites of skeletal muscle Ca<sup>2+</sup> release channel. *Biophys J* 70:2600-2615.
61. Valdivia H.H., Kaplan J.H, Ellies-Davies G.C.R. and Lederer W.J. 1995. Rapid adaptation of cardiac ryanodine receptors: modulation by Mg<sup>+</sup> and phosphorylation. *Science.* 267:1997-2000.
62. Velez P., Gyorke S., Escobar A., Vergara J., Fill M. 1997. Adaptation of single cardiac ryanodine receptor channels. *Biophys. J.* 72:691-697.
63. Zahradníková A., Zahradník I. 1995. Description of modal gating of the cardiac calcium release channel in planar lipid membranes. *Biophys. J.* 69:1780-1788.
64. Villalba-Galea CA, Suarez-Isla BA, Fill M, Escobar AL. 1998. Kinetic model for ryanodine receptor adaptation. *Biophys J* 74:A58.
65. Watras J. et al. 1991. Inositol 1,4,5-Trisphosphate-gated Channels in Cerebellum: Presence of Multiple Conductance States, *J. Neurosci.* 11:3239-3245.
66. Yao Y., Choi J. and Parker I. 1995. Quantal puffs of intracellular Ca<sup>2+</sup> evoked by inositol trisphosphate in *Xenopus* oocytes. *J Physiol* 1995 Feb 1;482 ( Pt 3):533-53  
Yasui K, Palade P, Gyorke S. 1994. Negative control mechanism with features of adaptation controls Ca<sup>2+</sup> release in cardiac myocytes. *Biophys J* 67:457-460.
67. Zahradníková A, Zahradník I. 1996. A minimal gating model for the cardiac calcium release channel. *Biophys J* 71:2996-3012.
68. Zahradníková A., Zahradník I., Györke I., Györke S. 1999. Rapid activation of the cardiac ryanodine receptor by submillisecond calcium stimuli. *J Gen Physiol.* 114:787-798.
69. Zorzato F., Flijii J., Otsu K., Phillips M., Green N.M., Lai F.A., Meissner G., MacLennan D.H. 1990. Molecular cloning of cDNA encoding human and rabbit forms of the Ca<sup>2+</sup> release channel (ryanodine receptor) of skeletal muscle sarcoplasmic reticulum. *Journal of Biological Chemistry.* 265(4):2244-56.
70. Zucker R.S. 1993. Calcium concentration clamp: spike and reversible pulses using the photolabile chelator DM-nitrophen. *Cell Calcium.* 14: 87-100.

**Correspondence:**

Michael Fill  
Loyola University Chicago  
Department of Physiology  
2160 South First Avenue  
Maywood, IL 60153

# Altered Communication Between L-Type Calcium Channels and Ryanodine Receptors in Heart Failure

J.-P. Bénitah, B.G. Kerfant, G. Vassort, S. Richard, A.M. Gómez  
INSERM U-390, Montpellier, France

**ABSTRACT** Heart failure (HF) is a progressive syndrome that appears as the final phase of most cardiac diseases and is manifested as a decreased contractile function. Contraction in cardiomyocytes arises by the  $\text{Ca}^{2+}$  induced  $\text{Ca}^{2+}$  release mechanism, where  $\text{Ca}^{2+}$  entry ( $I_{\text{Ca}}$ ) through  $\text{Ca}^{2+}$  channels (DHPRs) activates  $\text{Ca}^{2+}$  release channels (RyRs) in the junctional sarcoplasmic reticulum (SR). This is the base of cardiac excitation-contraction (EC) coupling. To elucidate the mechanisms underlying depressed function of the failing heart, analysis of EC coupling main elements have been undertaken.  $I_{\text{Ca}}$  density is usually maintained in HF. However, failing myocytes show a reduced SR  $\text{Ca}^{2+}$  release. Then, if the trigger of SR  $\text{Ca}^{2+}$  release is maintained, why is SR  $\text{Ca}^{2+}$  release depressed in HF? Analyses of the DHPR-RyR coupling efficiency have revealed a decrease in the  $I_{\text{Ca}}$  efficacy to trigger  $\text{Ca}^{2+}$  release in failing myocytes. In terminal heart failure without hypertrophy, a decrease in SR  $\text{Ca}^{2+}$  load can account for the decreased SR  $\text{Ca}^{2+}$  release. Fewer  $\text{Ca}^{2+}$  sparks (elementary units of SR  $\text{Ca}^{2+}$  release) are triggered by an equivalent  $I_{\text{Ca}}$  in hypertrophied failing myocytes, suggesting a functional or spatial reorganization of the space T-tubule junctional SR. This theory is supported by new data showing that the T-tubule density is reduced in failing cells.

## INTRODUCTION

The heart adapts to work in different situations to ensure adequate blood distribution. This adaptation can be fast, in response to an acute need, i.e. in a stress situation, adrenergic stimulation will have a fast inotropic effect. In response to a sustained pathological stimulus, the heart adapts to adjust cardiac output. In this case, the heart experiments biochemical, electrophysiological and structural changes, globally known as "remodeling" (1), that usually involve hypertrophy. Although hypertrophy is initially beneficial, sustained cardiac hypertrophy is a leading predictor for the development of sudden death and heart failure (HF) (2, 3).

For a long time, the process of heart remodeling has been divided in three phases (4). After the first phase ("development", hours to days after the initiating stimuli) the heart hypertrophies to meet the body needs. This period is called "compensated" hypertrophy. The compensation provided by hypertrophy is often limited and the cardiac pump function is compromised. During this new situation of "decompensated" hypertrophy, HF develops. The failing heart function is depressed and has less capacity to respond to acute needs. In systolic HF, the failing muscle pumps out blood with less strength than normal. In diastolic HF, the pump function may be normal, but it cannot relax normally and refilling of the ventricles is impaired. This last situation is characteristic of the HF found in the elderly.

Because  $\text{Ca}^{2+}$  activates contraction in the cardiac muscle, the major mechanism underlying contractile alterations during cardiac remodeling and its final outcome, heart failure, could be alterations in the  $\text{Ca}^{2+}$  signaling, or in the contractile proteins itself. We will focus here in collected data regarding  $\text{Ca}^{2+}$  signaling in heart remodeling.

## Etiology and stage of disease does matter

HF is a progressive syndrome that appears as the final phase of most cardiac diseases. The initiating insult can be acute as in myocardial infarction, gradual as in hemodynamic load (pressure or volume overload) or as in the case of many hereditary cardiomyopathies. Other acquired diseases, such as viral myocarditis can also induce heart remodeling. One must take into consideration the above discussion when integrating data regarding  $\text{Ca}^{2+}$  handling collected in different experimental models of hypertrophy and HF and define precisely the stage of the disease. Many apparent contradictory data may just reflect the different stages in the disease progression. In this view, ideally the best tissues to analyze would be human tissues. However, one major difficulty resides in the access to normal hearts, which is highly limited for obvious reasons (5, 6). Only terminally failing hearts obtained from transplants are available. Regardless of the variability in etiology, age and gender, all failing tissues are obtained from patients with long-term medications, which clearly hampers analysis and proper understanding of the disease progression. Consequently, many animal models have been used in an attempt to overcome these problems and better standardize the experimental conditions. The etiology and stage of the pathology can be determined more accurately, and the effect of medication is avoided although one cannot always extrapolate from the many animal models to human heart. Moreover, no animal model reproduces the wide variety of causes and manifestations of clinical syndromes in human. In addition to these limitations, several variables reviewed recently (7) underlie discrepancies found in different animal models: (i) pathophysiology of myocardial failure which varies among models; (ii) the studied molecular level, since discrepancies can potentially exist between mRNA level, protein level and function, both in normal and diseased tissues

(differences in terms of protein isoforms, sub-unit assembly, mRNA or protein degradation, regulation); (iii) the stage of the disease and time of measurement; and (iv) the experimental conditions themselves which are a major variable among groups.

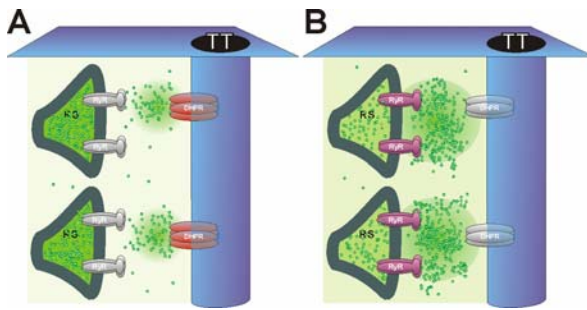


Fig.1 A. Animated cartoon showing the basis of cardiac excitation-contraction coupling. Membrane depolarization during an action potential activates L-type  $\text{Ca}^{2+}$  channels (DHPRs).  $\text{Ca}^{2+}$  influx increases the local  $[\text{Ca}^{2+}]_i$ , activating neighboring ryanodine receptors (RyRs).  $\text{Ca}^{2+}$  is extruded from the cell by the  $\text{Na}^+$ - $\text{Ca}^{2+}$  exchanger (NCX) and pumped back to the sarcoplasmic reticulum (SR) by the SR- $\text{Ca}^{2+}$  ATPase (SERCA). B. Animated confocal images of a Fluo-3 loaded rat ventricular myocyte stimulated at 1 Hz. Image dimensions are  $96 \times 74 \mu\text{m}$ .

### $\text{Ca}^{2+}$ HANDLING IN THE NORMAL HEART

Contraction arises when intracellular free  $\text{Ca}^{2+}$  level increases following activation by an action potential. Figure 1 shows the bases of cardiac excitation-contraction (EC) coupling. Membrane depolarization during an action potential activates voltage-dependent L-type  $\text{Ca}^{2+}$  channels (or dihydropyridine receptors, DHPRs) concentrated in the transverse tubules (TT). Charge carried by  $\text{Ca}^{2+}$  entry through these channels generates a current referred to as  $I_{\text{Ca}}$ . The resultant increase in  $[\text{Ca}^{2+}]_i$  activates  $\text{Ca}^{2+}$  release channels (or ryanodine receptors, RyRs) in the junctional sarcoplasmic reticulum (SR). This  $\text{Ca}^{2+}$ -induced  $\text{Ca}^{2+}$  release (CICR) mechanism is the basis of cardiac excitation-contraction (EC) coupling. By this mechanism, the initial  $\text{Ca}^{2+}$  signal is greatly amplified, then providing enough  $\text{Ca}^{2+}$  for contraction. CICR was first proposed by Fabiato (8) in skinned cardiac myocytes. Theoretical calculations on the CICR mechanisms suggested that  $\text{Ca}^{2+}$  release from the SR is not activated by elevation in the global  $[\text{Ca}^{2+}]_i$  (common pool theory) but by the *local* increase in  $[\text{Ca}^{2+}]_i$ , taking place in the restricted space between L-type  $\text{Ca}^{2+}$  channels and RyRs (9). The common pool theory would result in an all-or-none response, while a graded response is expected to result from the local control of EC coupling theory; the latter being physiologically more relevant. This theory was supported by the finding of non-propagating localized elevations of  $[\text{Ca}^{2+}]_i$  that correspond to the opening of one or few RyRs, named  $\text{Ca}^{2+}$  sparks (10). It was then demonstrated that a single L-type  $\text{Ca}^{2+}$  channel evokes one  $\text{Ca}^{2+}$  spark (11-13). Under the local control of EC coupling, the RyRs are relatively insensitive to  $\text{Ca}^{2+}$ , and only high  $[\text{Ca}^{2+}]_i$ , produced in the vicinity of a L-type  $\text{Ca}^{2+}$  channel, will be able to activate release through RyRs. Because  $\text{Ca}^{2+}$  diffuses away rapidly, the  $[\text{Ca}^{2+}]_i$  sensed by the RyR

is dependent on the physical distance from the DHPR (12). Thus, the efficient coupling of EC relies on a tight functional and spatial coupling of DHPRs and RyRs.

Relaxation occurs when cytoplasmic  $\text{Ca}^{2+}$  is both rapidly extruded from the cell through the  $\text{Na}^+$ - $\text{Ca}^{2+}$  exchanger and pumped back into the SR by the SR  $\text{Ca}^{2+}$  ATPase (SERCA). The sarcolemmal  $\text{Ca}^{2+}$  ATPase, different from SERCA, can also extrude some  $\text{Ca}^{2+}$ . However, its contribution appears to be minor (about 3% of total  $\text{Ca}^{2+}$  removal) and its physiological significance has yet to be determined. For equilibrium to occur, the amount of  $\text{Ca}^{2+}$  extruded through the  $\text{Na}^+$ - $\text{Ca}^{2+}$  exchanger should be equivalent to the amount of  $\text{Ca}^{2+}$  entering the cell through DHPRs, and the amount of  $\text{Ca}^{2+}$  transported by SERCA should be equivalent to  $\text{Ca}^{2+}$  released by the SR. These  $\text{Ca}^{2+}$ -extruding mechanisms not only allow relaxation but may also be indirectly involved in contraction, since they can modulate the amount of  $\text{Ca}^{2+}$  stored in the SR available for the next beat.

### $\text{Ca}^{2+}$ HANDLING IN HYPERTROPHIED AND FAILING MYOCYTES

$\text{Ca}^{2+}$  release and uptake originate contraction and relaxation. Consequently, alteration of  $\text{Ca}^{2+}$  handling has been suspected to drive the progression of functional abnormalities in hypertrophy and HF. Numerous analyses over the years have now provided a great body of evidence that  $\text{Ca}^{2+}$  handling is indeed altered. However, while some alterations are consistent among various models of hypertrophy and HF, some others are found only in failure and not in hypertrophy and they differ with the etiology.

Studies of  $[\text{Ca}^{2+}]_i$  transient have revealed several abnormalities. In a study comparing  $[\text{Ca}^{2+}]_i$  transient characteristics in human failing and hypertrophied non-failing hearts, an alteration of  $\text{Ca}^{2+}$  handling was evident in both, but it was more pronounced in failing hearts (14). This suggests that altered  $[\text{Ca}^{2+}]_i$  mobilization may develop early in the course of hypertrophy, before the onset of clinical signs of cardiac dysfunction. Abnormalities include decreased systolic  $\text{Ca}^{2+}$  and slowed decay phase. The slowing of the  $[\text{Ca}^{2+}]_i$  transient decay phase is perhaps the most consistent alteration (15-18). It has been correlated with a decrease in SERCA activity or expression, which is observed in some cases. However, it seems that contraction kinetics and  $[\text{Ca}^{2+}]_i$  transient characteristics are not constant in failing human ventricular cells, depending on dilated or ischemic cardiomyopathy etiology (19). These differences may account for the divergence in findings regarding SERCA in failing human myocytes that has been shown to be decreased or unaltered (for review see (20)). These alterations probably become critical at high beating rates because SR  $\text{Ca}^{2+}$  accumulation during shorter diastolic period may become dramatically inadequate to provide sufficient  $\text{Ca}^{2+}$  during systole. This process contributes largely to the negative force-frequency relationship reported in the failing human heart (21-23). Interestingly, after enhancing SERCA activity by either knocking out phospholamban or overexpressing SERCA, HF is prevented or rescued, respectively (24-27). Besides

alterations in relaxation, the lengthening of the  $[Ca^{2+}]_i$  transient decay could be responsible for lowering SR  $Ca^{2+}$  contents at higher frequencies and for frequency-dependent facilitation of  $I_{Ca}$  (see later). At the end of the action potential, the  $Na^+-Ca^{2+}$  exchanger (NCX) can work in reverse mode favoring  $Ca^{2+}$  entry, maintaining the  $[Ca^{2+}]_i$  transient and slowing relaxation. Thus, it has been proposed that the increased activity of the NCX can contribute to the decreased  $[Ca^{2+}]_i$  transient decay (28).

Besides slowed kinetics,  $[Ca^{2+}]_i$  transient amplitude seems modified in the remodeled heart, although different models have provided conflicting data. An increase of the SR  $Ca^{2+}$  release has been reported in models of early cardiac hypertrophy, together with hyperactivity, in spontaneous hypertensive rats (29-31). The increase in SR  $Ca^{2+}$  release during early stages of hypertrophy development has been correlated with longer action potential (AP) duration (32) while SR  $Ca^{2+}$  load is maintained (31). Some other models of hypertrophy have shown normal  $[Ca^{2+}]_i$  transient amplitude (33, 34), that can be reduced under some challenges, such as increase (35) or decrease (36) of extracellular  $[Ca^{2+}]_o$ . However, most analyses of the  $[Ca^{2+}]_i$  transient in tissue or isolated myocytes from failing hearts have evidenced a reduced capacity of the SR to release  $Ca^{2+}$  (37-46). Taken together, these data strongly suggest that SR  $Ca^{2+}$  release changes with the state of the heart adaptive response. In agreement with this notion, cell shortening and  $[Ca^{2+}]_i$  transient at two time points during autoimmune myocarditis in mice were normal at day 18<sup>th</sup> but reduced at day 35<sup>th</sup> (47). These observations suggest that the  $[Ca^{2+}]_i$  transient is progressively reduced with disease and that the weak contraction in failing myocytes may be due, at least in part, to a smaller SR  $Ca^{2+}$  release. Now, the challenge is to determine the molecular mechanisms that weaken the  $[Ca^{2+}]_i$  transient in failing hearts.

Theoretically, a decrease either in the triggering  $Ca^{2+}$  or in the EC coupling efficiency could account for reduced cellular contraction in HF. Defects may result from altered expression or function of proteins involved in  $Ca^{2+}$  homeostasis. There is indeed general agreement that disturbed SR function plays a significant role in the altered systolic and diastolic performance in human as well as in various animal models (48). To determine the defect(s) underlying the failure, investigators have long analyzed each of the elements involved in EC coupling. Here, we will overview these elements both in human and animal models of HF, focusing particularly on  $I_{Ca}$  and SR  $Ca^{2+}$  release. Simultaneous measurements of both  $I_{Ca}$  and SR  $Ca^{2+}$  release provide valuable information on the effectiveness of EC coupling.

### Triggers of SR $Ca^{2+}$ release

Calcium influx in cardiac myocytes is the initiating event in the EC coupling process. The sarcolemmal  $Ca^{2+}$  entry system includes two major proteins, namely the  $Na^+-Ca^{2+}$  exchanger and  $Ca^{2+}$  channels. Under certain circumstances,  $Ca^{2+}$  might also permeate through  $Na^+$  channels and activate SR  $Ca^{2+}$  release (49). Activation of this slip-mode

conductance in failing myocytes can improve  $Ca^{2+}$  signaling (40, 46).

### $Na^+-Ca^{2+}$ exchanger

The  $Na^+-Ca^{2+}$  exchanger (NCX) is a cation transporting protein. It exchanges 3  $Na^+$  for 1  $Ca^{2+}$  (50, 51) in either way. Although the normal "forward" mode is  $Ca^{2+}$  extrusion, which favors relaxation after each twitch, it can also work in the "reverse" mode inducing  $Ca^{2+}$  entry and thus probably triggering SR  $Ca^{2+}$  release (52), although with less efficiency than  $Ca^{2+}$  channels (53). In cardiac hypertrophy and HF, expression of the NCX seems altered. Increases in its mRNA and protein levels have been reported in human (54) and experimental (55) HF, although the functional meaning is controversial. For instance, Wang et al. (56) have confirmed the increase in NCX exchanger expression in a mice hypertrophy model but paradoxically the NCX current,  $I_{NCX}$ , was decreased. However, most investigators have found an increase in  $I_{NCX}$  both in hypertrophied and failing hearts (57-60). From an electrophysiological point of view, the increase in  $I_{NCX}$  may be arrhythmogenic (61); however, it is not clear whether the increase in NCX function is adaptive or deleterious for the  $Ca^{2+}$  handling of the hypertrophied and failing cell. In fact, because the NCX can work in both directions, it may be involved both in contraction and in relaxation (28). It seems that the increase in NCX function would be compensatory in cell relaxation. In human failing hearts with normal diastolic function, the NCX was upregulated while in hearts with impaired diastolic function the NCX expression was normal (62). Regarding the systolic function, a compensatory role has been proposed in compensatory hypertrophy, but the issue is more complicated. The underlying mechanism of the increased contraction would be an increase in SR  $Ca^{2+}$  load, favored by the *reverse* mode of the up regulated NCX (59). However in HF, up-regulation of the NCX could be deleterious because, working in *forward* mode would tend to decrease SR  $Ca^{2+}$  content (63). In summary, there is strong evidence that the NCX is up regulated both in hypertrophy and HF, but the physiopathologic consequences are unclear (64).

### $Ca^{2+}$ channels

$Ca^{2+}$  channels open transiently in response to depolarization and serve as the major pathway for  $Ca^{2+}$  entry into the myocytes. They permeate  $Ca^{2+}$  driven by its electrochemical gradient in a time- and voltage-dependent manner. In the myocardium, the coexistence of at least two populations of voltage-dependent  $Ca^{2+}$  channels (L-type and T-type) is well established. The T-type  $Ca^{2+}$  current ( $I_{Ca,T}$ ) has not been found in all mammalian species investigated, including human, but in the species where it is present, the efficacy of  $I_{Ca,T}$  to trigger SR  $Ca^{2+}$  release is much weaker than that of the L-type  $I_{Ca}$  (65).

### L-type $Ca^{2+}$ channels

The L-type  $Ca^{2+}$  channels (DHPRs) have been linked to the plateau phase of the action potential and play a crucial role in EC coupling. Initially termed 'slow inward current' (66, 67),  $I_{Ca}$

activates at depolarizations positive to  $-40$  mV, peaks near  $0$  mV and declines gradually at more positive voltages. Decay kinetics of the current include a fast  $\text{Ca}^{2+}$ -dependent component and a slow voltage-sensitive component. At the single channel level, this channel occupies three different basic modes: no opening or mode 0, short opening or mode 1 and long opening or mode 2 (68). The DHPR is constituted by a pore-forming subunit ( $\alpha_1\text{c}$  subunit), associated with auxiliary transmembrane subunits ( $\alpha_2$ - $\alpha$  subunit) and cytoplasmic regulatory subunits ( $\beta$  subunit) (69).

Many studies of  $I_{\text{Ca}}$  in hypertrophy and HF have been conducted but the results remain ambiguous (reviewed in (6, 70-73)). When investigating  $\text{Ca}^{2+}$  entry via  $I_{\text{Ca}}$  at least two parameters should be examined: (i) peak amplitude because it grades  $\text{Ca}^{2+}$  release from the SR; and, (ii) the decay kinetics because inactivation, which terminates  $\text{Ca}^{2+}$  entry, is likely to influence the AP repolarization. Regarding  $I_{\text{Ca}}$  density, the general trend is that cardiac hypertrophy ranges from no change to significant increase, whereas HF ranges from no change to significant decrease. It was thus tentatively proposed that  $I_{\text{Ca}}$  density would increase at early stages, be normalized during compensated hypertrophy, to finally decrease in late stage failure (70). This hypothesis was first postulated by Scamps et al. (74) to reconcile the unmodified  $I_{\text{Ca}}$  density observed in hypertrophied myocytes with the increase shown in hypertensive non-hypertrophied myocytes (75). This hypothesis predicts a decrease of  $I_{\text{Ca}}$  in severe HF such as human samples (always at the end-stage). However, in most studies of human failing myocytes and in animal models, the density of  $I_{\text{Ca}}$  is unchanged (6).

Both amplitude and kinetics of  $I_{\text{Ca}}$  may in part contribute to AP shape (76). Even if  $I_{\text{Ca}}$  peak density is maintained, slowing of its inactivation has been described in HF (reviewed in (73)) that might contribute to AP prolongation. Increased net  $\text{Ca}^{2+}$  entry would consequentially tend to enhance SR  $\text{Ca}^{2+}$  load and increase contraction.

Whole-cell current depends on both, number and individual properties of functional channels. Therefore, even if the macroscopic current seems unchanged, any modification of individual channel activity may be important in cardiac hypertrophy and HF. In human HF,  $\text{Ca}^{2+}$  channels were shown to switch activity from mode 1 to mode 2, showing higher availability and open probability (77). Since only one study analyzed single channel properties during human HF, one cannot definitively conclude whether this reflects a general feature. Moreover, extrapolation to whole-cell currents is difficult. In particular, one would expect larger  $I_{\text{Ca}}$  in HF cells. Surprisingly, the same study showed unchanged whole-cell  $I_{\text{Ca}}$ . One possibility to reconcile this disparity would be that HF cells have fewer but more active  $\text{Ca}^{2+}$  channels (78) as a result of an increase in channel phosphorylation. The latter could underlie the mode switching, too (79).

In this regard, myocytes from failing hearts are less responsive to  $\beta$ -adrenergic stimulation, which may be due to  $\beta$ -adrenergic receptor down-regulation or de-sensitization (80). Another

possibility is that the level of  $\text{Ca}^{2+}$  channel phosphorylation is increased in failing myocytes. Several facts support this interpretation: (1) the adrenergic tone is increased in HF patients (81) (2) single-channel records show increased activity (77), (3) some other proteins show increased phosphorylation state (82), and (4)  $\beta$ -adrenergic receptor blockers help in HF therapy (83). Furthermore, strengthening the  $\beta$ -adrenergic system has been proved beneficial to prevent the development of HF in transgenic mice, even in the presence of the instigating cause (45) (84). However, there is so far not enough evidence that  $\text{Ca}^{2+}$  channels are phosphorylated in human HF. In fact, forskolin, which also activates PKA phosphorylation of  $\text{Ca}^{2+}$  channels but bypasses  $\beta$ -adrenergic receptors, can increase  $I_{\text{Ca}}$  similarly in failing and control cells (85).

At the molecular level, a large discrepancy has been, once again, reported. In human HF (86) was revealed that mRNA expression for the  $\alpha_1\text{c}$  subunit and the abundance of dihydropyridine binding sites were reduced. More recently, unchanged expression of  $\alpha_1\text{c}$ -subunits was reported in end-stage or diastolic HF (77, 87-89). Ancillary subunits play important functional roles in the formation and stabilization of L-type  $\text{Ca}^{2+}$  channels (69, 90). Although mRNA levels of the  $\alpha_2/\alpha$ -subunit remained unchanged in diastolic human HF (87), either reduced or unchanged  $\beta$ -subunit mRNA levels were reported in human HF (77, 87). Nevertheless, the ratio of  $\beta$ -subunit mRNA over  $\alpha_1\text{c}$ -subunit mRNA was significantly reduced in both studies. Moreover, cardiac myocytes contain several isoforms of the  $\alpha_1\text{c}$ -subunit. Hypertrophy after myocardial infarction in rats is associated with re-emergence of the fetal isoform of the  $\alpha_1\text{c}$  gene (91). Similarly, the relative abundance of isoforms is changed in human ischemic HF (88), although the functional significance of isoform switching has not been established yet.

Regardless of the potential changes of  $I_{\text{Ca}}$  during cardiac hypertrophy and failure, two points that are usually underestimated have to be considered: (1) the electrophysiological landmark of hypertrophy and HF is the prolongation of AP duration induced, at least in part, by the down-regulation of the transient outward  $\text{K}^+$  current (73, 92-94) that regulates the height of the AP plateau during which  $I_{\text{Ca}}$  is active. Prolonged depolarization during the extended AP will thus enhance  $I_{\text{Ca}}$  contribution (95-97); (2) assuming unaltered  $I_{\text{Ca}}$  density in hypertrophy implies that the magnitude of  $I_{\text{Ca}}$  (and by extension, the total number of functional channels) is significantly increased in parallel with enlargement of cardiac myocytes. Therefore, a decrease in  $I_{\text{Ca}}$  density or DHPRs means a down- or no-regulation, whereas unchanged or increased  $I_{\text{Ca}}$  density means up-regulation. Interestingly, recent studies on a transgenic mouse model indicate that cardiac-specific overexpression of the L-type  $\text{Ca}^{2+}$  channel induces the development of hypertrophy and sets the stage for late-onset HF (98).

#### Activity of RyRs

Biochemical analysis of human failing hearts has revealed that the RyRs are

References	Model	$I_{Ca}$	$[Ca^{2+}]_i$ transient	$Ca^{2+}$ sparks	SR load
(31)	<b>Compensated hypertrophy:</b> SHR (rat)	=	↑	Bigger	=
(59)	AVB dog	=	↑		↑
(36)	Abdominal aortic constriction (rat)	=	(1 mM $Ca^{2+}]_o$ ) ↓ (0.5 mM $Ca^{2+}]_o$ )		=
(153)	Thoracic aortic constriction rabbit	= (DHPR density)	↓ (RyR density)		=
(38)	<b>Heart failure:</b> Dahl & SHHF rat	=	↓	Fewer, normal characteristics	=
(44)	Rat PMI	=	↓		
(46)	Rat PMI	=	↓	Fewer, normal characteristics	=
(103)	Rabbit PMI	↓	↓	Asynchronous	
(43)	Paced rabbit	↓	↓		
(61)	Aortic insufficiency + aortic constriction in Rabbit	=	↓		↓
(41)	Paced dog	=	↓		↓
(45)	<b>Transgenic mice:</b> MLP K.O.	=	↓	Normal characteristics	=
(40)	Viral myocarditis	=	↓		
(42)	Calsequestrin overexpression	=	↓	Fewer, diffused	↑
(18, 39, 107)	<b>Human</b> Terminal Heart Failure	=	↓		↓

Table 1: Several analysis of EC coupling in cardiac hypertrophy and heart failure

hyperphosphorylated (82) (detailed in other chapter of this issue), although no difference has been reported in RyR phosphorylation in the fast-paced dog HF model (99). Bilayer experiments have shown that RyRs phosphorylation would increase its open probability and accelerate adaptation (100). *In vivo*, RyRs are located in clusters that open synchronously (coupled gating) to produce one  $Ca^{2+}$  spark. Phosphorylation of RyRs unbinds FK 506 binding protein from the RyRs and induces uncoupled gating (101). So far the pathological implication is not clear. The RyR hyperphosphorylation in terminal human HF would be associated to changes in  $Ca^{2+}$  sparks characteristics. However, this kind of analysis has not been undertaken and the  $Ca^{2+}$  sparks characteristics in animal models of HF do not recapitulate the changes after PKA phosphorylation (38, 42, 45, 46).

#### Effectiveness of coupling

Even if  $I_{Ca}$  density is maintained, the AP duration is increased in cardiac hypertrophy and HF (38, 73, 102). The consequence should be an increased  $Ca^{2+}$  entry during the longer depolarization period in failing cells. Since HF cells contract less, despite AP prolongation, one must conclude that the prolongation of  $Ca^{2+}$  influx still does not provide enough  $Ca^{2+}$  for normal activation of contractile proteins. In fact, even AP-evoked  $[Ca^{2+}]_i$  transients are reduced in HF (46, 103). The question remains, if  $Ca^{2+}$  entry seems not to be decreased in HF, then why the heart fails?

Simultaneous measurements of  $I_{Ca}$  and SR  $Ca^{2+}$  release in different models have suggested that the mechanism of EC coupling, more precisely the  $Ca^{2+}$ -induced  $Ca^{2+}$ -release (CICR), is altered in HF (see Table 1). It was shown that  $I_{Ca}$ , which triggers SR  $Ca^{2+}$  release, was normal in failing human myocytes, but the  $[Ca^{2+}]_i$  transient was

depressed (18, 37). This means that for the same triggering  $\text{Ca}^{2+}$ , less  $\text{Ca}^{2+}$  is released. Similar results have also been observed in animal models of HF (38, 40, 42, 45, 46, 78). Now the underlying defect of this *uncoupling* must be identified. A detailed analysis of EC coupling entails determination of the efficacy of  $I_{\text{Ca}}$  to trigger  $\text{Ca}^{2+}$  release by simultaneously measuring  $I_{\text{Ca}}$  and SR  $\text{Ca}^{2+}$  release in its elementary events. In this way, one can determine how many  $\text{Ca}^{2+}$  sparks are triggered by a given  $\text{Ca}^{2+}$  entry. Likewise, the analysis of  $\text{Ca}^{2+}$  sparks characteristics provides an insight of RyR activity. We have undertaken this kind of analysis in two different models of pressure-overload decompensated hypertrophy (38). The first was the Dahl rat model. These animals are a strain of Sprague-Dawley that was selected by its sensitivity to sodium intake. The salt-sensitive rats develop hypertension when fed with a high salt diet. With time, their hearts hypertrophy and ultimately develop HF. The salt-resistant rats do not develop any alteration at the same high salt diet (104). At the time of experiments, the salt-sensitive animals experienced cardiac hypertrophy although no signs yet of congestive HF. However, isolated myocytes were failing. They showed a normal  $I_{\text{Ca}}$  (although slowed inactivation kinetics, see later) but the associated  $[\text{Ca}^{2+}]_i$  transient and contraction (shortening) was weak (38). To analyze the reason why the SR  $\text{Ca}^{2+}$  release was reduced, one approach was to estimate the SR  $\text{Ca}^{2+}$  load that was shown to be unchanged. Next was to count and analyze the  $\text{Ca}^{2+}$  sparks evoked by  $I_{\text{Ca}}$  at several potentials. Such analysis showed that the number of  $\text{Ca}^{2+}$  sparks triggered by equivalent  $I_{\text{Ca}}$  was greatly reduced in failing myocytes compared to match controls (38). That is, the coupling between L-type  $\text{Ca}^{2+}$  channels and RyRs was defective. Nevertheless, the cells maintained the ability to compensate by  $\beta$ -adrenergic stimulation. These results were compared with another model of pressure-overload disease in overt HF. Similar data was obtained, although in this case the  $\beta$ -adrenergic stimulation was ineffective to overcome the defect (38). This suggests that the defective EC coupling may be underlying HF and was unmasked when systemic compensation was not effective anymore. The decreased SR  $\text{Ca}^{2+}$  release was underlying the decreased cellular contraction. Because the global  $[\text{Ca}^{2+}]_i$  transient is constituted by the temporal and spatial summation of  $\text{Ca}^{2+}$  sparks (105) the depressed  $[\text{Ca}^{2+}]_i$  transient is due to fewer  $\text{Ca}^{2+}$  sparks. Today, it is generally accepted that a  $\text{Ca}^{2+}$  spark is produced by a group of RyRs acting in concert. Analysis of RyRs showed that the density of RyRs was unchanged in these failing myocytes, as was their  $\text{Ca}^{2+}$  sensitivity (38). This is further supported by the unchanged characteristics of  $\text{Ca}^{2+}$  sparks. The later finding suggests that there is no change in the activity of RyRs and confirms that the SR  $\text{Ca}^{2+}$  load is unchanged in these models of HF. In fact, once the RyR opens,  $\text{Ca}^{2+}$  is released down its concentration gradient. If the SR load were reduced, the  $\text{Ca}^{2+}$  spark amplitude would be reduced because it depends on SR  $\text{Ca}^{2+}$  load (106). Because RyRs were found normal in number and  $\text{Ca}^{2+}$  sensitivity, it seems that there are fewer  $\text{Ca}^{2+}$  sparks in failing myocytes because the release units

failed to be triggered. Since the trigger ( $I_{\text{Ca}}$ ) is normal, these data suggest that the relationship DHPRs – RyRs is altered in HF. Few other studies have analyzed the elementary EC coupling in other models of HF. Recently we have shown that the same defect is also present in a model of HF after myocardial infarct in the rat (46). In the calsequestrin overexpression transgenic mice, the number of  $\text{Ca}^{2+}$  sparks was also shown to be reduced even though the SR  $\text{Ca}^{2+}$  load was highly increased (42). But in this case, the fewer  $\text{Ca}^{2+}$  sparks could be due to the reduced RyR density of this transgenic model. During compensated hypertrophy, in the spontaneously hypertensive rats, bigger  $\text{Ca}^{2+}$  sparks underlie bigger  $[\text{Ca}^{2+}]_i$  transients and enhanced contractility, while the triggering  $I_{\text{Ca}}$  was also unchanged (31). Taken together, these data provide evidence that the relationship between DHPR and RyRs is modulated during the development of cardiac hypertrophy with: (i) an increase in the EC coupling gain underlying the increased contractility of this adaptive process; and (ii) a decrease as HF develops, underlying the decreased contractility.

#### **Defects underlying the EC uncoupling**

Data from human HF cells have been collected from terminally failing hearts obtained during transplantation. Very often, different etiologies are mixed together and the patients have a long history of medication, which render conclusions difficult. Nevertheless, it is always useful and necessary to know what happens in the human heart; even if limited to the end-stage of HF. Ventricular myocytes isolated from terminally failing human hearts had a decreased EC coupling gain (37). In fact, while the triggering  $I_{\text{Ca}}$  was maintained in density, the triggered  $[\text{Ca}^{2+}]_i$  transient was depressed. Moreover, the elevation in  $[\text{Ca}^{2+}]_i$  due to the L-type  $\text{Ca}^{2+}$  channel (with empty SR) was similar in both failing and normal hearts. The depressed  $[\text{Ca}^{2+}]_i$  transient was thus due to a smaller SR  $\text{Ca}^{2+}$  release (39) although in these non-hypertrophied failing cells, a decrease in SR  $\text{Ca}^{2+}$  content may, at least in part, explain the decrease in the efficacy of the  $I_{\text{Ca}}$  to trigger SR  $\text{Ca}^{2+}$  release (107). Similar explanation has been suggested in a model of paced-induced HF (41). Interestingly, this model also induces HF without cellular hypertrophy (60).

In cardiac hypertrophy and HF with cellular hypertrophy, the reorganization of the cellular structure as cell grows may be important determinants of defective EC coupling. In fact, there is a growing body of evidence suggesting that alterations in cardiac cytoskeletal proteins may induce dilated cardiomyopathy (108). Moreover, several transgenic mice with alterations in the cytoskeleton develop HF, such as the muscle LIM protein (MLP) knock out mice. They develop dilated cardiomyopathy and HF with hypertrophy (109) and decrease in the EC coupling efficiency (45). MLP is a protein involved in cytoarchitecture organization. Likewise, desmin (constituent of the intermediate filaments in muscle) deficiency induces cardiomyopathy (110) with cell hypertrophy and alterations in  $\text{Ca}^{2+}$  handling (111). Interestingly, acquired cardiac hypertrophy induces changes in

the cytoskeleton. More precisely, it has been reported that HF following chronic hypertension is associated with an increase in the density of another cytoskeleton component, the microtubules (112). Very interestingly, microtubule proliferation in the failing cell may be involved in the contractile abnormalities since microtubule depolymerization normalizes contraction in failing cells (112). Moreover, it has been shown that microtubule proliferation can decrease  $[Ca^{2+}]_i$  transient (113), whereas microtubule depolymerization increases  $[Ca^{2+}]_i$  transient (114) and modifies  $Ca^{2+}$  sparks characteristics (115). Because CICR occurs mainly at the region of junctional SR (where RyRs are located) close to the TT (where the DHPRs are located), a rearrangement in the spatial organization of DHPRs and RyRs in the dyadic cleft or a disruption in the TT system during remodeling would have severe consequences in EC coupling in the failing myocytes (Fig. 2). In this line, alterations in the TT system have been reported in hypertrophied cells from human failing myocardium (116). In a HF model of paced dog with significant cellular hypertrophy, a decrease in TT density has been shown (78), and it seems that a similar pattern could be present in human HF (117).

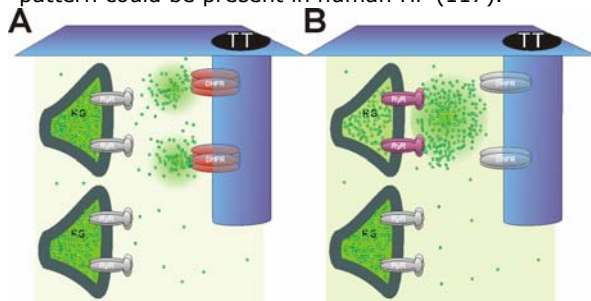


Fig. 2. Simplified animated cartoon showing the main excitation-contraction coupling elements as in Fig.1. Spatial remodeling can underlie the decrease in the EC coupling gain observed in heart failure (46).

$[Ca^{2+}]_i$  in the dyadic cleft induced by the  $KyR$  opening inactivates the L-type  $Ca^{2+}$  channel (118). In fact, analysis of the  $I_{Ca}$  inactivation time constant provides an insight of the magnitude of release. In this regard, most studies have shown a lengthening of the fast component of  $I_{Ca}$  inactivation (38, 73, 119) that could reflect decreased  $[Ca^{2+}]_i$  transient in HF. This hypothesis is supported by a theoretical model predicting that, under conditions of reduced SR  $Ca^{2+}$  release, there is less  $Ca^{2+}$ -dependent inactivation of  $I_{Ca}$ , which helps to prolong the plateau phase of the AP (120). Indeed, SR  $Ca^{2+}$  release inactivates up to 50% of net  $Ca^{2+}$  entry through  $Ca^{2+}$  channels (121). Besides slowing of  $I_{Ca}$  inactivation at a given frequency, increasing stimulation frequency in cardiac myocytes slows  $I_{Ca}$  inactivation with a subsequent increase in net  $Ca^{2+}$  entry. This phenomenon is termed  $I_{Ca}$  facilitation and is dependent on SR  $Ca^{2+}$  release (119, 122). Facilitation of  $I_{Ca}$  occurs over a range of frequencies corresponding to rates encountered in pathophysiological states. Higher rates produce a marked lengthening of  $I_{Ca}$  inactivation and, as a direct consequence, a slight increase in peak current, which is unrelated to recruitment of new channels. Simultaneous measurements of  $I_{Ca}$

facilitation and SR  $[Ca^{2+}]_i$  release have revealed that this phenomenon results from a decrease of the  $[Ca^{2+}]_i$  transient at high frequencies in rat ventricular myocytes (122). Moreover, thapsigargin and ryanodine induced similar "pharmacological"  $I_{Ca}$  facilitation (119, 122). In this regard,  $I_{Ca}$  facilitation in HF can be used as an index of the coupling DHPR-RyR. Interestingly,  $I_{Ca}$  facilitation is rarely observed in human HF when comparing either with ventricular cells from other mammals or atrial cells from HF and non-HF patients (72, 119, 123, 124). Furthermore, even at low stimulation rates, inactivation of  $I_{Ca}$  is slow in HF cells which is consistent with weaker SR  $Ca^{2+}$ -release and, thereby, weaker  $Ca^{2+}$ -dependent inactivation (119).

#### PERSPECTIVES: IMPORTANCE OF $Ca^{2+}$ CYCLING IN THE PROGRESSION OF HF

Remodeling during cardiac hypertrophy and failure is usually accompanied by complex changes in gene expression reprogramming (1). In recent years, it has become apparent that  $Ca^{2+}$  also plays a role in this longer-term regulation. This represents a second mechanism, via long-term adaptation, by which  $Ca^{2+}$  might alter the function of cardiac muscle. It has been suggested that alterations in  $Ca^{2+}$  handling proteins progressively exacerbate a hypertrophic or cardiomyopathic phenotype, in part, through sustained activation of  $Ca^{2+}$ -sensitive signaling pathways. The intricate signaling network that causes cardiac hypertrophy (125) involves  $Ca^{2+}$ -dependent gene regulation as a necessary component (126, 127). In the first phase of hypertrophy response (min to hours), early response genes, e.g. c-fos, c-myc, c-jun, are activated (128). In cardiac myocytes, transcriptional induction via c-jun has been related to intracellular  $Ca^{2+}$  (129, 130). Moreover,  $Ca^{2+}$  influx through L-type  $Ca^{2+}$  channels is critical for early response gene stimulation by a variety of stimuli, including neurotransmitters and growth factors (131, 132). Intracellular  $[Ca^{2+}]_i$  may also affect expression of late genes. Subject of intense research over the past decade, the signaling cascades underlying alteration in gene expression in cardiac hypertrophy and HF converge on the MAPK cascade (133, 134). Activation of this pathway by hypertrophy stimulus depends on transsarcolemmal influx of  $Ca^{2+}$  (135). A  $Ca^{2+}$  sensitive mechanism, which involves  $Ca^{2+}$ /Calmodulin pathway, seems to be important for activation of MAPK cascade (136). Over-expression of calmodulin (CaM) in transgenic mice causes myocytes hypertrophy (137). Calmodulin, when activated by  $Ca^{2+}$ , modulates the activity of a number of enzymes, including CaM-dependent protein kinases involved in transcriptional regulation (47, 138, 139). Recently, it has been shown that the CaM kinase pathway is sufficient to activate many features of cardiac hypertrophy and failure in vivo (140, 141). Recent studies have shown that the  $Ca^{2+}$ /calcineurin pathway is a necessary component for the expression of hypertrophy markers (126) although this has been subject of controversy (142). As matter of fact, overexpressing calcineurin in a transgenic mouse produced a rapid development of hypertrophy and HF (143). Calcineurin is a specific  $Ca^{2+}$ -dependent phosphatase that dephosphorylates

transcription factors, which turn on a panel of hypertrophy genes.

Thus, when considering all the published studies on HF, a central and perhaps essential role for intracellular  $\text{Ca}^{2+}$  is inescapable, not only on altered cardiac contraction, but also on altered gene expression. In cardiomyocytes, EC coupling thus regulates the transcription activity by process termed *excitation-transcription* coupling. This process represents an elementary pathway whereby, through  $\text{Ca}^{2+}$  signaling, the electrical activity of a cell feeds back upon and shapes the cellular genetic program (144, 145). This has been nicely evidenced in smooth muscle (146, 147). For instance, activation of  $\text{Ca}^{2+}$  influx through the L-type  $\text{Ca}^{2+}$  channel by membrane depolarization increased  $\text{Ca}^{2+}$  sparks frequency, which in turn activated the cAMP-responsive element-binding protein and subsequent c-fos expression.

Recently, we provided new data on the implication of this pathway in an aldosterone-induced down-regulation of the transient outward  $\text{K}^+$  current ( $\text{I}_{\text{to},1}$ ) functional expression, which might be involved in hypertrophy and HF (148). This mineralocorticoid hormone might be one of the primary factors in the remodeling of hypertrophy and HF (149-151). Incubation of adult rat isolated cardiomyocytes in the presence of aldosterone induces a specific and genomic up-regulation of functional expression of L-type  $\text{Ca}^{2+}$  channels (152). When this stimulation is sufficient, then it induces an increase in  $\text{Ca}^{2+}$  sparks occurrence, which is able to down-regulate the functional expression of  $\text{I}_{\text{to},1}$  (148).

We should expect, in the near future, new insights into the mechanisms by which intracellular  $\text{Ca}^{2+}$  influences the progression of hypertrophy and HF.

#### ACKNOWLEDGMENTS

We wish to thank Dr. W.J. Lederer for numerous discussions about  $\text{Ca}^{2+}$  signaling in heart failure. We acknowledge FRM (Fondation pour la recherche médicale, S.R., INE20001117051) for financial support. AMG and SR are CNRS (Centre National de la Recherche Scientifique) scientists.

#### REFERENCES

1. Swynghedauw, B.: Molecular mechanisms of myocardial remodeling. *Physiol Rev* 79, 215-62 (1999)
2. Kannel, W. B.: Left ventricular hypertrophy as a risk factor: the Framingham experience. *J Hypertens Suppl* 9, S3-8; discussion S8-9. (1991)
3. Pye, M. P. and Cobbe, S. M.: Mechanisms of ventricular arrhythmias in cardiac failure and hypertrophy. *Cardiovasc Res* 26, 740-50. (1992)
4. Meerson, F. Z.: The myocardium in hyperfunction, hypertrophy and heart failure. *Circ Res* 25, Suppl 2:1-163. (1969)
5. Lorente, P., Delgado C., Bénitah, J., Bailly, P., & Gomez, A. in *Cardiac electrophysiology. From cell to bedside*. (eds. Zipes D. & Jalife J.) 277-291 (WB. Saunders Company, Philadelphia, 1995).
6. Bénitah, J. P., Gómez, A. M., Fauconnier, J., Kerfant, B. G., Perrier, E., Vassort, G. and Richard, S.: Voltage-gated  $\text{Ca}^{2+}$  currents in the human pathophysiologic heart: a review. *Basic Res Cardiol*, in press (2001)
7. Hasenfuss, G.: Animal models of human cardiovascular disease, heart failure and hypertrophy. *Cardiovasc Res* 39, 60-76. (1998)
8. Fabiato, A. and Fabiato, F.: Use of chlorotetracycline fluorescence to demonstrate  $\text{Ca}^{2+}$ -induced release of  $\text{Ca}^{2+}$  from the sarcoplasmic reticulum of skinned cardiac cells. *Nature* 281, 146-8. (1979)
9. Stern, M. D.: Theory of excitation-contraction coupling in cardiac muscle. *Biophys J* 63, 497-517. (1992)
10. Cheng, H., Lederer, W. J. and Cannell, M. B.: Calcium sparks: elementary events underlying excitation-contraction coupling in heart muscle. *Science* 262, 740-4 (1993)
11. Lopez-Lopez, J. R., Shacklock, P. S., Balke, C. W. and Wier, W. G.: Local calcium transients triggered by single L-type calcium channel currents in cardiac cells. *Science* 268, 1042-5 (1995)
12. Santana, L. F., Cheng, H., Gómez, A. M., Cannell, M. B. and Lederer, W. J.: Relation between the sarcolemmal  $\text{Ca}^{2+}$  current and  $\text{Ca}^{2+}$  sparks and local control theories for cardiac excitation-contraction coupling. *Circ Res* 78, 166-71 (1996)
13. Wang, S. Q., Song, L. S., Lakatta, E. G. and Cheng, H.:  $\text{Ca}^{2+}$  signalling between single L-type  $\text{Ca}^{2+}$  channels and ryanodine receptors in heart cells. *Nature* 410, 592-6. (2001)
14. Gwathmey, J. K., Bentivegna, L. A., Ransil, B. J., Grossman, W. and Morgan, J. P.: Relationship of abnormal intracellular calcium mobilisation to myocyte hypertrophy in human ventricular myocardium. *Cardiovasc Res* 27, 199-203. (1993)
15. Gwathmey, J. K. and Morgan, J. P.: Altered calcium handling in experimental pressure-overload hypertrophy in the ferret. *Circ Res* 57, 836-43 (1985)
16. Gwathmey, J. K., Copelas, L., MacKinnon, R., Schoen, F. J., Feldman, M. D., Grossman, W. and Morgan, J. P.: Abnormal intracellular calcium handling in myocardium from patients with end-stage heart failure. *Circ Res* 61, 70-6. (1987)
17. Bentivegna, L. A., Ablin, L. W., Kihara, Y. and Morgan, J. P.: Altered calcium handling in left ventricular pressure-overload hypertrophy as detected with aequorin in the isolated, perfused ferret heart. *Circ Res* 69, 1538-45 (1991)
18. Beuckelmann, D. J. and Erdmann, E.:  $\text{Ca}^{2+}$ -currents and intracellular  $[\text{Ca}^{2+}]_i$ -transients in single ventricular myocytes isolated from terminally failing human myocardium. *Basic Res Cardiol* 87 Suppl 1, 235-43. (1992)
19. Sen, L., Cui, G., Fonarow, G. C. and Laks, H.: Differences in mechanisms of SR dysfunction in ischemic vs. idiopathic dilated cardiomyopathy. *Am J Physiol Heart Circ Physiol* 279, H709-18. (2000)
20. Houser, S. R., Piacentino, V., 3rd and Weisser, J.: Abnormalities of calcium cycling in the hypertrophied and failing heart. *J Mol Cell Cardiol* 32, 1595-607. (2000)
21. Schillinger, W., Lehnart, S. E., Prestle, J., Preuss, M., Pieske, B., Maier, L. S., Meyer, M., Just, H. and Hasenfuss, G.: Influence of SR  $\text{Ca}^{2+}$ -ATPase and  $\text{Na}^{+}$ - $\text{Ca}^{2+}$ -exchanger on the force-frequency relation. *Basic Res Cardiol* 93, 38-45. (1998)
22. Mulieri, L. A., Hasenfuss, G., Leavitt, B., Allen, P. D. and Alpert, N. R.: Altered myocardial force-frequency relation in human heart failure. *Circulation* 85, 1743-50. (1992)
23. Pieske, B., Kretschmann, B., Meyer, M., Holubarsch, C., Weirich, J., Posival, H., Minami, K., Just, H. and Hasenfuss, G.: Alterations in intracellular calcium handling associated with the inverse force-frequency relation in human dilated cardiomyopathy. *Circulation* 92, 1169-78. (1995)
24. Minamisawa, S., Hoshijima, M., Chu, G., Ward, C. A., Frank, K., Gu, Y., Martone, M. E., Wang, Y., Ross, J., Jr., Kranias, E. G., Giles, W. R. and Chien, K. R.: Chronic phospholamban-sarcoplasmic reticulum calcium ATPase interaction is the critical calcium cycling defect in dilated cardiomyopathy. *Cell* 99, 313-22 (1999)
25. del Monte, F., Harding, S. E., Schmidt, U., Matsui, T., Kang, Z. B., Dec, G. W., Gwathmey, J. K., Rosenzweig, A. and Hajjar, R. J.: Restoration of Contractile Function in Isolated Cardiomyocytes From

- Failing Human Hearts by Gene Transfer of SERCA2a. *Circulation* 100, 2308-2311 (1999)
26. Reilly, A. M., Petrou, S., Panchal, R. G. and Williams, D. A.: Restoration of calcium handling properties of adult cardiac myocytes from hypertrophied hearts. *Cell Calcium* 30, 59-66. (2001)
  27. Sato, Y., Kiriazis, H., Yatani, A., Schmidt, A. G., Hahn, H., Ferguson, D. G., Sako, H., Mitarai, S., Honda, R., Mesnard-Rouiller, L., Frank, K. F., Beyermann, B., Wu, G., Fujimori, K., Dorn, G. W., 2nd and Kranias, E. G.: Rescue of contractile parameters and myocyte hypertrophy in calsequestrin overexpressing myocardium by phospholamban ablation. *J Biol Chem* 276, 9392-9. (2001)
  28. Gaughan, J. P., Furukawa, S., Jeevanandam, V., Hefner, C. A., Kubo, H., Margulies, K. B., McGowan, B. S., Mattiello, J. A., Dipla, K., Piacentino, V., Li, S. and Houser, S. R.: Sodium/calcium exchange contributes to contraction and relaxation in failed human ventricular myocytes. *Am J Physiol* 277, H714-24. (1999)
  29. Gao, W. D., Perez, N. G., Seidman, C. E., Seidman, J. G. and Marbán, E.: Altered cardiac excitation-contraction coupling in mutant mice with familial hypertrophic cardiomyopathy. *J Clin Invest* 103, 661-6 (1999)
  30. Nagata, K., Liao, R., Eberli, F. R., Satoh, N., Chevalier, B., Apstein, C. S. and Suter, T. M.: Early changes in excitation-contraction coupling: transition from compensated hypertrophy to failure in Dahl salt-sensitive rat myocytes. *Cardiovasc Res* 37, 467-77. (1998)
  31. Shorofsky, S. R., Aggarwal, R., Corretti, M., Baffa, J. M., Strum, J. M., Al-Seikhan, B. A., Kobayashi, Y. M., Jones, L. R., Wier, W. G. and Balke, C. W.: Cellular mechanisms of altered contractility in the hypertrophied heart: big hearts, big sparks. *Circ Res* 84, 424-34 (1999)
  32. Brooksby, P., Levi, A. J. and Jones, J. V.: Investigation of the mechanisms underlying the increased contraction of hypertrophied ventricular myocytes isolated from the spontaneously hypertensive rat. *Cardiovasc Res* 27, 1268-77 (1993)
  33. Anand, I. S., Liu, D., Chugh, S. S., Prahash, A. J., Gupta, S., John, R., Popescu, F. and Chandrasekhar, Y.: Isolated myocyte contractile function is normal in postinfarct remodeled rat heart with systolic dysfunction. *Circulation* 96, 3974-84 (1997)
  34. Perez, N. G., Hashimoto, K., McCune, S., Altschuld, R. A. and Marbán, E.: Origin of contractile dysfunction in heart failure: calcium cycling versus myofilaments. *Circulation* 99, 1077-83 (1999)
  35. Tajima, M., Bartunek, J., Weinberg, E. O., Ito, N. and Lorell, B. H.: Atrial Natriuretic Peptide Has Different Effects on Contractility and Intracellular pH in Normal and Hypertrophied Myocytes From Pressure-Overloaded Hearts. *Circulation* 98, 2760-2764 (1998)
  36. McCall, E., Ginsburg, K. S., Bassani, R. A., Shannon, T. R., Qi, M., Samarel, A. M. and Bers, D. M.: Ca flux, contractility, and excitation-contraction coupling in hypertrophic rat ventricular myocytes. *Am J Physiol* 274, H1348-60 (1998)
  37. Beuckelmann, D. J., Nabauer, M. and Erdmann, E.: Intracellular calcium handling in isolated ventricular myocytes from patients with terminal heart failure. *Circulation* 85, 1046-55. (1992)
  38. Gómez, A. M., Valdivia, H. H., Cheng, H., Lederer, M. R., Santana, L. F., Cannell, M. B., McCune, S. A., Altschuld, R. A. and Lederer, W. J.: Defective excitation-contraction coupling in experimental cardiac hypertrophy and heart failure. *Science* 276, 800-6. (1997)
  39. Beuckelmann, D. J.: Contributions of Ca(2+)-influx via the L-type Ca(2+)-current and Ca(2+)-release from the sarcoplasmic reticulum to [Ca2+]i-transients in human myocytes. *Basic Res Cardiol* 92 Suppl 1, 105-10. (1997)
  40. Wessely, R., Klingel, K., Santana, L. F., Dalton, N., Hongo, M., Jonathan Lederer, W., Kandolf, R. and Knowlton, K. U.: Transgenic expression of replication-restricted enteroviral genomes in heart muscle induces defective excitation-contraction coupling and dilated cardiomyopathy. *J Clin Invest* 102, 1444-53 (1998)
  41. Hobai, I. A. and O'Rourke, B.: Decreased sarcoplasmic reticulum calcium content is responsible for defective excitation-contraction coupling in canine heart failure. *Circulation* 103, 1577-84. (2001)
  42. Jones, L. R., Suzuki, Y. J., Wang, W., Kobayashi, Y. M., Ramesh, V., Franzini-Armstrong, C., Cleemann, L. and Morad, M.: Regulation of Ca2+ signaling in transgenic mouse cardiac myocytes overexpressing calsequestrin. *J Clin Invest* 101, 1385-93 (1998)
  43. Yao, A., Su, Z., Nonaka, A., Zubair, I., Spitzer, K. W., Bridge, J. H., Muelheims, G., Ross, J., Jr. and Barry, W. H.: Abnormal myocyte Ca2+ homeostasis in rabbits with pacing-induced heart failure. *Am J Physiol* 275, H1441-8 (1998)
  44. Holt, E., Tonnessen, T., Lunde, P. K., Semb, S. O., Wasserstrom, J. A., Sejersted, O. M. and Christensen, G.: Mechanisms of cardiomyocyte dysfunction in heart failure following myocardial infarction in rats. *J Mol Cell Cardiol* 30, 1581-93. (1998)
  45. Esposito, G., Santana, L. F., Dilly, K., Cruz, J. D., Mao, L., Lederer, W. J. and Rockman, H. A.: Cellular and functional defects in a mouse model of heart failure. *Am J Physiol Heart Circ Physiol* 279, H3101-12 (2000)
  46. Gómez, A. M., Guatimosim, S., Dilly, K. W., Vassort, G. and Lederer, W. J.: Heart Failure After Myocardial Infarction: Altered Excitation-Contraction Coupling. *Circulation* 104, 688-693 (2001)
  47. Stull, L. B., Matteo, R. G., Sweet, W. E., Damron, D. S. and Schomisch Moravec, C.: Changes in calcium cycling precede cardiac dysfunction during autoimmune myocarditis in mice. *J Mol Cell Cardiol* 33, 449-60. (2001)
  48. Hasenfuss, G.: Alterations of calcium-regulatory proteins in heart failure. *Cardiovasc Res* 37, 279-89. (1998)
  49. Santana, L. F., Gómez, A. M. and Lederer, W. J.: Ca2+ flux through promiscuous cardiac Na+ channels: slip-mode conductance [see comments]. *Science* 279, 1027-33 (1998)
  50. Reeves, J. P. and Hale, C. C.: The stoichiometry of the cardiac sodium-calcium exchange system. *J Biol Chem* 259, 7733-9. (1984)
  51. Egger, M. and Niggli, E.: Regulatory function of Na-Ca exchange in the heart: milestones and outlook. *J Membr Biol* 168, 107-30. (1999)
  52. Leblanc, N. and Hume, J. R.: Sodium current-induced release of calcium from cardiac sarcoplasmic reticulum [see comments]. *Science* 248, 372-6 (1990)
  53. Sipido, K. R., Maes, M. and Van de Werf, F.: Low efficiency of Ca2+ entry through the Na(+)-Ca2+ exchanger as trigger for Ca2+ release from the sarcoplasmic reticulum. A comparison between L-type Ca2+ current and reverse-mode Na(+)-Ca2+ exchange. *Circ Res* 81, 1034-44 (1997)
  54. Studer, R., Reinecke, H., Bilger, J., Eschenhagen, T., Bohm, M., Hasenfuss, G., Just, H., Holtz, J. and Drexler, H.: Gene expression of the cardiac Na(+)-Ca2+ exchanger in end-stage human heart failure. *Circ Res* 75, 443-53. (1994)
  55. Pogwizd, S. M., Qi, M., Yuan, W., Samarel, A. M. and Bers, D. M.: Upregulation of Na+/Ca2+ Exchanger Expression and Function in an Arrhythmogenic Rabbit Model of Heart Failure. *Circ Res* 85, 1009-1019 (1999)
  56. Wang, Z., Nolan, B., Kutschke, W. and Hill, J. A.: Na+-Ca2+ exchanger remodeling in pressure overload cardiac hypertrophy. *J Biol Chem* 276, 17706-11. (2001)
  57. Hatem, S. N., Sham, J. S. and Morad, M.: Enhanced Na(+)-Ca2+ exchange activity in cardiomyopathic Syrian hamster. *Circ Res* 74, 253-61 (1994)
  58. Litwin, S. E. and Bridge, J. H.: Enhanced Na(+)-Ca2+ exchange in the infarcted heart. Implications

- for excitation-contraction coupling. *Circ Res* 81, 1083-93 (1997)
59. Sipido, K. R., Volders, P. G. A., de Groot, S. H. M., Verdonck, F., Van de Werf, F., Wellens, H. J. J. and Vos, M. A.: Enhanced Ca<sup>2+</sup> Release and Na/Ca Exchange Activity in Hypertrophied Canine Ventricular Myocytes : Potential Link Between Contractile Adaptation and Arrhythmogenesis. *Circulation* 102, 2137-2144 (2000)
  60. Hobai, I. A. and O'Rourke, B.: Enhanced Ca(2+)-activated Na(+)-Ca(2+) exchange activity in canine pacing-induced heart failure. *Circ Res* 87, 690-8. (2000)
  61. Pogwizd, S. M., Schlotthauer, K., Li, L., Yuan, W. and Bers, D. M.: Arrhythmogenesis and Contractile Dysfunction in Heart Failure : Roles of Sodium-Calcium Exchange, Inward Rectifier Potassium Current, and Residual {beta}-Adrenergic Responsiveness. *Circ Res* 88, 1159-1167 (2001)
  62. Hasenfuss, G., Schillinger, W., Lehnart, S. E., Preuss, M., Pieske, B., Maier, L. S., Prestle, J., Minami, K. and Just, H.: Relationship Between Na+-Ca2+-Exchanger Protein Levels and Diastolic Function of Failing Human Myocardium. *Circulation* 99, 641-648 (1999)
  63. Pogwizd, S. M.: Increased Na+-Ca2+ Exchanger in the Failing Heart. *Circ Res* 87, 641-643 (2000)
  64. Pu, J., Robinson, R. B. and Boyden, P. A.: Abnormalities in Ca(i)handling in myocytes that survive in the infarcted heart are not just due to alterations in repolarization. *J Mol Cell Cardiol* 32, 1509-23. (2000)
  65. Sipido, K. R., Carmeliet, E. and Van de Werf, F.: T-type Ca<sup>2+</sup> current as a trigger for Ca<sup>2+</sup> release from the sarcoplasmic reticulum in guinea-pig ventricular myocytes. *J Physiol* 508, 439-51. (1998)
  66. Reuter, H.: The dependence of slow inward current in Purkinje fibres on the extracellular calcium-concentration. *J Physiol* 192, 479-92. (1967)
  67. Rougier, O., Vassort, G., Garnier, D., Gargouil, Y. M. and Coraboeuf, E.: Existence and role of a slow inward current during the frog atrial action potential. *Pflugers Arch* 308, 91-110. (1969)
  68. Hess, P., Lansman, J. B. and Tsien, R. W.: Different modes of Ca channel gating behaviour favoured by dihydropyridine Ca agonists and antagonists. *Nature* 311, 538-44. (1984)
  69. Catterall, W. A.: Structure and regulation of voltage-gated Ca<sup>2+</sup> channels. *Annu Rev Cell Dev Biol* 16, 521-55. (2000)
  70. Hart, G.: Cellular electrophysiology in cardiac hypertrophy and failure. *Cardiovasc Res* 28, 933-46 (1994)
  71. Mukherjee, R. and Spinale, F. G.: L-type calcium channel abundance and function with cardiac hypertrophy and failure: a review. *J Mol Cell Cardiol* 30, 1899-916. (1998)
  72. Richard, S., Leclercq, F., Lemaire, S., Piot, C. and Nargeot, J.: Ca<sup>2+</sup> currents in compensated hypertrophy and heart failure. *Cardiovasc Res* 37, 300-11. (1998)
  73. Tomaselli, G. F. and Marbán, E.: Electrophysiological remodeling in hypertrophy and heart failure. *Cardiovasc Res* 42, 270-83. (1999)
  74. Scamps, F., Mayoux, E., Charlemagne, D. and Vassort, G.: Calcium current in single cells isolated from normal and hypertrophied rat heart. Effects of beta-adrenergic stimulation. *Circ Res* 67, 199-208 (1990)
  75. Keung, E. C.: Calcium current is increased in isolated adult myocytes from hypertrophied rat myocardium. *Circ Res* 64, 753-63. (1989)
  76. Hume, J. R. and Uehara, A.: Ionic basis of the different action potential configurations of single guinea-pig atrial and ventricular myocytes. *J Physiol* 368, 525-44. (1985)
  77. Schroder, F., Handrock, R., Beuckelmann, D. J., Hirt, S., Hullin, R., Priebe, L., Schwinger, R. H., Weil, J. and Herzig, S.: Increased availability and open probability of single L-type calcium channels from failing compared with nonfailing human ventricle. *Circulation* 98, 969-76. (1998)
  78. He, J., Conklin, M. W., Foell, J. D., Wolff, M. R., Haworth, R. A., Coronado, R. and Kamp, T. J.: Reduction in density of transverse tubules and L-type Ca(2+) channels in canine tachycardia-induced heart failure. *Cardiovasc Res* 49, 298-307. (2001)
  79. Yue, D. T., Herzig, S. and Marbán, E.: Beta-adrenergic stimulation of calcium channels occurs by potentiation of high-activity gating modes. *Proc Natl Acad Sci U S A* 87, 753-7. (1990)
  80. Bristow, M. R.: Changes in myocardial and vascular receptors in heart failure. *J Am Coll Cardiol* 22, 61A-71A (1993)
  81. Bristow, M. R., Hershberger, R. E., Port, J. D., Gilbert, E. M., Sandoval, A., Rasmussen, R., Cates, A. E. and Feldman, A. M.: Beta-adrenergic pathways in nonfailing and failing human ventricular myocardium. *Circulation* 82, 112-25 (1990)
  82. Marx, S. O., Reiken, S., Hisamatsu, Y., Jayaraman, T., Burkhoff, D., Rosembli, N. and Marks, A. R.: PKA phosphorylation dissociates FKBP12.6 from the calcium release channel (ryanodine receptor): defective regulation in failing hearts. *Cell* 101, 365-76 (2000)
  83. Bristow, M. R.: Mechanism of action of beta-blocking agents in heart failure. *Am J Cardiol* 80, 26L-40L (1997)
  84. Dorn, G. W., 2nd, Tepe, N. M., Lorenz, J. N., Koch, W. J. and Liggett, S. B.: Low- and high-level transgenic expression of beta2-adrenergic receptors differentially affect cardiac hypertrophy and function in Galphaq-overexpressing mice. *Proc Natl Acad Sci U S A* 96, 6400-5. (1999)
  85. Mewes, T. and Ravens, U.: L-type calcium currents of human myocytes from ventricle of non-failing and failing hearts and from atrium. *J Mol Cell Cardiol* 26, 1307-20. (1994)
  86. Takahashi, T., Allen, P. D., Lacro, R. V., Marks, A. R., Dennis, A. R., Schoen, F. J., Grossman, W., Marsh, J. D. and Izumo, S.: Expression of dihydropyridine receptor (Ca<sup>2+</sup> channel) and calsequestrin genes in the myocardium of patients with end-stage heart failure. *J Clin Invest* 90, 927-35. (1992)
  87. Hullin, R., Asmus, F., Ludwig, A., Hersel, J. and Boekstegers, P.: Subunit expression of the cardiac L-type calcium channel is differentially regulated in diastolic heart failure of the cardiac allograft. *Circulation* 100, 155-63. (1999)
  88. Yang, Y., Chen, X., Margulies, K., Jeevanandam, V., Pollack, P., Bailey, B. A. and Houser, S. R.: L-type Ca<sup>2+</sup> channel alpha 1c subunit isoform switching in failing human ventricular myocardium. *J Mol Cell Cardiol* 32, 973-84. (2000)
  89. Kaab, S., Dixon, J., Duc, J., Ashen, D., Nabauer, M., Beuckelmann, D. J., Steinbeck, G., McKinnon, D. and Tomaselli, G. F.: Molecular basis of transient outward potassium current downregulation in human heart failure: a decrease in Kv4.3 mRNA correlates with a reduction in current density. *Circulation* 98, 1383-93. (1998)
  90. Singer, D., Biel, M., Lotan, I., Flockner, V., Hofmann, F. and Dascal, N.: The roles of the subunits in the function of the calcium channel. *Science* 253, 1553-7. (1991)
  91. Gidh-Jain, M., Huang, B., Jain, P., Battula, V. and el-Sherif, N.: Reemergence of the fetal pattern of L-type calcium channel gene expression in non infarcted myocardium during left ventricular remodeling. *Biochem Biophys Res Commun* 216, 892-7. (1995)
  92. Bénitah, J. P., Gómez, A. M., Bailly, P., Da Ponte, J. P., Berson, G., Delgado, C. and Lorente, P.: Heterogeneity of the early outward current in ventricular cells isolated from normal and hypertrophied rat hearts. *J Physiol (Lond)* 469, 111-38 (1993)
  93. Gómez, A. M., Bénitah, J. P., Henzel, D., Vinet, A., Lorente, P. and Delgado, C.: Modulation of electrical heterogeneity by compensated hypertrophy in rat left ventricle. *Am J Physiol* 272, H1078-86 (1997)
  94. Takimoto, K. & Levitan, E.S. in *Potassium Channels in cardiovascular biology* (eds. Archer, S.L. & Rusch, N.J.) Kluwer Academic/Plenum, New York, 773-83 (2001).

95. Wickenden, A. D., Kaprielian, R., Kassiri, Z., Tsoporis, J. N., Tsushima, R., Fishman, G. I. and Backx, P. H.: The role of action potential prolongation and altered intracellular calcium handling in the pathogenesis of heart failure. *Cardiovasc Res* 37, 312-23. (1998)
96. Kaprielian, R., Wickenden, A. D., Kassiri, Z., Parker, T. G., Liu, P. P. and Backx, P. H.: Relationship between K<sup>+</sup> channel down-regulation and [Ca<sup>2+</sup>]<sub>i</sub> in rat ventricular myocytes following myocardial infarction. *J Physiol* 517, 229-45. (1999)
97. Volk, T., Nguyen, T. H.-D., Schultz, J.-H. and Ehmke, H.: Relationship between transient outward K<sup>+</sup> current and Ca<sup>2+</sup> influx in rat cardiac myocytes of endo- and epicardial origin. *J Physiol (Lond)* 519, 841-850 (1999)
98. Muth, J. N., Bodi, I., Lewis, W., Varadi, G. and Schwartz, A.: A Ca(2+)-dependent transgenic model of cardiac hypertrophy: A role for protein kinase Calpha. *Circulation* 103, 140-7. (2001)
99. Ming, T. J., Lokuta, A. J., Wolf, M. R., Haworth, R. A. and Valdivia, H. H.: Depression of ryanodine receptor density, but not function, may decrease calcium release in heart failure (HF). *Biophys J* 78, 376A (abstract) (2000)
100. Valdivia, H. H., Kaplan, J. H., Ellis-Davies, G. C. and Lederer, W. J.: Rapid adaptation of cardiac ryanodine receptors: modulation by Mg<sup>2+</sup> and phosphorylation. *Science* 267, 1997-2000 (1995)
101. Marx, S. O., Gaburjakova, J., Gaburjakova, M., Henrikson, C., Ondrias, K. and Marks, A. R.: Coupled Gating Between Cardiac Calcium Release Channels (Ryanodine Receptors). *Circ Res* 88, 1151-1158 (2001)
102. Aronson, R. S.: Characteristics of action potentials of hypertrophied myocardium from rats with renal hypertension. *Circ Res* 47, 443-54 (1980)
103. Litwin, S. E., Zhang, D. and Bridge, J. H. B.: Dyssynchronous Ca<sup>2+</sup> Sparks in Myocytes From Infarcted Hearts. *Circ Res* 87, 1040-1047 (2000)
104. Inoko, M., Kihara, Y., Morii, I., Fujiwara, H. and Sasayama, S.: Transition from compensatory hypertrophy to dilated, failing left ventricles in Dahl salt-sensitive rats. *Am J Physiol* 267, H2471-82 (1994)
105. Cheng, H., Lederer, M. R., Xiao, R. P., Gómez, A. M., Zhou, Y. Y., Ziman, B., Spurgeon, H., Lakatta, E. G. and Lederer, W. J.: Excitation-contraction coupling in heart: new insights from Ca<sup>2+</sup> sparks. *Cell Calcium* 20, 129-40 (1996)
106. Santana, L. F., Gómez, A. M., Kranias, E. G. and Lederer, W. J.: Amount of calcium in the sarcoplasmic reticulum: influence on excitation-contraction coupling in heart muscle. *Heart Vessels Suppl* 12, 44-9 (1997)
107. Lindner, M., Erdmann, E. and Beuckelmann, D. J.: Calcium content of the sarcoplasmic reticulum in isolated ventricular myocytes from patients with terminal heart failure. *J Mol Cell Cardiol* 30, 743-9. (1998)
108. Chen, J. and Chien, K. R.: Complexity in simplicity: monogenic disorders and complex cardiomyopathies. *J Clin Invest* 103, 1483-5. (1999)
109. Arber, S., Hunter, J. J., Ross, J., Jr., Hongo, M., Sansig, G., Borg, J., Perriard, J. C., Chien, K. R. and Caroni, P.: MLP-deficient mice exhibit a disruption of cardiac cytoarchitectural organization, dilated cardiomyopathy, and heart failure. *Cell* 88, 393-403 (1997)
110. Thomell, L., Carlsson, L., Li, Z., Mericskay, M. and Paulin, D.: Null mutation in the desmin gene gives rise to a cardiomyopathy. *J Mol Cell Cardiol* 29, 2107-24 (1997)
111. Gómez, A. M., Aimond, F., Alvarez, J., Artilles, A., Li, Z. L. and G., V.: Cardiac function in desmin-deficient transgenic mice. *Biophys J* 76, A462 (abstract) (1999)
112. Tsutsui, H., Ishihara, K. and Cooper, G. t.: Cytoskeletal role in the contractile dysfunction of hypertrophied myocardium. *Science* 260, 682-7 (1993)
113. Howarth, F. C., Calaghan, S. C., Boyett, M. R. and White, E.: Effect of the microtubule polymerizing agent taxol on contraction, Ca<sup>2+</sup> transient and L-type Ca<sup>2+</sup> current in rat ventricular myocytes. *J Physiol (Lond)* 516, 409-19 (1999)
114. Gómez, A. M., Kerfant, B. G. and Vassort, G.: Microtubule Disruption Modulates Ca(2+) Signaling in Rat Cardiac Myocytes. *Circ Res* 86, 30-36 (2000)
115. Kerfant, B. G., Vassort, G. and Gómez, A. M.: Microtubule disruption by colchicine reversibly enhances calcium signaling in intact rat cardiac myocytes. *Circ Res* 88, E59-65. (2001)
116. Kaprielian, R. R., Stevenson, S., Rothery, S. M., Cullen, M. J. and Severs, N. J.: Distinct patterns of dystrophin organization in myocyte sarcolemma and transverse tubules of normal and diseased human myocardium. *Circulation* 101, 2586-94 (2000)
117. Wong, C., Soeller, C., Burton, L. and Cannell, M. B.: Changes In Transverse-Tubular System Architecture In Myocytes From Diseased Human Ventricles. *Biophysical Journal* 80, 588a (abstract) (2001)
118. Adachi-Akahane, S., Cleemann, L. and Morad, M.: Cross-signaling between L-type Ca<sup>2+</sup> channels and ryanodine receptors in rat ventricular myocytes. *J Gen Physiol* 108, 435-54 (1996)
119. Barrere-Lemaire, S., Piot, C., Leclercq, F., Nargeot, J. and Richard, S.: Facilitation of L-type calcium currents by diastolic depolarization in cardiac cells: impairment in heart failure. *Cardiovasc Res* 47, 336-49. (2000)
120. Ahmmed, G. U., Dong, P. H., Song, G., Ball, N. A., Xu, Y., Walsh, R. A. and Chiamvimonvat, N.: Changes in Ca(2+) cycling proteins underlie cardiac action potential prolongation in a pressure-overloaded guinea pig model with cardiac hypertrophy and failure. *Circ Res* 86, 558-70. (2000)
121. Bers, D. M. and Perez-Reyes, E.: Ca channels in cardiac myocytes: structure and function in Ca influx and intracellular Ca release. *Cardiovasc Res* 42, 339-60 (1999)
122. Delgado, C., Artilles, A., Gómez, A. M. and Vassort, G.: Frequency-dependent increase in cardiac Ca(2+)Current is due to reduced Ca(2+)Release by the sarcoplasmic reticulum [In Process Citation]. *J Mol Cell Cardiol* 31, 1783-93 (1999)
123. Piot, C., Lemaire, S., Albat, B., Seguin, J., Nargeot, J. and Richard, S.: High frequency-induced upregulation of human cardiac calcium currents. *Circulation* 93, 120-8. (1996)
124. Lemaire, S., Piot, C., Leclercq, F., Leuranguer, V., Nargeot, J. and Richard, S.: Heart rate as a determinant of L-type Ca<sup>2+</sup> channel activity: mechanisms and implication in force-frequency relation. *Basic Res Cardiol* 93 Suppl 1, 51-9. (1998)
125. Molkenkin, J. D. and Dorn, I. G., 2nd: Cytoplasmic signaling pathways that regulate cardiac hypertrophy. *Annu Rev Physiol* 63, 391-426. (2001)
126. Molkenkin, J. D.: Calcineurin and beyond: cardiac hypertrophic signaling. *Circ Res* 87, 731-8. (2000)
127. Frey, N., McKinsey, T. A. and Olson, E. N.: Decoding calcium signals involved in cardiac growth and function. *Nat Med* 6, 1221-7. (2000)
128. Chien, K. R., Knowlton, K. U., Zhu, H. and Chien, S.: Regulation of cardiac gene expression during myocardial growth and hypertrophy: molecular studies of an adaptive physiologic response. *Faseb J* 5, 3037-46. (1991)
129. Marbán, E. and Koretsune, Y.: Cell calcium, oncogenes, and hypertrophy. *Hypertension* 15, 652-8. (1990)
130. McDonough, P. M., Hanford, D. S., Sprenkle, A. B., Mellon, N. R. and Glembotski, C. C.: Collaborative roles for c-Jun N-terminal kinase, c-Jun, serum response factor, and Sp1 in calcium-regulated myocardial gene expression. *J Biol Chem* 272, 24046-53. (1997)
131. Morgan, J. I. and Curran, T.: Calcium as a modulator of the immediate-early gene cascade in neurons. *Cell Calcium* 9, 303-11. (1988)
132. Ginty, D. D.: Calcium regulation of gene expression: isn't that spatial? *Neuron* 18, 183-6. (1997)
133. Sugden, P. H. and Clerk, A.: Cellular mechanisms of cardiac hypertrophy. *J Mol Med* 76, 725-46 (1998)
134. Hefti, M. A., Harder, B. A., Eppenberger, H. M. and Schaub, M. C.: Signaling pathways in cardiac

- myocyte hypertrophy. *J Mol Cell Cardiol* 29, 2873-92. (1997)
135. Yamazaki, T., Tobe, K., Hoh, E., Maemura, K., Kaida, T., Komuro, I., Tamemoto, H., Kadowaki, T., Nagai, R. and Yazaki, Y.: Mechanical loading activates mitogen-activated protein kinase and S6 peptide kinase in cultured rat cardiac myocytes. *J Biol Chem* 268, 12069-76. (1993)
  136. Soderling, T. R.: The Ca-calmodulin-dependent protein kinase cascade. *Trends Biochem Sci* 24, 232-6. (1999)
  137. Gruver, C. L., DeMayo, F., Goldstein, M. A. and Means, A. R.: Targeted developmental overexpression of calmodulin induces proliferative and hypertrophic growth of cardiomyocytes in transgenic mice. *Endocrinology* 133, 376-88. (1993)
  138. Soderling, T. R., Chang, B. and Brickey, D.: Cellular signaling through multifunctional Ca<sup>2+</sup>/calmodulin-dependent protein kinase II. *J Biol Chem* 276, 3719-22. (2001)
  139. Corcoran, E. E. and Means, A. R.: Defining Ca<sup>2+</sup>/calmodulin-dependent protein kinase cascades in transcriptional regulation. *J Biol Chem* 276, 2975-8. (2001)
  140. Passier, R., Zeng, H., Frey, N., Naya, F. J., Nicol, R. L., McKinsey, T. A., Overbeek, P., Richardson, J. A., Grant, S. R. and Olson, E. N.: CaM kinase signaling induces cardiac hypertrophy and activates the MEF2 transcription factor in vivo. *J Clin Invest* 105, 1395-406. (2000)
  141. Chien, K. R.: Meeting Koch's postulates for calcium signaling in cardiac hypertrophy. *J Clin Invest* 105, 1339-42. (2000)
  142. Leinwand, L. A.: Calcineurin inhibition and cardiac hypertrophy: A matter of balance. *Proc Natl Acad Sci U S A* 98, 2947-9. (2001)
  143. Sussman, M. A., Lim, H. W., Gude, N., Taigen, T., Olson, E. N., Robbins, J., Colbert, M. C., Gualberto, A., Wieczorek, D. F. and Molkenkin, J. D.: Prevention of cardiac hypertrophy in mice by calcineurin inhibition. *Science* 281, 1690-3. (1998)
  144. Atar, D., Backx, P. H., Appel, M. M., Gao, W. D. and Marbán, E.: Excitation-transcription coupling mediated by zinc influx through voltage-dependent calcium channels. *J Biol Chem* 270, 2473-7. (1995)
  145. Anderson, M. E.: Connections count : excitation-contraction meets excitation-transcription coupling. *Circ Res* 86, 717-9. (2000)
  146. Cartin, L., Lounsbury, K. M. and Nelson, M. T.: Coupling of Ca(2+) to CREB activation and gene expression in intact cerebral arteries from mouse : roles of ryanodine receptors and voltage-dependent Ca(2+) channels. *Circ Res* 86, 760-7. (2000)
  147. Stevenson, A. S., Cartin, L., Wellman, T. L., Dick, M. H., Nelson, M. T. and Lounsbury, K. M.: Membrane depolarization mediates phosphorylation and nuclear translocation of CREB in vascular smooth muscle cells. *Exp Cell Res* 263, 118-30. (2001)
  148. Bénitah, Perrier, E., Gómez, A. and Vassort, G.: Effects of aldosterone on transient outward K<sup>+</sup> current density in rat ventricular myocytes. *J Physiol* 537, 151-160 (2001)
  149. Holmer, S. R. and Schunkert, H.: Adaptive and genetic alterations of the renin angiotensin system in cardiac hypertrophy and failure. *Basic Res Cardiol* 91, 65-71. (1996)
  150. Pitt, B., Zannad, F., Remme, W. J., Cody, R., Castaigne, A., Perez, A., Palensky, J. and Wittes, J.: The effect of spironolactone on morbidity and mortality in patients with severe heart failure. Randomized Aldactone Evaluation Study Investigators. *N Engl J Med* 341, 709-17. (1999)
  151. Delcayre, C. and Silvestre, J. S.: Aldosterone and the heart: towards a physiological function? *Cardiovasc Res* 43, 7-12. (1999)
  152. Bénitah, J. P. and Vassort, G.: Aldosterone upregulates Ca(2+) current in adult rat cardiomyocytes. *Circ Res* 85, 1139-45. (1999)
  153. Milnes, J. T. and MacLeod, K. T.: Reduced ryanodine receptor to dihydropyridine receptor ratio may underlie slowed contraction in a rabbit model of left ventricular cardiac hypertrophy. *J Mol Cell Cardiol* 33,473-85. (2001)

# Ryanodine Receptors in Smooth Muscle

Agustín Guerrero-Hernández, Leticia Gómez-Viquez, Guadalupe Guerrero-Serna and Angélica Rueda

Departamento de Bioquímica, CINVESTAV-IPN, México D.F. 07000 Email: [aguerrer@mail.cinvestav.mx](mailto:aguerrer@mail.cinvestav.mx)

**Abstract** The sarcoplasmic reticulum (SR) of smooth muscle is endowed with two different types of  $\text{Ca}^{2+}$  release channels, i.e. inositol 1,4,5-trisphosphate receptors ( $\text{IP}_3\text{Rs}$ ) and ryanodine receptors (RyRs). In general, both release channels mobilize  $\text{Ca}^{2+}$  from the same internal store in smooth muscle. While the importance of  $\text{IP}_3\text{Rs}$  in agonist-induced contraction is well established, the role of RyRs in excitation-contraction coupling of smooth muscle is not clear. The participation of smooth muscle RyRs in the amplification of  $\text{Ca}^{2+}$  transients induced by either opening of  $\text{Ca}^{2+}$ -permeable channels or  $\text{IP}_3$ -triggered  $\text{Ca}^{2+}$  release has been studied. The efficacy of both processes to activate RyRs by calcium-induced calcium release (CICR) is highly variable and not widely present in smooth muscle. Although RyRs in smooth muscle generate  $\text{Ca}^{2+}$  sparks that are similar to those observed in striated muscles, the contribution of these local  $\text{Ca}^{2+}$  events to depolarization-induced global rise in  $[\text{Ca}^{2+}]_i$  is rather limited. Recent data suggest that RyRs are involved in regulating the luminal  $[\text{Ca}^{2+}]$  of SR and also in smooth muscle relaxation. This review summarizes studies that were carried out mainly in muscle strips or in freshly isolated myocytes, and that were aimed to determine the physiological role of RyRs in smooth muscle.

## Introduction

### $\text{Ca}^{2+}$ regulation of smooth muscle contraction

Visceral smooth muscle constitutes one of the layers of numerous hollow organs such as trachea, uterus, intestines, urinary bladder, etc. whereas vascular smooth muscle is present in blood vessels. The mechanical activity of all these organs depends on the contraction-relaxation features of their smooth muscle tissues. Similarly to striated muscle, smooth muscle cells contracts in response to an increase in the intracellular  $\text{Ca}^{2+}$  concentration ( $[\text{Ca}^{2+}]_i$ ). However, significant differences between smooth and striated muscles exist; among them, contraction is slower in the former and myofilaments in smooth muscle do not show the regular pattern of sarcomeric muscles. One of the reasons for the slower mechanical response of smooth muscle is that the  $\text{Ca}^{2+}$  sensor (calmodulin) is not an integral part of the myofilaments, as is troponin C in striated muscles. The  $\text{Ca}^{2+}$ -calmodulin complex activates the myosin light chain kinase to phosphorylate serine 19 of myosin light chain, which in turn removes inhibition of the myosin ATPase. This event is followed by ATP hydrolysis and sliding of myosin on actin filaments to generate force (for review, see 1-3).

### Sources of $\text{Ca}^{2+}$ for smooth muscle contraction

Elevation of  $[\text{Ca}^{2+}]_i$  in smooth muscle can be due to  $\text{Ca}^{2+}$  influx from the external milieu or  $\text{Ca}^{2+}$  release from internal stores, which are located in the sarcoplasmic reticulum (SR). External  $\text{Ca}^{2+}$  gains access to the cytoplasm through either voltage-dependent  $\text{Ca}^{2+}$  channels (VDCCs) or different types of  $\text{Ca}^{2+}$  permeable cation channels; whereas internal stores provide  $\text{Ca}^{2+}$  by at least two types of release-channels, the inositol 1,4,5-trisphosphate receptor ( $\text{IP}_3\text{R}$ ) and the ryanodine receptor (RyR) (for review see 1, 2). The participation of internal  $\text{Ca}^{2+}$  stores in smooth muscle contraction is highly variable. In

general, internal stores release  $\text{Ca}^{2+}$  during the initial phase of contraction, but their overall participation is rather small. In some cases,  $\text{Ca}^{2+}$  internal stores supply basically all  $\text{Ca}^{2+}$  for agonist-induced contraction, e.g. guinea pig pulmonary artery and porcine coronary artery (4,5). The main mechanism by which neurotransmitters, hormones and other agonists release  $\text{Ca}^{2+}$  from internal stores involves the activation of phospholipase C, which in turn hydrolyzes phosphatidylinositol bisphosphate to generate both diacylglycerol and inositol 1,4,5-trisphosphate ( $\text{IP}_3$ ). The latter induces the opening of  $\text{IP}_3\text{Rs}$  to produce a global elevation in  $[\text{Ca}^{2+}]_i$  and contraction in smooth muscle (1). Therefore,  $\text{IP}_3\text{Rs}$  have an essential participation in pharmacomechanical coupling (1). By contrast, the role played by RyRs in triggering smooth muscle contraction by physiological stimuli is not clear. This review summarizes studies focused on the physiological role of RyRs in smooth muscle, that have been carried out either in tissue preparations or in freshly isolated myocytes.

### Characteristics and types of ryanodine receptors in smooth muscle

Initially, the characterization of RyRs from smooth muscle was carried out with pharmacological tools such as caffeine and ryanodine, similarly to the studies done in striated muscles. Subsequently, biochemical and molecular studies of RyRs from smooth muscles have been reported.

### Pharmacological characterization

The presence of RyRs in smooth muscle was first suggested by studies showing that caffeine induces transient contractures of smooth muscle bundles in the absence of extracellular  $\text{Ca}^{2+}$  (6). Caffeine works by increasing the  $\text{Ca}^{2+}$  sensitivity of RyRs such that these release-channels are opened by

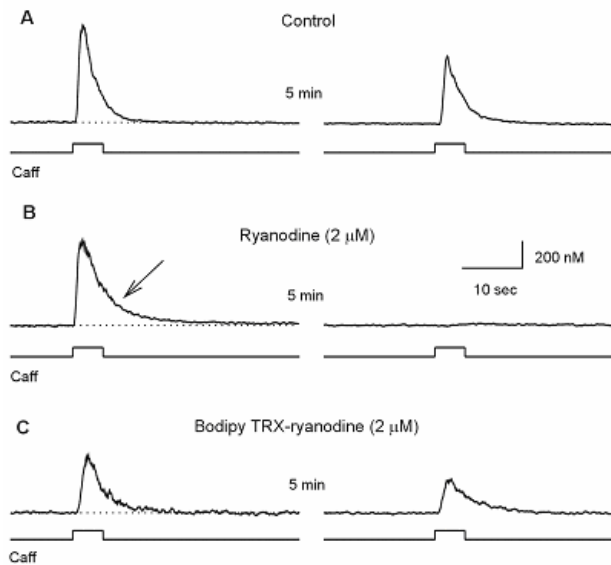


Figure 1. Effect of ryanodine on caffeine-induced  $\text{Ca}^{2+}$  release from internal stores. Single smooth muscle cells isolated from guinea pig urinary bladder were loaded with fura-2 and changes in  $[\text{Ca}^{2+}]_i$  were recorded in response to the application of 20 mM caffeine (Caff) (as indicated by the traces below the  $[\text{Ca}^{2+}]_i$  recordings) with a puffer pipette placed close to the cell. Bath solution was Hepes-buffered saline solution (2 mM  $\text{Ca}^{2+}$ ). A. Caffeine induced a transient increase in  $[\text{Ca}^{2+}]_i$  that started to return to the basal level even in the presence of caffeine. A time period of 5 min was allowed to recover internal  $\text{Ca}^{2+}$  stores. This recovery was not complete based on the smaller amplitude of the  $[\text{Ca}^{2+}]_i$  transient induced by a second application of caffeine. B. Cells that were incubated with ryanodine responded normally to the first application of caffeine. This was true even when cells were incubated with ryanodine for a prolonged period of time (> 30 min). However, two main differences were evident respect to control responses. First, the rate of decay of  $[\text{Ca}^{2+}]_i$  was significantly delayed, which is notorious at  $[\text{Ca}^{2+}]_i$  below 300 nM (arrow). Second, an additional application of caffeine produced no increase in  $[\text{Ca}^{2+}]_i$ . These data and the absence of a significant capacitative  $\text{Ca}^{2+}$  influx in this type of myocytes (16) suggest that ryanodine and caffeine combined lock the RyR open, leading to a complete depletion of internal  $\text{Ca}^{2+}$  stores. C. Fluorescently-labeled ryanodine (BODIPY TRX-ryanodine) appears to be incapable of correctly interacting with the open state of RyRs as this derivative did not produce a complete depletion of the internal  $\text{Ca}^{2+}$  stores. Collectively, these data support the hypothesis that RyRs must be activated before interacting with ryanodine and also that low concentrations of this alkaloid locks the RyRs in an open state, to the extent that internal  $\text{Ca}^{2+}$  stores cannot be recovered. The dotted line indicates resting  $[\text{Ca}^{2+}]_i$ . Both  $[\text{Ca}^{2+}]_i$  and time scales apply for all recordings.

basal  $[\text{Ca}^{2+}]_i$  (7). The action of caffeine is to produce a transient increase in  $[\text{Ca}^{2+}]_i$  that originates from internal stores. However, caution must be exercised since it has been shown that caffeine can also activate a  $\text{Ca}^{2+}$  permeable cation channel, which is present in the plasma membrane of gastric smooth muscle cells (8-10).

Ryanodine is a plant alkaloid that binds with high affinity and selectivity to RyRs (11). Micromolar concentrations of this alkaloid in combination with caffeine produce a complete depletion of caffeine-

sensitive  $\text{Ca}^{2+}$  stores in skinned smooth muscle of pulmonary artery, portal vein and taenia caeci from guinea pig (5). Similar results have been obtained in freshly isolated smooth muscle cells, including guinea pig urinary bladder (12) and mouse duodenum (13). The effect of either ryanodine or fluorescently-labeled ryanodine on caffeine-sensitive internal  $\text{Ca}^{2+}$  stores is shown in Figure 1. The application of caffeine to smooth muscle cells incubated with 2  $\mu\text{M}$  ryanodine (concentration that "locks" RyR in a subconductance state) (14, 15) did not appreciably alter the initial  $[\text{Ca}^{2+}]_i$  response to caffeine. However, internal  $\text{Ca}^{2+}$  stores were unable to recover in the presence of ryanodine, most likely because the SR was leaky, which is reflected in both a slower rate of recovery of the  $[\text{Ca}^{2+}]_i$  (indicated by the arrow, Figure 1) and a lack of  $[\text{Ca}^{2+}]_i$  response to a second application of caffeine (Figure 1). Fluorescently-labeled ryanodine did not behave similarly to parental ryanodine because in the presence of the former, there was a partial recovery of the internal  $\text{Ca}^{2+}$  store (Figure 1).

The effect of ryanodine on the ion channel activity of RyRs from smooth muscle has also been studied in planar lipid bilayers. The toad stomach RyR displays a subconductance state of high open probability in response to micromolar concentrations of ryanodine (15), similar to the effect described for cardiac and skeletal RyRs (17). However, ryanodine does not induce this subconducting state in RyRs from aorta (18) or from coronary artery smooth muscle (19). In the case of RyRs from aorta, millimolar concentrations of ryanodine induced the fully blocked state of this  $\text{Ca}^{2+}$  release channel (18), whereas for RyRs from coronary artery, concentrations of ryanodine up to 10  $\mu\text{M}$  increased the ion channel activity, while higher concentrations inhibited this activity (19). It is not clear whether these differences between visceral and vascular RyRs imply the existence of different RyR isoforms or the loss of some regulatory factor during the RyR isolation procedure. Thus, further studies at the single channel level are needed to clarify the effect of ryanodine on RyRs from different types of smooth muscle cells.

### Biochemical characterization

The ryanodine receptor has been localized to the SR of smooth muscle cells and its abundance correlates with the amount of SR, which fluctuates between 1.5 and 7.5 % of the total myocyte volume (20-23). Interestingly, phasic smooth muscle contains less SR than tonic smooth muscle and the SR of the former is preferentially localized close to the plasma membrane (20, 22-24). Apparently, some parts of the SR (peripheral SR) are in close apposition ( $\sim 20$  nm) to the plasma membrane, generating what is known as junctional gaps. These regions contain structures that resemble the feet described in skeletal muscle (20). Additionally, recent data in myocytes from cerebral arteries (21) and guinea pig urinary bladder (25) indicate that VDCCs co-localize with RyRs.

Further characterization of RyRs has been carried out using binding of  $[\text{3H}]$ ryanodine to microsomal preparations from different smooth muscles. Overall, these studies have yielded a  $K_d$

close to 5 nM and a Hill coefficient of 1 (15, 26-29), which are similar to those obtained for RyRs from striated muscles (30). The density of [<sup>3</sup>H]ryanodine binding sites is in the vicinity of 100 fmol/mg protein, although a density as high as 5.7 pmol/mg protein has been reported in crude microsomal preparations of smooth muscle from rat portal vein (31). In general, the number of [<sup>3</sup>H]ryanodine binding sites in smooth muscle is 10 times lower or even less than in striated muscles (18). Presumably, this low density of RyRs is a consequence of the sparse SR in smooth muscle (26). Moreover, the binding of [<sup>3</sup>H]ryanodine to microsomal membranes from smooth muscle can be increased by the same factors that also modulate the activity of RyRs from striated muscles (32), such as Ca<sup>2+</sup>, caffeine, ATP, high ionic strength and pH (26,28). Ruthenium red and Mg<sup>2+</sup> inhibit [<sup>3</sup>H]ryanodine binding in smooth muscle microsomes (26,28), similar to the effect observed in striated muscles. All these data suggest the presence of typical RyRs in smooth muscle, albeit at a low density.

### **Molecular characterization**

The ryanodine receptor is a homotetrameric protein of approximately 2 MDa molecular weight. Three isoforms of RyRs that are encoded by different genes (ryr1, ryr2 and ryr3) have been identified and cloned (33-36). All three types of RyRs have been detected in RNA extracted from smooth muscle (Table 1). However, these results should be interpreted with some caution, since the detection of different RyR transcripts may reflect contamination from cells other than smooth muscle (e. g. endothelial cells, neurons, etc.). Studies in isolated smooth muscle cells have shown that there is no predominant RyR isoform in smooth muscle (Table 1).

RyR knockout mice have recently emerged as suitable tools to study the role of RyRs in smooth muscle physiology. Arterial smooth muscle from mice lacking RyR3 contracts normally to caffeine and norepinephrine (50). Another study has shown that the frequency of Ca<sup>2+</sup> sparks (localized [Ca<sup>2+</sup>]<sub>i</sub> events that are produced by the opening of a cluster of RyRs) is significantly increased in RyR3 knockout mice (41). Studies in smooth muscle derived from RyR2 knockout mice are lacking because mutant embryos die at day 10 due to abnormalities in the heart tube (51). In addition, there are no data on smooth muscle function in RyR1 knockout mice (52,53).

Studies in rat portal vein myocytes with antisense oligonucleotides targeting each of the three types of RyRs demonstrated that the presence of both RyR1 and RyR2 is required for myocytes to respond to membrane depolarization with Ca<sup>2+</sup> sparks and a global increase in [Ca<sup>2+</sup>]<sub>i</sub> (42). The inhibition of RyR3 expression in rat portal vein myocytes did not alter either evoked or spontaneous Ca<sup>2+</sup> sparks (42). Apparently, RyR3 acquires the ability to respond to caffeine only in conditions of increased SR Ca<sup>2+</sup> loading in myocytes from both rat portal vein (54) and myometrium of non-pregnant mice (45). However, some of these studies were carried out in cells that had been cultured for several days, which might have changed the type and level of expression

of RyRs. Indeed, RyRs cannot be found in rat aortic smooth muscle cells in proliferating conditions, but they are detected when cells reach a non-proliferative state (40). Thus, the type and functional role of RyRs need to be assessed for each type of smooth muscle.

### **Physiological role of ryanodine receptors in smooth muscle**

The role of RyRs in smooth muscle cells is not clearly established. This release channel has been involved in the amplification of Ca<sup>2+</sup> transients that are originated by either opening of VDCCs or IP<sub>3</sub>-induced Ca<sup>2+</sup> release in some smooth muscle cells. Alternatively, RyRs also seem to participate in both the regulation of luminal [Ca<sup>2+</sup>] and the local activation of large-conductance Ca<sup>2+</sup>-dependent K<sup>+</sup> channels (BK<sub>Ca</sub> channels). These roles suggest a more important participation of RyRs in smooth muscle relaxation than in excitation-contraction coupling as summarized below.

### **Excitation-contraction coupling**

#### **Amplification by RyRs of the Ca<sup>2+</sup> influx through voltage-dependent Ca<sup>2+</sup> channels.**

Membrane depolarization in smooth muscle increases [Ca<sup>2+</sup>]<sub>i</sub> as a consequence of VDCCs opening. However, it has been calculated that the Ca<sup>2+</sup> coming through these channels, either in a single or a train of 5-10 action potentials, might not be sufficient to induce contraction because the cytoplasmic Ca<sup>2+</sup> buffer capacity may reduce the activity of Ca<sup>2+</sup> ions (4,20). Therefore, in this scenario it is obligatory to postulate the existence of an additional source of Ca<sup>2+</sup>, most likely the SR. The question then turns: How does the SR amplify the Ca<sup>2+</sup> influx through VDCCs? One possibility could be the activation of IP<sub>3</sub>Rs, because smooth muscle produces IP<sub>3</sub> in response to Ca<sup>2+</sup> influx (55) and membrane depolarization increases the activity of phospholipase C (56,57). However, this scenario seems unlikely as heparin, an antagonist of IP<sub>3</sub>Rs, does not reduce the [Ca<sup>2+</sup>]<sub>i</sub> transient induced by membrane depolarization (58,59).

Another possibility for the amplification of Ca<sup>2+</sup> influx through VDCCs could be the activation of RyR by the calcium-induced calcium release (CICR) mechanism, which is well established for cardiac myocytes (60). The first direct evidence of CICR in smooth muscle was obtained by studies in skinned smooth muscle bundles (61). However, it has been suggested that CICR might not be functioning as the primary physiological Ca<sup>2+</sup> release mechanism, since higher Ca<sup>2+</sup> is required to activate CICR than to induce contraction (62). Nevertheless, these results do not completely exclude the participation of CICR in releasing Ca<sup>2+</sup> during excitation-contraction coupling in smooth muscle, as local elevations of [Ca<sup>2+</sup>]<sub>i</sub> in the vicinity of RyRs may be high enough to activate these release channels (62). Alternatively, a cytosolic factor regulating CICR may have been lost during the smooth muscle permeabilization procedure (62).

Studies of [Ca<sup>2+</sup>]<sub>i</sub> in single smooth muscle cells under the whole-cell configuration of the patch

Smooth muscle Source	RYR Isoform			Detection Method	Ref.
	RYR1	RYR2	RYR3		
Aorta	N. D. + (rt)	+ (rt) + (p, rt)	+ (rb) + (p, rt)	Northern-blot RT-PCR	36, 37 38, 39, 40
Aorta without endothelium	- (rt)	- (rt)	+ (rt)	RT-PCR	40
Cerebral arteries	N.D. + (m)	+ (rt) + (m)	N. D. + (m)	Immunocitology RT-PCR	21 41
Mesenteric arterial vessels	+ (rt)	+ (rt)	+ (rt)	RT-PCR	39
Portal vein myocytes	+ (rt)	+ (rt)	+ (rt)	RT-PCR	42
Bronchi	- (h)	- (h)	+ (h)	RT-PCR	43
Esophagus	N. D. + (p, m)	N. D. + (m)	+ (rb) + (p,m)	Northern-blot RT-PCR	36 38, 44
Small intestine	- (p)	- (p)	+ (p)	RT-PCR	38
Duodenum	- (m)	+ (m)	+ (m)	RT-PCR	45
Taenia coli	N. D.	N. D.	+ (rb)	Northern-blot	36
Stomach	+ (m)	+ (m)	+ (m)	RT-PCR	44
Ureter	N. D.	N. D.	+ (rb)	Northern-blot	36
Ureteric myocytes	- (rt)	- (rt)	+ (rt)	RT-PCR	29
Urinary bladder	N. D. - (h)	N. D. + (h)	+ (rb) - (h)	Northern-blot RT-PCR	36 46
Cultured urinary bladder myocytes	- (h)	+ (h)	- (h)	RT-PCR	46
Uterus	N. D.	N. D.	+ (rb)	Northern-blot	36
Non-pregnant myometrium	+ (h) - (h)	+ (h) - (h)	+ (h) + (h, m)	RT-PCR RT-PCR	47,48 49,45
Pregnant myometrium	+ (h) - (h)	+ (h) + (h)	+ (h) + (h)	RT-PCR RT-PCR	48 49
Cultured myometrial myocytes	- (h)	- (h)	+ (h)	RT-PCR	49

Abbreviations: N.D. not determined; + detected isoform; - not detected isoform; h, human; m, mouse; p, pig; rb, rabbit; rt, rat; RT-PCR, reverse transcriptase-polymerase chain reaction.

Table 1. Expression of RyR types in different smooth muscles

clamp technique demonstrated that membrane depolarization produces a bell-shape curve of both VDCC currents and changes in  $[Ca^{2+}]_i$ , with the peak  $[Ca^{2+}]_i$  response close to 0 mV (63-68). Similar shape of the voltage-dependent changes in  $[Ca^{2+}]_i$  has been described in cardiac myocytes (69-70). This relationship between voltage and  $[Ca^{2+}]_i$  implies that  $Ca^{2+}$  influx is required in smooth muscle to elevate  $[Ca^{2+}]_i$  during membrane depolarization. Different studies looking at  $[Ca^{2+}]_i$  (58,65,71,72) or  $Ca^{2+}$ -dependent ion channels (73) have suggested the presence of CICR in different smooth muscle cells. However, these studies did not show the extent of CICR contribution to the depolarization-induced  $[Ca^{2+}]_i$  transient. In addition, it appears that CICR is not universally present in smooth muscle cells (67,74-76). To further complicate this picture, there are cases where CICR is evident only for the first depolarization pulse (77) or the first train of voltage pulses (68). Studies aimed to quantify the relevance of CICR in the  $Ca^{2+}$  transient induced by activation of VDCCs demonstrated that an average of only 20 % of the  $[Ca^{2+}]_i$  transient at 500 msec was due to  $Ca^{2+}$  release from internal stores (78). The same type of study was carried out to calculate the cytoplasmic  $Ca^{2+}$  buffer capacity (79), but in this case the idea was to determine the initiation of CICR in VDCC-induced  $[Ca^{2+}]_i$  transient (9, 78). The  $Ca^{2+}$  buffer capacity was obtained for the initial 50 msec of membrane depolarization and compared with a late determination from 100 to 200 msec after VDCCs have been activated. In the absence of ryanodine, the initial  $Ca^{2+}$  buffer was  $87.8 \pm 2.7$  ( $n = 10$ ) while the late  $Ca^{2+}$  buffer was significantly lowered to  $54.1 \pm 5.4$  ( $n = 10$ ). This artificial reduction of the cytoplasmic  $Ca^{2+}$  buffer implies that  $Ca^{2+}$  ions from internal stores contribute to increase  $[Ca^{2+}]_i$  but are not part of the integrated voltage-dependent  $Ca^{2+}$  current. Indeed, the presence of ryanodine in the internal solution of the patch clamp pipette inhibited this extra source of  $Ca^{2+}$ , since the initial and late  $Ca^{2+}$  buffer were similar ( $81.1 \pm 10.0$  vs  $79.2 \pm 9.1$ ,  $n = 8$ ). These data indicate that CICR is a delayed event in smooth muscle (78), as this amplification mechanism was evident only 50 to 100 msec after the activation of VDCCs. This contrast with a time constant of  $\sim 7$  msec between the activation of VDCCs and  $Ca^{2+}$  sparks in cardiac cells (80).

Confocal studies of  $[Ca^{2+}]_i$  in smooth muscle cells under voltage clamp have also shown delays of tens of msec between the activation of VDCCs and  $Ca^{2+}$  sparks (59,81,82). These studies have suggested that smooth muscle RyRs are loosely coupled to VDCCs, implying that it is the bulk  $[Ca^{2+}]_i$  that triggers RyRs activation in smooth muscle (59,83). This is a completely different situation to the one described in cardiac cells, where the efficiency of CICR depends to a great extent on the close proximity between RyRs and VDCCs (80, 84). The concept of "loose coupling" of CICR may be in line with the demonstration that  $Ca^{2+}$  influx through other channels, e.g. stretch-activated channels, can also trigger CICR (78). One of the problems with the loose coupling hypothesis is that  $Ca^{2+}$  sensitivity of RyRs is

not high enough (15,18,61) to activate these channels by bulk  $[Ca^{2+}]_i$ . Another limitation is that CICR should be unstable due to the lack of local control of RyRs.

Additional data undermine the role of CICR in amplifying the  $Ca^{2+}$ -influx through VDCCs in smooth muscle cells. For instance, inhibition of SR  $Ca^{2+}$  pumps with cyclopiazonic acid, although abolishing  $Ca^{2+}$  sparks, it does not reduce the global rise in  $[Ca^{2+}]_i$  triggered by membrane depolarization (82). If anything, it increases the elevation in  $[Ca^{2+}]_i$  (82). Furthermore, the application of ryanodine to rat gastric myocytes increases the efficiency of VDCCs to elevate  $[Ca^{2+}]_i$  (76). The fact that  $Ca^{2+}$  influx through VDCCs is able to increase global  $[Ca^{2+}]_i$  before triggering  $Ca^{2+}$  sparks (59, 81) and that ryanodine does not change the initial  $Ca^{2+}$  buffering capacity (78) suggest that RyRs from smooth muscle are insensitive to  $Ca^{2+}$  influx through VDCCs, even when the activation of VDCCs generates a strong increase in the subsarcolemmal  $[Ca^{2+}]_i$  (85). Interestingly, line scan recordings of  $[Ca^{2+}]_i$  in cardiac cells have shown that when a sparklet (a local  $[Ca^{2+}]_i$  event due to the opening of a single VDCC) does not trigger a  $Ca^{2+}$  spark, the probability of a second, similar sparklet to induce a  $Ca^{2+}$  spark is the same as the probability of the first sparklet that successfully triggered a  $Ca^{2+}$  spark (see figure 6 in reference 80). Collectively, these studies suggest that RyRs might be able to switch between  $Ca^{2+}$ -sensitive and  $Ca^{2+}$ -insensitive states. Thus, beside localization, it appears that there are other factors that determine the ability of RyRs to respond to  $Ca^{2+}$ . If this is true, then identifying these factors might explain the variability of CICR in smooth muscle.

### **Amplification by RyRs of $IP_3$ R-mediated $Ca^{2+}$ release**

The sarcoplasmic reticulum of smooth muscle cells is a continuous membrane organelle (1), although only some parts are specialized in storing  $Ca^{2+}$  (86-89). Smooth muscle SR can be divided in peripheral and central SR, and both types of release-channels (RyRs and  $IP_3$ Rs) are localized in these two sections (1, 22, 90). Conceivably, the activation of  $IP_3$ Rs could either stimulate adjacent RyRs by increasing cytoplasmic  $[Ca^{2+}]_i$  or inhibit RyRs by decreasing luminal  $[Ca^{2+}]_i$ . Such reduction in luminal  $[Ca^{2+}]_i$  has already been demonstrated to affect the activity of RyRs in smooth muscle (91). We have summarized work done on how these two release channels interact in smooth muscle.

It has been proposed that CICR via RyRs propagates the vasopressin-induced  $IP_3$ -initiated  $Ca^{2+}$  release in A7r5 cells (92). Recently, further evidence has been reported supporting the participation of RyRs in amplifying the  $[Ca^{2+}]_i$  signal initiated by activation of  $IP_3$ Rs in smooth muscle cells. Both anti-RyR antibody and ryanodine strongly inhibit the rate of rise of agonist-induced  $Ca^{2+}$  release in myocytes from either portal vein or duodenum (31).

However, there are also many examples where RyRs do not seem to participate in the  $IP_3$ -mediated  $Ca^{2+}$  release. The presence of ryanodine

does not alter the agonist-induced contraction in portal vein, pulmonary artery and taenia caeci from guinea pig (5). In rat portal vein myocytes, tetracaine, although inhibits  $\text{Ca}^{2+}$  release mediated by caffeine, does not affect noradrenaline-triggered  $\text{Ca}^{2+}$  mobilization (93). Acetylcholine-induced  $\text{Ca}^{2+}$  release is not affected by 50  $\mu\text{M}$  ruthenium red in equine tracheal myocytes (94). In rat ureteric myocytes, neither ryanodine nor anti-RyR antibody modifies acetylcholine-mediated  $\text{Ca}^{2+}$  waves (29). Additionally, ryanodine does not block either multiple  $\text{IP}_3$ -triggered  $\text{Ca}^{2+}$  releases in colonic smooth muscle (95) or acetylcholine-induced  $\text{Ca}^{2+}$  release in guinea pig urinary bladder myocytes (Figure 2). These data suggest that either RyRs are not opened during  $\text{IP}_3$ -mediated  $\text{Ca}^{2+}$  release or if they are, then the open time is too short for ryanodine to recognize the open conformation of RyR. However, the latter seems unlikely, as the opening of RyRs by caffeine does induce a complete depletion of internal stores in the presence of ryanodine (Figure 2). Similarly, ryanodine does not have any effect on the histamine-induced  $\text{Ca}^{2+}$  release (96 and Figure 2). Possible explanations for the absence of  $\text{IP}_3$ -induced activation of RyR could be either that  $\text{IP}_3$ R does not increase  $[\text{Ca}^{2+}]_i$  high enough to activate RyRs or that  $\text{IP}_3$ Rs decrease the  $\text{Ca}^{2+}$ -sensitivity of RyRs by lowering luminal  $[\text{Ca}^{2+}]$ , a possibility that might be supported by localization of both receptors at the same internal  $\text{Ca}^{2+}$  store (97). Indeed, different agonists that release  $\text{Ca}^{2+}$  from internal stores also inhibit the spontaneous transient outward currents (STOCs) (98,99), which are due to  $\text{Ca}^{2+}$  sparks activating  $\text{BK}_{\text{Ca}}$  channels (100). This inhibition appears to depend on the  $\text{Ca}^{2+}$ -releasing activity of the agonists, since blocking  $\text{IP}_3$ R with heparin inhibits the action of agonists on STOCs (98,99). Alternatively, it has been suggested that protein kinase C, activated by agonist-induced diacylglycerol, reduces the  $\text{Ca}^{2+}$  sensitivity of RyRs (101). Thus, although it seems that RyRs can amplify the  $\text{IP}_3$ -induced  $\text{Ca}^{2+}$  signal in smooth muscle cells, this action of RyRs does not appear to be present in all types of smooth muscle.

### cADPR and smooth muscle function

From data summarized in the previous section, it seems that RyRs do not play a strong role in excitation-contraction coupling of smooth muscle. It is feasible that other factors might increase the in vivo efficiency of CICR in smooth muscle cells. One candidate is cyclic adenosine diphosphate-ribose (cADPR), a metabolite derived from  $\beta\text{-NAD}^+$  with the ability to induce  $\text{Ca}^{2+}$  release from internal stores in a wide variety of mammalian cells, including cardiac and smooth muscle myocytes. cADPR is generated by ADP-ribosyl cyclase and degraded by cADPR hydrolase. Both enzyme activities appear to reside in the same protein (102), which was firstly identified in mammalian cells as the lymphocyte antigen CD38 (103).

The  $\text{Ca}^{2+}$  releasing activity of cADPR is blocked by procaine, ruthenium red (104) and high concentrations of either ryanodine (19,104) or caffeine (104). Moreover, cADPR-induced  $\text{Ca}^{2+}$  release

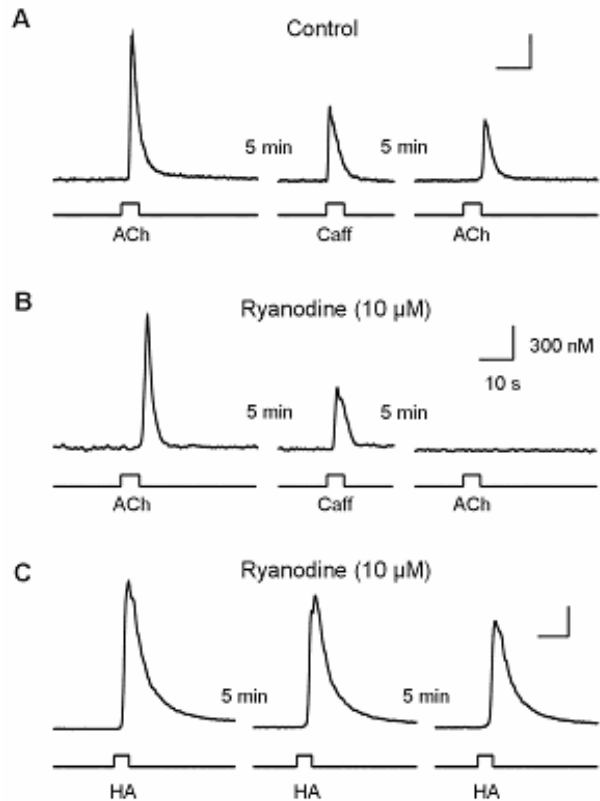


Figure 2. RyRs and  $\text{IP}_3$ Rs share the same internal  $\text{Ca}^{2+}$  store and RyRs do not seem to participate in agonist-induced  $\text{Ca}^{2+}$  release. Single smooth muscle cells from guinea pig urinary bladder were loaded with fura-2 and challenged with either 10  $\mu\text{M}$  Acetylcholine (ACh), or 20 mM caffeine (Caff) or 1 mM histamine (HA) by pressure ejection from a puffer pipette placed close to the cell. The application of agonists are indicated by the traces below the  $[\text{Ca}^{2+}]_i$  recordings. A. Cells responded to both agonists with transient increases in  $[\text{Ca}^{2+}]_i$  provided that time periods of 5 min were allowed between the different applications. Note that recovery of internal stores was only partial because cells were not depolarized to rise  $[\text{Ca}^{2+}]_i$  and facilitate refilling of the stores. B. ACh did not affect caffeine-induced  $\text{Ca}^{2+}$  release in the presence of 10  $\mu\text{M}$  ryanodine, but Caff inhibited ACh-mediated  $\text{Ca}^{2+}$  release in this condition. C. The  $[\text{Ca}^{2+}]_i$  responses to HA were not affected by the presence of ryanodine. These data imply that ACh-induced increase in  $[\text{Ca}^{2+}]_i$  derives from internal  $\text{Ca}^{2+}$  stores only, and all agonists release  $\text{Ca}^{2+}$  from the same internal store. The fact that in the presence of ryanodine, neither ACh nor HA induces an irreversible depletion of internal  $\text{Ca}^{2+}$  stores suggests that  $\text{IP}_3$ -mediated  $\text{Ca}^{2+}$  release does not involve RyRs.

is not affected by heparin, but it is enhanced by low concentrations of caffeine (104, 105). These data support the notion that cADPR activates RyRs in

bovine coronary artery (19) and in smooth muscle from both rabbit longitudinal intestine (106) and porcine trachea (104). Direct evidence that RyR is the target of cADPR comes from a recent work showing that 1  $\mu$ M cADPR increases 8-fold the activity of bovine coronary artery RyRs incorporated in planar lipid bilayers (19). Nevertheless, it has also been suggested that cADPR may activate a novel and RyR-independent  $\text{Ca}^{2+}$  release mechanism in vascular smooth muscle (105).

The first report by Kuemmerle and Makhlof (106) demonstrated that cADPR stimulated  $\text{Ca}^{2+}$  release in permeabilized longitudinal smooth muscle cells from rabbit ileum. This effect was specific because permeabilized circular smooth muscle cells did not respond to cADPR. Since this report, it has been shown that both visceral and vascular smooth muscles respond to cADPR by releasing  $\text{Ca}^{2+}$  from internal stores (104,105,107). Moreover, it has been proposed that cADPR-mediated  $\text{Ca}^{2+}$  signaling participates in the regulation of a variety of functions in smooth muscle such as, agonist-induced contraction (106,108-110) and agonist-induced  $[\text{Ca}^{2+}]_i$  oscillations (104). It has also been suggested that cADPR controls resting  $[\text{Ca}^{2+}]_i$  levels (19,109), vascular and visceral tone (110,111) and decreases  $\text{BK}_{\text{Ca}}$  channel activity (112,113). Recently, it has been reported that cADPR participates in hypoxic pulmonary vasoconstriction as well (107,114). Nevertheless, the role of cADPR in inducing contraction does not seem to be universal (86,115). In addition, there are unanswered questions regarding how cADPR works in smooth muscle, e.g. there is no evidence that membrane depolarization increases cADPR and the mechanism that triggers activation of ADP-ribosyl cyclase in smooth muscle cells is unknown.

### Superficial buffer barrier

Another possible physiological function of RyR in smooth muscle cells is the regulation of luminal  $[\text{Ca}^{2+}]$  of the SR ( $[\text{Ca}^{2+}]_{\text{SR}}$ ). It has been shown that the activity of RyR from cardiac myocytes is sensitive to the  $[\text{Ca}^{2+}]_{\text{SR}}$  (116), which is also supported by studies in permeabilized cardiac myocytes showing that the frequency of  $\text{Ca}^{2+}$  sparks increases in response to a higher  $\text{Ca}^{2+}$  loading of SR. Thus, the modulation of RyR activity by luminal  $[\text{Ca}^{2+}]$  could be a mechanism to regulate the  $[\text{Ca}^{2+}]_{\text{SR}}$  (117). This mechanism may be present in smooth muscle cells as well, since the frequency of  $\text{Ca}^{2+}$  sparks is also sensitive to the  $[\text{Ca}^{2+}]_{\text{SR}}$  (91).

In agreement with the superficial buffer barrier hypothesis proposed for smooth muscle (for review see 118), the peripheral SR separates cytoplasm into a subsarcolemmal region and the bulk cytoplasmic compartment. This compartmentalization would permit the buffering by the peripheral SR of  $\text{Ca}^{2+}$  entering in the subsarcolemmal region. To avoid  $\text{Ca}^{2+}$  overloading of the SR, the sequestered  $\text{Ca}^{2+}$  should be vectorially leaked in the subsarcolemmal space to be extruded from the cell (118). It seems feasible that RyRs are the "leak" channels responding to an increase in the  $[\text{Ca}^{2+}]_{\text{SR}}$  of smooth muscle (119).

Indeed, the incubation of vascular smooth muscle with ryanodine induces vasoconstriction (100). This could be due to the effect of ryanodine on the superficial buffer barrier, as this alkaloid impedes the function of SR as a  $\text{Ca}^{2+}$  store by locking RyRs in an open state (5). Considering that a small  $\text{Ca}^{2+}$  influx through VDCCs is continually sequestered by the activity of peripheral SR  $\text{Ca}^{2+}$  pumps, and since this action limits  $\text{Ca}^{2+}$  access to the myofilaments (16,76,119-121), then eliminating this mechanism with ryanodine should result in a higher effect of VDCCs on contraction (119). Thus, ryanodine either induces or facilitates smooth muscle contraction by nullifying the sink activity of peripheral SR. This is completely opposite to the effect of ryanodine in heart since this alkaloid inhibits contraction by depleting the internal  $\text{Ca}^{2+}$  stores of cardiac myocytes. Nevertheless, stronger or faster  $\text{Ca}^{2+}$  entries are needed to saturate the buffering activity of peripheral SR and to induce contraction in smooth muscle cells (16). Therefore, RyR activity appears to be involved in the vectorial release of  $\text{Ca}^{2+}$  to the subsarcolemmal region.

### Smooth muscle relaxation

Recently, it has been proposed that RyRs might participate in smooth muscle relaxation by generating  $\text{Ca}^{2+}$  sparks (100). In general,  $\text{Ca}^{2+}$  sparks are localized close to the plasma membrane (82,122) where they activate  $\text{BK}_{\text{Ca}}$  channels in a coordinated fashion to produce STOCs, first described by Benhan and Bolton (123). STOCs in turn induce membrane hyperpolarization with the consequent deactivation of VDCCs. This last action decreases  $\text{Ca}^{2+}$  influx, which in turn facilitates smooth muscle relaxation (124). Accordingly, it appears that  $\text{BK}_{\text{Ca}}$  channels are functionally associated to RyRs (125). Indeed, a colocalization study with antibodies showed limited zones where  $\text{BK}_{\text{Ca}}$  channels are close to RyRs (122). Thus, a fraction of RyRs in some smooth muscle cells is tuned or organized in a way that  $\text{Ca}^{2+}$  sparks but not global  $[\text{Ca}^{2+}]_i$  elevations are generated (126). The importance of RyRs generating only  $\text{Ca}^{2+}$  sparks is the implication that overloaded SR can be discharged by an increased frequency of  $\text{Ca}^{2+}$  sparks. These events, as indicated above, generate STOCs with the concomitant hyperpolarization of the cell membrane and deactivation of VDCCs. These effects together with the contribution of the superficial buffer barrier would have as a final result the reduction of  $\text{Ca}^{2+}$  loading in SR. This dynamic regulation of  $\text{Ca}^{2+}$  influx and SR  $\text{Ca}^{2+}$  loading may be responsible for the myogenic tone (124).

However,  $\text{Ca}^{2+}$  sparks also activate  $\text{Ca}^{2+}$ -dependent  $\text{Cl}^-$  channels, which can induce membrane depolarization and smooth muscle contraction (127). Furthermore,  $\text{BK}_{\text{Ca}}$  channels can also be directly activated by local  $\text{Ca}^{2+}$  entry through VDCCs (128). These data indicate that not all  $\text{BK}_{\text{Ca}}$  channels are strictly associated with RyRs. Indeed, it has been found that a substantial number of  $\text{Ca}^{2+}$  sparks does not elicit STOCs in myocytes from both feline esophagus (129) and toad stomach (130). In addition, studies in intact cells have shown that  $\text{BK}_{\text{Ca}}$

channels display an extremely high Hill number and a  $\text{Ca}^{2+}$  sensitivity near  $1 \mu\text{M}$  (131), both of which are higher than the same obtained for these channels in planar lipid bilayers (132). Therefore,  $\text{Ca}^{2+}$  sparks do not need to be in such close apposition to  $\text{BK}_{\text{Ca}}$  channels, as nearby  $\text{Ca}^{2+}$  sparks would only require to increase  $[\text{Ca}^{2+}]_i$  to  $\sim 1 \mu\text{M}$  to trigger STOCs.

It has been established that cyclic nucleotides (cAMP and cGMP) play a significant role in smooth muscle relaxation. These second messengers increase the frequency of both  $\text{Ca}^{2+}$  sparks and STOCs in smooth muscle cells isolated from basilar arteries (133), supporting the role of  $\text{Ca}^{2+}$  sparks in smooth muscle relaxation. However, the same nucleotides either barely increase the frequency of STOCs in myocytes from rabbit portal vein (134), or do not have any effect on STOCs frequency in pulmonary artery smooth muscle cells (135). Interestingly, in these three cases cyclic nucleotides appear to increase the  $[\text{Ca}^{2+}]_{\text{SR}}$ . Certainly, although the function of RyRs in smooth muscle relaxation seems to be appealing, more studies are needed to establish the actual role of RyRs in terminating smooth muscle mechanical activity.

### Perspectives

The role of RyRs in smooth muscle has begun to be unraveled. From the data reviewed here, it appears that unknown factors may regulate the activity of RyRs in this type of cells. This notion is supported by the fact that RyR3 in uterine smooth muscle cannot directly respond to  $\text{Ca}^{2+}$  or caffeine (45, 47), although they respond to these agents when expressed in HEK293 cells (136). Identifying the nature of these factors is critical to understand the role of RyRs in smooth muscle physiology. However, there are still other questions that need to be addressed, among them: 1) Is there more than one type of RyR expressed in the same smooth muscle cell? 2) What is the intracellular distribution of the different types of RyRs? 3) How tight is the relationship between RyR and  $\text{BK}_{\text{Ca}}$  channels? 4) What is the importance of RyR in regulating the luminal  $[\text{Ca}^{2+}]$  in smooth muscle cells? These issues are further complicated by the diversity of smooth muscles. Thus, although RyRs are present on the SR of smooth muscle cells, these release channels do not seem to participate in excitation-contraction coupling. Clearly, this is the opposite to the key role played by RyRs in the contraction of striated muscles.

### Acknowledgments

This work was partially supported by CONACyT grant 31864N. We thank Beatriz Aguilar for reading the manuscript.

### References

1. Somlyo, A. P. & A. V. Somlyo. Signal transduction and regulation in smooth muscle. *Nature* 372, 231-236 (1994).
2. Horowitz, A., C. B. Menice, R. Laporte & K. G. Morgan. Mechanisms of smooth muscle contraction. *Physiol Rev* 76, 967-1003 (1996).
3. Bolton, T. B., S. A. Prestwich, A. V. Zholos & D. V. Gordienko. Excitation-contraction coupling in

- gastrointestinal and other smooth muscles. *Annu Rev Physiol* 61, 85-115 (1999).
4. Itoh, T., H. Ueno & H. Kuriyama Calcium-induced calcium release mechanism in vascular smooth muscles-assessments based on contractions evoked in intact and saponin-treated skinned muscles. *Experientia* 41, 989-996 (1985).
5. Iino, M., T. Kobayashi & M. Endo. Use of ryanodine for functional removal of the calcium store in smooth muscle cells of the guinea-pig. *Biochem Biophys Res Comm* 152, 417-422 (1988).
6. Endo, M., T. Kitazawa, S. Yagi, M. Iino & Y. Kakuta. Some properties of chemically skinned smooth muscle fibers. In Excitation-contraction coupling in smooth muscle. R. Casteels, T. Godfraind, & J.C. Ruegg, editors. Elsevier Science Publishers, Amsterdam 199-209 (1977).
7. Rousseau, E. & G. Meissner. Single cardiac sarcoplasmic reticulum  $\text{Ca}^{2+}$ -release channel: activation by caffeine. *Am J Physiol* 256, H328-333 (1989).
8. Guerrero, A., F. S. Fay & J. J. Singer. Caffeine activates a  $\text{Ca}^{2+}$ -permeable, nonselective cation channel in smooth muscle cells. *J Gen Physiol* 104, 375-394 (1994).
9. Guerrero, A., J. J. Singer & F. S. Fay. Simultaneous measurement of  $\text{Ca}^{2+}$  release and influx into smooth muscle cells in response to caffeine. A novel approach for calculating the fraction of current carried by calcium. *J Gen Physiol* 104, 395-422 (1994).
10. Zou, H., L. M. Lifshitz, R. A. Tuft, K. E. Fogarty & J. J. Singer. Imaging  $\text{Ca}^{2+}$  entering the cytoplasm through a single opening of a plasma membrane cation channel. *J Gen Physiol* 114, 575-88 (1999).
11. Pessah, I. N. & I. Zimanyi. Characterization of multiple [ $^3\text{H}$ ]ryanodine binding sites on the  $\text{Ca}^{2+}$  release channel of sarcoplasmic reticulum from skeletal and cardiac muscle: evidence for a sequential mechanism in ryanodine action. *Mol Pharmacol* 39, 679-689 (1991).
12. Ganitkevich, V. Ya. & H. Hirche. High cytoplasmic  $\text{Ca}^{2+}$  levels reached during  $\text{Ca}^{2+}$ -induced  $\text{Ca}^{2+}$  release in single smooth muscle cell as reported by a low affinity  $\text{Ca}^{2+}$  indicator Mag-Indo-1. *Cell Calcium* 19, 391-398 (1996).
13. Morel, J. L., N. Macrez & J. Mironneau. Specific Gq protein involvement in muscarinic  $\text{M}_3$  receptor-induced phosphatidylinositol hydrolysis and  $\text{Ca}^{2+}$  release in mouse duodenal myocytes. *Br J Pharmacol* 121, 451-458 (1997).
14. Rousseau, E., J. Ladine, Q. Y. Liu & G. Meissner. Activation of the  $\text{Ca}^{2+}$  release channel of skeletal muscle sarcoplasmic reticulum by caffeine and related compounds. *Arch Biochem Biophys* 267, 75-86 (1988).
15. Xu, L., F. A. Lai, A. Cohn, E. Etter, A. Guerrero, F. S. Fay & G. Meissner. Evidence for a  $\text{Ca}^{2+}$ -gated ryanodine-sensitive  $\text{Ca}^{2+}$  release channel in visceral smooth muscle. *Proc Natl Acad Sci U S A* 91, 3294-3298 (1994).
16. Yoshikawa, A., C. van Breemen & G. Isenberg. Buffering of plasmalemmal  $\text{Ca}^{2+}$  current by sarcoplasmic reticulum of guinea pig urinary bladder myocytes. *Am J Physiol* 271, C833-C841 (1996).
17. Lai, F.A. & G. Meissner. The muscle ryanodine receptor and its intrinsic  $\text{Ca}^{2+}$  channel activity. *J Bioenerg Biomembr* 21, 227-246. (1989).
18. Herrmann-Frank, A., E. Darling & G. Meissner. Functional characterization of the  $\text{Ca}^{2+}$ -gated  $\text{Ca}^{2+}$  release channel of vascular smooth muscle sarcoplasmic reticulum. *Pflügers Arch* 418, 353-359 (1991).
19. Li, P. L., W. X. Tang, H. H. Valdivia, A. P. Zou & W. B. Campbell. cADP-ribose activates reconstituted ryanodine receptors from coronary arterial smooth muscle. *Am J Physiol* 280, H208-H215 (2001).
20. Somlyo, A. P. Excitation-contraction coupling and the ultrastructure of smooth muscle. *Circ Res* 57, 497-507 (1985).

21. Gollasch, M., G. C. Wellman, H. J. Knot, J. H. Jaggard, D. H. Damon, A. D. Bonev & M. T. Nelson. Ontogeny of local sarcoplasmic reticulum  $Ca^{2+}$  signals in cerebral arteries:  $Ca^{2+}$  sparks as elementary physiological events. *Circ Res* 83, 1104-1114 (1998).
22. Lesh R.E., G. F. Nixon, S. Fleischer, J. A. Airey, A. P. Somlyo & A. V. Somlyo. Localization of ryanodine receptors in smooth muscle. *Circ Res* 82, 175-185 (1998).
23. Gordienko, D. V., I. A. Greenwood & T. B. Bolton. Direct visualization of sarcoplasmic reticulum regions discharging  $Ca^{2+}$  sparks in vascular myocytes. *Cell Calcium* 29, 13-28 (2001).
24. Devine, C. E., A. V. Somlyo & A. P. Somlyo. Sarcoplasmic reticulum and excitation-contraction coupling in mammalian smooth muscles. *J Cell Biol* 52, 690-718 (1972).
25. Carrington, W. A., R. M. Lynch, E. D. Moore, G. Isenberg, K. E. Fogarty & F. S. Fay. Superresolution three-dimensional images of fluorescence in cells with a minimal light exposure. *Science* 268, 1483-1487 (1995).
26. Zhang, Z. D., C. Y. Kwan & E. E. Daniel. Subcellular-membrane characterization of [ $^3H$ ]ryanodine-binding sites in smooth muscle. *Biochem J* 290, 259-266 (1993).
27. Zhang, Z. D., C. Y. Kwan & E. E. Daniel. Characterization of [ $^3H$ ]ryanodine binding sites in smooth muscle of dog mesentery artery. *Biochem Biophys Res Commun* 194, 1242-1247 (1993).
28. Kuemmerle, J.F., K. S. Murthy & G. M. Makhlof. Agonist-activated, ryanodine-sensitive,  $IP_3$ -insensitive  $Ca^{2+}$  release channels in longitudinal muscle of intestine. *Am J Physiol* 266, C1421-C1431 (1994).
29. Boittin F. X., F. Coussin, J. L. Morel, G. Halet, N. Macrez & J. Mironneau.  $Ca^{2+}$  signals mediated by  $Ins(1,4,5)P_3$ -gated channels in rat ureteric myocytes. *Biochem J* 349, 323-332 (2000).
30. Coronado, R., J. Morrisette, M. Sukhareva & D.M. Vaughan. Structure and function of ryanodine receptors. *Am J Physiol* 266, C1485-C1504 (1994).
31. Boittin F.X., N. Macrez, G. Halet & Mironneau J. Norepinephrine-induced  $Ca^{2+}$  waves depend on  $InsP_3$  and ryanodine receptor activation in vascular myocytes. *Am J Physiol* 277, C139-C151 (1999).
32. Chu, A., M. Diaz-Munoz, Hawkes, M. J., K. Brush & S. L. Hamilton. Ryanodine as a probe for the functional state of the skeletal muscle sarcoplasmic reticulum calcium release channel. *Mol Pharmacol* 37, 735-741 (1990).
33. Takeshima, H., S. Nishimura, T. Matsumoto, H. Ishida, K. Kangawa, N. Minamino, H. Matsuo, M. Ueda, M. Hanaoka, T. Hirose & S. Numa. Primary structure and expression from complementary DNA of skeletal muscle ryanodine receptor. *Nature* 339, 439-445 (1989).
34. Otsu, K., H. F. Willard, V. K. Khanna, F. Zorzato, N. M. Green & D. H. MacLennan. Molecular cloning of cDNA encoding the  $Ca^{2+}$  release channel (ryanodine receptor) of rabbit cardiac muscle sarcoplasmic reticulum. *J Biol Chem* 265, 13472-13483 (1990).
35. Giannini, G., E. Clementi, R. Ceci, G. Marziali & V. Sorrentino. Expression of a ryanodine receptor- $Ca^{2+}$  channel that is regulated by TGF- $\beta$ . *Science* 257, 91-94 (1992).
36. Hakamata, Y., J. Nakai, H. Takeshima & K. Imoto. Primary structure and distribution of a novel ryanodine receptor/calcium release channel from rabbit brain. *FEBS Lett* 312, 229-235 (1992).
37. Moschella M. C. & A. R. Marks. Inositol 1,4,5-trisphosphate receptor expression in cardiac myocytes. *J Cell Biol* 120, 1137-1146 (1993).
38. Ledbetter M. W., J. K. Preiner, C. F. Louis & J. R. Mickelson. Tissue distribution of ryanodine receptor isoforms and alleles determined by reverse transcription polymerase chain reaction. *J Biol Chem* 269, 31544-31551 (1994).
39. Neylon C. B., S. M. Richards, M. A. Larsen, A. Agrotis & A. Bobik. Multiple types of ryanodine receptor/ $Ca^{2+}$  release channels are expressed in vascular smooth muscle. *Biochem Biophys Res Commun* 215, 814-821 (1995).
40. Vallot, O., L. Combettes, P. Jourdon, J. Inamo, I. Marty, M. Claret & A. M. Lompre. Intracellular  $Ca^{2+}$  handling in vascular smooth muscle cells is affected by proliferation. *Arterioscler Thromb Vasc Biol* 20, 1225-1235 (2000).
41. Lohn, M., W. Jessner, M. Furstenau, M. Wellner, V. Sorrentino, H. Haller, F. C. Luft & M. Gollasch. Regulation of calcium sparks and spontaneous transient outward currents by RyR3 in arterial vascular smooth muscle cells. *Circ Res* 89, 1051-1057 (2001).
42. Coussin, F., N. Macrez, J. L. Morel & J. Mironneau. Requirement of ryanodine receptor subtypes 1 and 2 for  $Ca^{2+}$ -induced  $Ca^{2+}$  release in vascular myocytes. *J Biol Chem* 275, 9596-9603 (2000).
43. Hyvelin, J. M., C. Martin, E. Roux, R. Marthan & J. P. Savineau. Human isolated bronchial smooth muscle contains functional ryanodine/cafeine-sensitive  $Ca^{2+}$ -release channels. *Am J Respir Crit Care Med* 162, 687-694 (2000).
44. Giannini, G., A. Conti, S. Mammarella, M. Scrobogna & V. Sorrentino. The ryanodine receptor/calcium channel genes are widely and differentially expressed in murine brain and peripheral tissues. *J Cell Biol* 128, 893-904 (1995).
45. Mironneau, J., N. Macrez, J. L. Morel, V. Sorrentino & C. Mironneau. Identification and function of ryanodine receptor subtype 3 in non-pregnant mouse myometrial cells. *J Physiol* 538, 707-716 (2002).
46. Chambers, P., D. E. Neal & J. I. Gillespie. Ryanodine receptors in human bladder smooth muscle. *Exp Physiol* 84, 41-46 (1999).
47. Lynn, S., J. M. Morgan, H. K. Lamb, G. Meissner & J. I. Gillespie. Isolation and partial cloning of ryanodine-sensitive  $Ca^{2+}$  release channel protein isoforms from human myometrial smooth muscle. *FEBS Lett.* 372, 6-12 (1995).
48. Martin, C., K. E. Chapman, S. Thornton & R. H. Ashley. Changes in the expression of myometrial ryanodine receptor mRNAs during human pregnancy. *Biochim Biophys Acta* 1451, 343-352 (1999).
49. Awad, S. S., H. K. Lamb, J. M. Morgan, W. Dunlop & J. I. Gillespie. Differential expression of ryanodine receptor RyR2 mRNA in the non-pregnant and pregnant human myometrium. *Biochem J* 322, 777-783 (1997).
50. Takeshima, H., T. Ikemoto, M. Nishi, N. Nishiyama, M. Shimuta, Y. Sugitani, J. Kuno, I. Saito, H. Saito, M. Endo, Iino M & T. Noda. Generation and characterization of mutant mice lacking ryanodine receptor type 3. *J Biol Chem* 271, 19649-19652 (1996).
51. Takeshima, H., S. Komazaki, K. Hirose, M. Nishi, T. Noda & M. Iino. Embryonic lethality and abnormal cardiac myocytes in mice lacking ryanodine receptor type 2. *EMBO J* 17:3309-3316 (1998).
52. Takeshima, H., M. Iino, H. Takekura, M. Nishi, J. Kuno, O. Minowa, H. Takano & T. Noda. Excitation-contraction uncoupling and muscular degeneration in mice lacking functional skeletal muscle ryanodine-receptor gene. *Nature* 369, 556-559 (1994).
53. Takeshima, H., T. Yamazawa, T. Ikemoto, H. Takekura, M. Nishi, T. Noda & Iino M.  $Ca^{2+}$ -induced  $Ca^{2+}$  release in myocytes from dyspedic mice lacking the type-1 ryanodine receptor. *EMBO J* 14, 2999-3006 (1995).
54. Mironneau, J., F. Coussin, L. H. Jeyakumar, S. Fleischer, C. Mironneau & N. Macrez. Contribution of ryanodine receptor subtype 3 to  $Ca^{2+}$  responses in  $Ca^{2+}$ -overloaded cultured rat portal vein myocytes. *J Biol Chem* 276, 11257-11264 (2001).
55. Matsumoto, H., C. B. Baron & R. F. Coburn. Smooth muscle stretch-activated phospholipase C activity. *Am J Physiol* 268, C458-C465 (1995).

56. Itoh, T., N. Seki, S. Suzuki, S. Ito, J. Kajikuri & M. Kuriyama. Membrane hyperpolarization inhibits agonist-induced synthesis of inositol 1,4,5-trisphosphate in rabbit mesenteric artery. *J Physiol* 451, 307-328 (1992).
57. Ganitkevich, V. Y., & G. Isenberg. Membrane potential modulates inositol 1,4,5-trisphosphate-mediate  $\text{Ca}^{2+}$  transients in guinea-pig coronary myocytes. *J Physiol* 470, 35-44 (1993).
58. Ganitkevich, V. Y., & G. Isenberg. Efficacy of peak  $\text{Ca}^{2+}$  currents ( $I_{\text{Ca}}$ ) as trigger of sarcoplasmic reticulum  $\text{Ca}^{2+}$  release in myocytes from the guinea-pig coronary artery. *J Physiol* 484, 287-306 (1995).
59. Collier, M. L., G. Ji, Y. Wang & M. I. Kotlikoff. Calcium-induced calcium release in smooth muscle. Loose coupling between the action potential and calcium release. *J Gen Physiol* 115, 653-662 (2000).
60. Fabiato, A. Time and calcium dependence of activation and inactivation of calcium-induced release of calcium from the sarcoplasmic reticulum of a skinned canine cardiac Purkinje cell. *J Gen Physiol* 85, 247-289 (1985).
61. Iino, M. Calcium-induced calcium release mechanism in guinea-pig taenia caeci. *J Gen Physiol* 94, 363-383 (1989).
62. Iino, M. Calcium release mechanisms in smooth muscle. *Japan J Pharmacol* 54, 345-354 (1990).
63. Vogalis, F., N.G. Plubicover, J.R. Hume & K. M. Sanders. Relationship between calcium current and cytosolic calcium in canine gastric smooth muscle cells. *Am J Physiol* 260, C1012-C1018 (1991).
64. Ganitkevich, V.Ya. & G. Isenberg. Depolarization-mediated intracellular calcium transients in isolated smooth muscle cells of guinea-pig urinary bladder. *J Physiol* 435, 187-205 (1991).
65. Gregoire, G., G. Loirand & P. Pacaud.  $\text{Ca}^{2+}$  and  $\text{Sr}^{2+}$  entry induced  $\text{Ca}^{2+}$  release from the intracellular  $\text{Ca}^{2+}$  store in smooth muscle cells of rat portal vein. *J Physiol* 472, 483-500 (1993).
66. Fleischmann, B.K., Y.X. Wang, M. Pring & M.I. Kotlikoff. Voltage-dependent calcium currents and cytosolic-calcium in equine air way myocytes. *J Physiol* 492, 347-358 (1996).
67. Kamishima, T. & J.G. McCarron. Depolarization-evoked increases in cytosolic calcium concentration in isolated smooth muscle cells of rat portal vein. *J Physiol* 492, 61-74 (1996).
68. Shmigol, A. V., D. A. Eisner & S. Wray. Properties of voltage-activated  $[\text{Ca}^{2+}]_i$  transients in single smooth muscle cells isolated from pregnant rat uterus. *J Physiol* 511, 803-811 (1998).
69. Cannell, M. B., J. R. Berlin & W. J. Lederer. Effect of membrane potential changes on the calcium transient in single rat cardiac muscle cells. *Science* 238, 1419-1423 (1987).
70. Barcenas-Ruiz, L., & W. G. Wier. Voltage dependence of intracellular  $\text{Ca}^{2+}$  transients in guinea pig ventricular myocytes. *Circ Res* 61, 148-154 (1987).
71. Ganitkevich, V. & G. Isenberg. Contribution of  $\text{Ca}^{2+}$ -induced  $\text{Ca}^{2+}$  release to the  $[\text{Ca}^{2+}]_i$  transients in myocytes from guinea-pig urinary bladder. *J Physiol* 458, 119-137 (1992).
72. Kamishima, T. & J.G. McCarron. Regulation of the cytosolic  $\text{Ca}^{2+}$  concentration by  $\text{Ca}^{2+}$  stores in single smooth muscle cells from rat cerebral arteries. *J Physiol* 501, 497-508 (1997).
73. Zholos, A. V., L. V. Baidan & M. F. Shuba. Some properties of  $\text{Ca}^{2+}$ -induced  $\text{Ca}^{2+}$  release mechanism in single visceral smooth muscle cell of guinea-pig. *J Physiol* 457, 1-25 (1992).
74. Fleischmann B. K., R. K. Murray & M. I. Kotlikoff. Voltage window for sustained elevation of cytosolic calcium in smooth muscle cells. *Proc Natl Acad Sci U S A* 91, 11914-11918 (1994).
75. Janssen, L. J. & S. M. Sims.  $\text{Ca}^{2+}$ -dependent  $\text{Cl}^-$  current in canine tracheal smooth muscle cells. *Am J Physiol* 269, C163-C169 (1995).
76. White, C. & J. G. McGeown.  $\text{Ca}^{2+}$  uptake by the sarcoplasmic reticulum decreases the amplitude of depolarization-dependent  $[\text{Ca}^{2+}]_i$  transients in rat gastric myocytes. *Pflugers Arch* 440, 488-495 (2000).
77. Ganitkevich, V. Y.  $\text{Ca}^{2+}$ -induced  $\text{Ca}^{2+}$  release in single isolated smooth muscle cells. In: Smooth muscle excitation. Eds Bolton, T. B. Tomita, T. Academic press N.Y (1996).
78. Kirber, M.T., A. Guerrero-Hernández, D.S. Bowman, K.E. Fogarty, R.A. Tuft, J.J. Singer & F.S. Fay. Multiple pathways responsible for the stretch-induced increase in  $\text{Ca}^{2+}$  concentration in toad stomach smooth muscle cells. *J Physiol* 524, 3-17 (2000).
79. Neher, E. & G. J. Augustine. Calcium gradients and buffers in bovine chromaffin cells. *J Physiol* 450, 273-301 (1992).
80. Wang, S. O., L. S. Song, E. G. Lakatta & H. Cheng.  $\text{Ca}^{2+}$  signalling between single L-type  $\text{Ca}^{2+}$  channels and ryanodine receptors in heart cells. *Nature* 410, 592-596 (2001).
81. Bolton, T. & D. Gordienko. Confocal imaging of calcium events in single smooth muscle cells. *Acta Physiol Scand* 164, 567-576 (1998).
82. Imaizumi, Y., Y. Tori, Y. Ohi, N. Nagano, K. Atsuki, H. Yamamura, K. Muraki, M. Watanabe & T. B. Bolton.  $\text{Ca}^{2+}$  images and  $\text{K}^+$  current during depolarization in smooth muscle cells of the guinea-pig vas deferens and urinary bladder. *J Physiol* 510, 705-719 (1998).
83. Arnaudeau, S., F. X. Boittin, N. Macrez, J. L. Lavie, C. Mironneau & J. Mironneau. L-type and  $\text{Ca}^{2+}$  release channel-dependent hierarchical  $\text{Ca}^{2+}$  signalling in rat portal vein myocytes. *Cell Calcium* 22, 399-411 (1997).
84. Gomez, A. M., H. H. Valdivia, H. Cheng, M. R. Lederer, L. F. Santana, M. B. Cannell, S. A. McCune, R. A. Altschuld & W. J. Lederer. Defective excitation-contraction coupling in experimental cardiac hypertrophy and heart failure. *Science* 276, 800-806 (1997).
85. Etter, E. F., A. Minta, M. Poenie & F. S. Fay. Near-membrane  $[\text{Ca}^{2+}]_i$  transients resolved using the  $\text{Ca}^{2+}$  indicator FFP18. *Proc Natl Acad Sci U S A* 93, 5368-5373 (1996).
86. Steenberg, J. M. & F. S. Fay. The quantal nature of calcium release to caffeine in single smooth muscle cells results from activation of the sarcoplasmic reticulum  $\text{Ca}^{2+}$ -ATPase. *J Biol Chem* 271, 1821-1824 (1996).
87. Tribe, R. M., M. L. Borin & M. P. Blaustein. Functionally and spatially distinct  $\text{Ca}^{2+}$  stores are revealed in cultured vascular smooth muscle cells. *Proc Natl Acad Sci U S A* 91, 5908-5912 (1994).
88. Meldolesi, J. & T. Pozzan. The heterogeneity of ER  $\text{Ca}^{2+}$  stores has a key role in nonmuscle cell signaling and function. *J Cell Biol* 142, 1395-1398 (1998).
89. Young, R. C. & S. P. Mathur. Focal sarcoplasmic reticulum calcium stores and diffuse inositol 1,4,5-trisphosphate and ryanodine receptors in human myometrium. *Cell Calcium* 26, 69-75 (1999).
90. Nixon, G. F., G. A. Mignery & A. V. Somlyo. Immunogold localization of inositol 1,4,5-trisphosphate receptors and characterization of ultrastructural features of the sarcoplasmic reticulum in phasic and tonic smooth muscle. *J Mus Res Cell Motil* 15, 682-700 (1994).
91. ZhuGe, R., R.A. Tuft, K.E. Fogarty, K. Bellve, F.S. Fay & J.V. Walsh, Jr. The influence of sarcoplasmic reticulum  $\text{Ca}^{2+}$  concentration on  $\text{Ca}^{2+}$  sparks and spontaneous transient outward currents in single smooth muscle cells. *J Gen Physiol* 113, 215-228 (1999).
92. Blatter, L. A. & W. G. Wier. Agonist-induced  $[\text{Ca}^{2+}]_i$  waves and  $\text{Ca}^{2+}$ -induced  $\text{Ca}^{2+}$  release in mammalian vascular smooth muscle cells. *Am J Physiol* 263, H576-H586 (1992).
93. Pacaud, P & G. Loirand. Release of  $\text{Ca}^{2+}$  by noradrenaline and ATP from the same  $\text{Ca}^{2+}$  store sensitive to both  $\text{IP}_3$  and  $\text{Ca}^{2+}$  in rat portal vein myocytes. *J Physiol* 484, 549-555 (1995).

94. Wang, Y & M. I. Kotlikoff. Muscarinic signaling pathway for calcium release and calcium activated chloride current in smooth muscle. *Am J Physiol* 273, C509-C519 (1997).
95. Flynn, E. R., K. N. Bradley, T. C. Muir & J. G. McCarron. Functionally separate intracellular  $\text{Ca}^{2+}$  stores in smooth muscle. *J Biol Chem* 276, 36411-36418 (2001).
96. Rueda, A., L. García & A. Guerrero-Hernández. Luminal  $\text{Ca}^{2+}$  and the activity of Sarcoplasmic Reticulum  $\text{Ca}^{2+}$  Pump modulate histamine-induced all-or-none  $\text{Ca}^{2+}$  release in smooth muscle cells. *Cell Signal* 14, 517-527 (2002).
97. Komori, S., M. Itagaki, T. Unno & H. Ohashi. Caffeine and carbachol act on common  $\text{Ca}^{2+}$  stores to release  $\text{Ca}^{2+}$  in guinea-pig ileal smooth muscle. *Eur J Pharmacol* 277, 173-180 (1995).
98. Bolton, T. B. & Y. Imaizumi. Spontaneous transient outward currents in smooth muscle cells. *Cell Calcium* 20, 141-152 (1996).
99. Rueda, A., L. García, L. E. Soria-Jasso, J. A. Arias-Montaño & A. Guerrero-Hernández. The initial inositol 1,4,5-trisphosphate response induced by histamine is strongly amplified by  $\text{Ca}^{2+}$  release from internal stores in smooth muscle. *Cell Calcium* (2002) In press.
100. Nelson, M. T., C. M. Rubart, L. F. Santana, A. D. Bonev, H. J. Knot & W. J. Lederer. Relaxation of arterial smooth muscle by calcium sparks. *Science* 270, 633-637 (1995).
101. Jaggar J. H. & M. T. Nelson. Differential regulation of  $\text{Ca}^{2+}$  sparks and  $\text{Ca}^{2+}$  waves by UTP in rat cerebral artery smooth muscle cells. *Am J Physiol Cell Physiol* 279, C1528-39 (2000).
102. Lee, H. C. Physiological functions of cyclic ADP-ribose and NAADP as calcium messengers. *Ann Rev Pharmacol Toxicol* 41, 317-345 (2001).
103. Howard, M., J. C. Grimaldi, J. F. Bazan, F. E. Lund, L. Santos-Argumedo, R. M. E. Parkhouse, T. F. Walseth & H. C. Lee. Formation and hydrolysis of cyclic ADP-ribose catalyzed by lymphocyte antigen CD38. *Science* 262, 1056-1059 (1993).
104. Prakash, Y. S., M. S. Kannan, T. F. Walseth & G. C. Sieck. Role of cyclic ADP-ribose in the regulation of  $[\text{Ca}^{2+}]_i$  in porcine tracheal smooth muscle. *Am J Physiol* 43, C1653-1660 (1998).
105. Kannan, M. S., A. M. Fenton, Y. S. Prakash & G. C. Sieck. Cyclic-ADP-ribose stimulates sarcoplasmic reticulum calcium release in porcine coronary artery smooth muscle. *Am J Physiol* 270, H801-H806 (1996).
106. Kuemmerle, J. F. & G. M. Makhlof. Agonist-stimulated cyclic ADP ribose. Endogenous modulator of  $\text{Ca}^{2+}$  - induced  $\text{Ca}^{2+}$  release in intestinal longitudinal muscle. *J Biol Chem* 270, 25488-25494 (1995).
107. Wilson, H. L. M. Dipp, J. M. Thomas, C. Lad, A. Galione & A. M. Evans. ADP-ribosyl cyclase and cyclic ADP-ribose hydrolase act as a redox sensor. A primary role for cyclic ADP-ribose in hypoxic pulmonary vasoconstriction. *J Biol. Chem* 276, 11180-11188 (2001)
108. Chini, E. N., F. G. de Toledo, M. A. Thompson & T. P. Dousa. Effect of estrogen upon cyclic ADP ribose metabolism: beta-estradiol stimulates ADP ribosyl cyclase in rat uterus. *Proc Natl Acad Sci U S A* 94, 5872-5876 (1997).
109. Giuliumian A. D., L. G. Meszaros & L. C. Fuchs. Endothelin-1-induced contraction of mesenteric small arteries is mediated by ryanodine receptor  $\text{Ca}^{2+}$  channels and cyclic ADP-ribose. *J Cardiovasc Pharmacol* 36, 758-63 (2000).
110. Franco, L., S. Bruzzone, P. Song, L. Guida, E. Zocchi, T. F. Walseth, E. Crimi, C. Usai, A. De Flora & V. Brusasco. Extracellular cyclic ADP-ribose potentiates ACh-induced contraction in bovine tracheal smooth muscle. *Am J Physiol* 280, L98-L106 (2001).
111. Geiger, J., A. P. Zou, W. B. Campbell & P. L. Li. Inhibition of cADP-ribose formation produces vasodilation in bovine coronary arteries. *Hypertension* 35, 397-402 (2000).
112. Li, P., A. P. Zou & W. B. Campbell. Metabolism and actions of ADP-riboses in coronary arterial smooth muscle. *Adv Exp Med Biol* 419, 437-41 (1997).
113. Li, P. L., A. P. Zou & W. B. Campbell. Regulation of KCa-channel activity by cyclic ADP-ribose and ADP-ribose in coronary arterial smooth muscle. *Am J Physiol* 275, H1002-H1010 (1998).
114. Dipp, M & A. M. Evans. Cyclic ADP-ribose is the primary trigger for hypoxic pulmonary vasoconstriction in the rat lung in situ. *Circ Res* 89, 77-83 (2001).
115. Iizuka, K., A. Yoshii, K. Dobashi, T. Horie, M. Mori & T. Nakazawa.  $\text{InsP}_3$ , but not novel  $\text{Ca}^{2+}$  releasers, contributes to agonist-initiated contraction in rabbit airway smooth muscle. *J Physiol* 511, 915-933 (1998).
116. Gyorke, I. & S. Gyorke. Regulation of the cardiac ryanodine receptor channel by luminal  $\text{Ca}^{2+}$  involves luminal  $\text{Ca}^{2+}$  sensing sites. *Biophys J* 75, 2801-2810 (1998).
117. Lukyanenko, V., S. Viatchenko-Kartpinski, A. Smirnov, T. F. Wiesner & S. Gyorke. Dynamic regulation of sarcoplasmic reticulum  $\text{Ca}^{2+}$  content and release by luminal  $\text{Ca}^{2+}$ -sensitive leak in rat ventricular myocytes. *Biophys J* 81, 785-798 (2001).
118. van Breemen, C., Q. Chen & I. Laher. Superficial buffer barrier function of smooth muscle sarcoplasmic reticulum. *Trends Pharmacol Sci* 16, 98-105 (1995).
119. Janssen, L. J., P. A. Betti, S. J. Netherton & D. K. Walters. Superficial buffer barrier and preferentially directed release of  $\text{Ca}^{2+}$  in canine airway smooth muscle. *Am J Physiol* 276, L744-L753 (1999).
120. Chen, Q., M. Cannell, & C. van Breemen. The superficial buffer barrier in vascular smooth muscle. *Can J Physiol Pharmacol* 70, 509-514 (1992).
121. Shmigol, A. V., D. A. Eisner & S. Wray. The role of the sarcoplasmic reticulum as a  $\text{Ca}^{2+}$  sink in rat uterine smooth muscle cells. *J Physiol* 520, 153-63 (1999).
122. Ohi, Y., H. Yamamura, N. Nagano, S. Ohya, K. Muraki, M. Watanabe & Y. Imaizumi. Local  $\text{Ca}^{2+}$  transients and distribution of BK channels and ryanodine receptors in smooth muscle cells of guinea-pig vas deferens and urinary bladder. *J Physiol* 534, 313-26 (2001).
123. Benham C. D. & T. B. Bolton. Spontaneous transient outward currents in single visceral and vascular smooth muscle cells of the rabbit. *J Physiol* 381, 384-406 (1986).
124. Jaggar, J.H., V.A. Porter, W.J. Lederer & M.T. Nelson. Calcium sparks in smooth muscle. *Am J Physiol* 278, C235-C256 (2000).
125. Perez, G. J., A. D. Bonev, J. B. Patlak & M. T. Nelson. Functional coupling of ryanodine receptors to  $\text{K}_{\text{Ca}}$  channels in smooth muscle cells from rat cerebral arteries. *J Gen Physiol* 113, 229-237 (1999).
126. Jaggar, J. H., A. S. Stevenson & M. T. Nelson. Voltage dependence of  $\text{Ca}^{2+}$  sparks in intact cerebral arteries. *Am J Physiol* 274, C1755-61 (1998).
127. ZhuGe, R., S. M. Sims, R. A. Tuft, K. E. Fogarty & Jr. J.V. Walsh.  $\text{Ca}^{2+}$  sparks activate  $\text{K}^+$  and  $\text{Cl}^-$  channels, resulting in spontaneous transient currents in guinea-pig tracheal myocytes. *J Physiol* 513, 711-718 (1998).
128. Guia, A., X. Wan, M. Courtemanche & N. Leblanc. Local  $\text{Ca}^{2+}$  entry through L-type  $\text{Ca}^{2+}$  channels activates  $\text{Ca}^{2+}$ -dependent  $\text{K}^+$  channels in rabbit coronary myocytes. *Circ Res* 84, 1032-1042 (1999).
129. Kirber, M.T., E. F. Etter, K. A. Bellve, L. M. Lifshitz, R. A. Tuft, F. S. Fay, J. V. Walsh & K. E. Fogarty. Relationship of  $\text{Ca}^{2+}$  sparks to STOCs studied with 2D and 3D imaging in feline oesophageal smooth muscle cells. *J Physiol* 531, 315-327 (2001).
130. ZhuGe, R., K. E. Fogarty, R. A. Tuft, L. M. Lifshitz, K. Sayar & J. V. Walsh. Dynamics of signaling between  $\text{Ca}^{2+}$  sparks and  $\text{Ca}^{2+}$ -activated  $\text{K}^+$  channels studied with a novel image-based method for direct intracellular measurement of ryanodine receptor  $\text{Ca}^{2+}$  current. *J Gen Physiol* 116, 845-864 (2000).

131. Muñoz, A., L. Garcia & A. Guerrero-Hernandez. In situ characterization of the  $\text{Ca}^{2+}$  sensitivity of large conductance  $\text{Ca}^{2+}$ -activated  $\text{K}^+$  channels: implications for their use as near-membrane  $\text{Ca}^{2+}$  indicators in smooth muscle cells. *Biophys J* 75, 1774-1782 (1998).
132. Carl, A., H. K. Lee & S. M. Regulation of ion channels in smooth muscles by calcium. *Am J Physiol* 271, C9-C34 (1996).
133. Porter, V. A., A. D. Bonev, H. J. Knot, T. J. Heppner, A. S. Stevenson, T. Kleppisch, W. J. Lederer & M. T. Nelson. Frequency modulation of  $\text{Ca}^{2+}$  sparks is involved in regulation of arterial diameter by cyclic nucleotides. *Am J Physiol* 274, C1346-C1355 (1998).
134. Komori, S. & T. B. Bolton. Actions of guanine nucleotides and cyclic nucleotides on calcium stores in single patch-clamped smooth muscle cells from rabbit portal vein. *Br. J Pharmacol* 97, 973-982 (1989).
135. Lee, S. H. & Y. E. Earm. Caffeine induces periodic oscillations of  $\text{Ca}^{2+}$ -activated  $\text{K}^+$  current in pulmonary arterial smooth muscle cells. *Pflugers Arch* 426, 189-198 (1994).
136. Chen, S. R., X. Li, K. Ebisawa & L. Zhang. Functional characterization of the recombinant type 3  $\text{Ca}^{2+}$  release channel (ryanodine receptor) expressed in HEK293 cells. *J Biol Chem* 272, 24234-24246 (1997).

#### **Abbreviations:**

ACh, acetylcholine;  $\text{BK}_{\text{Ca}}$  channels, high conductance  $\text{Ca}^{2+}$ -dependent  $\text{K}^+$  channels; cADPR, cyclic adenosine diphosphate-ribose; Caff, caffeine; CICR, calcium-induced calcium release;  $[\text{Ca}^{2+}]_{\text{i}}$ , intracellular calcium concentration;  $[\text{Ca}^{2+}]_{\text{SR}}$ , luminal calcium concentration; HA, histamine;  $\text{IP}_3\text{R}$ , inositol 1,4,5-trisphosphate receptor; RyR, ryanodine receptor; SR, sarcoplasmic reticulum; VDCC, voltage-dependent calcium channels; STOCs, spontaneous transient outward currents.

#### **Key words:**

Smooth muscle, ryanodine receptor, CICR, cADPR,  $\text{Ca}^{2+}$  sparks, sarcoplasmic reticulum, internal  $\text{Ca}^{2+}$  stores.

#### **Send correspondence to:**

Dr. Agustín Guerrero-Hernández  
 Depto. de Bioquímica  
 CINVESTAV-IPN  
 Apdo. Postal 14-740  
 México D. F. 07000  
 México  
 phone: 52-55-5747-7000 ext 5210  
 fax: 52-55-5747-7083  
 email: aguerrer@mail.cinvestav.mx

#### **Running title:**

Ryanodine receptors in smooth muscle

# Regulation of Sarcoplasmic Reticulum Calcium Release by Luminal Calcium in Cardiac Muscle

Sandor Györke<sup>1</sup>, Inna Györke<sup>1</sup>, Valeriy Lukyanenko<sup>1</sup>, Dmitriy Terentyev<sup>1</sup>, Serge Viatchenko-Karpinski<sup>1</sup>, and Theodore F. Wiesner<sup>2</sup>

<sup>1</sup> Department of Physiology, Texas Tech University Health Sciences Center, Lubbock Texas 79430-6551. Györke Email: [physg@physiology.ttuhscc.edu](mailto:physg@physiology.ttuhscc.edu) ; <sup>2</sup> Department of Chemical Engineering, Texas Tech University, Lubbock, TX 79409-3121.

**ABSTRACT** The amount of  $\text{Ca}^{2+}$  released from the sarcoplasmic reticulum (SR) is a principal determinant of cardiac contractility. Normally, the SR  $\text{Ca}^{2+}$  stores are mobilized through the mechanism of  $\text{Ca}^{2+}$ -induced  $\text{Ca}^{2+}$  release (CICR). In this process,  $\text{Ca}^{2+}$  enters the cell through plasmalemmal voltage-dependent  $\text{Ca}^{2+}$  channels to activate the  $\text{Ca}^{2+}$  release channels in the SR membrane. Consequently, the control of  $\text{Ca}^{2+}$  release by cytosolic  $\text{Ca}^{2+}$  has traditionally been the main focus of cardiac excitation-contraction (EC) coupling research. Evidence obtained recently suggests that SR Ca release is controlled not only by cytosolic  $\text{Ca}^{2+}$ , but also by  $\text{Ca}^{2+}$  in the lumen of the SR. The presence of a luminal  $\text{Ca}^{2+}$  sensor regulating release of SR luminal  $\text{Ca}^{2+}$  potentially has profound implications for our understanding of EC coupling and intracellular  $\text{Ca}^{2+}$  cycling. Here we review evidence, obtained using *in situ* and *in vitro* approaches, in support of such a luminal  $\text{Ca}^{2+}$  sensor in cardiac muscle. We also discuss the role of control of  $\text{Ca}^{2+}$  release channels by luminal  $\text{Ca}^{2+}$  in termination and stabilization of CICR, as well as in shaping the response of cardiac myocytes to various inotropic influences and diseased states such as  $\text{Ca}^{2+}$  overload and heart failure.

## INTRODUCTION

In cardiac muscle, most of the  $\text{Ca}^{2+}$  required for contractile activation is derived from a specialized intracellular  $\text{Ca}^{2+}$  release and storage organelle, the SR. During electrical activation, the  $\text{Ca}^{2+}$  that enters the cell through plasmalemmal voltage dependent  $\text{Ca}^{2+}$  channels binds to and activates the  $\text{Ca}^{2+}$  release channels, also known as ryanodine receptors (RyRs), clustered in release units in the membrane of the SR. When the  $\text{Ca}^{2+}$  release channels open, a much larger amount of  $\text{Ca}^{2+}$  is released from the SR, resulting in activation of contractile proteins. This mechanism is known as CICR (for reviews see 1-4). Intuitively, CICR, at least in individual RyR clusters, should be self-regenerating and continue until completion because of the positive feedback of released  $\text{Ca}^{2+}$  on further release. However, relaxation of cardiac muscle requires a robust termination of  $\text{Ca}^{2+}$  release, so that resting cytosolic  $\text{Ca}^{2+}$  can be restored by  $\text{Ca}^{2+}$  transporters present in both the SR membrane and plasmalemma. Intense research has been brought to bear on the mechanisms that terminate and stabilize CICR. Much attention has been focused on the role of cytosolic  $\text{Ca}^{2+}$  in regulating  $\text{Ca}^{2+}$  release. In particular, it has been suggested that binding of  $\text{Ca}^{2+}$  to inhibition sites on the RyR causes channel activity to decrease through processes referred to as  $\text{Ca}^{2+}$ -dependent inactivation or adaptation accounting for the early termination of  $\text{Ca}^{2+}$  release. However, the role of these mechanisms that involve changes in cytosolic  $[\text{Ca}^{2+}]$  remains controversial (See ref. 5 for a review).

The key to resolving the paradoxes of CICR may reside on the luminal side of the SR. Growing evidence suggests that the SR  $\text{Ca}^{2+}$  release process is regulated not only by cytosolic  $\text{Ca}^{2+}$  but also by  $\text{Ca}^{2+}$

inside the lumen of the SR. The regulatory mechanism appears to be much more sophisticated than simply its influence upon the concentration gradient between the SR and the cytosol. An emerging view is that the size and the functional state of the SR  $\text{Ca}^{2+}$  store is controlled by  $\text{Ca}^{2+}$  sensing sites on the luminal side of the  $\text{Ca}^{2+}$  release channel. By linking the loading status of the SR to the activity of RyRs, the luminal  $\text{Ca}^{2+}$  sensor stabilizes CICR and influences the way in which the cell responds to pharmacological agents that affect SR  $\text{Ca}^{2+}$  cycling. Furthermore, alterations in this mechanism may contribute to certain pathological conditions such as  $\text{Ca}^{2+}$ -dependent arrhythmias and heart failure. In this article, we summarize experimental evidence for luminal  $\text{Ca}^{2+}$  regulation of  $\text{Ca}^{2+}$  release. We also review potential molecular mechanisms and discuss functional implications of this control mechanism in normal and diseased heart.

## $\text{Ca}^{2+}$ IN THE SR

The amount of  $\text{Ca}^{2+}$  stored in the SR is determined by the balance between  $\text{Ca}^{2+}$  uptake by the SR  $\text{Ca}^{2+}$  pump (sarco/endoplasmic reticulum  $\text{Ca}^{2+}$ -ATPase, SERCA), binding of  $\text{Ca}^{2+}$  to luminal buffers such as calsequestrin (CSQ), and  $\text{Ca}^{2+}$  leak from the SR via the RyRs. For the purpose of this review, it is important to distinguish between the free and total SR  $[\text{Ca}^{2+}]$  ( $[\text{Ca}^{2+}]_{\text{SR}}$ ). During release,  $\text{Ca}^{2+}$  bound to luminal buffers is expected to dissociate from these binding sites, thus contributing to the  $\text{Ca}^{2+}$  released. Therefore, the amount of bound  $\text{Ca}^{2+}$  may be an important determinant of the functional size of the pool. However, it is the free  $[\text{Ca}^{2+}]_{\text{SR}}$  that determines the concentration gradient and electrochemical driving force for  $\text{Ca}^{2+}$  across the SR membrane. Similarly, it is

the free  $\text{Ca}^{2+}$  that is likely to govern various  $\text{Ca}^{2+}$ -dependent processes in the lumen of the SR, including modulation of the functional activity of the  $\text{Ca}^{2+}$  release channels. In the sections below we briefly summarize the data available regarding estimates of the total and free  $[\text{Ca}^{2+}]$  in the SR and the properties and role of the main luminal  $\text{Ca}^{2+}$  buffer, CSQ.

### **Total $[\text{Ca}^{2+}]_{\text{SR}}$ and calsequestrin**

The total SR  $\text{Ca}^{2+}$  content in intact cells is commonly estimated by measuring the amount of  $\text{Ca}^{2+}$  released from the SR to the cytoplasm upon addition of caffeine. The amount of released  $\text{Ca}^{2+}$  is inferred by using fluorescent  $\text{Ca}^{2+}$  dyes or by integrating the  $\text{Na}^+/\text{Ca}^{2+}$  exchange current (e.g. refs. 6-9). Most studies performed under normal cellular conditions have estimated the resting total SR  $\text{Ca}^{2+}$  content to be in the range of 50-260  $\mu\text{mol/liter}$  of cytosol in myocytes from various mammalian species. (e.g. 4). Assuming the SR comprises 3.5% of cell volume (4), the total SR  $\text{Ca}^{2+}$  content is 1.4-7.4  $\text{mmol/liter}$  of SR volume. As discussed below, a substantial part of this  $\text{Ca}^{2+}$  may be bound to low affinity intraluminal buffers. The concentration of  $\text{Ca}^{2+}$  binding sites within the SR has been estimated to be 3 or 14  $\text{mM}$  in intact ventricular myocytes (10) and isolated cardiac SR microsomes, respectively (11), with a  $K_D$  of 0.63  $\text{mM}$  (11). The difference in luminal  $\text{Ca}^{2+}$  buffering between intact cells and SR vesicles is likely to reflect SR fragmentation caused by tissue homogenization (12). The  $\text{Ca}^{2+}$  binding properties of the SR in cardiac myocytes match reasonably well those of CSQ, supporting the notion that CSQ is a major site for storing  $\text{Ca}^{2+}$ . Cardiac CSQ binds  $\sim 40$   $\text{Ca}^{2+}$  ions/mole with an apparent affinity of 0.5  $\text{mM}$  (13). Based on the reported yield of isolated cardiac CSQ (14; 40  $\text{mg/kg}$  wet wt), the concentration of CSQ  $\text{Ca}^{2+}$  binding sites in cardiac SR can be estimated to be in the range of 3.2-6.4  $\text{mM}$  (4). Thus, assuming a total concentration of  $\text{Ca}^{2+}$  in the SR of 4  $\text{mM}$  and a concentration of SR  $\text{Ca}^{2+}$  binding sites of 4-5  $\text{mM}$  with a  $K_D$  of 0.65  $\text{mM}$ , the free  $[\text{Ca}^{2+}]_{\text{SR}}$  would be about 0.6 - 1.0  $\text{mM}$  and the fraction of intra SR  $\text{Ca}^{2+}$  bound to buffers would be approximately 50-75%. During a twitch, up to 60% of the total  $\text{Ca}^{2+}$  is released from the SR (7). Therefore, depending on the true amount of bound luminal  $\text{Ca}^{2+}$ , a substantial fraction (up to 50%) of  $\text{Ca}^{2+}$  that is released during a twitch may be released from CSQ. While the equilibrium binding properties of  $\text{Ca}^{2+}$  to CSQ are relatively well characterized, very little is known about the kinetics of binding. Apparently, no experimental studies of the association and dissociation rate constants have been reported in the literature. The paucity of kinetic data for  $\text{Ca}^{2+}$  binding to CSQ makes it difficult to assess the relative roles of binding and diffusion in establishing the concentration profile of free  $\text{Ca}^{2+}$  within the SR. Also the role of minor luminal  $\text{Ca}^{2+}$  binding proteins (sarcalumenin, histidine rich Ca-binding protein, and calreticulin, 4) in cardiac SR  $\text{Ca}^{2+}$  homeostasis remains to be determined.

10-20 fold over-expression of CSQ leads to development of severe heart failure in mice and reduction of the amplitude of  $\text{Ca}^{2+}$  transients in cells

isolated from the failing hearts (15-17). At steady state, increasing  $\text{Ca}^{2+}$  binding site concentration would be expected to increase the amount of releasable  $\text{Ca}^{2+}$ . This is expected because the overexpressed CSQ provides a larger store of SR  $\text{Ca}^{2+}$ . However, in a beating cardiac cell, increased  $\text{Ca}^{2+}$  store size may slow the dynamic recovery of  $[\text{Ca}^{2+}]_{\text{SR}}$  because of the longer times required to refill the store. This is a potential explanation for why EC coupling is depressed in mice overexpressing CSQ.

### **Free $[\text{Ca}^{2+}]_{\text{SR}}$**

Few experimental studies have been performed to measure free  $[\text{Ca}^{2+}]_{\text{SR}}$  in cardiac muscle. One obstacle has been the lack of low affinity fluorescent  $\text{Ca}^{2+}$  indicators that would be suitable for measuring  $\text{Ca}^{2+}$  in the millimolar range in which  $\text{Ca}^{2+}$  appears to be present in this compartment. Another difficulty is introducing the probe into the SR. Shannon and Bers (11) measured  $[\text{Ca}^{2+}]_{\text{SR}}$  in rat isolated cardiac microsomes with the Ca-Mg indicator fura-2 trapped in the vesicles by homogenization of cardiac tissue in the presence of the indicator. They estimated that the resting free  $[\text{Ca}^{2+}]_{\text{SR}}$  reaches 0.7  $\text{mM}$  for cytosolic  $[\text{Ca}^{2+}]$  of 100  $\text{nM}$ . This value might underestimate the true intra-vesicular  $[\text{Ca}^{2+}]$  because the fluorescence signal saturated also near 0.7  $\text{mM}$   $\text{Ca}^{2+}$ . On the other hand, the content of  $\text{Ca}^{2+}$  in the vesicles was likely to have been higher than normal because of the presence, in the experimental solutions, of ruthenium red to block the RyRs. Inhibition of  $\text{Ca}^{2+}$  leak via RyRs by this drug is known to lead to a substantial increase of the SR  $\text{Ca}^{2+}$  content (9). Chen et al. (18) used a low affinity Ca-sensitive NMR probe (TF-BAPTA) to measure free  $[\text{Ca}^{2+}]$  inside the SR in intact, perfused working hearts and reported a diastolic value of  $\sim 1.5$   $\text{mM}$ . Raising cytosolic free  $\text{Ca}^{2+}$  by exposing the heart to elevated extracellular KCl, resulted in an increase in  $[\text{Ca}^{2+}]_{\text{SR}}$  to about 5  $\text{mM}$ . During systole  $[\text{Ca}^{2+}]_{\text{SR}}$  decreased only moderately (by  $\sim 30\%$ ), consistent with the notion that the  $\text{Ca}^{2+}$  is heavily buffered in the SR. It is unclear how such measurements of  $[\text{Ca}^{2+}]$ , averaged throughout the entire SR luminal compartment, reflect the local  $[\text{Ca}^{2+}]$  changes near  $\text{Ca}^{2+}$  release sites. A mathematical model of  $\text{Ca}^{2+}$  release from the junctional SR (jSR) predicts that local release events (i.e.  $\text{Ca}^{2+}$  sparks) might be associated with significant depletion of local  $\text{Ca}^{2+}$  in the jSR elements (19). Clearly, more experimental and modeling studies are needed to define the changes in  $[\text{Ca}^{2+}]_{\text{SR}}$  during both global and local  $\text{Ca}^{2+}$  release from the SR.

### **EXPERIMENTAL EVIDENCE FOR MODULATION OF THE $\text{Ca}^{2+}$ RELEASE MECHANISM BY LUMINAL $\text{Ca}^{2+}$**

A number of studies have explored the dependence of SR  $\text{Ca}^{2+}$  release on SR  $\text{Ca}^{2+}$  content in intact and permeabilized cardiac cells. In addition, the effects of luminal  $\text{Ca}^{2+}$  have been studied in RyR channels reconstituted into lipid bilayers. Most of these studies found that luminal  $\text{Ca}^{2+}$  influences the functional activity of the  $\text{Ca}^{2+}$  release channels. However, the interpretation of the results has been

complicated by the existence of at least two potential mechanisms: 1) extra-SR effects involving the cytosolic  $\text{Ca}^{2+}$  activation sites of the RyR; and 2) intra-SR effects mediated by distinct luminal  $\text{Ca}^{2+}$  sensing sites on the RyR or associated proteins. It is likely that these two mechanisms co-exist in cardiac myocytes. Here we will summarize evidence, obtained using *in situ* and *in vitro* approaches, in favor and against a luminal  $\text{Ca}^{2+}$  sensor regulating RyR activity.

### Cell studies

In 1992, Fabiato (20) provided the first experimental evidence for regulation of  $\text{Ca}^{2+}$  release by  $\text{Ca}^{2+}$  stored inside the SR of cardiac muscle. He showed that mechanically skinned cardiac myocytes exhibit spontaneous  $\text{Ca}^{2+}$  release, which required a SR  $\text{Ca}^{2+}$  overload. High cytosolic  $\text{Ca}^{2+}$  did not inactivate this release. This mechanism existed in addition to the time- and  $\text{Ca}^{2+}$ -dependent  $\text{Ca}^{2+}$  release that is first activated and then inactivated by an increase of  $\text{Ca}^{2+}$  at the cytosolic side of the SR. Fabiato (20) proposed that this second type of release is initiated by binding of  $\text{Ca}^{2+}$  to regulatory sites in the lumen of the SR.

In intact cardiac myocytes, a number of investigators have explored the effects of changes of SR  $\text{Ca}^{2+}$  content on  $\text{Ca}^{2+}$  release from the SR (for a review see 4). Most studies found that that SR  $\text{Ca}^{2+}$  release increases steeply with the increase in the SR  $\text{Ca}^{2+}$  content. For example, Shannon et al. (21) used conditioning pulses to progressively increase SR  $\text{Ca}^{2+}$  load. This study employed caffeine applications to empty the SR for assessment of its  $\text{Ca}^{2+}$  content. They found a steep nonlinear relationship between the fraction of  $\text{Ca}^{2+}$  released and SR  $\text{Ca}^{2+}$  content. The highly non-linear relationship between  $\text{Ca}^{2+}$  release and SR  $\text{Ca}^{2+}$  content, revealed in these studies, indicates that the effects of load may not be simply due to the increased amount of  $\text{Ca}^{2+}$  available for release. Rather, they likely involve alterations of RyR gating. It is important to note that, while consistent with regulation of the release mechanism by luminal  $\text{Ca}^{2+}$ , these effects can also be readily explained by extra-SR effects through cytosolic  $\text{Ca}^{2+}$  ( $[\text{Ca}^{2+}]_i$ ). Indeed,  $[\text{Ca}^{2+}]_i$  near the release sites would be expected to be higher for any RyR opening at increased SR  $\text{Ca}^{2+}$  loads. This higher  $[\text{Ca}^{2+}]_i$  would tend to activate more neighboring RyRs via CICR, thereby accounting for or contributing to disproportionately large SR  $\text{Ca}^{2+}$  release.

At the local  $\text{Ca}^{2+}$  release level, several studies have demonstrated that the rate of occurrence of elementary  $\text{Ca}^{2+}$  release events (i. e. sparks) depends positively on SR  $\text{Ca}^{2+}$  content (22-24). In these studies, the SR  $\text{Ca}^{2+}$  content was increased by elevating the  $[\text{Ca}^{2+}]$  in the extracellular solution or by altering the rate of electrical stimulation of the cells. Subsequently, Song et al. (25) found no significant change in the frequency of sparks when the SR  $\text{Ca}^{2+}$  content was reduced by thapsigargin (a selective inhibitor of the SR  $\text{Ca}^{2+}$  pump), while correcting the spark statistics for changes in detectability of events. Because the detectability of small sparks against background noise is reduced in confocal microscopy,

the data had to be corrected to avoid overestimating the reduction of spark frequency. These authors attributed the changes in spark frequency observed in previous studies to two factors. The first was altered detectability of sparks with different amplitudes against the background noise. The second was increases in cytosolic  $\text{Ca}^{2+}$  that usually accompany alterations in SR  $\text{Ca}^{2+}$  load upon elevating extracellular  $[\text{Ca}^{2+}]$ . Lukyanenko and co-workers (26) then re-examined the effects of alterations of SR  $\text{Ca}^{2+}$  content on  $\text{Ca}^{2+}$  sparks in permeabilized myocytes at constant (i.e. buffered) cytosolic  $[\text{Ca}^{2+}]$  and with corrections made to account for missed events. Enhancing the SR  $\text{Ca}^{2+}$  content by selectively stimulating the efficiency of the SR  $\text{Ca}^{2+}$  pump (using an anti-phospholamban antibody) increased the frequency of  $\text{Ca}^{2+}$  release events. Furthermore, in myocytes exposed to elevated cytosolic  $\text{Ca}^{2+}$  to increase the initial SR  $\text{Ca}^{2+}$  content, partial depletion of the SR by thapsigargin reduced the frequency of sparks (corrected for missed events). Thus, it is possible that the Song et al's (25) experiments were performed at relatively low SR  $\text{Ca}^{2+}$  loads, at which luminal  $\text{Ca}^{2+}$  was outside the range in which it could effectively influence release site activity. All together, the relationship between spark frequency and SR  $\text{Ca}^{2+}$  content seems to support active luminal regulation of release at luminal sites.

In addition to monitoring fractional  $\text{Ca}^{2+}$  release and spark frequency at different SR  $\text{Ca}^{2+}$  loads, another useful strategy for demonstrating the role of luminal  $\text{Ca}^{2+}$  in controlling  $\text{Ca}^{2+}$  release has been the use of RyR inhibitors. It has been shown that certain RyR inhibitors, such as tetracaine, only transiently suppress spontaneous (i.e.  $\text{Ca}^{2+}$  sparks and waves) and experimentally evoked  $\text{Ca}^{2+}$  release (26-30). The restoration of release in the continuous presence of the drugs was associated with an increase in the SR  $\text{Ca}^{2+}$  content caused by reduced leak of  $\text{Ca}^{2+}$  through the RyRs. One possibility is that the recovery of release in the presence of tetracaine is simply due to increased amount of releasable  $\text{Ca}^{2+}$  in the SR (28,29). The decreased number of open  $\text{Ca}^{2+}$  release channels may be offset by an enhanced  $\text{Ca}^{2+}$  flux through each channel that was not inhibited by the drug. Such a simple compensation of blockage could occur only if inhibition by the drug is partial, and at least some of the release sites remain available for liberation of  $\text{Ca}^{2+}$ . Further, at the local release level, such a mechanism would be expected to manifest itself only by an increase in the magnitude of sparks without any increase in their frequency. In contrast to these expectations, we found that the effects of tetracaine were transient not only with respect to the amplitude of release events, but also with respect to their frequency (26-27). In addition, the recovery of release was observed even with tetracaine concentrations that caused an initial complete inhibition of release (30). Such observations indicate that the recovery of release from inhibition is not simply due to an increase in the amount of releasable  $\text{Ca}^{2+}$ . Instead the release mechanism itself becomes altered by luminal  $\text{Ca}^{2+}$  in a way that makes it less sensitive to inhibition by tetracaine. These results

cannot be explained easily by effects of  $\text{Ca}^{2+}$  on the cytosolic side of the SR and provide strong evidence in support of existence of distinct intraluminal  $\text{Ca}^{2+}$  sensing sites that regulate the behavior of the RyR allosterically.

### Studies in RyRs reconstituted in bilayers

A number of investigators have shown that increasing  $\text{Ca}^{2+}$  on the luminal side of the RyR leads to an increase in RyR channel open probability (23,31-35). These effects occurred in the range of 0.1 – 10 mM  $\text{Ca}^{2+}$  (apparent  $K_D \sim 2$  mM, Hill coefficient  $\sim 2$ ; i.e. 33) and were manifested predominantly by increased open times (34) or an increased frequency of events (33). While in some studies the presence of cytosolic  $\text{Ca}^{2+}$ , alone, was sufficient (albeit at high concentrations) to mediate the effects of luminal  $\text{Ca}^{2+}$  (34), other studies found that the activation by luminal  $\text{Ca}^{2+}$  required, in addition to cytosolic  $\text{Ca}^{2+}$ , the presence of allosteric modulators of RyR activity such as sulmazole, caffeine, or ATP on the cytosolic side of the channel (23,31-33). Similar to experiments with cardiac myocytes, two mechanisms of luminal  $\text{Ca}^{2+}$  regulation have been proposed. One suggestion is that  $\text{Ca}^{2+}$  flowing through the open RyR channel activates the channel by interacting with its cytosolic  $\text{Ca}^{2+}$  activation sites ("feed-through" regulation). The other suggestion is that luminal  $\text{Ca}^{2+}$  acts at distinct sites on the luminal side of the  $\text{Ca}^{2+}$  release channel complex (true luminal regulation). Locating the site of action of luminal  $\text{Ca}^{2+}$  is confounded by the fact that, with millimolar luminal  $\text{Ca}^{2+}$ , high  $\text{Ca}^{2+}$  flux from the luminal to the cytosolic side of the channel makes it difficult to exclude the possibility that luminal  $\text{Ca}^{2+}$  has some access to cytosolic sites.

In support for the "feed-through" regulation hypothesis, Xu and Meissner (34) found, in canine RyRs purified by sucrose gradient, that the effects of luminal  $\text{Ca}^{2+}$  are much larger at negative holding potentials than at positive holding potentials. Negative holding potentials favor luminal-to cytosolic  $\text{Ca}^{2+}$  fluxes. They were able to correlate the effects of luminal  $\text{Ca}^{2+}$  on RyR open probability ( $P_o$ ) with the magnitude of luminal-to cytosolic fluxes. In the presence of caffeine and nanomolar cytosolic  $\text{Ca}^{2+}$ , estimated luminal-to-cytosolic fluxes of 0.25 pA increased channel  $P_o$ . At high cytosolic [ $\text{Ca}^{2+}$ ], estimated luminal  $\text{Ca}^{2+}$  fluxes of 8 pA caused a decline in channel activity. The authors proposed that  $\text{Ca}^{2+}$  passing through the channel could both activate and inactivate the channel at cytosolic sites. These studies provide strong evidence for the ability of  $\text{Ca}^{2+}$  passing through the pore to influence channel activity at cytosolic regulatory sites. However, they do not necessarily rule out the possibility that luminal  $\text{Ca}^{2+}$  can also modulate channel activity at distinct luminal sites.

The existence of luminal sites was addressed directly (33) by performing measurements at high positive membrane potentials and at high cytosolic  $\text{Ca}^{2+}$  conditions, in which the electrochemical gradient does not support luminal-to-cytosolic  $\text{Ca}^{2+}$  fluxes. Luminal  $\text{Ca}^{2+}$  was found to potentiate native canine

cardiac RyRs, regardless of whether  $\text{Ca}^{2+}$  flowed from the luminal to cytosolic side or from the cytosolic to luminal side of the channel. These results support the notion that luminal flux is not required for the effects of luminal  $\text{Ca}^{2+}$ . Recently Ching and co-workers (35) also reported convincing evidence of lumenally-located  $\text{Ca}^{2+}$  regulatory sites in native sheep cardiac RyR using a tryptic digestion approach. After the RyRs were exposed to luminal trypsin, they lost their ability to respond to luminal  $\text{Ca}^{2+}$ . Apparently the luminal  $\text{Ca}^{2+}$  activation sites were damaged by trypsin digestion. Thus, the single channel data accumulated to date show that, in some instances, luminal  $\text{Ca}^{2+}$  can have access to the cytosolic  $\text{Ca}^{2+}$  regulatory sites. At the same time, they also provide evidence for the existence of distinct regulatory sites on the luminal side of the channel. Taken together, the studies described above seem to support the existence of a true luminal  $\text{Ca}^{2+}$  sensor that controls the function of the RyR channel.

### MOLECULAR STRUCTURE OF THE LUMINAL $\text{Ca}^{2+}$ SENSOR

Very little is known about the structure of the luminal  $\text{Ca}^{2+}$  binding sites. Two obvious possibilities are that  $\text{Ca}^{2+}$  binds directly to the luminal aspect of the ryanodine receptor protein, or that it binds to an auxiliary protein with luminal location. The luminal loops connecting the putative transmembrane spanning domains M1-M2 and M3-M4 of the RyR possesses many negatively charged residues (36-38). Calcium ions could bind to these regions, altering the channel conformation to increase its open probability. Consistent with this possibility, the effects of luminal  $\text{Ca}^{2+}$  have been described in RyRs purified with CHAPS solubilization (31). It should be noted, however, that CHAPS solubilization does not necessarily lead to dissociation of all the proteins from the RyR (39). In addition, the results of experiments with purified RyRs could have been influenced by potential effects of luminal  $\text{Ca}^{2+}$  at the cytosolic activation sites, making it difficult to discriminate true luminal from feed-through effects of  $\text{Ca}^{2+}$ . Therefore the possibility that luminal  $\text{Ca}^{2+}$  exerts its modulatory influences indirectly, via interaction of the RyR with  $\text{Ca}^{2+}$ -sensitive luminal proteins, cannot be discarded.

Cardiac RyRs localized in the jSR appear to complex with a number of luminal proteins including CSQ, triadin and junctin (39). As discussed above, CSQ may bind a large portion of  $\text{Ca}^{2+}$  in the SR and provide a reserve for release. In addition, biochemical evidence obtained predominantly in skeletal muscle suggests that CSQ may actively participate in SR  $\text{Ca}^{2+}$  release by modulating the RyR (40,41). The actions of CSQ on the RyR could be direct or require the presence of intermediate linker proteins such as triadin or junctin. Consistent with the former possibility, the addition of CSQ to the luminal side of the skeletal RyR has been reported to enhance  $P_o$  of the channel in a  $\text{Ca}^{2+}$ -dependent manner (42,43). Junctin and triadin are structurally related integral membrane proteins that co-localize with the RyR and CSQ at the jSR membrane in cardiac and skeletal muscle (39,44-45). It appears that junctin and triadin

interact directly in the jSR membrane and form a complex that anchors CSQ to the ryanodine receptor (39). Therefore, these proteins could mediate the proposed effects of CSQ on the RyR. The role of CSQ as a luminal  $\text{Ca}^{2+}$  sensor for the RyR was questioned by Ching and co-workers (35). These workers demonstrated that trypsin does not cleave CSQ, although exposure to the enzyme does abolish the luminal sensitivity of the RyR. This implies that the observed changes in luminal regulation of RyR were not caused by damage to CSQ, unless trypsin damaged certain structures involved in the interaction of the RyR and CSQ on the channel protein, itself, or on intermediate linker proteins. An alternative possibility is that the luminal  $\text{Ca}^{2+}$  sensor is formed by either junctin or triadin instead of CSQ. Their luminal domains are also rich in negatively charged residues that could form the  $\text{Ca}^{2+}$ -binding regions. Furthermore, these proteins do have putative sites for cleavage that could account for the loss of luminal  $\text{Ca}^{2+}$  sensitivity upon trypsin digestion.

### **FUNCTIONAL IMPLICATIONS FOR NORMAL PHYSIOLOGY AND DISEASE**

The presence of a luminal  $\text{Ca}^{2+}$  sensor regulating release of luminal  $\text{Ca}^{2+}$  potentially has profound implications for our understanding of cardiac EC coupling and intracellular  $\text{Ca}^{2+}$  cycling in cardiac muscle. Here we will review the possible role for such a sensor in termination and long-term stabilization of CICR. We will also examine its potential role in such pathological conditions as regenerative  $\text{Ca}^{2+}$  waves and impaired  $\text{Ca}^{2+}$  release in heart failure

#### **Termination of CICR**

As a system in which  $\text{Ca}^{2+}$  is both the trigger and the output signal, CICR should be inherently unstable and self-regenerating. Yet,  $\text{Ca}^{2+}$  release is tightly graded with the magnitude of the  $\text{Ca}^{2+}$  trigger and robustly terminates. Despite intense effort, the mechanisms involved in control of CICR remain poorly understood. Lowering  $\text{Ca}^{2+}$  in the lumen of the SR would decrease channel activity, thereby providing a potential negative control mechanism to counter the positive feedback of CICR. Several recent studies are consistent with this scenario. For example, depletion of  $[\text{Ca}^{2+}]_{\text{SR}}$  resulted in a disproportionately large decrease in the amount of  $\text{Ca}^{2+}$  released from the SR (7). This supports the notion that SR depletion may somehow contribute to the termination signal for  $\text{Ca}^{2+}$  release. Evidence for functional depletion of SR  $\text{Ca}^{2+}$  stores was also presented in recent studies of refractoriness of  $\text{Ca}^{2+}$  release. Following release of  $\text{Ca}^{2+}$ , time must pass before CICR can be activated again (1,46). This refractory behavior has been commonly attributed to inactivation by cytosolic  $\text{Ca}^{2+}$ . Recently, DelPrincipe and co-workers (47) showed that the SR  $\text{Ca}^{2+}$  release mechanism exhibits a much more prominent refractoriness following its activation on a global scale than following local activation of just a few release sites by photolysis of caged  $\text{Ca}^{2+}$ . They attributed this discrepancy to functional depletion of SR  $\text{Ca}^{2+}$ , which leaves the  $\text{Ca}^{2+}$  release channels unresponsive to  $\text{Ca}^{2+}$  trigger until the SR  $\text{Ca}^{2+}$  store is

re-charged with  $\text{Ca}^{2+}$ . A direct experimental confirmation of the role of luminal  $\text{Ca}^{2+}$  in termination of CICR may come from studies that use low affinity  $\text{Ca}^{2+}$  buffers (ADA, citrate, or maleate) loaded into the SR. According to preliminary data obtained in our laboratory, clamping the level of  $\text{Ca}^{2+}$  in the SR by these exogenous buffers leads to dramatic increases in the amplitude and time-to-peak of sparks, as well as the duration of local  $\text{Ca}^{2+}$  release fluxes underlying  $\text{Ca}^{2+}$  sparks (48). These findings imply that the level of  $\text{Ca}^{2+}$  in the SR controls termination of  $\text{Ca}^{2+}$  release. At the whole-cell level,  $\text{Ca}^{2+}$  release loses its ability to respond to  $\text{Ca}^{2+}$  stimuli in a graded fashion, in the presence of exogenous buffers in the SR (49). These data suggest that regulation of RyR openings by local intra-SR  $[\text{Ca}^{2+}]$  might be responsible for termination of  $\text{Ca}^{2+}$  sparks, and that robust termination of sparks is required for graded behavior of macroscopic  $\text{Ca}^{2+}$  release. Recently a mathematical model of  $\text{Ca}^{2+}$  sparks also has been suggested, in which RyR gating depends on luminal  $\text{Ca}^{2+}$  and the coupling between RyRs, in addition to the well-established activation by local  $\text{Ca}^{2+}$  in the dyadic cleft (50).

#### **Dynamic control of SR $\text{Ca}^{2+}$ content and release**

In addition to providing an immediate "break" for regenerative CICR, the luminal  $\text{Ca}^{2+}$  sensor appears to continuously regulate the functional activity of the SR  $\text{Ca}^{2+}$  stores by linking SR  $\text{Ca}^{2+}$  content to the activity of the RyRs. A key element of this mechanism is luminal  $\text{Ca}^{2+}$  dependent  $\text{Ca}^{2+}$  leak across the SR membrane. Openings of RyRs, manifested as spontaneous  $\text{Ca}^{2+}$  sparks, mediate a substantial leak that is controlled by the level of  $\text{Ca}^{2+}$  inside the SR (1,23,26). At the same time the activity of RyRs influences the SR  $\text{Ca}^{2+}$  content, thereby forming a closed control loop (26). This dynamic control mechanism comes to play when either the SR  $\text{Ca}^{2+}$  release or uptake mechanisms are disturbed pharmacologically (27, 26). For example, when the RyR channel blocker tetracaine is applied, the leak of  $\text{Ca}^{2+}$  through the channels (i.e. appearing as  $\text{Ca}^{2+}$  sparks) is decreased, resulting in accumulation of  $\text{Ca}^{2+}$  in the SR. The luminal  $\text{Ca}^{2+}$  sensor detects this elevation and increases the open channel probability of the RyR. This, in turn, leads to the recovery of sparking activity and counterbalances the inhibition by tetracaine. The sequence of events is the opposite when the RyR agonist caffeine is applied. Potentiation of RyRs leads to enhanced  $\text{Ca}^{2+}$  leak, causing the SR  $\text{Ca}^{2+}$  content to decline. The decreased  $[\text{Ca}^{2+}]_{\text{SR}}$  leads to reduced RyR activity, thereby counterbalancing the primary potentiation of  $\text{Ca}^{2+}$  sparks by caffeine. This intrinsic self-regulation of  $\text{Ca}^{2+}$  release channels explains why modulation of RyRs leads to only transient changes in both triggered and spontaneous activities of  $\text{Ca}^{2+}$  release sites in cardiac myocytes (27,26).

Such a dynamic control mechanism, although possessing a certain time lag (due to the dynamics of changing SR load), should be advantageous for stabilizing  $\text{Ca}^{2+}$  cycling when either  $\text{Ca}^{2+}$  release or uptake is altered. The significance of luminal  $\text{Ca}^{2+}$  regulation can also be considered in the context of

periodic  $\text{Ca}^{2+}$  cycling in cardiac cells. The periodic beating of the heart requires that  $\text{Ca}^{2+}$ , once released, is rapidly re-sequestered in the SR. To move  $\text{Ca}^{2+}$  rapidly, the SR  $\text{Ca}^{2+}$  pump may have to maintain high levels of cycling through the whole range of  $[\text{Ca}^{2+}]$  to which the pump is exposed in the cytosol. This  $\text{Ca}^{2+}$  transport mechanism, which is designed for rapid  $\text{Ca}^{2+}$  uptake, might be too coarse for precise adjustments of the SR  $\text{Ca}^{2+}$  content. Such fine adjustments might be necessary to avoid SR  $\text{Ca}^{2+}$  overload, which could result in loss of stability of CICR. The luminal  $\text{Ca}^{2+}$ -dependent leak may serve to fine tune the SR  $\text{Ca}^{2+}$  content by releasing excess  $\text{Ca}^{2+}$ . Thus RyRs, in addition to their role as a major  $\text{Ca}^{2+}$  release pathway, may also operate as "safety valves" to maintain stable  $\text{Ca}^{2+}$  load and release.

### Maintained regulation of $\text{Ca}^{2+}$ release

Given such dynamic regulation of release, however, why do certain substances such as cADP-ribose (cADPR), which are thought to interact specifically with RyRs, have maintained modulatory effects on release? This paradox can be resolved if such substances do not act directly upon the RyRs, but, in fact, influence the release channel indirectly through luminal modulation.

cADPR appears to present just such an example in which the release is enhanced solely by increasing the uptake, without any direct effects on the RyRs. In recent years, cADPR has emerged as a potential endogenous regulator of SR  $\text{Ca}^{2+}$  release (51-53). For example, it has been demonstrated that cADPR applied to the cytosol increases cell-averaged  $\text{Ca}^{2+}$  transients and contractions (54-56). The compound was initially viewed as a specific agonist of RyR channels, acting by sensitizing the RyR to cytosolic  $\text{Ca}^{2+}$ , thereby enhancing CICR (57). However, subsequent studies have indicated no effect of cADPR upon RyRs, or have detected influences that should be abolished in the presence of physiological concentrations of ATP (58,59). The conflicting data have led some investigators to rule out cADPR altogether as modulator of SR  $\text{Ca}^{2+}$  release (60).

This body of apparently contradictory results was reconciled by the recent finding that cADPR acts by enhancing SR  $\text{Ca}^{2+}$  uptake (61). Potentiation of  $\text{Ca}^{2+}$  release by cADPR appears to be mediated by increased SR  $\text{Ca}^{2+}$  load due to persistent enhancement of uptake, with subsequent luminal  $\text{Ca}^{2+}$ -dependent activation of RyRs. The evidence for this mechanism includes the following observations in response to cADPR application to intact and permeabilized cardiac myocytes: increased frequency of local  $\text{Ca}^{2+}$  release events (i.e. sparks), increased SR  $\text{Ca}^{2+}$  load, and reduced influence of cADPR in the presence of the SERCA2a inhibitor thapsigargin (61,62). At the same time, cADPR has negligible impact upon the activity of single RyRs in lipid bilayers, but significantly increased  $\text{Ca}^{2+}$  uptake by cardiac SR microsomes. The exact biochemical mechanism for the effect of cADPR upon SERCA activity is to date unknown, but could involve direct potentiation of the SERCA pump, or relief of the inhibition of the SERCA by dephosphorylated phospholamban. This mechanism of

indirect modulation of RyR activity via the luminal sensor could therefore serve as a paradigm for other effectors of  $\text{Ca}^{2+}$  release that demonstrate maintained effects.

### Generation of $\text{Ca}^{2+}$ waves

An excess of  $\text{Ca}^{2+}$  in the SR  $\text{Ca}^{2+}$  stores ( $\text{Ca}^{2+}$  overload) is a common feature in a variety of cell injuries (63).  $\text{Ca}^{2+}$  overload is known to promote the generation of spontaneous  $\text{Ca}^{2+}$  waves in cardiac myocytes (64-67,1). Regenerative  $\text{Ca}^{2+}$  waves are believed to be the underlying cause of both early and delayed afterdepolarizations (EAD and DAD), the basis of triggered arrhythmias in the heart (68,69). Considering the fact that increased  $[\text{Ca}^{2+}]_{\text{SR}}$  enhances RyR  $P_o$ , how does the presence of the luminal  $\text{Ca}^{2+}$  sensor affect the generation of  $\text{Ca}^{2+}$  waves in  $\text{Ca}^{2+}$ -overloaded myocytes? Two specific scenarios have been discussed in this regard (20,69,70,1,67). According to the first mechanism,  $\text{Ca}^{2+}$  transported from the moving wavefront into the SR could trigger release by activation of RyRs from within the SR. The wave propagates as  $\text{Ca}^{2+}$  released from the SR is taken up into adjacent SR elements, raising local luminal  $\text{Ca}^{2+}$  above threshold for activation of the release mechanism at luminal sites. According to the second mechanism, elevated luminal  $\text{Ca}^{2+}$  sensitizes the  $\text{Ca}^{2+}$  release channels to cytosolic  $\text{Ca}^{2+}$ , enhancing the ability of cytosolic  $\text{Ca}^{2+}$  to activate adjacent release sites to cytosolic  $\text{Ca}^{2+}$  via CICR. From most experimental evidence, the second mechanism is more likely. For example, Engel and co-workers (70) investigated the temperature dependence of  $\text{Ca}^{2+}$  wave properties in isolated rat cardiomyocytes using digital  $\text{Ca}^{2+}$  imaging. They observed waves at 37°C, 27°C, and 17°C. The velocities decreased by a factor of 1.8 over this range. At the same time, the half-maximal decay rates, which characterize local  $\text{Ca}^{2+}$  removal by the  $\text{Ca}^{2+}$  ATPase, increased by a factor of 3.5. The higher temperature sensitivity of  $\text{Ca}^{2+}$  removal compared with that of  $\text{Ca}^{2+}$  wave propagation is inconsistent with the hypothesis that  $\text{Ca}^{2+}$  wave propagation relies on  $\text{Ca}^{2+}$  ATPase-dependent uptake of  $\text{Ca}^{2+}$  from the spreading wave front into the SR. Also, using fluo-3 confocal microscopy, Cheng and co-workers (1) demonstrated that the local  $\text{Ca}^{2+}$  rise during spontaneous  $\text{Ca}^{2+}$  waves and electrically evoked  $\text{Ca}^{2+}$  transients has the same rapid time course. This is consistent with both phenomena having the same underlying mechanism, namely CICR. Lukyanenko and co-workers (67) used a pharmacological approach to discriminate between the cytosolic and luminal  $\text{Ca}^{2+}$  activation hypotheses. We examined the transition of focal caffeine-induced localized  $\text{Ca}^{2+}$  release into propagating  $\text{Ca}^{2+}$  waves under various experimental conditions. The conditions included increased SR  $\text{Ca}^{2+}$  loading, inhibition of SR  $\text{Ca}^{2+}$  uptake by thapsigargin, and sensitization of RyRs by caffeine. We were able to induce self-sustaining  $\text{Ca}^{2+}$  waves when the SR  $\text{Ca}^{2+}$  load was increased by exposing the cells to elevated extracellular  $\text{Ca}^{2+}$ . Inhibition of SR  $\text{Ca}^{2+}$  uptake by thapsigargin in cells preloaded with above normal levels of SR  $\text{Ca}^{2+}$  did not prevent local  $\text{Ca}^{2+}$  elevations from triggering

propagating waves, but, instead, led to increased wave velocity. These results imply that  $\text{Ca}^{2+}$  wave propagation does not require translocation of  $\text{Ca}^{2+}$  from the spreading wave front into the SR. We were also able to induce propagating  $\text{Ca}^{2+}$  waves in cells with normal levels of SR  $\text{Ca}^{2+}$  load when the  $\text{Ca}^{2+}$  release mechanism was sensitized to cytosolic  $\text{Ca}^{2+}$  by low doses of caffeine (0.5 mM). This concentration of caffeine increases the  $P_o$  of RyR in lipid bilayers to about the same extent as does millimolar luminal  $\text{Ca}^{2+}$ . Therefore, it is clear that potentiation of RyR activity by elevated luminal  $\text{Ca}^{2+}$  could indeed contribute to higher incidence of  $\text{Ca}^{2+}$  waves in  $\text{Ca}^{2+}$ -overloaded myocytes.

How is this destabilizing influence of the luminal  $\text{Ca}^{2+}$  sensor reconciled with its potential stabilizing role discussed above? It appears that the dynamic control mechanism discussed above can operate effectively only within a certain range of SR  $\text{Ca}^{2+}$  load. When the increase in SR  $\text{Ca}^{2+}$  content falls outside this normal, "correctable" range as a result of cardiac cell injury, enhanced RyR channel activity, mediated by elevated luminal  $\text{Ca}^{2+}$ , tends to exacerbate the problem of instability, resulting in even more regenerative  $\text{Ca}^{2+}$  waves.

### Heart failure

Alterations in RyRs have been suggested to be a cause of reduced SR  $\text{Ca}^{2+}$  release and of diminished contractile response in failing hearts (71-75), although some other studies have found no alterations in expression or intrinsic gating behavior of RyRs in heart failure (76,77). As discussed above, one of the manifestations of SR  $\text{Ca}^{2+}$  release regulation by luminal  $\text{Ca}^{2+}$  is that any maintained and selective modulation of RyRs would be expected to have only transient effects on SR  $\text{Ca}^{2+}$  release. Therefore, alterations in RyR number or functional activity would not be expected to result in sustained changes in SR  $\text{Ca}^{2+}$  release, unless the dependence of the RyR on luminal  $\text{Ca}^{2+}$  were also altered or the aberrations of  $\text{Ca}^{2+}$  handling were to exceed the ability of the luminal  $\text{Ca}^{2+}$ -mediated feedback mechanism to compensate the primary defects in RyRs (26). In accord with our preliminary data (78), luminal  $\text{Ca}^{2+}$  regulation of RyRs is indeed compromised in a dog model of heart failure. We can speculate that this reduced sensitivity of RyRs to luminal  $\text{Ca}^{2+}$  is an adaptive response to minimize the energy costs of  $\text{Ca}^{2+}$  cycling in failing hearts. Because luminal  $\text{Ca}^{2+}$ -dependent cycling may be important for stabilizing CICR, this adaptation may come at the price of reduced stability of CICR in heart failure. Thus, altered modulation of RyRs by luminal  $\text{Ca}^{2+}$  could potentially account for or contribute to fatal cardiac arrhythmias in failing hearts.

### CONCLUSION

To summarize, luminal  $\text{Ca}^{2+}$  regulation of SR  $\text{Ca}^{2+}$  release has emerged as an important component of cardiac EC coupling and, therefore, should be included in any comprehensive description of the control of  $\text{Ca}^{2+}$  handling in cardiac muscle. Its consideration is also important to understand the

impact of various inotropic influences and pathological conditions, such as heart failure upon  $\text{Ca}^{2+}$  cycling. Several key unknowns await determination for a complete understanding of this regulatory pathway. These include the molecular determinants of the luminal  $\text{Ca}^{2+}$  sensor and the precise levels of free  $[\text{Ca}^{2+}]$  inside the SR to which the sensor is exposed to during  $\text{Ca}^{2+}$  cycling in heart cells.

### ACKNOWLEDGMENTS

We thank Drs. R. Nathan and A. Zahradnikova for critical reading of the manuscript. This work was supported by grants from the National Institutes of Health (HL 52620 and HL 03739 to S.G.) and the American Heart Association, Texas Affiliate (V.L.).

### References

1. Cheng, H., M.R. Lederer, R.P. Xiao, A.M. Gomez, Y.Y. Zhou, B. Ziman, H. Spurgeon, E.G. Lakatta & W.J. Lederer: Excitation-contraction coupling in heart: new insights from  $\text{Ca}^{2+}$  sparks. *Cell Calcium* 20, 129-140 (1996)
2. Wier, W.G. & C.W. Balke:  $\text{Ca}^{2+}$  release mechanisms,  $\text{Ca}^{2+}$  sparks, and local control of excitation-contraction coupling in normal heart muscle. *Circ Res* 85, 770-776 (1999)
3. Niggli, E.: Localized intracellular calcium signaling in muscle: calcium sparks and calcium quarks. *Annu Rev Physiol* 61, 311-335 (1999)
4. Bers, D.M.: *Excitation-Contraction Coupling and Cardiac Contractile Force*. Kluwer Academic Publishers, Dordrecht, The Netherlands (2001)
5. Fill, M, A. Zahradnikova, C.A. Villalba-Galea, I. Zahradnik, A.L. Escobar & S. Gyorke: Ryanodine receptor adaptation. *J Gen Physiol* 116, 873-882 (2000)
6. Varro, A., N. Negretti, S.B. Hester & D.A. Eisner: An estimate of the calcium content of the sarcoplasmic reticulum in rat ventricular myocytes. *Pflugers Arch.* 423, 158-160 (1993)
7. Bassani, R.A. & D.M. Bers: Rate of diastolic Ca release from the sarcoplasmic reticulum of intact rabbit and rat ventricular myocytes. *Biophys J* 68, 2015-2022 (1995)
8. Terracciano, C.M. & K.T. MacLeod: Measurements of  $\text{Ca}^{2+}$  entry and sarcoplasmic reticulum  $\text{Ca}^{2+}$  content during the cardiac cycle in guinea pig and rat ventricular myocytes. *Biophys J* 72, 1319-1326 (1997)
9. Lukyanenko, V., I. Gyorke, S. Subramanian, A. Smirnov, T.F. Wiesner & S. Gyorke: Inhibition of  $\text{Ca}^{2+}$  sparks by ruthenium red in permeabilized rat ventricular myocytes. *Biophys J* 79, 1273-1284 (2000)
10. Shannon, T.R., K.S. Ginsburg & D.M. Bers. Reverse mode of the sarcoplasmic reticulum calcium pump and load-dependent cytosolic calcium decline in voltage-clamped cardiac ventricular myocytes. *Biophys J* 78, 322-333 (2000)
11. Shannon, T.R. & D.M. Bers: Assessment of intra-SR free  $[\text{Ca}]$  and buffering in rat heart. *Biophys J* 73, 1524-1531 (1997)
12. Volpe, P. & B.J. Simon: The bulk of  $\text{Ca}^{2+}$  released to the myoplasm is free in the sarcoplasmic reticulum and does not unbind from calsequestrin. *FEBS Lett* 278, 274-278 (1991)
13. Mitchell, R.D., H.K. Simmerman, & L.R. Jones:  $\text{Ca}^{2+}$  binding effects on protein conformation and protein interactions of canine cardiac calsequestrin. *J Biol Chem* 263, 1376-1381 (1988)
14. Campbell, K.P.: *Protein components and their roles in sarcoplasmic reticulum function*. In: *Sarcoplasmic Reticulum in Muscle Physiology*. Entman, M.L. & W.B. Van Winkle (eds). Boca Raton, FL, CRC Press, Inc., 65-99 (1986)
15. Jones, L.R., Y.J. Suzuki, W. Wang, Y.M. Kobayashi, V. Ramesh, C. Franzini-Armstrong, L. Cleemann & M. Morad: Regulation of  $\text{Ca}^{2+}$  signaling in transgenic mouse cardiac

- myocytes overexpressing calsequestrin. *J Clin Invest* 101, 1385-1393 (1998)
16. Sato, Y., D.G. Ferguson, H. Sako, G.W. Dorn, V.J. Kadambi, A. Yatani, B.D. Hoyt, R.A. Walsh & E.G. Kranias: Cardiac-specific overexpression of mouse cardiac calsequestrin is associated with depressed cardiovascular function and hypertrophy in transgenic mice. *J Biol Chem* 273:28470-28477 (1998)
  17. Wang, W., L. Cleemann, L.R. Jones & M. Morad: Modulation of focal and global  $Ca^{2+}$  release in calsequestrin-overexpressing mouse cardiomyocytes. *J Physiol* 524, 399-414 (2000)
  18. Chen, W., C. Steenbergen, L.A. Levy, J. Vance, R.E. London & E. Murphy: Measurement of free  $Ca^{2+}$  in sarcoplasmic reticulum in perfused rabbit heart loaded with 1,2-bis(2-amino-5,6-difluorophenoxy)ethane-N,N,N',N'-tetraacetic acid by  $^{19}F$  NMR. *J Biol Chem* 271, 7398-7403 (1996)
  19. Rice, J.J., M.S. Jafri & R.L. Winslow: Modeling gain and gradedness of  $Ca^{2+}$  release in the functional unit of the cardiac diadic space. *Biophys J* 77, 1871-1884 (1999)
  20. Fabiato, A.: Two kinds of calcium-induced release of calcium from the sarcoplasmic reticulum of skinned cardiac cells. *Adv Exp Med Biol* 311, 245-262 (1992)
  21. Shannon, T.R., K.S. Ginsburg & D.M. Bers: Potentiation of fractional sarcoplasmic reticulum calcium release by total and free intra-sarcoplasmic reticulum calcium concentration. *Biophys J* 78, 334-343 (2000)
  22. Cheng, H., M.R. Lederer, W.J. Lederer & M.B. Cannell: Calcium sparks and  $[Ca^{2+}]_i$  waves in cardiac myocytes. *Am J Physiol* 270, C148-C159 (1996)
  23. Lukyanenko, V., I. Gyorke & S. Gyorke: Regulation of calcium release by calcium inside the sarcoplasmic reticulum in ventricular myocytes. *Pflugers Arch* 432, 1047-1054 (1996)
  24. Satoh, H., L.A. Blatter & D.M. Bers: Effects of  $[Ca^{2+}]_i$ , SR  $Ca^{2+}$  load, and rest on  $Ca^{2+}$  spark frequency in ventricular myocytes. *Am J Physiol* 272:H657-H668 (1997)
  25. Song, L.S., M.D. Stern, E.G. Lakatta & H. Cheng: Partial depletion of sarcoplasmic reticulum calcium does not prevent calcium sparks in rat ventricular myocytes. *J Physiol* 505, 665-675 (1997)
  26. Lukyanenko, V., S. Viatchenko-Karpinski, A. Smirnov, T.F. Wiesner & S. Gyorke: Dynamic regulation of sarcoplasmic reticulum  $Ca^{2+}$  content and release by luminal  $Ca^{2+}$ -sensitive leak in rat ventricular myocytes. *Biophys J* 81:785-798 (2001)
  27. Gyorke S., V. Lukyanenko & I. Gyorke: Dual effects of tetracaine on spontaneous calcium release in rat ventricular myocytes. *J Physiol* 500, 297-309 (1997)
  28. Overend, C.L., D.A. Eisner & S.C. O'Neill: The effect of tetracaine on spontaneous  $Ca^{2+}$  release and sarcoplasmic reticulum calcium content in rat ventricular myocytes. *J Physiol* 502, 471-479 (1997)
  29. Overend, C.L., S.C. O'Neill & D.A. Eisner: The effect of tetracaine on stimulated contractions, sarcoplasmic reticulum  $Ca^{2+}$  content and membrane current in isolated rat ventricular myocytes. *J Physiol* 507, 759-769 (1998)
  30. Lukyanenko, V., S. Subramanian, I. Gyorke, T.F. Wiesner & S. Gyorke: The role of luminal  $Ca^{2+}$  in the generation of  $Ca^{2+}$  waves in rat ventricular myocytes. *J Physiol* 518, 173-186 (1999)
  31. Sitsapesan, R. & A.J. Williams: Regulation of the gating of the sheep cardiac sarcoplasmic reticulum  $Ca^{2+}$ -release channel by luminal  $Ca^{2+}$ . *J Membr Biol* 137, 215-226 (1994)
  32. Sitsapesan, R. & A.J. Williams: Regulation of current flow through ryanodine receptors by luminal  $Ca^{2+}$ . *J Membr Biol* 159, 179-185 (1997)
  33. Gyorke, I. & S. Gyorke: Regulation of the cardiac ryanodine receptor channel by luminal  $Ca^{2+}$  involves luminal  $Ca^{2+}$  sensing sites. *Biophys J* 75, 2801-2810 (1998)
  34. Xu, L. & G. Meissner: Regulation of cardiac muscle  $Ca^{2+}$  release channel by sarcoplasmic reticulum luminal  $Ca^{2+}$ . *Biophys J* 75, 2302-2312 (1998)
  35. Ching, L.L., A.J. Williams & R. Sitsapesan: Evidence for  $Ca^{2+}$  activation and inactivation sites on the luminal side of the cardiac ryanodine receptor complex. *Circ Res* 87, 201-206 (2000)
  36. Takeshima, H., S. Nishimura, T. Matsumoto, H. Ishida, K. Kangawa, N. Minamino, H. Matsuo, M. Ueda, M. Hanaoka & T. Hirose: Primary structure and expression from complementary DNA of skeletal muscle ryanodine receptor. *Nature* 339(6224), 439-445 (1989)
  37. Marks, A.R., S. Fleischer & P. Tempst: Surface topography analysis of the ryanodine receptor/junctional channel complex based on proteolysis sensitivity mapping. *J Biol Chem* 265, 13143-13149 (1990)
  38. Sienaert I., H. De Smedt, J.B. Parys & L. Missiaem: Regulation of  $Ca^{2+}$ -release channels by luminal  $Ca^{2+}$ . Integrative Aspects of Calcium Signalling, Eds. Verkhratsky and Toescu, Plenum Press, New York (1998).
  39. Zhang, L., J. Kelley, G. Schmeisser, Y.M. Kobayashi & L.R. Jones: Complex formation between junctin, triadin, calsequestrin, and the ryanodine receptor. Proteins of the cardiac junctional sarcoplasmic reticulum membrane. *J Biol Chem* 272, 23389-23397 (1997)
  40. Ikemoto, N., M. Ronjat, L.G. Meszaros & M. Koshita: Postulated role of calsequestrin in the regulation of calcium release from sarcoplasmic reticulum. *Biochemistry* 28, 6764-6771 (1989)
  41. Donoso, P., H. Prieto & C. Hidalgo: Luminal calcium regulates calcium release in triads isolated from frog and rabbit skeletal muscle. *Biophys J* 68, 507-515 (1995)
  42. Kawasaki, T. & M. Kasai: Regulation of calcium channel in sarcoplasmic reticulum by calsequestrin. *Biochem Biophys Res Commun* 199, 1120-1127 (1994)
  43. Szegedi, C., S. Sarkozi, A. Herzog, I. Jona, M. Varsanyi: Calsequestrin: more than 'only' a luminal  $Ca^{2+}$  buffer inside the sarcoplasmic reticulum. *Biochem J* 337, 19-22 (1999)
  44. Caswell, A.H., N.R. Brandt, J.P. Brunschwig & S. Purkerson: Localization and partial characterization of the oligomeric disulfide-linked molecular weight 95,000 protein (triadin) which binds the ryanodine and dihydropyridine receptors in skeletal muscle triadic vesicles. *Biochemistry* 30, 7507-7513 (1991)
  45. Knudson, C.M., K.K. Stang, A.O. Jorgensen & K.P. Campbell: Biochemical characterization of ultrastructural localization of a major junctional sarcoplasmic reticulum glycoprotein (triadin). *J Biol Chem* 268, 12637-12645 (1993)
  46. Tanaka H, Sekine T, Kawanishi T, Nakamura R, Shigenobu K. Intrasarcomere  $[Ca^{2+}]$  gradients and their spatio-temporal relation to  $Ca^{2+}$  sparks in rat cardiomyocytes. *J Physiol* 508, 145-152 (1998)
  47. DelPrincipe, F., M. Egger, G.C. Ellis-Davies & E. Niggli: Two-photon and UV-laser flash photolysis of the  $Ca^{2+}$  cage, dimethoxynitrophenyl-EGTA-4. *Cell Calcium* 25, 85-91 (1999)
  48. Terentyev, D., S. Viatchenko-Karpinski, H. Valdivia, A. Escobar & S. Gyorke: Luminal Ca determines termination of cardiac Ca sparks. Biophys. Soc. Meeting, San-Francisco (2002)
  49. Terentyev, D., S. Viatchenko-Karpinski & S. Gyorke: Modulation of Ca Release by Low Affinity Ca Buffers in Rat Ventricular Myocytes. *Biophys J* 80, 593a (2001)
  50. Sobie, E.A., A.R. Marks, W.J. Lederer & M.S. Jafri: Mathematical simulation of cardiac  $Ca^{2+}$  Sparks. *Biophys J* 80, 590a (2001)
  51. Lee, H.C.: Physiological functions of cyclic ADP-ribose and NAADP as calcium messengers. *Annu Rev Pharmacol Toxicol* 41, 317-345 (2001)
  52. Rakovic, S., Y. Cui, S. Iino, A. Galione, G.A. Ashamu, B.V. Potter & D.A. Terrar: An antagonist of cADP-ribose inhibits arrhythmogenic oscillations of intracellular  $Ca^{2+}$  in heart cells. *J Biol Chem* 274, 17820-17827 (1999)
  53. Rakovic, S., A. Galione, G.A. Ashamu, B.V. Potter & D.A. Terrar: A specific cyclic ADP-ribose antagonist inhibits cardiac excitation-contraction coupling. *Curr Biol* 6, 989-996 (1996)

54. Cui, Y., A. Galione & D.A. Terrar: Effects of photoreleased cADP-ribose on calcium transients and calcium sparks in myocytes isolated from guinea-pig and rat ventricle. *Biochem J* 342, 269-273 (1999)
55. Iino, S., Y. Cui, A. Galione & D.A. Terrar: Actions of cADP-ribose and its antagonists on contraction in guinea pig isolated ventricular myocytes. Influence of temperature. *Circ Res* 81, 879-884 (1997)
56. Prakash, Y.S., M.S. Kannan, T.F. Walseth & G.C. Sieck: cADP ribose and  $[Ca^{2+}]_i$  regulation in rat cardiac myocytes. *Am J Physiol* 279, H1482-H1489 (2000)
57. Meszaros, L.G., J. Bak & A. Chu: Cyclic ADP-ribose as an endogenous regulator of the non-skeletal type ryanodine receptor  $Ca^{2+}$  channel. *Nature* 364, 76-79 (1993)
58. Fruen, B.R., J.R. Mickelson, N.H. Shomer, P. Velez & C.F. Louis: Cyclic ADP-ribose does not affect cardiac or skeletal muscle ryanodine receptors. *FEBS Lett* 352, 123-126 (1994)
59. Sitsapesan, R., S.J. McGarry & A.J. Williams: Cyclic ADP-ribose competes with ATP for the adenine nucleotide binding site on the cardiac ryanodine receptor  $Ca^{2+}$ -release channel. *Circ Res* 75, 596-600 (1994)
60. Guo, X., M.A. Laflamme & P.L. Becker: Cyclic ADP-ribose does not regulate sarcoplasmic reticulum  $Ca^{2+}$  release in intact cardiac myocytes. *Circ Res* 79, 147-151 (1996)
61. Lukyanenko, V., I. Györke, T.F. Wiesner & S. Györke: Potentiation of  $Ca^{2+}$  release by cADPR in heart is mediated by enhanced  $Ca^{2+}$  uptake into the sarcoplasmic reticulum. *Circ Res* 89, 614-622 (2001)
62. Lukyanenko, V. & S. Györke:  $Ca^{2+}$  sparks and  $Ca^{2+}$  waves in saponin-permeabilized rat ventricular myocytes. *J Physiol* 521, 575-585 (1999)
63. Ishide, N.: Intracellular calcium modulators for cardiac muscle in pathological conditions. *Jpn Heart J* 37, 1-17 (1996)
64. Wier, W.G., M.B. Cannell, J.R. Berlin, E. Marban & W.J. Lederer: Cellular and subcellular heterogeneity of  $[Ca^{2+}]_i$  in single heart cells revealed by fura-2. *Science* 235, 325-328 (1987)
65. Stern, M.D., M.C. Capogrossi & E.G. Lakatta: Spontaneous calcium release from the sarcoplasmic reticulum in myocardial cells: mechanisms and consequences. *Cell Calcium* 9, 247-56 (1988)
66. Lipp, P. & E. Niggli: Modulation of  $Ca^{2+}$  release in cultured neonatal rat cardiac myocytes. Insight from subcellular release patterns revealed by confocal microscopy. *Circ Res* 74, 979-990 (1994)
67. Lukyanenko, V., S. Subramanian, I. Györke, T. Wiesner & S. Györke: The role of sarcoplasmic reticulum luminal  $Ca^{2+}$  in generation of  $Ca^{2+}$  wave in rat ventricular myocytes. *J Physiol* 518, 173-186 (1999)
68. Boyden, P.A. & H.E. ter Keurs: Reverse excitation-contraction coupling:  $Ca^{2+}$  ions as initiators of arrhythmias. *J Cardiovasc Electrophysiol* 12, 382-385 (2001)
69. Lakatta, E.G. & T. Guarnieri: Spontaneous myocardial calcium oscillations: are they linked to ventricular fibrillation? *J Cardiovasc Electrophysiol* 4, 473-489 (1993)
70. Engel, J., A.J. Sowerby, S.A. Finch, M. Fechner & A. Stier: Temperature dependence of  $Ca^{2+}$  wave properties in cardiomyocytes: implications for the mechanism of autocatalytic  $Ca^{2+}$  release in wave propagation. *Biophys J* 68, 40-45 (1995)
71. Vatner, D.E., N. Sato, K. Kiuchi, R.P. Shannon & S.F. Vatner: Decrease in myocardial ryanodine receptors and altered excitation-contraction coupling early in the development of heart failure. *Circulation* 90, 1423-1430 (1994)
72. Hittinger, L., B. Ghaleh, J. Chen, J.G. Edwards, R.K. Kudej, M. Iwase, S.J. Kim, S.F. Vatner & D.E. Vatner: Reduced subendocardial ryanodine receptors and consequent effects on cardiac function in conscious dogs with left ventricular hypertrophy. *Circ Res* 84, 999-1006 (1999)
73. Yamamoto, T., M. Yano, M. Kohno, T. Hisaoka, K. Ono, T. Tanigawa, Y. Saiki, Y. Hisamatsu, T. Ohkusa & M. Matsuzaki: Abnormal  $Ca^{2+}$  release from cardiac sarcoplasmic reticulum in tachycardia-induced heart failure. *Cardiovasc Res* 44, 146-155 (1999)
74. Marks, A.R.: Cardiac intracellular calcium release channels: role in heart failure. *Circ Res* 87, 8-811 (2000).
75. Marx, S.O., S. Reiken, Y. Hisamatsu, T. Jayaraman, D. Burkhoff, N. Rosembliit & A.R. Marks: PKA phosphorylation dissociates FKBP12.6 from the calcium release channel (ryanodine receptor): defective regulation in failing hearts. *Cell* 101, 365-376 (2000)
76. Gomez, A.M., H.H. Valdivia, H. Cheng, M.R. Lederer, L.F. Santana, M.B. Cannell, S.A. McCune, R.A. Altschuld & W.J. Lederer: Defective excitation-contraction coupling in experimental cardiac hypertrophy and heart failure. *Science* 276(5313), 800-806 (1997)
77. Farrell, E.F., M.-T. Jiang & A.J. Lokutta, M.B. Meyers & H.H. Valdivia: Abnormal calcium release, but normal ryanodine receptors, in canine and human heart failure. *Biophys J* 80, 508a (2001)
78. Gyorke, I., S.D. Prabhu, G. Salama & S. Gyorke: RyR regulation by luminal Ca is altered in heart failure. *Biophys. Soc. Meeting. San Francisco* (2002)

# Calmodulin Modulation of Proteins Involved in Excitation-Contraction Coupling

Wei Tang, Serap Sencer, Susan L. Hamilton

Department of Molecular Physiology and Biophysics, Baylor College of Medicine, Houston, Texas, U.S.A.

**Abstract** Muscle excitation-contraction coupling is, in large part, regulated by the activity of two proteins. These are the ryanodine receptor (RyR), which is an intracellular  $\text{Ca}^{2+}$  release channel and the dihydropyridine receptor (DHPR), which is a voltage gated L-type calcium channel. In skeletal muscle, the physical association between RyR1 and L-type  $\text{Ca}^{2+}$  channels is required for muscle excitation-contraction coupling. RyRs also regulate intracellular  $\text{Ca}^{2+}$  homeostasis, thereby contributing to a variety of cellular functions in different tissues. A wide variety of modulators directly regulate RyR1 activity and, consequentially, alter both excitation-contraction coupling and calcium homeostasis. Calmodulin, one of these cellular modulators, is a ubiquitously expressed 17 kDa  $\text{Ca}^{2+}$  binding protein containing four E-F hands, which binds to RyR1 at both nanomolar and micromolar  $\text{Ca}^{2+}$  concentrations. Apocalmodulin ( $\text{Ca}^{2+}$  free calmodulin) is a partial agonist, while  $\text{Ca}^{2+}$ calmodulin is an inhibitor of RyR1. This conversion of calmodulin from an activator to an inhibitor is due to  $\text{Ca}^{2+}$  binding to the two C-terminal sites on calmodulin. Calmodulin can also modulate the L-type  $\text{Ca}^{2+}$  channel in the transverse tubule membrane, producing, upon elevation of the local  $\text{Ca}^{2+}$  concentrations, either inactivation or facilitation of the channel. Calmodulin binds to a region on RyR1 corresponding to amino acids 3614-3643 and to a region in the carboxy-terminal tail of the L-type  $\text{Ca}^{2+}$  channel  $\alpha_1$  subunit. However, these calmodulin binding motifs on both proteins bind to undetermined motifs on the other protein, suggesting that they represent more general protein-protein interaction motifs. These findings raise questions about the role of calmodulin in excitation-contraction coupling in skeletal muscle.

## RYANODINE RECEPTORS

Ryanodine receptors (RyRs) are  $\text{Ca}^{2+}$  release channels that reside in endoplasmic/sarcoplasmic reticulum. These proteins have a high affinity for ryanodine, a plant alkaloid, and are homotetramers of a subunit with a molecular mass greater than 500 kDa. To date there are three isoforms of ryanodine receptors identified in mammalian tissues: RyR1, RyR2 and RyR3. The three RyRs are encoded by separate genes and have different tissue distributions. The overall sequence homology among these RyRs is about 60%. Although RyR1, RyR2 and RyR3 are often referred to as skeletal, cardiac and brain isoforms (1-5), respectively, this designation is misleading since all of these isoforms are found in other tissues. RyR1 is found in some parts of brain, such as Purkinje cells of the cerebellum (6, 7), and in smooth muscle (8), while RyR2 is the most widely distributed form in brain (6, 7). RyR3 is a minor isoform in both brain and skeletal muscle (6, 7, 9). In skeletal muscle RyR3 appears to exist in the highest concentration in the diaphragm (9). RyR1 and RyR2 are essential proteins in skeletal and cardiac excitation-contraction coupling, respectively. In RyR1 deficient mice, E-C coupling is completely abolished resulting in perinatal death from respiratory failure. Muscular degeneration is also found in these mutant mice, suggesting a role for RyR1 in skeletal muscle morphogenesis (10). RyR2 is not required for E-C coupling in embryonic heart, but appears to serve as a regulator of internal  $\text{Ca}^{2+}$  stores for other aspects of calcium homeostasis (11). RyR3 is expressed in relative abundance in neonate skeletal muscle and may play an amplifying or auxiliary role in E-C coupling (12). RyR3 has also been implicated in

spatial learning and hippocampal synaptic plasticity (13). In nonexcitable cells, RyRs are involved in the  $\text{Ca}^{2+}$  wave propagation needed for other cellular functions, such as secretion activity in pancreatic acinar cells (14).

## DIHYDROPYRIDINE RECEPTORS

Dihydropyridine receptors (DHPRs) are oligomeric proteins that are found primarily in the transverse tubules in skeletal muscle. They are  $\text{Ca}^{2+}$  channels of the L-type, which means that they are activated by high voltage, show slow voltage-dependent inactivation and are modulated by phenylalkylamines (eg, verapamil), benzothiazepines (eg, diltiazem), and dihydropyridines (eg, nitrendipine) (15). The DHPR is composed of a 190 kDa  $\alpha_1$  subunit, a 55 kDa  $\beta$  subunit, a 170 kDa disulfide-linked  $\alpha_2\delta$  dimer and a 33 kDa transmembrane  $\gamma$  subunit (16). In skeletal muscle DHPRs in the t-tubules are arranged in regular arrays above RyR1 in the SR membranes. In the arrays the DHPRs are found in groups of four, called tetrads, and are positioned above every other RyR1 (17, 18). In the absence of the DHPR  $\alpha_1$  subunit (dysgenic muscle), other subunits of DHPR are no longer anchored to the junctional region and tetrads are absent (19).

## EXCITATION-CONTRACTION COUPLING

The process whereby depolarization of the muscle membrane leads to contraction of the muscle is known as excitation-contraction (E-C) coupling. There are two kinds of E-C coupling: mechanical

coupling, where a change in the conformation of the DHPR directly signals the  $\text{Ca}^{2+}$  release channel to open, and  $\text{Ca}^{2+}$ -induced calcium release (CICR), where  $\text{Ca}^{2+}$  entering through the L-type channel activates the  $\text{Ca}^{2+}$  release channel (20, 21). Mechanical coupling is required for skeletal but not cardiac muscle E-C coupling (21). The functional interactions between RyR1 and DHPR are believed to be reciprocal. DHPR opens RyR1, defined as orthograde signaling, and RyR1 can prevent DHPR inactivation, defined as retrograde signaling (22, 23). Chimeras of RyR1 and RyR2 or  $\alpha_{1sk}$  and  $\alpha_{1c}$  have been used extensively to map the regions on RyR1 and DHPR responsible for these interactions. This approach is based on the findings that only RyR1 and  $\alpha_{1sk}$  can restore mechanical E-C coupling in skeletal muscle (23-26). The II-III loop of the  $\alpha_{1sk}$  subunit has been shown to be required for the mechanical coupling. Several regions on RyR1 are thought to be involved in either orthograde or retrograde signaling, or both. A region between amino acids 1635-2636 on RyR1 has been shown to be required for both orthograde and retrograde signaling. In addition, a region between residues 2659-3720 on RyR1 has been implicated in retrograde signaling (23). Other regions of both proteins may be involved in their coupling (27, 28). A synthetic peptide representing a sequence between amino acids 3614 and 3643 on RyR1 has been shown to directly interact with the DHPR (29) and conversely, the carboxy-terminal tail of the DHPR  $\alpha_1$  subunit has been shown to interact with RyR1 (28, 29).

As mentioned previously, only every other RyR1 appears to be physically associated with a tetrad of DHPRs (17, 18), producing two different populations of RyR1 (coupled and uncoupled). These two populations must be regulated in different ways. Uncoupled RyR1s are likely to be activated by CICR, with the triggering  $\text{Ca}^{2+}$  released from neighboring coupled RyR1s. An additional level of complexity, however, comes from the finding that both of the primary players in E-C coupling are modulated by other proteins. One example of proteins that modulate the activity of both the DHPR and RyR1 is the  $\text{Ca}^{2+}$  binding protein, calmodulin (CaM). CaM in both its  $\text{Ca}^{2+}$  bound and  $\text{Ca}^{2+}$  free states can bind and regulate both RyR1 and DHPR (30-34). Studies of the role of calmodulin in E-C coupling have concentrated primarily on its interaction with uncoupled proteins, raising the question of how calmodulin regulates coupled channels. Determining the role of modulatory proteins in E-C coupling remains a major challenge to the understanding of the molecular mechanisms involved in E-C coupling in skeletal muscle.

## CALMODULIN

Calmodulin (CaM) is a 17 kDa ubiquitously expressed  $\text{Ca}^{2+}$  binding protein with a single 148-amino-acid polypeptide chain. It contains four calcium binding EF hands between residues 20-31, 56-67, 93-104 and 129-140 (35). EF hand is defined as two  $\alpha$ -helical sequences oriented in a perpendicular way and connected by a  $\text{Ca}^{2+}$  binding loop. Calmodulin consists of two globular (N and C) lobes connected by an

eight-turn  $\alpha$ -helix. Each lobe has two calcium binding sites (35). Calmodulin goes through  $\text{Ca}^{2+}$  dependent conformational changes upon binding to  $\text{Ca}^{2+}$  resulting in the exposure of several hydrophobic residues in the helices of both lobes (36). It has numerous cellular targets and plays an important role of regulating cellular functions (37). CaM binds most target proteins in a  $\text{Ca}^{2+}$  dependent manner. Upon binding  $\text{Ca}^{2+}$ , CaM exposes the binding site for its target sequence and can modulate the function of the target.  $\text{Ca}^{2+}$ CaM binding proteins include calcineurin and CaM dependent kinase II (37, 38). Other proteins, such as neuromodulin, primarily bind the  $\text{Ca}^{2+}$  free form of CaM (39). Still other proteins bind both the  $\text{Ca}^{2+}$  free and  $\text{Ca}^{2+}$  bound forms of CaM. Both RyR1 and the DHPR fit into this latter category. One type of calmodulin binding site is an amphipathic helix with two clusters of positive charges separated by a hydrophobic region (40). Another motif that can bind either apoCaM,  $\text{Ca}^{2+}$ CaM or both is the IQ motif, which has a consensus sequence of IQXXRGXXXR (40).

### Functional effects of Calmodulin on RyR1

CaM directly interacts with RyR1 and modulates its function. CaM increases RyR1 activity at low  $\text{Ca}^{2+}$  concentrations (nM) and inhibits channel activity at high  $\text{Ca}^{2+}$  concentrations ( $\mu\text{M}$ ) (30, 41, 42). Since both CaM and RyR1 are  $\text{Ca}^{2+}$  binding proteins (36, 43), these  $\text{Ca}^{2+}$  dependent functional effects could arise from  $\text{Ca}^{2+}$  binding to CaM, RyR1 or both. Using a CaM mutant, which does not bind  $\text{Ca}^{2+}$  at any of the four  $\text{Ca}^{2+}$  binding sites, we demonstrated that  $\text{Ca}^{2+}$  binding to CaM converts it from an activator to inhibitor of the RyR1 (30). We also found that  $\text{Ca}^{2+}$  binding to sites 3 and 4 on CaM is responsible for its conversion from an activator to an inhibitor.  $\text{Ca}^{2+}$  binding to RyR1 does, however, alter its interaction with CaM.  $\text{Ca}^{2+}$  binding to RyR1 increases its affinity for both apoCaM and  $\text{Ca}^{2+}$ CaM and, conversely, the binding of CaM to RyR1 increases the affinity of the  $\text{Ca}^{2+}$  binding site on RyR1 (30, 31).

Closely related to the modulation of RyR1 by CaM is its regulation by oxidants and nitric oxide (NO). Skeletal muscle produces reactive oxygen intermediates (ROI) and nitric oxide (NO) even at rest. Reactive oxidant production increases upon strenuous contraction, leading to muscle fatigue (44). RyR1 is believed to be one of the target proteins of both oxidants and NO. Oxidants, NO and calmodulin appear to work together to finely tune the RyR1 activity during the dynamic changes of skeletal muscle. Oxidants, such as  $\text{H}_2\text{O}_2$ , increase RyR1 activity and produce intersubunit disulfide bonds within the RyR1 tetramer (45-47). Calmodulin can protect the channel from oxidation-induced intersubunit cross-linking and, conversely, oxidation can prevent calmodulin binding to RyR1 (48).

The effect of NO, however, on RyR1 function is controversial. Both activating and inhibiting action on the channel have been reported (49, 50). Eu *et al.* (51) demonstrated that under physiological  $\text{O}_2$  tension ( $\sim 10\text{mmHg}$ ), NO activated the RyR1 and this modulation appeared to be calmodulin dependent. NO

has been shown to oppose the ROI effect of enhancing muscle contractile function (44). Consistent with this, NO blocks oxidation activation of RyR1 (46).

### **Calmodulin binding sites on RyR1**

Ryanodine receptors were first suggested to be calmodulin-modulated proteins by photo affinity labeling studies (52). Using azido- $^{125}\text{I}$ calmodulin, Seiler *et al.* (52) demonstrated that high molecular proteins in both cardiac and skeletal muscle, later known as RyRs, could bind calmodulin and were the principal bands labeled in junctional SR. Although several earlier papers suggested that there were multiple apocalmodulin binding sites per subunit of RyR1 (41, 45, 53), more recent studies (30, 54) have shown that both apoCaM and  $\text{Ca}^{2+}\text{CaM}$  bind to a single site per subunit of RyR1. A number of laboratories have attempted to identify CaM binding sites in the primary sequence of RyR1. Analysis of primary structure of RyR1 identified several putative calmodulin binding sites between residues 2807-2840, 2909-2930, 3031-3049, 3614-3637 and 4295-4325 on RyR1 (2, 55). Based on calpain digestion pattern of RyR1 and CaM's ability to inhibit calpain digestion, three more candidate CaM binding sites were proposed between residues 1383-1400, 1974-1996 and 3358-3374 (56). Using  $^{125}\text{I}$ calmodulin overlays, Chen *et al.* identified six potential calcium-dependent CaM binding sites, three strong CaM binding domains in regions between residues 2063-2091, 3611-3642, and 4303-4328, and three weaker CaM binding domains in regions between residues 921-1173, 2804-2930, and 2961-3084 (57). Zorzato and his group identified three calmodulin binding sites, residues 2937-3225 binding to both apoCaM and  $\text{Ca}^{2+}\text{CaM}$ , residues 3546-3655 binding only to  $\text{Ca}^{2+}\text{CaM}$ , and peptides with amino acids 3610-3629 and 4534-4552 interacting directly with dansylcalmodulin under micromolar  $\text{Ca}^{2+}$  based on fluorescence spectra (58). Our laboratory found that calmodulin bound to RyR1 could protect a site on RyR1 from tryptic cleavage. Both  $\text{Ca}^{2+}\text{CaM}$  and apoCaM prevented tryptic cleavage after amino acids 3630 and 3637, suggesting that apoCaM and  $\text{Ca}^{2+}\text{CaM}$  bind to the same or overlapping regions on RyR1 and this site contains residues 3614-43 (48, 54, 59, 60). Non-denaturing gel shift assays using a synthetic peptide corresponding to amino acids 3614-3643 on RyR1 confirmed that this sequence could bind both forms of calmodulin (59). Point mutations in this region abolish CaM binding (54). This sequence is highly conserved in the different RyR isoforms, suggesting that all three are modulated by CaM.

Our previous studies with oxidizing agents showed that calmodulin could protect RyR1 from oxidation-induced intersubunit crosslinking. C3635, one of the cysteine residues that form intersubunit disulfide bonds, is protected from oxidation by CaM binding (60). This suggests that CaM binds to a RyR1 intersubunit contact site. This cysteine residue is also the primary site for NO nitrosylation of RyR1 (61).

A crucial aspect needed to evaluate the molecular mechanism by which CaM regulates RyR1

activity is the location of CaM in the three dimensional structure of RyR1. Wagenknecht and coworkers showed that the CaM binding sites on RyR1 were located in the cytoplasmic domain of RyR1 and that the apoCaM and  $\text{Ca}^{2+}\text{CaM}$  binding sites are closely spaced to one another (62, 63). The regulation of RyR1 activity by CaM is, therefore, likely to be allosteric.

### **Calmodulin and DHPR**

CaM can bind to both cardiac and skeletal muscle DHPR, although most of the functional effects of CaM on DHPR have been studied in cardiac muscle. CaM serves as a  $\text{Ca}^{2+}$  sensor for both  $\text{Ca}^{2+}$  dependent inactivation and facilitation of the cardiac L-type  $\text{Ca}^{2+}$  channel (32, 64). A mutated CaM that can not bind  $\text{Ca}^{2+}$  at any of the four  $\text{Ca}^{2+}$  binding sites blocks the effects of  $\text{Ca}^{2+}\text{CaM}$  on the cardiac L-type  $\text{Ca}^{2+}$  channel (64), suggesting that both  $\text{Ca}^{2+}\text{CaM}$  and apoCaM bind to L-type  $\text{Ca}^{2+}$  channels. It has been proposed that CaM is tethered to the channel under resting  $\text{Ca}^{2+}$  and the elevation of intracellular  $\text{Ca}^{2+}$  leads to  $\text{Ca}^{2+}$  binding to CaM, producing cardiac L-type channel inactivation and facilitation (34). The carboxy tail of DHPR  $\alpha_1$  subunit is required for both apoCaM and  $\text{Ca}^{2+}\text{CaM}$  interactions. Two  $\text{Ca}^{2+}$ -dependent CaM binding sites have been identified in the carboxy-terminal tail of the  $\alpha_1$ -subunit of DHPR, the CB region (between the amino acids 1484-1509 or 1627-1652 of the human skeletal muscle or cardiac  $\alpha_1$  subunit, respectively.) and IQ-like motif (between the amino acids 1522-1542 or 1665-1685 of the human skeletal muscle or cardiac  $\alpha_1$  subunit, respectively.) (33, 65, 66). Another region, called the A motif (between the amino acids 1558-1579 of the rabbit cardiac  $\alpha_1$  subunit) may also contribute to the interaction of CaM with the DHPR  $\alpha_1$  carboxy-terminal tail (34). Synthetic peptides, corresponding to the CB region and the IQ motif bind both partially and fully  $\text{Ca}^{2+}$ -saturated CaM (33). Mutation of the isoleucine 1672 of the cardiac IQ motif to alanine abolishes  $\text{Ca}^{2+}/\text{CaM}$  dependent inactivation and unmasks a strong facilitation by CaM. Mutation of this isoleucine to a glutamate abolishes both facilitation and inactivation (65). Peptides with either mutation still bind to  $\text{Ca}^{2+}\text{CaM}$  as well as wild type IQ peptide. Neither the CB nor IQ peptide has a high affinity for apoCaM (33, 67). Peptide A (1558-1579) and peptide C (1585-1606) from rabbit cardiac  $\alpha_1$  subunit may bind CaM at low  $\text{Ca}^{2+}$  concentrations, making them candidates for the CaM tethering site on cardiac DHPR under resting conditions (34). A recombinant protein which encompasses the  $\text{Ca}^{2+}$  binding EF hand, the A and the CB motif of the skeletal muscle DHPR  $\alpha_1$  subunit was found to bind to CaM at less than 10 nM  $\text{Ca}^{2+}$  (29). A functional effect of calmodulin on the skeletal muscle DHPR has not yet been demonstrated.

### **CaM and E-C coupling**

A number of studies have shown conclusively that CaM is able to bind to both the DHPR and RyR1. These studies have, however, been performed with uncoupled proteins. Recent studies in our laboratory have revealed another possible role for the CaM

binding motifs on both of these proteins (29). We have shown that these motifs can be used for interaction between RyR1 and DHPR and that CaM is competitive for this interaction. Hence the carboxy-terminal tail of the DHPR  $\alpha_1$  subunit, a well established CaM interaction domain, binds to RyR1 and conversely, the CaM binding motif on RyR1 interacts with the DHPR  $\alpha_1$ -subunit carboxy-terminal tail. These two CaM binding motifs do not bind directly to each other, and therefore, each must have another binding partner on the other protein. These findings raise the possibility that CaM regulation of coupled channels is very different from that of uncoupled channels. In uncoupled channels CaM is a  $\text{Ca}^{2+}$  sensor for inactivation and facilitation of the L-type channel and an activator or inhibitor of RyR1 (depending on the  $\text{Ca}^{2+}$  concentration). However, when these two ion channels are coupled to one another, CaM at sufficiently high concentrations would tend to disrupt one site of DHPR-RyR1 interaction. Since both the CB peptide and an expressed carboxy-terminal tail fragment of the DHPR  $\alpha_1$  inhibit RyR1 channel activity and [ $^3\text{H}$ ]ryanodine binding to RyR1 (28, 29), the interaction of the carboxy-terminal tail of the DHPR  $\alpha_1$  subunit may serve to stabilize a closed state of RyR1. If this is true, CaM might be expected to facilitate RyR1 channel opening at low  $\text{Ca}^{2+}$ , both by disrupting this interaction and by direct effects on channel activity.

## SUMMARY

The role that CaM plays in E-C coupling is likely to be extremely complex since CaM can interact with both the DHPR and RyR1 and it can do so at both high and low  $\text{Ca}^{2+}$ . Not only can both  $\text{Ca}^{2+}$ CaM and apoCaM interact with the two channels, but in both cases the functional consequences of the interaction is also altered by  $\text{Ca}^{2+}$  binding to CaM. In addition, the CaM binding motifs may be used by coupled channels to interact with each other rather than with CaM. In this situation CaM would be capable of disrupting one of the sites where the DHPR couples to RyR1. These findings demonstrate the remarkable flexibility of CaM as a  $\text{Ca}^{2+}$  sensor, but emphasize the difficulty in clearly defining its role in E-C coupling. Disruption of CaM binding sites would be expected to alter CaM binding to both uncoupled and coupled channels and to affect the interactions between the DHPR and RyR1. Interpretation of the molecular mechanisms of altered E-C coupling by CaM could be, therefore, misleading. Mutation of CaM or decreasing its expression would be expected to alter a number of  $\text{Ca}^{2+}$  sensitive processes that use CaM as a  $\text{Ca}^{2+}$  sensor, possibly producing secondary effects as well as primary effects on E-C coupling. These changes would alter both  $\text{Ca}^{2+}$  independent and  $\text{Ca}^{2+}$  dependent effects of CaM on both RyR1 and the DHPR. Interpretation of the molecular mechanisms involved in CaM regulation of the DHPR and RyR1 requires additional structural information. We do not know the molecular details of the interaction of CaM with either channel. Particularly important will be the elucidation of both the molecular determinants for apoCaM versus  $\text{Ca}^{2+}$  CaM binding on both RyR1 and

the DHPR and the molecular mechanisms for the movement of CaM from an apoCaM binding site to a  $\text{Ca}^{2+}$ CaM binding site. The intriguing structural data obtained with the small conductance  $\text{Ca}^{2+}$  activated  $\text{K}^+$  channel (68) clearly show the importance of high-resolution structure for the interpretation of the complex role of CaM as a  $\text{Ca}^{2+}$  sensor.

## ACKNOWLEDGEMENTS

We would like to acknowledge the helpful comments of Dr. Rao Papineni, Dr. Wael Mourad, Dr. Mihail Chelu, Dr. Irina Serysheva, Dr. LiangWen Xiong, Dr. Jia-Zheng Zhang, Patricia Pate, KeKe Dong, Hongwei Zhang, Oluwatoyin Thomas, Mariah Baker, and Lynda Attaway.

## References

1. Marks, A. R., P. Tempst, K. S. Hwang, M.B. Taubman, M. Inui, C. Chadwick, S. Fleischer, and B. Nadal-Ginard. Molecular cloning and characterization of the ryanodine receptor/junctional channel complex cDNA from skeletal muscle sarcoplasmic reticulum. *Proc. Natl. Acad. Sci. USA* 86: 8683-8687, (1989).
2. Takeshima, H., S. Nishimura, H. Matsumoto, K. Ishida, N. Kangawa, H. Minamino, M. Matsuo, M. Ueda, M. Hanakoa, T. Hirose, and S. Numa. Primary structure and expression from complementary DNA of skeletal muscle ryanodine receptor. *Nature* 339: 439-445, (1989).
3. Nakai, J., T. Imagawa, Y. Hakawat, M. Shigekawa, H. Takeshima, and S. Numa. Primary structure and functional expression from cDNA of the cardiac ryanodine receptor/calcium release channel. *FEBS Lett.* 271: 169-177, (1990).
4. Otsu, K., H. F. Willard, V. K. Khanna, F. Zorzato, N. M. Green, and D. H. MacLennan. Molecular cloning of cDNA encoding the  $\text{Ca}^{2+}$  release channel (ryanodine receptor) of rabbit cardiac muscle sarcoplasmic reticulum. *J. Biol. Chem.* 265: 13472-13483, (1990).
5. Hakamata, Y., J. Nakai, H. Takeshima, and K. Imoto. Primary structure and distribution of a novel ryanodine receptor/calcium release channel from rabbit brain. *FEBS Lett.* 312: 229-235, (1992).
6. Furuichi, T., D. Furutama, Y. Hakamata, J. Nakai, H. Takeshima, and K. Mikoshiba. Multiple types of ryanodine receptor/ $\text{Ca}^{2+}$  release channels are differentially expressed in rabbit brain. *J. Neurosci.* 14: 4794-4805, (1994).
7. Giannini, G., A. Conti, S. Mammarella, M. Scrobogna, and V. Sorrentino. The ryanodine receptor/calcium channel genes are widely and differentially expressed in murine brain and peripheral tissues. *J. Cell. Biol.* 128: 893-904, (1995).
8. Neylon, C. B., S. M. Richards, M. A. Larsen, A. Argotis, and A. Bobik. Multiple types of ryanodine receptor/ $\text{Ca}^{2+}$  release channels are expressed in vascular smooth muscle. *Biochem. Biophys. Res. Commun.* 215:814-821, (1995).
9. Conti, A., L. Gorza, and V. Sorrentino. Differential distribution of ryanodine receptor type 3 (RyR3) gene product in mammalian skeletal muscles. *Biochem. J.* 316: 19-23, (1996).
10. Takeshima, H., M. Iino, H. Takekura, M. Nishi, J. Kuno, O. Minowa, H. Takano, and T. Noda. Excitation-contraction uncoupling and muscular degeneration in mice lacking functional skeletal muscle ryanodine-receptor gene. *Nature* 369: 556-559, (1994).
11. Takeshima, H., S. Komazaki, K. Hirose, M. Nishi, T. Noda, and M. Iino. Embryonic lethality and abnormal cardiac myocytes in mice lacking ryanodine receptor type 2. *EMBO J.* 17: 3309-3316, (1998).
12. Takeshima, H., T. Yamazawa, T. Ikemoto, H. Takekura, M. Nishi, T. Noda, and M. Iino.  $\text{Ca}^{2+}$ -induced  $\text{Ca}^{2+}$  release in myocytes from dyspedic mice lacking the

- type-1 ryanodine receptor. *EMBO J.* 14: 2999-3006, (1995).
13. Balschun, D., D. P. Wolfer, F. Bertocchini, V. Barone, A. Conti, W. Zuschratter, L. Missiaen, H. P. Lipp, J. U. Frey, and V. Sorrentino. Deletion of the ryanodine receptor type 3 (RyR3) impairs forms of synaptic plasticity and spatial learning. *EMBO J.* 18: 5264-5273, (1999).
  14. Straub, S. V., D. R. Giovannucci, and D. I. Yule. Calcium wave propagation in pancreatic acinar cells: functional interaction of inositol 1,4,5-triphosphate receptors, ryanodine receptors, and mitochondria. *J. Gen. Physiol.* 116: 547-560, (2000).
  15. Reuter, H. Calcium channel modulation by neurotransmitters, enzymes and drugs. *Nature* 301:569-574, (1983).
  16. Takahashi, M., M. J. Seager, J. F. Jones, B. F. Reber, and W. A. Catterall. Subunit structure of dihydropyridine-sensitive calcium channels from skeletal muscle. *Proc. Natl. Acad. Sci. U.S.A.* 84: 5478-5482, (1987).
  17. Franzini-Armstrong, C., and J. W. Kish. Alternate disposition of tetrads in peripheral couplings of skeletal muscle. *J. Muscle Res. Cell Motil.* 16: 319-324, (1995).
  18. Franzini-Armstrong, C., and F. Protasi. Ryanodine receptors of striated muscles: a complex channel capable of multiple interactions. *Physiol. Rev.* 77: 699-729, (1997).
  19. Flucher, B. E., J. L. Phillips, and J. A. Powell. Dihydropyridine receptor alpha subunits in normal and dysgenic muscle in vitro: expression of alpha 1 is required for proper targeting and distribution of alpha 2. *J. Cell Biol.* 115:1345-1356, (1991).
  20. Beeler, G. W. Jr., and H. Reuter. Membrane calcium current in ventricular myocardial fibres. *J. Physiol.* 207: 191-209, (1970).
  21. Chandler, W. K., R. F. Rakowski, and M. F. Schneider. Effects of glycerol treatment and maintained depolarization on charge movement in skeletal muscle. *J. Physiol.* 254: 285-316, (1976).
  22. Nakai, J., R. T. Dirksen, H. T. Nguyen, I. N. Pessah, K. G. Beam, and P. D. Allen. Enhanced dihydropyridine receptor channel activity in the presence of ryanodine receptor. *Nature* 380: 72-75, (1996).
  23. Nakai, J., N. Sekiguchi, T. A. Rando, P.D. Allen, and K. G. Beam. Two regions of the ryanodine receptor involved in coupling with L-type Ca<sup>2+</sup> channels. *J. Biol. Chem.* 273: 13403-13406, (1998).
  24. Grabner, M., R.T. Dirksen, N. Suda, and K. G. Beam. The II-III loop of the skeletal muscle dihydropyridine receptor is responsible for the bi-directional coupling with the ryanodine receptor. *J. Biol. Chem.* 274: 21913-21919, (1999).
  25. Tanabe, T., A. Mikami, S. Numa, and K. G. Beam. Cardiac-type excitation-contraction coupling in dysgenic skeletal muscle injected with cardiac dihydropyridine receptor cDNA. *Nature* 344: 451-453, (1990).
  26. Nakai, J, T. Ogura, F. Protasi, C. Franzini-Armstrong, P. D, Allen, K. G. Beam. Functional nonequality of the cardiac and skeletal ryanodine receptors. *Proc. Natl. Acad. Sci. U S A* 94: 1019-1022, 1997.
  27. Leong, P., and D. H. MacLennan. A 37-amino acid sequence in the skeletal muscle ryanodine receptor interacts with the cytoplasmic loop between domains II and III in the skeletal muscle dihydropyridine receptor. *J. Biol. Chem.* 273: 7791-7794, (1998).
  28. Slavik, K. J., J. P. Wang, B. Aghdasi, J. Z. Zhang, F. Mandel, N. Malouf, and S. L. Hamilton. A carboxy-terminal peptide of the alpha 1-subunit of the dihydropyridine receptor inhibits Ca<sup>2+</sup>-release channels. *Am. J. Physiol.* 272: 1475-1481, (1997).
  29. Sencer, S., R. V. L. Papineni, D. B. Halling, P. Pate, J. Krol, J. Zhang, and S. L. Hamilton. Coupling of RyR1 and L-type calcium channels via calmodulin binding domains. *J. Biol. Chem.* 276: 38237-38241, (2001).
  30. Rodney, G. G., B. Y. Williams, G. M. Strasburg, K. Beckingham, and S. L. Hamilton. Regulation of RYR1 activity by Ca<sup>2+</sup> and calmodulin. *Biochem.* 39: 7807-7812, (2000).
  31. Rodney, G. G., J. Krol, B. Williams, K. Beckingham, and S. L. Hamilton. The carboxy-terminal calcium binding sites of calmodulin control calmodulin's switch from an activator to an inhibitor of RYR1. *Biochemistry* 40: 12430-12435, (2001).
  32. Zühlke, R. D., G. S. Pitt, K. Deisseroth, R. W. Tsien, and H. Reuter. Calmodulin supports both inactivation and facilitation of L-type calcium channels. *Nature* 399: 159-162, (1999).
  33. Pate, P., J. Mocha-Morales, Y. Wu, J. Zhang, G. G. Rodney, I. I. Serysheva, B. Y. Williams, M. E. Anderson, and S. L. Hamilton. Determinants for calmodulin binding on voltage-dependent Ca<sup>2+</sup> channels. *J. Biol. Chem.* 275: 39786-39792, (2000).
  34. Pitt, G. S., R. D. Zühlke, A. Hudmon, H. Schulman, H. Reuter, and R. W. Tsien. Molecular basis of calmodulin tethering and Ca<sup>2+</sup>-dependent inactivation of L-type Ca<sup>2+</sup> channels. *J. Biol. Chem.* 276: 30794-30802, (2001).
  35. Babu, Y. S., J. S. Sack, T. J. Greenhough, C. E. Bugg, A. R. Means, and W. J. Cook. Three-dimensional structure of calmodulin. *Nature* 315: 37-40, (1985).
  36. Yap, K. I., J. B. Ames, M. B. Swindells, M. Ikura. Diversity of conformational states and changes within the EF-hand protein superfamily. *Proteins* 37: 499-507, (1999).
  37. Hook, S. S., and A. R. Means. Ca<sup>2+</sup>/CaM-dependent kinases: from activation to function. *Annu. Rev. Pharmacol. Toxicol.* 41: 471-505, (2001).
  38. Sugiura, R., S. O. Sio, H. Shuntoh, and T. Kuno. Molecular genetic analysis of the calcineurin signaling pathways. *Cell Mol. Life Sci.* 58: 278-288, (2001).
  39. Masure, H. R., K. A. Alexander, B. T. Wakim, and D. R. Storm. Physicochemical and hydrodynamic characterization of P-57, a neurospecific calmodulin binding protein. *Biochemistry* 25: 7553-7560, (1986).
  40. Rhoads, A. R., and F. Friedberg. Sequence motifs for calmodulin recognition. *FASEB J.* 11: 331-340, (1997).
  41. Tripathy, A., L. Xu, G. Mann, and G. Meissner. Calmodulin activation and inhibition of skeletal muscle Ca<sup>2+</sup> release channel (ryanodine receptor). *Biophys. J.* 69: 106-119, (1995).
  42. Buratti, R., G. Prestipino, P. Menegazzi, S. Treves, and F. Zorzato. Calcium dependent activation of skeletal muscle Ca<sup>2+</sup> release channel (ryanodine receptor) by calmodulin. *Biochem. Biophys. Res. Commun.* 213: 1082-1090, (1995).
  43. Meissner, G., E. Rios, A. Tripathy, and D. A. Pasek. Regulation of skeletal muscle Ca<sup>2+</sup> release channel (ryanodine receptor) by Ca<sup>2+</sup> and monovalent cations and anions. *J. Biol. Chem.* 272: 1628-1638, (1997).
  44. Reid, M. B., Nitric oxide, reactive oxygen species, and skeletal muscle contraction. *Med. Sci. Sports Exerc.* 33: 371-376, 2001.
  45. Zhang, J. Z., Y. Wu, B. Williams, G. Rodney, F. Mandel, G. M. Strasburg, and S. L. Hamilton. Oxidation of the skeletal muscle Ca<sup>2+</sup> release channel alters calmodulin binding. *Am. J. Physiol.* 276: C46-53, (1999).
  46. Aghdasi, B., M. B. Reid, and S. L. Hamilton. Nitric oxide protects the skeletal muscle Ca<sup>2+</sup> release channel from oxidation induced activation. *J. Biol. Chem.* 272: 25462-25467, (1997).
  47. Wu, Y., B. Aghdasi, S. J. Dou, J. Z. Zhang, S. Q. Liu, and S. L. Hamilton. Functional interactions between cytoplasmic domains of the skeletal muscle Ca<sup>2+</sup> release channel. *J. Biol. Chem.* 272: 25051-25061, (1997).
  48. Moore, C. P., Rodney, G., J. Zhang, L. Santacruz-Tolosa, G. Strasburg, and S. L. Hamilton. Apocalmodulin and Ca<sup>2+</sup>Calmodulin bind to the same region on the skeletal muscle Ca<sup>2+</sup> release channel. *Biochem.* 38:8532-8537, (1999).
  49. Meszaros, L. G., I. Minarovic, and A. Zahradnikova. Inhibition of the skeletal muscle ryanodine receptor calcium release channel by nitric oxide. *FEBS Lett.* 380: 49-52, (1996).

50. Stoyanovsky, D., T. Murphy, P. R. Anno, Y. M. Kim, G. Salama. Nitric oxide activates skeletal and cardiac ryanodine receptors. *Cell Calcium* 21: 19-29, (1997).
51. Eu, J. P., J. Sun, L. Xu, J. S. Stamler, and G. Meissner. The skeletal muscle calcium release channel: coupled O<sub>2</sub> sensor and NO signaling functions. *Cell* 102: 499-509, (2000).
52. Seiler, S., A. D. Wegener, D. D. Whang, D. R. Hathaway, and L. R. Jones. High molecular weight proteins in cardiac and skeletal muscle junctional sarcoplasmic reticulum vesicles bind calmodulin, are phosphorylated, and are degraded by Ca<sup>2+</sup>-activated protease. *J. Biol. Chem.* 257: 8550-8557, (1984).
53. Yang, H., M. M. Reedy, C. L. Burke, and G. M. Strasburg. Calmodulin interaction with the skeletal muscle sarcoplasmic reticulum calcium channel protein. *Biochemistry* 33: 518-525, (1994).
54. Yamaguchi, N., C. Xin, and G. Meissner. Identification of Apo- and Ca<sup>2+</sup>-Calmodulin regulatory domain in skeletal muscle. *J. Biol. Chem.* (2001).
55. Zorzato, F., J. Fujii, K. Otsu, M. Phillips, N. M. Green, F. A. Lai, G. Meissner, and D. H. MacLennan. Molecular cloning of cDNA encoding human and rabbit forms of the Ca<sup>2+</sup> release channel (Ryanodine receptor) of skeletal muscle sarcoplasmic reticulum. *J. Biol. Chem.* 265: 2244-2256, (1990).
56. Brandt, N. R., A. H. Caswell, T. Brandt, K. Brew, and R. L. Mellgren. Mapping of the calpain proteolysis products of the junctional foot protein of the skeletal muscle triad junction. *J. Membr. Biol.* 127: 35-47, (1992).
57. Chen, S. R., and D. H. MacLennan. Identification of calmodulin-, Ca<sup>2+</sup>-, and ruthenium red-binding domains in the Ca<sup>2+</sup> release channel (ryanodine receptor) of rabbit skeletal muscle sarcoplasmic reticulum. *J. Biol. Chem.* 269: 22698-22704, (1994).
58. Mengazzi, P., F. Larini, S. Treves, R. Guerrini, M. Quadroni, and F. Zorzato. Identification and characterization of three calmodulin binding sites of the skeletal muscle ryanodine receptor. *Biochem.* 33:9078-9084, (1994).
59. Rodney, G. G., C. P. Moore, B. Y. Williams, J. Z. Zhang, J. Krol, S. E. Pedersen, and S. L. Hamilton. Calcium binding to calmodulin leads to an N-terminal shift in its binding site on the ryanodine receptor. *J. Biol. Chem.* 276:2069-2074, (2001).
60. Moore, C. P., J. Z. Zhang, and S. L. Hamilton. A role for cysteine 3635 of RYR1 in redox modulation and calmodulin binding. *J. Biol. Chem.* 274:36831-36834. (1999).
61. Sun, J., C. Xin, J. P. Eu, J. S. Stamler, and G. Meissner. Cysteine-3635 is responsible for skeletal muscle ryanodine receptor modulation by NO. *Proc. Natl. Acad. Sci U.S.A.* 98: 11158-11162, (2001).
62. Wagenknecht, T., J. Berkowiz, R. Grassucci, A. P. Timerman, and S. Fleischer. Localization of calmodulin binding sites on the ryanodine receptor from skeletal muscle by electron microscopy. *Biophys. J.* 67: 2286-2295, (1994).
63. Samsó, M., and T. Wagenknecht. Apocalmodulin and Ca<sup>2+</sup>-calmodulin bind to neighboring locations on the ryanodine receptor. *J. Biol. Chem.* 277: 1349-1353, (2002).
64. Peterson, B. Z., C. D. DeMaria, J. P. Adelman, and D. T. Yue. Calmodulin is the Ca<sup>2+</sup> sensor for Ca<sup>2+</sup>-dependent inactivation of the L-type calcium channels. *Neuron* 22: 549-558, (1999).
65. Zühlke, R. D., G. S. Pitt, R. W. Tsien, and H. Reuter. Ca<sup>2+</sup>-sensitive inactivation and facilitation of L-type Ca<sup>2+</sup> channels both depend on specific amino acid residues in a consensus calmodulin-binding motif in the  $\alpha_{1C}$  subunit. *J. Biol. Chem.* 275: 21121-21129, (2000).
66. Zühlke, R. D., and H. Reuter. Ca<sup>2+</sup>-sensitive inactivation of L-type Ca<sup>2+</sup> channels depends on multiple cytoplasmic amino acid sequences of the  $\alpha_{1C}$  subunit. *Proc. Natl. Acad. Sci. U S A* 95: 3287-3294, (1998).
67. Romanin, C., R. Gamsjaeger, H. Kahr, D. Schaufler, O. Carlson, D. R. Abernethy, N. M. Soldatov. Ca<sup>2+</sup> sensors of L-type Ca<sup>2+</sup> channel. *FEBS Lett.* 487: 301-306, (2000).
68. Schumacher, M. A., A. F. Rivard, H. P. Bachinger, and J. P. Adelman. Structure of the gating domain of a Ca<sup>2+</sup> activated K<sup>+</sup> channel complexed with Ca<sup>2+</sup>/calmodulin. *Nature* 410: 1120-1124, (2001).

# Regulation of Calcium Release by Interdomain Interaction within Ryanodine Receptors

Noriaki Ikemoto<sup>1, 2</sup> and Takeshi Yamamoto<sup>1</sup>

1: Boston Biomedical Research Institute, Watertown, MA

2: Harvard Medical School, Boston, MA. Email: [ikemoto@bbri.org](mailto:ikemoto@bbri.org)

**ABSTRACT** In excitation-contraction (E-C) coupling, various types of activation signals, which are received presumably at the bulky cytoplasmic domain of the ryanodine receptor (RyR), are translated (or transduced) into the opening of the Ca<sup>2+</sup> release channel located in the trans-membrane domain of the RyR. In order to elucidate the detailed mechanism of the signal transduction process, it is essential (i) to identify various sub-domains of the RyR that are involved in the Ca<sup>2+</sup> channel regulation, (ii) to characterize the events occurring in these sub-domains during the activation process, and (iii) to characterize the modes of active interactions among these sub-domains. Recent developments in the E-C coupling research have provided us with new insight into each of these aspects, as outlined in this review. Of many putative regulatory sub-domains of the RyR, two domains (designated as N-terminal domain and central domain) are particularly interesting, because disease-linked mutations that have occurred in these domains (malignant hyperthermia and central core disease in skeletal muscle, and inheritable cardiac disease) induce abnormal modes of Ca<sup>2+</sup> channel regulation. Pieces of evidence accumulated to this date suggest the following hypothesis. The N-terminal and central domains form, at least partly, the interacting domain pair, and unzipping and zipping actions of such domain-pair are involved in the opening and closing actions of the Ca<sup>2+</sup> channel, respectively. We also propose that there are local conformational changes in the signal reception domains (e.g. the II-III loop-binding core), and such conformational changes are coupled with the aforementioned actions of the interacting domain pair. It seems that by virtue of such a coordination of the events occurring in various regions of the RyR, the Ca<sup>2+</sup> channel can recognize the activation signal received at the cytoplasmic region of the RyR.

## EXCITATION-CONTRACTION COUPLING AND RYANODINE RECEPTORS OF SKELETAL AND CARDIAC MUSCLE

E-C coupling in skeletal muscle and cardiac muscle share some basic features underlying both tissues, and have some tissue-specific characteristics as well (1). The most important basic feature common for skeletal and cardiac muscles is that both types of E-C coupling are mediated by two key components: the dihydropyridine receptor (DHPR) and the ryanodine receptor (RyR)(2-4). The DHPR is a hetero-oligomer consisting of the  $\alpha 1$ ,  $\alpha 2$ ,  $\beta$ ,  $\gamma$ , and  $\delta$  subunits (5). Four units of the DHPR tend to form the electron microscopically visible structure referred as tetrad upon linking the DHPR with the RyR (6, 7). The formation of the tetrad is pronounced in skeletal muscle, but rarely seen in cardiac muscle, because fewer RyRs are linked with the DHPRs. The  $\alpha 1$  subunit performs at least two important functions of the DHPR as a voltage sensor and an L-type Ca<sup>2+</sup> channel (2-4). The RyR shows an electron microscopic structure initially recognized as a junctional foot (8), which actually is an assembly of the four identical ~500 kDa macro-peptide chains (9). Recent cryo-electron microscope/3D imaging studies have resolved intriguing features of the tetrameric complex of both skeletal and cardiac RyR isoforms (10, 11). In skeletal muscle, the voltage-sensing by the  $\alpha 1$  subunit leads to its physical interaction with the RyR to

Both RyR isoforms have a very high affinity for ryanodine (12, 13) and behave like a Ca<sup>2+</sup> channel when incorporated into lipid bilayers (14, 15), indicating that the Ca<sup>2+</sup> channel responsible for SR Ca<sup>2+</sup> release resides in the transmembrane domain of the RyR.

The major differences between the skeletal and cardiac types of E-C coupling are ascribable presumably to the facts that both molecular components of E-C coupling (DHPR and RyR) are expressed by the different tissue-specific genes (16) and that the anatomical arrangements of both components are quite different as described below. In skeletal muscle, practically all DHPR tetrads are physically linked with about 50% of the total population of the RyR tetramers, leaving the remaining 50% of the RyR molecules uncoupled with the DHPR (17, 18). In cardiac muscle, the relative density of the RyR (the ratio of the RyR to the DHPR) is 5-10 fold less than the skeletal muscle (17). Consequently, practically all of the RyR tetramers are structurally uncoupled with the DHPR. The DHPR  $\alpha 1$  subunit serves as a voltage-sensor and an L-type Ca<sup>2+</sup> channel for both skeletal and cardiac E-C coupling as described above, but the mode of the DHPR-mediated regulation of the RyR is quite different between skeletal and cardiac muscle cells. In skeletal muscle, the  $\alpha 1$  subunit activates the SR Ca<sup>2+</sup> release channel, presumably by mediation of one or more cytoplasmic loops of the

DHPR  $\alpha 1$  subunit (19, 20). The above-mentioned DHPR-uncoupled RyRs are activated perhaps by the  $\text{Ca}^{2+}$  that has been released from the neighboring DHPR-coupled RyRs by the so-called  $\text{Ca}^{2+}$ -induced  $\text{Ca}^{2+}$  release mechanism (21). In cardiac muscle, the voltage-sensing immediately opens the DHPR  $\text{Ca}^{2+}$  channel, causing  $\text{Ca}^{2+}$  flux from the extra-cellular space into the cytoplasm, and the entered  $\text{Ca}^{2+}$  activates the RyR by the  $\text{Ca}^{2+}$ -induced  $\text{Ca}^{2+}$  release mechanism. Interestingly, in some cases of skeletal muscle E-C coupling (e.g. invertebrate and neonatal vertebrate skeletal muscles) the  $\text{Ca}^{2+}$  inflow across the plasma membrane is required for the activation of E-C coupling (22) like cardiac E-C coupling.

The skeletal RyR isoform (RyR1) and the cardiac RyR isoform (RyR2) show a  $\sim 60\%$  homology (23, 24). An early analysis (25) identified the three major divergent (non-homologous) regions; the so-called D1, D2 and D3 regions as indicated in Fig. 1. Fig. 1 also shows a heterogeneity map we constructed on the basis of the residue distance score of individual corresponding residues of the two isoforms. As seen, there are several more divergent regions in the RyR. The researchers have correlated the isoform-specific structural characteristics with functional characteristics, and attempted to identify various domains involved in the regulation of the RyR as described below.

## **VARIOUS REGULATORY DOMAINS OF THE RYR**

### **Domains involved in the physical interaction with the DHPR**

As described above, voltage-dependent activation of skeletal muscle-type E-C coupling is mediated by physical interaction between the DHPR and the RyR, presumably by mediation of one of the cytoplasmic loops of the DHPR  $\alpha 1$  subunit called the II-III loop (18, 19, 25). On the other hand,  $\text{Ca}^{2+}$  mediates cardiac E-C coupling as a chemical mediator. Then, which portions of the RyR are involved in such a physical interaction in the case of the RyR1? This important question has been addressed by several groups, yielding rather controversial results. The chimera approach by Nakai *et al.* (27) suggested that the critical region is in a rather long stretch encompassing the residues 1635-2636. On the other hand, the II-III loop affinity column assay by Leong and MacLennan (28) suggested a short 1076-1112 segment. Using deletion strategy, Yamazawa *et al.* (29) identified the residues 1303-1406 region (D2 region) as a critical region for skeletal E-C coupling. Interestingly, according to the recent studies of immuno-localization of anti-D2 antibody in the 3D image, the site of antibody reaction is located in the so-called clamp region, which is regarded as the area for the interaction with the DHPR (30, 31). Thus, the critical regions suggested in the literature are spread in a relatively wide region of the primary structure encompassing residues #1076-2636.

The above fact that the suggested DHPR-binding regions are distributed in a broad region of the RyR polypeptide chain would indicate that the putative DHPR-interaction domain is constructed by a number of small sub-domains derived from different regions of the RyR chain. We recently initiated a new approach to test this hypothesis. Using some of the II-III loop peptides, we localized their binding sites within the RyR primary structure. Using the peptide-mediated and site-directed probe-labeling technique, we could fluorescently label the binding sites of peptide A and peptide C (the peptides corresponding to the Thr<sup>671</sup>-Leu<sup>690</sup> and the Glu<sup>724</sup>-Pro<sup>760</sup> regions of the II-III loop, respectively) on the RyR. The A site and C site are located at the opposite sides of the major calpain cleavage site (residue #1400: interestingly this is right in the D2 region described above) (32, 33). The A and C sites appear to be very close to each other in the quaternary structure (our preliminary data). We tentatively propose that the putative II-III loop binding core of the RyR consists of at least two non-covalently but tightly associated domains flanking the D2 region.

### **Domains involved in the regulation of channel gating**

In the case of skeletal muscle-type E-C coupling, the activation signal received at the signal reception domain (i.e. the II-III loop binding core described above) is recognized by the  $\text{Ca}^{2+}$  channel located at the opposite end of the RyR. There must be a relay switch-like mechanism, in which a number of putative regulatory domains and their intricate interactions are involved. In searching for such regulatory domains, we as other researchers have paid a particular attention to the fact that the sites of RyR1 mutations in the MH and CCD patients are localized in three major areas. As shown in Fig. 1, most mutations are found in either N-terminal region (designated as N-terminal domain) or central region (central domain)(Refs. 34-52). Few mutations were found in the transmembrane  $\text{Ca}^{2+}$  channel domain, presumably in the channel pore region (53, 54). As widely recognized, mutations in either N-terminal or central domain produce abnormal modes of regulation of the RyR  $\text{Ca}^{2+}$  channel, as generally characterized as hyper-activation and hyper-sensitization effects (reviews: 55-57). In the other words, the channel tends to be activated more than the normal channel by the applied activation signal, and the sensitivity of the RyR to the activation signal increases. Thus, it appears that the two domains (the N-terminal domain and the central domain) represent the prime candidates for the regulatory domains involved in the relay switch mechanism described above.

The primary structure of the RyR2 corresponding to both of the skeletal N-terminal and central domains are relatively well conserved (Fig. 1, heterogeneity map). We would propose that the cardiac domains corresponding to these N-terminal and central domains also play a key role for the following reasons. Recently several RyR2 mutations

have been reported related to some inheritable cardiac diseases (58-60). Seven out of total ten mutations shown here are located in either of the predicted N-terminal or central domain of the RyR2 (see red regions, Fig. 1); two out of seven being in the N-terminal domain, and five in the central domain region. Of particular interest is that one of the cardiomyopathy (ARVD2) mutations in the N-terminal domain of the RyR2, Arg176Gln, corresponds exactly to the Arg163Cys human MH mutation of the RyR1. It is also noted that the amino acid residues of the RyR2 corresponding to those of the RyR1 at the potential MH and CCD mutation sites (21 in total) are exactly identical without exception. Thus, it is very likely that the essentially identical sets of regulatory domains are operating for the signal transduction (relay switch) mechanism in both RyR1 and RyR2.

### **Other important regulatory domains**

Both RyR isoforms share some common mechanisms as described above, but their functional properties are differentiated in many aspects. It is worthwhile to correlate the structural divergence with the characteristic functional properties seen in the cardiac RyR. For instance, the D1 region corresponds approximately to the predicted 'modulatory' domain (61) and in fact the putative Ca<sup>2+</sup>-modulatory 4485-4494 segment (PEPEP sequence) is located in the region of the RyR1 corresponding to the D1 region (62). The RyR2 was reported to be more sensitive to the activating concentration of the cytoplasmic Ca<sup>2+</sup>; for instance, the threshold of [Ca<sup>2+</sup>]<sub>cys</sub> for channel opening is about 0.1 μM for the RyR2, while it is about 1.0 μM for the RyR1 (63, 64). According to the recent reports, experimental Glu3987Ala mutation in the RyR2 reduced the Ca<sup>2+</sup>-sensitivity considerably in the mouse RyR2 (65). The effect of the corresponding skeletal mutation, Glu4032Ala, on the Ca<sup>2+</sup>-sensitivity of the RyR1 was not observed in an earlier study (66), but according to the recent study (67) this mutation reduced the Ca<sup>2+</sup>-sensitivity in the RyR1 as well. This would indicate that the residue Glu<sup>3987</sup> is at least a part of the high-affinity Ca<sup>2+</sup>-sensing device of both RyR2 and RyR1.

An interesting suggestion that the highly negatively charged region of the RyR1 at positions 1873-1903 may be involved in the low-affinity Ca<sup>2+</sup>/Mg<sup>2+</sup> binding was made by Laver et al. (68). In agreement with this suggestion, the RyR1 mutant, in which the D3 (Ile<sup>1641</sup>-Ala<sup>2437</sup>) region was deleted, showed a considerably reduced (~10 fold) sensitivity to the inhibitory Ca<sup>2+</sup> or Mg<sup>2+</sup> (69). The considerably reduced sensitivity to the inhibitory Mg<sup>2+</sup> or Ca<sup>2+</sup> is the widely recognized property characteristic for the RyR2. Therefore, the structural difference in the acidic region present in the D3 region (highly acidic in the RyR1 but less acidic in the RyR2) might be the cause for the difference in the sensitivity to the inhibitory Mg<sup>2+</sup> or Ca<sup>2+</sup>. The structural modification in the D3 region could also be the cause for the above-mentioned loss of the DHPR-binding ability in the RyR2 (see section 3.1.).

Both RyR1 and RyR2 have two kinds of tightly associated proteins that are involved in 'external' regulation of the skeletal and cardiac Ca<sup>2+</sup> channels. One is a ubiquitous regulatory protein calmodulin (CaM) and the other is the FK506-binding protein (FKBP). The fact both proteins bind to the RyR with a very high affinity and in a strictly stoichiometrical amount (one mol per one mol of the 550 kDa RyR monomer) has suggested an essential requirement of these proteins for the RyR regulation. This also suggests that the regions of the RyR to which these proteins bind must be considered as the regulatory domains of the RyR.

*Calmodulin (CaM) binding domain:* CaM has interesting Ca<sup>2+</sup>-dependent dual effects on the RyR1, but produces somewhat different effects on the RyR2. Namely, at lower Ca<sup>2+</sup> (< 0.1 μM) CaM activates the RyR1, but it inhibits at higher Ca<sup>2+</sup> (70-72). In the case of the RyR2, CaM produces no effect at lower Ca<sup>2+</sup>, but it inhibits at higher Ca<sup>2+</sup> as in the case of the RyR1 (73). Earlier studies suggested several potential CaM binding regions of the RyR1 (74, 75). According to the more recent information, however, only one of these predicted CaM binding regions, which corresponds to the residue 3614-3642 region (23), seems to play a major role at least for the CaM binding to the RyR1 at higher Ca<sup>2+</sup> (e.g. the 3614-3643 region, Refs. 76, 77). At lower Ca<sup>2+</sup>, CaM binding to the RyR1 takes place to about the same region, although in the strict sense the CaM binding site at low Ca<sup>2+</sup> is somewhat shifted to the C-terminal side of the RyR1 polypeptide chain (77). Also in the case of the RyR2, one of the major predicted (from the overlay assay) CaM binding region corresponds to the region encompassing the residues 3298-3961 (corresponding to the skeletal sequence: 3336-4005) (78). Thus, it appears that both RyR1 and RyR2 share at least one common CaM-binding domain.

*FKBP binding domain:* The potential role of FKBP in the regulation of the RyR has been investigated chiefly by dissociation/reconstitution and knock-out experiments (79-83). Although not generally agreed, several important functions could be assigned to the FKBP. FKBP may stabilize the RyR channel in the closed state. Thus, dissociation of the protein-bound FKBP by FK506 or rapamycin (79-81) or protein kinase A-mediated phosphorylation (in case of the RyR2, Ref. 84) increased the Po and the channel open time (81-84). An important recent finding in this context is that experimental induction of cardiomyopathy by pacing decreased the amount of RyR2-associated FKBP, which in turn caused the leakiness of the Ca<sup>2+</sup> channel (85, 86). FKBP may also be involved in the mediation of coupled gating of the multiple number of neighboring RyRs (83). With regard to the putative FKBP binding domain, the recent report by Gaburjakova et al (87) is particularly interesting. According to this study, mutation of Val<sup>2461</sup> of the RyR1 produced a severe effect on the ability of FKBP to bind to the RyR, suggesting that this region represents the FKBP binding domain. Furthermore, replacement of that Val to Ile, just as

seen in the corresponding amino acid residue of the RyR2, conferred the RyR2-like specific FKBP12.6 binding (88) to the RyR1. The above-mentioned Val<sup>2461</sup> is positioned just adjacent to the Pro<sup>2462</sup> that has previously suggested as a critical residue for FKBP binding (89). It is interesting to point out that this putative FKBP binding domain is located in the C-terminal region of the 'central domain' described in section 3.2. Since we are proposing in the next section (4.) that the tight interaction between the 'N-terminal domain' and the 'central domain' stabilizes the closed state of the channel, it is tempting to speculate that FKBP binding to the RyR may be facilitating the tightening of the intra-molecular domain-domain interaction.

## **POSTULATED INTERDOMAIN INTERACTIONS WITHIN THE RYR**

### **Global conformational change of the RYR**

The classic 'plunger' hypothesis proposed by Schneider and Chandler (90) predicted a global change in the RyR as a mechanism for the Ca<sup>2+</sup> channel opening. As shown in the recent cryo-electron microscope studies, there seem to be appreciable differences in the 3D image between inactive and active states of the RyR (91, 92). Thus, in the activated state, the portion of the cytoplasmic domain (the generally called 'clamp' region) extends towards the T-tubule with conspicuous changes in its configuration (91, 92). Also there is a slight rotation of the channel domain relative to the cytoplasmic domain with concomitant appearance of a pore-like structure in a way reminiscent of the action of opening a camera aperture (91).

No information is available about dynamic changes occurring in the global structure of the RyR, which are presumably occurring during the E-C coupling process. We have been trying to follow rapid local conformational changes occurring in different regions of the RyR. Site-directed incorporation of the fluorescence conformational probe using various RyR-specific ligands as site-directing carriers permitted us to introduce the probe to the designated regions (93). For instance, the probe that had been introduced into the channel domain by mediation of neomycin reported the gating behavior during the activation by T-tubule depolarization and the agonist polylysine (94). As described in the following sections (4.2. and 4.3.), this site-specific conformational probe approach has provided some new insights into the dynamic conformational changes occurring in several regulatory domains during T-tubule depolarization-induced activation process.

### **LOCAL Conformational changes in the II-III LOOP PEPTIDE binding domain**

As described above (27-29), the literature suggests that the RyR domains interacting with the

DHPR II-III loop span over a very broad 1076-2636 region (1561-residue long) of the RyR polypeptide chain. Since the total length of the II-III loop is only about 120-residue long, the putative II-III loop binding domain must be confined in a small area forming the II-III binding core, which presumably consists of multiple numbers of small segments derived from different regions of the RyR polypeptide chain. Unfortunately, only very limited amount of information is available about the structure and function of the putative DHPR-interacting domain. Moreover, there is a considerable amount of controversy in the interpretations about which parts of the DHPR are responsible for the voltage-regulated interaction with the RyR (19, 20, 95-104). However, we would make the tentative proposal described below.

In case of the RyR1, the two kinds of II-III loop peptides, peptide A (Thr<sup>671</sup>-Leu<sup>690</sup>) and peptide C (Phe<sup>725</sup>-Pro<sup>742</sup>), bind to the C-terminal and N-terminal sides of the major calpain cleavage site (at the vicinity of residue 1400), respectively (32, 33). The location of this region corresponds approximately to the IP<sub>3</sub>-binding region of the IP<sub>3</sub> receptor. Furthermore, in the postulated IP<sub>3</sub>-binding core, the critical basic residues for the IP<sub>3</sub> binding are located at both sides of the site, which is highly susceptible to the proteolytic digestion. This shows a striking similarity to the postulated structure of the II-III loop-binding core described above. We hypothesize the II-III binding core will close upon voltage-mediated binding of the DHPR in a similar manner as the closing of the IP<sub>3</sub> binding core upon the ligand binding (cf. ref. 105). Such conformational changes in the II-III binding core would be recognized as the activation signal by the Ca<sup>2+</sup> channels. Our recent observation that the fluorescence conformational probe attached to the II-III loop binding region increased upon T-tubule depolarization (32) is consistent with this idea.

### **Conformational changes in the signal transduction domains**

The physiological activation signal, which is received at the II-III loop binding core of the RyR1, is translated into the opening action of the Ca<sup>2+</sup> channel located at the other side of the RyR. Presumably a number of regulatory domains, including those listed in Section 3, are involved in the signal transduction mechanism, the mechanism by which the signal received is translated into the channel opening action. Recent studies began to reveal how intra-molecular interactions of these domains are involved in the signal transduction mechanism.

According to an earlier study of Zorzato *et al* (106), an antibody raised against the region containing Gly<sup>341</sup> human MH mutation site produced a considerable increase in the rate of Ca<sup>2+</sup>-induced Ca<sup>2+</sup>

release, and shifted the concentration for half-maximal activation (AC<sub>50</sub>) of Ca<sup>2+</sup> from 1.2 to 0.1 μM; the same type of effects as seen in MH (i.e. hyper-

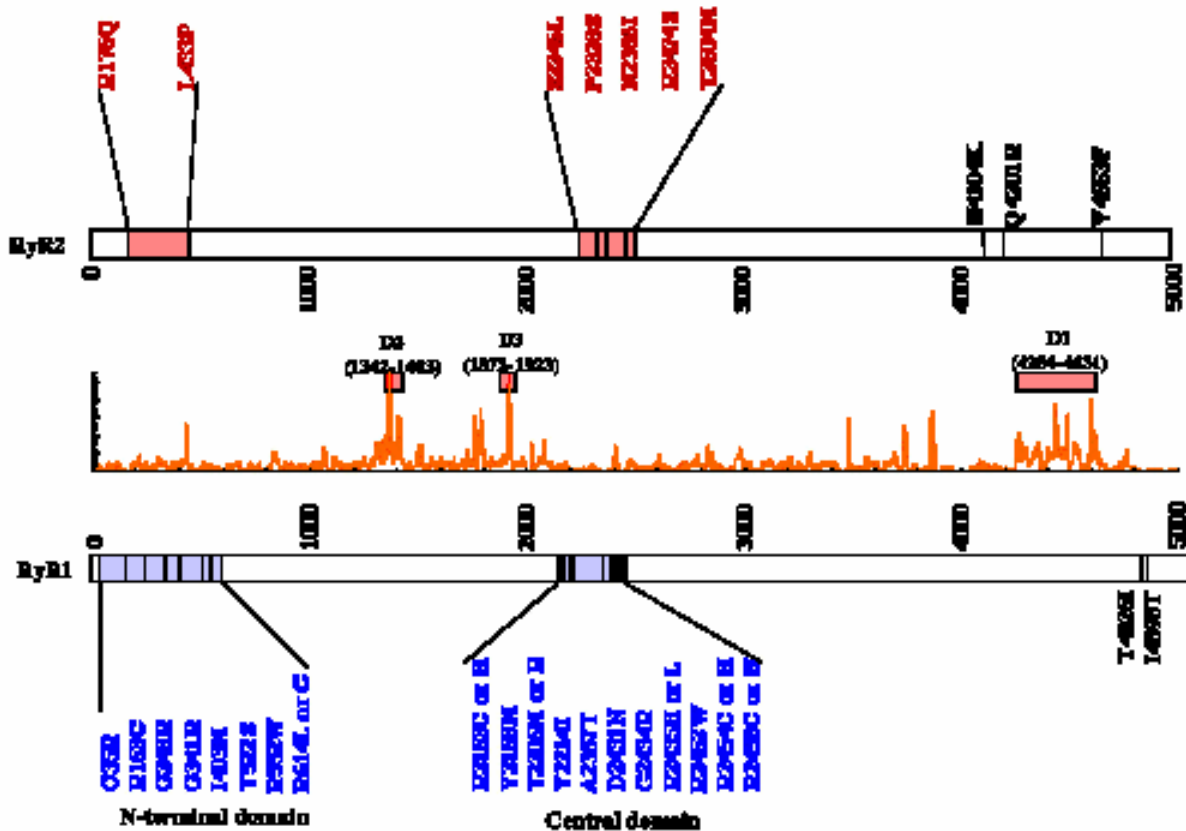


Figure 1. Comparison of the primary structures of the RyR1 and the RyR2 and the locations of MH/CCD mutation sites (RyR1) and cardiac ventricular tachycardia/ myopathy (ARVD) mutation sites (RyR2). Most of the MH/CCD mutations are found either in the regions, which we designate N-terminal domain and central domain, suggesting that these domains are the prime candidates for the putative regulatory or signal transduction domains. Recently reported cardiac mutations are also localized in the regions of the RyR2, which correspond approximately to the N-terminal and central MH/CCD domains of the RyR1. As a reference, the

activation and hyper-sensitization effects). Furthermore, the peptide containing Gly<sup>341</sup> bound to the 3010-3225-residue and the 799-1172-residue regions of the RyR1, suggesting that the N-terminal region interact with central regions of the RyR and that such inter-domain interactions may be involved in the Ca<sup>2+</sup> channel regulation.

Recently we synthesized several peptides corresponding to different regions of the N-terminal and central MH/CCD mutation domains (cf. 3.2.), designated as domain peptides (DP) (100, 107, 108). One of these, DP4, which corresponds to the Leu<sup>2442</sup>-Pro<sup>2477</sup> region containing three potential MH/CCD mutation sites, was found to bind to the N-terminal region of the RyR, as indicated by the DP4-mediated site-specific MCA labeling study (109). Thus, it appears that the two MH/CCD mutation domains, i.e. the N-terminal and central domains, come close to each other, at least partially, in the quaternary structure of the RyR.

As seen in a number of case reports (review: 57), any MH/CCD mutations occurred in either N-terminal or central domain seem to produce more or less identical type of effects on the mode of channel

regulation (namely, an increased response to the RyR-agonist caffeine, Ref. 110), regardless of the position of the mutation site. In this context, it is important to refer to the work of Tong et al (111). They produced mutations corresponding to the 15 human MH/CCD mutations (9 in the N-terminal domain; 6 in the central domain) in a full-length rabbit RyR1 cDNA, and transfected wild-type and mutant cDNAs into HEK-293 cells. Ca<sup>2+</sup> release in the cells expressing MH/CCD mutant RyRs was significantly more sensitive to caffeine than the wild-type for all mutations tested. This indicates that all mutations that occurred in either of these domains have a basically identical contribution to the production of the abnormal mode of channel regulation regardless of the position of mutation sites.

The hypothetical model illustrated in Model 1 provides the simplest and the most straightforward explanation for such situations. In this model we assume that a close contact between the N-terminal domain and the central domain (*zipping*) stabilizes the closed state of the Ca<sup>2+</sup> channel. The activation signal applied to the RyR removes the close contact, which causes *unzipping* of the interacting domain pair

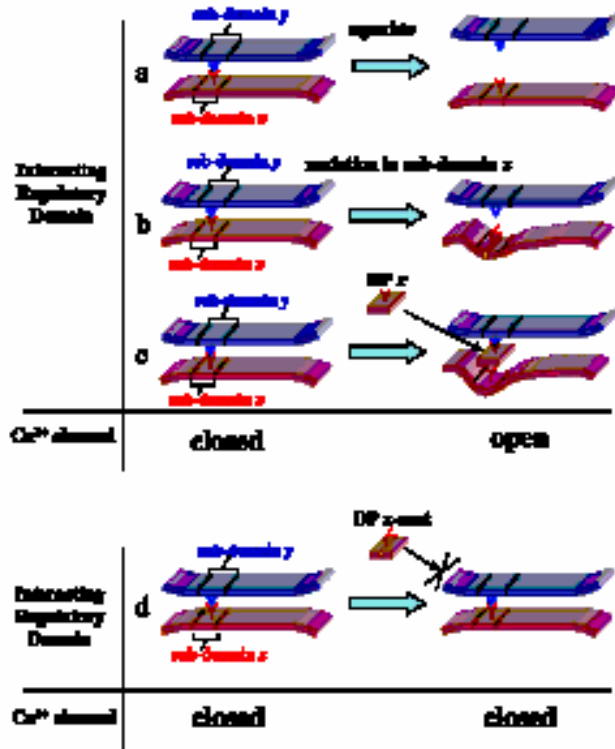
and  $\text{Ca}^{2+}$  channel opening. A mutation that has occurred in either of these interacting domains will weaken the affinity of the inter-domain interaction, resulting in the increased tendency of unzipping and consequently in the hyper-activation/hyper-sensitization effects. Therefore, the degree of unzipping (hence the extent of channel-activation) caused by mutations is more or less the same regardless of the location the mutation has taken place.

The peptide probe study described in the following parts (cf. review 100) has been found to be a very effective way to test the above hypothesis and to investigate the details how the unzipping action causes channel activation. The principle of this approach is illustrated in Model 1. Suppose that sub-domain  $x$  of the central domain is interacting with sub-domain  $y$  of the N-terminal domain, then synthetic or expressed peptide corresponding to the sub-domain  $x$ , i.e. domain peptide  $x$  (DP $x$ ), would bind to the sub-domain  $y$  in competition with sub-domain  $x$ . This will weaken the interaction between sub-domains  $x$  and  $y$ , causing the increased tendency of unzipping and channel activation. An excellent negative control to test the physiological relevance of the observed activation effect of DP $x$  is as follows. Since mutation in sub-domain  $x$  weakens the interaction between sub-domains  $x$  and  $y$ , the same mutation made in DP $x$  (namely DP $x$ -mut) will reduce the affinity of its binding to sub-domain  $y$ , causing the loss of the activating function that would have present in the peptide.

Table 1 depicts the results obtained with one of such domain peptides, DP4, which corresponds to the Leu<sup>2442</sup>-Pro<sup>2477</sup> region of the central domain. Interestingly, DP4 and its mutant DP4-mut (see the sequence diagrams below) function exactly as predicted from the above hypotheses. Thus, DP4 enhanced ryanodine binding, induced  $\text{Ca}^{2+}$  release from the SR, induced contraction in skinned muscle fiber at an inhibitory  $\text{Mg}^{2+}$  concentration (112), increased the frequency of  $\text{Ca}^{2+}$  sparks in saponin-permeabilized fibers (113), and increased the open probability of single channels (Valdivia, in preparation). DP4-mut, in which one mutation was made to mimic the Arg<sup>2458</sup>-to-Cys<sup>2458</sup> MH mutation (see the sequence diagram), produced no appreciable effect on any of these parameters with one exception where its effect could not be determined.

DP4:  
<sup>2442</sup>LIQAGKGEALRIRAILRSLVPLDDLVIISLPLQIP<sup>2477</sup>  
 DP4-mut:  
<sup>2442</sup>LIQAGKGEALRIRAILC<sup>2458</sup>SLVPLDDLVIISLPLQIP<sup>2477</sup>

Consistent with the hypothesis that the two MH/CCD domains (N-terminal and central domains) interact with each other, the central domain peptide DP4 binds to the N-terminal region of the RyR, as evidenced by the fact that the DP4-mediated site-directed probe labeling resulted in an exclusive fluorescence labeling of the ~150 kDa N-terminal



Model 1. Hypothetical model showing how the changes in the mode of interaction between the two major MH/CCD domains (N-terminal domain and central domain) control the state of the  $\text{Ca}^{2+}$  channel of the RyR1. Probably the same or similar mechanism operates for the regulation of cardiac  $\text{Ca}^{2+}$  channel. a. The model assumes that a close contact between the N-terminal domain and the central domain (zippering) stabilizes the closed state of the  $\text{Ca}^{2+}$  channel, and the removal of the close contact (unzipping) de-blocks the channel to open. Such an unzipping action is produced by the activation signal received by the RyR (e.g. T-tubule depolarization). b. MH/CCD mutations in either of the N-terminal or the central domain cause weakening of the interaction between these domains, resulting in the unzipping and channel activation. c. Domain peptide (in this example, the peptide corresponding to sub-domain  $x$  of the central domain; namely domain peptide  $x$  or DP $x$ ) binds to sub-domain  $y$  of the N-terminal domain. As a result of competition between DP $x$  and sub-domain  $x$  for their binding to sub-domain  $y$ , the interaction between sub-domains  $x$  and  $y$  (hence the interaction between the N-terminal and central domains) is weakened. This causes unzipping of the interacting domain pair and activation of the channel. d. MH/CCD-like mutation in DP $x$  abolishes its ability to bind to sub-domain  $y$ , resulting in the loss of the activating function of DP $x$ .

segment of the RyR (109). Furthermore, activation of the RyR caused (a) a rapid decrease in the fluorescence intensity of the MCA probe attached to the N-terminal segment and (b) an increase in the accessibility to a large-size collisional fluorescence quencher (109). Both of these facts are consistent with the proposal that the unzipping of the two interacting domains is the causative mechanism for the  $\text{Ca}^{2+}$  channel activation. In further support of this concept, another domain peptide DP1-2 corresponding to the Leu<sup>590</sup>-Gly<sup>628</sup> portion of the N-

terminal domain activated the RyR and induced SR Ca<sup>2+</sup> release, indicating that both central domain peptide DP4 and N-terminal domain peptide DP1-2 produced essentially identical MH/CCD-like hyper-activation effects (107, 108).

SYSTEM	FUNCTION	DP4	DP4-mut
Triad	Ryanodine binding <sup>(i)</sup>	+	-
	SR Ca <sup>2+</sup> release <sup>(i)</sup>	+	-
	Apparent affinity to agonist <sup>(i)</sup>	+	-
Skinned fiber	Force response to caffeine <sup>(ii)</sup>	+	ND
	Force response to sub-max depolarization <sup>(ii)</sup>	+	ND
Permeabilized fiber	Frequency of Ca <sup>2+</sup> sparks <sup>(iii)</sup>	+	-
Single channel	Po <sup>(iv)</sup>	+	-

(+):increase, (-):no change

Table 1. A central domain peptide DP4 produces MH/CCD-like hyper-activation effects on the RyR Ca<sup>2+</sup> channel as seen in various systems: from a level of the single channel to a level of the whole cell. Single mutation in the peptide abolishes its activating function in all cases, except for the skinned fiber experiment, in which its effect could not be determined (ND) because of the solubility problem

As described in 3.2., many mutations related to the inheritable cardiac myopathies occur in the regions of the RyR2 corresponding to the N-terminal and central MH/CCD domains of the RyR1 (cf. Fig. 1). This suggests that these domains and their inter-domain interactions play an important role also in the cardiac Ca<sup>2+</sup> channel regulation. Consistent with this idea, both central domain peptide DP4 and N-terminal domain peptide DP1-2 activated the RyR2 as they activated the RyR1 (107), suggesting that that the cardiac Ca<sup>2+</sup> channel is controlled by the basically identical mechanism as in the RyR1.

### Coordination of local conformational changes

We now return to the question how the Ca<sup>2+</sup> channel located in the trans-SR membrane region can sense the activating signal received at the T-tubule site of the RyR. As described in section 4.2., upon T-tubule depolarization, the putative E-C coupling activator (presumably located in the DHPR II-III loop) binds to the II-III loop binding core. This induces the change of the configuration of the II-III loop-binding core. Thus, the electric signal elicited in the DHPR is converted to the conformational signal. As described in section 4.3., upon T-tubule depolarization (or upon addition of activating domain peptides), there seems to be local conformational changes in the cytoplasmic domain of the RyR, such as the zipping action of the

interacting N-terminal domain/central domain pair. T-tubule depolarization induces local conformational change also in the trans-SR membrane channel region, as demonstrated by using the fluorescence conformational probe attached to the neomycin (the Ca<sup>2+</sup> channel blocker) binding region (114) of the RyR (94). We propose that all of these events occurring in these domains of the RyR take place in a highly coordinated manner upon the arrival of the activating signal to the signal reception domain. By virtue of this coordination, the conformational changes occurring in the T-tubule side and the SR-membrane side of the RyR can be coupled, permitting the Ca<sup>2+</sup> channel to recognize and respond to the activation signal that has received at the opposite end of the receptor.

### CONCLUSIONS AND PERSPECTIVES

The Ca<sup>2+</sup> release channel is activated by mediation of a global conformational change of the RyR, which presumably consists of consorted local conformational changes occurring in many different places of the RyR. In this review, we dealt chiefly with two mechanisms. First, the activation signal (i.e. the voltage-dependent interaction of the DHPR with the RyR1) seems to be received at the II-III loop binding core consisting of at least two sub-domains of the RyR polypeptide chain flanking the major calpain cleavage site (at residue #1400). This produces a conformational change in the loop binding core (closing of the core), and such a change in the local structure is recognized as the activation signal by the Ca<sup>2+</sup> release channel. Second, the frequent occurrence of both skeletal and cardiac myopathy mutations in the two domains of the RyR, viz. N-terminal and central domains, and the well-known functional outcome of these mutations have permitted us to identify these two domains as the prime domains involved in the Ca<sup>2+</sup> channel regulation. The accumulated evidence suggests that the mode of interaction between these two domains is the important factor that controls the Ca<sup>2+</sup> channel function. Thus, a close contact between these domains, *zipping*, stabilizes the closed state of the channel; while, removal of such a contact, *unzipping*, produces de-blocking, namely the activation, of the Ca<sup>2+</sup> channel. The conformational change occurring in the N-terminal/central domain pair is tightly coupled with the conformational change occurring in the II-III loop-binding core described above. In summary, the voltage-dependent activation signal is translated into the local conformational change in the II-III loop-binding core. Then, this conformational information is transmitted to the Ca<sup>2+</sup> channel by mediation of the coupled conformational change in the N-terminal/central domain pair.

The above mechanism provides a reasonable explanation for the pathogenesis of some RyR-linked muscle diseases. For example, site-mutations taken place in either side of the N-terminal/central domain pair will weaken the inter-domain interaction, resulting in an increased tendency of unzipping. This

seems to be the major cause for the hyper-activation effects seen in the RyR1 of the patients with MH and CCD, and for the leaky Ca<sup>2+</sup> channels seen in the RyR2 of cardiac myopathy patients. The fact that many of the critical cardiac mutation sites are localized in the regions of the RyR2 corresponding to the N-terminal and central domains of the RyR1 suggests that the essentially identical domain-domain interaction-mediated mechanism is operating for the regulation of both RyR1 and RyR2 Ca<sup>2+</sup> channels. This idea may be tested in future studies, by producing the skeletal MH/CCD mutations in the RyR2, or alternatively by producing the cardiac myopathy mutations in the RyR1.

Most of the information described in this review has been derived from the studies with the peptides corresponding to the selected regions of the *in vivo* E-C coupling components. Needless to say, stringent tests (such as the mutation control as described here) must be carried out to verify the relevance of these peptides as a physiologically meaningful probe. Once it is done, these peptides serve as a powerful tool for many purposes; e.g. to localize the sites of peptide binding in the primary structure of the RyR, to introduce the fluorescence conformational probe to the designated sites, to monitor local conformational changes in the designated domains, etc. With the aid of a sufficiently large number of useful peptides and with finer localization of the peptide binding sites within the primary structure of the RyR, it should become possible to construct the intra-molecular or inter-molecular domain-domain interaction map. Upon accumulation of a sufficient amount of information from the *in vitro* studies, some of these key domain peptides can be tested for their effects in the *in vivo* system, as done with DP4. It would also be worthwhile to apply the domain peptide-mediated site-specific fluorescence labeling technique developed from the *in vitro* work to introduce the conformational probe to the designated domain of the RyR *in situ* and monitor the local events occurring during E-C coupling *in vivo*.

#### ACKNOWLEDGEMENTS

The authors thank Drs. Graham Lamb, Martin F. Schneider and Hector H. Valdivia for the collaboration in the studies of DP4 and its mutant and for their comments on the manuscript. This work was supported by National Institutes of Health Grant AR16922.

#### References

1. Lamb, G. D.: Excitation-contraction coupling in skeletal muscle: comparisons with cardiac muscle. *Clin Exp Pharmacol Physiol* 27, 216-224 (2000)
2. Rios, E. & G. Pizarro: Voltage sensor of excitation-contraction coupling in skeletal muscle. *Physiol Rev* 71, 849-908 (1991)
3. Schneider, M. F.: Control of calcium release in functioning skeletal muscle fibers. *Annu Rev Physiol* 56, 463-484 (1994)
4. Melzer, W., A. Herrmann-Frank & H. C. Luttgau: The role of Ca<sup>2+</sup> ions in excitation-contraction coupling of

- skeletal muscle fibres. *Biochim Biophys Acta* 1241, 59-116 (1995)
5. Catterall, W. A.: Structure and function of voltage-sensitive ion channels. *Science* 242, 50-61 (1988)
6. Franzini-Armstrong, C. & G. Nunzi: Junctional feet and particles in the triads of a fast-twitch muscle fibre. *J Muscle Res Cell Motil* 4, 233-252 (1983)
7. Block, B. A., T. Imagawa, K. P. Campbell & C. Franzini-Armstrong: Structural evidence for direct interaction between the molecular components of the transverse tubule/sarcoplasmic reticulum junction in skeletal muscle. *J Cell Biol* 107, 2587-2600 (1988)
8. Franzini-Armstrong, C.: Studies of the triad I. Structure of the junction in frog twitch fibers. *J Cell Biol* 47, 488-499 (1970)
9. Wagenknecht, T., R. Grassucci, J. Frank, A. Saito, M. Inui & S. Fleischer: Three dimensional architecture of the calcium channel/foot structure of sarcoplasmic reticulum. *Nature* 338, 167-170 (1989)
10. Radermacher, M., V. Rao, R. Grassucci, J. Frank, A. P. Timerman, S. Fleischer & T. Wagenknecht: Cryo-electron microscopy and three-dimensional reconstruction of the calcium release channel/ryanodine receptor from skeletal muscle. *J Cell Biol* 127, 411-423 (1994)
11. Sharma, M. R., P. Penczek, R. Grassucci, H. B. Xin, S. Fleischer & T. Wagenknecht: Cryoelectron microscopy and image analysis of the cardiac ryanodine receptor. *J Biol Chem* 273, 18429-18434 (1998)
12. Coronado, R., J. Morrisette, M. Sukhareva & D. M. Vaughan: Structure and function of ryanodine receptors. *Am J Physiol* 266, C1485-C1504 (1994)
13. Lai, F. A., H. P. Erickson, E. Rousseau, Q. Y. Liu & G. Meissner: Purification and reconstitution of the calcium release channel from skeletal muscle. *Nature* 331, 315-319 (1988)
14. Coronado, R., S. Kawano, C. J. Lee, C. Valdivia & H. H. Valdivia: Planar bilayer recording of ryanodine receptors of sarcoplasmic reticulum. *Methods Enzymol* 207, 699-707 (1992)
15. Meissner, G., E. Rousseau, F. A. Lai, Q. Y. Liu & K. A. Anderson: Biochemical characterization of the Ca<sup>2+</sup> release channel of skeletal and cardiac sarcoplasmic reticulum. *Mol Cell Biochem* 82, 59-65 (1988)
16. Giannini, G. & V. Sorrentino: Molecular structure and tissue distribution of ryanodine receptors calcium channels. *Med Res Rev* 15, 313-323 (1995)
17. Bers, D. M. & V. M. Stiffel: Ratio of ryanodine to dihydropyridine receptors in cardiac and skeletal muscle and implications for E-C coupling. *Am J Physiol* 264, C1587-C1593 (1993)
18. Franzini-Armstrong, C. & A. O. Jorgensen: Structure and development of E-C coupling units in skeletal muscle. *Annu Rev Physiol* 56, 509-534 (1994)
19. Tanabe, T., K. G. Beam, J. A. Powell & S. Numa: Restoration of excitation-contraction coupling and slow calcium current in dysgenic muscle by dihydropyridine receptor complementary DNA. *Nature* 336, 134-139 (1988)
20. Tanabe, T., K. G. Beam, B. A. Adams, T. Niidome & S. Numa: Regions of the skeletal muscle dihydropyridine receptor critical for excitation-contraction coupling. *Nature* 346, 567-569 (1990)
21. Endo, M., M. Tanaka & Y. Ogawa: Calcium induced release of calcium from the sarcoplasmic reticulum of skinned skeletal muscle fibres. *Nature* 228, 34-36 (1970)
22. Dangain, J. & I. R. Neering: Effect of low extracellular calcium and ryanodine on muscle contraction of the mouse during postnatal development. *Can J Physiol Pharmacol* 69, 1294-1300 (1991)
23. Takeshima, H., S. Nishimura, T. Matsumoto, H. Ishida, K. Kangawa, N. Minamino, H. Matsuo, M. Ueda, M. Hanaoka, T. Hirose & S. Numa: Primary structure and expression from complementary DNA of skeletal muscle ryanodine receptor. *Nature* 339, 439-445 (1989)

24. Nakai, J., T. Imagawa, Y. Hakamata, M. Shigekawa, H. Takeshima & S. Numa: Primary structure and functional expression from cDNA of the cardiac ryanodine receptor/calcium release channel. *FEBS Lett* 271, 1-2 (1990)
25. Sorrentino, V. & P. Volpe: Ryanodine receptors: how many, where and why? *Trends Pharmacol Sci* 14, 98-103 (1993)
26. Lu, X., L. Xu & G. Meissner: Activation of the skeletal muscle calcium release channel by a cytoplasmic loop of the dihydropyridine receptor. *J Biol Chem* 269, 6511-6516 (1994)
27. Nakai, J., N. Sekiguchi, T. A. Rando, P. D. Allen & K. G. Beam: Two regions of the ryanodine receptor involved in coupling with L-type Ca<sup>2+</sup> channels. *J Biol Chem* 273, 13403-13406 (1998)
28. Leong, P. & D. H. MacLennan: The cytoplasmic loops between domains II and III and domains III and IV in the skeletal muscle dihydropyridine receptor bind to a contiguous site in the skeletal muscle ryanodine receptor. *J Biol Chem* 273, 29958-29964 (1998)
29. Yamazawa, T., H. Takeshima, M. Shimuta & M. Iino: A region of the ryanodine receptor critical for excitation-contraction coupling in skeletal muscle. *J Biol Chem* 272, 8161-8164 (1997)
30. Murayama, T., T. Oba, E. Katayama, H. Oyamada, K. Oguchi, M. Kobayashi, K. Otsuka & Y. Ogawa: Further characterization of the type 3 ryanodine receptor (RyR3) purified from rabbit diaphragm. *J Biol Chem* 274, 17297-17308 (1999)
31. Trujillo, R., B. L. Benacquista, J. Berkowitz, M. R. Sharma, M. Samsó, F. Zorzato, S. Treves, & T. Wagenknecht: Localization of epitopes on the skeletal ryanodine receptor (RyR) by 3D cryo-immuno-electron microscopy. *Biophys J* 80, 426a (2001)
32. Yamamoto, T. & N. Ikemoto: T-tubule depolarization-induced local events in the ryanodine receptor, as monitored with the fluorescent conformational probe incorporated by mediation of peptide A. *J Biol Chem* in press
33. Yamamoto, T., J. Rodriguez & N. Ikemoto: Ca<sup>2+</sup>-dependent dual functions of peptide C: The peptide corresponding to the Glu724-Pro760 region (the so-called determinant of E-C coupling) of the dihydropyridine receptor  $\alpha$ I subunit II-III loop. *J Biol Chem* in press
34. Barone, V., O. Massa, E. Intravaia, A. Bracco, A. Di Martino, V. Tegazzin, S. Cozzolino & V. Sorrentino: Mutation screening of the RYR1 gene and identification of two novel mutations in Italian malignant hyperthermia families. *J Med Genet* 36, 115-118 (1999)
35. Brandt, A., L. Schleithoff, K. Jurkat-Rott, W. Klingler, C. Baur & F. Lehmann-Horn: Screening of the ryanodine receptor gene in 105 malignant hyperthermia families: novel mutations and concordance with the in vitro contracture test. *Hum Mol Genet* 8, 2055-2062 (1999)
36. Chamley, D., N. A. Pollock, K. M. Stowell & R. L. Brown: Malignant hyperthermia in infancy and identification of novel RYR1 mutation. *Br J Anaesth* 84, 500-504 (2000)
37. Fortunato, G., R. Berruti, V. Brancadoro, M. Fattore, F. Salvatore & A. Carsana: Identification of a novel mutation in the ryanodine receptor gene (RYR1) in a malignant hyperthermia Italian family. *Eur J Hum Genet* 8, 149-152 (2000)
38. Gencik, M., A. Gencik, W. Mortier & J. T. Eppelen: Novel mutation in the RYR1 gene (R2454C) in a patient with malignant hyperthermia. *Hum Mutat (Online)* 15, 122. (2000)
39. Gillard, E. F., K. Otsu, J. Fujii, V. K. Khanna, S. de Leon, J. Derdemezi, B. A. Britt, C. L. Duff, R. G. Worton & D. H. MacLennan: A substitution of cysteine for arginine 614 in the ryanodine receptor is potentially causative of human malignant hyperthermia. *Genomics* 11, 751-755 (1991)
40. Gillard, E. F., K. Otsu, J. Fujii, C. Duff, S. de Leon, V. K. Khanna, B. A. Britt, R. G. Worton & D. H. MacLennan: Polymorphisms and deduced amino acid substitutions in the coding sequence of the ryanodine receptor (RYR1) gene in individuals with malignant hyperthermia. *Genomics* 13, 1247-1254 (1992)
41. Keating, K. E., K. A. Quane, B. M. Manning, M. Lehane, E. Hartung, K. Censier, A. Urwyler, M. Klausnitzer, C. R. Muller, J. J. Heffron & T. V. McCarthy: Detection of a novel RYR1 mutation in four malignant hyperthermia pedigrees. *Hum Mol Genet* 3, 1855-1858 (1994)
42. Keating, K. E., L. Giblin, P. J. Lynch, K. A. Quane, M. Lehane, J. J. Heffron & T. V. McCarthy: Detection of a novel mutation in the ryanodine receptor gene in an Irish malignant hyperthermia pedigree: correlation of the IVCT response with the affected and unaffected haplotypes. *J Med Genet* 34, 291-296 (1997)
43. Lynch, P. J., R. Krivosic-Horber, H. Reyford, N. Monnier, K. Quane, P. Adnet, G. Haudecoeur, I. Krivosic, T. McCarthy & J. Lunardi: Identification of heterozygous and homozygous individuals with the novel RYR1 mutation Cys35Arg in a large kindred [see comments]. *Anesthesiology* 86, 620-626 (1997)
44. Manning, B. M., K. A. Quane, H. Ordling, A. Urwyler, V. Tegazzin, M. Lehane, J. O'Halloran, E. Hartung, L. M. Giblin, P. J. Lynch, P. Vaughan, K. Censier, D. Bendixen, G. Comi, L. Heytens, K. Monsieurs, T. Fagerlund, W. Wolz, J. J. Heffron, C. R. Muller & T. V. McCarthy: Identification of novel mutations in the ryanodine-receptor gene (RYR1) in malignant hyperthermia: genotype-phenotype correlation. *Am J Hum Genet* 62, 599-609 (1998)
45. Manning, B. M., K. A. Quane, P. J. Lynch, A. Urwyler, V. Tegazzin, R. Krivosic-Horber, K. Censier, G. Comi, P. Adnet, W. Wolz, J. Lunardi, C. R. Muller & T. V. McCarthy: Novel mutations at a CpG dinucleotide in the ryanodine receptor in malignant hyperthermia. *Hum Mutat* 11, 45-50 (1998)
46. Phillips, M. S., V. K. Khanna, S. De Leon, W. Frodis, B. A. Britt & D. H. MacLennan: The substitution of Arg for Gly2433 in the human skeletal muscle ryanodine receptor is associated with malignant hyperthermia. *Hum Mol Genet* 3, 2181-2186 (1994)
47. Quane, K. A., J. M. Healy, K. E. Keating, B. M. Manning, F. J. Couch, L. M. Palmucci, C. Doriguzzi, T. H. Fagerlund, K. Berg, H. Ordling, D. Bendixen, W. Mortier, U. Linz, C. R. Muller & T.V. McCarthy: Mutations in the ryanodine receptor gene in central core disease and malignant hyperthermia. *Nat Genet* 5, 51-55 (1993)
48. Quane, K. A., K. E. Keating, B. M. Manning, J. M. Healy, K. Monsieurs, J. J. Heffron, M. Lehane, L. Heytens, R. Krivosic-Horber, P. Adnet, F. R. Ellis, N. Monnier, J. Lunardi & T.V. McCarthy: Detection of a novel common mutation in the ryanodine receptor gene in malignant hyperthermia: implications for diagnosis and heterogeneity studies. *Hum Mol Genet* 3, 471-476 (1994)
49. Quane, K. A., K. E. Keating, J. M. Healy, B. M. Manning, R. Krivosic-Horber, I. Krivosic, N. Monnier, J. Lunardi & T. V. McCarthy: Mutation screening of the RYR1 gene in malignant hyperthermia: detection of a novel Tyr to Ser mutation in a pedigree with associated central cores. *Genomics* 23, 236-239 (1994)
50. Quane, K. A., H. Ordling, K. E. Keating, B. M. Manning, R. Heine, D. Bendixen, K. Berg, R. Krivosic-Horber, F. Lehmann-Horn, T. Fagerlund & T. V. McCarthy: Detection of a novel mutation at amino acid position 614 in the ryanodine receptor in malignant hyperthermia. *Br J Anaesth* 79, 332-337 (1997)
51. Sambuughin, N., Y. Sei, K. L. Gallagher, H. W. Wyre, D. Madsen, T. E. Nelson, J. E. Fletcher, H. Rosenberg & S. M. Muldoon: North American malignant hyperthermia population: screening of the ryanodine receptor gene

- and identification of novel mutations. *Anesthesiology* 95, 594-599 (2001)
52. Zhang, Y., H. S. Chen, V. K. Khanna, S. De Leon, M. S. Phillips, K. Schappert, B. A. Britt, A. K. Browell & D. H. MacLennan: A mutation in the human ryanodine receptor gene associated with central core disease. *Nat Genet* 5, 46-50 (1993)
  53. Brown, R. L., A. N. Pollock, K. G. Couchman, M. Hodges, D. O. Hutchinson, R. Waaka, P. Lynch, T. V. McCarthy & K. M. Stowell: A novel ryanodine receptor mutation and genotype-phenotype correlation in a large malignant hyperthermia New Zealand Maori pedigree. *Hum Mol Genet* 9, 1515-1524 (2000)
  54. Lynch, P. J., J. Tong, M. Lehane, A. Mallet, L. Giblin, J. J. Heffron, P. Vaughan, G. Zafra, D. H. MacLennan & T. V. McCarthy: A mutation in the transmembrane/luminal domain of the ryanodine receptor is associated with abnormal Ca<sup>2+</sup> release channel function and severe central core disease. *Proc Natl Acad Sci USA* 96, 4164-4169 (1999)
  55. Mickelson, J. R. & C. F. Louis: Malignant hyperthermia: excitation-contraction coupling, Ca<sup>2+</sup> release channel, and cell Ca<sup>2+</sup> regulation defects. *Physiol Rev* 76, 537-592 (1996)
  56. Loke, J. & D. H. MacLennan: Malignant hyperthermia and central core disease: disorders of Ca<sup>2+</sup> release channels. *Am J Med* 104, 470-486 (1998)
  57. Jurkat-Rott, K., T. McCarthy & F. Lehmann-Horn: Genetics and pathogenesis of malignant hyperthermia. *Muscle Nerve* 23, 4-17 (2000)
  58. Laitinen, P. J., K. M. Brown, K. Piippo, H. Swan, J. M. Devaney, B. Brahmhatt, E. A. Donarum, M. Marino, N. Tiso, M. Viitasalo, L. Toivonen, D. A. Stephan & K. Kontula: Mutations of the cardiac ryanodine receptor (RyR2) gene in familial polymorphic ventricular tachycardia. *Circulation* 103, 485-490 (2001)
  59. Tiso, N., D. A. Stephan, A. Nava, A. Bagattin, J. M. Devaney, F. Stanchi, G. Larderet, B. Brahmhatt, K. Brown, B. Baucce, M. Muriago, C. Basso, G. Thiene, G. A. Danieli & A. Rampazzo: Identification of mutations in the cardiac ryanodine receptor gene in families affected with arrhythmogenic right ventricular cardiomyopathy type 2 (ARVD2). *Hum Mol Genet* 10, 189-194 (2001)
  60. Priori, S. G., C. Napolitano, N. Tiso, M. Memmi, G. Vignati, R. Bloise, V. V. Sorrentino & G. A. Danieli: Mutations in the Cardiac Ryanodine Receptor Gene (hRyR2) Underlie Catecholaminergic Polymorphic Ventricular Tachycardia. *Circulation* 103, 196-200 (2001)
  61. Du, G. G., V. K. Khanna & D. H. MacLennan: Mutation of divergent region 1 alters caffeine and Ca<sup>2+</sup> sensitivity of the skeletal muscle Ca<sup>2+</sup> release channel (ryanodine receptor). *J Biol Chem* 275, 11778-11783 (2000)
  62. Chen, S. R., L. Zhang & D. H. MacLennan: Antibodies as probes for Ca<sup>2+</sup> activation sites in the Ca<sup>2+</sup> release channel (ryanodine receptor) of rabbit skeletal muscle sarcoplasmic reticulum. *J Biol Chem* 268, 13414-13421 (1993)
  63. Ashley, R. H. & A. J. Williams: Divalent cation activation and inhibition of single calcium release channels from sheep cardiac sarcoplasmic reticulum. *J Gen Physiol* 95, 981-1005 (1990)
  64. Smith, J. S., R. Coronado & G. Meissner: Single channel measurements of the calcium release channel from skeletal muscle sarcoplasmic reticulum. Activation by Ca<sup>2+</sup> and ATP and modulation by Mg<sup>2+</sup>. *J Gen Physiol* 88, 573-588 (1986)
  65. Li, P. & S. R. Chen: Molecular basis of Ca<sup>2+</sup> activation of the mouse cardiac Ca<sup>2+</sup> release channel (ryanodine receptor). *J Gen Physiol* 118, 33-44. (2001)
  66. Du, G. G. & D. H. MacLennan: Functional consequences of mutations of conserved, polar amino acids in transmembrane sequences of the Ca<sup>2+</sup> release channel (ryanodine receptor) of rabbit skeletal muscle sarcoplasmic reticulum. *J Biol Chem* 273, 31867-31872 (1998)
  67. Fessenden, J. D., L. Chen, Y. Wang, C. Paolini, C. Franzini-Armstrong, P. D. Allen & I. N. Pessah: Ryanodine receptor point mutant E4032A reveals an allosteric interaction with ryanodine. *Proc Natl Acad Sci U S A* 98, 2865-2870 (2001)
  68. Laver, D. R., V. J. Owen, P. R. Junankar, N. L. Taske, A. F. Dulhunty & G. D. Lamb: Reduced inhibitory effect of Mg<sup>2+</sup> on ryanodine receptor-Ca<sup>2+</sup> release channels in malignant hyperthermia. *Biophys J* 73, 1913-1924 (1997)
  69. Bhat, M. B., J. Zhao, S. Hayek, E. C. Freeman, H. Takeshima & J. Ma: Deletion of amino acids 1641-2437 from the foot region of skeletal muscle ryanodine receptor alters the conduction properties of the Ca release channel. *Biophys J* 73, 1320-1328 (1997)
  70. Tripathy, A., L. Xu, G. Mann & G. Meissner: Calmodulin activation and inhibition of skeletal muscle Ca<sup>2+</sup> release channel (ryanodine receptor). *Biophys J* 69, 106-119 (1995)
  71. Rodney, G. G., B. Y. Williams, G. M. Strasburg, K. Beckingham & S. L. Hamilton: Regulation of RYR1 activity by Ca<sup>2+</sup> and calmodulin. *Biochemistry* 39, 7807-7812 (2000)
  72. Moore, C. P., G. Rodney, J. Z. Zhang, L. Santacruz-Tolosa, G. Strasburg & S. L. Hamilton: Apocalmodulin and Ca<sup>2+</sup> calmodulin bind to the same region on the skeletal muscle Ca<sup>2+</sup> release channel. *Biochemistry* 38, 8532-8537 (1999)
  73. Fruen, B. R., J. M. Bardy, T. M. Byrem, G. M. Strasburg & C. F. Louis: Differential Ca<sup>2+</sup> sensitivity of skeletal and cardiac muscle ryanodine receptors in the presence of calmodulin. *Am J Physiol Cell Physiol* 279, C724-C733 (2000)
  74. Menegazzi, P., F. Larini, S. Treves, R. Guerrini, M. Quadroni & F. Zorzato: Identification and characterization of three calmodulin binding sites of the skeletal muscle ryanodine receptor. *Biochemistry* 33, 9078-9084 (1994)
  75. Chen, S. R. & D. H. MacLennan: Identification of calmodulin-, Ca<sup>2+</sup>-, and ruthenium red-binding domains in the Ca<sup>2+</sup> release channel (ryanodine receptor) of rabbit skeletal muscle sarcoplasmic reticulum. *J Biol Chem* 269, 22698-22704 (1994)
  76. Yamaguchi, N., C. Xin & G. Meissner: Identification of apocalmodulin and Ca<sup>2+</sup>-calmodulin regulatory domain in skeletal muscle Ca<sup>2+</sup> release channel, ryanodine receptor. *J Biol Chem* 276, 22579-22585 (2001)
  77. Rodney, G. G., C. P. Moore, B. Y. Williams, J. Z. Zhang, J. Krol, S. E. Pedersen & S. L. Hamilton: Calcium binding to calmodulin leads to an N-terminal shift in its binding site on the ryanodine Receptor. *J Biol Chem* 276, 2069-2074 (2001)
  78. Balshaw, D. M., L. Xu, N. Yamaguchi, D. A. Pasek & G. Meissner: Calmodulin binding and inhibition of cardiac muscle calcium release channel (ryanodine receptor). *J Biol Chem* 276, 20144-20153 (2001)
  79. Timerman, A. P., H. Onoue, H. B. Xin, S. Barg, J. Copello, G. Wiederrecht & S. Fleischer: Selective binding of FKBP12.6 by the cardiac ryanodine receptor. *J Biol Chem* 271, 20385-20391 (1996)
  80. Barg, S., J. A. Copello & S. Fleischer: Different interactions of cardiac and skeletal muscle ryanodine receptors with FK-506 binding protein isoforms. *Am J Physiol* 272, C1726-C1733 (1997)
  81. Xiao, R. P., H. H. Valdivia, K. Bogdanov, C. Valdivia, E. G. Lakatta & H. Cheng: The immunophilin FK506-binding protein modulates Ca<sup>2+</sup> release channel closure in rat heart. *J Physiol* 500, 343-354 (1997)
  82. Shou, W., B. Aghdasi, D. L. Armstrong, Q. Guo, S. Bao, M. J. Charng, L. M. Mathews, M. D. Schneider, S. L. Hamilton & M. M. Matzuk: Cardiac defects and altered ryanodine receptor function in mice lacking FKBP12. *Nature* 391, 489-492 (1998)

83. Marx, S. O., K. Ondrias & A. R. Marks: Coupled gating between individual skeletal muscle Ca<sup>2+</sup> release channels (ryanodine receptors). *Science* 281, 818-821 (1998)
84. Marx, S. O., S. Reiken, Y. Hisamatsu, T. Jayaraman, D. Burkhoff, N. Rosembliit & A. R. Marks: PKA phosphorylation dissociates FKBP12.6 from the calcium release channel (ryanodine receptor): defective regulation in failing hearts. *Cell* 101, 365-376 (2000)
85. Yamamoto, T., M. Yano, M. Kohno, T. Hisaoka, K. Ono, T. Tanigawa, Y. Saiki, Y. Hisamatsu, T. Ohkusa & M. Matsuzaki: Abnormal Ca<sup>2+</sup> release from cardiac sarcoplasmic reticulum in tachycardia-induced heart failure. *Cardiovasc Res* 44, 146-155 (1999)
86. Yano, M., K. Ono, T. Ohkusa, M. Suetsugu, M. Kohno, T. Hisaoka, S. Kobayashi, Y. Hisamatsu, T. Yamamoto, N. Noguchi, S. Takasawa, H. Okamoto & M. Matsuzaki: Altered stoichiometry of FKBP12.6 versus ryanodine receptor as a cause of abnormal Ca<sup>2+</sup> leak through ryanodine receptor in heart failure. *Circulation* 102, 2131-2136 (2000)
87. Gaburjakova, M., J. Gaburjakova, S. Reiken, F. Huang, S. O. Marx, N. Rosembliit & A. R. Marks: FKBP12 binding modulates ryanodine receptor channel gating. *J Biol Chem* 276, 16931-16935 (2001)
88. Valdivia, H. H.: Cardiac ryanodine receptors and accessory proteins: augmented expression does not necessarily mean big function. *Circ Res* 88, 134-136 (2001)
89. Cameron, A. M., F. C. Nucifora, Jr., E. T. Fung, D. J. Livingston, R. A. Aldape, C. A. Ross & S. H. Snyder: FKBP12 binds the inositol 1,4,5-trisphosphate receptor at leucine-proline (1400-1401) and anchors calcineurin to this FK506-like domain. *J Biol Chem* 272, 27582-27588. (1997)
90. Schneider, M. F. & W. K. Chandler: Voltage dependent charge movement of skeletal muscle: a possible step in excitation-contraction coupling. *Nature* 242, 244-246 (1973)
91. Serysheva, II, M. Schatz, M. van Heel, W. Chiu & S. L. Hamilton: Structure of the skeletal muscle calcium release channel activated with Ca<sup>2+</sup> and AMP-PCP. *Biophys J* 77, 1936-1944 (1999)
92. Stokes, D. L. & T. Wagenknecht: Calcium transport across the sarcoplasmic reticulum: structure and function of Ca<sup>2+</sup>-ATPase and the ryanodine receptor. *Eur J Biochem* 267, 5274-5279. (2000)
93. Kang, J. J., A. Tarcsafalvi, A. D. Carlos, E. Fujimoto, Z. Shahrokh, B. J. Thevenin, S. B. Shohet & N. Ikemoto: Conformational changes in the foot protein of the sarcoplasmic reticulum assessed by site-directed fluorescent labeling. *Biochemistry* 31, 3288-3293 (1992)
94. Yano, M., R. El-Hayek & N. Ikemoto: Conformational changes in the junctional foot protein/Ca<sup>2+</sup> release channel mediate depolarization-induced Ca<sup>2+</sup> release from sarcoplasmic reticulum. *J Biol Chem* 270, 3017-3021 (1995)
95. El-Hayek, R., B. Antoniu, J. Wang, S. L. Hamilton & N. Ikemoto: Identification of calcium release-triggering and blocking regions of the II-III loop of the skeletal muscle dihydropyridine receptor. *J Biol Chem* 270, 22116-22118 (1995)
96. El-Hayek, R. & N. Ikemoto: Identification of the minimum essential region in the II-III loop of the dihydropyridine receptor alpha 1 subunit required for activation of skeletal muscle-type excitation-contraction coupling. *Biochemistry* 37, 7015-7020 (1998)
97. Nakai, J., T. Tanabe, T. Konno, B. Adams & K. G. Beam: Localization in the II-III loop of the dihydropyridine receptor of a sequence critical for excitation-contraction coupling. *J Biol Chem* 273, 24983-24986 (1998)
98. Dulhunty, A. F., D. R. Laver, E. M. Gallant, M. G. Casarotto, S. M. Pace & S. Curtis: Activation and inhibition of skeletal RyR channels by a part of the skeletal DHPR II-III loop: effects of DHPR Ser687 and FKBP12. *Biophys J* 77, 189-203 (1999)
99. Grabner, M., R. T. Dirksen, N. Suda & K. G. Beam: The II-III loop of the skeletal muscle dihydropyridine receptor is responsible for the Bi-directional coupling with the ryanodine receptor. *J Biol Chem* 274, 21913-21919 (1999)
100. Ikemoto, N. & T. Yamamoto: Postulated role of inter-domain interaction within the ryanodine receptor in Ca<sup>2+</sup> channel regulation. *Trends Cardiovasc Med* 10, 310-316 (2000)
101. Proenza, C., C. M. Wilkens & K. G. Beam: Excitation-Contraction Coupling Is Not Affected By Scrambled Sequence In Residues 681-690 Of The Dihydropyridine Receptor II-III Loop. *J Biol Chem* 275, 29935-29937 (2000)
102. Wilkens, C. M., N. Kasielke, B. E. Flucher, K. G. Beam & M. Grabner: Excitation-contraction coupling is unaffected by drastic alteration of the sequence surrounding residues L720-L764 of the alpha 1S II-III loop. *Proc Natl Acad Sci USA* 98, 5892-5897 (2001)
103. Stange, M., A. Tripathy & G. Meissner: Two domains in dihydropyridine receptor activate the skeletal muscle Ca<sup>2+</sup> release channel. *Biophys J* 81, 1419-1429 (2001)
104. Ahern, C. A., J. Arikath, P. Vallejo, C. A. Gurnett, P. A. Powers, K. P. Campbell & R. Coronado: Intramembrane charge movements and excitation-contraction coupling expressed by two-domain fragments of the Ca<sup>2+</sup> channel. *Proc Natl Acad Sci U S A* 98, 6935-6940 (2001)
105. Yoshikawa, F., H. Iwasaki, T. Michikawa, T. Furuichi & K. Mikoshiba: Cooperative formation of the ligand-binding site of the inositol 1,4,5-trisphosphate receptor by two separable domains. *J Biol Chem* 274, 328-334 (1999)
106. Zorzato, F., P. Menegazzi, S. Treves & M. Ronjat: Role of malignant hyperthermia domain in the regulation of Ca<sup>2+</sup> release channel (ryanodine receptor) of skeletal muscle sarcoplasmic reticulum. *J Biol Chem* 271, 22759-22763 (1996)
107. El-Hayek, R., Y. Saiki, T. Yamamoto & N. Ikemoto: A postulated role of the near amino-terminal domain of the ryanodine receptor in the regulation of the sarcoplasmic reticulum Ca<sup>2+</sup> channel. *J Biol Chem* 274, 33341-33347 (1999)
108. Yamamoto, T., R. El-Hayek & N. Ikemoto: Postulated role of interdomain interaction within the ryanodine receptor in Ca<sup>2+</sup> channel regulation. *J Biol Chem* 275, 11618-11625 (2000)
109. Yamamoto, T., & N. Ikemoto: Regulatory domains of the RyR revealed by peptide probes. *Biophys J* 80, 383a (2001)
110. Allen G. C., M. G. Larach, & A. R. Kunselman: The sensitivity and specificity of the caffeine-halothane contracture test: a report from the North American Malignant Hyperthermia Registry. *The North American Malignant Hyperthermia Registry of MHAUS. Anesthesiology* 88, 579-588 (1998)
111. Tong, J., H. Oyamada, N. Demaurex, S. Grinstein, T. V. McCarthy & D. H. MacLennan: Caffeine and halothane sensitivity of intracellular Ca<sup>2+</sup> release is altered by 15 calcium release channel (ryanodine receptor) mutations associated with malignant hyperthermia and/or central core disease. *J Biol Chem* 272, 26332-26339 (1997)
112. Lamb, G. D., G. S. Posterino, T. Yamamoto, & N. Ikemoto: Effects of a domain peptide of the ryanodine receptor on Ca<sup>2+</sup> release in skinned skeletal muscle fibers. *Am J Physiol Cell Physiol* 281, C207-C214 (2001)
113. Shtifman, A., T. Yamamoto, N. Ikemoto, & M. F. Schneider: Interdomain interaction modulates frequency but not properties of Ca sparks in frog skeletal muscle. *Biophys J* 80, 65a (2001)
114. Wang, J. P., D. H. Needleman, A. B. Seryshev, B. Aghdasi, K. J. Slavik, S. Q. Liu, S. E. Pedersen & S. L. Hamilton: Interaction between ryanodine and neomycin

binding sites on Ca<sup>2+</sup> release channel from skeletal muscle sarcoplasmic reticulum. *J Biol Chem* 271, 8387-8393 (1996)

- (i) Yamamoto, T., R. El-Hayek & N. Ikemoto: Postulated role of interdomain interaction within the ryanodine receptor in Ca<sup>2+</sup> channel regulation. *J Biol Chem* 275, 11618-11625 (2000)
- (ii) Lamb, G. D., G. S. Posterino, T. Yamamoto, & N. Ikemoto: Effects of a domain peptide of the ryanodine receptor on Ca<sup>2+</sup> release in skinned skeletal muscle fibers. *Am J Physiol Cell Physiol* 281, C207-C214 (2001)
- (iii) Shtifman, A., T. Yamamoto, N. Ikemoto, & M. F. Schneider: Interdomain interaction modulates frequency but not properties of Ca sparks in frog skeletal muscle. *Biophys J* 80, 65a (2001)
- (iv) Valdivia, H. in preparation

**Key words:** Excitation-contraction coupling, ryanodine receptor, Ca<sup>2+</sup> channel regulation, inter-domain interaction

**Send correspondence to:** Noriaki Ikemoto, Boston Biomedical Research Institute, 64 Grove St., Watertown, MA 02472, email: [ikemoto@bbri.org](mailto:ikemoto@bbri.org), Tel: (617) 658-7774, Fax: (617) 972-1761

**Running title:** Domain-domain interaction for Ca<sup>2+</sup> channel regulation

# Voltage-Sensor Control of Ca<sup>2+</sup> Release in Skeletal Muscle: Insights from Skinned Fibers

Graham D. Lamb

Department of Zoology, La Trobe University, Melbourne, Victoria, 3086, AUSTRALIA

Email: [zooql@zoo.latrobe.edu.au](mailto:zooql@zoo.latrobe.edu.au)

**ABSTRACT** Important aspects of the excitation-contraction (EC) coupling process in skeletal muscle have been revealed using mechanically-skinned fibers in which the transverse-tubular system can be depolarized by ion substitution or electrical stimulation, activating the voltage-sensors which in turn open the Ca<sup>2+</sup> release channels in the adjacent sarcoplasmic reticulum (SR). Twitch and tetanic force responses elicited in skinned fibers closely resemble those in intact fibers, showing that the coupling mechanism is entirely functional. It was found that ATP has to be bound to the Ca<sup>2+</sup> release channels for them to be activated by the voltage-sensors and that the coupling mechanism likely involves the voltage-sensors removing the inhibitory effects of cytoplasmic Mg<sup>2+</sup> on the release channels; such findings are relevant to the basis of muscle fatigue and to certain diseases such as malignant hyperthermia (MH). EC coupling is evidently not mediated by upmodulation of Ca<sup>2+</sup>-induced Ca<sup>2+</sup> release (CICR) or by an oxidation or phosphorylation reaction. The Ca<sup>2+</sup> load in the SR of skinned fibers can be set at the endogenous level or otherwise. The normal coupling mechanism functions well in mammalian fast-twitch fibers even when the SR is only partially loaded, whereas CICR is highly dependent on SR luminal Ca<sup>2+</sup> and caffeine is poorly effective at inducing release at the endogenous SR Ca<sup>2+</sup> load level.

## INTRODUCTION

### Background

The mechanically-skinned fiber technique was first developed by Natori (1) and involves physically peeling or rolling back the sarcolemma, leaving the other structures more-or-less unaltered. This gives experimental access to the intracellular environment, which can then be manipulated in many ways to investigate particular aspects of muscle function, such as those involving the contractile machinery (2) or Ca<sup>2+</sup> uptake and release by the sarcoplasmic reticulum (SR) (3). Importantly and quite remarkably, it is possible to study the normal excitation-contraction (EC) coupling process in such fibers. Upon skinning, the transverse-tubular system seals off (4,5), and if the skinned fiber segment is placed in a solution broadly mimicking the normal intracellular environment, in particular with high [K<sup>+</sup>], some Na<sup>+</sup>, and physiological levels of ATP and free Mg<sup>2+</sup> (~1 mM), the Na/K pump in the t-system keeps the [Na<sup>+</sup>] high and the [K<sup>+</sup>] low within the t-system, thereby re-establishing the normal transmembrane potential, with the lumen of the t-system positive with respect to the 'cytoplasmic' space (the 'intracellular' region that was opened to the bathing solution by the skinning procedure) (Figure 1). It was found that the t-system could then be depolarized by substituting the high [K<sup>+</sup>] bathing solution with a low [K<sup>+</sup>]-high [Cl<sup>-</sup>] solution, eliciting Ca<sup>2+</sup> release from the SR and contraction (6-8). However, increasing the 'cytoplasmic' [Cl<sup>-</sup>] directly stimulates the ryanodine receptor/Ca<sup>2+</sup> release channels in the SR (8-11) and under some circumstances (such as when the SR is heavily loaded with Ca<sup>2+</sup>), such Cl<sup>-</sup> substitution can induce Ca<sup>2+</sup> release in a manner unrelated to the normal voltage-sensor controlled mechanism (8). This problem was obviated by instead substituting the high [K<sup>+</sup>] solution with a high [Na<sup>+</sup>]-low [K<sup>+</sup>] solution, which depolarizes the t-system without any

appreciable direct effect on the Ca<sup>2+</sup> release channels or the SR itself (8). Furthermore, skinning the muscle fibers under paraffin oil rather than in a low [Ca<sup>2+</sup>] 'relaxing' solution ensured that the dihydropyridine receptor (DHPR)/voltage-sensors in the t-system were kept in a functional state and that the endogenous level of Ca<sup>2+</sup> in the SR was maintained, the latter

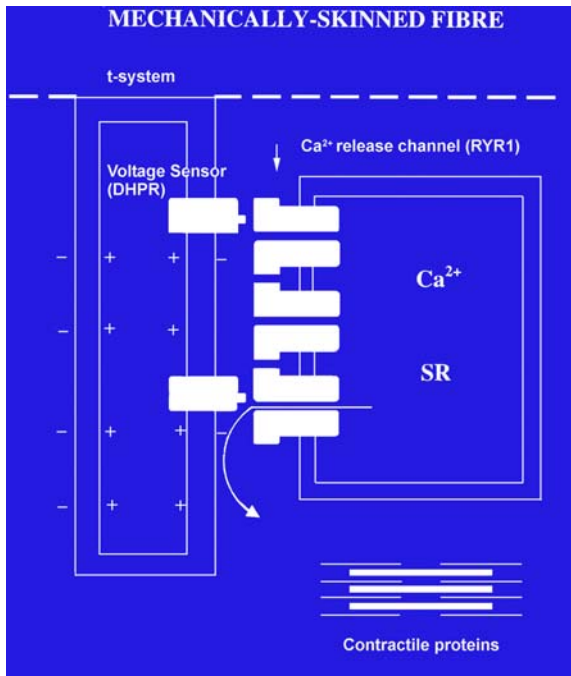


Figure 1. Schematic diagram of a mechanically-skinned muscle fiber. The sarcolemma is removed (dashed line) and t-system seals off and repolarizes (positive inside) if the segment is bathed in a high [K<sup>+</sup>] solution (see text). The voltage-sensors/dihydropyridine receptors (DHPR) in the t-system control the Ca<sup>2+</sup> release channels (ryanodine receptor type 1, RYR1) in the sarcoplasmic reticulum (SR).

being particularly important for distinguishing between normal and abnormal mechanisms of  $\text{Ca}^{2+}$  release (8,11).

### Electrical stimulation and advantages of the preparation

The properties of this depolarization-induced  $\text{Ca}^{2+}$  release (in particular its dependence on the  $[\text{K}^+]$  and t-system contents and integrity, and the effects of DHPs and D600 (8,12,13) showed that it was mediated by the DHPR/voltage-sensors in the t-system activating the SR  $\text{Ca}^{2+}$  release channels, in other words, the normal coupling mechanism (Figure 2).

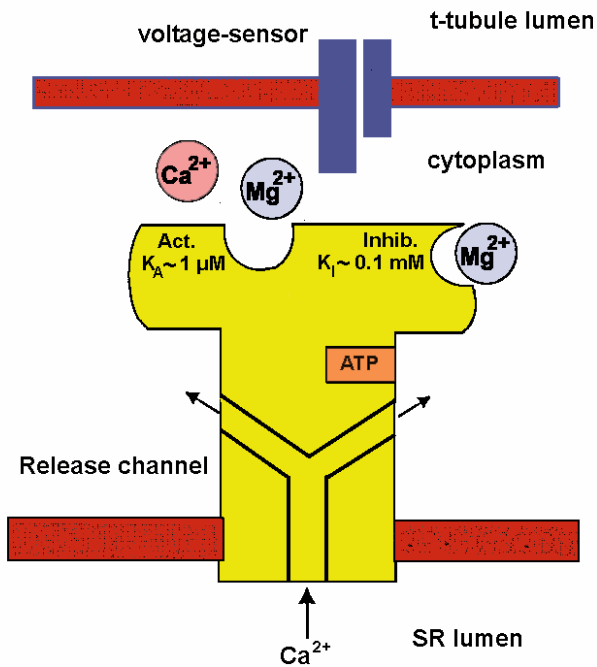


Figure 2. Regulation of the  $\text{Ca}^{2+}$  release channel. The channel is stimulated by ATP binding to a regulatory site (dissociation constant  $\sim 1$  mM) and  $\text{Ca}^{2+}$  binding to a  $\text{Ca}^{2+}$ -activation site (act.) (dissociation constant ( $K_A$ )  $\sim 1$   $\mu\text{M}$  in the absence of  $\text{Mg}^{2+}$ ). The channel is inhibited by  $\text{Mg}^{2+}$  binding at the  $\text{Ca}^{2+}$ -activation site (with  $>30$  fold lower affinity than for  $\text{Ca}^{2+}$ ) and by  $\text{Ca}^{2+}$  or  $\text{Mg}^{2+}$  binding at a non-specific inhibitory site (inhib.) ( $K_I \sim 0.1$  mM for both ions).  $\text{Mg}^{2+}$ , normally present at 1 mM, lowers the apparent  $\text{Ca}^{2+}$  affinity of the activation site  $\sim 30$  fold and causes almost full occupation of the  $\text{Ca}^{2+}/\text{Mg}^{2+}$  site. It is proposed that voltage-sensor activation opens the channel by lowering the  $\text{Mg}^{2+}$  affinity of these sites and thereby removing its inhibitory effects.

However, one draw-back with the ion substitution method of depolarization is that diffusional delays means that depolarization takes  $\sim 0.5$  s and is thus considerably slower than in an intact fiber. Recently, this problem has been circumvented by stimulating the skinned fiber rapidly with a brief transverse electric field ( $\sim 2$  ms, 40 V/cm) applied via parallel platinum electrodes whilst the fiber is kept in the normal high  $[\text{K}^+]$  solution (14). Such stimulation evidently induces an action potential (AP) in the sealed t-system all along the length of the skinned fiber, which elicits  $\text{Ca}^{2+}$  release and a twitch response, with stimulation at progressively higher frequencies

inducing unfused and then fused tetanic force responses. As expected, these responses were dependent on the potential of the t-system and were blocked by tetrodotoxin in the t-system lumen (14). The close similarity between the twitch and tetanic responses in these skinned fibers (Figure 3) and those in intact fibers, proved unequivocally that the responses in the skinned fibers were mediated by the normal voltage-sensor dependent mechanism. An interesting incidental finding in these experiments was that action potentials also travel longitudinally between adjacent sarcomeres in mammalian muscles fibers via a longitudinal tubular network (14); this may well be an important fail-safe mechanism in muscle to ensure uniform activation of the whole fiber even under adverse conditions.

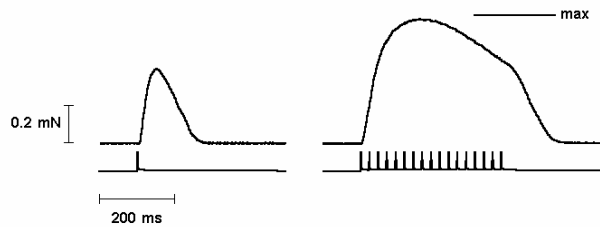


Fig 3. Twitch and tetanic force responses in a skinned fiber. Transverse electric field stimulation (40 V/cm, 2 ms) was applied to a skinned fiber segment from the extensor digitorum longus muscle of a rat, eliciting an action potential in the sealed t-system which resulted in SR  $\text{Ca}^{2+}$  release and contraction. A single stimulus induced a twitch response (left trace) and 50 Hz stimulation induced a fused tetanic force response. 'Max' indicates the maximum  $\text{Ca}^{2+}$ -activated force in the fiber.

In summary, the key advantages of this mechanically-skinned fiber preparation are as follows. It allows ready access to the 'intracellular' environment, and manipulation of factors and structures therein, whilst still retaining the normal mechanism of voltage-sensor control of  $\text{Ca}^{2+}$  release. This mechanism can be stimulated by depolarizing the t-system by ion substitution or more rapidly by triggering an AP in the t-system, which of course is the process occurring in-vivo. Furthermore, the amount of  $\text{Ca}^{2+}$  in the SR can be maintained at endogenous level or varied as desired (8,15,16). Thus, with the skinned fiber preparation it is possible to examine how some manipulation affects the whole of the EC coupling sequence, as well individual elements such as the responsiveness of the contractile apparatus to applied  $\text{Ca}^{2+}$  or the release of  $\text{Ca}^{2+}$  from the SR to direct stimulation with  $\text{Ca}^{2+}$  or caffeine. In this way the skinned fiber preparation can complement and extend the information obtained with other techniques, providing a powerful experimental tool that bridges the gap between studies on intact fibers and those on isolated SR or contractile or channel proteins.

### KEY FINDINGS

A number of findings are immediately apparent from the fact that the EC coupling mechanism in skinned fibers is evidently entirely functional even though the normal cytoplasm has

been replaced with a solution with only particular minimal requirements.

- a) The coupling mechanism between the voltage sensor and the release channel does not require the presence of substances that readily dissociate and diffuse out of the fiber (other than those added experimentally, eg.  $K^+$ ,  $Mg^{2+}$ , ATP), as it continues to function well for more than 30 minutes after skinning and cytoplasmic perfusion. (Even large proteins should diffuse out of the  $\sim 50 \mu\text{m}$  thick skinned fiber within a matter of minutes (17), and the bathing solution has a volume  $\sim 10^6$  times that of the skinned fiber and is regularly changed.) This does not mean however that some important factors, such as calmodulin or FKPB12 (18), have not remained bound at key regulatory sites.
- b) Cytoplasmic  $Mg^{2+}$  and ATP are both critical to the normal coupling mechanism (see later).
- c) The coupling mechanism is not noticeably altered by the washout or addition of reducing agents glutathione (GSH) or dithiothreitol (DTT) and is evidently not mediated by an oxidation reaction (19).
- d) The stimulatory effect of caffeine and cytoplasmic  $Ca^{2+}$  on the  $Ca^{2+}$  release channels in mammalian muscle is greatly augmented by increasing the  $Ca^{2+}$  load level in the SR, probably via a stimulatory  $Ca^{2+}$  site within the SR lumen, but in contrast the normal coupling mechanism functions well even when the SR is relatively depleted of  $Ca^{2+}$  (11) (see later).
- e) Concomitant with the last three observations, the normal coupling mechanism is not mediated by up-modulation of 'simple'  $Ca^{2+}$ -induced  $Ca^{2+}$  release (CICR) and is relatively insensitive to factors that favor CICR (such as oxidation) or inhibit CICR (such as low pH, raised  $[Mg^{2+}]$ , lactate, DP4) (11,12,20-22). It is suggested that this is because voltage-sensor activation itself up-regulates and utilizes the  $Ca^{2+}$  sensitivity of the release channels, meaning that there is 'voltage-sensor controlled-CICR', rather than 'simple CICR' that is independent of the voltage-sensors (23-25).
- f) Rapid  $Ca^{2+}$  release from the SR occurs in the absence of any  $Cl^-$  or other anion highly permeable to the SR, demonstrating that such  $Ca^{2+}$  efflux is not dependent on the flow of anion-mediated counter-current.

### **IMPORTANCE OF ATP AND $Mg^{2+}$**

#### **Voltage-sensor coupling requires ATP binding to the release channel**

ATP is present in the cytoplasm of intact resting fibers at  $\sim 6$  to  $8 \text{ mM}$ . Millimolar concentrations of cytoplasmic ATP stimulates  $Ca^{2+}$  release and augments CICR and caffeine-induced  $Ca^{2+}$ -release in skinned fibers (3,26,27), SR vesicles (28) and single release channels (29). However, this does not indicate whether ATP is in any way important in normal EC coupling, where the voltage-sensors activate the  $Ca^{2+}$  release channels apparently by some direct physical interaction (30). Experiments with skinned fibers show that despite such a direct interaction, ATP is absolutely required for normal coupling. In toad muscle depolarization-induced  $Ca^{2+}$  release by ion substitution was completely blocked in

the absence of ATP (23) and the total amount of release was reduced approximately two-fold at  $0.5 \text{ mM}$  ATP (31). In mammalian (rat) muscle, the inhibitory effect of lowering the total  $[ATP]$  to  $0.5 \text{ mM}$  was only apparent in the ion substitution experiments when  $Ca^{2+}$  release had already been reduced by raising  $[Mg^{2+}]$  (32) (see next section), probably because of temporal limitations in those experiments, with recent experiments with electrical stimulation showing that low  $[ATP]$  does inhibit the release mechanism at the normal  $[Mg^{2+}]$  of  $1 \text{ mM}$  (33). The critical importance to EC coupling of ATP binding to a regulatory site on the  $Ca^{2+}$  release channel was further established using adenosine, an extremely weak agonist, as a competitor of ATP at that site. Adenosine competitively inhibited ATP-stimulation of voltage-sensor dependent  $Ca^{2+}$  release (34) in a manner quantitatively similar to its action on caffeine-stimulated release in skinned fibers (26,34) and on single  $Ca^{2+}$  release channels (35), showing that the inhibitory effect of low  $[ATP]$  was due to failure to stimulate a regulatory site on the release channel rather than being related to a decrease in phosphorylation or some other process dependent on ATP hydrolysis. 'Depolarization-induced'  $Ca^{2+}$  release in a triad (SR - t-tubular) preparation was also found to be inhibited in the absence of ATP (36), though it is not clear how much this effect was due to ATP favoring direct CICR in that preparation which was very heavily loaded with  $Ca^{2+}$  (11) (and see above). The fact that ATP binding to the release channel (Figure 2) is required for normal EC coupling gives insight into how the voltage-sensor may regulate the release channel and is also relevant to the basis of muscle fatigue occurring in some conditions (see below).

#### **Role of $Ca^{2+}$ activation and $Mg^{2+}$ inhibition**

Cytoplasmic  $Ca^{2+}$  stimulates the opening of the  $Ca^{2+}$  release channel by binding to a high affinity site(s) (dissociation constant,  $K_a \sim 0.2\text{-}1 \mu\text{M}$  in mammalian (3,10,28), but possibly  $\sim 10 \mu\text{M}$  in frog muscle (27,37)). It is likely that this  $Ca^{2+}$ -activation site is required for normal coupling because recent experiments expressing mutated release channels in myotubes found that greatly lowering the affinity of the activation site for  $Ca^{2+}$  largely or completely blocked coupling (38).  $Mg^{2+}$  is known to inhibit the opening of the  $Ca^{2+}$  release channels by acting both at this ' $Ca^{2+}$ -activation site' and at a low affinity  $Ca^{2+}/Mg^{2+}$  inhibitory site (Figure 2) (3,28,39).  $Mg^{2+}$  competes with  $Ca^{2+}$  for the activation site but with a  $>30\text{-}80$  fold lower apparent affinity ( $K_i \sim 20\text{-}50 \mu\text{M}$ ) (10,27,28,39,40) and it apparently not only prevents  $Ca^{2+}$  stimulation of the channel but also directly inhibits channel opening when bound at this site (28).  $Mg^{2+}$  also competes with  $Ca^{2+}$  for the low affinity site, but the site is quite non-specific, with both ions binding with similar affinity and both causing similar inhibition of channel opening (10,27,28,39,40). It seems most appropriate to regard this latter site as a ' $Mg^{2+}$ -inhibitory site' (41) because there is  $\sim 1 \text{ mM}$   $Mg^{2+}$  normally present in the cytoplasm, and consequently the site would be primarily occupied by  $Mg^{2+}$  rather than  $Ca^{2+}$  under physiological circumstances (Figure 2). Furthermore, as the dissociation constant for this  $Ca^{2+}/Mg^{2+}$  inhibitory site is  $\sim 0.1\text{-}0.2 \text{ mM}$  at physiological ionic strength

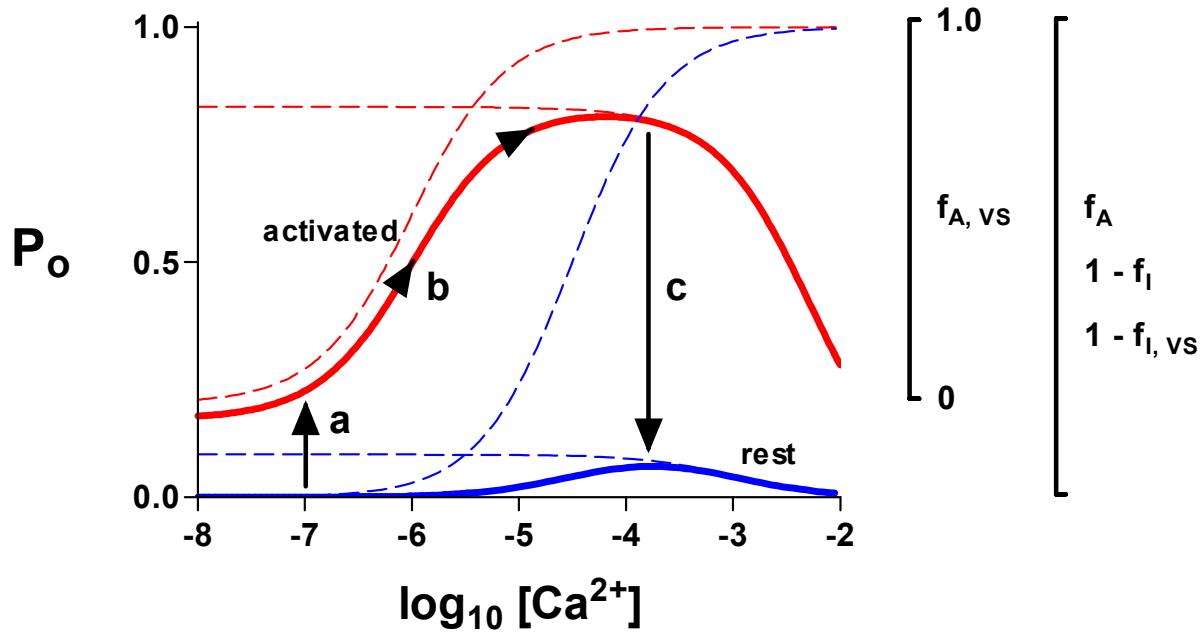


Figure 4. Effect of voltage-sensor activation on the  $\text{Ca}^{2+}$  dependence of release channel opening ( $P_o$ ). In a resting fiber (ie. with the voltage-sensor not activated and physiological cytoplasmic  $[\text{Mg}^{2+}]$  of  $\sim 1$  mM),  $\text{Mg}^{2+}$  will compete strongly with  $\text{Ca}^{2+}$  for the  $\text{Ca}^{2+}$ -activation site, lowering its apparent  $\text{Ca}^{2+}$  affinity  $\sim 30$  fold ( $K_A$  increased to  $\sim 30$   $\mu\text{M}$ ; see ascending dashed blue curve) and the  $\text{Ca}^{2+}/\text{Mg}^{2+}$  inhibitory site ( $K_i \sim 0.1$  mM) will be almost fully occupied by  $\text{Mg}^{2+}$  (see lower dashed blue line) resulting in a low channel open probability ( $P_o < 0.1$ ) even at optimum cytoplasmic  $[\text{Ca}^{2+}]$  (see blue bell curve). It is proposed that voltage-sensor activation substantially reduces the affinity for  $\text{Mg}^{2+}$  at both sites so that i) the limitation on peak  $P_o$  caused by  $\text{Mg}^{2+}$  occupation of the  $\text{Ca}^{2+}/\text{Mg}^{2+}$  site is largely removed (red descending dashed curve,  $K_i \sim 5$  mM) and ii) the apparent  $\text{Ca}^{2+}$ -affinity of the  $\text{Ca}^{2+}$ -activation site returns towards  $\sim 1$   $\mu\text{M}$  and the stimulatory effect of ATP will open the channel even in the absence of  $[\text{Ca}^{2+}]$  (eg.  $P_o \sim 0.2$ ) (a), with the released  $\text{Ca}^{2+}$  further stimulating channel opening (b). This is 'voltage-sensor controlled CICR'. When the voltage-sensor is deactivated, the  $\text{Mg}^{2+}$  inhibition at both sites is restored and  $P_o$  rapidly declines (c) even in the presence of high local  $[\text{Ca}^{2+}]$ . Ascending blue and red dashed curves show the fraction of  $\text{Ca}^{2+}$ -activation sites occupied by  $\text{Ca}^{2+}$  at rest ( $f_A$ ) and with the voltage-sensor activated ( $f_{A,vs}$ ) respectively. Descending blue and red dashed curves show the fraction of  $\text{Ca}^{2+}/\text{Mg}^{2+}$  inhibitory sites that are unoccupied in the two cases respectively ( $1 - f_i$  and  $1 - f_{i,vs}$ ).  $P_o$  is calculated as  $(f_A \times (1 - f_i))$  and  $((f_{A,vs} + 0.2) \times (1 - f_{i,vs}))$ .

(10,28,42), it could be expected to be substantially occupied by  $\text{Mg}^{2+}$  in-vivo. Thus,  $\text{Mg}^{2+}$  will inhibit simple CICR in skeletal muscle by acting at both sites, but it is because of its occupancy of the low affinity  $\text{Ca}^{2+}/\text{Mg}^{2+}$  inhibitory site that such release will be considerably depressed no matter how high the  $[\text{Ca}^{2+}]$  may rise in the vicinity of the release channels (3,12,23,25) (Figure 4).

The inhibitory action of  $\text{Mg}^{2+}$  on  $\text{Ca}^{2+}$  release is clearly present in skinned fibers even when EC coupling is entirely functional and the release channels are under the control of the voltage-sensors, because lowering the free  $[\text{Mg}^{2+}]$  induces full release of SR  $\text{Ca}^{2+}$  in both mammalian and amphibian muscle independently of any changes in free or total  $[\text{ATP}]$  or  $[\text{MgATP}]$  (21,23,43). Of course, E-C coupling does work in-vivo in the presence of  $\sim 1$  mM cytoplasmic  $[\text{Mg}^{2+}]$ , and further it appears that most or all the release channels must open almost fully (albeit transiently) if the observed peak rates of  $\text{Ca}^{2+}$  efflux are to be achieved (44). Consequently, it appears that the stimulatory effect of voltage-sensor activation must in some way bypass or overcome the inhibitory effect of  $\text{Mg}^{2+}$  on the release channel, in particular at the low affinity  $\text{Ca}^{2+}/\text{Mg}^{2+}$  site where raised  $[\text{Ca}^{2+}]$  will only compound, not relieve, the inhibitory action of  $\text{Mg}^{2+}$ .

Importantly too, experiments in skinned fibers showed that depolarization-induced  $\text{Ca}^{2+}$

release is inhibited almost completely in mammalian and amphibian fibers if the  $[\text{Mg}^{2+}]$  is raised to 10 mM (21,23) including when stimulating rapidly by electrical stimulation (unpublished observations); inhibition of  $\text{Ca}^{2+}$  release is also seen in intact fibers with raised  $[\text{Mg}^{2+}]$  (45). This effect of raised  $[\text{Mg}^{2+}]$  is not due to inactivation of the voltage-sensors, nor to an inability of  $\text{Ca}^{2+}$  to flow out through the release channels – instead it appears simply that the channels do not open with voltage-sensor stimulation in the presence of such a high cytoplasmic  $[\text{Mg}^{2+}]$  (23). These observations led to the following proposal.

#### Voltage-sensor control of $\text{Mg}^{2+}$ inhibition and CICR

As voltage-sensor activation overcomes the  $\text{Mg}^{2+}$  inhibitory effect at 1 mM  $\text{Mg}^{2+}$  but not at 10 mM  $\text{Mg}^{2+}$ , we have proposed that the voltage-sensor activates the release channel by lowering its affinity for  $\text{Mg}^{2+}$  at both the  $\text{Ca}^{2+}$ -activation site (23,24) and the low affinity  $\text{Ca}^{2+}/\text{Mg}^{2+}$  site (21,25,41) (Figure 4). The proposal of a  $\text{Mg}^{2+}$ -affinity change is also supported by recent findings in voltage-clamped cut fibers from mammalian muscle (46).

The above proposal seems the simplest way to account for information to date. The fact that high cytoplasmic  $[\text{Mg}^{2+}]$  inhibits coupling does not fit with a proposal in which the inhibitory effect of  $\text{Mg}^{2+}$  is

bypassed altogether (eg. that the voltage-sensor simply directly opens the release channel irrespective of  $Mg^{2+}$  binding) but is consistent with a  $Mg^{2+}$  affinity change. Furthermore, it is known that the  $Mg^{2+}$  affinity of the sites on the release channel can indeed be reduced by certain treatments (eg. high  $[Cl^-]$  (10) or agents (eg. bastadin (47))).

It is apparent from many experiments that it would not be sufficient for the voltage-sensors to only increase the  $Ca^{2+}$  affinity and/or decrease the  $Mg^{2+}$  affinity of the  $Ca^{2+}$  activation site without changing the inhibitory effect of  $Mg^{2+}$  at the  $Ca^{2+}/Mg^{2+}$  site. For example, 'depolarization-induced'  $Ca^{2+}$  release and CICR in triads are strongly inhibited under conditions (0.3 mM  $Ca^{2+}$ , 1.2 mM  $Mg^{2+}$ , 5 mM AMPPCP) in which the  $Ca^{2+}$ -activation site would be occupied almost exclusively by  $Ca^{2+}$  but where the low affinity  $Ca^{2+}/Mg^{2+}$  site would be appreciably occupied (36). Comparable results are also seen in ryanodine binding studies (with 1 mM  $Ca^{2+}$ , 5 mM AMP (10)). Also, increasing the  $Ca^{2+}$ -affinity of the activation site with 30 mM caffeine elicits little  $Ca^{2+}$  release in mammalian skinned fibers in the presence of 1 mM  $Mg^{2+}$  even though the voltage-sensor activation works extremely well under the same conditions (11). (Here it is presumed that caffeine increases only the  $Ca^{2+}$  affinity and not the  $Mg^{2+}$  affinity of the  $Ca^{2+}$ -activation site, in agreement with results in amphibian muscle fibers (27) – recent results in mammalian muscle SR (40) however have suggested that the  $Mg^{2+}$  affinity is increased as well, but this was with no ATP present and only 5 mM caffeine, and occurred only with SR from normal muscle and not in muscle from malignant hyperthermia-susceptible animals). Thus, it appears that the voltage-sensors must at least lower the affinity of the  $Ca^{2+}/Mg^{2+}$  site to get physiological  $Ca^{2+}$  release rates (41).

The question then arises as to whether it is sufficient to remove the inhibitory effect of  $Mg^{2+}$  only at the low affinity  $Ca^{2+}/Mg^{2+}$  site. This would require that the channels in vivo (with ATP present etc.) open to some extent even when  $Mg^{2+}$  is bound to the  $Ca^{2+}$ -activation site. If they do, the released  $Ca^{2+}$  could be expected to bind to the activation site, very rapidly inducing maximal channel opening. However, if the channels are not appreciably open under such conditions, it must be proposed that the voltage-sensors also remove or reduce the inhibitory effect of  $Mg^{2+}$  at the activation site, by reducing its affinity for  $Mg^{2+}$  and possibly also increasing its affinity for  $Ca^{2+}$  (23). Given that it was found in skinned mammalian fibers with functional coupling that decreasing the free  $[Mg^{2+}]$  to 50  $\mu M$  induced considerably less  $Ca^{2+}$  release than did decreasing  $[Mg^{2+}]$  to 15  $\mu M$  (21), it appears that reducing the level of occupancy of the low affinity  $Ca^{2+}/Mg^{2+}$  site to ~25% with 50  $\mu M$   $Mg^{2+}$  is not in itself sufficient to give substantial  $Ca^{2+}$  release at resting  $[Ca^{2+}]$  (~0.1  $\mu M$ ), suggesting that for potent channel activation in functional fibers it is indeed necessary to reduce the  $Mg^{2+}$  inhibition at the activation site. As the voltage-sensors can induce  $Ca^{2+}$  release even when the cytoplasmic  $[Ca^{2+}]$  is buffered to nM levels (16), it seems that increasing the  $Ca^{2+}$ -sensitivity of the activation site without lowering its affinity for  $Mg^{2+}$  would not be sufficient to induce release.

Thus, it seems most parsimonious to propose that the voltage-sensor activates the release channel by reducing  $Mg^{2+}$ -inhibition at both sites (23,25). This would affect the  $Ca^{2+}$  dependence of release channel opening dramatically (Figure 4). When the voltage-sensors are not activated,  $Mg^{2+}$  would severely limit  $Ca^{2+}$  binding to the  $Ca^{2+}$ -activation sites (ascending dashed blue line in Figure 4) and also nearly saturate the  $Ca^{2+}/Mg^{2+}$  inhibitory sites (descending dashed blue line) so that the channel would open to only a small extent even at optimal  $[Ca^{2+}]$  (note the low peak of blue bell curve). Activating the voltage-sensors would move the 'activation' function to the left and 'inhibition' function to the right (to the red ascending and descending dashed curves respectively), with the latter effect greatly increasing the peak of the resulting bell curve (ie. giving a high probability of channel opening). Thus, the stimulatory effect of ATP will induce some degree of channel activation even when the cytoplasmic  $[Ca^{2+}]$  is at or below the normal resting level (<0.1  $\mu M$ ) ('a' in Figure 4), with the  $Ca^{2+}$  efflux then able to maximally stimulate the channel by acting on the  $Ca^{2+}$ -activation site ('b' in Figure 4). This is 'voltage-sensor controlled CICR', not simple uncontrolled CICR, and importantly  $Ca^{2+}$  release can be rapidly stopped, irrespective of any high local  $[Ca^{2+}]$ , by deactivating the voltage-sensor and restoring the  $Mg^{2+}$  inhibition (23) ('c' in Figure 4) (see also section on termination of  $Ca^{2+}$  release). The proposed effect of voltage-sensor activation on the bell curves in Figure 4 is similar to that observed when adding high cytoplasmic  $[Cl^-]$  (10), possibly suggesting that high  $[Cl^-]$  stabilises the same 'activated' state favored by voltage-sensor activation. Increasing the level of  $Ca^{2+}$  loading in the SR also may have a similar effect (presumably mediated via a SR luminal  $Ca^{2+}$  site (48-50)), because it not only increases the apparent  $Ca^{2+}$ -sensitivity of the activation site (3, 28) but also seemingly reduces the extent of inhibition occurring via the low affinity  $Ca^{2+}/Mg^{2+}$  site, given that caffeine and  $Ca^{2+}$  can induce rapid and considerable  $Ca^{2+}$  release even in the presence of ~1 mM  $Mg^{2+}$  when the SR is very loaded (11,36,51).

The fact that ATP is a strong stimulant to channel opening and is absolutely required for voltage-sensor activation of the channels (see above) suggests that the release channels have to be in a 'primed' state to be opened by the voltage-sensors, and consequently is consistent with the idea that the release channels can be activated simply by removing a resting inhibition, that is, the  $Mg^{2+}$ -inhibition. Experiments with SR vesicles from both mammalian (28,36) and amphibian muscle (52) indicate that the  $Ca^{2+}$  release rate would be indeed high enough to explain release in-vivo if the vesicles are stimulated by cytoplasmic ATP (mM) and  $Ca^{2+}$  (>1  $\mu M$ ) in the absence of inhibition by  $Mg^{2+}$ . A recent study with amphibian skinned muscle fibers however concluded that removing  $Mg^{2+}$  inhibition would not by itself increase channel opening sufficiently to give physiological  $Ca^{2+}$  release rates (27), though the fibers in that study did not have functional EC coupling and the rate of  $Ca^{2+}$  release may have been limited by diffusional delays when applying ATP. The question of whether removing  $Mg^{2+}$ -inhibition is sufficient in itself to give physiological  $Ca^{2+}$  release

may be best resolved in the future by experiments in which the  $[Mg^{2+}]$  is very rapidly lowered in fibers with functional EC coupling. It is possible that in functioning fibers the combined stimulatory effects on the release channels of cytoplasmic ATP (and calmodulin) and luminal  $Ca^{2+}$  loading are still not enough to stimulate maximal  $Ca^{2+}$  release in the absence of  $Mg^{2+}$  inhibition – in that case it would have to be concluded that the voltage-sensors, in addition to removing the inhibitory effect of  $Mg^{2+}$ , must also have a direct stimulatory action on the release channels.

### **Malignant hyperthermia**

The above mechanism also gives further insight into basis of malignant hyperthermia (MH). MH is an inherited disorder of skeletal muscle, in most cases caused by mutations in the  $Ca^{2+}$  release channel, where volatile anesthetics and stress can trigger uncontrolled contractures, leading to hyperthermia and often to death (53).  $Ca^{2+}$  release in muscle fibers from MH-susceptible individuals is not inhibited as strongly by cytoplasmic  $Mg^{2+}$  as it is in normal muscle (54). This is due both to a two to three fold reduction in the  $Mg^{2+}$  affinity of the  $Ca^{2+}/Mg^{2+}$  inhibitory site (42) and a two fold decrease in the  $Mg^{2+}$  affinity and a two fold increase in the  $Ca^{2+}$  affinity of the  $Ca^{2+}$ -activation site (40). In view of the discussion above, this readily explains why the bell-curve describing the  $Ca^{2+}$  dependence of channel opening of release channels from MH muscle at rest (ie. with no voltage-sensor activation) is somewhat higher and wider than that for normal channels shown by the blue bell curve in Figure 4. So long as the  $Mg^{2+}$  inhibition is not reduced so much that the MH channel is appreciably open at the resting  $[Ca^{2+}]$  (ie. the point on the bell curve at  $\sim 0.1 \mu M$   $Ca^{2+}$  remains close to a  $P_0$  of zero), this would mean that muscle function would be little if at all affected, with the MH channel remaining closed in the resting muscle and opening normally upon voltage-sensor activation when its characteristics would be the same as the normal channel (ie. red bell curve in Figure 4). However, if some extraneous factor such as a volatile anaesthetic or stress stimulated the release channel in any way (or raised the cytoplasmic  $[Ca^{2+}]$ ), this could well be enough to induce a self-reinforcing cycle of CICR in the MH channel, which would produce the observed uncontrolled muscle contraction. In comparison, the normal release channel would be much less susceptible to any such stimuli.

Recent results indicate that the mutations in the release channel responsible for MH cause hyperactivation because they interfere with the normal interactions between different domains of the protein (55). It was found that the properties of the normal  $Ca^{2+}$  release channel altered to those of MH channels when a synthetic peptide (DP4), corresponding a particular region of the channel, was added (55). The exogenous peptide evidently competed with the corresponding region on the channel for its binding site on a different region of the channel, thereby preventing the channel from adopting its normal stable closed state. Addition of DP4 to skinned fibers caused similar sensitising effects, giving them the characteristics of MH-susceptible fibers (22). These experiments suggest the view that voltage-sensor activation opens the release channel by 'destabilising'

the resting state that the channel protein normally adopts in the presence of  $Mg^{2+}$ .

### **TERMINATION OF $Ca^{2+}$ RELEASE**

Deactivation of the voltage-sensor rapidly stops  $Ca^{2+}$  release in skeletal muscle (56,57). As mentioned above, this can be explained by there being marked inhibition of CICR by  $Mg^{2+}$  when the voltage-sensors are not activated – simply deactivating the voltage-sensors would restore this strong level of  $Mg^{2+}$  inhibition, which would then greatly decrease  $Ca^{2+}$  release even if the presence of a high local  $[Ca^{2+}]$  (Figure 4). Furthermore, the fact that the sensitivity of CICR is greatly inhibited by partially depleting the SR of  $Ca^{2+}$  (3,11) (with depolarization-induced release being little affected (11,58)) means that any tendency for the  $Ca^{2+}$  release to be self-sustaining would be further reduced following the initial channel activation and  $Ca^{2+}$  efflux. (This can also account for the phenomenon of 'repolarization-induced stop of  $Ca^{2+}$  release (11,59)). Termination of  $Ca^{2+}$  release will be further aided if release channels also display 'inactivation', in which the open probability of the release channels greatly decreases from an initial high level to a relatively low level, due either to a type of  $Ca^{2+}$ -specific (56,57,60) or use-dependent inactivation (61-63). Finally, depleting the SR  $Ca^{2+}$  would also reduce the absolute rate of  $Ca^{2+}$  release because of the reduced  $Ca^{2+}$  gradient, and this could be exacerbated by local depletion of  $Ca^{2+}$  inside the lumen of the SR near the release channels caused by diffusion limitations on  $Ca^{2+}$  as it binds and unbinds to calsequestrin within the SR. Together these phenomena explain why the amount of  $Ca^{2+}$  released during a single twitch response (ie. to stimulation by a single action potential) remains virtually unchanged when fibers are given treatments that up-modulate the sensitivity to simple CICR, such as addition of DP4 (22) or oxidation of the release channels (G. S. Posterino & G. D. Lamb, unpublished observations).

### **INVESTIGATIONS INTO MUSCLE FATIGUE**

Finally, the skinned fiber preparation has also provided important information about the basis of muscle fatigue. Muscle fatigue, which is a decline in muscle performance with repeated activity, has many facets and causes (64,65). It can be caused by direct effects on the contractile apparatus and, of particular interest here, by a reduction in  $Ca^{2+}$  release from the SR (64). The reduction in  $Ca^{2+}$  release is not caused by a decline in intracellular pH (20,21,66-68), even though this depresses CICR in skinned fibers (20,21) and  $Ca^{2+}$ - and ATP-activation of isolated release channels (69), once again showing that voltage-sensor controlled  $Ca^{2+}$  release is not mediated by simple CICR. The reduction in  $Ca^{2+}$  release is also not due to the inhibitory effect of lactate ions on the release channels, as the twitch response to electrical stimulation in skinned fibers is quite unaffected by the presence of even 30 mM lactate (70).

Two factors that are likely to be important in muscle fatigue in some circumstances are a) a decrease in cytoplasmic [ATP] and b) the accompanying increase in free  $[Mg^{2+}]$  that occurs with a fall in [ATP] owing to the fact that most cellular ATP is in the form MgATP and the hydrolysis products of ATP bind  $Mg^{2+}$  with much lower affinity than does

ATP. Following vigorous stimulation of human fast-twitch fibers, the average [ATP] in the cytoplasm falls to <1 mM (71), and the concentration may well be lower near the Ca<sup>2+</sup> release channels in the triad junction. The ability of the voltage-sensors to induce Ca<sup>2+</sup> release is inhibited when the [ATP] falls into this range (31-33), and this would be exacerbated if the local [Mg<sup>2+</sup>] reached ~3 mM (23,32,45,46), with the reasons for this explained above. In other circumstances where [ATP] does not fall, reduced Ca<sup>2+</sup> release may occur due to inorganic phosphate, which rises to high concentrations in the cytoplasm (64), moving into the SR and precipitating with Ca<sup>2+</sup>, thereby reducing the amount of readily releasable Ca<sup>2+</sup> (72,73). Glycogen depletion, which occurs with sustained activity, can also by some unknown means cause a reduction in depolarization-induced Ca<sup>2+</sup> release (17,74). Lastly, it appears that if the cytoplasmic [Ca<sup>2+</sup>] is raised for prolonged periods, voltage-sensor control of Ca<sup>2+</sup> release is hindered (5,75), apparently due to physical disruption of the triad junction (5), leading to 'low-frequency fatigue' which may last for a day or more.

### CONCLUSIONS / PERSPECTIVES

The skinned fiber preparation with functional EC coupling has given important insight into the properties and basis of the coupling mechanism in skeletal muscle. Because the 'intracellular' environment can be readily manipulated in these fibers, it has been possible to investigate which factors influence normal coupling and which do not. This has given information not only about how the voltage-sensors control the Ca<sup>2+</sup> release channels, but also about the possible basis of muscle fatigue and particular diseases. These experiments have highlighted how Ca<sup>2+</sup> release controlled by the voltage-sensor differs from direct stimulation or modulation of the channels by Ca<sup>2+</sup>, H<sup>+</sup>, lactate and caffeine etc. It appears that voltage-sensor regulation of the release channels may be achieved by varying the affinity of certain sites for Mg<sup>2+</sup> - a mechanism in which channel activation is initiated by removal of resting inhibition rather than by a direct stimulatory effect. It may be that many other cellular processes are also regulated by varying the affinity of key sites for Mg<sup>2+</sup>, an ion present in most cells at a relatively constant, high (millimolar) level, properties which, perhaps contrary to general thinking, make it useful for dynamic regulation of molecular processes.

### ACKNOWLEDGMENTS

I wish to thank Professor George Stephenson, Dr Giuseppe Posterino and Dr Cassandra Thumwood for helpful suggestions and comments. Supported by the National Health and Medical Research Council of Australia.

### References

1. Natori, R.: The property and contraction process of isolated myofibrils. *Jikei-Kai Med J* 1, 119-126 (1954)
2. Moiescu, D. G.: kinetics of reaction in calcium-activated skinned muscle fibres. *Nature* 262, 610-613 (1976)
3. Endo, M.: Calcium release from sarcoplasmic reticulum. *Curr Top Memb Trans* 25, 181-230 (1985)
4. Stephenson, E. W: Activation of fast skeletal muscle: contribution of studies on skinned fibres. *Am J Physiol* 240, C1-C9 (1981)

5. Lamb, G. D., P. R. Junankar & D. G. Stephenson: Raised intracellular [Ca<sup>2+</sup>] abolishes excitation-contraction coupling in skeletal muscle of rat and toad. *J Physiol* 489, 349-362 (1995)
6. Stephenson, E. W: Excitation of skinned muscle fibers by imposed ion gradients. I. Stimulation of <sup>45</sup>Ca efflux at constant [K][Cl] product. *J Gen Physiol* 86, 813-832 (1985)
7. Fill, M. D. & P. M. Best. Contractile activation and recovery in skinned frog muscle stimulated by ionic substitution. *Am J Physiol* 254, C107-C114 (1988)
8. Lamb, G. D. & D. G. Stephenson: Calcium release in skinned muscle fibres of the toad by transverse tubular depolarization or by direct stimulation. *J Physiol* 423, 495-517 (1990)
9. Sukhareva, M., J. Morrissette & R. Coronado: Mechanism of chloride-dependent release of Ca<sup>2+</sup> in the sarcoplasmic reticulum of rabbit skeletal muscle. *Biophys J* 67, 751-765 (1994)
10. Meissner, G., E. Rios, A. Tripathy. & D. A. Pasek: Regulation of skeletal muscle Ca<sup>2+</sup> release channel (ryanodine receptor) by Ca<sup>2+</sup> and monovalent cations and anions. *J Biol Chem* 272, 1628-1638 (1997)
11. Lamb, G. D., M. A. Cellini & D. G. Stephenson: Different Ca<sup>2+</sup> releasing action of caffeine and depolarisation in skeletal muscle fibres of the rat. *J Physiol* 531, 715-728 (2001)
12. Lamb, G. D. & D. G. Stephenson: Control of calcium release and the effect of ryanodine in skinned muscle fibres of the toad. *J Physiol* 423, 519-542 (1990)
13. Posterino, G. S. & G. D. Lamb. Effect of nifedipine on depolarization-induced force responses in skinned skeletal muscle fibres of rat and toad. *J Muscle Res Cell Motil* 19, 53-65 (1998)
14. Posterino, G. S., G. D. Lamb & D. G. Stephenson: Twitch and tetanic force responses and longitudinal propagation of action potentials in skinned skeletal muscle fibres of the rat. *J Physiol* 527, 131-137 (2000)
15. Fryer, M. W. & D. G. Stephenson: Total and sarcoplasmic reticulum calcium contents of skinned fibres from rat skeletal muscle. *J Physiol* 493, 357-370 (1996)
16. Owen, V. J., G. D. Lamb, D. G. Stephenson & M. W. Fryer: Relationship between depolarization-induced force responses and Ca<sup>2+</sup> content in skeletal muscle fibres of rat and toad. *J Physiol* 498, 571-586 (1997)
17. Stephenson, D. G., L. T. Nguyen & G. M. M. Stephenson: Glycogen content and excitation-contraction coupling in mechanically skinned fibres of the cane toad. *J Physiol* 519, 177-187 (1999)
18. Marx, S. O., K. Ondrias & A. R. Marks: Coupled gating between individual skeletal muscle Ca<sup>2+</sup> release channels (ryanodine receptors). *Science* 281, 818-821 (1998)
19. Posterino, G. S. & G. D. Lamb: Effects of reducing agents and oxidants on excitation-contraction coupling in skeletal muscle fibres of rat and toad. *J Physiol* 496, 809-825 (1996)
20. Lamb, G. D., E. Recupero & D. G. Stephenson: Effect of myoplasmic pH on excitation-contraction coupling in skeletal muscle fibres of the toad. *J Physiol* 448, 211-224 (1992)
21. Lamb, G. D. & D. G. Stephenson: Effect of intracellular pH and [Mg<sup>2+</sup>] on excitation-contraction coupling in skeletal muscle fibres of the rat. *J Physiol* 489, 331-339 (1994)
22. Lamb, G. D., G. S. Posterino, T. Yamamoto & N. Ikemoto: Effects of a domain peptide of the ryanodine receptor on Ca<sup>2+</sup> release in skinned skeletal muscle fibres. *Am J Physiol Cell Physiol* 281, C207-C214 (2001)
23. Lamb, G. D. & D. G. Stephenson: Effect of Mg<sup>2+</sup> on the control of Ca<sup>2+</sup> release in skeletal muscle fibres of the toad. *J Physiol* 434, 507-528 (1991)
24. Lamb, G. D. & D. G. Stephenson: Importance of Mg<sup>2+</sup> in excitation-contraction coupling in skeletal muscle. *News Physiol Sci* 7, 270-274 (1992)
25. Lamb, G. D.: Excitation-contraction coupling in skeletal muscle: comparisons with cardiac muscle. *Clinical Exp Pharmacol Physiol* 27, 216-224 (2000)
26. Duke, A. M. & D. S. Steele: Effects of caffeine and adenine nucleotides on Ca<sup>2+</sup> release by the

- sarcoplasmic reticulum in saponin-permeabilized frog skeletal muscle fibres. *J Physiol* 513, 43–53 (1998)
27. Murayama, T., N. Kurebayashi & Y. Ogawa: Role of  $Mg^{2+}$  in  $Ca^{2+}$ -induced  $Ca^{2+}$  release through ryanodine receptors of frog skeletal muscle: modulations by adenine nucleotides and caffeine. *Biophys J* 78, 1810–1824 (2000)
  28. Meissner, G., E. Darling & J. Eveleth: Kinetics of rapid  $Ca^{2+}$  release by sarcoplasmic reticulum. Effects of  $Ca^{2+}$ ,  $Mg^{2+}$  and adenine nucleotides. *Biochemistry* 25, 236–244 (1986)
  29. Meissner, G., E. Rousseau, F. A. Lai, Q. Y. Liu & K. A. Anderson: Biochemical characterisation of the  $Ca^{2+}$  release channel of skeletal and cardiac sarcoplasmic reticulum. *Mol Cell Biochem* 82, 59–65 (1988)
  30. Tanabe, T., K.G. Beam, B.A. Adams, T. Nicodome: & S. Numa: Regions of the skeletal muscle dihydropyridine receptor critical for excitation-contraction coupling. *Nature* 346, 567–569 (1990)
  31. Owen, V. J., G. D. Lamb & D. G. Stephenson: Effect of low [ATP] on depolarization-induced  $Ca^{2+}$  release in skeletal muscle fibres of the toad. *J Physiol* 493, 309–315 (1996)
  32. Blazev, R. & G. D. Lamb: Low [ATP] and elevated [ $Mg^{2+}$ ] reduce depolarization-induced  $Ca^{2+}$  release in rat skinned skeletal muscle fibres. *J Physiol* 520, 203–215 (1999)
  33. Dutka, T. L. & G. D. Lamb: Effect of low [ATP] on action-potential mediated  $Ca^{2+}$  release in fast-twitch muscle fibres. *XXXIV International Congress of Physiological Sciences poster* 665 (2001) <http://iups.esc.auckland.ac.nz/abstracts/pdfs/iabs-omi-057-2001-18-37-09.pdf>
  34. Blazev, R. & G. D. Lamb: Adenosine inhibits depolarization-induced  $Ca^{2+}$  release in mammalian skeletal muscle. *Muscle & Nerve* 22, 1674–1683 (1999)
  35. Laver, D. R., G. K. E. Lenz & G. D. Lamb: Regulation of the calcium release channel from rabbit skeletal muscle by the nucleotides ATP, AMP, IMP and adenosine. *J Physiol* (in press) (2001)
  36. Anderson, K. & G. Meissner: T-tubule depolarization-induced SR  $Ca^{2+}$  release is controlled by dihydropyridine receptor- and  $Ca^{2+}$ -dependent mechanisms in cell homogenates from rabbit skeletal muscle. *J Gen Physiol* 105, 363–383 (1995)
  37. Ogawa, Y.: Role of ryanodine receptors. *Crit Rev Biochem Mol Biol* 29, 229–274 (1994)
  38. O'Brien, J. J., P. D. Allen, K. Beam & S. R. W. Chen: Effect of mutation E4032A on the function of RYR1 expressed in HEK 293 cells and in dyspedic myotubes. *Biophys J* 76, A302 (1999)
  39. Laver, D. R., T. M. Baynes & A. F. Dulhunty: Magnesium-inhibition of ryanodine-receptor calcium channels: Evidence for two independent mechanisms. *J Memb Biol* 156, 213–229 (1997a)
  40. Balog, E. M., B. R. Fruen, N. H. Shomer & C. F. Louis: Divergent effect of the malignant hyperthermia-susceptible arg<sup>615</sup>→Cys mutation on the  $Ca^{2+}$  and  $Mg^{2+}$  dependence of the RYR1. *Biophys J* 81, 2050–2058 (2001)
  41. Lamb, G. D.:  $Ca^{2+}$ -inactivation,  $Mg^{2+}$ -inhibition and malignant hyperthermia. *J Muscle Res Cell Motil* 14, 554–556 (1993)
  42. Laver, D. R., V. J. Owen, P. R. Junankar, N. L. Taske, A. F. Dulhunty & G. D. Lamb: Reduced inhibitory effect of  $Mg^{2+}$  on ryanodine receptor -  $Ca^{2+}$  release channels in malignant hyperthermia. *Biophys J* 73, 1913–1924 (1997)
  43. Launikonis, B. S. & D. G. Stephenson: Effects of  $Mg^{2+}$  on  $Ca^{2+}$  release from sarcoplasmic reticulum of skeletal muscle fibres from yabby (crustacean) and rat. *J Physiol* 526, 200–312 (2000)
  44. Mejia-Alvarez, R., C. Kettlum, E. Rios, M. Stern & M. Fill: Unitary  $Ca^{2+}$  current through cardiac ryanodine receptor channels under quasi-physiological ionic conditions. *J Gen Physiol* 113, 177–186 (1999)
  45. Westerblad, H. & D. G. Allen: Myoplasmic free  $Mg^{2+}$  concentration during repetitive stimulation of single fibres from mouse skeletal muscle. *J Physiol* 453, 413–434 (1992)
  46. Jona, L., C. Szegedi, S. Sarkozi, P. Szentesi, L. Csernoch & L. Kovacs: Altered inhibition of the rat skeletal ryanodine receptor/calcium release channel by magnesium in the presence of ATP. *Pflugers Arch* 441, 729–738 (2001)
  47. Mack, M. M., T. F. Molinski, E. D. Buck & I. N. Pessah: Novel modulators of skeletal muscle FKBP12/calcium channel complex from *Ianthella basta*. *J Biol Chem* 269, 23236 – 23249 (1994)
  48. Sitsapesan, R. & A. J. Williams: Regulation of current flow through ryanodine receptors by luminal  $Ca^{2+}$ . *J Membr Bio* 159, 179–185 (1997)
  49. Nelson, T. E., M. Lin. & P. Volpe: Evidence for intraluminal  $Ca^{++}$  regulatory site defect in sarcoplasmic reticulum from malignant hyperthermia pig muscle. *J Pharmacol Exp Therap* 256, 645–649 (1991)
  50. Donoso, P., H. Prieto & C. Hidalgo: Luminal calcium regulates calcium release in triads isolated from frog and rabbit skeletal muscle. *Biophys J* 68, 507–515 (1995)
  51. Rousseau, E., J. LaDine, Y.Q. Liu & G. Meissner: Activation of  $Ca^{2+}$  release channel of skeletal muscle sarcoplasmic reticulum by caffeine and related compounds. *Arch Biochem Biophys* 267, 75–86 (1988)
  52. Donoso P. & C. Hidalgo: pH-sensitive calcium release in triads from frog skeletal muscle-rapid filtration studies. *J Biol Chem* 268, 25432–25438 (1993)
  53. Jurkat-Rott, K., T. McCarthy & F. Lehmann-Horn: Genetics and pathogenesis of malignant hyperthermia. *Muscle & Nerve* 23, 4–17 (2000)
  54. Owen, V. J., N. L. Taske, and G. D. Lamb: Reduced  $Mg^{2+}$  inhibition of  $Ca^{2+}$  release in muscle fibers of pigs susceptible to malignant hyperthermia. *Am J Physiol Cell Physiol* 272: C203–C211 (1997)
  55. Yamamoto, T., R. El-Hayek & N. Ikemoto. Postulated role of interdomain interaction within the ryanodine receptor in  $Ca^{2+}$  channel regulation. *J Biol Chem* 275, 11618–11625 (2000)
  56. Rios, E. & G. Pizarro: Voltage sensor of excitation-contraction coupling in skeletal muscle. *Physiol Rev* 71, 849–908 (1991)
  57. Schneider, M.F.: Control of calcium release in functioning muscle fibres. *Ann Rev Physiol* 56, 463–484 (1994)
  58. Pape, P. C., D-E. Jong & W.K. Chandler: Calcium release and its voltage dependence in frog cut muscle fibers equilibrated with 20 mM EGTA. *J Gen Physiol* 106, 259–336 (1995)
  59. Suda, N. & R. Penner: Membrane polarization stops caffeine-induced  $Ca^{2+}$  release in skeletal muscle cells. *Proc Natl Acad Sci USA* 91, 5725–5729 (1994)
  60. Jong, D. S., P. C. Pape, W. K. Chandler & S. M. Baylor: Reduction of calcium inactivation of sarcoplasmic reticulum calcium release by fura-2 in voltage-clamped cut twitch fibers from frog muscle. *J Gen Physiol* 102, 333–370 (1993)
  61. Pizarro, G., N. Shirokova, A. Tsugorka & E. Rios: “Quantal” calcium release operated by membrane voltage in frog skeletal muscle. *J Physiol* 501, 289–303 (1997)
  62. Laver, D.R. & G.D. Lamb: Inactivation of  $Ca^{2+}$  release channels (ryanodine receptors RYR1 and RYR2) with rapid steps in [ $Ca^{2+}$ ] and voltage. *Biophys J* 74, 2352–2364 (1998)
  63. Szentesi, P., L. Kovacs & L. Csernoch: Deterministic inactivation of calcium release channels in mammalian skeletal muscle. *J Physiol* 528, 447–456 (2000)
  64. Allen, D. G., J. Lännergren & H. Westerblad: Muscle cell function during prolonged activity: cellular mechanisms of fatigue. *Exp Physiol* 80, 497–527 (1995)
  65. Stephenson, D. G., Lamb, G. D. & Stephenson, G. M. M.: Events of the excitation-contraction-relaxation (E-C-R) cycle in fast- and slow- twitch mammalian muscle fibres relevant to muscle fatigue. *Acta Physiol Scand* 162: 229–245 (1998)
  66. Bruton, J. D., J. Lännergren & H. Westerblad: Effects of  $CO_2$ -induced acidification on the fatigue resistance of single mouse fibers at 28 degrees C. *J Appl Physiol* 85:478–483 (1998)
  67. Chin, E.R. & D.G. Allen: The contribution of pH-dependent mechanisms to fatigue at different

- intensities in mammalian single muscle fibres. *J Physiol* 512, 831-840 (1998)
68. Nielsen, O.B., F. dePaoli & K.Overgaard: Protective effects of lactic acid on force production in rat skeletal muscle. *J Physiol* 536, 161-166 (2001)
  69. Laver, D.R., K.R. Eager, L. Taoube & G.D. Lamb: Effects of cytoplasmic and luminal pH on Ca<sup>2+</sup> release from rabbit skeletal muscle. *Biophys J* 78, 1835-1851 (2000)
  70. Posterino, G. S., T.L. Dutka & G.D. Lamb: L(+)-lactate does not affect twitch and tetanic responses in mechanically skinned mammalian muscle fibres. *Pflügers Archiv* 442, 197-203(2001)
  71. Karatzaferi, C., A. de Haan, R. A. Ferguson, W. van Mechelen & A. J. Sargeant: Phosphocreatine and ATP content in human single muscle fibres before and after maximum dynamic exercise. *Pflügers Archiv* 442, 467-474 (2001)
  72. Fryer, M. W., V. J. Owen, G. D. Lamb & D. G. Stephenson: Effects of creatine phosphate and P<sub>i</sub> on Ca<sup>2+</sup> movements and tension development in reticulum calcium skinned skeletal muscle fibres. *J Physiol* 482, 123-140 (1995)
  73. Westerblad, H. & D. G. Allen: The effects of intracellular injections of phosphate on intracellular calcium and force in single fibres of mouse skeletal muscle. *Pflügers Archiv* 431, 964-970 (1996)
  74. Chin, E.R. & D.G. Allen: Effects of reduced muscle glycogen concentration on force, Ca<sup>2+</sup> release and contractile protein function in intact mouse skeletal muscle. *J Physiol* 498: 17-29 (1997)
  75. Chin, E.R. & D.G. Allen: The role of elevations in intracellular [Ca<sup>2+</sup>] in the development of low frequency fatigue in mouse single muscle fibres. *J Physiol* 491: 813-824 (1996)

**Running title:** Control of Ca<sup>2+</sup> release in muscle

**Key words:**

cell physiology  
skeletal muscle  
Ca<sup>2+</sup> release  
excitation-contraction coupling  
skinned fiber  
voltage-sensor

**Corresponding Author:**

Dr G. D. Lamb  
Department of Zoology, La Trobe University  
Victoria, 3086, Australia

Tel: (61)-3-94792249  
Fax: (61)-3-94791551  
E.mail: [zoogl@zoo.latrobe.edu.au](mailto:zoogl@zoo.latrobe.edu.au)

# Junctional Membrane Structure and Store Operated Calcium Entry in Muscle Cells

Jianjie Ma and Zui Pan

Department of Physiology and Biophysics, UMDNJ-Robert Wood Johnson Medical School Email: [maj2@umdnj.edu](mailto:maj2@umdnj.edu)

**ABSTRACT** The store-operated  $\text{Ca}^{2+}$  channel (SOC) located on the plasma membrane (PM) mediates capacitative entry of extracellular  $\text{Ca}^{2+}$  following depletion of intracellular  $\text{Ca}^{2+}$  stores in the endoplasmic or sarcoplasmic reticulum (ER/SR). It plays important roles in a variety of cell signaling processes, including proliferation, apoptosis, gene regulation and motility. In skeletal muscle, the L-type  $\text{Ca}^{2+}$  channel on the surface membrane has slow kinetics of activation in response to voltage stimulation, and therefore does not support entry of extracellular  $\text{Ca}^{2+}$ . Recent studies have provided functional evidence for the existence of SOC in muscle cells. Severe dysfunction of SOC is identified in muscle cells lacking either ryanodine receptors located on the SR membrane, or mitsugumin 29 - a membrane protein located in the triad junction of skeletal muscle. These results indicate that SOC activation requires an intact interaction between PM and SR, and is linked to conformational changes of ryanodine receptors. The cumulative entry of  $\text{Ca}^{2+}$  through SOC not only provides the mechanism for refilling of intracellular  $\text{Ca}^{2+}$  stores, but may also add to the  $\text{Ca}^{2+}$  needed for muscle contraction under conditions of intensive exercise and fatigue. The proper coupling of PM with ER/SR, in the triad junction in skeletal muscle or dyad junction in cardiac muscle, is essential not only for the membrane excitation-induced intracellular  $\text{Ca}^{2+}$  release but also for the store depletion-initiated capacitative  $\text{Ca}^{2+}$  entry.

## INTRODUCTION

$\text{Ca}^{2+}$  ions are important second messengers in many signal transduction pathways. They participate in essentially every cellular process, ranging from gene regulation and protein trafficking, to cell differentiation and apoptosis, to membrane excitability and cell motility. In general, there are two sources of this signaling ion in the cell: channels in the plasma membrane (PM) that open to allow external  $\text{Ca}^{2+}$  to flow into the cytoplasm, and internal stores in the form of endoplasmic reticulum (ER) or sarcoplasmic reticulum (SR) that release  $\text{Ca}^{2+}$  into the cytosol. The effective coupling of extracellular  $\text{Ca}^{2+}$  entry and intracellular  $\text{Ca}^{2+}$  release requires an intimate communication between PM and ER/SR.

In many excitable cells, entry of extracellular  $\text{Ca}^{2+}$  can be achieved via activation of voltage-gated  $\text{Ca}^{2+}$  channels by membrane depolarization. This initial  $\text{Ca}^{2+}$  signal is further amplified as the entering  $\text{Ca}^{2+}$  triggers additional mobilization of intracellular  $\text{Ca}^{2+}$  stores through activation of IP<sub>3</sub> receptor or ryanodine receptor (RyR) channels, a process known as  $\text{Ca}^{2+}$ -induced  $\text{Ca}^{2+}$  release (CICR) (5, 19, 90). In most non-excitable cells, the initial  $\text{Ca}^{2+}$  signal usually originates from release of  $\text{Ca}^{2+}$  from internal stores via activation of IP<sub>3</sub> receptors located on the ER. The entry of extracellular  $\text{Ca}^{2+}$  into non-excitable cells can be triggered by either direct activation through receptor molecules located on the PM or indirect activation by a variety of second messengers, in a process generally referred to as the receptor-operated  $\text{Ca}^{2+}$  entry (ROCE) pathway (28). Another commonly observed mechanism of regulated  $\text{Ca}^{2+}$  entry in non-excitable cells is a process known as the capacitative  $\text{Ca}^{2+}$  entry or store-operated  $\text{Ca}^{2+}$  entry (SOCE) (91). In this mechanism, the depletion of intracellular

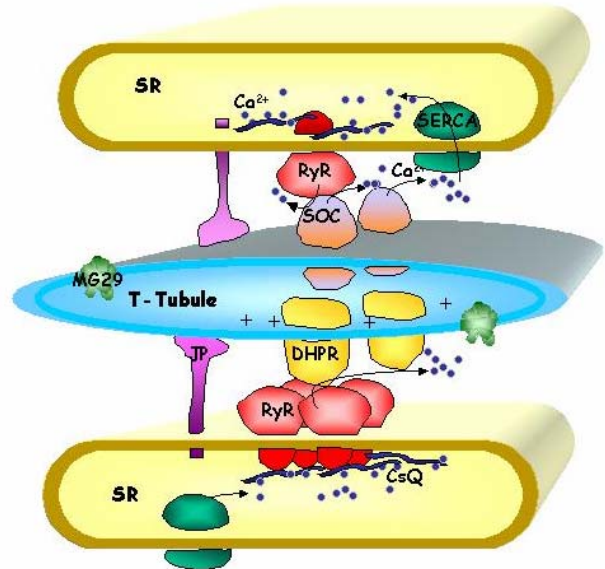


Figure 1. Molecular components of excitation-contraction coupling in muscle cells. A close contact of T-tubule and SR membrane is essential for the coupling of extracellular  $\text{Ca}^{2+}$  entry and intracellular  $\text{Ca}^{2+}$  release. The DHPR located on the T-tubule membrane functions as an L-type  $\text{Ca}^{2+}$  channel, as well as the voltage sensor of the plasma membrane. The RyR located on the SR membrane functions as the  $\text{Ca}^{2+}$  release channel. Junctophilins (JP) are proteins located in the SR membrane, and presumably provide the link of SR with plasma membrane for the formation of the triad junction. MG29 is a synaptophysin-family member protein located on the T-tubule membrane. The store-operated  $\text{Ca}^{2+}$  channel (SOC) resides on the T-tubule membrane that is in the close proximity of the RyR. Calsequestrin (CSQ) is a  $\text{Ca}^{2+}$  binding protein located in the SR lumen. SERCA  $\text{Ca}^{2+}$  pump is responsible for maintaining the high  $\text{Ca}^{2+}$  load in the SR membrane.

stores due to activation of IP<sub>3</sub> receptor or RyR or other Ca<sup>2+</sup>-releasing signals activates a signaling pathway leading to the opening of PM-located store-operated Ca<sup>2+</sup> channels.

In recent years, the SOCE pathway has received great interest not only because of its unusual nature as retrograde signaling, but also due to its wide occurrence in both excitable and non-excitable cells and its possible role in physiological and pathophysiological situations (9, 20, 27, 38, 81, 134). More recently, the capacitative Ca<sup>2+</sup> entry has been identified in skeletal and cardiac muscle cells, and its physiological functions are being recognized (34, 60, 80, 118).

### **Calcium movements in muscle cells – intracellular release and extracellular entry**

Coupling of electrical excitation across the PM to intracellular Ca<sup>2+</sup> release from the SR and subsequent muscle contraction (E-C coupling) occurs in the junction between the transverse-tubular (T-tubule) invagination of PM and the terminal cisternae of SR in a structure known as the “triad junction”, where two major protein components are located: the dihydropyridine receptors (DHPR), which function as voltage sensors of the T-tubule membrane, and the RyRs, which function as the Ca<sup>2+</sup> release channels in the SR (6, 7, 8, 22, 33, 68, 77) (see Figure 1). In skeletal muscle, the triad junction provides the structural framework for the interaction between DHPR and RyR that mediates direct signal transduction of voltage-induced Ca<sup>2+</sup> release (VICR). The operation of VICR in skeletal muscle appears to involve a direct physical interaction between DHPR and RyR, without requiring the transmembrane movement of extracellular Ca<sup>2+</sup> (95, 96, 99). In the heart, however, depolarization of PM initiates rapid Ca<sup>2+</sup> influx through activation of the DHPR/L-type Ca<sup>2+</sup> channel, which triggers opening of the RyR/Ca<sup>2+</sup> release channel via CICR (18, 66, 124). Peripheral coupling between PM and SR in the form of dyad junction mediates efficient communication from DHPR to RyR in the cardiac muscle.

The DHPR/L-type Ca<sup>2+</sup> channel located in the T-tubules of skeletal muscle has slow activation kinetics (23, 29, 67), and does not support Ca<sup>2+</sup> influx under normal physiological conditions. Therefore, the twitch force in skeletal muscle is triggered mainly by the acute release of Ca<sup>2+</sup> from the SR, primarily via VICR, and secondarily amplified by CICR through activation of neighboring RyRs not directly coupled to DHPR (96, 99). The internal Ca<sup>2+</sup> stores located in the SR of muscle cells and ER of other cells have a limited capacity for Ca<sup>2+</sup> storage. As a result, cells possess the capability of SOCE as a means of renewing depleted intracellular Ca<sup>2+</sup>. Although evidence indicates that physical docking of ER with PM is involved in the activation of SOC, the molecules and/or signals that couple ER/SR Ca<sup>2+</sup> depletion to opening of SOC remain largely unknown (82, 92, 93).

### **Transient receptor potential proteins (TRP) and store-operated Ca<sup>2+</sup> channel**

The initial leads to identify the molecular basis of SOCE were provided by the study of phototransduction in *Drosophila melanogaster*. Work in *Drosophila* photoreceptors showed that mutations in a protein encoded by the *trp* gene were associated with a defect in Ca<sup>2+</sup> entry following light stimulation (70, 87, 128). Expression of TRP in a baculovirus system produced Ca<sup>2+</sup> currents when intracellular Ca<sup>2+</sup> stores were depleted with thapsigargin (TG), a result indicative of a role of TRP in mediating SOCE (85, 120). To date, seven mammalian homologues bearing 35-43% identity to the *Drosophila* TRP have been cloned and termed TRP-canonical or TRPC1-7 (9, 11, 14, 78, 79, 138, 139). A common characteristic of all TRPC proteins is that they form Ca<sup>2+</sup>-permeable nonselective cation channels. Functional studies using various heterologous expression systems have provided evidence supporting the role of TRPCs in SOCE and/or ROCE. First, all TRPCs mediate Ca<sup>2+</sup> entry in response to phospholipase C (PLC) stimulation by receptor agonists (9). Second, TRPC1, 2, 4 and 5 are activated by TG (64, 88, 89, 121, 126). Third, activities of endogenous SOCs were inhibited by antisense TRPC1 oligonucleotides, by expression of antisense RNA of TRPCs (64, 86, 138), or by treatment with antibodies against TRPC1 or TRPC2 (130). Fourth, expression of the amino-terminus of TRPC3 inhibited the endogenous SOCE in human endothelium in a dominant-negative manner (41). Finally, TRPC4 knockout mice showed reduced vasorelaxation in association with diminished store-operated Ca<sup>2+</sup> currents in aortic endothelium (35).

The conundrum is that TG does not always activate TRPC-based channels. In most cells, the channels formed by TRPC3, 6, and 7 appear to be largely insensitive to TG but respond very well to the stimulation of PLC (10, 78, 137). However, in chicken DT40 cells, heterologous expression of human TRPC3 seem to lead to TG-stimulated Ba<sup>2+</sup> influx (122). TRPC4 and TRPC5 have been shown to be store-operated channels by some research groups (86, 126), but not by others (78, 98, 104). The discrepancies may reflect the complexity of SOCs both in subunit composition and in functional regulation. Native SOCs may contain four non-identical TRPC subunits or TRPC plus other unidentified subunits [54]. Channels formed due to over-expression of a single TRPC type could have anomalous compositions, leading to abnormal single channel conductance, ion selectivity, pharmacological profiles, and sensitivity to some essential regulatory elements (93). In the case of *Drosophila* TRP-like and TRP<sub>γ</sub>, a SOC was formed when both were expressed together, but not when each TRP was expressed individually (129, 131). Thus, it remains a challenge to find the “right” mix of TRPC proteins to make a channel with the same properties as the Ca<sup>2+</sup> release-activated Ca<sup>2+</sup> (CRAC) channel, the best characterized SOC (46, 81, 140).

Channel-like proteins distantly related to TRPCs have also been cloned. They are now collectively called members of the TRP superfamily and are further classified according to their sequence homology into four subfamilies: TRPV, TRPM, TRPP, and TRPML (20, 71). Some of them have been

suggested to participate in the formation of SOCs. For example, TRPV6 (CaT1) was shown to be similar to the CRAC channel when expressed in HEK 293 cells (135). However, a more recent study argues that it has a quite distinct pore property from the CRAC channel (123). Members of the TRPV subfamily form heat-activated channels (capsaicin receptor, TRPV1, and TRPV2) (16,17), stretch-inactivated or osmolarity-regulated channels (OTRPC4 or TRPV4) (103, 108, 127), a growth factor-regulated channel (GRC, the same sequence as TRPV2) (52), and Ca<sup>2+</sup> transporting epithelial channels (ECaC or CaT: TRPV5 and TRPV6) (45, 83, 84). A number of TRP proteins are implicated in etiology of human diseases, such as autosomal dominant polycystic kidney disease (PC2 or TRPP1) (117), metastatic melanoma (melastatin, or TRPM1) (44), and mucopolidosis type IV (mucopolin or TRPML1) (3, 106).

### **Activation of store-operated Ca<sup>2+</sup> channel – cross talk between cell surface and intracellular membranes**

The activation mechanism of SOCs is an unresolved problem. Three major hypotheses have been proposed. First, a small diffusible factor may be responsible for activating SOCs. A Ca<sup>2+</sup> influx factor seems to be present in the acid extracts of activated Jurkat cells and platelets, or a Ca<sup>2+</sup> store-depleted yeast mutant strain (24, 94, 116), but its identity has not been determined. Second, IP<sub>3</sub>Rs may directly bind to the SOCs and activate them through a conformational coupling mechanism (48), in a manner similar to the activation of skeletal muscle RyR by the DHPR in E-C coupling (95, 96, 99). Third, insertion of preformed channel-containing vesicles in the PM in a fashion similar to the secretion of neurotransmitters may be required for the activation of SOCs (133).

During the past few years, increasing evidence has accumulated supporting the conformational coupling hypothesis, owing mainly to studies conducted on TRPC channels. Functional coupling by IP<sub>3</sub>Rs was first shown for TRPC3 expressed in HEK293 cells (55) and then for a native SOC found in A431 epithelium (53). These were followed by the demonstration that IP<sub>3</sub>Rs and TRPC proteins coimmunoprecipitated in several systems (10, 56, 65, 97) and finally the identification of IP<sub>3</sub>R-TRPC binding domains (10, 115, 136). Additional evidence also suggests that RyRs could substitute for the IP<sub>3</sub>Rs to activate TRPC3 and native SOCs (57, 58). Moreover, the binding of IP<sub>3</sub>Rs to TRPCs is inhibited by calmodulin, which prevents the channels from being spontaneously active, and inactivates the channels after they are activated (115, 136). Therefore, Ca<sup>2+</sup> release channels, IP<sub>3</sub>Rs and RyRs, and calmodulin appear to control the gating of SOCs through direct interaction with TRPC proteins.

### **JUNCTOPHILINS AND MITSUGUMINS – LINKERS OF JUNCTIONAL STRUCTURE BETWEEN CELL SURFACE AND INTRACELLULAR MEMBRANES**

Perhaps the best studied example of Ca<sup>2+</sup> signaling is that defined by VICR in skeletal muscle. Research over the past 30 years or so has defined

certain key molecular components involved in E-C coupling (see Figure 1), and has also begun to elucidate the machinery underlying the signal transduction step from activation of DHPR to activation of RyR (77). A central focus in current E-C coupling research is to understand the molecular and structural components that define the close T-tubule/SR interaction, and to study the roles of accessory proteins that may interact with DHPR or RyR to modulate the VICR, CICR, and SOCE.

In addition to DHPRs and RyRs, other proteins of the T-tubule/SR junction also play critical roles in muscle E-C coupling. Transgenic mice that lack expression of either DHPRs or RyRs still form seemingly normal triad junctions (32, 47), indicating that structural components other than the DHPR/RyR interaction are needed for a close apposition of T-tubules and SR membranes. Chinese hamster ovary (CHO) cells transfected with both DHPR and RyR cDNAs showed neither Ca<sup>2+</sup> release in response to membrane depolarization, nor close association between the PM and ER (105, 107, 109). Thus, the DHPR/RyR interaction is neither necessary nor sufficient for the formation of triad and dyad junctions. Although several transmembrane proteins with no established physiological roles have been identified as components of triad junctions (42, 50), none appears to be a candidate molecule for mediating the physiological coupling of the junctional complex. Furthermore, the gap size between T-tubule and SR was reduced when the triad lacked RyRs (from ~12 nm in normal muscle to ~7 nm in *ryr1(-/-)ryr3(-/-)* muscle) (47), suggesting an elastic property of the proposed bridge between the two junctional membranes.

In an attempt to identify structural components supportive of triad junction-like membrane arrangements, Takeshima and colleagues have used a combination of monoclonal antibody immunocytochemistry and cDNA library screening techniques, and identified a group of novel membrane proteins termed mitsugumins and junctophilins that in cardiac and skeletal muscle are exclusively localized to the triad and dyad junctions, respectively (75, 76, 113, 114).

### **Mitsugumin 29 and transverse tubule structure in skeletal muscle**

Mitsugumin29 (MG29) is a synaptophysin-family member protein, with a molecular weight of 29 kDa, localized specifically in the triad junction of skeletal muscle, and to a lesser extent also present in the tubular membranes of the kidney (113). In mature skeletal muscle, MG29 is present predominantly on the T-tubule membrane (12, 59). Similar to other synaptophysin family proteins, MG29 forms an oligomeric structure - a homohexamer (13), that may be essential for the function of MG29 in muscle development and contraction.

To examine the physiological function of MG29, Nishi et al have created a mutant mouse with targeted disruption of the *mg29* gene (75). Abnormalities of membrane ultrastructure around the triad junction were detected in skeletal muscle from

the *mg29(-/-)* mice: the T-tubules were swollen and sometimes missing from the A-I junction, and the SR networks were poorly formed with vacuolated and fragmented structures, leading to misalignment of triad junctions (see Figure 4). In the *mg29(-/-)* muscle, apparently normal tetanus tension was observed, whereas twitch tension was significantly reduced. Interestingly, the mutant muscle showed faster decrease of twitch tension under  $\text{Ca}^{2+}$ -free conditions compared with the control muscle (75). The morphological and functional abnormalities of the mutant muscle indicate that MG29 is essential for both refinement of the membrane structure and effective E-C coupling in skeletal muscle.

### **Junctophilin type 1 (JP1) and triad junction in skeletal muscle**

A family of membrane proteins named junctophilins (JP) was identified as the major protein components at junctional membrane complexes in excitable cells (114). Three subtypes of JP have been identified, JP1, JP2 and JP3, which exhibit tissue specific distribution. JP1 is predominantly expressed in skeletal muscle, JP2 is distributed in both skeletal and heart muscles, and JP3 is abundantly expressed in the brain and testis. The lung and stomach, tissues containing smooth muscle, showed weak hybridization signals with the JP2-specific probe, suggesting expression of JP2 in smooth muscle cells as well (114).

The primary amino acid sequence of JP proteins revealed a unique secondary structure with a large cytoplasmic region and a carboxyl-terminal transmembrane segment spanning the SR/ER. The cytoplasmic region of JP contains repeated motifs of 14 amino acid residues termed "membrane occupation and recognition nexus" or MORN motifs, and exhibit selective binding affinity to the plasma membrane. The MORN motif is a novel protein-folding module shared by functionally different proteins and probably having a specific physiological role.

Electron microscopy revealed junctional complexes between the ER and PM in cells expressing JP1 (114). The average gap size between PM and ER in the junctional structure was  $\sim 7.6$  nm. When a soluble form of JP1 lacking the carboxy-terminal transmembrane segment was expressed, immunolabeling was detected specifically at the PM, but lacked ER-PM junction. This demonstrates a specific binding affinity of the cytoplasmic domain of JP1 for the PM. The JP1 mediated junctional complexes showed structural characteristics similar to those of the peripheral coupling detected commonly in muscle cell types. The gap between T-tubule and SR in the triad junction from normal muscle is  $\sim 12$  nm, whereas the mutant muscle lacking RyR has a gap size of  $\sim 7$  nm. This suggests that RyR likely restricts the gap size. Since the "foot" structure of RyR is absent in heterologous cells expressing JP1, the gap size of 7.6 nm probably correspond to that of the mutant triad junction lacking RyR. Together, these studies suggest that the JP family proteins, by their nature of specific anchorage to the SR/ER membrane and selective interaction with the PM, may play

essential roles in the formation of junctional membrane complexes.

To examine the physiological role of JP1 in skeletal muscle, Ito et al (49) have generated mutant mice lacking JP1. The JP1 knockout mice showed no milk suckling and died shortly after birth. Ultrastructural analysis demonstrated that triad junctions were reduced in number, and that the SR was often structurally abnormal in the skeletal muscles of the mutant mice. The mutant muscle developed less contractile force evoked by low-frequency electrical stimuli and showed abnormal sensitivities to extracellular  $\text{Ca}^{2+}$ . These data indicate that JP1 contributes to the construction of triad junctions and is essential for the efficiency of signal conversion during E-C coupling in skeletal muscle.

### **Junctophilin type 2 (JP2) and dyad junction in cardiac muscle**

JP2 is abundantly expressed in the heart. It appears to be essential for dyad junction formation because disruption of its expression in mice produces embryonic lethality, as a result of defective junctional membrane coupling and unsynchronized intracellular  $\text{Ca}^{2+}$  transients (114). To survey functional abnormalities in the *jp2(-/-)* mice, the hearts from E9.5 embryos were subjected to  $\text{Ca}^{2+}$ -imaging analysis using an intracellular  $\text{Ca}^{2+}$  indicator. In wild-type hearts, all of the myocytes showed spontaneous and synchronized  $\text{Ca}^{2+}$  transients, and the transients disappeared in a  $\text{Ca}^{2+}$ -free bathing solution, because cardiac E-C coupling requires  $\text{Ca}^{2+}$  influx via DHPR. However, in mutant hearts from the *jp2(-/-)* embryos, a large number of myocytes showed irregular  $\text{Ca}^{2+}$  transients that were not synchronized with heartbeats and occurred randomly. The random transients were even retained in the  $\text{Ca}^{2+}$ -free bathing solution, albeit with reduced frequency. Therefore, the abnormal  $\text{Ca}^{2+}$  transients in the mutant hearts are primarily independent of  $\text{Ca}^{2+}$  influx through DHPR.

Deficiency of peripheral coupling, observed in the mutant myocytes prior to cardiac arrest, supports the notion that JP proteins contribute to the formation of junctional membrane complexes in various cell types. Generation of the junctional structure may require at least two processes: first the SR and PM must approach each other, and then the JP proteins anchor the two membranes together in a stable complex. A few peripheral couplings retained in the *jp2(-/-)* myocytes might correspond to an unstable form of the junctional membrane complexes that is junctophilin-independent. Alternatively, other JP subtypes might contribute to the formation of the peripheral coupling in the *jp2(-/-)* myocytes, i.e. low levels of JP1 expression in the adult hearts were suggested by Northern blot analysis.

The deficient junctional membrane structure and abnormal intracellular  $\text{Ca}^{2+}$  transients observed in cardiac myocytes of the JP2 knockout mice resemble some of the functional changes associated with diseased human heart, i.e., widening of the dyadic membrane cleft and reduced efficiency of intracellular  $\text{Ca}^{2+}$  release measured in congestive

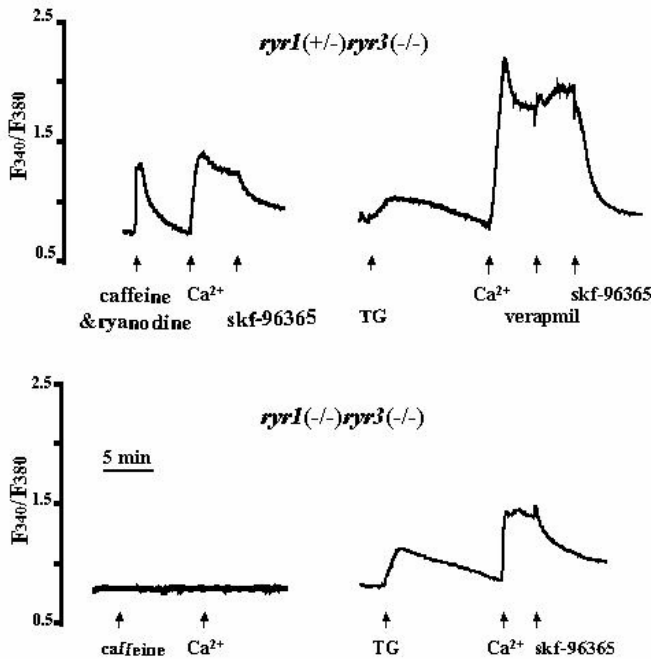


Figure 2. Ryanodine receptor-mediated activation of store-operated  $\text{Ca}^{2+}$  channel in skeletal muscle. In *ryr1(+/-)ryr3(-/-)* myotubes, inhibition of the SERCA  $\text{Ca}^{2+}$  pump by 10  $\mu\text{M}$  thapsigargin (TG), or activation of RyR/ $\text{Ca}^{2+}$  release channel by caffeine and ryanodine resulted in depletion of SR  $\text{Ca}^{2+}$ , and triggered store-operated  $\text{Ca}^{2+}$  entry (SOCE) after addition of 2 mM  $[\text{Ca}^{2+}]_o$ . A large component of SOCE was sensitive to blockade by 20  $\mu\text{M}$  SKF-96365 but not by 50  $\mu\text{M}$  verapamil. In *ryr1(-/-)ryr3(-/-)* cells, caffeine could not induce  $\text{Ca}^{2+}$  release from SR due to the lack of RyR1 and RyR3. The amplitude of SOCE in *ryr1(-/-)ryr3(-/-)* myotubes was significantly smaller than that in *ryr1(+/-)ryr3(-/-)* myotubes, when the SR  $\text{Ca}^{2+}$  store was completely depleted with TG.

heart failure (CHF) (40, 43). Although the pathogenesis of CHF is probably multi-factorial, alterations in E-C coupling are a central finding in all animal models of CHF and in failing human heart. Presumably, mutations or altered expression of mitsugumins might induce human diseases by affecting the  $\text{Ca}^{2+}$  signaling of excitable cells.

### RYANODINE RECEPTOR-MEDIATED ACTIVATION OF STORE-OPERATED $\text{Ca}^{2+}$ CHANNEL

Conformation coupling between  $\text{IP}_3$  receptors and SOCs is analogous to E-C coupling between DHPRs and RyRs in skeletal muscle. A retrograde interaction between RyR and DHPR also exists in skeletal muscle, as the absence of RyR hinders the function of DHPR (30, 73). Of the three known RyR isoforms, RyR1, expressed in skeletal muscle, is the only one capable of interacting with DHPR. RyR2, the cardiac isoform, is not capable of coupling to DHPR (74, 112). RyR3, widely expressed in both excitable and nonexcitable cells and whose main function appear to be limited to CICR, is not known to interact directly with a DHPR (21, 31, 102, 125, 132).

Growing evidence suggests that  $\text{Ca}^{2+}$  stores of many nonmuscle cells, including neurons (2), neuroendocrine (4), lymphocytes (39, 100) and epithelial cells (62) express RyRs. Thus,

pharmacological agents such as caffeine and the second messenger cADPR (61) can release  $\text{Ca}^{2+}$  from internal stores of these cells. Furthermore,  $\text{Ca}^{2+}$  release by activation of RyRs in nonmuscle cells activates SOCE in a manner similar to  $\text{Ca}^{2+}$  release from the  $\text{IP}_3$ -sensitive stores (4, 119). The functional coupling between RyR and SOC, if it exists, is likely to be influenced by the structural interaction between PM and SR. In the case of muscle cells, those proteins participate in the formation of dyad and triad junction, e.g. mitsugumins and junctophilins may modulate the interaction between RyR and SOC and the overall  $\text{Ca}^{2+}$  signaling process.

### Interaction between TRP and ryanodine receptor

Using co-expression and reconstitution studies, Kiselyov et al. (57) provided direct evidence supporting a conformational coupling between RyR and SOC in non-excitable cells.  $\text{Ca}^{2+}$  release from RyR-sensitive stores was shown to activate TRPC3 channels in electrophysiological measurements. And the RyR-TRPC3 complex can be demonstrated in co-immunoprecipitation studies. Furthermore, the coupling appears to be specific for RyR1, since RyR2 did not appear to interact with TRPC3 and to gate the channel. The data show that regulation of SOC or ROC by RyRs is not unique to skeletal muscle. Thus, the gating of PM  $\text{Ca}^{2+}$  channels by intracellular  $\text{Ca}^{2+}$  release channels may be viewed as a general and widespread paradigm in  $\text{Ca}^{2+}$  signaling.

### Dysfunction of SOC in muscle cells lacking RyR1 and RyR3

The first direct demonstration of SOCE in skeletal muscle was provided by Kurebayashi and Ogawa (60). They used muscle fibers isolated from the extensor digitorum longus (EDL) of adult mice, and depleted the SR  $\text{Ca}^{2+}$  stores by repetitive treatments with high- $\text{K}^+$  solutions in combination with inhibitors of the SERCA  $\text{Ca}^{2+}$  pump. The SOCE in skeletal muscle was sensitive to blockade by  $\text{Ni}^{2+}$ , resistant to nifedipine, and suppressed by plasma membrane depolarization. This SOCE pathway is sufficient to refill the depleted SR  $\text{Ca}^{2+}$  store within several minutes in skeletal muscle fibers. The  $\text{Mn}^{2+}$  influx through SOC measured by quenching of Fura-2 fluorescence was observed only when the SR was severely depleted of  $\text{Ca}^{2+}$ . The voltage-dependence of SOCE in skeletal muscle exhibited inward rectification, which was similar to the CRAC current described in other preparations (46).

To test the putative regulation of SOC by RyR in muscle cells, we used primary cultured myotubes derived from neonates of the *ryr1(-/-)ryr3(-/-)* and *ryr1(+/-)ryr3(-/-)* mice (110, 111). It is known that deletion of either RyR1 or RyR3 does not disrupt the triad junction structure (47). Therefore, the *ryr1(-/-)ryr3(-/-)* and *ryr1(+/-)ryr3(-/-)* mice offer unique models to examine the potential regulation of SOC by RyR1, the main isoform of RyR present in skeletal muscle. The *ryr1(+/-)ryr3(-/-)* myotubes responded to caffeine stimulation with rapid release of  $\text{Ca}^{2+}$  from SR (Figure 2). SOCE was observed upon addition of 2

mM  $[Ca^{2+}]_o$ . Simultaneous application of caffeine and ryanodine, ligands that induce permanent opening of the RyR/ $Ca^{2+}$  release channel, resulted in SR  $Ca^{2+}$  release similar to caffeine alone, but the extent of SOCE was significantly larger. TG, a potent inhibitor of the SR  $Ca^{2+}$  pump, produced sustained depletion of  $Ca^{2+}$  from SR and induced even greater activation of SOCE in *ryr1(+/-)ryr3(-/-)* cells. Near complete inhibition of SOCE in *ryr1(+/-)ryr3(-/-)* cells was observed upon addition of 20  $\mu$ M SKF 96365, a known blocker of SOC (63, 69). The *ryr1(-/-)ryr3(-/-)* myotube, lacking both *ryr1* and *ryr3*, failed to respond to caffeine or ryanodine, but contained TG-sensitive SR  $Ca^{2+}$  store similar to that present in *ryr1(+/-)ryr3(-/-)* cells. SOC activity in *ryr1(-/-)ryr3(-/-)* cells, however, was significantly smaller than that in *ryr1(+/-)ryr3(-/-)* cells. After depletion of SR  $Ca^{2+}$  with thapsigargin, *ryr1(-/-)ryr3(-/-)* cells exhibited a residual component of SOCE (~40% of that present in *ryr1(+/-)ryr3(-/-)* cells), which was partially sensitive to inhibition by SKF 96365 (Figure 2).

Our data provide direct evidence for a RyR-coupled activation of SOC in skeletal muscle. Based on the different degree of SOCE triggered by caffeine, caffeine and ryanodine, or TG in *ryr1(+/-)ryr3(-/-)* cells, we conclude that SOCs in skeletal muscle can function in a graded manner depending on the SR  $Ca^{2+}$  content or the conformation of RyR (80).

## STORE-OPERATED $Ca^{2+}$ ENTRY AND MUSCLE FATIGUE

### Involvement of extracellular $Ca^{2+}$ entry in muscle fatigue

Fatigue is an important functional property of skeletal muscle, and is defined as a reversible decrease in the isometric contractile force in response to an increase in the frequency or duration of stimulation (1). Optimal muscle performance revolves around the maintenance of intracellular  $Ca^{2+}$  homeostasis, such that inadequate  $Ca^{2+}$  release from the SR would lead to reduced force output observed in muscle fatigue. The decline in intracellular  $Ca^{2+}$  release could result from improper coupling between DHPR and RyR, reduction of the SR  $Ca^{2+}$  content, direct modification of RyR function, or dysfunction of SOCE.

Experiments with intact muscle fiber show that the size of the  $Ca^{2+}$  store declines during fatigue and recovers upon rest (1). With skinned muscle fiber preparation, it was shown that increased intracellular phosphate can lead to reduction of  $Ca^{2+}$  released from the SR (36, 37). Skeletal muscles which lack the enzyme creatine kinase, do not exhibit the usual rise of phosphate during fatigue and, under these conditions, the decline of  $Ca^{2+}$  release is absent or delayed (25, 26). It has been suggested that the rise in myoplasmic phosphate can lead to  $Ca^{2+}$ -phosphate precipitation within the SR, and the resultant reduction in free  $Ca^{2+}$  within the SR would contribute to the reduced  $Ca^{2+}$  release during fatigue (1, 51).

It is well known that  $[Ca^{2+}]_o$  is essential for priming of the DHPR/voltage sensor in the active state

(15), but the demonstration of a functional role for extracellular  $Ca^{2+}$  influx in skeletal muscle E-C coupling has eluded detection despite being well studied. Although the twitch force initiated by a single electrical stimulation does not depend on the movement of extracellular  $Ca^{2+}$ , the fatigue pattern of isolated muscle fibers shows a clear dependence on extracellular  $Ca^{2+}$  (Figure 3). Changing the bath solution from 2 mM  $[Ca^{2+}]_o$  to 0  $[Ca^{2+}]_o$  significantly increased the fatigability of the muscle, as indicated by the reduction in the sustained force output at the end of the tetanic stimulation. The reduction of SR  $Ca^{2+}$  stores associated with muscle fatigue can trigger the activation of SOCE, which could play a role in the overall  $Ca^{2+}$  handling properties of skeletal muscle. By blocking the SOCE pathway with SKF-96365, one observes a significant change in the fatigue behavior of skeletal muscle (Figure 3).

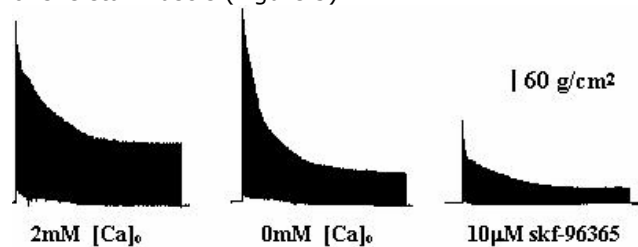


Figure 3. Involvement of extracellular  $Ca^{2+}$  entry in muscle fatigue. Differential fatigability of soleus muscles were observed with tetanic stimulation at a frequency that produced maximum force output (80 Hz), either in the presence of 2 mM  $[Ca^{2+}]_o$  (left panel), 0  $Ca^{2+}$  plus 0.5 mM EGTA (middle panel), or 2 mM  $[Ca^{2+}]_o$  plus 10  $\mu$ M SKF-96365 (right panel). The degree of fatigue was significantly higher with the removal of  $Ca^{2+}$  from the extracellular solution, or after inhibition of the SOCE by SKF-96365. See refs 72 and 80 for more details.

### Dysfunction of SOC and muscle fatigue in *mg29(-/-)* muscle

Unlike the normal skeletal muscle whose E-C coupling machinery does not rely on the entry of extracellular  $Ca^{2+}$ , skeletal muscle from the mutant *mg29(-/-)* mice exhibits clear dependence on extracellular  $Ca^{2+}$  for contraction (75, 80). As MG29 is involved in the coupling between T-tubule and SR, presumably the expression of MG29 will have functional impact on the RyR-mediated activation of SOC in muscle cells.

A distinct phenotype of the *mg29(-/-)* mice is their failure to complete an endurance test, i.e., their skeletal muscles exhibit increased susceptibility to fatigue. Nagaraj et al (72) showed that muscle fibers isolated from the *mg29(-/-)* not only fatigued to a greater extent, but also recovered significantly less than the wild type muscles. Following fatigue, the mutant EDL and soleus muscles produced lower twitch forces than the wild-type muscles. Additionally, fatiguing produced a rightward shift in the force-frequency relationship in the mutant mice compared with the wild type controls.

Quantitative measurements of intracellular

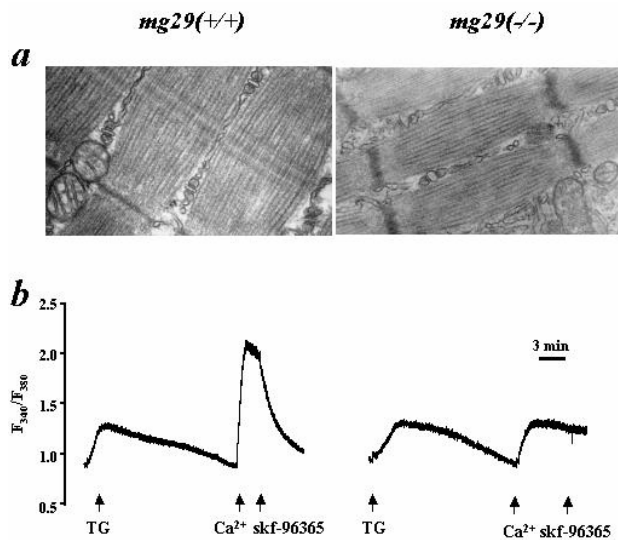


Figure 4. Dysfunction of store-operated  $\text{Ca}^{2+}$  channel in muscle cells lacking MG29. a. Abnormal membrane structure in skeletal muscle from  $mg29(-/-)$  mice. Electron micrographs revealed swollen T-tubules and vacuolated SR networks in  $mg29(-/-)$  muscle (right panel) compared with the wild type control or  $mg29(+/+)$  muscle (left panel). b. SOCE in individual skeletal muscle myotubes was significantly lower in  $mg29(-/-)$  cells, compared with that in  $mg29(+/+)$  cells. A large component of SOCE in  $mg29(+/+)$  cells was sensitive to blockade by SKF-96365 (20  $\mu\text{M}$ ), but not by verapamil.

$[\text{Ca}^{2+}]_i$  with Fura-2 fluorescent indicator in individual myotubes derived from different mutant mice enabled us to identify a defective regulation of SOC in  $mg29(-/-)$  cells, and begin to define the mechanism of SOC operation in skeletal muscle (80). As shown in Figure 4, treatment of cells with TG in 0  $[\text{Ca}^{2+}]_o$  solution induced measurable SOCE in both control and  $mg29(-/-)$  cells after addition of 2 mM  $[\text{Ca}^{2+}]_o$ . Note that the extent of SOCE in  $mg29(-/-)$  cells is less than 40% of that seen in control cells. SKF-96365, a known blocker of SOC, blocked this SOCE in control cells by >90%. In contrast, the SKF-sensitive component of CCE is severely compromised in  $mg29(-/-)$  cells. Further studies show that the  $mg29(+/+)$  and  $mg29(-/-)$  muscles showed comparable responses to fatigue stimulation at 0  $[\text{Ca}^{2+}]_o$  and after inhibition of SOC with SKF-96365. This suggests that the increased susceptibility to fatigue stimulation is likely a consequence of dysfunction of SOC in  $mg29(-/-)$  muscle cells.

#### PERSPECTIVE – EMERGING QUESTIONS OF SOC FUNCTION IN $\text{Ca}^{2+}$ HOMEOSTASIS OF MUSCLE CELLS

In recent years, much research has focused on the mechanism linking depletion of intracellular  $\text{Ca}^{2+}$  stores to the activation of plasma membrane  $\text{Ca}^{2+}$  channels. Most of the studies were performed with non-excitabile cells. There is considerable evidence for a conformational coupling mechanism by which depletion of intracellular  $\text{Ca}^{2+}$  stores induces a conformational change in  $\text{IP}_3$  receptor or RyR, which interacts with and activates a plasma membrane  $\text{Ca}^{2+}$  channel. A close association between T-tubules of PM

and terminal cisternae of SR not only determines the spatial coupling between DHPR and  $\text{Ca}^{2+}$  release channel, but also fine tunes the efficacy of  $\text{Ca}^{2+}$  signaling in muscle cells. It remains to be studied how the JP proteins affect the retrograde  $\text{Ca}^{2+}$  signaling in muscle and other excitable cells.

At present, the TRPs remain the most popular candidate protein for SOC. There is evidence that channels formed by TRP proteins can be gated by  $\text{Ca}^{2+}$  store depletion, although this is not consistent in all studies. However, it seems clear that none of the TRPs so far studied shows the properties required for  $\text{I}_{\text{CRAC}}$ . The key missing property is  $\text{Ca}^{2+}$  selectivity, which has not been observed for any TRPC family member. It is highly possible that the molecular entity determining SOC may consist of a macromolecular complex that spans the cell surface and intracellular membranes, i.e. a multimeric structure.

In summary, significant progresses have been made in elucidating the physiological roles of SOCE and ROCE. In particular, in the process of cell proliferation, apoptosis and smooth muscle contraction, the role of SOCE has been well documented. In striated muscle cells, we now know that SOC participates in muscle fatigue. We do not yet know how alteration of SOC could affect long term muscle development and gene adaptation. Identification of the molecular components of SOC remains the key task for future studies.

#### ACKNOWLEDGEMENTS

We greatly appreciate our previous and present collaborators for their contribution to this study. In particular, we thank Dr. Mike Zhu for sharing his initial thoughts on the study with TRP channels with us. Our studies were supported by grants from the National Institutes of Health (RO1-AG15556, RO1-CA95379, and RO1-HL69000), and the American Heart Association.

#### References

- Allen, D.G., and Westerblad, H.: Role of phosphate and calcium stores in muscle fatigue. *J. Physiol.* 536, 657-665 (2001)
- Balschun, D., Wolfer, D.P., Bertocchini, F., Barone, V., Conti, A., Zuschratter, W., Missiaen, L., Lipp, H.P., Frey, J.U., and Sorrentino, V.: Deletion of the ryanodine receptor type 3 (RyR3) impairs forms of synaptic plasticity and spatial learning. *EMBO J.* 18, 5264-5273. (1999)
- Bargal, R., Avidan, N., Ben-Asher, E., Olender, Z., Zeigler, M., Frumkin, A., Raas-Rothschild, A., Glusman, G., Lancet, D. and Bach, G.: Identification of the gene causing mucopolipidosis type IV. *Nat. Genet.* 26, 118-123, (2000)
- Bennett, D.L., Bootman, M.D., Berridge, M.J., and Cheek, T.R.:  $\text{Ca}^{2+}$  entry into PC12 cells initiated by ryanodine receptors or inositol1,4,5-trisphosphate receptors: *J. Biochem.* 329, 349-357. (1998)
- Berridge, M. J.: Neuronal calcium signaling. *Neuron* 21, 13-26. (1998)
- Bhat, M.B., Zhao, J., Takeshima, H., and Ma, J. Functional calcium release channel formed by the carboxyl-terminal portion of ryanodine receptor: *Biophys. J.* 73, 1329-1336. (1997)
- Bhat, M.B., Zang, W., Takeshima, H., Wier, W.G., and Ma, J.: Caffeine-induced release of intracellular  $\text{Ca}^{2+}$  from chinese hamster ovary cells expressing the skeletal muscle ryanodine receptor. Cooperative

- opening of  $\text{Ca}^{2+}$  release channels. *J. Gen. Physiol.* 110, 749-762. (1997)
8. Bhat, M.B., Hayek, S.M., Takeshima, H., Wier, W.G., and Ma, J.: Expression and functional characterization of the cardiac ryanodine receptor in chinese hamster ovary cells. *Biophys. J.* 77, 808-816 (1999)
  9. Birnbaumer, L., Zhu, X., Jiang, M., Boulay, G., Peyton, M., Vannier, B., Brown, D., Platano, D., Sadeghi, H., Stefani, E. and Birnbaumer, M.: On the Molecular Basis and Regulation of Cellular Capacitative Calcium Entry: Roles for Trp Proteins. *Proc. Natl. Acad. Sci. USA* 93, 15195-15202 (1996)
  10. Boulay, G., Brown, D., Qin, N., Jiang, M., Dietrich, A., Zhu, M.X., Chen, Z., Birnbaumer, M., Mikoshiba, K., and Birnbaumer, L.: Modulation of  $\text{Ca}^{2+}$  entry by TRP-binding polypeptides of the inositol 1,4,5-trisphosphate receptor ( $\text{IP}_3\text{R}$ ). Evidence for roles of TRP and  $\text{IP}_3\text{R}$  in store-depletion-activated  $\text{Ca}^{2+}$  entry. *Proc. Natl. Acad. Sci. U.S.A.* 96 (1999)
  11. Boulay, G., Zhu, X., Peyton, M., Jiang, M., Hurst, R., Stefani, E. and Birnbaumer, L.: Cloning and Expression of A Novel Mammalian Homolog of *Drosophila Transient Receptor Potential* (Trp) Involved in Calcium Entry Secondary to Activation of Receptor Coupled by The  $\text{G}_q$  Class of G Protein. *J. Biol. Chem.* 272, 29672-29680 (1997)
  12. Brandt, N.R., Caswell, A.H.: Localization of mitsugumin29 to transverse tubules in rabbit skeletal muscle. *Arch. Biochem. Biophys.* 371: 348-350. (1999)
  13. Brandt, N.R., Franklin, G., Brunschwig, J.P., and Caswell, A.H.: The role of mitsugumin 29 in transverse tubules of rabbit skeletal muscle. *Arch. Biochem Biophys.* 385: 406-409. (2001)
  14. Brough, G.H., Wu, S., Cioffi, D., Moore, T.M., Li, M., Dean, N., and Stevens, T.: Contribution of endogenously expressed Trp1 to a  $\text{Ca}^{2+}$ -selective, store-operated  $\text{Ca}^{2+}$  entry pathway. *FASEB J.* 15, 1727-1738 (2001)
  15. Brum, G., Fitts, R., Pizarro, G., and Rios, E.: Voltage sensors of the frog skeletal muscle membrane require calcium to function in excitation-contraction coupling. *J Physiol.* 398, 475-505. (1988)
  16. Caterina, M.J., Schumacher, M.A., Tominaga, M., Rosen, T.A., Levine, J.D., and Julius, D.: The capsaicin receptor: a heat-activated ion channel in the pain pathway. *Nature* 389, 816-824 (1997)
  17. Caterina, M.J., Rosen, T.A., Tominaga, M., Brake, A.J., and Julius, D.: A capsaicin-receptor homologue with a high threshold for noxious heat. *Nature* 398, 436-441 (1999)
  18. Cheng, H., Lederer, W.J., and Cannell, M.B.: Calcium sparks: elementary events underlying excitation-contraction coupling in heart muscle. *Science* 262, 740-744. (1993)
  19. Clapham, D.E.: Calcium Signaling. *Cell* 80, 259-268 (1995)
  20. Clapham, D.E., Runnels, L.W., and Strubing, C.: The trp ion channel family. *Nat. Rev. Neurosci.* 2, 387-396 (2001)
  21. Conklin MW, Ahern  $\text{Ca}^{2+}$ , Vallejo P, Sorrentino V, Takeshima H, Coronado R.: Comparison of  $\text{Ca}^{2+}$  sparks produced independently by two ryanodine receptor isoforms (type 1 or type 3). *Biophys J.* 78: 1777-1785. (2000)
  22. Coronado, R., Morrissette, J., Sukhareva, M., and Vaughan, D.M.: Structure and function of ryanodine receptors. *Am. J. Physiol.* 266, C1485-C1504. (1994)
  23. Cota, G. and Stefani, E.: Voltage-dependent inactivation of slow calcium channels in intact twitch muscle fibers of the frog. *J. Gen. Physiol.* 94: 937-951. (1989)
  24. Csutora, P., Su, Z., Kim, H.Y., Bugrim, A., Cunningham, K.W., Nuccitelli, R., Keizer, J.E., Hanley, M.R., Blalock, J.E., and Marchase, R.B.: Calcium influx factor is synthesized by yeast and mammalian cells depleted of organellar calcium stores. *Proc. Natl. Acad. Sci. USA*, 96, 121-126. (1999)
  25. Dahlstedt, A.J., Katz, A., Wieringa, B. and Westerblad, H.: Is creatine kinase responsible for fatigue? Studies of isolated skeletal muscle deficient in creatine kinase. *FASEB J.* 14, 982-990 (2000)
  26. Dahlstedt, A. J., and Westerblad, H.: Inhibition of creatine kinase reduces the fatigue-induced decrease of tetanic  $[\text{Ca}^{2+}]_i$  in mouse skeletal muscle. *Journal of Physiology* 533, 639-649 (2001).
  27. Doi, S., Damron, D.S., Horibe, M., Murray, PA.: Capacitative  $\text{Ca}^{2+}$  entry and tyrosine kinase activation in canine pulmonary arterial smooth muscle cells. *Am. J. Physiol.* 278, L118-130 (2000)
  28. Fasolato, C., Innocenti, B., and Pozzan, T.: Receptor-activated  $\text{Ca}^{2+}$  influx: how many mechanisms for how many channels? *Trends Pharmacol. Sci.* 15, 77-83 (1994)
  29. Feldmeyer, D., Melzer, W., Pohl, B., and Zollner, P.: Fast gating kinetics of the slow  $\text{Ca}^{2+}$  current in cut skeletal muscle fibers of the frog. *J. Physiol.* 425, 347-367. (1990)
  30. Fleig, A., Takeshima, H. & Penner, R.: Absence of  $\text{Ca}^{2+}$  current facilitation in skeletal muscle of transgenic mice lacking the ryanodine receptor type 1. *J. Physiol.* 496, 339-345. (1996)
  31. Flucher, B. E., Conti, A., Takeshima, H. & Sorrentino, V.: Type 3 and type 1 ryanodine receptors are localized in triads of same mammalian skeletal muscle fibers. *J. Cell Biol.* 146, 621-629 (1999)
  32. Franzini-Armstrong, C., Pincon-Raymond, M. and Rieger, F.: Muscle fibers from dysgenic mouse in vivo lack a surface component of peripheral couplings. *Dev. Biol.* 146, 364-376. (1991)
  33. Franzini-Armstrong, C. and Jorgensen, A.O.: Structure and development of E-C coupling units in skeletal muscle. *Ann. Rev. Physiol.* 56: 509-534. (1994)
  34. Freichel, M., Schweig, U., Stauffenberger, S., Freise, D., Schorb, W., and Flockerzi, V.: Store-operated cation channels in the heart and cells of the cardiovascular system. *Cell Physiol. Biochem.* 9, 270-283 (1999)
  35. Freichel, M., Suh, S.H., Pfeifer, A., Schweig, U., Trost, C., Weissgerber, P., Biel, M., Philipp, S., Freise, D., Droogmans, G., Hofmann, F., Flockerzi, V., and Nilius, B.: Lack of an endothelial store-operated  $\text{Ca}^{2+}$  current impairs agonist-dependent vasorelaxation in TRP4-/- mice. *Nat. Cell Biol.* 3, 121-127 (2001)
  36. Fryer, M. W., Owen, V. J., Lamb, G. D. and Stephenson, D. G.: Effects of creatine phosphate and  $\text{P}_i$  on  $\text{Ca}^{2+}$  movements and tension development in rat skinned skeletal muscle fibres. *J. Physiol.* 482, 123-140 (1995).
  37. Fryer, M. W., West, J. M, and Stephenson, D. G.: Phosphate transport into the sarcoplasmic reticulum of skinned fibres from rat skeletal muscle. *Journal of Muscle Research and Cell Motility* 18, 161-167. (1997).
  38. Gibson, A., McFadzean, I., Wallace, P., and Wayman, C.P.: Capacitative  $\text{Ca}^{2+}$  entry and the regulation of smooth muscle tone. *Trends Pharmacol. Sci.* 19, 266-269 (1998)
  39. Girard, T., Cavagna, D., Padovan, E., Spagnoli, G., Urwyler, A., Zorzato, F., Traves, S.: B-lymphocytes from malignant hyperthermia-susceptible patients have an increased sensitivity to skeletal muscle ryanodine receptor activators. *J Biol Chem.* 276: 48077-82. (2001)
  40. Gomez, A.M., Valdivia, H. H., Cheng, H., Lederer, M.R., Santana, L.F., Cannell, M.B., McCune, S.A., Altschuld, R.A., Lederer, W.J.: Defective excitation-contraction coupling in experimental cardiac hypertrophy and heart failure. *Science* 276, 800-806. (1997)
  41. Groschner, K., Hingel, S., Lintschinger, B., Balzer, M., Romanin, C, Zhu, X., and Schreibmayer, W.: Trp Proteins Form Store-Operated Cation Channels in Human Vascular Endothelial Cells. *FEBS Lett.* 437, 101-106 (1998)
  42. Guo, W. & Campbell, K. P.: Association of triadin with the ryanodine receptor and calsequestrin in the lumen

- of the sarcoplasmic reticulum. *J. Biol. Chem.* 270, 9027-9030. (1995)
43. Hasenfuss G.: Alterations of calcium-regulatory proteins in heart failure. *Cardiovasc Res.* 37, 279-289. (1998)
  44. Hunter, J.J., Shao, J., Smutko, J.S., Dussault, B.J., Nagle, D.L., Woolf, E.A., Holmgren, L.M., Moore, K.J., and Shyjan, A.W.: Chromosomal localization and genomic characterization of the mouse melastatin gene (Mln1). *Genomics* 54, 116-123 (1998)
  45. Hoenderop, J.G., van der Kemp, A.W., Hartog, A., van de Graaf, S.F., van Os, C.H., Willems, P.H., and Bindels, R.J.: Molecular identification of the apical Ca<sup>2+</sup> channel in 1, 25-dihydroxyvitamin D3-responsive epithelia. *J. Biol. Chem.* 274, 8375-8378 (1999)
  46. Hoth, M. and Penner, R.: Calcium release-activated calcium current in rat mast cells. *J. Physiol.* 465, 359-386 (1993)
  47. Ikemoto, T., Komazaki, S., Takeshima, H., Nishi, M., Noda, T., Iino, M. and Endo, M.: Functional and morphological features of myocytes from mutant mice lacking both ryanodine receptors type 1 and type 3. *J. Physiol.* 501, 305-312. (1997)
  48. Irvine, R.F.: 'Quantal' Ca<sup>2+</sup> release and the control of Ca<sup>2+</sup> entry by inositol phosphates--a possible mechanism. *FEBS Lett.* 263, 5-9 (1990)
  49. Ito K, Komazaki S, Sasamoto K, Yoshida M, Nishi M, Kitamura K, Takeshima H.: Deficiency of triad junction and contraction in mutant skeletal muscle lacking junctophilin type 1. *J Cell Biol.* 154: 1059-1067. (2001)
  50. Jones, L. R., Zhang, L., Sanborn, K., Jorgensen, A. O., and Kelley, J.: Purification, primary structure, and immunological characterization of the 26-kDa calsequestrin binding protein (junctin) from cardiac junctional sarcoplasmic reticulum. *J. Biol. Chem.* 270, 30787-30796. (1995)
  51. Kabbara, A. A., and Allen, D. G.: The role of calcium stores in fatigue of isolated single muscle fibres from the cane toad. *J. Physiol.* 519, 169-176 (1999)
  52. Kanzaki, M., Zhang, Y.-Q., Mashima, H., Li, L., Shibata, H. and Kojima, I.: Translocation of a calcium-permeable cation channel induced by insulin-like growth factor-I. *Nat. Cell Biol.* 1, 165-170, 1999
  53. Kaznacheeva, E., Zubov, A., Nikolaev, A., Alexeenko, V., Bezprozvanny, I., and Mozhayeva, G.N.: Plasma membrane calcium channels in human carcinoma A431 cells are functionally coupled to inositol 1,4,5-trisphosphate receptor-phosphatidylinositol 4,5-bisphosphate complexes. *J. Biol. Chem.* 275, 4561-4564 (2000)
  54. Kerschbaum, H. H. and Cahalan, M. D.: Monovalent permeability, rectification, and ionic block of store-operated calcium channels in Jurkat T lymphocytes. *J. Gen. Physiol.* 111, 521-537 (1998)
  55. Kiselyov, K., Xu, X., Kuo, T.H., Mozhayeva, G., Pessah, I., Mignery, G., Zhu, X., Birnbaumer, L., and Muallem, S.: Functional Interaction Between *HTRP3* channel and IP<sub>3</sub> receptors. *Nature* 396, 478-482 (1998)
  56. Kiselyov, K., Mignery, G.A., Zhu, M.X. and Muallem, S.: The N-terminal domain of the IP<sub>3</sub> Receptor gates Store-Operated hTrp3 Channels. *Mol. Cell* 4, 423-429 (1999)
  57. Kiselyov, K.I., Shin, D.M., Wang, Y., Pessah, I.N., Allen, P.D., and Muallem, S.: Gating of store-operated channels by conformational coupling to ryanodine receptors. *Mol. Cell* 6, 421-431 (2000)
  58. Kiselyov, K., Shin, D.M., Shcheynikov, N., Kurosaki, T., and Muallem, S.: Regulation of Ca<sup>2+</sup>-release-activated Ca<sup>2+</sup> current (*I*<sub>CRAC</sub>) by ryanodine receptors in inositol 1,4,5-trisphosphate-receptor-deficient DT40 cells. *Biochem. J.* 360, 17-22. (2001)
  59. Komazaki, S., Nishi, M., Kangawa, K. and Takeshima, H.: Immunolocalization of mitsugumin29 in developing skeletal muscle and effects of the protein expressed in amphibian embryonic cells. *Dev. Dynam.* 215, 87-95. (1999)
  60. Kurebayashi N and Ogawa Y.: Depletion of Ca<sup>2+</sup> in the sarcoplasmic reticulum stimulates Ca<sup>2+</sup> entry into mouse skeletal muscle fibres. *J Physiol.* 533, 185-99. (2001)
  61. Lee, H.C.: Mechanisms of calcium signaling by cyclic ADP-ribose and NAADP. *Physiol. Rev.* 77, 1133-1164. (1997).
  62. Lee, M.G., Xu, X., Zeng, W., Diaz, J., Kuo, T.H., Wuytack, F., Racymaekers, L., and Muallem, S.: Polarized expression of Ca<sup>2+</sup> pumps in pancreatic and salivary gland cells. Role in initiation and propagation of [Ca<sup>2+</sup>]<sub>i</sub> waves. *J. Biol. Chem.* 272, 15771-15776. (1997).
  63. Leung YM, Kwan CY, and Loh, T.T.: Dual effects of SK&F 96365 in human leukemic HL-60 cells. Inhibition of calcium entry and activation of a novel cation influx pathway. *Biochem Pharmacol.* 51, 605-612. (1996)
  64. Liu, X., Wang, W., Singh, B. B., Lockwich, T., Jadlowiec, J., O'Connell, B., Wellner, R., Zhu, M. X., and Ambudkar, I. S.: Trp1, a candidate protein for the store-operated Ca<sup>2+</sup> influx mechanism in salivary gland cells. *J. Biol. Chem.* 275, 3403-3411 (2000)
  65. Lockwich, T.P., Liu, X., Singh, B.B., Jadlowiec, J., Weiland, S., and Ambudkar, I.S.: Assembly of Trp1 in a signaling complex associated with caveolin-scaffolding lipid raft domains. *J. Biol. Chem.* 275, 11934-11942. (2000)
  66. Lopez-Lopez, J.R., Shacklock, P.S., Blake, C.W., and Wier, W.G.: Local calcium transients triggered by single L-type calcium channel currents in cardiac cells. *Science* 268, 1042-1045. (1995)
  67. Ma, J., Gonzalez, A., and Chen, R.: Fast activation of dihydropyridine-sensitive calcium channels of skeletal muscle. Multiple pathways of channel gating. *J. Gen. Physiol.* 108, 221-232. (1996)
  68. Meissner, G.: Ryanodine receptor/Ca<sup>2+</sup> release channels and their regulation by endogenous effectors. *Ann. Rev. Physiol.* 56: 485-508. (1994)
  69. Merritt, J.E., Armstrong, W.P., Benham, C.D., Hallam, T.J., Jacob, R., Jaxa-Chamiec, A., Leigh, B.K., McCarthy, S.A., Moores, K.E. & Rink, T.J.: SK&F 96365, a novel inhibitor of receptor-mediated calcium entry. *Biochem. J.* 271, 515-522 (1990)
  70. Montell, C., and Rubin, G. M.: Molecular characterization of the *Drosophila* trp locus: a putative integral membrane protein required for phototransduction. *Neuron* 2, 1313-1323 (1989)
  71. Montell, C., Birnbaumer, L., Flockerzi, V., Bindels, R.J., Bruford, E.A., Caterina, M.J., Clapham, D.E., Harteneck, C., Heller, S., Julius, D., Mori, Y., Penner, R., Prawitt, D., Scharenberg, A.M., Schultz, G., Shimizu, N., and Zhu, M. X.: A unified nomenclature for the superfamily of TRP cation channels. *Mol. Cell* 9, 229-231. (2002)
  72. Nagaraj, R.Y., Nosek, C., Brotto, M.A., Nishi, M., Takeshima, H., Nosek, T.M., and Ma, J.: Increased susceptibility to fatigue of slow and fast twitch muscles from mice lacking the MG29 gene. *Physiol. Genomics* 4, 43-49. (2000).
  73. Nakai, J., Dirksen, R.T., Nguyen, H.T., Pessah, I.N., Beam, K.G., and Allen, P.D.: Enhanced dihydropyridine receptor channel activity in the presence of ryanodine receptor. *Nature* 380, 72-75. (1996)
  74. Nakai, J., Ogura, T., Protasi, F., Franzini-Armstrong, C., Allen, P.D., Beam, K.G.: Functional nonequality of the cardiac and skeletal ryanodine receptors *Proc. Natl. Acad. Sci (USA)* 94: 1019-1022. (1997)
  75. Nishi, M., Komazaki, S., Kurebayashi, N., Ogawa, Y., Noda, T., Iino, M. and Takeshima, H.: Abnormal features in skeletal muscle from mice lacking mitsugumin29. *J. Cell Biol.* 147, 1473-1480. (1998)
  76. Nishi, M., Mizushima, A., Nakagawara, K. & Takeshima, H.: Characterization of human junctophilin subtype genes. *Biochem. Biophys. Res. Commun.* 273, 920-927. (2000)
  77. Numa, S., Tanabe, T., Takeshima, H., Mikami, A., Nidome, T., Nishimura, S., Adams, B.A., and Beam, K.G.: Molecular insights into excitation-contraction

- coupling. *Cold. Spring Harbor Symp. Quant. Biol.* 45, 1-7. (1990)
78. Okada, T., Shimizu, S., Wakamori, M., Maeda, A., Kurosaki, T., Takada, N., Imoto, K., and Mori, Y.: Molecular cloning and functional characterization of a novel receptor-activated TRP Ca<sup>2+</sup> channel from mouse brain. *J. Biol. Chem.* 273, 10279-10287 (1998)
  79. Okada, T., Inoue, R., Yamazaki, K., Maeda, A., Kurosaki, T., Yamakuni, T., Tanaka, I., Shimizu, S., Ikenaka, K., Imoto, K., and Mori, Y.: Molecular and functional characterization of a novel mouse transient receptor potential protein homologue TRP7. Ca<sup>2+</sup>-permeable cation channel that is constitutively activated and enhanced by stimulation of G protein-coupled receptor. *J. Biol. Chem.* 274, 27359-27370 (1999)
  80. Pan, Z., Nagaraj, R.Y., Yang, D.M., Nosek, T.A., Takeshima, H., Cheng, H., and Ma, J.: Dysfunction of store-operated Ca<sup>2+</sup> channel in muscle cells lacking mg29 gene. *Nature Cell Biol.* 4, 379-383. (2002)
  81. Parekh, A. B. and Penner, R.: Store depletion and calcium influx. *Physiol. Rev.* 77, 901-930. (1997)
  82. Patterson, R.L., van Rossum, D.B., and Gill, D. L.: Store-operated Ca<sup>2+</sup> entry: evidence for a secretion-like coupling model. *Cell* 98: 487-499. (1999)
  83. Peng, J.B., Chen, X.Z., Berger, U.V., Vassilev, P.M., Brown, E.M. and Hediger, M.A.: A rat kidney-specific calcium transporter in the distal nephron. *J. Biol. Chem.* 275, 28186-28194, (2000)
  84. Peng, J.B., Chen, X.Z., Berger, U.V., Vassilev, P.M., Tsukaguchi, H., Brown, E.M. and Hediger, M.A.: Molecular cloning and characterization of a channel-like transporter mediating intestinal calcium absorption. *J. Biol. Chem.* 274, 22739-22746 (1999)
  85. Petersen, C. C., Berridge, M. J., Borgese, M. F., and Bennett, D. L.: Putative capacitative calcium entry channels: expression of *Drosophila trp* and evidence for the existence of vertebrate homologues *Biochem. J.* 311, 41-44. (1995)
  86. Philipp, S., Trost, C., Warnat, J., Rautmann, J., Himmerkus, N., Schroth, G., Kretz, O., Nastainczyk, W., Cavalié, A., Hoth, M., and Flockerzi, V.: TRP4 (CCE1) protein is part of native calcium release-activated Ca<sup>2+</sup>-like channels in adrenal cells. *J. Biol. Chem.* 275, 23965-23972 (2000)
  87. Phillips, A. M., Bull, A., and Kelly, L. E.: Identification of a *Drosophila* gene encoding a calmodulin-binding protein with homology to the *trp* phototransduction gene. *Neuron* 8, 631-642 (1992)
  88. Philipp, S., Cavalié, A., Freichel, M., Wissenbach, U., Zimmer, S., Trost, C., Marquart, A., Murakami, M., and Flockerzi, V.: A mammalian capacitative calcium entry channel homologous to *Drosophila TRP* and *TRPL*. *EMBO J.* 15, 6166-6171 (1996)
  89. Philipp, S., Hambrecht, J., Braslavski, L., Schroth, G., Freichel, M., Murakami, M., Cavalié, A., and Flockerzi, V.: A novel capacitative calcium entry channel expressed in excitable cells. *EMBO J.* 17, 4274-4282. (1998)
  90. Pozzan, T., Rizzuto, R., Volpe, P. and Meldolesi, J.: Molecular and cellular physiology of intracellular calcium stores. *Physiol. Rev.* 74, 595-636. (1994)
  91. Putney, J.W. Jr. Capacitative calcium entry revisited.: *Cell Calcium* 11, 611-624 (1990)
  92. Putney, J.W. Jr, Broad, L.M., Braun, F.J., Lievremont, J.P., and Bird, G.S. Mechanisms of capacitative calcium entry. *J Cell Sci.* 114(Pt 12), 2223-9 (2001)
  93. Putney, J. W. Jr. and McKay, R. R.: Capacitative calcium entry channels. *Bioessays* 21, 38-46. (1999)
  94. Randriamampita, C. and Tsien, R.Y.: Emptying of intracellular Ca<sup>2+</sup> stores releases a novel small messenger that stimulates Ca<sup>2+</sup> influx. *Nature* 364, 809-814 (1993)
  95. Rios, E., Ma, J., and Gonzalez, A.: The mechanical hypothesis of excitation-contraction coupling in skeletal muscle. *J. Muscle. Res. Cell Motil.* 12, 127-135. (1991)
  96. Rios, E., Pizzaro, G., and Stefani, E.: Charge movement and the nature of signal transduction in skeletal muscle excitation-contraction coupling. *Ann. Rev. Physiol.* 54, 109-133. (1992)
  97. Rosado, J.A. and Sage, S.O.: Coupling between inositol 1,4,5-trisphosphate receptors and human transient receptor potential channel 1 when intracellular Ca<sup>2+</sup> stores are depleted. *Biochem. J.* 350, 631-635 (2000)
  98. Schaefer, M., Plant, T.D., Obukhov, A.G., Hofmann, T., Gudermann, T., and Schultz, G.: Receptor-mediated regulation of the nonselective cation channels TRPC4 and TRPC5. *J. Biol. Chem.* 275, 17517-17526 (2000)
  99. Schneider, M. F.: Control of calcium release in functioning skeletal muscle fibers. *Annu. Rev. Physiol.* 56, 463-84. (1994)
  100. Sei, Y., Gallagher, K.L., Basile, A.S.: Skeletal muscle type ryanodine receptor is involved in calcium signaling in human B lymphocytes. *J Biol Chem.* 274, 5995-6002. (1999)
  101. Shimuta, M., Komazaki, S., Nishi, M., Iino, M., Nakagawara, K & Takeshima, H.: Structure and expression of mitsugumin29 gene. *FEBS Lett.* 431, 263-267. (1998)
  102. Shirokova, N., Shirokov, R., Roosi, D., Gonzalez, A. Kirsch, W.G., Garcia, J., Sorrentino, V., and Rios, E.: Spatially segregated control of Ca<sup>2+</sup> release in developing skeletal muscle of mice. *J. Physiol.* 521, 483-495. (1999)
  103. Strotmann, R., Harteneck, C., Nunnenmacher, K., Schultz, G. and Plant, T.D.: OTRPC4, a nonselective cation channel that confers sensitivity to extracellular osmolarity. *Nat. Cell Biol.* 2, 695-702 (2000)
  104. Strubing, C., Krapivinsky, G., Krapivinsky, L., and Clapham, D.E.: *Trpc1* and *trpc5* form a novel cation channel in mammalian brain. *Neuron* 29, 645-655 (2001)
  105. Suda, N., Franzius, D., Fleig, A., Nishimura, S., Bodding, M., Hoth, M., Takeshima, H. and Penner, R.: Caffeine-induced release of intracellular Ca<sup>2+</sup> from Chinese hamster ovary cells expressing skeletal muscle ryanodine receptor. *J. Gen. Physiol.* 109, 619-631. (1997)
  106. Sun, M., Goldin, E., Stahl, S., Falardeau, J.L., Kennedy, J.C., Acierno, J.S. Jr., Bove, C., Kaneski, C.R., Nagle, J., Bromley, M.C., Colman, M., Schiffmann, R. and Slaughter, S.A.: Mucopolidosis type IV is caused by mutations in a gene encoding a novel transient receptor potential channel. *Hum. Mol. Genet.* 9, 2471-2478 (2000)
  107. Sun, X-H., Protasi, F., Takahashi, M., Takeshima, H., Ferguson, D. G. & Franzini-Armstrong, C.: Molecular architecture of membranes involved in excitation-contraction coupling of cardiac muscle. *J. Cell Biol.* 129, 659-671. (1995)
  108. Suzuki, M., Sato, J., Kutsuwada, K., Ooki, G. and Imai, M.: Cloning of a stretch-inhibitable nonselective cation channel. *J. Biol. Chem.* 274, 6330-6335 (1999)
  109. Takekura, H., Takeshima, H., Nishimura, S., Takahashi, M., Tanabe, T., Flockerzi, V., Hofmann, F. and Franzini-Armstrong, C.: Co-expression in CHO cells of two muscle proteins involved in excitation-contraction coupling. *J. Muscle Res. Cell Motil.* 16, 465-480. (1995)
  110. Takeshima, H., Iino, M., Takekura, H., Nishi, M., Kuno, J., Minowa, O., Takano, H. and Noda, T.: Excitation-contraction uncoupling and muscular degeneration in mice lacking functional skeletal muscle ryanodine-receptor gene. *Nature* 369, 556-559. (1994)
  111. Takeshima, H., Ikemoto, T., Nishi, M., Nishiyama, N., Shimuta, M., Sugitani, Y., Kuno, J., Saito, I., Saito, H., Endo, M., Iino, M. & Noda, T.: Generation and characterization of mutant mice lacking ryanodine receptor type 3. *J. Biol. Chem.* 271, 19649-19652. (1996)
  112. Takeshima, H., Komazaki, S., Hirose, K., Nishi, M., Noda, T. and Iino, M.: Embryonic lethality and

- abnormal cardiac myocytes in mice lacking ryanodine receptor type 2. *EMBO J.* 17, 3309-3316. (1998)
113. Takeshima, H., Shimuta, M., Komazaki, S., Ohmi, K., Nishi, M., Iino, M., Miyata, A. and Kangawa, K.: Mitsugumin29, a novel synaptophysin family member from the triad junction in skeletal muscle. *Biochem. J.* 331, 317-322. (1998)
  114. Takeshima, H., Komazaki, S., Nishi, M., Iino, M. & Kangawa, K.: Junctophilins: a novel family of junctional membrane proteins. *Mol. Cell* 6, 11-22. (2000)
  115. Tang, J., Lin, Y., Zhang, Z., Tikunova, S., Birnbaumer, L., and Zhu, M.X.: Identification of common binding sites for calmodulin and inositol 1,4,5-trisphosphate receptors on the carboxyl termini of Trp channels. *J. Biol. Chem.* 276, 21303-21310. (2001)
  116. Trepakova, E. S., Csutora, P., Hunton, D. L., Marchase, R. B., Cohen, R. A. and Bolotina, V. M.: Calcium influx factor directly activates store-operated cation channels in vascular smooth muscle cells. *J. Biol. Chem.* 275, 26158-26163. (2000)
  117. Tsiokas, L., Arnould, T., Zhu, C., Kim, E., Walz, G., and Sukhatme, V.P.: Specific association of the gene product of PKD2 with the TRPC1 channel. *Proc. Natl. Acad. Sci. USA.* 96, 3934-3939. (1999)
  118. Uehara, A., Yasukochi, M., Imanaga, I., Nishi, M., Takeshima, H.: Store-operated  $Ca^{2+}$  entry uncoupled with ryanodine receptor and junctional membrane complex in heart muscle cells. *Cell Calcium* 31, 89-96. (2002)
  119. Usachev, Y.M., and Thayer, S.A.:  $Ca^{2+}$  influx in resting rat sensory neurons that regulates and is regulated by ryanodine-sensitive  $Ca^{2+}$  stores. *J. Physiol.* 519, 115-130. (1999)
  120. Vaca, L., Sinkins, W. G., Hu, Y., Kunze, D. L., and Schilling, W. P.: Activation of recombinant trp by thapsigargin in Sf9 insect cells. *Am. J. Physiol.* 267, C1501-C1505. (1994)
  121. Vannier, B., Peyton, M., Boulay, G., Brown, D., Qin, N., Jiang, M., Zhu, X., and Birnbaumer, L.: Mouse trp2, the homologue of the human trpc2 pseudogene, encodes mTrp2, a store depletion-activated capacitative  $Ca^{2+}$  entry channel. *Proc. Natl. Acad. Sci. U.S.A.* 96, 2060-2064 (1999)
  122. Vazquez, G., Lievreumont, J.P. St. J., Bird, G., and Putney, J.W. Jr.: Human Trp3 forms both inositol trisphosphate receptor-dependent and receptor-independent store-operated cation channels in DT40 avian B lymphocytes. *Proc. Natl. Acad. Sci. U.S.A.* 98, 11777-11782. (2001)
  123. Voets, T., Prenen, J., Fleig, A., Vennekens, R., Watanabe, H., Hoenderop, J.G., Bindels, R.J., Droogmans, G., Penner, R., and Nilius, B.: CaT1 and the Calcium Release-activated Calcium Channel Manifest Distinct Pore Properties. *J. Biol. Chem.* 276, 47767-47770. (2001)
  124. Wang SQ, Song LS, Lakatta EG, Cheng H.:  $Ca^{2+}$  signaling between single L-type  $Ca^{2+}$  channels and ryanodine receptors in heart cells. *Nature.* 410(6828), 592-6. (2001)
  125. Ward, C.W., Schneider, M.F., Castillo, D., Protasi, F., Wang, Y., Chen, S.R., Allen, P.D.: Expression of ryanodine receptor RyR3 produces  $Ca^{2+}$  sparks in dyspedic myotubes. *J. Physiol.* 525, 91-103. (2000)
  126. Warnat, J., Philipp, S., Zimmer, S., Flockerzi, V., and Cavalie, A.: Phenotype of a recombinant store-operated channel: highly selective permeation of  $Ca^{2+}$ . *J. Physiol. (Lond).* 518, 631-638. (1999)
  127. Wissenbach, U., Boedding, M., Freichel, M. and Flockerzi, V.: Trp12, a novel Trp related protein from kidney. *FEBS Lett.* 485, 127-134. (2000)
  128. Wong, F., Schaefer, E. L., Roop, B. C., LaMendola, J. N., Johnson-Seaton, D., and Shao, D.: Proper function of the *Drosophila* trp gene product during pupal development is important for normal visual transduction in the adult. *Neuron* 3, 81-94. (1989)
  129. Xu, X. Z., Chien, F., Butler, A., Salkoff, L., and Montell, C.: TRP $\gamma$ , a *Drosophila* TRP-related subunit, forms a regulated cation channel with TRPL. *Neuron* 26, 647-657. (2000)
  130. Xu, S. Z. and Beech, D. J.: TrpC1 is a membrane-spanning subunit of store-operated  $Ca^{2+}$  channels in native vascular smooth muscle cells. *Circ. Res.* 88, 84-87. (2001)
  131. Xu, X.Z., Li, H.S., Guggino, W.B., and Montell, C.: Coassembly of TRP and TRPL produces a distinct store-operated conductance. *Cell* 89, 1155-1164 (1997)
  132. Yang, D.M., Pan, Z., Takeshima, H., Cai, H., Nagaraj, R.Y., Ma, J. and Cheng, H.: RyR3 amplifies RyR1-mediated  $Ca^{2+}$ -induced  $Ca^{2+}$  release in neonatal mammalian skeletal muscle. *J. Biol. Chem.* 276, 40210-40214. (2001)
  133. Yao, Y., Ferrer-Montiel, A.V., Montal, M., and Tsien, R.Y.: Activation of store-operated  $Ca^{2+}$  current in *Xenopus* oocytes requires SNAP-25 but not a diffusible messenger. *Cell* 98, 475-485. (1999)
  134. Yoshimura, M., Oshima, T., Matsuura, H., Ishida, T., Kambe, M., and Kajiyama, G.: Extracellular  $Mg^{2+}$  inhibits capacitative  $Ca^{2+}$  entry in vascular smooth muscle cells. *Circulation* 95, 2567-2572. (1997)
  135. Yue, L., Peng, J.B., Hediger, M.A., and Clapham, D.E.: CaT1 manifests the pore properties of the calcium-release-activated calcium channel. *Nature* 410, 705-709. (2001)
  136. Zhang, Z., Tang, J., Tikunova, S., Johnson, J.D., Chen, Z., Qin, N., Dietrich, A., Stefani, E., Birnbaumer, L., and Zhu, M. X.: Activation of Trp3 by  $IP_3$  receptors through displacement of inhibitory calmodulin from a common binding domain. *Proc. Natl. Acad. Sci. U.S.A.* 98, 3168-3173. (2001)
  137. Zhu, X., Jiang, M. and Birnbaumer, L.: Receptor-Activated  $Ca^{2+}$  Influx via Human Trp3 Stably Expressed in HEK293 Cells: Evidence for A Non-Capacitative  $Ca^{2+}$  Entry. *J. Biol. Chem.* 273, 133-142. (1998)
  138. Zhu, X., Jiang, M., Peyton, M., Boulay, G., Hurst, R., Stefani, E. and Birnbaumer, L.: *trp*, a Novel Mammalian Gene Family Essential for Agonist-Activated Capacitative  $Ca^{2+}$  Entry. *Cell*, 85, 661-671. (1996)
  139. Zitt, C., Zobel, A., Obukhov, A. G., Harteneck, C., Kalkbrenner, F., Luckhoff, A., and Schultz, G.: Cloning and functional expression of a human  $Ca^{2+}$ -permeable cation channel activated by calcium store depletion. *Neuron* 16, 1189-1196. (1996)
  140. Zweifach, A. and Lewis, R.S.: Rapid inactivation of depletion-activated calcium current ( $I_{CRAC}$ ) due to local calcium feedback. *J. Gen. Physiol.* 105, 209-226. (1995)

### Correspondence:

Department of Physiology and Biophysics  
 UMDNJ-Robert Wood Johnson Medical School  
 675 Hoes Lane  
 Piscataway, NJ 08854  
 Tel. (732) 235-4494  
 Fax (732) 235-4483  
 Email: [maj2@umdnj.edu](mailto:maj2@umdnj.edu)

# Ryanodine receptors, FKBP12, and heart failure

Andrew R. Marks

Center for Molecular Cardiology, Departments of Medicine and Pharmacology,  
Columbia University College of Physicians and Surgeons, New York, N.Y. 10032, USA.

**ABSTRACT** RyR2 function is regulated by highly conserved signaling pathways that modulate excitation-contraction (EC) coupling. cAMP dependent protein kinase (PKA) phosphorylation of RyR2 plays an important role in regulating channel function in response to stress signaled by the sympathetic nervous system (the classic "fight or flight response") (1). PKA phosphorylation of RyR2 induces dissociation of the regulatory protein FKBP12.6 resulting in channels with increased sensitivity to  $\text{Ca}^{2+}$ -induced  $\text{Ca}^{2+}$  release. Under normal physiological conditions (no cardiac damage) PKA phosphorylation of RyR2 is part of an integrated physiological response that leads to increased EC coupling gain and increased cardiac output. PKA-hyperphosphorylation of RyR2 in failing hearts is a maladaptive response that results in depletion of FKBP12.6 from the RyR2 macromolecular complex and defective channel function (pathologically increased sensitivity to  $\text{Ca}^{2+}$ -induced  $\text{Ca}^{2+}$  release) that may cause depletion of SR  $\text{Ca}^{2+}$  and diastolic release of SR  $\text{Ca}^{2+}$  that can initiate delayed afterdepolarizations (DADs) that trigger ventricular arrhythmias (1). RyR2 mutations in patients with catecholaminergic induced sudden cardiac death provide further evidence linking the sympathetic nervous system, RyR2 and ventricular arrhythmias (2-4). The chronic hyperadrenergic state of heart failure is associated with defective  $\text{Ca}^{2+}$  signaling in part due to PKA hyperphosphorylation of RyR2.

## INTRODUCTION

Although we now understand a great deal more about the systems that regulate cardiac function than we did 20 years ago, this abundance of new knowledge brings with it additional challenges. It is becoming ever more apparent that the concept of linear signaling pathways does not apply to complex biological systems. In this light disease states that perturb normal signaling often cannot be explained by a single defect in one pathway. Accordingly, therapies of many diseases likely will not succeed when they are targeted only at one pathway in a complex parallel signaling system. This review focuses on the ryanodine receptor (RyR2)/ calcium ( $\text{Ca}^{2+}$ ) release channel, on the cardiac sarcoplasmic reticulum (SR). The RyR2 is one component of a complex integrated system that regulates cytosolic [ $\text{Ca}^{2+}$ ] which in turn controls cardiac muscle contraction and relaxation. Many other molecules exert regulatory effects on  $\text{Ca}^{2+}$  homeostasis mechanisms in cardiomyocytes. It is beyond the scope of this focused review to address the full complexities of this regulatory system and interested readers are encouraged to read further on the subject of cardiac muscle function to get an overview that will help place the present discussion in the proper global context.

## RYANODINE RECEPTORS: STRUCTURE AND FUNCTION

RyRs are members of a gene family that includes three isoforms: RyR1, expressed predominantly in skeletal muscle but also in non-muscle including the central nervous system; RyR2, expressed predominantly in cardiac muscle but also in non-muscle including the central nervous system; and RyR3, expressed in specialized muscle and non-

muscle tissues including the brain. Primary structures of the three RyR isoforms have been deduced from their corresponding cDNAs (5-8) revealing >65% amino acid sequence homology among them. Homotetramers of four RyRs, each with a molecular mass of ~560,000 Da, comprise a single RyR channel with a molecular mass in excess of 2.3 million Da. RyR channels have enormous cytoplasmic domains containing binding sites for proteins and other channel modulators (e.g.  $\text{Ca}^{2+}$ ) that control the state of activity of the channel-forming domain of the molecule.

Intact RyR have been isolated and purified from skeletal (9-11) and cardiac muscles (12,13) after mild CHAPS solubilization of heavy SR using  $^3\text{H}$  ryanodine as a high affinity ligand. Recombinant RyR1 has been expressed in insect cells (14), *Xenopus oocytes* (15), HEK cells (16,17), and CHO cells (18). Purified receptor has been incorporated in planar lipid bilayers and demonstrates characteristics identical to the  $\text{Ca}^{2+}$  release channel of the heavy SR (9,17,19-23). The activity of RyR is modulated by a variety of agents. Cytoplasmic  $\text{Ca}^{2+}$  activates the channel at nM- $\mu\text{M}$  concentrations, while mM concentrations inhibit the channel (24). Channels are activated by ATP (25) and inhibited by  $\text{Mg}^{2+}$  (26). In addition to these physiological regulators, useful modulators of RyR channel function include caffeine, specific antibodies (27,28), ryanodine (29-31), ruthenium red, and the immunosuppressant drugs FK506 and rapamycin (14,32-34).

The regulation of cardiac EC coupling by the release of  $\text{Ca}^{2+}$  from the sarcoplasmic reticulum (SR) via the ryanodine receptor (RyR2) in cardiomyocytes, known as  $\text{Ca}^{2+}$ -induced  $\text{Ca}^{2+}$  release (CICR), has been appreciated for more than a decade (35,36) and it is well known that the amplitude of the  $\text{Ca}^{2+}$  transient

generated by SR  $\text{Ca}^{2+}$  release determines contractile force in cardiomyocytes. Systems that regulate SR  $\text{Ca}^{2+}$  release include: 1) the triggers (predominantly  $\text{Ca}^{2+}$  influx through the voltage-gated  $\text{Ca}^{2+}$  channel on the plasma membrane and secondarily  $\text{Ca}^{2+}$  influx via the  $\text{Na}^+$ - $\text{Ca}^{2+}$  exchanger); 2) the SR  $\text{Ca}^{2+}$  release channel or type 2 ryanodine receptor (RyR2); 3) the SR  $\text{Ca}^{2+}$  reuptake pump (SERCA2a) and its regulator phospholamban. These trigger, release, reuptake systems are modulated by signaling pathways including the beta adrenergic receptor ( $\beta$ -AR) signaling pathway (i.e. phosphorylation by PKA).

### **RyR2 complex is formed via leucine/isoleucine zippers**

RyR1 and RyR2 contain highly conserved leucine/isoleucine zippers (LIZs,  $\alpha$  helical heptad repeats of Leu/Ile residues) that bind to LIZs present in the adaptor/targeting proteins for kinases (PKA) and phosphatases (PP1 and PP2A) that regulate RyR channel function and play a role in defects in channel function in heart failure (1,37). A heptad repeat of hydrophobic residues is the important feature of LIZs (38). Leu/Ile line up on one face of the helix (3.5 residues/turn) and oligomerize with other coiled coil helices. A 2<sup>nd</sup> important feature of LIZs is that hydrophobic residues occupy the "a" as well as the "d" (Leu/Ile) positions of the repeating heptad of *a-g* residues that form the helix. Leu residues can be replaced by Ile or Val and can include "skips" and "hiccups" (39). Specificity is imparted via the amino acids in the other positions in the coiled-coil forming  $\alpha$  helix. We have identified leucine heptad repeats in the cardiac RyR2 and the skeletal RyR1 that are involved in targeting kinases and phosphatases to the channel (37) and the targeting of PKA, PP2A and PP1 to RyR2 can be disrupted by mutating these leucine zipper motifs (37).

Elucidating the role of LIZs in mediating the targeting of specific kinases and phosphatases to RyR2 provides tools that can be used to specifically eliminate PKA-dependent modulation of RyR2 function. We have used a specific RyR2 peptide containing LIZ3 to compete the mAKAP/PKA complex from the channel (37) demonstrating that it is possible to specifically determine the effects of PKA phosphorylation of RyR2 (37). This approach can be adapted to *in vivo* studies by expressing the specific peptides in cardiomyocytes to determine the effects of inhibiting PKA phosphorylation of RyR2 in intact cardiomyocytes (37).

### **FKBP12.6 regulates RyR2**

A 12 and a 12.6-kDa protein respectively are tightly associated with highly purified RyR1 and RyR2 and modulate the function of the channels, possibly by enhancing cooperativity among its four subunits (5,14,33,40-42). The 12 kDa protein, was originally identified as a peptide KC7 that co-purifies with RyR1 (5), and was later shown to be FKBP12, the cytosolic binding protein for the immunosuppressant drugs FK506 and rapamycin (43). FKBP12 is expressed at high levels in all muscles (40). FKBP12 and FKBP12.6 are *cis-trans* peptidyl-prolyl isomerases and are

members of the immunophilin family of proteins (42). The molar ratio of FKBP12 to RyR1 in highly purified RyR1 preparations is  $\sim 1:1$  (44), indicating that one FKBP12 molecule binds to each subunit of the  $\text{Ca}^{2+}$ -release channel or four FKBP12 molecules are part of each RyR1-channel complex.

In the absence of FKBP12/12.6, RyR1/RyR2 channels exhibit partial openings known as subconductance states. However, when RyR1 and FKBP12 were co-expressed in insect cells, these subconductance states are eliminated (14). Similarly when FKBP12.6 was removed from RyR2 with FK506 or rapamycin subconductances appeared (33). These results indicate a cellular function for FKBP12/12.6 and establish that functional  $\text{Ca}^{2+}$ -release channels are a complex composed of RyR and FKBP. These results have recently been confirmed by other laboratories (45-47). In addition to stabilizing RyR channels, FKBP12s are required for coupled gating (48,49); a phenomenon in which two or more physically connected RyR channels can gate simultaneously. Coupled gating provides a mechanism for the coordinated activation and inactivation of RyR channels (and thus Ca release) during EC coupling (48,49).

### **PKA PHOSPHORYLATION REGULATES RYR2 FUNCTION**

Activation of the sympathetic nervous system in response to stress raises circulating catecholamines that activate  $\beta$ -adrenergic receptors and elevate intracellular cAMP. Among the many targets for the cAMP-dependent kinase PKA are the trigger for EC coupling, the L-type channel, the release channel, RyR2, and phospholamban which regulates the  $\text{Ca}^{2+}$ -uptake pump SERCA2a (Fig. 1A). Thus, activation of the sympathetic nervous system ("fight or flight" response) increases cardiac output by increasing the gain of EC coupling due to PKA phosphorylation that activates the trigger, the release channel and the SR  $\text{Ca}^{2+}$ -uptake pathway. PKA phosphorylation of RyR2 is physiologically regulated *in vivo* in response to activation of the sympathetic nervous system ("fight or flight" response) and channels from failing hearts are PKA hyperphosphorylated (due to a maladaptive response that creates a chronic hyperadrenergic state) resulting in dissociation of the FKBP12.6 and altered channel function (1). Maladaptation of this physiological pathway, that has never been subjected to evolutionary pressure since heart failure is a new disease of the last century or two, plays an important role in the pathophysiology of heart failure (50,51).

Stimulation of the sympathetic nervous system results in phosphorylation of RyR2 by PKA and activation of the channel (Fig. 1B). PKA phosphorylation potently modulates RyR2 function and is physiologically regulated *in vivo* (1,37,50-59). PKA hyperphosphorylation of RyR2 in failing hearts shifts the sensitivity of RyR2 to  $\text{Ca}^{2+}$ -induced  $\text{Ca}^{2+}$  release to the left (1) resulting in "leaky" channels (Fig. 1C) (channels with increased sensitivity to  $\text{Ca}^{2+}$ -induced  $\text{Ca}^{2+}$  release) that may cause diastolic  $\text{Ca}^{2+}$  release that generates delayed after depolarizations

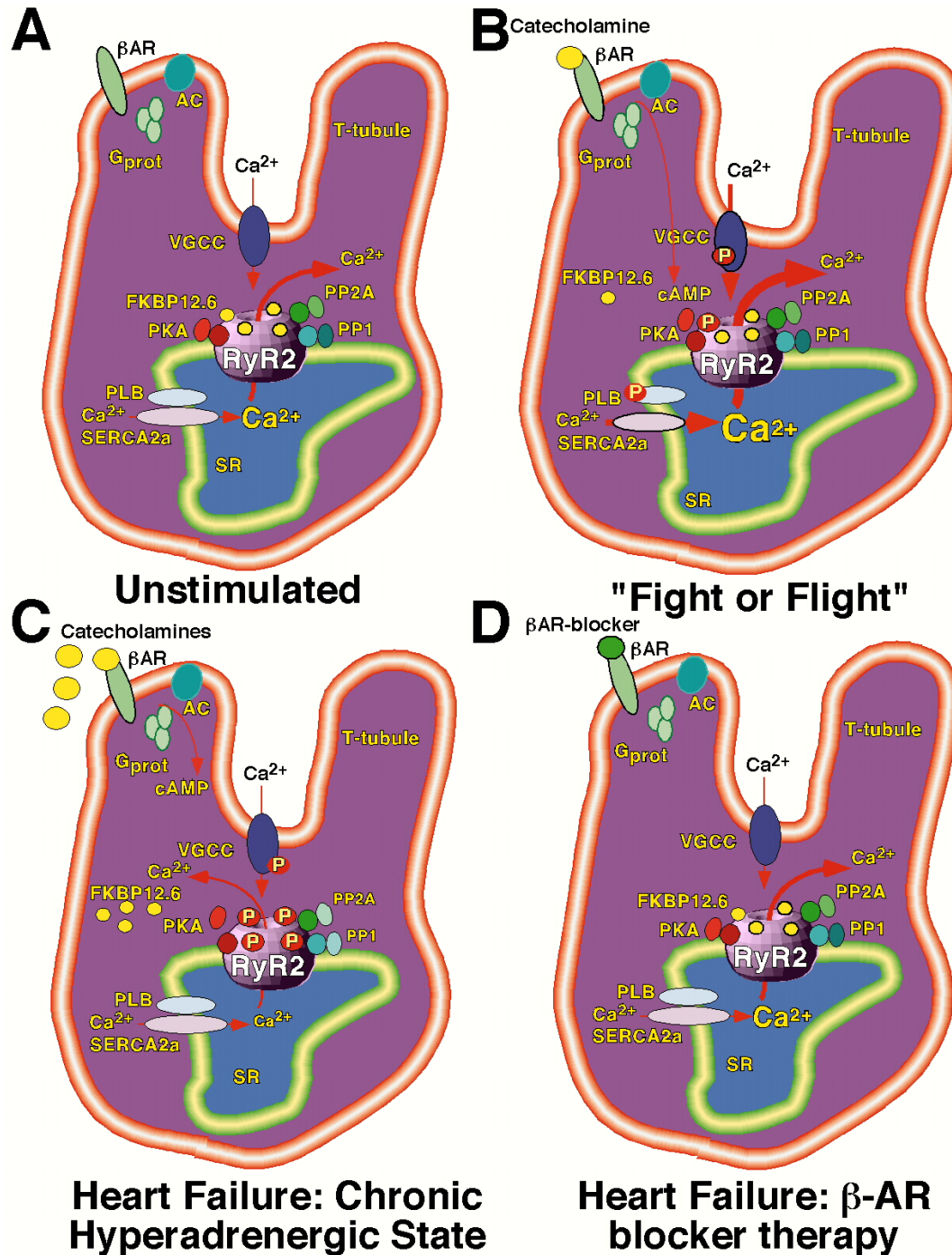


Figure 1. Modulation of cardiac excitation-contraction coupling by PKA phosphorylation.

A) Key features of cardiac EC coupling are shown. Action potentials depolarize the transverse tubule (T-tubule) and activate voltage-gated  $\text{Ca}^{2+}$  channels (VGCC).  $\text{Ca}^{2+}$  influxes through VGCC and activates RyR2 (SR  $\text{Ca}^{2+}$  release channel). RyR2 releases  $\text{Ca}^{2+}$  from the sarcoplasmic reticulum (SR) raising  $[\text{Ca}^{2+}]_{\text{cyt}}$  from  $\sim 100$  nM to  $\sim 1$   $\mu\text{M}$ .  $\text{Ca}^{2+}$  binding to troponin C induces a conformational change that activates muscle contraction.  $\text{Ca}^{2+}$  is pumped back into the SR by the  $\text{Ca}^{2+}$ -ATPase (SERCA2a). SERCA2a is inhibited by phospholamban (PLB). RyR2 macromolecular complexes include four RyR2, each RyR2 binds one FKBP12.6, PKA catalytic and regulatory subunits (RII) and mAKAP, PP2A and its targeting protein PR130, PP1 and its targeting protein spinophilin (only one of the four of each of these proteins are shown except in 1C where four FKBP12.6 are shown) (1,37).  $\beta$ -adrenergic receptor ( $\beta$ -AR) signaling pathway is shown including  $\beta$ -AR in the plasmamembrane that activates adenylyl cyclase (AC) via G proteins ( $G_{\text{prot}}$ ).

B) The "fight or flight" response involves activation of the sympathetic nervous system resulting in the release of catecholamines into the circulation that activate  $\beta$ -AR and elevate cAMP levels that in turn activate PKA (by causing the release of the PKA catalytic subunit from its regulatory subunit) (1). PKA phosphorylates and activates: 1) the VGCC, increasing  $\text{Ca}^{2+}$  influx which activates RyR2; 2) RyR2, increasing  $\text{Ca}^{2+}$ -dependent activation thereby increasing EC coupling gain; 3) PLB, releasing inhibition of SERCA2a and increasing SR  $\text{Ca}^{2+}$ -uptake. Increasing EC coupling gain increases cardiac output.

C) Decreased cardiac function in heart failure results in chronic activation of the fight or flight response (sympathetic nervous system) because the damaged heart cannot adequately respond to increase cardiac output. The chronic hyperadrenergic state results leading to PKA hyperphosphorylation of RyR2 (1). PKA hyperphosphorylation is associated with reduced PP1 and PP2A levels in the RyR2 complex and depletion of FKBP12.6 from the RyR2 complex. This pathologically increases  $\text{Ca}^{2+}$ -dependent activation of RyR2 resulting in depletion of SR  $\text{Ca}^{2+}$  stores, uncoupling of RyR2 from each other (further reducing EC coupling gain) and potentially providing diastolic SR  $\text{Ca}^{2+}$  release that can activate depolarizations that trigger fatal ventricular cardiac arrhythmias.

D)  $\beta$ -AR blockade restores FKBP12.6, PP1 and PP2A levels and RyR2 function in failing hearts (61).

that trigger VT (50,51). SR  $\text{Ca}^{2+}$  leak during diastole can generate "delayed after depolarizations" that can trigger fatal cardiac arrhythmias (e.g. VT).

### **PKA Phosphorylation of RyR2 dissociates FKBP12.6 from the channel**

The RyR2 macromolecular complex includes FKBP12.6, PKA and its targeting protein mAKAP, PP1 and its targeting protein spinophilin and PP2A with its targeting protein PR130 (1,37). Binding of FKBP12.6 to RyR2 is physiologically regulated by PKA phosphorylation of the channel which dissociates FKBP12.6 from RyR2 (1) resulting in increased activity (increased  $P_o$ ) of RyR2. Similarly, PKA phosphorylation of RyR1 also regulates FKBP12 binding (Marks et al in preparation). Increased RyR2 activity induced by dissociation of FKBP12.6 results from a shift to the left in the  $\text{Ca}^{2+}$  dependence for RyR2 activation. Regulation of FKBP12.6 binding to RyR2 is an important physiological modulator of EC coupling because FKBP12.6 binding to RyR2 is involved in the regulation of EC coupling gain (1,50,51), defined as the amount of SR  $\text{Ca}^{2+}$  released for a given trigger ( $\text{Ca}^{2+}$  influx via the voltage-gated  $\text{Ca}^{2+}$  channel) (60). In failing hearts PKA hyperphosphorylation of RyR2 also decreases coupled gating between RyR2 (48,49) due to dissociation of FKBP12.6 from the channel (unpublished data). Reduced coupled gating can further reduce EC coupling gain and may lead to incomplete closure of RyR2 during diastole (50,51). Administration of oral  $\beta$ -adrenergic receptor blocker (metoprolol 25 mg b.i.d.) reverses the PKA hyperphosphorylation of RyR2, restores normal stoichiometry of the RyR2 macromolecular complex and restores normal single channel function in a canine model of heart failure (61).

RyR2 is PKA phosphorylated on Ser<sup>2809</sup> (1) and by  $\text{Ca}^{2+}$ -CaM kinase (CamKII) on the same residue (53). PKA phosphorylation of RyR2 increases the activity ( $P_o$ ) of the channel (1), increases <sup>3</sup>H ryanodine binding (a surrogate for RyR2 function) in cardiac myocytes (59) and increases  $P_o$  of RyR2 channels activated by flash photolysis of caged  $\text{Ca}^{2+}$  (58). In the latter experiments (58) the steady state  $P_o$  of PKA treated channels (PKA phosphorylation of RyR2 was not determined in these experiments) was decreased possibly due to subsequent dephosphorylation of RyR2 by bound phosphatases that were not inhibited. PKA dependent phosphorylation reverses  $\text{Mg}^{2+}$  dependent inhibition of RyR2, and induces subconductance states in planar lipid bilayer experiments (52). Isoproterenol treatment of isolated rat myocytes increases the phosphorylation of RyR2 (59) and the amplitude of  $\text{Ca}^{2+}$  sparks (62). Other kinases including CamKII phosphorylate RyR2 although there is disagreement as to whether CamKII inhibits or activates RyR2 (52,55,57,63).

Another effect of PKA hyperphosphorylation of RyR2 in failing hearts would be to functionally uncouple the channels from one another. RyR2 are arranged on the sarcoplasmic reticulum membrane in closely packed arrays such that their large

cytoplasmic domains contact one another. We have shown that multiple RyR2s can be isolated under conditions such that they remain physically coupled to one another (48,49). When these coupled channels are examined in planar lipid bilayers multiple channels exhibit simultaneous gating termed "coupled gating" (48,49). Removal of the regulatory subunit, FKBP12.6, functionally but not physically uncouples multiple RyR2 channels (49). Coupled gating between RyR2 channels may be an important regulatory mechanism in EC coupling as well as other signaling pathways involving intracellular  $\text{Ca}^{2+}$  release. This may have important implications for understanding the molecular pathophysiology of heart failure in which PKA hyperphosphorylation of RyR2 which dissociates FKBP12.6 will inhibit coupled gating thereby reducing EC coupling gain and promoting diastolic SR  $\text{Ca}^{2+}$  leaks (DADs) that can trigger fatal cardiac arrhythmias.

### **Cellular effects of PKA phosphorylation of RyR2**

There have also been apparently contradictory findings showing that acute treatment with caffeine, which activates RyR2, fails to alter cardiac EC coupling (64), or acute administration of isoproterenol decreases  $\text{Ca}^{2+}$  spark heterogeneity (65) or improves EC coupling in failing cardiomyocytes (66). Despite the apparent contradictions these findings from other groups are not at odds with our data showing PKA hyperphosphorylation, FKBP12.6 depletion and increased  $\text{Ca}^{2+}$  sensitivity of RyR2 in failing cardiomyocytes (1). Since heart failure is a chronic disease alterations in RyR2 structure and function in failing hearts persist for months or years (1,50). The consequences of such *chronic* structural remodeling on RyR2 function are quite distinct from the effects of *acute* administration of stimulatory compounds such as caffeine or isoproterenol. The acute administration of drugs can transiently modulate RyR2 function allowing other  $\text{Ca}^{2+}$  handling molecules in the cell to restore homeostasis when RyR2 function returns to normal. In contrast, the chronic alteration of RyR2 structure and function that occurs in failing hearts can contribute to resetting SR  $\text{Ca}^{2+}$  content at a lower level due in part to increased "leak" through PKA hyperphosphorylated RyR2. This reduction in SR  $\text{Ca}^{2+}$  content can contribute to reduced EC coupling gain (1,50). Other alterations that occur in failing hearts such as a decrease in SERCA2a expression and function and/or an increase in  $\text{Na}^+/\text{Ca}^{2+}$  exchanger compound these changes as well (e.g. by reducing the amount of  $\text{Ca}^{2+}$  reuptake into the SR).

It is important to emphasize the distinction between acute administration of isoproterenol versus the chronic hyperadrenergic state of heart failure. We have shown that in heart failure there is an alteration in the stoichiometry of the RyR2 macromolecular complex such that there is a reduction in the amount of phosphatases (PP1 and PP2A) and FKBP12.6 in the complex (1). Moreover, the altered stoichiometry of the RyR2 macromolecular complex is associated with PKA hyperphosphorylation of RyR2 [an increase in the stoichiometry of PKA phosphorylation of the channel

from ~1 (normal) to ~3.5 (heart failure) moles of phosphate/mole RyR2] (1). It is unlikely that acute administration of isoproterenol would have the same effects on Ca<sup>2+</sup> handling as chronic exposure to the hyperadrenergic state of heart failure. For example there might be PKA hyperphosphorylation of RyR2 (but possibly only if phosphatase inhibitors are included), some dissociation of FKBP12.6 from the channel but probably not the decrease in phosphatases in the RyR2 macromolecular complex.

Recently, Litwin and colleagues reported that isoproterenol (100 nmol/L) induced a slight decrease in EC coupling gain and decreased the heterogeneity in Ca<sup>2+</sup> transients observed in a rabbit infarct model (65). The decrease in EC coupling gain in the infarcted heart is consistent with our data showing PKA hyperphosphorylation of RyR2, which we predict would lead to a reduction in SR Ca<sup>2+</sup> content (which Litwin and colleagues did not document but which has been shown by others groups in heart failure (67), as opposed to infarct models), as well as uncoupling of coupled RyR2 channels (49).

Critically important in these types of studies is that during isolation of the cardiomyocytes there can be a restoration of normal function due to the ongoing activity of phosphatases in the heart in the absence of phosphatase inhibitors. Our data showing direct targeting of both PP1 and PP2A to RyR2 (1,37) indicate that the phosphatases could be active during cardiomyocyte isolation and could dephosphorylate the channel once the cells are removed from the hyperadrenergic heart failure state *in vivo*. If this were the case it would explain at least in part why the cells are responsive to isoproterenol and why there is only a modest decrease in EC coupling gain and no decrease in SR Ca<sup>2+</sup> content. In short there may be a partial restoration of normal function in cardiomyocytes once they are removed from the heart failure milieu in the animal. Moreover, PKA phosphorylation of specific targets within the cardiomyocyte is compartmentalized such that some proteins (e.g. RyR2) are PKA hyperphosphorylated in failing hearts whereas other Ca<sup>2+</sup> handling proteins such as phospholamban are hypophosphorylated in the same hearts (Marks et al unpublished observation). Our recent data showing that PKA, PP1 and PP2A are specifically targeted to RyR2 via targeting proteins that bind to highly conserved leucine/isoleucine zippers (1,37) on the channel provide strong support for the concept of compartmentalization of PKA signaling.

### **RyR2 MUTATIONS LINKED TO SUDDEN CARDIAC DEATH**

Recently eleven RyR2 missense mutations have been linked to two inherited forms of sudden cardiac death (SCD): 1) Catecholaminergic Polymorphic Ventricular Tachycardia (CPVT) (2) or Familial Polymorphic VT (FPVT) (3); and 2) Arrhythmogenic Right Ventricular Dysplasia Type 2 (ARVD2) (4). Interestingly, all eleven RyR2 mutations cluster into 3 regions of the channel that correspond to three Malignant Hyperthermia (MH)/Central Core Disease (CCD) mutation regions of

the highly homologous skeletal muscle ryanodine receptor/Ca<sup>2+</sup> release channel RyR1. Both RyR2 mutations linked to genetic forms of catecholaminergic-induced VT and PKA hyperphosphorylation of RyR2 in heart failure may alter the regulation of the channel resulting in increased SR Ca<sup>2+</sup> leak that triggers SCD. RyR2 mutations linked to exercise-induced SCD may share common functional properties with RyR1 mutations linked to MH and CCD.

The fact that RyR2 mutations have been discovered in individuals with exercise-induced VT suggest an association between PKA phosphorylation of the channel (which is increased by activation of the sympathetic nervous system) and the defective channel function that predisposes to VT. Another intriguing possibility is that PKA phosphorylation of RyR2 exacerbates the defect in mutant RyR2 that are linked to exercise-induced VT.

### **MOLECULAR MECHANISMS UNDERLYING $\beta$ -ADRENERGIC RECEPTOR BLOCKADE THERAPY FOR HEART FAILURE.**

$\beta$ -AR blockade is one of the most effective treatments for heart failure. However, the use of  $\beta$ -AR blockers in patients with heart failure is counterintuitive, as they are known to decrease contractility in normal hearts. We have recently shown that systemic oral administration of a  $\beta$ -AR blocker reverses PKA hyperphosphorylation of RyR2, restores the stoichiometry of the RyR2 macromolecular complex and normalizes single channel function (Fig. 1D) in a canine model of heart failure (61). These results may, in part, explain the improved cardiac function observed in heart failure patients treated with  $\beta$ -AR blockers.

### **Conclusions and perspectives**

Elucidation of the molecular basis of cardiac EC coupling has improved our understanding of basic mechanisms that regulate cardiac function. Applications of these new understandings to the problems of heart failure and cardiac arrhythmogenesis have provided additional new understandings with important therapeutic implications. Complicating these new understandings are the challenging problems of studying integrative physiology using reductionist models. Model systems, that are necessitated by the complexity of cellular and organ physiology, each provide additional challenges that must be overcome. As investigators our goal is to integrate data from all useful models and adapt hypotheses to fit new understandings. To deny the validity of new observations because at first blush they challenge closely held beliefs is an approach that likely leads one into darkness. Most often tomorrow's investigations uncover new threads of understanding that tie together apparently disparate observations. Such an inclusive approach to investigation most often provides pathways towards the light and to lasting truths.

A better understanding of the potential role of PKA hyperphosphorylation of RyR2 in heart failure and its role in the generation of fatal cardiac arrhythmias

may emerge from studying the biophysical properties of RyR2 mutations linked to catecholamine-induced ventricular arrhythmias. However, integrating single channel data, cellular and animal physiology and emerging with a unifying mechanism that causes heart failure and SCD will be a challenge. Nevertheless, elucidating the molecular pathogenesis of heart failure and VT will be the basis for strategies that lead to novel therapeutics.

## ACKNOWLEDGMENTS

The work described in this review was supported by grants from the NIH and the AHA. The author is a Doris Duke Foundation Distinguished Clinical Scientist.

## References

- Marx SO, Reiken S, Hisamatsu Y, et al.: PKA Phosphorylation Dissociates FKBP12.6 from the Calcium Release Channel (Ryanodine Receptor): Defective Regulation in Failing Hearts. *Cell*. 2000;101:365-376.
- Priori SG, Napolitano C, Tiso N, et al.: Mutations in the Cardiac Ryanodine Receptor Gene (hRyR2) Underlie Catecholaminergic Polymorphic Ventricular Tachycardia. *Circulation*. 2001;103:196-200.
- Laitinen PJ, Brown KM, Piippo K, et al.: Mutations of the cardiac ryanodine receptor (RyR2) gene in familial polymorphic ventricular tachycardia. *Circulation*. 2001;103:485-490.
- Tiso N, Stephan DA, Nava A, et al.: Identification of mutations in the cardiac ryanodine receptor gene in families affected with arrhythmogenic right ventricular cardiomyopathy type 2 (ARVD2). *Hum Mol Genet*. 2001;10:189-194.
- Marks AR, Tempst P, Hwang KS, et al.: Molecular cloning and characterization of the ryanodine receptor/junctional channel complex cDNA from skeletal muscle sarcoplasmic reticulum. *Proc. Natl. Acad. Sci.* 1989;86:8683-8687.
- Nakai J, Imagawa T, Hakamata Y, et al.: Primary structure and functional expression from cDNA of the cardiac ryanodine receptor/calcium release channel. *FEBS*. 1990;271:169-177.
- Otsu K, Willard HF, Khanna VK, et al.: Molecular cloning of cDNA encoding the Ca<sup>2+</sup> release channel (ryanodine receptor) of rabbit cardiac muscle sarcoplasmic reticulum. *J Biol Chem*. 1990;265:13472-13483.
- Hakamata Y, Nakai J, Takeshima H, et al.: Primary Structure and distribution of a novel ryanodine receptor/calcium release channel from rabbit brain. *FEBS*. 1992;312:229-235.
- Imagawa T, Smith J, Coronado R, et al.: Purified ryanodine receptor from skeletal muscle sarcoplasmic reticulum is the Ca<sup>2+</sup>-permeable pore of the calcium release channel. *J. Biol. Chem*. 1987;262:16636-16643.
- Inui M, Saito A, Fleischer S: Purification of the ryanodine receptor and identity with feet structures of junctional terminal cisternae of sarcoplasmic reticulum from fast skeletal muscle. *J.Biol. Chem*. 1987;262:1740-1747.
- Lai FA, Erickson HP, Rousseau E, et al.: Purification and reconstitution of the calcium release channel from skeletal muscle. *Nature*. 1988;331:315-319.
- Inui M, Saito A, Fleischer S: Isolation of the ryanodine receptor from cardiac sarcoplasmic reticulum and identity with the feet structures. *J. Biol. Chem*. 1987;262:15637-15642.
- Inui M, Fleischer S: Purification of Ca<sup>2+</sup> release channel (ryanodine receptor) from heart and skeletal muscle sarcoplasmic reticulum. *Methods in Enzymology*. 1988;157:490-505.
- Brillantes AB, Ondrias K, Scott A, et al.: Stabilization of calcium release channel (ryanodine receptor) function by FK506-binding protein. *Cell*. 1994;77:513-523.
- Kobrinisky E, Ondrias K, Marks AR: Expressed ryanodine receptor can substitute for the inositol 1,4,5-trisphosphate receptor in *Xenopus laevis* oocytes during progesterone-induced maturation. *Dev. Biol*. 1995;172:531-540.
- Chen SR, Leong P, Imredy JP, et al.: Single-channel properties of the recombinant skeletal muscle Ca<sup>2+</sup> release channel (ryanodine receptor). *Biophys J*. 1997;73:1904-1912.
- Gaburjakova M, Gaburjakova J, Reiken S, et al.: FKBP12 binding modulates ryanodine receptor channel gating. *J Biol Chem*. 2001;276:16931-16935.
- Bhat MB, Hayek SM, Zhao J, et al.: Expression and functional characterization of the cardiac muscle ryanodine receptor Ca(2+) release channel in Chinese hamster ovary cells. *Biophys J*. 1999;77:808-816.
- Hymel L, Inui M, Fleischer S, et al.: Purified ryanodine receptor of skeletal muscle forms Ca<sup>2+</sup>-activated oligomeric Ca<sup>2+</sup> channels in planar bilayers. *Proc. Natl. Acad. Sci. USA*. 1988;85:441-444.
- Lai F, Erickson H, Block B, et al.: Evidence for a Ca<sup>2+</sup> channel within the ryanodine receptor complex from cardiac sarcoplasmic reticulum. *Biochem. Biophys. Res. Commun*. 1988;151:441-449.
- Smith JS, Imagawa T, Ma J, et al.: Purified ryanodine receptor from rabbit skeletal muscle is the calcium release channel of sarcoplasmic reticulum. *J. Gen. Physiol*. 1988; 2:1-26.
- Brillantes A-MB, Ondrias K, Jayaraman T, et al.: FKBP12 Optimizes function of the cloned expressed calcium release channel (ryanodine receptor). *Biophysical Journal*. 1994;66:A19.
- Ondrias K, Brillantes AM, Scott A, et al.: Single channel properties and calcium conductance of the cloned expressed ryanodine receptor/calcium-release channel. *Soc Gen Physiol*. 1996;51:29-45.
- Bezprozvanny I, Watras J, Ehrlich B: Bell-shaped calcium response curves of Ins(1,4,5)P<sub>3</sub>- and calcium-gated channels from endoplasmic reticulum of cerebellum. *Nature*. 1991;351:751-754.
- Meissner G: Adenine nucleotide stimulation of Ca<sup>2+</sup>-induced Ca<sup>2+</sup> release in sarcoplasmic reticulum. *J Biol Chem*. 1984;259:2365-2374.
- Meissner G: Ryanodine receptor/Ca<sup>2+</sup> release channels and their regulation by endogenous effectors. *Annu Rev Physiol*. 1994;56:485-508.
- Chen SRW, Zhang L, MacLennan DH: Characterization of a Ca<sup>2+</sup> Binding and Regulatory Site in the Ca<sup>2+</sup> Release Channel (Ryanodine Receptor) of Rabbit Skeletal Muscle Sarcoplasmic Reticulum. *J. Biol. Chem*. 1992;267:23318-23326.
- Fill M, Mejia-Alvarez R, Zorzato F, et al.: Antibodies as probes for ligand gating of single sarcoplasmic reticulum Ca<sup>2+</sup>-release channels. *Biochem J*. 1991;273:449-457.
- Chu A, Diaz-Munoz M, Hawkes M, et al.: Ryanodine as a probe for the functional state of the skeletal muscle sarcoplasmic reticulum calcium release channel. *Mol. Pharmacol*. 1990;37:735-741.
- Hawkes MJ, Nelson TE, Hamilton SL: [3H]Ryanodine as a Probe of Changes in the Functional State of the Ca<sup>2+</sup>-release Channel in Malignant Hyperthermia. *J. Biol. Chem*. 1992;267:6702-6709.
- Meissner G, El-Hashem A: Ryanodine as a functional probe of the skeletal muscle sarcoplasmic reticulum Ca<sup>2+</sup> release channel. *Mol and Cell. Biochem*. 1992;114:119-123.
- Chen SR, Zhang L, MacLennan DH: Asymmetrical blockade of the Ca<sup>2+</sup> release channel (ryanodine receptor) by 12-kDa FK506 binding protein. *Proc. Natl. Acad. Sci*. 1994;91:11953-11957.
- Kaftan E, Marks AR, Ehrlich BE: Effects of rapamycin on ryanodine receptor/Ca(2+)-release channels from cardiac muscle. *Circ Res*. 1996;78:990-997.

34. Marks AR: Immunophilin modulation of calcium channel gating. *Methods: A Companion to Methods in Enzymology*. 1996;9:177-187.
35. Fabiato A: Calcium-induced release of calcium from the cardiac sarcoplasmic reticulum. *Am J Physiol*. 1983;245:C1-C14.
36. Nabauer M, Callewart G, Cleeman L, et al.: Regulation of calcium release is gated by calcium current, not gating charge, in cardiac, myocytes. *Science*. 1989;244:800-803.
37. Marx SO, Reiken S, Hisamatsu Y, et al.: Phosphorylation-dependent Regulation of Ryanodine Receptors. A novel role for leucine/isoleucine zippers. *J Cell Biol*. 2001;153:699-708.
38. Landschulz WH, Johnson PF, McKnight SL: The leucine zipper: a hypothetical structure common to a new class of DNA binding proteins. *Science*. 1988;240:1759-1764.
39. Leung IW, Lassam N: Dimerization via tandem leucine zippers is essential for the activation of the mitogen-activated protein kinase kinase, MLK-3. *J Biol Chem*. 1998;273:32408-32415.
40. Jayaraman T, Brillantes A-MB, Timerman AP, et al.: FK506 Binding Protein Associated with the Calcium Release Channel (Ryanodine Receptor). *J. Biol. Chem*. 1992;267:9474-9477.
41. Timerman AP, Jayaraman T, Wiederrecht G, et al.: The ryanodine receptor from canine heart sarcoplasmic reticulum is associated with a novel FK-506 binding protein. *Biochem. Biophys. Res. Commun*. 1994;198:701-706.
42. Marks AR: Cellular functions of immunophilins. *Physiol. Rev*. 1996;76:631-649.
43. Schreiber S: Chemistry and biology of the immunophilins and their immunosuppressive ligands. *Science*. 1991;251:283-287.
44. Timerman AP, Ogunbumni E, Freund E, et al.: The calcium release channel of sarcoplasmic reticulum is modulated by FK-506-binding protein. Dissociation and reconstitution of FKBP-12 to the calcium release channel of skeletal muscle sarcoplasmic reticulum. *Journal of Biological Chemistry*. 1993;268:22992-22999.
45. Ahern GP, Junankar PR, Dulhunty AF: Subconductance states in single-channel activity of skeletal muscle ryanodine receptors after removal of FKBP12. *Biophysical Journal*. 1997;72:146-162.
46. Shou W, Aghdasi B, Armstrong DL, et al.: Cardiac defects and altered ryanodine receptor function in mice lacking FKBP12. *Nature*. 1998;391:489-492.
47. Chen L, Molinski TF, Pessah IN: Bastadin 10 Stabilizes the Open Conformation of the Ryanodine-sensitive Ca(2+) Channel in an FKBP12-dependent Manner. *J Biol Chem*. 1999;274:32603-32612.
48. Marx SO, Ondrias K, Marks AR: Coupled gating between individual skeletal muscle Ca<sup>2+</sup> release channels (ryanodine receptors). *Science*. 1998;281:818-821.
49. Marx SO, Gaburjakova J, Gaburjakova M, et al.: Coupled Gating Between Cardiac Calcium Release Channels (Ryanodine Receptors). *Circ Res*. 2001;in press.
50. Marks AR: Cardiac intracellular calcium release channels: role in heart failure. *Circ Res*. 2000;87:8-11.
51. Marks AR: Ryanodine Receptors/Calcium Release channels in Heart Failure and Sudden Cardiac Death. *J Mol Cell Cardiol*. 2001;33:615-624.
52. Hain J, Onoue H, Mayrleitner M, et al.: Phosphorylation modulates the function of the calcium release channel of sarcoplasmic reticulum from cardiac muscle. *J Biol Chem*. 1995;270:2074-2081.
53. Hohenegger M, Suko J: Phosphorylation of the purified cardiac ryanodine receptor by exogenous and endogenous protein kinases. *Biochem J*. 1993;296:303-308.
54. Islam MS, Leibiger I, Leibiger B, et al.: In situ activation of the type 2 ryanodine receptor in pancreatic beta cells requires cAMP-dependent phosphorylation. *Proc Natl Acad Sci U S A*. 1998;95:6145-6150.
55. Lokuta AJ, Rogers TB, Lederer WJ, et al.: Modulation of cardiac ryanodine receptors of swine and rabbit by a phosphorylation-dephosphorylation mechanism. *J. Phys*. 1995;487:609-622.
56. Takasago T, Imagawa T, Shigekawa M: Phosphorylation of the cardiac ryanodine receptor by cAMP-dependent protein kinase. *J Biochem (Tokyo)*. 1989;106:872-877.
57. Takasago T, Imagawa T, Furukawa K, et al.: Regulation of the cardiac ryanodine receptor by protein kinase-dependent phosphorylation. *J Biochem (Tokyo)*. 1991;109:163-170.
58. Valdivia HH, Kaplan JH, Ellis-Davies GC, et al.: Rapid adaptation of cardiac ryanodine receptors: modulation by Mg<sup>2+</sup> and phosphorylation. *Science*. 1995;267:1997-2000.
59. Yoshida A, Takahashi M, Imagawa T, et al.: Phosphorylation of ryanodine receptors in rat myocytes during beta-adrenergic stimulation. *J Biochem (Tokyo)*. 1992;111:186-190.
60. Bers DM. *Excitation-Contraction Coupling and Cardiac Contractile Force*. Boston: Kluwer Academic Publishers; 1991.
61. Reiken S, Gaburjakova M, Gaburjakova J, et al.: Beta adrenergic receptor blockers restore cardiac calcium release channel (ryanodine receptor) structure and function in heart failure. *Circulation*. 2001;in press.
62. Tanaka H, Nishimaru K, Sekine T, et al.: Two-dimensional millisecond analysis of intracellular Ca<sup>2+</sup> sparks in cardiac myocytes by rapid scanning confocal microscopy: increase in amplitude by isoproterenol. *Biochem Biophys Res Commun*. 1997;233:413-418.
63. Witche DR, Striffler BA, Jones LR: Cardiac-specific phosphorylation site for multifunctional Ca<sup>2+</sup>/calmodulin-dependent protein kinase is conserved in the brain ryanodine receptor. *J. Biol. Chem*. 1992;267:4963-4967.
64. Trafford AW, Diaz ME, Sibbring GC, et al.: Modulation of CICR has no maintained effect on systolic Ca<sup>2+</sup>: simultaneous measurements of sarcoplasmic reticulum and sarcolemmal Ca<sup>2+</sup> fluxes in rat ventricular myocytes. *J Physiol (Lond)*. 2000;522 Pt 2:259-270.
65. Litwin SE, Zhang D, Bridge JH: Dyssynchronous Ca(2+) Sparks in Myocytes From Infarcted Hearts. *Circ Res*. 2000;87:1040-1047.
66. Gomez AM, Valdivia HH, Cheng H, et al.: Defective excitation-contraction coupling in experimental cardiac hypertrophy and heart failure. *Science*. 1997;276:800-806.
67. Hobai IA, O'Rourke B: Decreased sarcoplasmic reticulum calcium content is responsible for defective excitation-contraction coupling in canine heart failure. *Circulation*. 2001;103:1577-1584.

**Correspondence:**

Andrew R. Marks  
 Center for Molecular Cardiology, Box 65  
 Columbia University College of Physicians & Surgeons, Rm 9-401  
 630 West 168th Street  
 New York, NY 10032  
 tel 212 305-0270  
 fax 212 305-3690  
 E-mail: [arm42@columbia.edu](mailto:arm42@columbia.edu)

**Running title:** Ryanodine receptors, PKA and FKBP12

**Key words:** calcium, excitation-contraction coupling, heart failure

# Regulation of Mammalian Ryanodine Receptors

Gerhard Meissner

Department of Biochemistry and Biophysics, University of North Carolina, Chapel Hill, NC 27599-7260.  
email: [meissner@med.unc.edu](mailto:meissner@med.unc.edu)

**ABSTRACT** Ryanodine receptors (RyRs) are large, high conductance  $\text{Ca}^{2+}$  channels that control the level of intracellular  $\text{Ca}^{2+}$  by releasing  $\text{Ca}^{2+}$  from an intracellular compartment, the sarco/endoplasmic reticulum. Mammalian tissues express three closely related ryanodine receptors (RyRs) known as skeletal muscle (RyR1), cardiac muscle (RyR2) and brain (RyR3). The RyRs are isolated as 30S protein complexes comprised of four 560 kDa RyR2 subunits and 12.6 kDa Fk506 binding protein (FKBP12.6) subunits. Multiple endogenous effector molecules and posttranslational modifications regulate the RyRs. This chapter reviews the regulation of the mammalian RyRs by endogenous effector molecules.

Type	RyR1	RyR2	RyR3
Major tissue	Skeletal muscle	Cardiac muscle	Diaphragm, Brain
Sedimentation coefficient	30 S	30 S	30 S
Subunit composition, RyR peptide + FKBP	4+4	4+4	4+4
Amino acids/RyR peptide	5035	4970	4870
Activation	DHPR (Voltage Sensor/ $\text{Ca}^{2+}$ )	$\text{Ca}^{2+}$	$\text{Ca}^{2+}$

Table 1. Properties of mammalian  $\text{Ca}^{2+}$  release channels/RyRs

## INTRODUCTION

Ryanodine receptors (RyRs) are large, high conductance  $\text{Ca}^{2+}$  channels that control the level of intracellular  $\text{Ca}^{2+}$  by releasing  $\text{Ca}^{2+}$  from an intracellular compartment, the sarco/endoplasmic reticulum. They are known as ryanodine receptors because they bind the plant alkaloid ryanodine with high affinity and specificity and to distinguish them from another intracellular  $\text{Ca}^{2+}$  release channel family, the inositol 1,4,5-tris phosphate receptors ( $\text{IP}_3\text{R}$ ). There are three widely expressed mammalian RyR isoforms: RyR1 is the dominant isoform in skeletal muscle, RyR2 is found in high levels in cardiac muscle, and RyR3 is expressed in many tissues at low levels including diaphragm and brain. They are also known as skeletal muscle (RyR1), cardiac muscle (RyR2) and brain (RyR3) RyRs because they were first isolated from these tissues. All three have been purified as 30 S protein complexes composed of four 560 kDa subunits and four small 12 kDa FK506 binding proteins (FKBP) with a total molecular weight of  $\sim 2,200$  kDa (Table 1). They are cation-selective channels that have high conductance for mono- and divalent cations and are regulated by a large number

of endogenous and exogenous effectors.  $\text{Ca}^{2+}$  ions are the principal activators of the cardiac and brain isoforms. In cardiac muscle during an action potential, dihydropyridine- and voltage-sensitive (L-type)  $\text{Ca}^{2+}$  channels (DHPRs) located in the surface membrane and tubular infoldings of the surface membrane (T-tubule) mediate the influx of  $\text{Ca}^{2+}$  that open SR  $\text{Ca}^{2+}$  release channels. Regulation of the skeletal isoform differs significantly from that of the two other isoforms. A unique property of the mammalian skeletal muscle RyR is that its activity is regulated via direct protein-protein interactions with the voltage-sensing T-tubule L-type  $\text{Ca}^{2+}$  channel/dihydropyridine receptor. Morphological evidence indicates the presence of a second population of RyR1s in mammalian skeletal muscle that are not directly linked to L-type  $\text{Ca}^{2+}$  channels, which raises the question how unlinked RyRs are activated. One suggestion is that  $\text{Ca}^{2+}$  ions released by DHPR-linked RyR1s activate DHPR-unlinked RyRs by a  $\text{Ca}^{2+}$ -induced mechanism resembling that in cardiac muscle (Rios and Pizarro, 1991). In an alternative mechanism, neighboring RyR1s are physically linked

leading to simultaneous opening and closing, termed coupled gating (Marx et al., 1998).

In both skeletal and cardiac muscle,  $\text{Ca}^{2+}$  release through the RyR ion channels is highly regulated by ligands and protein-protein interactions including inhibitors such as  $\text{Mg}^{2+}$  and monovalent cations, anions such as  $\text{Cl}^-$  and adenine nucleotides that activate the channels, and proteins such as calmodulin (CaM) (Fig. 1). RyRs also contain phosphorylation sites and a large number of free sulfhydryls suggesting that protein kinases, and reactive nitrogen and oxygen species have a role in regulating channel activity *in vivo*. This chapter focuses on the regulation of the mammalian RyRs by the above endogenous effectors. RyRs interact with other proteins including the voltage-sensing L-type  $\text{Ca}^{2+}$  channel/dihydropyridine receptor and various sarcoplasmic reticulum proteins. These areas of research are beyond the scope of this review.

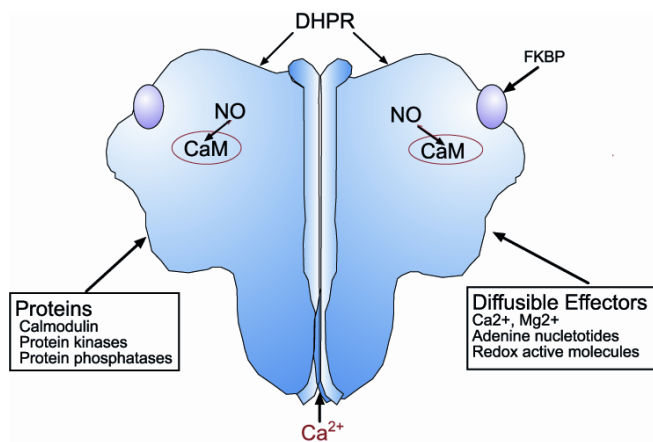


Fig. 1. Effectors of skeletal muscle RyR/ $\text{Ca}^{2+}$  release

### REGULATION OF RYRS BY $\text{Ca}^{2+}$

Regulation of RyR ion channel activity has been studied *in vitro* by three complementary methods. The  $\text{Ca}^{2+}$  efflux behavior of passively or actively (via the  $\text{Ca}^{2+}$  pump) loaded, junctionally-derived T-tubule-attached (triads) or -detached ("heavy") SR vesicles has been examined using rapid mixing and filtration methods. Second, [ $^3\text{H}$ ]ryanodine binding studies suggest that ryanodine is a suitable ligand for probing the functional states of the release channel. Third, regulation of the channel is studied in single channel recordings following the incorporation of SR vesicles or purified RyRs into planar lipid bilayers. Although single channel recordings provide direct information, an advantage of the vesicle flux and [ $^3\text{H}$ ]ryanodine binding measurements is that they yield data averaging the kinetic behavior of a large number of channels.

RyR1s are activated by  $\text{Ca}^{2+}$  binding to high-affinity,  $\text{Ca}^{2+}$  specific sites and inhibited by  $\text{Ca}^{2+}$  binding to low-affinity, less selective sites, giving rise to the characteristic bimodal  $\text{Ca}^{2+}$  dependence of channel activity shown in Fig. 2 (Xu et al., 1998). The binding sites are accessible from the cytosolic side in

the large cytosolic foot region of RyRs. A bimodal  $\text{Ca}^{2+}$  activation/inactivation curve is also obtained in  $\text{Ca}^{2+}$  efflux and [ $^3\text{H}$ ]ryanodine binding studies with skeletal muscle SR vesicles, with RyR activities being maximal at  $\mu\text{M}$   $\text{Ca}^{2+}$  (Nagasaki and Kasai, 1983; Kirino et al., 1983; Meissner et al., 1986). RyR2 (Fig. 2) and RyR3 (Chen et al., 1997; Jeyakumar et al., 1998; Murayama et al., 1999) are activated by  $\text{Ca}^{2+}$  to a greater extent and require higher  $\text{Ca}^{2+}$  concentrations for inactivation than RyR1. Single channel measurements indicate that SR luminal  $\text{Ca}^{2+}$  regulates the RyRs by binding to luminal channel sites (Gyorke and Gyorke, 1998; Sitsapesan and Williams, 1997) or by accessing cytosolic  $\text{Ca}^{2+}$  activation and inactivation sites following their passage to the cytosolic receptor side (Tripathy and Meissner, 1996; Xu and Meissner, 1998). The reasons for the different results are not clear but may reflect a predominance of one of the two mechanisms, depending on the experimental conditions.

It is likely that the bimodal  $\text{Ca}^{2+}$ -dependence of the RyRs is a consequence of at least two classes of  $\text{Ca}^{2+}$  binding sites, a high affinity activation site and a low affinity inactivation site. Several lines of evidence suggest that the carboxyl-terminal one-third of RyR1 has a critical role in activation by  $\text{Ca}^{2+}$ . Antibodies raised against a negatively charged sequence PEPEPEPEPEPE at aa 4489-4499 blocked  $\text{Ca}^{2+}$ -dependent activation of the channel (Chen et al., 1993). A single site mutation E4032A in RyR1, equivalent to E3987A in RyR2 and E3885A in RyR3, forms a functional channel with normal conductance but with greatly reduced  $\text{Ca}^{2+}$  sensitivity (Li and Chen, 2001). A deletion mutant encoding the carboxyl-terminal 1377 amino acids of RyR1 (residues 3661-5037) was activated by  $\mu\text{M}$   $\text{Ca}^{2+}$  (Bhat et al., 1997). Less is known about the location of  $\text{Ca}^{2+}$  inactivation site(s). Unlike the full-length RyR1, truncated RyR1 ( $\Delta 1-3660$ ) failed to close at high  $\text{Ca}^{2+}$ , suggesting that the N-terminal foot structure has a role in  $\text{Ca}^{2+}$  regulation (Bhat et al., 1997). On the other hand, RyR1/RyR2 chimeras containing the RyR2 carboxyl-terminal domain showed reduced inhibition at elevated  $\text{Ca}^{2+}$  (Du and MacLennan, 1999; Nakai et al.,

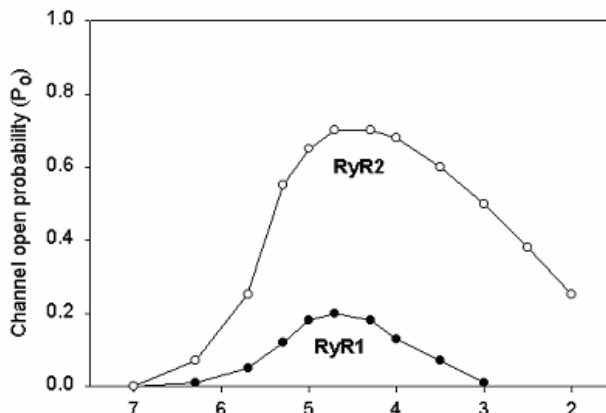


Fig. 2.  $\text{Ca}^{2+}$  dependence of single skeletal muscle (RyR1) and cardiac muscle (RyR2)  $\text{Ca}^{2+}$  release channels.

1999), similar to RyR2 (see Fig. 2), suggesting that the carboxyl-terminal region (3720-5037) has a role in  $\text{Ca}^{2+}$  inactivation. The mutation studies are complicated because mutations may induce long-range conformational changes that distort the assembly of the large multimeric RyR complexes.

### **MODULATION OF $\text{Ca}^{2+}$ -DEPENDENT RYR ACTIVITIES BY MONOVALENT IONS**

$\text{Ca}^{2+}$ -activated RyR ion channels are modulated by other molecules such as pH, ionic strength, and cation and anion composition. RyR1 and RyR2 activities were reduced by decreasing the pH from  $\sim 7.5$  to 6 (Xu et al., 1996; Ma and Zhao, 1994). Typically, an increase in salt concentration increased RyR activity, despite the fact that monovalent cations inhibited RyR activity by interacting with the  $\text{Ca}^{2+}$  activation and inactivation sites. When used as  $\text{Cl}^-$  salts, the order of effectiveness of monovalent ions in competing with  $\text{Ca}^{2+}$  at the RyR1  $\text{Ca}^{2+}$  activation sites was  $\text{Li}^+ > \text{Na}^+ > \text{K}^+ > \text{Cs}^+$  (Meissner et al., 1997). Hill coefficients of greater than 1 indicate that monovalent cations inhibit RyR1 by a cooperative interaction involving at least two cations. An interesting exception is choline<sup>+</sup> that activated RyR1 at nM  $\text{Ca}^{2+}$  concentrations, thus behaving like a weak  $\text{Ca}^{2+}$  agonist. The action of choline<sup>+</sup> appears to be unique for RyR1 because choline<sup>+</sup> did not activate the cardiac RyR (Liu et al., 1998).  $\text{Cl}^-$  anions oppose the inhibitory effects of inorganic monovalent cations by binding to specific anion regulatory sites. An increase in RyR1 activity with salt concentration indicate that the activating effects of  $\text{Cl}^-$  predominate over the inhibitory effects conveyed by  $\text{K}^+$  or  $\text{Na}^+$  (Meissner et al., 1997). Chaotropic anions ( $\text{ClO}_4^-$ ,  $\text{SCN}^-$ ,  $\text{I}^-$ ,  $\text{NO}_3^-$ ) and inorganic phosphate anions (Fruen et al., 1994) were more effective in raising RyR1 activity, whereas replacement of  $\text{Cl}^-$  by buffer anions ( $\text{MES}^-$ ,  $\text{Pipes}^-$ ) was inhibitory (Meissner et al., 1997).

A distinguishing feature of mammalian RyRs is that at 0.25–0.5 M KCl,  $\text{Ca}^{2+}$  ions activate RyR2 (Fig. 2) and RyR3 (Chen et al., 1997; Jeyakumar et al., 1998; Murayama et al., 1999) to a greater extent than RyR1. A lower binding affinity of  $\text{Ca}^{2+}$  to the  $\text{Ca}^{2+}$  inactivation sites of RyR2 and RyR3 appears to be the primary cause. As observed for RyR1, monovalent cations had an inhibitory effect on RyR2 by interacting with the  $\text{Ca}^{2+}$  activation and inactivation sites.  $\text{Cl}^-$  had an activating effect (Liu et al., 1998). Modulation of RyR3 activity by monovalent cations and anions has not been systematically studied.

### **MODULATION OF RYR ACTIVITY BY $\text{Mg}^{2+}$ , $\text{Sr}^{2+}$ AND $\text{Ba}^{2+}$ IN THE ABSENCE OF ADENINE NUCLEOTIDES**

$\text{Mg}^{2+}$ ,  $\text{Sr}^{2+}$  and  $\text{Ba}^{2+}$  compete with  $\text{Ca}^{2+}$  for the high- and low-affinity  $\text{Ca}^{2+}$  binding sites of RyR1 and RyR2, but with different effects (Meissner et al., 1986) (Laver et al., 1997) (Liu et al., 1998). Besides  $\text{Ca}^{2+}$ , cytoplasmic  $\text{Sr}^{2+}$  activated RyR1 and RyR2 by binding with more than 100 times lower affinity to the

channel activation sites. In contrast,  $\text{Mg}^{2+}$  and  $\text{Ba}^{2+}$  had an inhibitory effect. The order of mono- and divalent cations in competing with  $\text{Ca}^{2+}$  at the RyR1 and RyR2  $\text{Ca}^{2+}$  activation sites was  $\text{Mg}^{2+} > \text{Ba}^{2+} > \text{Li}^+ > \text{K}^+$  (Liu et al., 1998).

Elevated levels of divalent cations typically inhibit the RyRs. Under conditions that eliminate binding to the high affinity  $\text{Ca}^{2+}$  activation sites, mM  $\text{Mg}^{2+}$ ,  $\text{Sr}^{2+}$ ,  $\text{Ba}^{2+}$  inhibited RyR1 and RyR2 with an efficacy essentially identical to  $\text{Ca}^{2+}$ , suggesting that the low-affinity inhibitory site has a broad divalent cation specificity. On the other hand, ionic strength affected the efficacy of divalent cations in inhibiting RyR1, as indicated by an inactivation constant of  $\sim 0.1$  and  $\sim 1.35$  mM in 0.1 mM and 0.5 mM KCl media, respectively (Meissner et al., 1997)

### **REGULATION OF RYR ACTIVITY IN THE PRESENCE OF ADENINE NUCLEOTIDES**

In the absence of  $\text{Mg}^{2+}$  and ATP at neutral pH, rabbit skeletal muscle SR vesicles release their  $\text{Ca}^{2+}$  stores with a first-order rate constant of 1–2  $\text{s}^{-1}$  (Nagasaki and Kasai, 1983; Kirino et al., 1983; Meissner et al., 1986). In vivo SR  $\text{Ca}^{2+}$  release occurs on a millisecond time scale. An early key observation therefore was that  $\text{Ca}^{2+}$ -induced  $\text{Ca}^{2+}$  release was potentiated by mM ATP (Ogawa and Ebashi, 1976; Nagasaki and Kasai, 1983; Meissner, 1984). The presence of  $\mu\text{M}$   $\text{Ca}^{2+}$  and mM ATP or the nonhydrolyzable ATP analog AMP-PCP yielded maximal release rates with a first-order rate constant of 20–100  $\text{s}^{-1}$  (Nagasaki and Kasai, 1983; Meissner et al., 1986; Moutin and Dupont, 1988).  $\text{Ca}^{2+}$  release from cardiac SR vesicles was maximally activated by  $\mu\text{M}$   $\text{Ca}^{2+}$  and mM AMP-PCP, yielding a release rate with a first order rate constant of  $\sim 100$   $\text{s}^{-1}$ . In this case the potentiating effects of the nonhydrolyzable ATP analog were less pronounced because  $\text{Ca}^{2+}$  alone yielded a release rate with a first order constant of  $\sim 50$   $\text{s}^{-1}$ . In single channel measurements,  $\mu\text{M}$   $\text{Ca}^{2+}$  and mM ATP fully activated RyR1 (Smith et al., 1986) and RyR2 (Rousseau et al., 1986) with an increase in the channel open time ( $P_o$ ) to  $\sim 1$ . ATP itself is a poor activator, because RyRs were only minimally activated by adenine nucleotide in [<sup>3</sup>H]ryanodine binding and single channel measurements at [ $\text{Ca}^{2+}$ ]  $< 50$  nM (Tripathy et al., 1995; Jeyakumar et al., 1998; Chen et al., 1997).

Various other adenine nucleotides (AMP-PCP, ADP, AMP, cAMP, adenosine, adenine) potentiate SR  $\text{Ca}^{2+}$  release, suggesting that activation occurs by effector binding rather than by RyR phosphorylation (Meissner, 1984). Cyclic ADP-ribose has a role in regulating intracellular  $\text{Ca}^{2+}$  release in a variety of cells (Galione and Churchill, 2000). However, most studies using isolated membrane fractions or purified receptors did not show a direct, physiologically relevant interaction of the RyRs with cADP-ribose. Cyclic ADP-ribose appears to have a more indirect role by increasing SR  $\text{Ca}^{2+}$  uptake in heart, which was suggested to lead to RyR2 activation (Lukyanenko et

al., 2001). Other trinucleotides (CTP, GTP, ITP, UTP) had no substantial effect on the release of SR  $\text{Ca}^{2+}$  (Morii, 1983; Meissner, 1984).

Most ATP in cells is bound to  $\text{Mg}^{2+}$ . It is therefore likely that MgATP, rather than free ATP, is a major physiological effector of the RyR ion channels. However, determining the regulation of the channel complexes by MgATP is complicated by the presence of uncomplexed  $\text{Mg}^{2+}$  ions that inhibit RyRs by binding to the high-affinity and low-affinity  $\text{Ca}^{2+}$  binding sites. Additionally, CaATP complexes may form near the release site during SR  $\text{Ca}^{2+}$  release.  $\text{Ca}^{2+}$  release studies with skeletal muscle SR vesicles showed that at  $\mu\text{M}$  [ $\text{Ca}^{2+}$ ],  $\text{Mg}^{2+}$  and adenine nucleotide strongly potentiated  $\text{Ca}^{2+}$  release when present at concentrations approximating those in muscle (5 mM each, 0.7 mM free  $\text{Mg}^{2+}$  and ATP each) (Meissner et al., 1986). An increase in free  $\text{Mg}^{2+}$  from 0.1 to 4 mM inhibited SR  $\text{Ca}^{2+}$  release, which supports that free  $\text{Mg}^{2+}$  in muscle is an important determinant of RyR1 activity. One interesting suggestion is that voltage-activation of the DHPR lowers the affinity of RyR1 for  $\text{Mg}^{2+}$ , thus overcoming the inhibitory effect exerted by cytosolic  $\text{Mg}^{2+}$  (Lamb, 2000).

The effects of MgATP on the RyR2 are more modest. MgATP antagonized channel inactivation by mM  $\text{Ca}^{2+}$ , without substantially affecting the maximal level of channel activity (Xu et al., 1996; Liu et al., 1998). Further,  $> 2$  mM free  $\text{Mg}^{2+}$  was required to detect a significant decrease in channel activity in the presence of ATP or the nonhydrolyzable analog AMP-PCP. Other  $\text{Ca}^{2+}$ -dependent mechanisms include regulation by calsequestrin and calmodulin, SR luminal and cytosolic  $\text{Ca}^{2+}$  binding proteins, respectively (see below).

### MODULATION OF RYRS BY CALMODULIN

Calmodulin (CaM) is a small 16.7 kDa cytosolic protein that influences SR  $\text{Ca}^{2+}$  release through a direct interaction with RyRs as well as other proteins that regulate SR  $\text{Ca}^{2+}$  release such as the sarcolemmal voltage dependent  $\text{Ca}^{2+}$  channel (DHPR), calmodulin dependent protein kinase (CaMKII), and calmodulin stimulated protein phosphatase (calcineurin) (see below).

Early studies indicated that the  $\text{Ca}^{2+}$ -bound form of calmodulin (CaCaM) inhibits the RyR1 and RyR2 ion channels in the absence of ATP, which suggested inhibition via a direct interaction rather than through phosphorylation (Meissner, 1986; Meissner and Henderson, 1987; Smith et al., 1989). More recent [ $^3\text{H}$ ]ryanodine and single channel measurements confirmed CaM inhibition at free [ $\text{Ca}^{2+}$ ]  $> 1 \mu\text{M}$  but have also indicated significant differences in the regulation of RyRs by the  $\text{Ca}^{2+}$ -free form of CaM (apoCaM). At low free  $\text{Ca}^{2+}$  concentrations ( $< 1 \mu\text{M}$ ), apoCaM had a stimulatory effect on RyR1 (Buratti et al., 1995; Tripathy et al., 1995) and RyR3 (Chen et al., 1997) channel activities, whereas RyR2 was unaffected (Fruen et al., 2000) or inhibited (Balshaw et al., 2001) by CaM at [ $\text{Ca}^{2+}$ ]  $< 1 \mu\text{M}$ .

Studies investigating the structural basis of the functional effects of CaM on the RyRs have focused on RyR1. Skeletal muscle SR vesicles (Moore et al., 1999a; Balshaw et al., 2001) and the purified channel complex (Balshaw et al., 2001) bind a single metabolically labeled [ $^{35}\text{S}$ ]CaM per RyR1 subunit with nM affinity, independent of cytosolic  $\text{Ca}^{2+}$ . ApoCaM and CaCaM share a single CaM binding domain in RyR1 (aa residues 3616-3643), with CaM apparently shifting its points of interaction N-terminally upon binding  $\text{Ca}^{2+}$ , as shown in binding studies with RyR1 derived peptides (Rodney et al., 2001) and by site directed mutagenesis (Yamaguchi et al., 2001). Cryo-electron microscopy revealed that the position of calmodulin binding in RyR1 is shifted approximately 32 Å after binding  $\text{Ca}^{2+}$ , suggesting that binding and release of  $\text{Ca}^{2+}$  to CaM produces major conformational changes in the large RyR1 channel complex (Samso and Wagenknecht, 2002). ApoCaM and CaCaM bind to and dissociate from RyR1 and RyR2 on a time scale of seconds to minutes (Balshaw et al., 2001). It is therefore likely that CaM is constitutively bound to the receptor.

An unresolved question is why apoCaM affects the RyRs differently, because the CaM binding domain identified in RyR1 is highly conserved among the RyRs. Direct binding studies suggest that cardiac SR membranes bind 1 CaCaM and 0.25 ApoCaM per RyR2 subunit (Fruen et al., 2000) or 2 CaCaM and 1 ApoCaM (Balshaw et al., 2001) per subunit. Purification of RyR2 decreased the stoichiometry of CaCaM binding to 1 CaM/RyR2 subunit and eliminated CaCaM-dependent inhibition of [ $^3\text{H}$ ]ryanodine binding, effects not observed for RyR1. A conformational change in the purified receptor rather than removal of a necessary cofactor may be responsible for the lack of function. Single channel measurements showed that application of a transmembrane potential restored channel inhibition by CaM (Balshaw et al., 2001). Direct binding of CaM to the native RyR3 was not reported since no tissue expresses RyR3 alone.

### OXIDATION OF RYRS

Working skeletal muscle produces reactive oxygen intermediates (Reid, 1996). Reactive oxygen intermediates are also extensively formed during reoxygenation of ischemic tissue and include superoxide, hydroxyl radicals and hydrogen peroxide. In support of a functional role of these compounds, redox-active compounds and antioxidant enzymes modulate excitation-contraction coupling and force production in striated muscle.

RyR1 is an excellent target for reactive oxygen intermediates formed in muscle because it contains a large number of free sulfhydryls. The tetrameric mammalian RyR1 has 100 cysteines per 560 kDa RyR1 peptide and 1 per 12 kDa FK505 binding protein (404 per complex). Up to 50 cysteines per RyR1 subunit (200 per complex) are free (Eu et al., 2000). Accordingly in skeletal muscle, a large number of RyR1 thiols are likely in a reduced state because cells maintain a reducing environment

through thiol-reducing compounds, the most abundant being glutathione.

No unifying picture has yet evolved to explain the complex redox modulation of the RyRs. RyR1 redox state and function are dependent on O<sub>2</sub> tension, glutathione transmembrane redox potential, and Ca<sup>2+</sup>, Mg<sup>2+</sup> and calmodulin that control RyR1 channel activity. Altering O<sub>2</sub> tension alone modulated RyR1 activity by oxidizing and reducing up to 8 thiols per RyR1 subunit (Eu et al., 2000) by a mechanism that remains to be determined. RyR1 thiols sense the activity state of the receptor. [<sup>3</sup>H]ryanodine rate binding studies revealed that at highly oxidizing redox potentials (high GSSG/GSH ratio), RyR1 was more sensitive to activation by Ca<sup>2+</sup> (Xia et al., 2000). Channel closing at <math>\mu\text{M}</math> Ca<sup>2+</sup> or mM Ca<sup>2+</sup> or Mg<sup>2+</sup> caused the redox potential to become less negative, favoring the formation of free thiols. Highly reactive (hyperreactive) thiols help to confer Ca<sup>2+</sup> sensitivity because a redox response was no longer observed when the closed channel was pretreated with 7-diethylamino-3-(4'-maleimidylphenyl)-4-methylcoumarin (CPM), an alkylating reagent, that specifically labels the closed RyR1 at nM concentrations. In single channel measurements, RyR1 responded to redox potentials produced by SR luminal and cytoplasmic glutathione, indicating the presence of a unique transmembrane redox sensor in RyR1 (Feng et al., 2000). An SR transporter selective for glutathione was identified and the involvement of hyperreactive thiols in the function of the transmembrane redox sensor in RyR1 was described (Feng et al., 2000).

Studies have attempted to identify the cysteines involved in redox modulation of the RyRs. NEN alkylation and diamide oxidation of skeletal muscle SR membranes and trypsin digestion suggest that C3635 is involved in redox and calmodulin modulation of RyR1 activity (Moore et al., 1999b). On the other hand, while a C3635 to alanine substitution resulted in loss of S-nitrosylation by NO (see below), modulation by Ca<sup>2+</sup>, calmodulin, oxygen tension or glutathione was not altered (Sun et al., 2001a). A likely explanation for these results is that alkylation of C3635 introduces major steric effects, whereas a C3635 to alanine substitution does not.

Dependence of RyR1 ion channel activity on free thiol content was determined by exploring the effects of three physiological determinants of cellular redox state - oxygen tension, reduced (GSH) or oxidized (GSSG) glutathione, and NO/O<sub>2</sub><sup>-</sup> (released by SIN-1). Nearly half of the 404 cysteines within the tetrameric RyR1 channel complex were reduced (free thiol) in the presence of 5 mM GSH at pO<sub>2</sub>~10 mm Hg, i.e. under conditions comparable to resting muscle (Sun et al., 2001b). Oxidation of ~10 RyR1 thiols (~48 to ~38 free thiols per RyR1 subunit) had little effect on channel activity. Channel activity increased reversibly as the number of free thiols was reduced to ~23 per subunit, whereas more extensive oxidation (~13 free thiols per subunit) inactivated the channel irreversibly. Thus, RyR1 has at least three functional classes of thiols: 1) a large group of

functionally inert thiols that may protect RyR1 from oxidation under conditions of low oxidative stress in normal working muscle, 2) another large group of redox active thiols that controls channel response to conditions of moderate oxidative stress during extensive exercise, and 3) a group of thiols that may be susceptible to oxidative injury under extreme conditions.

Redox active species affect the activity of RyR2, with the release of endogenous CaM causing release of Ca<sup>2+</sup> from SR (Kawakami and Okabe, 1998). Direct binding studies indicated that the affinity of apoCaM and CaCaM binding to RyR1 is lower under oxidizing conditions, as determined in the presence of reduced or oxidized glutathione (Balshaw et al., 2001). CaM-dependent RyR2 activity was also influenced by glutathione redox potential, although to a lesser extent than RyR1. Redox modulation of RyR3 activity by reactive oxygen species has not been systematically studied.

### S-NITROSYLATION OF RYRS

Nitric oxide (NO) is a ubiquitous regulator of cell function. Mammalian tissues express three isoforms of nitric oxide synthase, known as endothelial (eNOS), neuronal (nNOS) and inducible (iNOS) nitric oxide synthases. In normal skeletal muscle the predominant isoform is nNOS, whereas in cardiac muscle, the major isoform is eNOS (Stamler and Meissner, 2001). Both isoforms are targeted to sarcolemmal caveola by caveolae structural protein caveolin. Immunolocalization of nNOS to isolated cardiac but not skeletal muscle SR vesicles has been reported, suggesting a unique localization of nNOS to cardiac SR (Xu et al., 1999). iNOS is absent or very low in normal skeletal muscle and heart but may increase, depending on disease state (Stamler and Meissner, 2001).

The mechanism of NO action in muscle is not well understood. NO activates guanylate cyclase, which accounts for some of its physiological effects. However, NO is also known to affect cellular functions involving S-nitrosylation and oxidation of free thiols. Both RyR1 (Eu et al., 2000) and RyR2 (Xu et al., 1998) are endogenously S-nitrosylated, supporting that NO is a physiological modulator of skeletal and cardiac muscle excitation-contraction coupling [Kelly, 1996 #5200; Reid, 1998 #2540; Eu, 1999 #3924; Petroff, 2001 #5170; Ziolo, 2001 #5099].

Modulation of RyR1 activity by NO and NO-related molecules was demonstrated in vesicle-Ca<sup>2+</sup> flux, single channel and [<sup>3</sup>H]ryanodine binding measurements. Activating (Stoyanovsky et al., 1997; Aghdasi et al., 1997) and inhibitory (Meszaros et al., 1996) effects were reported, suggesting that NO and NO-related molecules modify the channel in multiple ways. In two studies, NO-generating agents both activated and inhibited the RyR1 in lipid bilayers, depending on donor concentration, membrane potential, and the presence of channel agonists and other sulfhydryl modifying reagents (Suko et al., 1999; Hart and Dulhunty, 2000).

In vitro S-nitrosylation of RyR1 depends on O<sub>2</sub> tension and on whether NO or NO-generating molecules are used. NO S-nitrosylated RyR1 at physiologically relevant oxygen tension (pO<sub>2</sub> ~ 10 mm Hg) but not in ambient air (pO<sub>2</sub> ~ 150 mm Hg) (Eu et al., 2000), whereas the NO-generating molecule NOC-12 S-nitrosylated RyR1 in an oxygen-independent manner (Sun et al., 2002). Changes in oxygen tension oxidize/reduce as many as 6-8 thiols in each RyR1 subunit (Eu et al., 2000), which may explain the responsiveness of RyR1 to NO at tissue pO<sub>2</sub> but not ambient air. Site-directed mutagenesis studies demonstrated that at physiological O<sub>2</sub> concentrations, NO specifically S-nitrosylates Cys3635 out of ~50 free cysteines per RyR1 subunit (Sun et al., 2001a). C3635 is in the CaM binding domain of RyR1, which may explain why NO transduces its functional effect only in the presence of calmodulin (Eu et al., 2000). Thus, different cysteines within the channel appear to be responsible for the nitrosative and oxidative regulation of RyR1.

NO and NO-generating molecules were also reported to activate (Stoyanovsky et al., 1997) and inactivate (Zahradnikova et al., 1997) RyR2. NO-related molecules S-nitrosylate and oxidize the cardiac RyR in ambient O<sub>2</sub> tension. S-nitrosylation and oxidation (2-3 and ~3 sites/RyR subunit, respectively) led to activation of single RyR2s that was reversed by the sulfhydryl reducing agent dithiothreitol, whereas oxidation of a greater number of thiols was not reversed by dithiothreitol (Xu et al., 1998). The level of S-nitrosylation depended on channel conformation because it was reduced by the RyR inhibitor Mg<sup>2+</sup>. Thus, NO-related molecules affect the cardiac RyR via covalent modifications of thiol groups, leading to reversible or irreversible alteration of RyR2 ion channel activity. S-Nitrosylation of RyR2 was suggested to be physiologically significant in the normal heart (Petroff et al., 2001; Ziolo et al., 2001), whereas excess oxidation during periods of oxidative stress can lead to deleterious loss of control. NO may have a role in ischemia-reperfusion injury, however, its function is controversial, as both protective (Lefer et al., 1993) and deleterious (Woolfson et al., 1995) effects were described.

Taken together, current evidence suggests that the effects of NO and NO-related molecules on the RyRs depend on the experimental conditions, including redox state, the presence of allosteric effectors of the RyRs and the identity of NO-related molecules. Future work needs to address the isoform and tissue specificity of interaction of the RyRs with NO and NO-related molecules, the molecular basis of this specificity, and as it relates to the role of NO in overall cellular function.

### PHOSPHORYLATION OF RYRS

Endogenous kinases and phosphatases that phosphorylate and/or modulate RyR1 include cAMP-dependent protein kinase A (PKA), calmodulin-dependent kinase II (CaMKII), and protein phosphatase 1 (Leddy et al., 1993; Hain et al., 1994; Damiani et al., 1997; Zhao et al., 1998; Dulhunty et

al., 2001; Marx et al., 2001). Phosphorylation of Ser2843 by endogenous kinases (Varsanyi and Meyer, 1995) and *in vitro* phosphorylation of Ser2843 by cAMP-, cGMP- and CaM-dependent protein kinases (Suko et al., 1993) have been reported. However, the presence of additional phosphorylation sites is likely, as CaMKII also phosphorylated threonine residue(s). Functional studies comparing the effects of endogenous and exogenous kinases also support the presence of more than one phosphorylation site (Hain et al., 1994).

RyR2 forms a large multi-protein complex that includes PKA, protein phosphatases 1 and 2A (PP1 and PP2A), and anchoring proteins for PKA and PP1 and PPA2 that bind to RyR2 via leucine/isoleucine zipper motifs (Marx et al., 2000; Marx et al., 2001). Regulation of channel activity by additional protein kinases and phosphatases has been reported. These include CaMKII (Witcher et al., 1991; Hain et al., 1995; Allen and Katz, 1996), protein kinase C (PKC) isoforms  $\alpha$  and  $\beta$  (Allen and Katz, 1996), and calcineurin (Bandyopadhyay et al., 2000). Guse et al. (2001) described the transient tyrosine phosphorylation of a ryanodine receptor upon T cell stimulation.

In vitro phosphorylation of Ser2809 (corresponding to Ser2843 in RyR1) by CaMK activated the calmodulin-inhibited RyR ion channel isolated from cardiac muscle (Witcher et al., 1991). On the other hand, Takasago et al. (1991) found that an endogenous CaMK decreased [<sup>3</sup>H]ryanodine binding, while exogenous addition of PKA, cGMP-dependent protein kinase (PKG) and PKC increased [<sup>3</sup>H]ryanodine binding. Peptide mapping indicated the predominant phosphorylation of one peptide by PKA, PKC and PKG, whereas endogenous CaMK phosphorylated another peptide. Valdivia et al. (1995) observed that PKA regulated the RyR2 dynamically by increasing the responsiveness of RyR to photoreleased Ca<sup>2+</sup>, which was followed by a lower steady state open channel level. Hain et al. (1995) found that phosphorylation removed channel blockade by Mg<sup>2+</sup> when either applying PKA or CaMK II. Furthermore, calmodulin was shown to block the channel in the dephosphorylated state, which was overcome by treatment with CaMK but not PKA. More recent studies indicate that PKA phosphorylation destabilizes the RyR2 in failing hearts. PKA dissociated FKBP12.6 from RyR2 and increased the appearance of subconductance states (Marx et al., 2000). In failing hearts, reduced levels of PP1 and PPA2 in the RyR2 macromolecular complex rather than an increased PKA activity appeared to be responsible for RyR2 hyperphosphorylation and formation of "leaky" channels.

Protein kinases also influence SR Ca<sup>2+</sup> release through interactions with proteins that influence SR Ca<sup>2+</sup> release. The sarcolemmal voltage-dependent L-type Ca<sup>2+</sup> channel (DHPR), like RyR2, is phosphorylated by PKA, PKC and CaMK II. Phosphorylation of the SR Ca<sup>2+</sup> pump regulatory protein phospholamban indirectly increases RyR2 activity by elevating the SR Ca<sup>2+</sup> load and thereby

RyR activity. Indeed in permeabilized cardiomyocytes, PKA activation increased RyR2 activity (measured as sparks) in wild-type not mutant cells lacking phospholamban (Li et al., 2002). PKA activation caused no change in spark frequency in phospholamban-deficient cells, even though <sup>32</sup>P-phosphorylation was increased. These data challenge the results of Marks et al. (2000) that extensive PKA-mediated phosphorylation of RyR2 leads to the formation of leaky RyR2 channels. A caveat in the study of Li et al. (2002) is that the studies were done with cardiomyocytes isolated from normal hearts and the stoichiometry of RyR2 phosphorylation was not determined. Other potential targets are RyR associated proteins. Phosphorylation of skeletal muscle calsequestrin (Szegedi et al., 1999), triadin (Damiani et al., 1995) and sarcolumenin (Orr and Shoshan-Barmatz, 1996) has been reported.

## CONCLUSION

Ryanodine receptors are Ca<sup>2+</sup> release channels that control the levels of intracellular Ca<sup>2+</sup> by releasing Ca<sup>2+</sup> from an intracellular Ca<sup>2+</sup> storing compartment, the endo/sarcoplasmic reticulum. They form large macromolecular protein complexes of four 560-kDa receptor peptides and various associated proteins. Ca<sup>2+</sup> ions are the primary activators of the mammalian cardiac muscle (RyR2) and brain (RyR3) isoforms. Regulation of the skeletal muscle isoform (RyR1) differs significantly from that of the two other isoforms. A unique property of the mammalian RyR1 is that its activity is regulated by a direct interaction with the voltage sensing L-type Ca<sup>2+</sup> channel/dihydropyridine receptor. RyRs are modulated by multiple endogenous effectors including Mg<sup>2+</sup>, H<sup>+</sup>, ATP, calmodulin, protein kinases and phosphatases. Modulation by NO and other redox active molecules suggests a critical role for cysteine residues in RyR activity. Taken together, RyRs are subject to regulation by multiple effector molecules. Exactly, how RyR regulation influences cellular functions remains to be established.

## ACKNOWLEDGEMENTS

This work was supported by National Institutes of Health Grants AR 18687 and HL 27430.

## References

1. Aghdasi, B., M. B. Reid, and S. L. Hamilton. 1997. Nitric oxide protects the skeletal muscle Ca<sup>2+</sup> release channel from oxidation induced activation. *J Biol Chem.* 272:25462-25467.
2. Allen, B. G., and S. Katz. 1996. Phosphorylation of cardiac junctional and free sarcoplasmic reticulum by PKC $\alpha$ , PKC $\beta$ , PKA and the Ca<sup>2+</sup>/calmodulin-dependent protein kinase. *Mol Cell Biochem.* 155:91-103.
3. Balshaw, D. M., L. Xu, N. Yamaguchi, D. A. Pasek, and G. Meissner. 2001. Calmodulin binding and inhibition of cardiac muscle calcium release channel (ryanodine receptor). *J Biol Chem.* 276:20144-53.
4. Bandyopadhyay, A., D. W. Shin, J. O. Ahn, and D. H. Kim. 2000. Calcineurin regulates ryanodine receptor/Ca(2+)-release channels in rat heart. *Biochem J.* 352:61-70.

5. Bhat, M. B., J. Y. Zhao, H. Takeshima, and J. J. Ma. 1997. Functional Calcium Release Channel Formed By the Carboxyl-Terminal Portion Of Ryanodine Receptor. *Biophys J.* 73:1329-1336.
6. Buratti, R., G. Prestipino, P. Menegazzi, S. Treves, and F. Zorzato. 1995. Calcium dependent activation of skeletal muscle Ca<sup>2+</sup> release channel (ryanodine receptor) by calmodulin. *Biochem Biophys Res Comm.* 213:1082-90.
7. Chen, S. R., L. Zhang, and D. H. MacLennan. 1993. Antibodies as probes for Ca<sup>2+</sup> activation sites in the Ca<sup>2+</sup> release channel (ryanodine receptor) of rabbit skeletal muscle sarcoplasmic reticulum. *J Biol Chem.* 268:13414-21.
8. Chen, S. R. W., X. Li, K. Ebisawa, and L. Zhang. 1997. Functional characterization of the recombinant type 3 Ca<sup>2+</sup> release channel (ryanodine receptor) expressed in HEK293 cells. *J Biol Chem.* 272:24234-46.
9. Damiani, E., E. Picello, L. Saggin, and A. Margreth. 1995. Identification of triadin and of histidine-rich Ca(2+)-binding protein as substrates of 60 kDa calmodulin-dependent protein kinase in junctional terminal cisternae of sarcoplasmic reticulum of rabbit fast muscle. *Biochem Biophys Res Comm.* 209:457-65.
10. Damiani, E., G. Tobaldin, E. Bortoloso, and A. Margreth. 1997. Functional behaviour of the ryanodine receptor/Ca(2+)-release channel in vesiculated derivatives of the junctional membrane of terminal cisternae of rabbit fast muscle sarcoplasmic reticulum. *Cell Calcium.* 22:129-50.
11. Du, G. G., and D. H. MacLennan. 1999. Ca(2+) inactivation sites are located in the COOH-terminal quarter of recombinant rabbit skeletal muscle Ca(2+) release channels (ryanodine receptors). *J Biol Chem.* 274:26120-6.
12. Dulhunty, A. F., D. Laver, S. M. Curtis, S. Pace, C. Haarmann, and E. M. Gallant. 2001. Characteristics of irreversible ATP activation suggest that native skeletal ryanodine receptors can be phosphorylated via an endogenous CaMKII. *Biophys J.* 81:3240-52.
13. Eu, J. P., J. Sun, L. Xu, J. S. Stamler, and G. Meissner. 2000. The skeletal muscle calcium release channel: coupled O<sub>2</sub> sensor and NO signaling functions. *Cell.* 102:499-509.
14. Feng, W., G. Liu, P. D. Allen, and I. N. Pessah. 2000. Transmembrane redox sensor of ryanodine receptor complex. *J Biol Chem.* 275:35902-7.
15. Fruen, B. R., J. M. Bardy, T. M. Byrem, G. M. Strasburg, and C. F. Louis. 2000. Differential Ca(2+) sensitivity of skeletal and cardiac muscle ryanodine receptors in the presence of calmodulin. *Am J Physiol.* 279:C724-33.
16. Fruen, B. R., J. R. Mickelson, T. J. Roghair, H. L. Cheng, and C. F. Louis. 1994. Anions that potentiate excitation-contraction coupling may mimic effect of phosphate on Ca<sup>2+</sup> release channel. *Am J Physiol.* 266:C1729-35.
17. Galione, A., and G. C. Churchill. 2000. Cyclic ADP ribose as a calcium-mobilizing messenger. *Science's STKE [Electronic Resource]: Signal Transduction Knowledge Environment.* 2000:E1.
18. Guse, A. H., A. Y. Tsygankov, K. Weber, and G. W. Mayr. 2001. Transient tyrosine phosphorylation of human ryanodine receptor upon T cell stimulation. *J Biol Chem.* 276:34722-7.
19. Gyorke, I., and S. Gyorke. 1998. Regulation of the cardiac ryanodine receptor channel by luminal Ca<sup>2+</sup> involves luminal Ca<sup>2+</sup> sensing sites. *Biophys J.* 75:2801-10.
20. Hain, J., S. Nath, M. Mayrleitner, S. Fleischer, and H. Schindler. 1994. Phosphorylation modulates the function of the calcium release channel of sarcoplasmic reticulum from skeletal muscle. *Biophys J.* 67:1823-33.
21. Hain, J., H. Onoue, M. Mayrleitner, S. Fleischer, and H. Schindler. 1995. Phosphorylation modulates the function of the calcium release channel of sarcoplasmic

- reticulum from cardiac muscle. *J Biol Chem.* 270:2074-81.
22. Hart, J. D. and A. F. Dulhunty. 2000. Nitric oxide activates or inhibits skeletal muscle ryanodine receptors depending on its concentration, membrane potential and ligand binding. *J Membrane Biol.* 173:227-36
  23. Jeyakumar, L. H., J. A. Copello, A. M. O'Malley, G. M. Wu, R. Grassucci, T. Wagenknecht, and S. Fleischer. 1998. Purification and characterization of ryanodine receptor 3 from mammalian tissue. *J Biol Chem.* 273:16011-20.
  24. Kawakami, M., and E. Okabe. 1998. Superoxide anion radical-triggered Ca<sup>2+</sup> release from cardiac sarcoplasmic reticulum through ryanodine receptor Ca<sup>2+</sup> channel. *Mol Pharmacol.* 53:497-503.
  25. Kirino, Y., M. Osakabe, and H. Shimizu. 1983. Ca<sup>2+</sup>-induced Ca<sup>2+</sup> release from fragmented sarcoplasmic reticulum: Ca<sup>2+</sup>-dependent passive Ca<sup>2+</sup> efflux. *J Biochem.* 94:1111-1118.
  26. Lamb, G. D. 2000. Excitation-contraction coupling in skeletal muscle: comparisons with cardiac muscle. *Clin Exp Pharm Physiol.* 27:216-24.
  27. Laver, D. R., T. M. Baynes, and A. F. Dulhunty. 1997. Magnesium inhibition of ryanodine-receptor calcium channels: evidence for two independent mechanisms. *J Membrane Biol.* 156:213-29.
  28. Leddy, J. J., B. J. Murphy, Y. Qu, J. P. Doucet, C. Pratt, and B. S. Tuana. 1993. A 60 kDa polypeptide of skeletal-muscle sarcoplasmic reticulum is a calmodulin-dependent protein kinase that associates with and phosphorylates several membrane proteins. *Biochem J.* 295:849-56.
  29. Lefer, D. J., K. Nakanishi, W. Johnston, and J. Vinten-Johansen. 1993. Antineutrophil and myocardial protecting actions of a novel nitric oxide donor after acute ischemia and reperfusion. *Circulation.* 88:2337-2350.
  30. Li, P., and S. R. Chen. 2001. Molecular basis of Ca(2)+ activation of the mouse cardiac Ca(2)+ release channel (ryanodine receptor). *J Gen Physiol.* 118:33-44.
  31. Li, Y., E. G. Kranias, G. A. Mignery, and D. M. Bers. 2002. Protein kinase A phosphorylation of the ryanodine receptor does not affect calcium sparks in mouse ventricular myocytes. *Circ Res.* 90:309-16.
  32. Liu, W., D. A. Pasek, and G. Meissner. 1998. Modulation of Ca(2+)-gated cardiac muscle Ca(2+)-release channel (ryanodine receptor) by mono- and divalent ions. *Am J Physiol.* 274:C120-8.
  33. Lukyanenko, V., I. Gyorke, T. F. Wiesner, and S. Gyorke. 2001. Potentiation of Ca(2+) release by cADP-ribose in the heart is mediated by enhanced SR Ca(2+) uptake into the sarcoplasmic reticulum. *Circ Res.* 89:614-22.
  34. Ma, J., and J. Zhao. 1994. Highly cooperative and hysteretic response of the skeletal muscle ryanodine receptor to changes in proton concentrations. *Biophys J.* 67:626-33.
  35. Marx, S. O., K. Ondrias, and A. R. Marks. 1998. Coupled gating between individual skeletal muscle Ca<sup>2+</sup> release channels (ryanodine receptors) [see comments]. *Science.* 281:818-21.
  36. Marx, S. O., S. Reiken, Y. Hisamatsu, M. Gaburjakova, J. Gaburjakova, Y. M. Yang, N. Rosemblyt, and A. R. Marks. 2001. Phosphorylation-dependent regulation of ryanodine receptors: a novel role for leucine/isoleucine zippers. *J Cell Biol.* 153:699-708.
  37. Marx, S. O., S. Reiken, Y. Hisamatsu, T. Jayaraman, D. Burkhoff, N. Rosemblyt, and A. R. Marks. 2000. PKA phosphorylation dissociates FKBP12.6 from the calcium release channel (ryanodine receptor): defective regulation in failing hearts. *Cell.* 101:365-76.
  38. Meissner, G. 1984. Adenine nucleotide stimulation of Ca<sup>2+</sup>-induced release in sarcoplasmic reticulum. *J Biol Chem.* 259:2365-2374.
  39. Meissner, G. 1986. Evidence of a role for calmodulin in the regulation of calcium release from skeletal muscle sarcoplasmic reticulum. *Biochemistry.* 25:244-51.
  40. Meissner, G., E. Darling, and J. Eveleth. 1986. Kinetics of rapid Ca<sup>2+</sup> release by sarcoplasmic reticulum. Effects of Ca<sup>2+</sup>, Mg<sup>2+</sup>, and adenine nucleotides. *Biochemistry.* 25:236-44.
  41. Meissner, G., and J. S. Henderson. 1987. Rapid calcium release from cardiac sarcoplasmic reticulum vesicles is dependent on Ca<sup>2+</sup> and is modulated by Mg<sup>2+</sup>, adenine nucleotide, and calmodulin. *J Biol Chem.* 262:3065-73.
  42. Meissner, G., E. Rios, A. Tripathy, and D. A. Pasek. 1997. Regulation of skeletal muscle Ca<sup>2+</sup> release channel (ryanodine receptor) by Ca<sup>2+</sup> and monovalent cations and anions. *J Biol Chem.* 272:1628-38.
  43. Meszaros, L. G., I. Minarovic, and A. Zahradnikova. 1996. Inhibition of the skeletal muscle ryanodine receptor calcium release channel by nitric oxide. *FEBS Letters.* 380:49-52.
  44. Moore, C. P., G. Rodney, J. Z. Zhang, L. Santacruz-Tolosa, G. Strasburg, and S. L. Hamilton. 1999a. Apocalmodulin and Ca<sup>2+</sup> calmodulin bind to the same region on the skeletal muscle Ca<sup>2+</sup> release channel. *Biochemistry.* 38:8532-7.
  45. Moore, P. C., J. Z. Zhang, and S. L. Hamilton. 1999b. A role for cysteine 3635 of RYR1 in redox modulation and calmodulin binding. *J Biol Chem.* 274:36831-4.
  46. Morii, H., and Tonomura, Y. 1983. The gating behavior of a channel for Ca<sup>2+</sup>-induced Ca<sup>2+</sup> release in fragmented sarcoplasmic reticulum. *J Biochem (Tokyo).* 93:1271-1285.
  47. Moutin, M. J., and Y. Dupont. 1988. Rapid filtration of Ca<sup>2+</sup>-induced Ca<sup>2+</sup> release from skeletal sarcoplasmic reticulum. *J Biol Chem.* 263:4228-4235.
  48. Murayama, T., T. Oba, E. Katayama, H. Oyamada, K. Oguchi, M. Kobayashi, K. Otsuka, and Y. Ogawa. 1999. Further characterization of the type 3 ryanodine receptor (RyR3) purified from rabbit diaphragm. *J Biol Chem.* 274:17297-308.
  49. Nagasaki, K., and M. Kasai. 1983. Fast release of calcium from sarcoplasmic reticulum vesicles monitored by chlortetracycline fluorescence. *J Biochem.* 94:1101-9.
  50. Nakai, J., L. Gao, L. Xu, C. Xin, D. A. Pasek, and G. Meissner. 1999. Evidence for a role of C-terminus in Ca(2+) inactivation of skeletal muscle Ca(2+) release channel (ryanodine receptor). *FEBS Letters.* 459:154-8.
  51. Ogawa, Y., and S. Ebashi. 1976. Ca-releasing action of b, g-methylene adenosine triphosphate on fragmented sarcoplasmic reticulum. *J Biochem.* 80:1149-1157.
  52. Orr, I., and V. Shoshan-Barmatz. 1996. Modulation of the skeletal muscle ryanodine receptor by endogenous phosphorylation of 160/150-kDa proteins of the sarcoplasmic reticulum. *Biochim Biophys Acta.* 1283:80-8.
  53. Petroff, M. G., S. H. Kim, S. Pepe, C. Dessy, E. Marban, J. L. Balligand, and S. J. Sollott. 2001. Endogenous nitric oxide mechanisms mediate the stretch dependence of Ca<sup>2+</sup> release in cardiomyocytes. *Nature Cell Biol.* 3:867-73.
  54. Reid, M. B. 1996. reactive oxygen and nitric oxide in skeletal muscle. *News Physiology Science.* 11:114-121.
  55. Rios, E., and G. Pizarro. 1991. Voltage sensor of excitation-contraction coupling in skeletal muscle. *Physiol Rev.* 71:849-908.
  56. Rodney, G. G., C. P. Moore, B. Y. Williams, J. Z. Zhang, J. Krol, S. E. Pedersen, and S. L. Hamilton. 2001. Calcium binding to calmodulin leads to an N-terminal shift in its binding site on the ryanodine Receptor. *J Biol Chem.* 276:2069-74.
  57. Rousseau, E., J. S. Smith, J. S. Henderson, and G. Meissner. 1986. Single channel and 45Ca<sup>2+</sup> flux measurements of the cardiac sarcoplasmic reticulum calcium channel. *Biophys J.* 50:1009-14.

58. Samsó, M., and T. Wagenknecht. 2002. Apocalmodulin and Ca<sup>2+</sup>-calmodulin bind to neighboring locations on the ryanodine receptor. *J Biol Chem.* 277:1349-53.
59. Sitsapesan, R., and A. J. Williams. 1997. Regulation of current flow through ryanodine receptors by luminal Ca<sup>2+</sup>. *J Membrane Biol.* 159:179-185.
60. Smith, J. S., R. Coronado, and G. Meissner. 1986. Single channel measurements of the calcium release channel from skeletal muscle sarcoplasmic reticulum. Activation by Ca<sup>2+</sup> and ATP and modulation by Mg<sup>2+</sup>. *J Gen Physiol.* 88:573-88.
61. Smith, J. S., E. Rousseau, and G. Meissner. 1989. Calmodulin modulation of single sarcoplasmic reticulum Ca<sup>2+</sup>-release channels from cardiac and skeletal muscle. *Circ Res.* 64:352-9.
62. Stamler, J. S., and G. Meissner. 2001. Physiology of nitric oxide in skeletal muscle. *Physiol Rev.* 81:209-237.
63. Stoyanovsky, D., T. Murphy, P. R. Anno, Y. M. Kim, and G. Salama. 1997. Nitric oxide activates skeletal and cardiac ryanodine receptors. *Cell Calcium.* 21:19-29.
64. Suko, J., I. Maurer-Fogy, B. Plank, O. Bertel, W. Wyskovsky, M. Hohenegger, and G. Hellmann. 1993. Phosphorylation of serine 2843 in ryanodine receptor-calcium release channel of skeletal muscle by cAMP-, cGMP- and CaM-dependent protein kinase. *Biochim Biophys Acta.* 1175:193-206.
65. Sun, J., C. Xin, J. P. Eu, J. S. Stamler, and G. Meissner. 2001a. Cysteine-3635 is responsible for skeletal muscle ryanodine receptor modulation by NO. *Proc Natl Acad Sci USA.* 98:11158-62.
66. Sun, J., L. Xu, J. P. Eu, J. S. Stamler, and G. Meissner. 2002. Modulation of skeletal muscle calcium release channel/ryanodine receptor (RyR1) by NOC-12 occurs independent of oxygen tension. *Biophys J.* 82:624a.
67. Sun, J., L. Xu, J. P. Eu, J. S. Stamler, and G. Meissner. 2001b. Classes of thiols that influence the activity of the skeletal muscle calcium release channel. *J Biol Chem.* 276:15625-30.
68. Szegedi, C., S. Sarkozi, A. Herzog, I. Jona, and M. Varsanyi. 1999. Calsequestrin: more than 'only' a luminal Ca<sup>2+</sup> buffer inside the sarcoplasmic reticulum. *Biochem J.* 337:19-22.
69. Takasago, T., T. Imagawa, K. Furukawa, T. Ogurusu, and M. Shigekawa. 1991. Regulation of the cardiac ryanodine receptor by protein kinase-dependent phosphorylation. *J Biochem Tokyo.* 109:163-70.
70. Tripathy, A., and G. Meissner. 1996. Sarcoplasmic reticulum luminal Ca<sup>2+</sup> has access to cytosolic activation and inactivation sites of skeletal muscle Ca<sup>2+</sup> release channel. *Biophys J.* 70:2600-15.
71. Tripathy, A., L. Xu, G. Mann, and G. Meissner. 1995. Calmodulin activation and inhibition of skeletal muscle Ca<sup>2+</sup> release channel (ryanodine receptor). *Biophys J.* 69:106-19.
72. Valdivia, H. H., J. H. Kaplan, G. C. Ellis-Davies, and W. J. Lederer. 1995. Rapid adaptation of cardiac ryanodine receptors: modulation by Mg<sup>2+</sup> and phosphorylation. *Science.* 267:1997-2000.
73. Varsanyi, M., and H. E. Meyer. 1995. Sarcoplasmic reticular Ca<sup>2+</sup> release channel is phosphorylated at serine 2843 in intact rabbit skeletal muscle. *Biol Chem Hoppe-Seyler.* 376:45-9.
74. Witcher, D. R., R. J. Kovacs, H. Schulman, D. C. Cefali, and L. R. Jones. 1991. Unique phosphorylation site on the cardiac ryanodine receptor regulates calcium channel activity. *J Biol Chem.* 266:11144-11152.
75. Woolfson, R. G., V. C. Patel, G. H. Neild, and D. M. Yellon. 1995. Inhibition of nitric acid synthesis reduces infarct size by an adenosine-dependent mechanism. *Circulation.* 91:1545-1551.
76. Xia, R., T. Stangler, and J. J. Abramson. 2000. Skeletal muscle ryanodine receptor is a redox sensor with a well defined redox potential that is sensitive to channel modulators. *J Biol Chem.* 275:36556-61.
77. Xu, K. Y., D. L. Huso, T. M. Dawson, D. S. Bredt, and L. C. Becker. 1999. Nitric oxide synthase in cardiac sarcoplasmic reticulum. *Proc Natl Acad Sci USA.* 96:657-62.
78. Xu, L., J. P. Eu, G. Meissner, and J. S. Stamler. 1998. Activation of the cardiac calcium release channel (ryanodine receptor) by poly-S-nitrosylation. *Science.* 279:234-7.
79. Xu, L., G. Mann, and G. Meissner. 1996. Regulation of cardiac Ca<sup>2+</sup> release channel (ryanodine receptor) by Ca<sup>2+</sup>, H<sup>+</sup>, Mg<sup>2+</sup>, and adenine nucleotides under normal and simulated ischemic conditions. *Circ Res.* 79:1100-9.
80. Xu, L., and G. Meissner. 1998. Regulation of cardiac muscle Ca<sup>2+</sup> release channel by sarcoplasmic reticulum luminal Ca<sup>2+</sup>. *Biophys J.* 75:2302-12.
81. Xu, L., A. Tripathy, D. Pasek, and G. Meissner. 1998. Potential for pharmacology of ryanodine receptor/calcium release channel. *Ann New York Acad Sci.* 853:130-148.
82. Yamaguchi, N., C. Xin, and G. Meissner. 2001. Identification of apocalmodulin and Ca<sup>2+</sup>-calmodulin regulatory domain in skeletal muscle Ca<sup>2+</sup> release channel, ryanodine receptor. *J Biol Chem.* 276:22579-85.
83. Zahradnikova, A., I. Minarovic, R. C. Venema, and L. G. Meszaros. 1997. Inactivation of the cardiac ryanodine receptor calcium release channel by nitric oxide. *Cell Calcium.* 22:447-54.
84. Zhao, S. M., N. R. Brandt, A. H. Caswell, and E. Y. C. Lee. 1998. Binding of the catalytic subunit of protein phosphatase-1 to the ryanodine-sensitive calcium release channel protein. *Biochemistry.* 37:18102-18109.
85. Ziolo, M. T., H. Katoh, and D. M. Bers. 2001. Positive and negative effects of nitric oxide on Ca(2+) sparks: influence of beta-adrenergic stimulation. *Am J Physiol.* 281:H2295-303.

## Correspondence

Phone: (919) 966 5021

Fax: (919) 966 2852

email: meissner@med.unc.edu

# Calcium quarks

Ernst Niggli, Marcel Egger

Department of Physiology, University of Bern, Bülhplatz 5, 3012 Bern, Switzerland. E-mail: [niggli@pyl.unibe.ch](mailto:niggli@pyl.unibe.ch)

**ABSTRACT** Elementary subcellular  $\text{Ca}^{2+}$  signals arising from the opening of single ion channels may offer the possibility to examine the stochastic behavior and the microscopic chemical reaction rates of these channel proteins in their natural environment. Such an analysis can yield detailed information about the molecular function that cannot be derived from recordings obtained from an ensemble of channels. In this review, we summarize experimental evidence suggesting that  $\text{Ca}^{2+}$  sparks, elementary  $\text{Ca}^{2+}$  signaling events of cardiac and skeletal muscle excitation contraction coupling, may be comprised of a number of smaller  $\text{Ca}^{2+}$  signaling events, the  $\text{Ca}^{2+}$  quarks.

## INTRODUCTION

When  $\text{Ca}^{2+}$  sparks were first identified as elementary events underlying cardiac  $\text{Ca}^{2+}$  (1-2) everyone working in the field of cardiac excitation-contraction (EC) coupling and  $\text{Ca}^{2+}$  signaling immediately became excited by the perspectives offered by these new findings. Besides having a strong impact on the conception of cardiac excitation-contraction coupling, this discovery was also expected to have implications comparable to those of the first description of ionic currents carried by single membrane channel molecules. Recordings of ion currents on the level of single channels by means of the patch-clamp technique had not only revolutionized the entire field of electrophysiology, but had also dramatically broadened our knowledge about the functioning of channel proteins (for review see 3).  $\text{Ca}^{2+}$  sparks were thus foreseen to enable us to extract information about single  $\text{Ca}^{2+}$  release channels *in-vivo*. Furthermore, it was anticipated that similar elementary  $\text{Ca}^{2+}$  events might underlie  $\text{Ca}^{2+}$  signaling in cells other than cardiac muscle (for review see 4). Indeed, it became rapidly clear that analogous  $\text{Ca}^{2+}$  signaling events could be found in many other excitable and unexcitable cells, such as skeletal muscle (5-6) neuronal cells, but also in a variety of unexcitable cells (for reviews see 4, 7-8). After all, scientists not working in the field of  $\text{Ca}^{2+}$  signaling might wonder why exactly everyone was exceedingly excited about these signals. In the present review, we try to highlight the possible impact of elementary  $\text{Ca}^{2+}$  signaling events on our understanding of  $\text{Ca}^{2+}$  signaling.

### Why is the elementary nature of $\text{Ca}^{2+}$ signaling important?

Until recently, several important features of cardiac  $\text{Ca}^{2+}$  signaling were poorly understood on the cellular level. A prominent example is called the "paradox of cardiac  $\text{Ca}^{2+}$  signaling". After the seminal studies carried out in the eighties by Fabiato and coworkers (9), it became generally accepted that in cardiac muscle a small trigger signal mediated by L-type  $\text{Ca}^{2+}$  current is amplified several-fold by the mechanism of  $\text{Ca}^{2+}$ -induced  $\text{Ca}^{2+}$  release (CICR) from the sarcoplasmic reticulum (SR). One might wonder what exactly would be paradoxical with this notion. It can be appreciated intuitively, that the

output signal of this amplification, an elevation of the intracellular  $\text{Ca}^{2+}$  concentration ( $[\text{Ca}^{2+}]_i$ ), is identical to the signal that triggers it. Thus, a high degree of positive feedback in CICR and a tendency for instability would be expected. Indeed, this behavior surfaced in attempts to develop computer models of cardiac  $\text{Ca}^{2+}$  signaling. As it turned out, the experimentally observed degree of amplification could not be simulated without compromising the stability of the model system, at least when "trigger  $\text{Ca}^{2+}$ " and "released  $\text{Ca}^{2+}$ " occupied a common cytosolic  $\text{Ca}^{2+}$  pool. Such models were referred to as "common pool models" (10). However, when CICR was modeled to occur via independent or loosely coupled functional units, each comprising a single L-type  $\text{Ca}^{2+}$  channel and one (" $\text{Ca}^{2+}$  synapse") or several ("cluster-bomb") SR  $\text{Ca}^{2+}$  release channels, the necessary amplification could be simulated without a tendency for all-or-none behavior. With such a model, regulation of  $\text{Ca}^{2+}$  release then became easily feasible by recruiting more or fewer functional  $\text{Ca}^{2+}$  release units. Thus, the apparent paradox was the discrepancy between the required amplification of CICR contrasting with both the experimentally observed maintained control over  $\text{Ca}^{2+}$  release and the mathematical model predictions. This paradox has been solved by implementing a  $\text{Ca}^{2+}$  signaling system which is based on the recruitment of functionally independent  $\text{Ca}^{2+}$  sparks, each spark itself exhibiting the necessary amplification and a high degree of positive feed-back, essentially representing an all-or none event.

### Why is the precise number of channels participating in the generation of $\text{Ca}^{2+}$ sparks important?

As mentioned above, the tremendous power of single ion channel analysis has provided insight into features of ion channel function that are not accessible otherwise. For example, with ensemble currents the analysis of microscopic channel gating kinetics and single channel conductance, possibly including some subconductance states, would not have been possible. Unfortunately, for single channels that are located in membranes of intracellular organelles, such as in the SR, the nucleus or mitochondria, the patch-clamp technique cannot be used easily (but see, for example, (11)). However, several groups

have developed methods to perform similar experimental recordings after reconstituting purified channel preparations (such as SR vesicles) into artificial lipid bilayer membranes. This powerful approach has allowed detailed studies of many aspects of RyR function and resulted in a large body of literature. There is, however, a problem common to all experimental studies carried out in the lipid bilayer system: the channels cannot be analyzed in their native environment. For example, during purification and reconstitution small accessory SR proteins with important functions may be lost. In addition, the composition of the solutions used to examine the channels in lipid bilayers is frequently quite different from the normal cytosol. Because of these difficulties, data obtained from reconstituted channels cannot simply be extrapolated to the behavior of the channels *in-vivo*. This word of caution is further supported by the results of recent attempts to examine the single channel conductance of the RyR in more physiological solutions (12). These experiments again emphasized, that the environment of the channels is extremely important for their normal functioning. From these considerations, it seems obvious that every method which allows to examine the RyRs on the single channel level *in-situ* would be highly valuable, such as imaging of Ca<sup>2+</sup> sparks in living cells with fluorescent Ca<sup>2+</sup> indicators. But when we intend to perform studies on Ca<sup>2+</sup> sparks using methods borrowed from single-channel current analysis, we need to know the number of channels contributing to the generation of a single Ca<sup>2+</sup> spark.

If we assume, for a moment, that opening of more than one RyR underlies a Ca<sup>2+</sup> spark, then the situation would be much more complex and an assortment of additional questions would need to be answered to understand Ca<sup>2+</sup> signaling on this molecular level. For example, we would need to understand how Ca<sup>2+</sup> flux into the diadic cleft via a single RyR interacts with the remaining neighboring RyRs within a cluster. Can a RyR open independently or does the first opening ignite the entire cluster, all channels synchronized by submicroscopic Ca<sup>2+</sup>-induced activation or by some allosteric interaction between the densely packed channel proteins (13)? If a single channel or a fraction of the channels within a cluster can open without igniting all of them, we need to identify the as of yet unknown mechanisms that makes some of the channels insensitive for activation. Related to this, it is essential to determine which mechanism (or which mechanisms) terminates the Ca<sup>2+</sup> release on the level of a single RyR and on the level of a cluster of RyRs. Taken together, in order to understand the activation, regulation and termination of EC-coupling and Ca<sup>2+</sup> signaling from the molecule to the cell and organ, it is important to have a complete picture of how the involved channels and other proteins talk to each other. This will be even more important when, based on such information, novel pharmacological strategies should be developed for the rational treatment of cardiac conditions in which the reliability and efficiency of EC-coupling are compromised.

#### **DEFINITION OF A Ca<sup>2+</sup> QUARK**

Before discussing the experimental results that led us to propose the existence of a Ca<sup>2+</sup> signaling event that is considerably smaller than a Ca<sup>2+</sup> spark, termed a "Ca<sup>2+</sup> quark", it is appropriate to state how such an event is defined. In the past, there has been some confusion in the literature regarding the precise definition of a Ca<sup>2+</sup> quark. A clear perception of this event is even more important, because the initial proposal of the existence of such events was based on a negative result, as detailed below (14). By definition, a Ca<sup>2+</sup> quark is the localized subcellular Ca<sup>2+</sup> signal resulting from the opening of a single SR Ca<sup>2+</sup> release channel.

#### **SR Ca<sup>2+</sup> RELEASE ACTIVATED BY UV-FLASH PHOTOLYSIS**

Spontaneous Ca<sup>2+</sup> sparks in cardiac muscle cells can be considered as accidents of Ca<sup>2+</sup> signaling which occur because, at the normal resting [Ca<sup>2+</sup>]<sub>i</sub> of about 100 nM, the probability for a RyR to open is not zero. Very early after the discovery of Ca<sup>2+</sup> sparks, it was proposed that signals identical to these spontaneous Ca<sup>2+</sup> sparks might also underlie the Ca<sup>2+</sup> release during EC-coupling (1). Indeed, this hypothesis was rapidly confirmed in experiments where the number of L-type Ca<sup>2+</sup> channels activated during a depolarization had been reduced with specifically designed voltage-clamp protocols or pharmacologically (15-16), see also fig. 1A. Both strategies revealed that the normal Ca<sup>2+</sup> transient was in fact composed of a large number of synchronized Ca<sup>2+</sup> sparks, each exhibiting properties similar to the spontaneous Ca<sup>2+</sup> sparks. After these studies were published, many were wondering whether the resemblance of spontaneous and triggered Ca<sup>2+</sup> sparks was a pure coincidence or whether an identical functional SR Ca<sup>2+</sup> release unit was opening in either case (possibly corresponding to a single RyR channel). Alternatively, the size of a Ca<sup>2+</sup> spark might have been determined by the trigger signal, the opening of L-type Ca<sup>2+</sup> channels. But this seemed less likely, because Ca<sup>2+</sup> influx via L-type Ca<sup>2+</sup> channels was not thought to be necessary for the incidents of spontaneous Ca<sup>2+</sup> sparks (but see 17). To address these questions, we decided to embark on a study in which we did not need to rely on L-type Ca<sup>2+</sup> channels to trigger Ca<sup>2+</sup> sparks. Instead, we decided to use flash-photolysis of caged Ca<sup>2+</sup> to provoke SR Ca<sup>2+</sup> release, while simultaneously imaging the subsequent Ca<sup>2+</sup> release events with laser-scanning confocal microscopy (fig. 1B and C). At photolytic power levels designed to activate only a small number of functional SR Ca<sup>2+</sup> release sites, we should be able to spatially resolve individual Ca<sup>2+</sup> release events. Naturally, we expected these release events to be Ca<sup>2+</sup> sparks.

To our considerable surprise, this was not the case. As illustrated in figure 1B and 1C, Ca<sup>2+</sup>

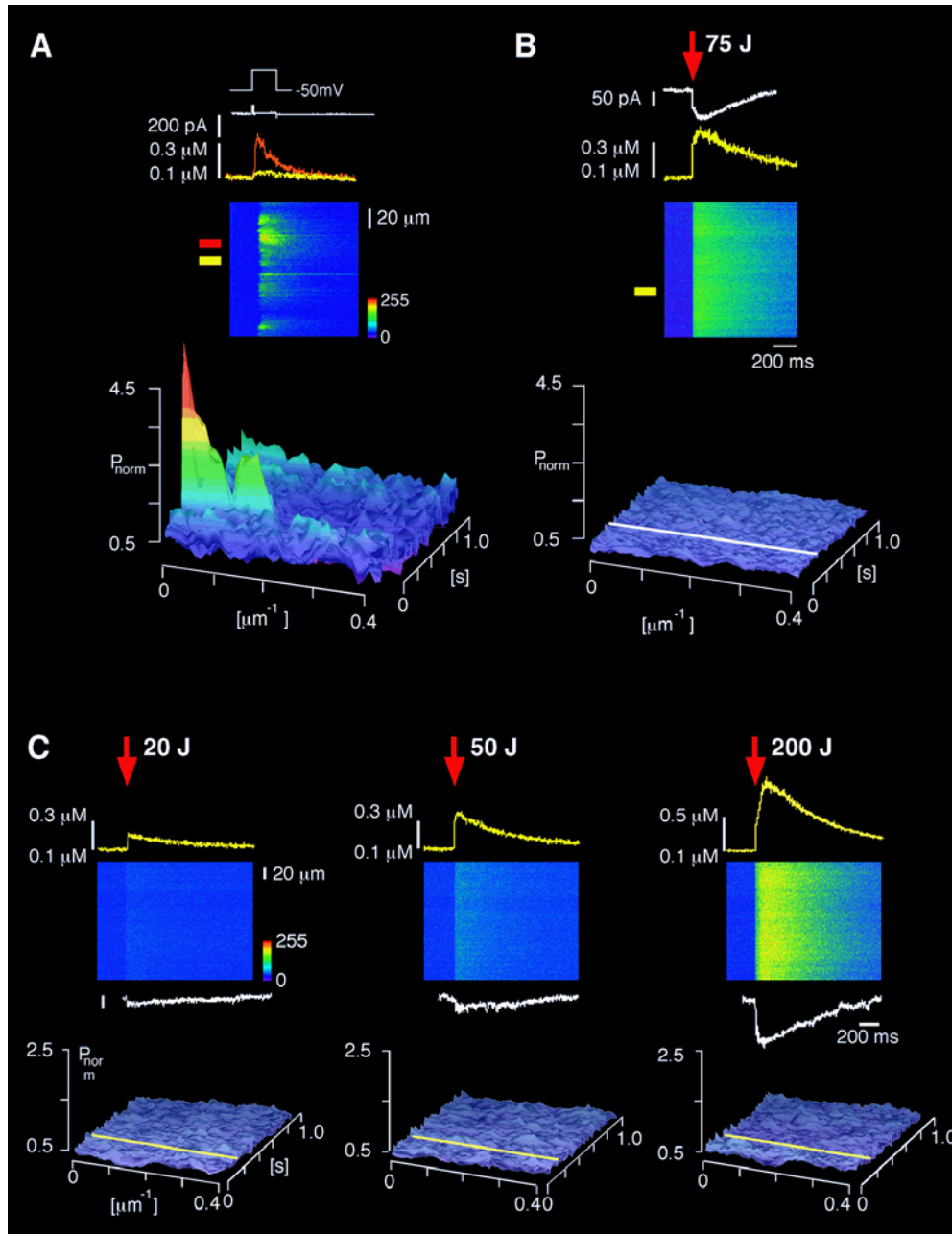


Figure 1. Comparison of  $\text{Ca}^{2+}$  transients induced by  $I_{\text{Ca}}$  and by homogeneous photochemical  $\text{Ca}^{2+}$  jumps in guinea-pig ventricular myocytes.

A, a voltage-clamp depolarization from  $-50$  mV to  $+5$  mV activated a small  $I_{\text{Ca}}$  due to a partial block by verapamil ( $10 \mu\text{M}$ ). The line-scan image reveals several localized  $\text{Ca}^{2+}$  signals. These  $\text{Ca}^{2+}$  sparks rose to  $350$  nM (red trace) while the changes of  $[\text{Ca}^{2+}]_i$  in regions between sparks were limited to about  $25$  nM (yellow trace). The power spectra in the spatial domain (computed with a fast Fourier transform, FFT, algorithm) exhibited a pronounced burst of low frequencies characteristic for localized  $\text{Ca}^{2+}$  signals. B, in the same cell a UV-flash was applied at a holding potential of  $-50$  mV resulting in an inward directed membrane current ( $50$  pA) due to  $\text{Ca}^{2+}$  removal mediated by the Na-Ca exchange ( $I_{\text{NaCa}}$ ). The  $\text{Ca}^{2+}$  transient (yellow) suggests a  $\text{Ca}^{2+}$  jump to  $375$  nM and the line-scan image reveals no spatial non-uniformities. This is confirmed in the flat power spectra (the white line indicates the moment of flash). The homogeneous photolytic  $\text{Ca}^{2+}$  trigger did not elicit  $\text{Ca}^{2+}$  sparks. C, UV-flashes of increasing energy were followed by  $I_{\text{NaCa}}$  and  $\text{Ca}^{2+}$  transients of increasing amplitude. The elicited  $\text{Ca}^{2+}$  signals were spatially uniform and the power spectra were flat at all energies (the yellow lines indicate the moment of the UV-flash). At a discharged energy of  $20$  J, the photolytically generated increase of  $[\text{Ca}^{2+}]_i$  was completed within  $2$  ms, while at  $50$  J a slower release component resulting from CICR followed the initial  $\text{Ca}^{2+}$  jump (photolytic released  $\text{Ca}^{2+}$ ). This slow SR  $\text{Ca}^{2+}$  release component was even more pronounced when the flash energy was raised further to  $200$  J.  $\text{Ca}^{2+}$  sparks were not elicited by UV-flash photolysis of caged  $\text{Ca}^{2+}$  independent of the energy discharged. Homogeneous flash photolysis seemed to trigger  $\text{Ca}^{2+}$  release units that were substantially smaller in size or amplitude than  $\text{Ca}^{2+}$  sparks (modified from 14).

release signals activated by flash-photolytic  $\text{Ca}^{2+}$  concentration jumps were always spatially homogeneous, irrespective of the power applied (14). Even reducing the power of the UV-flash to the threshold of CICR to trigger only few RyRs did not result in circumscribed  $\text{Ca}^{2+}$  release events which could be resolved with the confocal microscope. Nevertheless, inhibiting CICR by applying ryanodine dramatically reduced the amplitude of the  $\text{Ca}^{2+}$  release signals and changed their kinetics (by only leaving the rapid photolytic  $\text{Ca}^{2+}$  concentration change). This represents pharmacological evidence that CICR was doubtlessly activated by the photolytic  $\text{Ca}^{2+}$  liberation. From the observation of SR  $\text{Ca}^{2+}$  release remaining spatially homogeneous under all conditions, we concluded that  $\text{Ca}^{2+}$  release occurred most likely through a  $\text{Ca}^{2+}$  signaling event that was too small to be resolved microscopically. Since the smallest SR  $\text{Ca}^{2+}$  release signal we could imagine was due to the brief opening of a single RyR (i.e. a  $\text{Ca}^{2+}$  quark), we proposed that a large number of such events were underlying the spatially homogeneous SR  $\text{Ca}^{2+}$  release signal we had observed.

#### **SR $\text{Ca}^{2+}$ RELEASE ACTIVATED BY TWO-PHOTON PHOTOLYSIS**

This provocative conclusion was not immediately accepted by everyone working in the field. One consideration was that the hypothesis of a  $\text{Ca}^{2+}$  quark was essentially based on a negative result, or in other words, we had not optically resolved these events. Furthermore, the simultaneous use of UV-flash photolysis of caged  $\text{Ca}^{2+}$  compounds and laser-scanning confocal microscopy was a novel approach which could have its own intricacies and problems. In particular, the concern was expressed that the focal plane of the UV-flash might have been quite different from the focus of the laser beam exciting Fluo-3, even though the UV-flash was illuminating the entire cardiac myocyte. Indeed, we had previously determined the axial chromatic aberration of several microscope lenses used for confocal microscopy. The aberration was measured to be in the range of several  $\mu\text{m}$ , which is several-fold larger than the size of the point-spread function in the vertical direction (aberration was determined for confocal UV-excitation at wavelengths of 355 nm and 488 nm, respectively (18). Because of this chromatic aberration a UV-flash could, in principle, elicit  $\text{Ca}^{2+}$  sparks distant from the focal plane of the imaging system. Even a short distance would allow the  $\text{Ca}^{2+}$  sparks to diffuse together before reaching the plane of observation. Fortunately, a new photolytic technique bypassing the chromatic aberration problem inherent in UV-light became recently available. Instead of exciting a fluorescent molecule (or the chromophore of a caged compound) with a single UV photon, excitation can be achieved by near simultaneous absorption of several photons of longer wavelength (19). Instead of delivering UV-flashes at 355 nm to the entire cell, we created a stationary focus from a mode-locked Ti:sapphire laser running at a wave-length of 710 nm (20). The microscope objectives are well corrected

for red light and therefore the axial chromatic aberration problem was minimal. In addition, because of the quadratic dependence of excitation on power, photorelease of  $\text{Ca}^{2+}$  only occurred in a volume corresponding to the diffraction limited focus of the red laser light. As shown in figure 2 this allowed us to create a point source of  $\text{Ca}^{2+}$  within a cardiac myocyte and ensured perfect parfocality between the two-photon excitation photolysis (TPP) and the plane imaged with the  $\text{Ca}^{2+}$  indicator Fluo-3. Using this photolytic technique, we were again not able to elicit  $\text{Ca}^{2+}$  sparks as all-or-none events. Despite the fact that the localized photolytic signals shared many spatial and temporal features with  $\text{Ca}^{2+}$  sparks (fig. 2A), their amplitude was graded with the power of the photolytic laser over a extensive range of power levels. Only when the cells and  $\text{Ca}^{2+}$  stores were heavily loaded with  $\text{Ca}^{2+}$ , TPP could initiate regenerative  $\text{Ca}^{2+}$  release from the SR spreading along the cell as a triggered  $\text{Ca}^{2+}$  wave. When the power of the TPP laser was reduced down to the limit where photolytic signals could barely be resolved, we sometimes detected very small  $\text{Ca}^{2+}$  release events subsequent to the TPP trigger (fig. 2B). When comparing the  $\text{Ca}^{2+}$  signal mass of such small events with  $\text{Ca}^{2+}$  sparks (derived by integrating the  $\text{Ca}^{2+}$  concentration over time and space occupied by a signal), it turned out that 20 - 40 times less  $\text{Ca}^{2+}$  was released for such a signal than for a single  $\text{Ca}^{2+}$  spark. Therefore, these small events might correspond to  $\text{Ca}^{2+}$  quarks, but we have no possibility to rule out the involvement of more than one RyR channel.

#### **SR $\text{Ca}^{2+}$ RELEASE ACTIVATED BY NA-CA EXCHANGE RUNNING IN THE $\text{Ca}^{2+}$ INFLUX MODE**

All observations of homogeneous  $\text{Ca}^{2+}$  release or small  $\text{Ca}^{2+}$  events described above depended, in one way or another, on photochemical techniques. However, several independent findings also suggest the genuineness of SR  $\text{Ca}^{2+}$  release units smaller than  $\text{Ca}^{2+}$  sparks in cardiac muscle. One example is detailed below. In cardiac muscle, the Na-Ca exchange is one of the most important pathways for removal of  $\text{Ca}^{2+}$  during relaxation (21). In the steady state, the Na-Ca exchanger thereby balances  $\text{Ca}^{2+}$  influx occurring via L-type  $\text{Ca}^{2+}$  channels from beat to beat (22). However, depending on the prevailing electrochemical gradients for  $\text{Ca}^{2+}$  and  $\text{Na}^+$ , the Na-Ca exchange can also run in a  $\text{Ca}^{2+}$  influx mode. This mode has been known for many years to underlie slow tonic contractions of cardiac muscle, for example after removal of extracellular  $\text{Na}^+$ . More recently, several laboratories found experimental conditions, under which  $\text{Ca}^{2+}$  influx via Na-Ca exchange was able to trigger  $\text{Ca}^{2+}$  release from the SR, notably after eliciting  $\text{Na}^+$  current by depolarizing the cell membrane (23). Using a laser-scanning confocal microscope and the fluorescent  $\text{Ca}^{2+}$  indicator Fluo-3, it was even possible to detect the small amount of

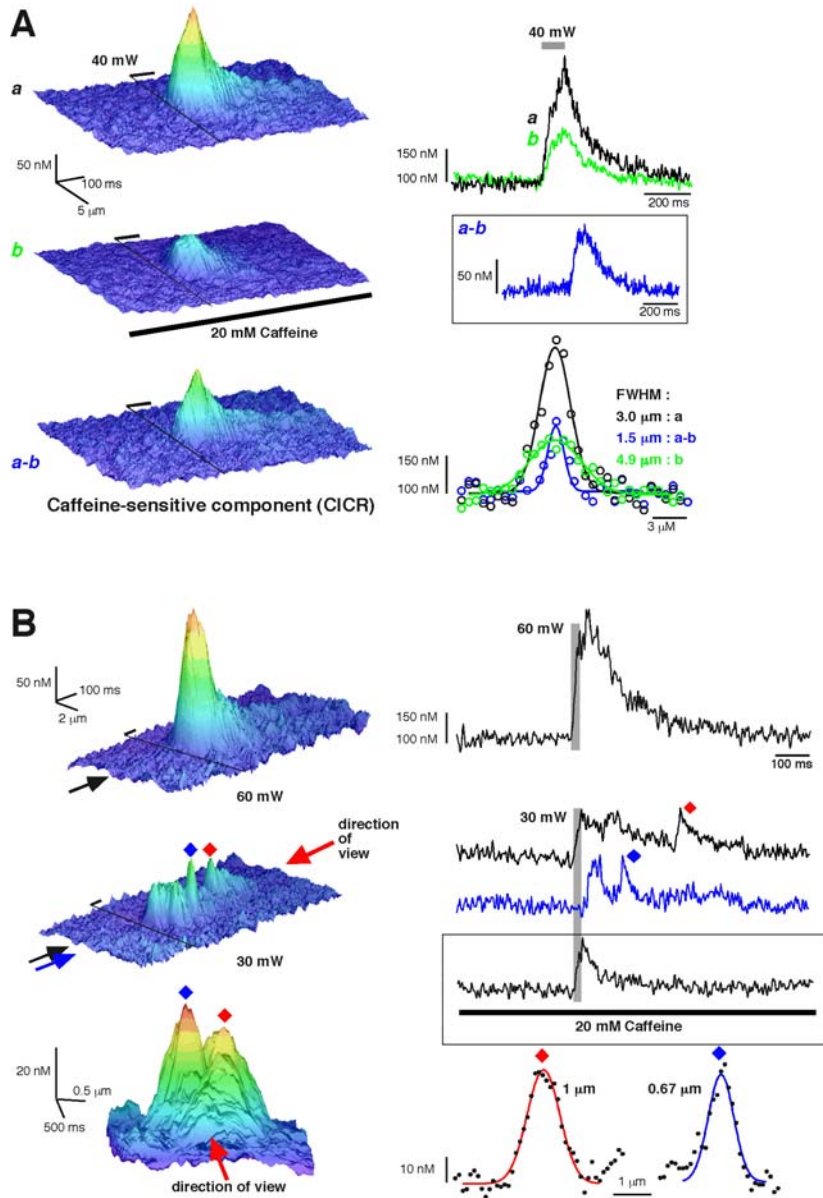


Figure 2.  $\text{Ca}^{2+}$  quarks triggered by TPP in guinea-pig ventricular myocytes.

Aa shows a  $\text{Ca}^{2+}$  signal generated by TPP at 40 mW (duration, 80 ms). Application of 20 mM caffeine reduced the photolytic  $\text{Ca}^{2+}$  transient significantly (Ab). Line tracings derived from the individual  $\text{Ca}^{2+}$  transients and the spatial spreading of the three  $\text{Ca}^{2+}$  release events are compared and illustrated in the right column. The caffeine-sensitive component arising from CICR is shown in Aa-b and in the inset (a-b). Interestingly, the event attributable to CICR was considerably smaller in amplitude than a typical  $\text{Ca}^{2+}$  spark. In addition to the smaller amplitude, the caffeine-sensitive difference signal also exhibited less spatial spreading (FWHM  $\approx 1.5 \mu\text{m}$ ) than a typical  $\text{Ca}^{2+}$  spark and than the TPP signal itself (FWHM  $\approx 4.9 \mu\text{m}$ ). The detection of a small caffeine-sensitive component indicates that TPP did trigger local CICR, possibly involving  $\text{Ca}^{2+}$  release events that are smaller than a  $\text{Ca}^{2+}$  spark, both in terms of amplitude and spatial spread. B shows a  $\text{Ca}^{2+}$  signal triggered by TPP at 60 mW (duration, 25 ms) and the corresponding time course of the  $\text{Ca}^{2+}$  signal, most likely containing a CICR component. Uncaging of DM-nitrophen slightly below threshold (30 mW) for SR  $\text{Ca}^{2+}$  release was followed by several tiny  $\text{Ca}^{2+}$  transients. A view from the end of the trace (in the direction of the red arrow) is depicted below to emphasize the spatial separation of the small  $\text{Ca}^{2+}$  release events. The time course of the tiny  $\text{Ca}^{2+}$  transients illustrated  $[\text{Ca}^{2+}]_i$  at the location of photolysis (upper trace, red diamond) and  $\approx 0.5 \mu\text{m}$  beneath this location (lower trace, blue diamond). The inset shows the TPP signal in the presence of 20 mM caffeine used for subtraction. The spatial characteristics of fundamental  $\text{Ca}^{2+}$  release signals are shown in more detail below. On average, the distance between the small  $\text{Ca}^{2+}$  signaling events triggered by TPP was  $\approx 0.4 \mu\text{m}$  while the average amplitude of  $\text{Ca}^{2+}$  quarks was  $\approx 37 \text{ nM}$  (modified from 20).

Ca<sup>2+</sup> which was entering the cell from the extracellular space (24). This tiny Ca<sup>2+</sup> signal presumably corresponds to the trigger for CICR mediated by the Na-Ca exchange running in the Na<sup>+</sup> removal (i.e. Ca<sup>2+</sup> influx) mode. Initially, Na<sup>+</sup> and Ca<sup>2+</sup> enter the diadic cleft and since the diffusion of Na<sup>+</sup> and Ca<sup>2+</sup> in this narrow space is likely to be restricted, concentration changes for Na<sup>+</sup> and Ca<sup>2+</sup> in this space were predicted to be sufficiently large to initiate CICR (25). When we applied the same instrumental and experimental approach to identify the nature of the elementary SR Ca<sup>2+</sup> release events prevailing under these conditions, we observed homogeneous SR Ca<sup>2+</sup> release signals reminiscent of those seen after UV-flash photolytic liberation of Ca<sup>2+</sup>. Moreover, the Ca<sup>2+</sup> signals were spatially homogeneous irrespective of the size of the depolarization and the Na<sup>+</sup> current (926). Control experiments with pharmacological tools provided the necessary evidence to confirm that SR Ca<sup>2+</sup> release had actually been triggered by Na-Ca exchange reverse mode. An interesting collateral observation provided a direct confirmation that the homogenous Ca<sup>2+</sup> release occurred via a pathway distinct from the usual activation of Ca<sup>2+</sup> sparks by L-type Ca<sup>2+</sup> channels. Sometimes, Ca<sup>2+</sup> sparks appeared to be superimposed on top of the homogeneous Ca<sup>2+</sup> release signals. These triggered sparks were clustered during the first few milliseconds of the Ca<sup>2+</sup> transient, i.e. exclusively during flow of I<sub>Na</sub>. They could be abolished by inhibitors of L-type Ca<sup>2+</sup> channels and their appearance could be boosted by increasing the series resistance of the patch-clamp electrodes. Based on these results we concluded that the superimposed Ca<sup>2+</sup> sparks were triggered by the activation of a few L-type Ca<sup>2+</sup> channels during voltage-escape which is inevitably introduced by large Na<sup>+</sup> currents. Therefore, the strikingly different spatial features of the two types of Ca<sup>2+</sup> release made it clear that the homogenous Ca<sup>2+</sup> release was not simply the consequence of a large number of synchronized Ca<sup>2+</sup> sparks. Instead, it appeared to be a different mode of Ca<sup>2+</sup> release, possibly arising from the activation of a considerable number of Ca<sup>2+</sup> sparks.

#### ELEMENTARY SR Ca<sup>2+</sup> RELEASE SIGNALS IN SKELETAL MUSCLE

As mentioned above, several laboratories have identified Ca<sup>2+</sup> sparks in skeletal muscle preparations (for example see(5-6)). Skeletal muscle excitation-contraction coupling shares many similarities with cardiac Ca<sup>2+</sup> signaling. However, despite the ultrastructural and molecular resemblance of the two cell types, there are remarkable differences that need to be considered before drawing conclusions from comparative studies. First of all, in skeletal muscle the RyR1 (and in some muscle types the RyR3) isoform is expressed, while cardiac muscle has the RyR2 (27). These isoforms show distinctly different behaviors for a variety of parameters, most notably for Ca<sup>2+</sup>

dependent activation and inactivation. Equally important, the initial steps of skeletal muscle EC-coupling are thought to rely on a direct mechanical coupling between the voltage-sensors and the RyRs. Afterwards, this voltage-induced Ca<sup>2+</sup> release is also amplified by Ca<sup>2+</sup>-induced Ca<sup>2+</sup> release. In contrast, in cardiac muscle the earliest step of EC-coupling is Ca<sup>2+</sup> influx via L-type Ca<sup>2+</sup> channels, which is subsequently amplified by CICR (27). Thus, there are several reasons why one might expect to find more than one type of Ca<sup>2+</sup> release in skeletal muscle. In one experimental study, Ca<sup>2+</sup> signals were analyzed in frog skeletal muscle cells held in a double-vaseline gap voltage-clamp setup (28). Using the fluorescent Ca<sup>2+</sup> indicator Fluo-3 and the line-scan mode of a confocal microscope, Ca<sup>2+</sup> sparks were readily observed during near-threshold voltage-clamp depolarizations (to -58 mV). However, small depolarizations to -72 mV only sporadically elicited Ca<sup>2+</sup> sparks. Nevertheless, a slight elevation of the Ca<sup>2+</sup> concentration was consistently observed with every tiny depolarization. The authors proposed that this change of [Ca<sup>2+</sup>]<sub>i</sub> must have resulted from Ca<sup>2+</sup> signaling events smaller than Ca<sup>2+</sup> sparks. This interpretation was further supported by a pharmacological experiment (see figure 3). Tetracaine is known to inhibit SR Ca<sup>2+</sup> release via CICR (29). When voltage-clamp depolarizations to -58 mV were applied, the line-scan images revealed an initial synchronized surge of Ca<sup>2+</sup> release, followed by infrequent and stochastically appearing Ca<sup>2+</sup> sparks, giving rise to a steady elevation of average [Ca<sup>2+</sup>]<sub>i</sub>. Superfusing the skeletal muscle cells with tetracaine eliminated the initial synchronized Ca<sup>2+</sup> spike and the subsequent Ca<sup>2+</sup> sparks. However, a small Ca<sup>2+</sup> release signal again remained, probably originating directly from voltage-induced Ca<sup>2+</sup> release. Taken together, it was

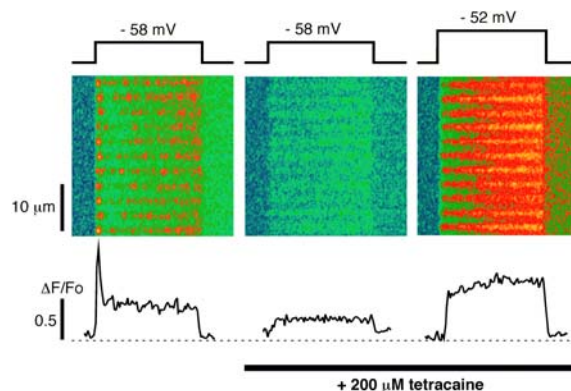


Figure 3. Tetracaine eliminates sparks, but spares small event Ca<sup>2+</sup> release in frog skeletal muscle.

Line scan images of normalized fluorescence in reference and in 200 μM tetracaine reveal triadic gradients of fluorescence, showing that tetracaine eliminated the peak of Ca<sup>2+</sup> release and the occurrence of Ca<sup>2+</sup> sparks. Fluorescence recorded at higher depolarization shows substantial Ca<sup>2+</sup> release in tetracaine, but without peak or Ca<sup>2+</sup> sparks. That tetracaine eliminated sparks at all voltages supports CICR as the activation mechanism, not just for some, but for all sparks (modified from 28).

proposed that in skeletal muscle voltage-induced  $\text{Ca}^{2+}$  release gives rise to "small event  $\text{Ca}^{2+}$  release" (presumably analogous to  $\text{Ca}^{2+}$  quarks) which subsequently triggers larger  $\text{Ca}^{2+}$  signals (i.e.  $\text{Ca}^{2+}$  sparks) by CICR.

### **$\text{Ca}^{2+}$ RELEASE SIGNALS IN A HETEROLOGOUS EXPRESSION SYSTEM**

Combining molecular biology techniques with  $\text{Ca}^{2+}$  imaging methods represents an almost ideal approach for engineering less complex experimental models. After the skeletal and cardiac muscle isoforms of the RyR (i.e. RyR1 and RyR2) had been cloned and sequenced (30-31), such an approach became possible and has been used to examine the elementary  $\text{Ca}^{2+}$  signaling events of RyRs heterologously expressed in Chinese hamster ovary (CHO) cells (see figure 4 and (32-33)). In these cells,  $\text{Ca}^{2+}$  release could be elicited by applying puffs of caffeine, a compound which increases the open probability of the RyRs by rendering them  $\text{Ca}^{2+}$  sensitive to an extent, which allows even resting  $[\text{Ca}^{2+}]_i$  to trigger  $\text{Ca}^{2+}$  release. In each of the two studies, caffeine-activated  $\text{Ca}^{2+}$  release from the  $\text{Ca}^{2+}$  stores was always spatially homogeneous and no  $\text{Ca}^{2+}$  sparks were resolved. Although the ultrastructural disposition of the RyRs expressed in these cells is not precisely known, it is obvious that major components of the microarchitecture of striated muscle cells are missing. Therefore, RyRs were certainly present in a much less organized distribution. Most likely, they were not aggregated in larger clusters of channels, since no dyads or triads were present and since the cytoskeletal elements for such a differentiated ultrastructure were missing. Therefore, the expressed RyRs may have been localized in the membrane of the endoplasmic reticulum of CHO cells in a quite isolated or at least less densely clustered fashion. The homogeneous  $\text{Ca}^{2+}$  release signals occurring via such spatially isolated channels then would be consistent with the view that the synchronized activation of more than one RyR is required to generate a detectable  $\text{Ca}^{2+}$  spark. Or, in other words,  $\text{Ca}^{2+}$  release in CHO cells expressing RyR1 or RyR2 may occur as (unresolved)  $\text{Ca}^{2+}$  quarks.

### **PERSPECTIVE**

After many attempts to determine the number of RyRs contributing to a  $\text{Ca}^{2+}$  spark, everyone would probably agree that with an isolated technique, such as confocal microscopic imaging of  $\text{Ca}^{2+}$  signals, it will be very difficult to answer all questions related to the generation of a  $\text{Ca}^{2+}$  spark or to address the associated issues of channel activation and inactivation. What appears to be more promising are efforts to combine information obtained with complementary techniques, such as electrophysiology,  $\text{Ca}^{2+}$  imaging, ultrastructural studies, molecular biology and transgenic animal approaches as well as biochemical tools. A strategy which has been used in several studies, was to apply a model of  $\text{Ca}^{2+}$  diffusion and  $\text{Ca}^{2+}$  buffering in an attempt to correlate the  $\text{Ca}^{2+}$  spark amplitude (or

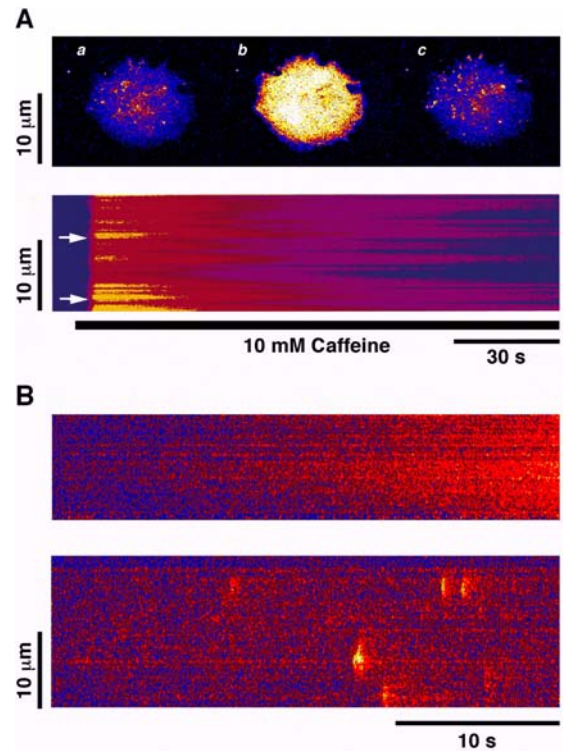


Figure 4. Caffeine-induced  $\text{Ca}^{2+}$  release in CHO cells.

A, Spatial and temporal patterns of caffeine-induced  $\text{Ca}^{2+}$  release in CHO cells expressing the full length skeletal muscle RyR. CHO cells expressing RyRs release  $\text{Ca}^{2+}$  upon exposure to caffeine. Images of Fluo-3 fluorescence in CHO cells expressing the full length RyR: (a) control, (b) 0.5 s after addition of 10 mM caffeine, and (c) 5 min after washout of the caffeine. The lower panel shows a compressed line-scan image of Fluo-3 fluorescence recorded from a single CHO cell exposed to 10 mM caffeine. The distribution of  $[\text{Ca}^{2+}]_i$  in response to caffeine was inhomogeneous. There appeared to be 'hot regions' where the level of  $[\text{Ca}^{2+}]_i$  was higher than in other places, as indicated by the arrows. These hot spots may correspond to regions where the density of  $\text{Ca}^{2+}$  release channels was high. B, Lack of  $\text{Ca}^{2+}$  sparks in CHO cells expressing RyR. Line-scan image of fluorescence ratio (Fluo-3) in CHO cells during the initial rise in  $[\text{Ca}^{2+}]_i$  in the presence of 0.5 mM caffeine.  $[\text{Ca}^{2+}]_i$  rises very slowly from resting levels, but no sparks are evident. In contrast, typical spontaneous  $\text{Ca}^{2+}$  sparks were seen in a cardiac myocyte (lower panel). Both line-scan images were obtained and presented at exactly the same spatial and temporal resolution, with the same confocal microscope (modified from 32).

signal mass) with single channel flux data, for example obtained from lipid bilayer experiments (1, 5, 34-35). When choosing such an approach, one has to keep in mind that the size of a local  $\text{Ca}^{2+}$  signal, such as a  $\text{Ca}^{2+}$  spark or  $\text{Ca}^{2+}$  quark, is ultimately determined by many factors. These include the diffusion of  $\text{Ca}^{2+}$  inside the cell, the  $\text{Ca}^{2+}$  buffer capacity of the cell and the  $\text{Ca}^{2+}$  binding kinetics and mobility of the  $\text{Ca}^{2+}$  indicator. Equally important, several properties of the  $\text{Ca}^{2+}$  release channels themselves directly affect the resulting  $\text{Ca}^{2+}$  signals, such as the amount of  $\text{Ca}^{2+}$  flux carried by an open channel and the gating behavior

of the channel protein. Gating and  $\text{Ca}^{2+}$  flux of membrane channels can be conveniently analyzed using electrophysiological techniques. As already mentioned, a lipid bilayer technique has been developed which allowed studies of channel conductance and gating with isolated RyRs, as well as pharmacological tests. While this technique is generally used to characterize the channel under steady-state conditions (for reviews see 36-37), some transient state studies have already been carried out by combining the lipid-bilayer with flash-photolysis techniques or with rapid solution changes (38-40). Such experiments more closely correspond to the physiological situation where the RyRs are only activated transiently. In experiments designed to mimic intracellular solutions as closely as possible, the previously established estimate for the  $\text{Ca}^{2+}$  current carried by a single cardiac RyR turned out to be too large and has been lowered to less than 0.6 pA (12). Although this current was still recorded under the highly artificial conditions of a lipid bilayer experiment, it represents the "best" data currently available. However, when substituting this current in numerical simulations of  $\text{Ca}^{2+}$  sparks, one would still need to make several assumptions regarding the  $\text{Ca}^{2+}$  diffusion in the cell and in the diadic cleft, but also assume a  $\text{Ca}^{2+}$  buffer capacity of the cell.

A preferable experiment would be to record the  $\text{Ca}^{2+}$  current flowing through a  $\text{Ca}^{2+}$  channel directly while simultaneously measuring the resulting  $\text{Ca}^{2+}$  signal. Such a combined set of data would allow a direct correlation of  $\text{Ca}^{2+}$  flux and  $\text{Ca}^{2+}$  signal, without having to rely on model dependent and poorly known assumptions. In fact, such an experimental study has recently been published (41). The strategy for this ingenious and challenging experiment was to record  $\text{Ca}^{2+}$  current via a single cardiac L-type  $\text{Ca}^{2+}$  channel in a cell-attached configuration of the patch-clamp technique, while at the same time imaging the resulting  $\text{Ca}^{2+}$  sparks, or, after inhibition of the SR, record the  $\text{Ca}^{2+}$  signals arising from the  $\text{Ca}^{2+}$  influx via a single L-type  $\text{Ca}^{2+}$  current (termed a " $\text{Ca}^{2+}$  sparklet"). By comparing the L-type  $\text{Ca}^{2+}$  current and the corresponding  $\text{Ca}^{2+}$  sparklet, the amount of  $\text{Ca}^{2+}$  flux required to generate a  $\text{Ca}^{2+}$  spark could be estimated directly. The authors concluded that for a typical  $\text{Ca}^{2+}$  spark the activation of about 4-6 RyRs was required. Thus, this finding also suggests that from within a dyad with its ultrastructural cluster of about hundred RyRs (13), only a small subset is actually activated. The question why only such a small fraction of the RyRs within a cluster are activated, remains open. Here, we obviously have the same conceptual issue that needs to be addressed in order to explain, why  $\text{Ca}^{2+}$  quarks can exist without immediately triggering a full-blown  $\text{Ca}^{2+}$  spark (by activating all neighboring channels).

While many readers may consider the precise number of  $\text{Ca}^{2+}$  channels contributing to a  $\text{Ca}^{2+}$  spark a hair-splitting detail, most would certainly agree that we need to understand the activation, inactivation and regulation of RyRs from the level of a single channel, through the somehow

coordinated behavior of channel (42-43), up to the complexity of intact cells and cardiac muscle. In order to have a complete picture it is essential to understand all mechanisms by which the channels grouped within a dyad can communicate with each other. We are convinced that future experiments using interdisciplinary approaches will provide the information necessary to solve this puzzle.

#### ACKNOWLEDGEMENTS

This work was supported by grants from the Swiss National Science Foundation and by the Roche Foundation. We would like to thank D. Lüthi for expert technical assistance and N. Lindegger for his comments on the manuscript.

#### References

1. Cheng, H. P., W. J. Lederer & M. B. Cannell: Calcium sparks - elementary events underlying excitation-contraction coupling in heart muscle. *Science* 262, 740-744 (1993)
2. Lipp, P. & E. Niggli: Modulation of  $\text{Ca}^{2+}$  release in cultured neonatal rat cardiac myocytes - insight from subcellular release patterns revealed by confocal microscopy. *Circ Res* 74, 979-990 (1994)
3. Sakmann, B. & E. Neher: Patch clamp techniques for studying ionic channels in excitable membranes. *Annu Rev Physiol* 46, 455-472 (1984)
4. Niggli, E.: Localized intracellular calcium signaling in muscle: Calcium sparks and calcium quarks. *Annu Rev Physiol* 61, 311-335 (1999)
5. Tsugorka, A., E. Rios & L. A. Blatter: Imaging elementary events of calcium release in skeletal muscle cells. *Science* 269, 1723-1726 (1995)
6. Klein, M. G., H. P. Cheng, L. F. Santana, Y. Jiang, W. J. Lederer & M. F. Schneider: Two mechanisms of quantized calcium release in skeletal muscle. *Nature* 379, 455-458 (1996)
7. Berridge, M. J.: Elementary and global aspects of calcium signalling. *J Physiol - Lond* 499, 291-306 (1997)
8. Lipp, P. & E. Niggli: A hierarchical concept of cellular and subcellular  $\text{Ca}^{2+}$  -signalling. *Prog Biophys Molec Biol* 65, 265-296 (1996)
9. Fabiato, A.: Time and calcium dependence of activation and inactivation of calcium-induced release of calcium from the sarcoplasmic reticulum of a skinned canine cardiac Purkinje cell. *J Gen Physiol* 85, 247-289 (1985)
10. Stern, M. D.: Theory of excitation-contraction coupling in cardiac muscle. *Biophys J* 63, 497-517 (1992)
11. Mazzanti, M., L. J. DeFelice, J. Cohen & H. Malter: Ion channels in the nuclear envelope. *Nature* 343, 764-767 (1990)
12. Mejía-Alvarez, R., C. Kettlun, E. Rios, M. D. Stern & M. Fill: Unitary  $\text{Ca}^{2+}$  current through cardiac ryanodine receptor channels under quasi-physiological ionic conditions. *J Gen Physiol* 113, 177-186 (1999)
13. Franzini-Armstrong, C., F. Protasi & V. Ramesh: Shape, size, and distribution of  $\text{Ca}^{2+}$  release units and couplons in skeletal and cardiac muscles. *Biophys J* 77, 1528-1539 (1999)
14. Lipp, P. & E. Niggli: Submicroscopic calcium signals as fundamental events of excitation-contraction coupling in guinea-pig cardiac myocytes. *J Physiol - Lond* 492, 31-38 (1996)
15. López-López, J. R., P. S. Shacklock, C. W. Balke & W. G. Wier: Local, stochastic release of  $\text{Ca}^{2+}$  in voltage-clamped rat heart cells: visualization with confocal microscopy. *J Physiol - Lond* 480, 21-29 (1994)
16. Cannell, M. B., H. P. Cheng & W. J. Lederer: Spatial non-uniformities in  $[\text{Ca}^{2+}]_i$  during excitation-contraction coupling in cardiac myocytes. *Biophys J* 67, 1942-1956 (1994)
17. Katoh, H., K. Schlotthauer & D. M. Bers: Transmission of information from cardiac dihydropyridine receptor to ryanodine receptor - Evidence from BayK 8644 effects on resting  $\text{Ca}^{2+}$  sparks. *Circ Res* 87, 106-111 (2000)
18. Niggli, E., D. W. Piston, M. S. Kirby, H. Cheng, D. R. Sandison, W. W. Webb & W. J. Lederer: A confocal laser scanning microscope designed for indicators with

- ultraviolet excitation wavelengths. *Am J Physiol* 266, C303-C310 (1994)
19. Denk, W., J. H. Strickler & W. W. Webb: Two-photon laser scanning fluorescence microscopy. *Science* 248, 73-76 (1990)
  20. Lipp, P. & E. Niggli: Fundamental calcium release events revealed by two-photon excitation photolysis of caged calcium in guinea-pig cardiac myocytes. *J Physiol- Lond* 508, 801-809 (1998)
  21. Egger, M. & E. Niggli: Regulatory function of Na-Ca exchange in the heart: Milestones and outlook. *J Membrane Biol* 168, 107-130 (1999)
  22. Bridge, J. H. B., J. R. Smolley & K. W. Spitzer: The stoichiometric relationship between charge movement associated with I<sub>Ca</sub> and I<sub>NaCa</sub> in cardiac myocytes. *Science* 248, 376-378 (1990)
  23. Leblanc, N. & J. R. Hume: Sodium current-induced release of calcium from cardiac sarcoplasmic reticulum. *Science* 248, 372-376 (1990)
  24. Lipp, P. & E. Niggli: Sodium current-induced calcium signals in isolated guinea-pig ventricular myocytes. *J Physiol - Lond* 474, 439-446 (1994)
  25. Lederer, W. J., E. Niggli & R. W. Hadley: Sodium-calcium exchange in excitable cells: fuzzy space. *Science* 248: 283 (1990)
  26. Lipp, P., M. Egger & E. Niggli: The role of Ca<sup>2+</sup> sparks and Ca<sup>2+</sup> quarks for excitation-contraction coupling in guinea-pig cardiac myocytes (Submitted).
  27. Bers, D. M.: *Excitation-contraction coupling and cardiac contractile force*. 2nd. edition, Kluwer Academic Publishers, Dordrecht, The Netherlands, 2001.
  28. Shirokova, N. & E. Rios: Small event Ca<sup>2+</sup> release: a probable precursor of Ca<sup>2+</sup> sparks in frog skeletal muscle. *J Physiol - Lond* 502, 3-11 (1997)
  29. Pizarro, G., L. Csernoch, I. Uribe & E. Rios: Differential effects of tetracaine on 2 kinetic components of calcium release in frog skeletal muscle fibres. *J Physiol - Lond* 457, 525-538 (1992)
  30. Takeshima, H., S. Nishimura, T. Matsumoto, H. Ishida, K. Kangawa, N. Minamino, H. Matsuo, M. Ueda, M. Hanaoka, T. Hirose & S. Numa: Primary structure and expression from complementary DNA of skeletal muscle ryanodine receptor. *Nature* 339, 439-445 (1989)
  31. Nakai, J., T. Imagawa, Y. Hakamata, M. Shigekawa, H. Takeshima & S. Numa: Primary structure and functional expression from cDNA of the cardiac ryanodine receptor/calcium release channel. *FEBS Lett* 271, 169-177 (1990)
  32. Bhat, M. B., J. Y. Zhao, W. J. Zang, C. W. Balke, H. Takeshima, W. G. Wier & J. J. Ma: Caffeine-induced release of intracellular Ca<sup>2+</sup> from Chinese hamster ovary cells expressing skeletal muscle ryanodine receptor - Effects on full-length and carboxyl-terminal portion of Ca<sup>2+</sup> release channels. *J Gen Physiol* 110, 749-762 (1997)
  33. Bhat, M. B., S. M. Hayek, J. Y. Zhao, W. J. Zang, H. Takeshima, W. G. Wier & J. J. Ma: Expression and functional characterization of the cardiac muscle ryanodine receptor Ca<sup>2+</sup> release channel in Chinese hamster ovary cells. *Biophys J* 77, 808-816 (1999)
  34. Cannell, M. B. & C. Soeller: Numerical analysis of ryanodine receptor activation by L-type channel activity in the cardiac muscle diad. *Biophys J* 73: 112-122 (1997)
  35. Rios, E., M. D. Stern, A. Gonzalez, G. Pizarro & N. Shirokova: Calcium release flux underlying Ca<sup>2+</sup> sparks of frog skeletal muscle. *J Gen Physiol* 114, 31-48 (1999)
  36. Meissner, G.: Ryanodine receptor Ca<sup>2+</sup> release channels and their regulation by endogenous effectors. *Annu Rev Physiol* 56, 485-508 (1994)
  37. Coronado, R., J. Morrisette, M. Sukhareva & D. M. Vaughan: Structure and function of ryanodine receptors. *Am J Physiol* 266, C1485-C1504 (1994)
  38. Györke, S. & M. Fill: Ryanodine receptor adaptation - control mechanism of Ca<sup>2+</sup>-induced Ca<sup>2+</sup> release in heart. *Science* 260, 807-809 (1993)
  39. Valdivia, H. H., J. H. Kaplan, G. C. R. Ellis-Davies & W. J. Lederer: Rapid adaptation of cardiac ryanodine receptors: modulation by Mg<sup>2+</sup> and phosphorylation. *Science* 267, 1997-2000 (1995)
  40. Laver D. R. & G. D. Lamb: Inactivation of Ca<sup>2+</sup> release channels (ryanodine receptors RyR1 and RyR2) with rapid steps in [Ca<sup>2+</sup>] and voltage. *Biophys J* 74, 2352-2364 (1998)
  41. Wang, S. Q., L. S. Song, E. G. Lakatta & H. P. Cheng: Ca<sup>2+</sup> signalling between single L-type Ca<sup>2+</sup> channels and ryanodine receptors in heart cells. *Nature* 410, 592-596 (2001)
  42. Marx, S. O., K. Ondrias & A. R. Marks: Coupled gating between individual skeletal muscle Ca<sup>2+</sup> release channels (Ryanodine receptors). *Science* 281 818-821 (1998)
  43. Marx, S. O., J. Gaburjakova, M. Gaburjakova, C. Henrikson, K. Ondrias & A. R. Marks: Coupled gating between cardiac calcium release channels (Ryanodine receptors). *Circ Res* 88,1151-1158 (2001)

**Keywords:** Cardiac muscle; calcium signaling; excitation-contraction coupling; confocal microscopy; photolysis.

**Running title:** Ca<sup>2+</sup> quarks

**Correspondence to:**

Ernst Niggli  
Department of Physiology  
University of Bern  
Bühlplatz 5  
3012 Bern  
Switzerland

Phone: +41 31 631 8730  
Fax: +41 31 631 4611  
WWW: [http://beam.to/calcium\\_quark](http://beam.to/calcium_quark)

# Ryanodine Receptor Isoforms of Non-Mammalian Skeletal Muscle

Yasuo Ogawa, Takashi Murayama, Nagomi Kurebayashi

Department of Pharmacology, Juntendo University, Tokyo, Japan Corresponding Author: Yasuo Ogawa, Email: [ysoqawa@med.juntendo.ac.jp](mailto:ysoqawa@med.juntendo.ac.jp)

**ABSTRACT:** Whereas mammalian skeletal muscles express primarily a single isoform of ryanodine receptor (RyR) as the  $\text{Ca}^{2+}$  releasing channel, many non-mammalian vertebrate skeletal muscles express two isoforms in almost similar amount,  $\alpha$ - and  $\beta$ -RyR which are homologues of mammalian isoforms RyR1 and 3, respectively.  $\alpha$ -RyR is believed to be directly involved in excitation-contraction coupling in skeletal muscles and is variable in its properties among animals and fibers, while  $\beta$ -RyR shows similar properties and is variable in its content.  $\alpha$ - and  $\beta$ -RyR purified from frog skeletal muscle, a favorite material for physiological and morphological experiments, are very similar in  $\text{Ca}^{2+}$  dependent [ $^3\text{H}$ ]ryanodine binding. On the SR membrane, however,  $\alpha$ -RyR is selectively suppressed in the ligand binding, indicating that the  $\text{Ca}^{2+}$ -induced  $\text{Ca}^{2+}$  release (CICR) activity in skeletal muscle is conducted primarily by  $\beta$ -RyR. We also stressed here that  $\text{Ca}^{2+}$  binding to the activating site is a necessary but not a sufficient condition for CICR. The maximum activity attainable under a specified condition is also a critical parameter to be determined. Taking these findings into consideration, we conclude that CICR is too slow to explain the physiological  $\text{Ca}^{2+}$  release on depolarization.

## INTRODUCTION

How the action potential in the sarcolemma (an electrical event) is transformed to the contraction of myofibrils in the myoplasm (a mechanical event) is the central theme in excitation-contraction coupling (ECC). Since establishment of the fact that myofibrillar contraction is regulated by  $\text{Ca}^{2+}$  (1), there is new focus on the mechanism underlying  $\text{Ca}^{2+}$  release from the sarcoplasmic reticulum (SR) on depolarization of the T-tubule. Identification of relaxing factor with  $\text{Ca}^{2+}$ -ATPase on the SR led to the finding of a  $\text{Ca}^{2+}$  release mechanism,  $\text{Ca}^{2+}$ -induced  $\text{Ca}^{2+}$  release (CICR) (2). The well-known experiment of local stimulation (3, 4) preceded identification of the T-tubule, invagination of the sarcolemma, which served as conduit for inward spreading of excitation, and of the foot structure, electron dense material spanning between T-tubule and the junctional face of SR in triad, which was thought to play the critical role in  $\text{Ca}^{2+}$  release in ECC (5, 6). Demonstration of charge movements suggested a hypothesis that the conformation change of the voltage sensor was transmitted to the  $\text{Ca}^{2+}$  release channel, resulting in  $\text{Ca}^{2+}$  release from the store (depolarization-induced  $\text{Ca}^{2+}$  release, DICR) (7). The finding that ryanodine strongly binds to CICR channels led to isolation of the ryanodine receptor (RyR) (8). Electron microscopic observation of RyR molecules revealed that the foot structure was the cytoplasmic part of RyR tetramers (8). Understanding of the molecular mechanism of

ECC has been deepened by molecular biological studies using dysgenic and dyspedic (RyR-knockout) mice (9-11). Interaction between dihydropyridine receptor (DHPR), the voltage sensor, and RyR, the  $\text{Ca}^{2+}$  release channel, is critical in ECC. It is now clear that RyR could operate two modes of  $\text{Ca}^{2+}$  release, CICR and DICR. Although  $\text{Ca}^{2+}$  influx is unnecessary for skeletal muscle contraction, the role of CICR in ECC remains a heated argument (12, 13).

Mammalian RyR has three genetically distinct isoforms: RyR1 is the primary isoform in skeletal muscle, RyR2 is the isoform in the cardiac muscle, and RyR3 is the isoform usually found in a minuscule amount in various kinds of cells, tissues and organs. In skeletal muscles, protein staining usually showed a single band of RyR1, although Western blot may detect a faint band of RyR3 in addition to the main band of RyR1 (14, 15). It should be mentioned that the primary isoform in the brain was RyR2, but RyR1 was detected in the Purkinje neuron in the cerebellum, and RyR3, faintly but characteristically, in the corpus striatum, hippocampus and thalamus (14, 15). Many non-mammalian skeletal muscles, in contrast, showed two bands of RyR,  $\alpha$ - and  $\beta$ -RyR, in similar density on protein staining after SDS-PAGE (14, 16). cDNA sequences showed that  $\alpha$ - and  $\beta$ -RyR were homologues of RyR1 and RyR3, respectively, although their genetic loci were not yet identified. In this article, the terms  $\alpha$ - and  $\beta$ -RyR refer to non-mammalian origins, whereas RyR1 and 3 to mammalian origins.

In this review we will summarize findings on  $\alpha$ - and  $\beta$ -RyR of non-mammalian vertebrate

skeletal muscle compared with the mammalian counterparts (RyR1 and 3). Discussion will concentrate on their CICR which has been well studied to learn the biological roles of the two isoforms. For want of space, we must defer many aspects to the authors of other chapters of this book. There are also many excellent reviews which can be consulted for general matter on RyR (17-23).

### **COEXPRESSION OF TWO DISTINCT ISOFORMS, $\alpha$ - and $\beta$ -RyR**

Sutko and his colleagues first detected two distinct isoforms,  $\alpha$ - and  $\beta$ -RyR, in the SR vesicles from skeletal muscles of chicken, frog and fish (24, 25). The densities of the two bands on the SDS-PAGE pattern were similar.  $\beta$ -RyR moves slightly faster than  $\alpha$ -RyR on SDS-PAGE; its mobility was similar to that of RyR2, whereas  $\alpha$ -RyR was similar to RyR1.  $\beta$ -RyR cannot be a fragment of  $\alpha$ -RyR, because they showed distinct peptide-map patterns on limited proteolysis, and also because they showed different immunologic reactivities (24).  $\beta$ -RyR cannot be the cardiac isoform, because they detected an additional separate isoform (probably corresponding to RyR2) in chicken heart (26, 27). On the basis of immunological coprecipitation, they concluded that  $\alpha$ - and  $\beta$ -RyR formed homotetramers (24). The cultured embryonic cells from a crooked neck dwarf chick (28, 29) where  $\alpha$ -RyR was lacking failed to show  $\text{Ca}^{2+}$  release on electrical stimulation in a  $\text{Ca}^{2+}$ -free medium, but they caused  $\text{Ca}^{2+}$  release in response to caffeine, indicating that  $\alpha$ -RyR is directly involved in ECC (see later) (30).

Block and her colleagues (31) extensively examined RyR isoforms expressed in non-mammalian vertebrate skeletal muscles. They found that coexpression of two isoforms was not a general rule in non-mammalian vertebrates: among reptiles, turtle and alligator coexpressed the two isoforms, whereas lizard and snake expressed  $\alpha$ -isoform alone. Extraocular muscles of fishes (toadfish, striped bass, tuna and blue marlin) and avians, and toadfish swim bladder muscles expressed  $\alpha$ -isoform alone, whereas these body muscles expressed the two isoforms. Murayama recently detected  $\beta$ -RyR in extraocular muscles of bullfrog (unpublished results). The content of  $\beta$ -RyR in frog extraocular muscles may be variable among fibers.

Murayama and Ogawa (32) purified  $\alpha$ - and  $\beta$ -RyR from bullfrog skeletal muscle by Mono-Q column chromatography, confirming homotetramers of each of the two isoforms. They are very similar in  $\text{Ca}^{2+}$ -dependent [ $^3\text{H}$ ]ryanodine binding (33). Using polyclonal antibodies specific to  $\alpha$ - and  $\beta$ -RyR, they examined cross-reactivity of the two isoforms from various species of animals (carp, 5 species of frog, two species of toad, chicken and 4

species of mammals) (34). Western blot analysis of the SDS-PAGE pattern of SR vesicles showed that anti- $\alpha$ -RyR antibody positively reacted only to the frogs examined, *Rana catesbeiana*, *R. nigromaculata*, *R. japonica*, and *R. temporaria*. It was negative or very weakly positive to the other animals including toads and a frog *Rhacophorus*. In contrast, anti  $\beta$ -RyR showed positive reactions to all non-mammalian vertebrates examined, although more weakly in those with carp muscle. Mammals were negative to anti  $\alpha$ -RyR or anti  $\beta$ -RyR. Mobilities of  $\alpha$ -RyRs on SDS-PAGE were variable among animals, whereas those of  $\beta$ -RyR were consistent among non-mammalian vertebrates.

Oyamada et al. (35) cloned and sequenced the cDNAs for  $\alpha$ - and  $\beta$ -RyRs in bullfrog skeletal muscles, and they concluded that  $\alpha$ -RyR and  $\beta$ -RyR were homologous to RyR1 and RyR3, respectively. Particularly, RyR3 and  $\beta$ -RyR lacked the D2 region. It was also confirmed that chicken  $\beta$ -RyR was homologous to RyR3 (36). Franck et al. (37) reported that  $\alpha$ -RyR in skeletal muscles of fish was fiber-type specific: distinct in its cDNA sequence between slow-twitch (red) and fast-twitch (white) muscles. They also showed that identities of the amino acid sequences of RyR1 and  $\alpha$ -RyR among rabbit, frog and fish were 73-78%, whereas those of RyR3 and  $\beta$ -RyR were 85-86% among rabbit, chicken and frog. These results suggest that  $\alpha$ -RyRs may be more variable among animals than  $\beta$ -RyRs which are similar to each other (34).

RyR3 isoform was at first detected as a novel isoform by its mRNA or cDNA in specified regions of the brain (38) and lung epithelial cells (39). Later it was found that RyR3 was ubiquitously distributed, but in a miniscule amount (40, 41). In the rabbit brain, RyR3 was about 2% of RyR2, the main isoform in the brain (the RyR amount in the brain was about 3% of that in the skeletal muscle) (42, 43). In adult skeletal muscles, diaphragm is the richest source of RyR3 (41) (less than 1% of RyR1 in rabbit diaphragm (44), and about 5% of RyR1 in bovine diaphragm (45)). Whereas RyR1 appeared at the early stage of the development, RyR3 appeared just before hatching, increased transiently and decreased with age (in mouse, the content reached maximum around 2 weeks after birth and then decreased to the adult level or disappeared) (46, 47). In chicken, similar time courses for  $\alpha$ - and  $\beta$ -RyR during development were reported (48).

We can conclude that RyR3 and  $\beta$ -RyR are similar in their properties, but their contents in skeletal muscles are greatly variable, depending on age, fiber type and animal species. Block et al. (49) clearly showed that  $\alpha$ -RyR in toadfish swim bladder aligned characteristically in two rows on the junctional face of the SR in the triad, and dihydropyridine receptors (DHPR)

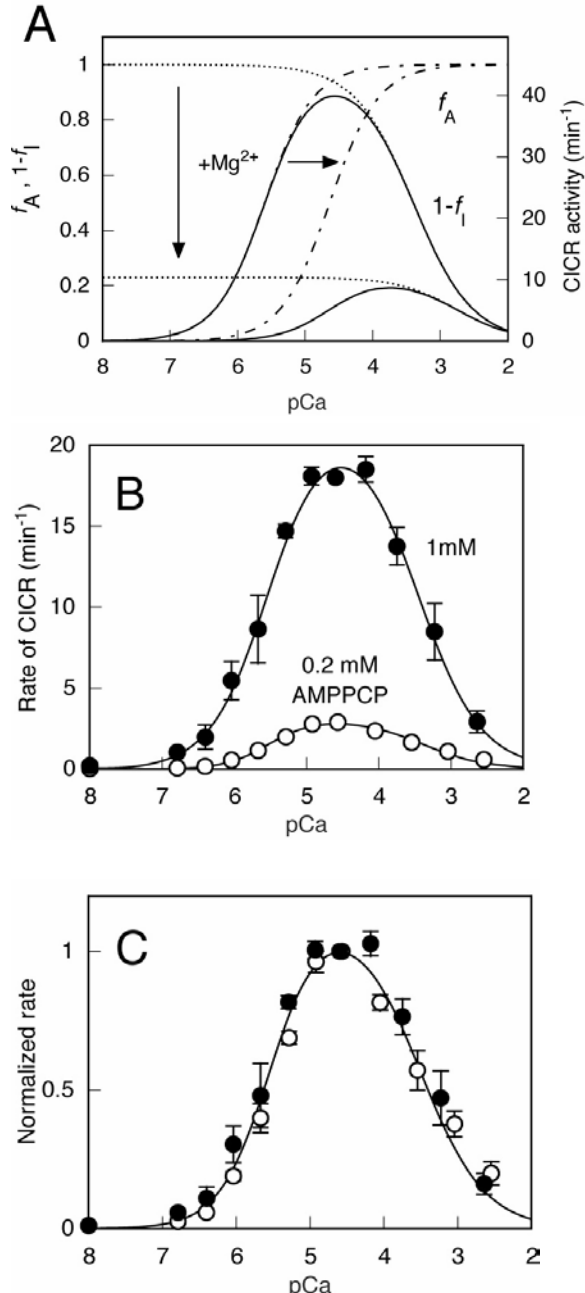


Fig. 1 Quantitative analysis of CICR  
 A. The pCa-CICR activity curves in an isotonic medium containing 4 mM AMPPCP with and without 1 mM Mg<sup>2+</sup> were drawn using parameters in Table 1 and the effect of Mg<sup>2+</sup> was analyzed according to equation 1. Mg<sup>2+</sup> shifted curve  $f_A$  (interrupted line) to a higher Ca<sup>2+</sup> concentration range and reduced the maximum value for  $(1 - f_I)$  (dotted line), resulting in a rightward shifted pCa-CICR activity curve with reduced peak activity. B. Dose-dependent effects of AMPPCP on CICR. C. Each curve shown in panel B was normalized with its own peak activity. The Ca<sup>2+</sup> dependence was unchanged by AMPPCP. Open circles, 0.2 mM AMPPCP; closed circles, 1 mM AMPPCP. For details, see ref. 61 (courtesy of the Biophysical Journal).

taking the form of the tetrad on the T-tubule are in precise register to every alternate foot. This

characteristic configuration of voltage sensor (tetrad/DHPR) and foot (RyR1 or  $\alpha$ -RyR) is now accepted as the basic structure for ECC in skeletal muscle (6, 50). Along this line, RyR1 and RyR3 isoforms were found to coexist in the same triads of the mammalian skeletal muscles (47). Recently, Felder and Franzini-Armstrong (51) reported that there were additional feet-like structures in 1-2 rows in either side of the junctional position on the SR, parajunctional feet, and that their occurrence is in parallel with the content of RyR3 or  $\beta$ -RyR in fibers. They also reported that the packing arrangement was different between the two kinds of feet.

### Ca<sup>2+</sup> DEPENDENCES OF $\alpha$ - AND $\beta$ -RYR

[<sup>3</sup>H]ryanodine binding to  $\alpha$ - and  $\beta$ -RyR from bullfrog skeletal muscles showed very similar biphasic Ca<sup>2+</sup> dependence: Ca<sup>2+</sup> less than 0.1 mM stimulates [<sup>3</sup>H]ryanodine binding ( $EC_{50} \sim 0.01$  mM) and Ca<sup>2+</sup> higher than this concentration decreases it ( $IC_{50} \sim 3$  mM) (33, see also Fig. 2B). [<sup>3</sup>H]ryanodine binding to RyR3 from rabbit brain and diaphragm showed similar Ca<sup>2+</sup> dependence (42, 44). [<sup>3</sup>H]ryanodine binding to RyR1 from rabbit skeletal muscle was about 10 times as sensitive to Ca<sup>2+</sup> as RyR3 (42, 44). Takeshima et al. (52) had observed similar results of CICR in neonatal skeletal muscle cells from wild type (mainly RyR1) and dyspedic mutant (RyR3) mice. Franck et al. (37) reported that  $\alpha$ -RyRs from slow-twitch red muscles of fishes was about 10 times more sensitive to Ca<sup>2+</sup> than those from fast-twitch white muscles and toadfish swim bladder. They also concluded that the Ca<sup>2+</sup> sensitivity of  $\alpha$ -RyR was not affected by coexisting  $\beta$ -RyR. Therefore we can conclude that RyR3 and  $\beta$ -RyR, irrespective of their origins, showed similar Ca<sup>2+</sup> sensitivity, whereas RyR1 and  $\alpha$ -RyR can show distinct Ca<sup>2+</sup> sensitivity among the sources. In other words, the difference of Ca<sup>2+</sup> sensitivity should be ascribed to the species specificity, rather than to the isoform specificity (43, 44).

The conclusions mentioned above were drawn from the results of CICR and of [<sup>3</sup>H]ryanodine binding in an isotonic medium. Because hypertonic media gave different Ca<sup>2+</sup> dependences (32, 33, 43, 53-55), attention to the composition of the medium is required. Ca<sup>2+</sup> dependence determined by lipid bilayer experiments may also give different conclusions (56-60). Bull and Marengo (56) first reported that the SR vesicles from frog skeletal muscle showed two types of channel activity: higher sensitivity to Ca<sup>2+</sup> and monophasic Ca<sup>2+</sup> dependence without inhibition at high Ca<sup>2+</sup> concentrations, which was similar to RyR2, and a lower sensitivity to Ca<sup>2+</sup> and biphasic Ca<sup>2+</sup> dependence with a marked inhibition at mM Ca<sup>2+</sup> concentrations, which was similar to RyR1. Later, these authors and Hidalgo (57) reported that these types of channel activity were

	A-site				I-site			
	Ca <sup>2+</sup>		Mg <sup>2+</sup>		Ca <sup>2+</sup>		Mg <sup>2+</sup>	
	K1(mM)	n1	K2(mM)	n2	K3(mM)	n3	K4(mM)	n4
α-RyR	0.010	2	0.3	1	2.4	1	2.8	1
β-RyR	0.018	2	.3	1	2.3	1	3.1	1
“CICR”	0.0025	~1.2	.075	1	0.4	1	.3	1

Table 1. Properties of A-sites and I-sites of CICR channels/RyR and α- and β-RyR purified from bullfrog skeletal muscles (“CICR” means CICR channels/RyR in the SR of skinned frog skeletal muscle fibers.)

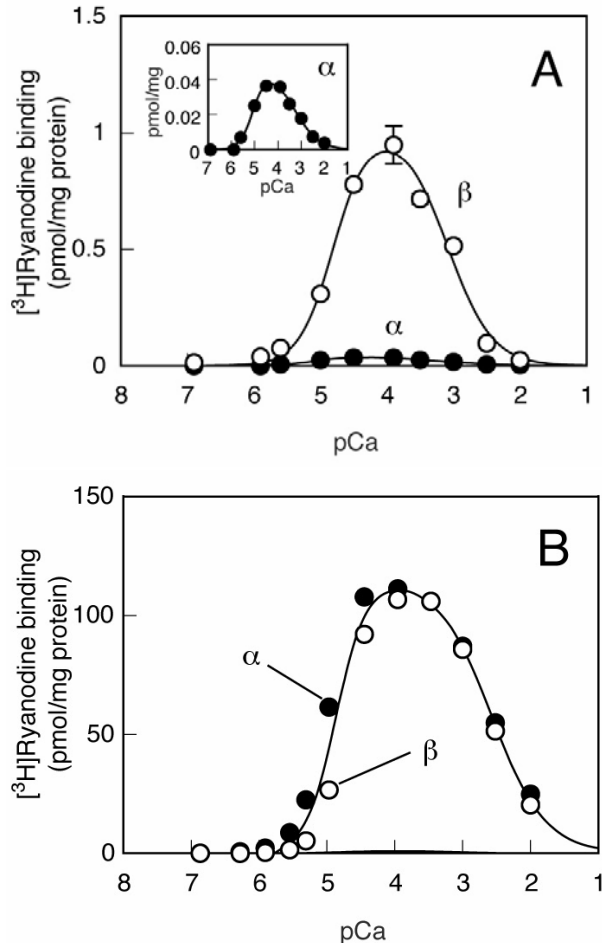


Fig. 2 Selective suppression of α-RyR in the SR. A. [3H]ryanodine binding to α- and β-RyR in the SR. B. [3H]ryanodine binding to purified α- and β-RyR. [3H]ryanodine binding to β-RyR in SR was equivalent to that of purified β-RyR, considering the content of β-RyR in SR and effect of the detergent used for purification. Note that Ca<sup>2+</sup> dependence of α-RyR in SR (inset) was very similar to that of β-RyR in SR, but that the peak value of the former was as low as 4% that of β-RyR. α- and β-RyR in SR were the same in the sensitivity to caffeine and AMPPCP as well as to Ca<sup>2+</sup>. α-RyR in SR showed a lower affinity for [3H]ryanodine without change in the maximum number of binding sites. For details, see ref. 66 (courtesy of the Journal of Biological Chemistry).

transformable and due to oxidation of channels, concluding that the two types of Ca<sup>2+</sup> dependence

could not be ascribed to the difference of the isoforms. Many investigators including us observed that β-RyR (from fish, chicken, and frog skeletal muscles) (58, 59) and RyR3 (23, 44, 45, 60) showed very steep Ca<sup>2+</sup> dependence with very weak or no inhibition at high Ca<sup>2+</sup> concentrations, and that the peak Po (open probability) can often reach as high as almost 1 in an isotonic medium without an adenine nucleotide or caffeine. Murayama et al. (44) showed that RyR3 which showed peak Po~1 had very low [3H]ryanodine binding under the corresponding conditions. The reason for the discrepancy between the two methodologies is not yet fully understood. It should be pointed out that lipid bilayer experiments report the activity of only the active channels, but not of silent ones, whereas the other methods give information on the averaged activity of all molecules. Po shows a time-averaged value of an (or several) active channel(s), but not an averaged number of open channels during a specified period. Because [3H]ryanodine binding was consistent with CICR, we believe that the Ca<sup>2+</sup> dependence based on [3H]ryanodine binding is more suitable.

## QUANTITATIVE ANALYSIS OF CICR

### Ca<sup>2+</sup> and Mg<sup>2+</sup>

The biphasic Ca<sup>2+</sup> dependence can be explained by Ca<sup>2+</sup> binding to high-affinity activating Ca<sup>2+</sup> sites (A-sites) and low-affinity inactivating Ca<sup>2+</sup> sites (I-sites) of RyR. Mg<sup>2+</sup> serves as a competitive antagonist in the A-site and an agonist in the I-site (Fig. 1A). These findings can be expressed by the following equation (61):

$$A = A_{\max} * f_A * (1 - f_I) \quad (1)$$

where A<sub>max</sub> is the maximum activity attainable under the specified conditions, and f<sub>A</sub> and f<sub>I</sub> were fractions of A- and I-sites, respectively, which were occupied by Ca<sup>2+</sup> and/or Mg<sup>2+</sup>.

$$f_A = \frac{Ca^{n1}}{\{Ca^{n1} + K1^{n1} * (1 + Mg^{n2} / K2^{n2})\}}$$

$$1 - f_I = 1 / (1 + Ca^{n3} / K3^{n3} + Mg^{n4} / K4^{n4})$$

where K1 and n1; and K3 and n3 represent dissociation constants and Hill coefficients for Ca<sup>2+</sup> of A- and I- sites, respectively, and K2 and n2; and K4 and n4, parameters for Mg<sup>2+</sup> of A- and I-sites, respectively. Here, Ca and Mg stand for [Ca<sup>2+</sup>] and [Mg<sup>2+</sup>], respectively. The results

obtained with purified  $\alpha$ - and  $\beta$ -RyR and with CICR in skinned frog skeletal muscle fibers are summarized in **Table 1** and drawn in Fig. 1A (61). The A-site favored  $\text{Ca}^{2+}$  20- to 30-fold over  $\text{Mg}^{2+}$ , whereas the I-site was nonselective between the two cations. It is interesting that the Hill coefficient for  $\text{Ca}^{2+}$  in the A-site was 2, whereas that for  $\text{Mg}^{2+}$  was 1, probably because of difference in the favorable configurations of the two cation complexes. Purified  $\alpha$ - and  $\beta$ -RyR are very similar within the accuracy of determinations. Intact SR showed higher sensitivity to  $\text{Ca}^{2+}$  and  $\text{Mg}^{2+}$  than purified isoforms (61). This difference can be reasonably accounted for by the following considerations: the different state of channels, RyR complexed with accessory proteins and purified RyR, presence and absence of the detergent, and [ $^3\text{H}$ ]ryanodine binding and  $\text{Ca}^{2+}$  release. Effect of  $\text{Mg}^{2+}$  (1 mM) on CICR of frog skinned fibers is shown in Fig. 1A.

### Effects of an adenine nucleotide

It is well known that adenine nucleotides including ATP, AMPPCP, ADP and AMP stimulate CICR channel/RyR through the effects on the same site(s). However, it is unknown whether MgATP exerts the same magnitude of effect as free ATP. This is critical in considering the in situ effect because MgATP is the major form in the sarcoplasm. Murayama et al. (61) addressed this problem comparing the effect of AMP which has very weak affinity for  $\text{Mg}^{2+}$  with that of AMPPCP which has an affinity for  $\text{Mg}^{2+}$  comparable to that of ATP. The conclusion is that the effect of an adenine nucleotide is independent of the form and that it is the total concentration which is important.

As shown in Fig. 1B, the rate of CICR in skinned fibers increased with the increase in concentration of AMPPCP. The  $\text{Ca}^{2+}$  dependence, however, remained unchanged, because normalized  $\text{Ca}^{2+}$  dependence was coincident (Fig. 1C). Namely, the main effect of an adenine nucleotide is the increase in  $A_{\text{max}}$  alone. Another change is the decrease in  $n_1$  to around 1, probably because of conformation change in RyR. These findings indicate that not only affinities for  $\text{Ca}^{2+}$  and  $\text{Mg}^{2+}$  of A- and I-sites but also  $A_{\text{max}}$  value in equation 1 is a parameter variable with experimental conditions. The conclusion that  $A_{\text{max}}$  is not fixed but variable is also supported by the finding that the inhibition of procaine was independent of  $\text{Ca}^{2+}$  concentrations (62). In other words, the occupation of the A-site with  $\text{Ca}^{2+}$  is a necessary but not a sufficient condition for CICR. Murayama et al. (61) also reported that AMPPCP definitely stimulates  $\text{Ca}^{2+}$  release in a dose-dependent manner in the virtual absence of  $\text{Ca}^{2+}$ . This indicates that an adenine nucleotide may also stimulate and amplify DICR which may be triggered by a mode different from that in CICR.

### Effects of caffeine

Murayama et al. (61) analyzed the effect of caffeine according to the procedure proposed. They reported that the effect of caffeine was two-fold: an increase in  $A_{\text{max}}$  and a decrease in  $K_1$ . No effect on  $K_2$ ,  $K_3$  or  $K_4$  was found. It is notable that caffeine exerts differential effects on  $\text{Ca}^{2+}$  affinity than on  $\text{Mg}^{2+}$  affinity in the A-sites. The I-sites, in contrast, are not affected by caffeine, excluding the possibility that the decrease of  $\text{Mg}^{2+}$  inhibition might be the underlying mechanism. Although the increase in the affinity for  $\text{Ca}^{2+}$  in the A-site is well known, attention has not been paid to the increase in  $A_{\text{max}}$  except by Endo (2, 63) and the authors (14, 22, 61, 64). Decrease in  $K_1$  was saturated at 10 mM caffeine, but the increase in  $A_{\text{max}}$  was not yet saturated at this concentration (64). There was no difference in effect between  $\alpha$ - and  $\beta$ -RyR from frog skeletal muscle. In comparison with mammalian RyR1, the extent of the decrease in  $K_1$  was similar between rabbit and frog. But increase in  $A_{\text{max}}$  in frog is greater than that in rabbit (64). Caffeine contracture was difficult to observe in mammalian skeletal muscle, and was sometimes abortive. In the presence of a SERCA inhibitor, cyclopiazonic acid or thapsigargin, however, caffeine contracture can be unfailingly observed (65). With skinned fibers, caffeine-induced  $\text{Ca}^{2+}$  release can be constantly observed in the absence of ATP. For the net  $\text{Ca}^{2+}$  release to be observed, the rate of this release must be in excess of the  $\text{Ca}^{2+}$ -pump activity. These findings indicate that the increase in  $A_{\text{max}}$  is a prevailing factor for caffeine-induced  $\text{Ca}^{2+}$  release.

### SELECTIVE SUPPRESSION OF $\alpha$ -RYR IN SR IN CICR ACTIVITY

Because CHAPS and exogenous phospholipids which were used for purification of RyR was not inert to [ $^3\text{H}$ ]ryanodine binding to RyR (54, 64), Murayama and Ogawa (66) examined whether RyR in SR and purified RyR were identical in this binding. The procedure for determination was as follows. The SR vesicles were subjected to [ $^3\text{H}$ ]ryanodine binding in an isotonic medium containing  $\text{Ca}^{2+}$  and AMPPCP at room temperature, supplemented with an excess amount of non-radiolabeled ryanodine to prevent extra [ $^3\text{H}$ ]ryanodine binding after the reaction had reached the steady state, and then were cooled down to about 4°C. Because the bound ligand would not dissociate at 4°C (67, 68), the following solubilization and separation of  $\alpha$ - and  $\beta$ -RyR were conducted at low temperature. After the SR vesicles were solubilized by CHAPS and phospholipids,  $\alpha$ -RyR was immunoprecipitated with a monoclonal antibody against the  $\alpha$ -RyR,  $\beta$ -RyR remaining in the supernatant. The contents of  $\alpha$ - and  $\beta$ -RyR in SR vesicles were 45 and 55% respectively. Surprisingly, [ $^3\text{H}$ ]ryanodine binding to  $\alpha$ -RyR in the SR was as low as ~4% that of  $\beta$ -

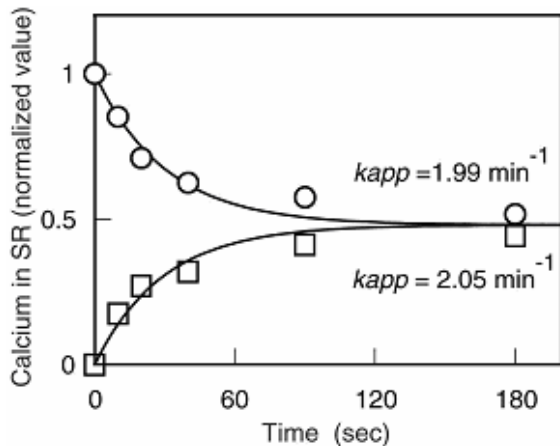


Fig. 3 Ca<sup>2+</sup> release from loaded SR (circles) and Ca<sup>2+</sup> influx into the empty SR (squares)  
The medium Ca<sup>2+</sup> concentration was 2 mM. The unit for "Calcium in SR" stands for the loading level after 2 min incubation with 0.0003 mM Ca<sup>2+</sup> in the presence of 4 mM MgATP at room temperature. For details, see ref. 62 (courtesy of the Biophysical Journal).

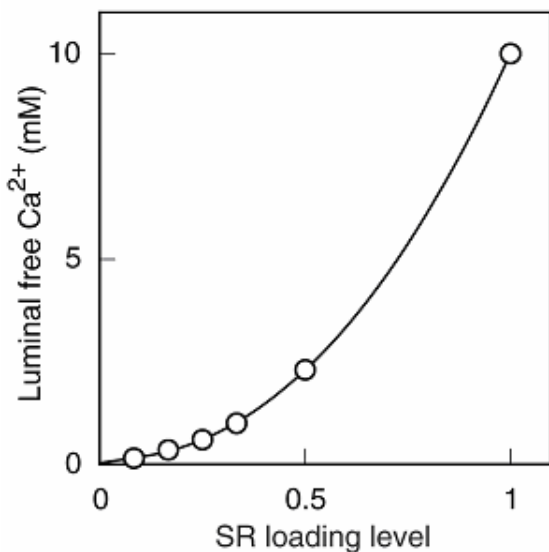


Fig.4 Non-linear relationship between the SR loading level and luminal free Ca<sup>2+</sup> concentration  
The luminal free Ca<sup>2+</sup> concentration at the unit SR loading level (see Fig. 3) was determined to be 10 mM. This level corresponds to 90% of the maximum loading and also to two- to three-fold of the physiological loading. The luminal Ca<sup>2+</sup> buffer sites were assumed to be 14 mM with K<sub>D</sub> of 1 mM. For details, see ref. 62.

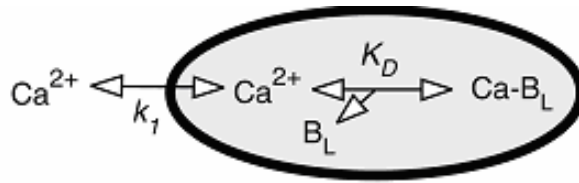
RyR in the SR vesicles, which was comparable to that of purified  $\beta$ -RyR (Fig. 2). The two isoforms, however, showed no difference in sensitivity to Ca<sup>2+</sup>, adenine nucleotide or caffeine. This reduced binding of  $\alpha$ -RyR was ascribed to the low affinity for [<sup>3</sup>H]ryanodine, with no change in the maximal number of binding sites. This means, in other words, that A<sub>max</sub> for  $\alpha$ -RyR in equation 1 will be markedly reduced in the SR vesicles. These results indicate that the CICR

activity in the SR of frog skeletal muscle is carried out largely by  $\beta$ -RyR. Murayama recently found that this was also the case with mammalian skeletal muscles (unpublished results). This is consistent with the finding by Shirokova et al. (69) that Ca<sup>2+</sup> sparks were easily observable in frog skeletal muscles, but scarcely in mammalian skeletal muscles because of the scanty RyR3 in the latter.

Coexistence of  $\beta$ -RyR cannot be the cause for the suppression of  $\alpha$ -RyR in SR membrane, because a mixture of purified  $\alpha$ - and  $\beta$ -RyR shows the result of their simple addition. Solubilization of SR with CHAPS partly remedied this non-equivalence, whereas 1 M NaCl was ineffective. Accessory proteins which form the Ca<sup>2+</sup> release channel complex might be responsible. 12 kDa FKBP (12 or 12.6), however, could not be responsible for the suppression, because FK506 treatment did not eliminate the suppression in contrast to marked removal of FKBP12 or 12.6 from  $\alpha$ -RyR. Nor can calmodulin be the factor, because supplementation of calmodulin did not selectively affect it. At the present time, the underlying mechanism including the possibility of change in the intermolecular interaction among  $\alpha$ -RyR monomers remains to be elucidated.

#### EFFECTS OF LUMINAL CA<sup>2+</sup>

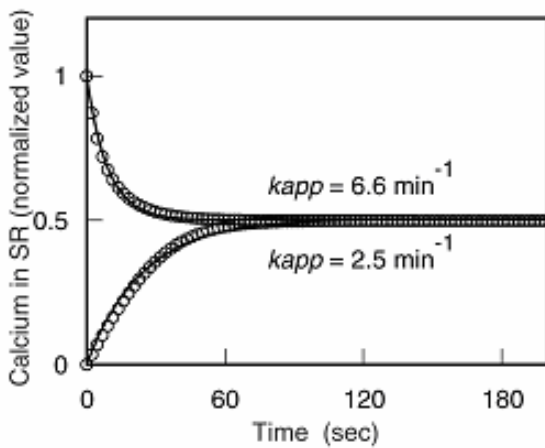
Calsequestrin and triadin are localized in the lumen of the terminal cisternae and their molecular interactions with RyR have been considered (17, 18, 22). Ca<sup>2+</sup> release might be regulated by these proteins and/or luminal Ca<sup>2+</sup> (70-73). Kurebayashi and Ogawa (62) addressed this problem using skinned fibers, determining the size and properties of the luminal Ca<sup>2+</sup> binding sites. They also showed how Ca<sup>2+</sup> release kinetics was apparently modulated by the Ca<sup>2+</sup>-buffer sites and suggested the effect of luminal Ca<sup>2+</sup> on the Ca<sup>2+</sup> release channels. Because voltage-sensitive and caffeine-sensitive Ca<sup>2+</sup> stores in skeletal muscles can be depleted simultaneously, the Ca<sup>2+</sup> store in skeletal muscles can be regarded as a single compartment (65). Kurebayashi and Ogawa (62) observed in frog skinned fiber that Ca<sup>2+</sup> influx into the empty SR occurred in a single exponential time course and that the rate constants were affected by Ca<sup>2+</sup>, Mg<sup>2+</sup>, adenine nucleotide, and procaine in the same manner as those in the CICR; they concluded that the Ca<sup>2+</sup> influx occurred through the CICR channels, but in the direction opposite to the Ca<sup>2+</sup> release. They also showed that the Ca<sup>2+</sup> release from the loaded SR and the Ca<sup>2+</sup> influx into the empty SR at a specified medium Ca<sup>2+</sup> concentration reached the same final steady state level following single exponential time courses with almost the same rate constants (Fig. 3). The steady state level was determined only by the Ca<sup>2+</sup> concentration of the incubating medium, indicating that the medium and luminal



$$k = k_1 * K_i / (K_i + Ca_L)$$

$$-\frac{dX}{dt} = k (Ca_L - Ca_C)$$

A.  $K_i = \infty$



B.  $K_i = 2 \text{ mM}$

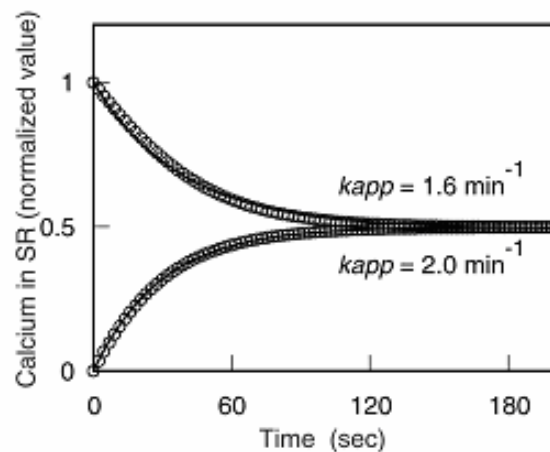


Fig.5 Calculated time courses of  $Ca^{2+}$  release from the loaded SR and of  $Ca^{2+}$  influx into the empty SR. The luminal  $Ca^{2+}$ -buffer sites ( $B_L$ ) and their dissociation constant ( $K_D$ ) were assumed to be 14 mM and 1 mM, respectively.  $Ca^{2+}$  association to and dissociation from  $B_L$  are assumed to be instantaneous.  $Ca^{2+}$  fluxes are driven by the free  $Ca^{2+}$  concentration gradient between the medium ( $Ca_C$ ) and luminal sides ( $Ca_L$ ) with a rate constant ( $k$ ) as shown in the following equation:  $-dX/dt = k * (Ca_L - Ca_C)$  where  $X$  stands for total calcium in SR.  $k$  was a function of luminal free  $Ca^{2+}$  concentrations as expressed by  $k = k_1 * K_i / (K_i + Ca_L)$  where  $k_1$  (an intrinsic rate constant) was arbitrarily determined to be  $10.5 \text{ min}^{-1}$  here. In this case,  $Ca_C = 2 \text{ mM}$  as is the case in Fig. 3. A. Calculated time courses under the assumption of no inhibition of the luminal  $Ca^{2+}$  (open circles, total  $Ca^{2+}$ ). The lines are best-fitted exponential curves with apparent rate constants ( $k_{app}$ ) indicated in the figure. Note that the calculated fluxes were approximated by single exponential curves with distinct  $k_{app}$  values ( $k_{app}$  for efflux  $>$   $k_{app}$  for influx). For unit calcium in SR, refer to Fig. 3. B. Assuming inhibition by luminal  $Ca^{2+}$ . In the equation,  $k = k_1 * K_i / (K_i + Ca_L)$ ,  $K_i = 2 \text{ mM}$  was assumed. Note that, then,  $k_{app}$  for efflux  $\approx$   $k_{app}$  for influx.

free  $Ca^{2+}$  concentrations must be equilibrated at this level. The relationship of the steady state levels at various  $Ca^{2+}$  concentrations allowed them to determine the luminal  $Ca^{2+}$  binding sites:  $B_{max} = 38 \text{ mM}$ ,  $K_D = 5 \text{ mM}$ ,  $n_H$  (Hill coefficient) = 0.65; or  $B_{max} = 14 \text{ mM}$ ,  $K_D = 1 \text{ mM}$ ,  $n_H = 1.0$ . The former corresponds to the case of heterogeneous classes of binding sites, and the latter to the case of the homogeneous binding sites composed of calsequestrin and the luminal low affinity sites of  $Ca^{2+}$ -ATPase. In either case, the same conclusions can be reached in the following discussion where we will deal with the latter case alone, just for simplicity.

Because the SR membrane is permeable

to  $K^+$ , the membrane potential difference can be easily compensated. Therefore, the driving force for  $Ca^{2+}$  release is primarily the  $Ca^{2+}$  concentration gradient between the medium and the lumen. A model simulation using parameters obtained here allows us the following predictions. First, the luminal free  $Ca^{2+}$  concentration changes in a non-linear relationship to SR loading level (Fig. 4). Second, the calculated time courses for  $Ca^{2+}$  release or for  $Ca^{2+}$  influx did not follow simple exponential time courses. They could be approximated, however, by single exponential curves (Fig. 5A). The apparent rate constant for  $Ca^{2+}$  release thus obtained was definitely greater

	Rate constant (min <sup>-1</sup> )
Physiological release	1200-3000
CICR in the	
0 mM Mg <sup>2+</sup> , at an	40
1 mM Mg <sup>2+</sup> , at an	~10
+ 5 mM caffeine	~50
0 mM Mg <sup>2+</sup> , at a	~5
1 mM Mg <sup>2+</sup> , at a	0.03
with the A-site free	~1.1

Table 2. Comparison of the release rate by CICR with that of physiological depolarization-induced Ca<sup>2+</sup> release

than that for Ca<sup>2+</sup> influx (Fig. 5A), being at variance with the experimental results shown in Fig. 3. This difference can be accommodated by the assumption that the luminal Ca<sup>2+</sup> exerts an inhibitory effect on RyR1 which is expressed in the following equation:

$$k/k_1 = 1 - Ca_L / (K_i + Ca_L)$$

where  $k_1$  stands for intrinsic rate constant for Ca<sup>2+</sup> release, and  $Ca_L$  and  $K_i$  are the luminal Ca<sup>2+</sup> concentration and the dissociation constant for inhibition. When  $K_i$  is assumed to be 2 mM, the apparent rate constants for Ca<sup>2+</sup> release and Ca<sup>2+</sup> influx in the medium containing 2 mM Ca<sup>2+</sup> became similar to the observed value (~2 min<sup>-1</sup>) (Fig. 5B). The inhibition of the luminal Ca<sup>2+</sup> also accounts for the observation that the apparent rate constants for Ca<sup>2+</sup> release were almost independent of the initial loading level (62, see also ref. 75). It also suggests that the apparent rate constant may be dependent on the endpoint of the Ca<sup>2+</sup> release.

### BIOLOGICAL ROLES OF CICR

Table 2 shows our estimates of CICR in frog skinned skeletal muscle fibers under various conditions in a medium simulating the myoplasm and compares those with the rate constant for depolarization-induced Ca<sup>2+</sup> release (61). Under the assumption of 4 and 1 mM for myoplasmic ATP and free Mg<sup>2+</sup> concentrations, respectively, the rate constant for CICR at an activating Ca<sup>2+</sup> (0.01 – 0.1 mM Ca<sup>2+</sup>) would be as low as no more than 10 min<sup>-1</sup> (see also Fig. 1A), whereas the physiological depolarization induced Ca<sup>2+</sup> release is estimated to be as high as 1200 – 3000 min<sup>-1</sup> (74, 75). If myoplasmic ATP concentration should be 8 mM (76), the rate constant for CICR would be at most twice that. Even if either A-site or I-site were freed of Mg<sup>2+</sup> inhibition (76, 77), the CICR would be much less than 100 min<sup>-1</sup> at an activating Ca<sup>2+</sup> or 10 min<sup>-1</sup> at a resting Ca<sup>2+</sup> (cf. Fig. 1A). These results indicate that the CICR is too slow to make a measurable contribution to physiological depolarization-

induced Ca<sup>2+</sup> release. This conclusion is supported by other lines of evidence in spite of the irrelevant criticism by Lamb et al. (76).

In frog skeletal muscle,  $\alpha$ -RyR in situ is selectively suppressed in the CICR activity. Therefore, CICR must be conducted exclusively by  $\beta$ -RyR. As shown previously, Ca<sup>2+</sup> sensitivity of  $\beta$ -RyR (EC<sub>50</sub> of about 0.03 mM in the presence of 1mM Mg<sup>2+</sup> (Fig. 1A)) was much lower than that of the contractile system (EC<sub>50</sub> of about 0.002 mM in the presence of 1 mM Mg<sup>2+</sup> (Kurebayashi & Ogawa (78))). In mammalian skeletal muscle where RyR3 is miniscule, RyR1 in situ is also suppressed in CICR. In vertebrate skeletal muscle, irrespective of whether mammalian or non-mammalian, CICR contributes in only a minor way to the physiological Ca<sup>2+</sup> release on depolarization.

However, CICR has a critical contribution to such pathological conditions as malignant hyperthermia ((79,80), also refer to other chapters of this book). The mutated sites of RyR1 in malignant hyperthermia are classified largely into three regions: region 1 (residues 35-614), region 2 (residues 2162-2458) and region 3 (residues 4637-4898) (79, 80). When RyR1 mutated in regions 1 and 2 was expressed in dyspedic myotube, EC<sub>50</sub> of the membrane potential for Ca<sup>2+</sup> transient was shifted to the hyperpolarized side (81, 82). It would be interesting if this finding might have some relation with a de-suppression mechanism for reduced CICR activity of RyR1 in situ. In any event, we must keep in mind that the seizure is evident only when it is triggered by psychic stress and drugs such as halothane, but otherwise ECC appears to be normal. Further investigation is required.

### PERSPECTIVES

There are two distinct modes for triggering Ca<sup>2+</sup> release from the SR: depolarization-induced Ca<sup>2+</sup> release (DICR) and Ca<sup>2+</sup>-induced Ca<sup>2+</sup> release (CICR). The direct interaction between DHPR and RyR is the trigger for the former, whereas the increased cytoplasmic Ca<sup>2+</sup> is the trigger for the latter. It is noteworthy, however, that Ca<sup>2+</sup> is a necessary though not a sufficient condition for CICR.  $\alpha$ -RyR and RyR1 are responsible both for DICR and for CICR, but their CICR activity is selectively suppressed in situ; the underlying mechanism for this remains to be elucidated.  $\beta$ -RyR and RyR3 appear not to be responsible for DICR, but their CICR activities were not suppressed. Therefore, CICR activity in frog skeletal muscles is largely conducted by  $\beta$ -RyR. CICR activity in frog skeletal muscle is thought to be too low to make a significant contribution to Ca<sup>2+</sup> release during depolarization.

Because the experimental system for CICR has been well established, understanding of CICR has deepened. Although some

experimental models have been proposed for DICR, they are not satisfactory, and establishment of such a model is desired as early as possible. Despite differences in their triggering modes, it is quite probable that some modulators of CICR might also affect DICR. They share the following two characteristics: the driving force for Ca<sup>2+</sup> release is primarily the luminal free Ca<sup>2+</sup> concentration and the luminal free Ca<sup>2+</sup> may exert an inhibitory effect on RyR.

## ACKNOWLEDGMENTS

Experiments conducted in our laboratory and cited in this article were largely supported by grants from the Ministry of Education, Science, Sports, Culture, and Technology of Japan. The Scientific Research Promotion Fund from the Promotion and Mutual Aid Corporation for Private Schools of Japan is also gratefully acknowledged.

## References

1. Ebashi, S. & M. Endo: Calcium ion and muscle contraction. *Prog Biophys Mol Biol* 18, 123-183 (1968)
2. Endo, M.: Calcium release from the sarcoplasmic reticulum. *Physiol Rev* 57, 71-108 (1977)
3. Huxley, A. F. & R. E. Taylor: Local activation of striated muscle fibres. *J Physiol* 144, 426-441 (1958)
4. Huxley, A. F.: The Croonian Lecture, 1967: The activation of striated muscle and its mechanical response. *Proc Roy Soc London B* 178, 1-27 (1971)
5. Peachey, L. D.: The sarcoplasmic reticulum and transverse tubules of the frog's sartorius. *J Cell Biol* 25, Part 2, 209-231 (1965)
6. Franzini-Armstrong, C. & A. O. Jorgensen: Structure and development of E-C coupling units in skeletal muscle. *Ann Rev Physiol* 56, 509-534 (1994)
7. Schneider, M. F. & W. K. Chandler: Voltage dependent charge movement of skeletal muscle: a possible step in excitation-contraction coupling. *Nature* 242, 244-246 (1973)
8. Fleischer, S. & M. Inui: Biochemistry and biophysics of excitation-contraction coupling. *Ann Rev Biophys Chem* 18, 333-364 (1989)
9. Powell, J. A.: Muscular dysgenesis: a model system for studying skeletal muscle development. *FASEB J* 4, 2798-2808. (1990)
10. Tanabe, T., K. G. Beam, J. A. Powell & S. Numa: Restoration of excitation-contraction coupling and slow calcium current in dysgenic muscle by dihydropyridine receptor complementary DNA. *Nature* 336, 134-139. (1988)
11. Takeshima, H., M. Iino, H. Takekura, M. Nishi, J. Kuno, O. Minowa, H. Takano & T. Noda: Excitation-contraction uncoupling and muscular degeneration in mice lacking functional skeletal muscle ryanodine-receptor gene. *Nature* 369, 556-559 (1994)
12. Schneider, M. F.: Control of calcium release in functioning skeletal muscle fibers. *Ann Rev Physiol* 56, 463-484 (1994)
13. Rios, E. & M. D. Stern: Calcium in close quarters: Microdomain feedback in excitation-contraction coupling and other cell biological phenomena. *Ann Rev Biophys Biomol Struct* 26, 47-82 (1997)
14. Ogawa, Y.: Role of ryanodine receptors. *Crit Rev Biochem Mol Biol* 29, 229-274 (1994)
15. Sorrentino, V. (Ed): *Ryanodine Receptors*. CRC Press. Boca Raton, N.Y., London, Tokyo (1996)
16. Sutko, J. L. & J. A. Airey: Ryanodine receptor Ca<sup>2+</sup> release channels: Does diversity in form equal diversity in function? *Physiol Rev* 76, 1027-1071 (1996)
17. Meissner, G.: Ryanodine receptor/Ca<sup>2+</sup> release channels and their regulation by endogenous effectors. *Ann Rev Physiol* 56, 485-508 (1994)
18. Coronado, R., J. Morrisette, M. Sukhareva & D. M. Vaughan: Structure and function of ryanodine receptors. *Am J Physiol* 266, C1485-C1504 (1994)
19. Wagenknecht, T. & M. Radermacher: Ryanodine receptors: Structure and macromolecular interactions. *Curr Opin Struct Biol* 7, 258-265 (1997)
20. Zucchi, R. & S. Ronca-Testoni: The sarcoplasmic reticulum Ca<sup>2+</sup> channel/ryanodine receptor: Modulation by endogenous effectors, drugs and disease states. *Pharmacol Rev* 49, 1-51 (1997)
21. Sitsapesan, R., and Williams, A. J. (Eds): *The Structure and Function of Ryanodine Receptor*. Imperial College Press. London (1998)
22. Ogawa, Y., N. Kurebayashi & T. Murayama: Ryanodine receptor isoforms in excitation-contraction coupling. *Adv Biophys* 36, 27-64 (1999)
23. Ogawa, Y., N. Kurebayashi & T. Murayama: Putative roles of type 3 ryanodine receptor isoforms. *Trends Cardiovasc Med* 10, 65-70 (2000)
24. Airey, J. A., C. F. Beck, K. Murakami, S. J. Tanksley, T. J. Deerinck, M. H. Ellisman & J. L. Sutko: Identification and localization of two triad junctional foot protein isoforms in mature avian fast twitch skeletal muscle. *J Biol Chem* 265, 14187-14194 (1990)
25. Olivares, E. B., S. J. Tanksley, J. A. Airey, C. F. Beck, Y. Ouyang, T. J. Deerinck, M. H. Ellisman & J. L. Sutko: Nonmammalian vertebrate skeletal muscles express two triad junctional foot protein isoforms. *Biophys J* 59, 1153-1163 (1991)
26. Airey, J. A., M. M. Grinsell, L. R. Jones, J. L. Sutko & D. Witcher: Three ryanodine Receptor Isoforms exist in avian striated muscles. *Biochemistry* 32, 5739-5745 (1993)
27. Dutro, S. M., J. A. Airey, C. F. Beck, J. L. Sutko & W. R. Trumble: Ryanodine receptor expression in embryonic avian cardiac muscle. *Develop Biol* 155, 431-441 (1993)
28. Airey, J. A., M. D. Baring, C. F. Beck, Y. Chelliah, T. J. Deerinck, M. H. Ellisman, L. J. Houenou, D. D. Mckemy, J. L. Sutko & J. Talvenheimo: Failure to make normal  $\alpha$ -ryanodine receptor is an early event associated with the Crooked Neck Dwarf (cn) mutation in chicken. *Develop Dynam* 197, 169-188 (1993)
29. Airey, J. A., T. J. Deerinck, M. H. Ellisman, L. J. Houenou, A. Ivanenko, J. L. Kenyon, D. D. Mckemy & J. L. Sutko: Crooked Neck Dwarf (cn) mutant chicken skeletal muscle cells in low density primary cultures fail to express normal  $\alpha$ -ryanodine receptor and exhibit a partial mutant phenotype. *Develop Dynam* 197, 189-202 (1993)
30. Ivanenko, A., D. D. Mckemy, J. L. Kenyon, J. A. Airey & J. L. Sutko: Embryonic chicken skeletal muscle cells fail to develop normal excitation-contraction coupling in the absence of the  $\alpha$  ryanodine receptor - Implications for a two-ryanodine receptor system. *J Biol Chem* 270, 4220-4223 (1995)
31. O'Brien, J., G. Meissner & B. A. Block: The fastest contracting muscles of nonmammalian vertebrates express only one isoform of the ryanodine receptor. *Biophys J* 65, 2418-2427 (1993)
32. Murayama, T. & Y. Ogawa: Purification and

- characterization of two ryanodine-binding protein isoforms from sarcoplasmic reticulum of bullfrog skeletal muscle. *J Biochem* 112, 514-522 (1992)
33. Murayama, T. & Y. Ogawa: Similar  $\text{Ca}^{2+}$  dependences of [ $^3\text{H}$ ]ryanodine binding to  $\alpha$ - and  $\beta$ -ryanodine receptors purified from bullfrog skeletal muscle in an isotonic medium. *FEBS Let* 380, 267-271 (1996)
  34. Murayama, T. & Y. Ogawa: Relationships among ryanodine receptor isoforms expressed in vertebrate skeletal muscles based on immunologic cross-reactivities. *J Biochem* 116, 1117-1122 (1994)
  35. Oyamada, H., T. Murayama, T. Takagi, M. Iino, N. Iwabe, T. Miyata, Y. Ogawa & M. Endo: Primary structure and distribution of ryanodine binding-protein isoforms of the bullfrog skeletal muscle. *J Biol Chem* 269, 17206-17214 (1994)
  36. Ottini, L., G. Marziali, A. Conti, A. Charlesworth & V. Sorrentino:  $\alpha$  and  $\beta$  isoforms of ryanodine receptor from chicken skeletal muscle are the homologues of mammalian RyR1 and RyR3. *Biochem J* 315, 207-216 (1996)
  37. Franck, J. P. C., J. Morrissette, J. E. Keen, R. L. Londraville, M. Beamsley & B. A. Block: Cloning and characterization of fiber type-specific ryanodine receptor isoforms in skeletal muscles of fish. *Am J Physiol* 275, C401-C415 (1998)
  38. Hakamata, Y., J. Nakai, H. Takeshima & K. Imoto: Primary structure and distribution of a novel ryanodine receptor/ calcium release channel from rabbit brain. *FEBS Let* 312, 229-235 (1992)
  39. Giannini, G., E. Clementi, R. Ceci, G. Marziali & V. Sorrentino: Expression of a ryanodine receptor- $\text{Ca}^{2+}$  channel that is regulated by TGF- $\beta$ . *Science* 257, 91-94 (1992)
  40. Giannini, G., A. Conti, S. Mammarella, M. Scrobogna & V. Sorrentino: The ryanodine receptor calcium channel genes are widely and differentially expressed in murine brain and peripheral tissues. *J Cell Biol* 128, 893-904 (1995)
  41. Conti, A., L. Gorza & V. Sorrentino: Differential distribution of ryanodine receptor type 3 (RyR3) gene product in mammalian skeletal muscles. *Biochem J* 316, 19-23 (1996)
  42. Murayama, T. & Y. Ogawa: Properties of RyR3 ryanodine receptor isoform in mammalian brain. *J Biol Chem* 271, 5079-5084 (1996)
  43. Ogawa, Y. & T. Murayama: Characteristics of ryanodine receptor 3 isoform (RyR3) and its homologues. In : The Structure and Function of Ryanodine Receptors Eds: Sitsapesan R, Williams A J, Imperial College Press, London 5-22 (1998)
  44. Murayama, T., T. Oba, E. Katayama, H. Oyamada, K. Oguchi, M. Kobayashi, K. Otsuka & Y. Ogawa: Further characterization of the type 3 ryanodine receptor (RyR3) purified from rabbit diaphragm. *J Biol Chem* 274, 17297-17308 (1999)
  45. Jeyakumar, L. H., J. A. Copello, A. M. O'Malley, G. M. Wu, R. Grassucci, T. Wagenknecht & S. Fleischer: Purification and characterization of ryanodine receptor 3 from mammalian tissue. *J Biol Chem* 273, 16011-16020 (1998)
  46. Bertocchini, F., C. E. Ovitt, A. Conti, V. Barone, H. R. Scholer, R. Bottinelli, C. Reggiani & V. Sorrentino: Requirement for the ryanodine receptor type 3 for efficient contraction in neonatal skeletal muscles. *EMBO J* 16, 6956-6963 (1997)
  47. Flucher, B. E., A. Conti, H. Takeshima & V. Sorrentino: Type 3 and type 1 ryanodine receptors are localized in triads of the same mammalian skeletal muscle fibres. *J Cell Biol* 146, 621-629 (1999)
  48. Sutko, J. L., J. A. Airey, K. Murakami, M. Takeda, C. Beck, T. Deerinck & M. H. Ellisman: Foot protein isoforms are expressed at different times during embryonic chick skeletal muscle development. *J Cell Biol* 113, 793-803 (1991)
  49. Block, B. A., T. Imagawa, K. P. Campbell & C. Franzini-Armstrong: Structural evidence for direct interaction between the molecular components of the transverse tubule/sarcoplasmic reticulum junction in skeletal muscle. *J Cell Biol* 107, 2587-2600 (1988)
  50. Franzini-Armstrong, C. & F. Protasi: Ryanodine receptor of striated muscles: a complex channel capable of multiple interactions. *Physiol Rev* 77, 699-729 (1997)
  51. Felder, E. & C. Franzini-Armstrong: Possible parajunctional location of RyR3 in skeletal muscle. *Biophys J* 80, 382a (2001)
  52. Takeshima, H., T. Yamazawa, T. Ikemoto, H. Takekura, M. Nishi, T. Noda & M. Iino:  $\text{Ca}^{2+}$ -induced  $\text{Ca}^{2+}$  release in myocytes from dyspedic mice lacking the type-1 ryanodine receptor. *EMBO J* 14, 2999-3006 (1995)
  53. Lai, F. A., Q. Y. Liu, L. Xu, A. El-Hashem, N. R. Kramarcy, R. Sealock & G. Meissner: Amphibian ryanodine receptor isoforms are related to those of mammalian skeletal or cardiac muscle. *Am J Physiol* 263, C365-C372 (1992)
  54. Murayama, T. & Y. Ogawa: Potential factors which affect the  $\text{Ca}^{2+}$ -sensitivity of ryanodine receptors. *Biomed Res* 14 (Suppl. 2), 71-72 (1993)
  55. Murayama, T., N. Kurebayashi & Y. Ogawa: Stimulation by polyols of the two ryanodine receptor isoforms of frog skeletal muscle. *J Muscle Res Cell Motil* 19, 15-24 (1998)
  56. Bull, R. & J. J. Marengo: Sarcoplasmic reticulum release channels from frog skeletal muscle display two types of calcium dependence. *FEBS Let* 331, 223-227 (1993)
  57. Marengo, J. J., C. Hidalgo & R. Bull: Sulfhydryl oxidation modifies the calcium dependence of ryanodine-sensitive calcium channels of excitable cells. *Biophys J* 74, 1263-1277 (1998)
  58. Percival, A. L., A. J. Williams, J. L. Kenyon, M. M. Grinsell, J. A. Airey & J. L. Sutko: Chicken skeletal muscle ryanodine receptor isoforms: Ion channel properties. *Biophys J* 67, 1834-1850 (1994)
  59. O'Brien, J., H. H. Valdivia & B. A. Block: Physiological differences between the  $\alpha$  and  $\beta$  ryanodine receptors of fish skeletal muscle. *Biophys J* 68, 471-482 (1995)
  60. Chen, S. R., X. Li, K. Ebisawa & L. Zhang: Functional characterization of the recombinant type 3  $\text{Ca}^{2+}$  release channel (ryanodine receptor) expressed in HEK293 cells. *J Biol Chem* 272, 24234-24246 (1997)
  61. Murayama, T., N. Kurebayashi & Y. Ogawa: Role of  $\text{Mg}^{2+}$  in  $\text{Ca}^{2+}$ -induced  $\text{Ca}^{2+}$  release through ryanodine receptors of frog skeletal muscle: Modulations by adenine nucleotides and caffeine. *Biophys J* 78, 1810-1824 (2000)
  62. Kurebayashi, N. & Y. Ogawa: Effect of luminal calcium on  $\text{Ca}^{2+}$  release channel activity of sarcoplasmic reticulum in situ. *Biophys J* 74, 1795-1807 (1998)
  63. Endo, M.: Calcium release from sarcoplasmic reticulum. *Curr Topic Membr Trans* 25, 181-230 (1985)
  64. Ogawa, Y., T. Murayama & N. Kurebayashi: Comparison of properties of  $\text{Ca}^{2+}$  release channels between rabbit and frog skeletal muscles. *Mol Cell Biochem* 190, 191-201 (1999)
  65. Kurebayashi, N. & Y. Ogawa: Depletion of  $\text{Ca}^{2+}$  in the sarcoplasmic reticulum stimulates  $\text{Ca}^{2+}$  entry into mouse skeletal muscle fibres. *J Physiol* 533, 185-199 (2001)
  66. Murayama, T. & Y. Ogawa: Selectively suppressed  $\text{Ca}^{2+}$ -induced  $\text{Ca}^{2+}$  release activity of  $\alpha$ -ryanodine receptor ( $\alpha$ -RyR) in frog skeletal muscle

- sarcoplasmic reticulum: potential distinct modes in  $\text{Ca}^{2+}$  release between  $\alpha$ - and  $\beta$ -RyR. *J Biol Chem* 276, 2953-2960 (2001)
67. Lai, F. A., H. P. Erickson, E. Rousseau, Q.-Y. Liu & G. Meissner: Purification and reconstitution of the calcium release channel from skeletal muscle. *Nature* 331, 315-319 (1988)
  68. Ogawa, Y. & H. Harafuji: Effect of temperature on [ $^3\text{H}$ ] ryanodine binding to sarcoplasmic reticulum from bullfrog skeletal muscle. *J Biochem* 107, 887-893 (1990)
  69. Shirokova, N., R. Shirokov, D. Rossi, A. Gonzalez, W. G. Kirsch, J. Garcia, V. Sorrentino & E. Rios: Spatially segregated control of  $\text{Ca}^{2+}$  release in developing skeletal muscle of mice. *J Physiol* 521, 483-496 (1999)
  70. Donoso, P., H. Prieto & C. Hidalgo: Luminal calcium regulates calcium release in triads isolated from frog and rabbit skeletal muscle. *Biophys J* 68, 507-515 (1995)
  71. Ikemoto, N., M. Ronjat, L. G. Meszaros & M. Koshita: Postulated role of calsequestrin in the regulation of calcium release from sarcoplasmic reticulum. *Biochemistry* 28, 6764-6771 (1989)
  72. Sitsapesan, R. & A. J. Williams: The gating of the sheep skeletal sarcoplasmic reticulum  $\text{Ca}^{2+}$ -release channel is regulated by luminal  $\text{Ca}^{2+}$ . *J Membr Biol* 146, 133-144 (1995)
  73. Tripathy, A. & G. Meissner: Sarcoplasmic reticulum luminal  $\text{Ca}^{2+}$  has access to cytosolic activation and inactivation sites of skeletal muscle  $\text{Ca}^{2+}$  release channel. *Biophys J* 70, 2600-2615 (1996)
  74. Csernoch, L., V. Jacquemond & M. F. Schneider: Microinjection of strong calcium buffers suppresses the peak of calcium release during depolarization in frog skeletal muscle fibers. *J Gen Physiol* 101, 297-333 (1993)
  75. Pape, P. C., D. S. Jong & W. K. Chandler: Calcium release and its voltage dependence in frog cut muscle fibers equilibrated with 20 mM EGTA. *J Gen Physiol* 106, 259-336 (1995)
  76. Lamb, G. D., M. A. Cellini & D. G. Stephenson: Different  $\text{Ca}^{2+}$  releasing action of caffeine and depolarisation in skeletal muscle fibres of the rat. *J Physiol* 531, 715-728 (2001)
  77. Lamb, G. D. & D. G. Stephenson: Effect of  $\text{Mg}^{2+}$  on the control of  $\text{Ca}^{2+}$  release in skeletal muscle fibres of the toad. *J Physiol* 434, 507-528 (1991)
  78. Kurebayashi, N. & Y. Ogawa: Increase by trifluoperazine in calcium sensitivity of myofibrils in a skinned fibre from frog skeletal muscle. *J Physiol* 403, 407-424 (1988)
  79. McCarthy, T. V., K. A. Quane & P. J. Lynch: Ryanodine receptor mutations in malignant hyperthermia and central core disease. *Hum Mutat* 15, 410-417 (2000)
  80. MacLennan, D. H.:  $\text{Ca}^{2+}$  signalling and muscle disease. *Eur J Biochem* 267, 5291-5297 (2000)
  81. Dietze, B., J. Henke, H. M. Eichinger, F. Lehmann-Horn & W. Melzer: Malignant hyperthermia mutation Arg615Cys in the porcine ryanodine receptor alters voltage dependence of  $\text{Ca}^{2+}$  release. *J Physiol* 526, 507-514 (2000)
  82. Avila, G., J. J. O'Brien & R. T. Dirksen: Excitation--contraction uncoupling by a human central core disease mutation in the ryanodine receptor. *Proc Natl Acad Sci USA* 98, 4215-4220 (2001)

**Running Title:** RyR isoforms of non mammalian muscle

**Key words:**  $\alpha$ -RyR,  $\beta$ -RyR,  $\text{Ca}^{2+}$ -induced  $\text{Ca}^{2+}$  release, adenine nucleotide, caffeine

**Corresponding Author:** Yasuo Ogawa  
Department of Pharmacology, Juntendo University School of Medicine, 2-1-1, Hongo, Tokyo 113-8421

Telephone: +81-3-5802-1034

Fax: +81-3-5802-0419

E-mail: ysogawa@med.juntendo.ac.jp

# Redox Sensing Properties of the Ryanodine Receptor Complex

Isaac N. Pessah, Kyung Ho Kim and Wei Feng

Department of Molecular Biosciences, School of Veterinary Medicine, One Shields Avenue, University of California, Davis, CA 95616. Email: [inpessah@ucdavis.edu](mailto:inpessah@ucdavis.edu)

**ABSTRACT** The release mechanism regulating SR  $\text{Ca}^{2+}$  homeostasis is significantly more sensitive than the uptake mechanisms. The exquisite sensitivity exhibited by ryanodine-sensitive  $\text{Ca}^{2+}$  channel complexes (*i.e.*, ryanodine receptors, RyRs) to functional perturbation by chemically diverse sulfhydryl-modifying compounds can include phases of activation and inhibition that are dependent on the concentration of the reagent used, the length of exposure, and the nature of the chemical reaction the reagent undertakes with sulfhydryl groups. However the exquisite sensitivity of RyR function to sulfhydryl modification has been generally viewed as significant only in pathophysiological processes. The present paper addresses possible physiological importance of the redox sensing properties of the ryanodine receptor complexes (RyRs) and proposes an underlying mechanism. New data is presented that directly measure the pKa of hyperreactive thiols that occur when the closed conformation of the RyR channel complex is assumed, and that appear to be an integral component of the redox sensor.

## Introduction

The  $\text{Ca}^{2+}$  release mechanism of sarcoplasmic reticulum (SR) was first shown to be sensitive to reagents that interact with protein thiols by exposing SR vesicles loaded with  $\text{Ca}^{2+}$  to heavy metals (1, 2). Even in these early experiments there were clear indications that the release mechanisms regulating SR  $\text{Ca}^{2+}$  homeostasis were significantly more sensitive than the uptake mechanisms. Since the initial observations were reported, several laboratories have provided evidence of the exquisite sensitivity exhibited by ryanodine-sensitive  $\text{Ca}^{2+}$  channel complexes (*i.e.*, ryanodine receptors; RyR) to functional perturbation by chemically diverse sulfhydryl-modifying compounds (recently reviewed in 3, 4). Several classes of non-physiologic organic compounds capable of oxidizing or arylating protein sulfhydryl groups have been utilized to modify the  $\text{Ca}^{2+}$  release properties of skeletal or cardiac SR by selective modification of RyR1 or RyR2 function, respectively. The functional consequence of sulfhydryl modification of RyRs can include phases of activation and inhibition that are dependent on the concentration of the reagent used, the length of exposure, and the nature of the chemical reaction the reagent undertakes with sulfhydryl groups. These observations have made important contributions toward understanding mechanisms by which oxidizing, reducing, and arylating reactions modify RyR function and its resulting influence on  $\text{Ca}^{2+}$  transport across SR. However the exquisite sensitivity of RyR function to sulfhydryl modification has generally been viewed as significant only in pathophysiological processes. The physiological importance of the redox-sensing property of RyR complexes in healthy cells remains unclear.

## Redox Model of Channel Gating

An original hypothesis proposed by Abramson and Salama suggested that the oxidation of critical sulfhydryl moieties within the RyR complex is a

necessary requisite for opening of the channel pore (5). In such a model, oxidation and reduction of the critical sulfhydryl moieties coincide with gating transitions between conducting and non-conducting states (Fig 1).

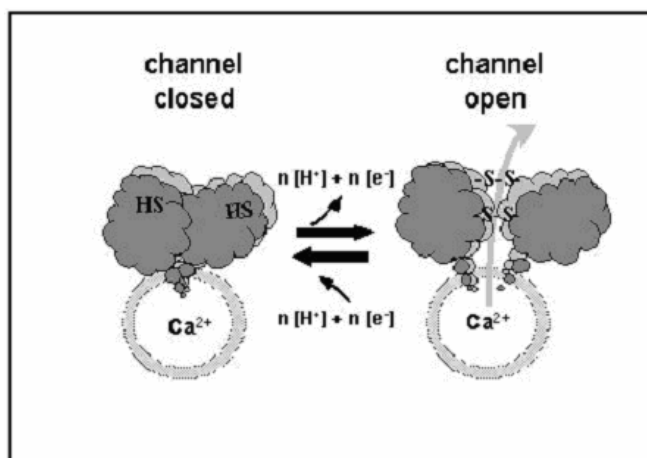


Figure 1. A model proposed by Abramson and Salama (5, 6) relating the oxidation state of critical cysteine thiol moieties to disulfides within RyR primary sequence and channel gating. Disulfides could form either within or between protomers.

Reagents that undergo redox cycling, such as the anthraquinones doxorubicin and daunorubicin, enhance RyR channel open probability (6, 7). In this model, the presence of a redox cyler would either enhance the normal rate of oxidation of critical sulfhydryls to disulfides, or delay the rate of reduction once the disulfides regulating channel open transitions are oxidized. Likewise aryl disulfides such as DTNB or DTDP readily form mixed disulfides with critical thiols within the RyR complex and mimic the "endogenous" protein disulfides that are proposed to be essential for channel opening (8, 9). One major difficulty in reconciling a mechanism of redox mediated gating of the RyR channel complex with physiological activation

and inactivation of  $\text{Ca}^{2+}$  release is the large discrepancy in kinetics with which the two processes proceed. RyR channel gating transitions are extremely rapid with the open state typically lasting no longer than a few milliseconds. Even in the presence of allosteric activators such as bastadin 10 that stabilize long open states, it is unlikely sulfhydryl oxidation is involved given the very rapid reversibility of the compound's effect (10). Quinones that both undergo redox cycling and arylation reactions such as naphthoquinones (11) and benzo[a]pyrene-7,8-dione (12) exhibit complex actions on RyR channel activity that largely depend on concentration and length of exposure, similar to those observed with maleimides under conditions that arylate several classes of RyR1 Cys residues (13). Therefore, sulfhydryl chemistry involving the formation and breaking of disulfide bonds within the RyR complex in the absence of catalysis is extremely slow and leads to long lived irreversible modification of function. In order for oxidation and reduction of critical Cys residues to coincide with each channel gating transition, an efficient means of catalytically transferring electrons from a primary donor to the reactive cysteine(s) within the RyR complex, and subsequently to a terminal acceptor, would be a necessary requisite to support gating. In this regard, a 23 kDa NADH oxidase appears to be closely associated with and modulates the function of RyR2 (14). However NADH oxidoreductase activity is not essential for supporting RyR2 channel gating. Moreover solubilized and purified RyR1 and RyR2 oligomers reconstituted in artificial bilayer lipid membranes (BLM) gate with similar properties to those observed with channels reconstituted directly from junctional SR fused with BLM in the absence of cofactors to support catalytic transfer of electrons (15). Taken together these observations indicate a modulatory role for sulfhydryl chemistry within the RyR complex.

### Redox Control of Calmodulin Binding and RyR Nitrosylation

Reactive sulfhydryl groups within RyR1 have been shown to contribute to the calmodulin-binding (16), and the topic is covered in detail elsewhere in this volume. Of particular interest to the issue of redox control of RyR, is the observation that arylation of Cys 3635 with N-ethylmaleimide resulted in loss of high affinity calmodulin binding and associated channel modulation (17). This finding raised the possibility that functional responses of RyR1 to calmodulin may be related to redox regulation observed with xenobiotic and endogenous sulfhydryl reagents such as glutathione, NADH, and nitric oxide radical ( $\text{NO}^\bullet$ ), and could at least in part be mediated through hyperreactive Cys3635. Recently Cys3635 has been shown to be the target of selective nitrosylation by  $\text{NO}^\bullet$  (18). Nitrosylation of RyRs has been shown to allosterically modulate channel gating kinetics and ryanodine-binding in a complex manner (covered in detail elsewhere in this volume). However Cys3635 does not appear to be related to redox sensing of GSH and GSSG since expression of site directed mutation C3635A in RyR1 maintained

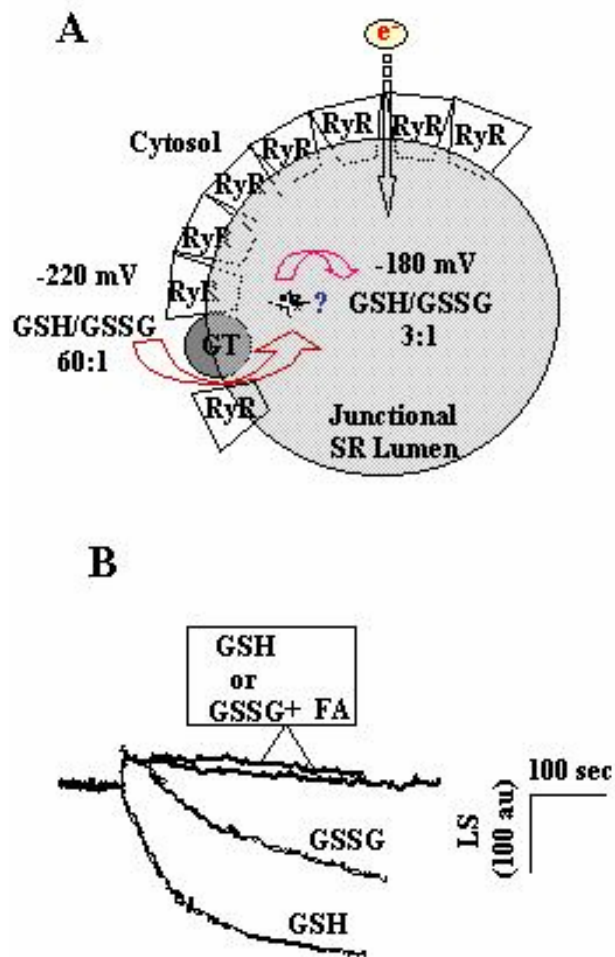


Figure 2. (A) Conceptual model highlighting recent evidence for co-existence within junctional SR of RyR and a transmembrane glutathione transporter (GT). The transporter produces a partition of redox potential between cytoplasmic and luminal compartments. (B) Light scattering measured spectrally shows that transport of GSH or GSSG (10 mM) from the extravesicular space into the vesicle lumen. The rate of decline in fluorescence (arbitrary units; au) represents the uptake of glutathione into the SR vesicles (thereby decreasing light scattering). Flufenamic acid (FA) blocks all glutathione transport.

responses to redox environment but lost responses to  $\text{NO}^\bullet$ . It is likely that more than one class of sulfhydryl residing within the RyR channel complex is subject to chemical modification, each contributing to specific aspects of function. The major challenge will be to understand how specific sulfhydryl moieties ascribe specific aspects of channel function. Considering the structural complexity of RyR and its associated proteins, this task is likely to be a formidable one.

### Transmembrane Redox Potential of SR

The cytosol of most healthy mammalian cells possesses a redox potential of approximately  $-230$  mV (19). The major cytosolic redox buffers within muscle and non-muscle cells are based on the relative concentration of reduced glutathione (GSH) and

oxidized glutathione (GSSG) or NADH and NAD<sup>+</sup> (20, 21). In the typical mammalian cell, the ratio of [GSH]/[GSSG] in the cytosol is  $\geq 60:1$  thereby maintaining very reduced redox potential of approximately -230 mV. By contrast, the redox potential of ER lumen is significantly more oxidized (approximately -180 mV); maintained with a 3:1 to 1:1 ratio of [GSH]/[GSSG] (19, 22). It is reasonable to predict that the typical microsomal membrane within which RyRs reside is normally subject to a large transmembrane redox potential difference of 40 to 50 mV with the lumen much more oxidized than the cytosol (Figure 2A). An important question is whether junctional SR of muscle possesses machinery needed to form a transmembrane redox gradient.

In non-muscle cells, one or more transporters have been found to facilitate diffusion of GSH and GSSG across the ER membrane (19, 22, 23). These transporters are thought to be essential for establishing and maintaining the redox potential gradient across the microsomal membrane. If junctional SR is subject to the same large redox gradient observed across ER, then isolated vesicles enriched in RyR should also contain transporters for glutathione. Like ER, junctional SR isolated from skeletal muscle has recently been shown to transport both oxidized and reduced glutathione in two independent studies (24, 25). Initial rates of transport of GSH were 5-times faster than those of GSSG, and were blocked by flufenamic acid (22, 24), suggesting a common pharmacology for SR and ER transporters (Fig. 2B). *o*-Phthaldialdehyde has been used to quantitatively measure luminal glutathione (GSH + GSSG) and the ratio of luminal GSH/GSSG can be measured in the presence of varying extravesicular redox potential (26, 27). A significant observation was that regardless of the extravesicular redox potential set experimentally, the luminal ratio of [GSH]/[GSSG] was maintained within narrow limits approximating 3:1, consistent with a significantly more oxidized microsomal lumen, as previously reported for non-muscle ER (19, 22, 23, 26, 28). A most intriguing recent observation is that glutathione transport across SR/ER membranes correlates with the abundance of RyR1, with the fastest transport in terminal cisternae (25). Moreover glutathione transport activity seems to be closely associated with RyR1 in SR.

In summary, junctional SR membranes, much like ER membranes from non-muscle origin, possess a selective transporter for GSH and GSSG. Although a common feature of this microsomal transporter is a preference for GSH over GSSG (based on initial rates), the ER/SR lumen appears to favor a 3:1 ratio of GSH/GSSG at steady state, even if the cytosolic redox potential is highly reduced. A 3:1 GSH/GSSG is consistent with the observation that healthy cells maintain an oxidized luminal potential (-160 to -180mV) relative to the cytosol (-220 to -230mV). How the ER/SR lumen maintains an oxidized potential despite the preference for transport of GSH is unclear. One possibility is that GSH is oxidized to GSSG within the ER/SR lumen and that the latter is preferentially retained. In support of this hypothesis,

there is evidence that GSSG can be converted from GSH locally within the ER lumen, although the mechanism(s) remain obscure (22).

### Transmembrane Redox Sensor of RyR complex

Redox potential can dramatically influence RyR1 function measured with isolated SR and intact muscle fibers. For example Koshita and coworkers found that Ca<sup>2+</sup> release from SR could be induced by oxidizing compounds such as alcian blue and plumbagin and was partially blocked in the presence of GSH (29). Abramson and coworkers have reported that GSH reduces whereas GSSG enhances the activity of RyR1 (30). In this regard, Marengo and coworkers contributed an insightful observation that RyR1 and RyR2 channels reconstituted in BLM display different patterns of Ca<sup>2+</sup> dependencies regardless of their origin and that the patterns could be deliberately altered with thiol oxidizing reagents (31). Their results imply that in the reducing environment of the muscle cell, Cys residues critical to function are maintained in the reduced state and may account for low open probability ( $P_o$ ) and low sensitivity to Ca<sup>2+</sup> activation. However the typical solutions using in the preparation of SR for *in vitro* study does not contain a redox buffer. It is likely that functionally important Cys within a large fraction of RyR complexes auto-oxidize resulting in channels that have high  $P_o$  and heightened sensitivity to Ca<sup>2+</sup> activation. One possible physiologic role for hyperreactive sulfhydryl chemistry (see section 1.6, below) within the RyR complex may be to respond to physiologically important changes in localized redox potential in response to redox-active signaling molecules such as nitric oxide (32-34) in the presence of redox buffers.

To study redox regulation of RyR channel activity, Feng et al (24) utilized the bilayer lipid membrane (BLM) preparation to precisely control the redox state on both the cytoplasmic and luminal faces of the reconstituted channel by adjusting the [GSH]/[GSSG] ratio to form varied redox potentials. Since GSH and GSSG by themselves in excess of 5 mM are highly reducing and oxidizing, respectively, they are likely to influence not only components of the redox sensor but also change the redox state of multiple classes of Cys unrelated to the redox sensor, thereby obfuscating conclusions. Great care was taken to tightly adjust the redox potential with GSH/GSSG ratios whose total concentration did not exceed the physiologically relevant range (1-5 mM) (35). For example, RyR1 channels failed to respond to an cytoplasmic redox potential (RP) of -180 mV (generated by addition 3:1 of [GSH]/[GSSG]; total [glutathione] = 4 mM). Physiologically a cytoplasmic RP of -180 mV would be considered highly oxidizing, yet RyR1 channel function remained unaltered (Fig 3). However, immediately after the addition of 3:1 [GSH]/[GSSG] to generate the same redox potential of -180 mV on the luminal (trans) side of the channel, channel  $P_o$  increased 13-fold. RyR1 responded to small (5-10 mV) changes in cytoplasmic redox potential when the luminal side of RyR1 was fixed at -180 mV. Chemical labeling studies with fluorogenic maleimide CPM (see section 1 and with

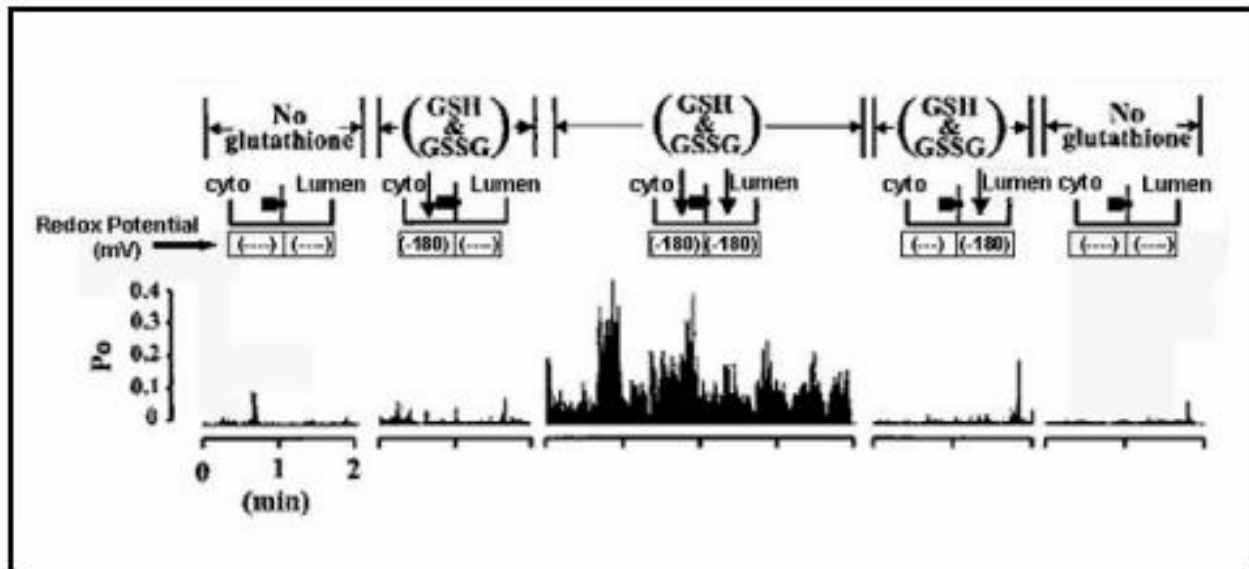


Figure 3. RyR1 responds to transmembrane redox potential in a reversible manner. Long channel records were obtained in the presence or absence of GSH/GSSG on the cytosolic (cyto) and lumenal (lumen) side of the channel as indicated to give  $-180$  mV.

RyR1 complexes in the closed conformation to promote forming thioether adducts with the most reactive (hyperreactive) thiols (36, 37) resulted in selective loss of redox sensing properties (24).

Kinetic analysis of [ $^3$ H]ryanodine binding to skeletal SR also revealed tight regulation of RyR1 conformation by redox potential using GSH/GSSG redox buffers that could be eliminated upon labeling of reactive thiols with CPM (38). Transmembrane redox sensing may represent a fundamental mechanism by which ER/SR  $\text{Ca}^{2+}$  channels respond to localized changes in transmembrane glutathione redox potential produced by physiologic and pathophysiologic modulators of  $\text{Ca}^{2+}$  release from stores. Moreover many endogenous cellular substrates and xenobiotic compounds of environmental concern can be metabolized *via* electrophilic or redox-active intermediates such as quinones. If hyperreactive thiols within the RyR complex constitute an important biochemical component of a redox sensor, they may convey information about localized changes in redox potential to the  $\text{Ca}^{2+}$  release process across the microsomal membrane. Ryanodine receptors represent a key  $\text{Ca}^{2+}$  regulatory channel widely expressed within microsomal membrane of a wide variety of cells where many xenobiotic molecules are metabolized to electrophilic intermediates by the cytochrome P450 system. Co-localization of ryanodine-sensitive  $\text{Ca}^{2+}$  channels and cytochrome P450 enzyme that catalyze formation of quinone-containing compounds could provide a fundamental mechanism by which localized redox potential is "sensed" by the major intracellular  $\text{Ca}^{2+}$  store. This mechanism may have both physiological and toxicological significance.

#### Hyperreactive Sulfhydryls of RyR Complex: A key Component of a Transmembrane Redox Sensor

As mentioned above RyR complexes were found to possess a class of Cys moieties that could be distinguished based on their chemical reactivity (36, 37). The rationale for these hinged on the fact that the pKa of the typical protein thiol is above pH 8 and would be expected to be largely protonated (reduced) and have slow chemical reactivity at physiologic cellular pH, especially toward maleimides (39, 40). In fact, disulfide bond-formation (sulfhydryl oxidation), so critical to protein folding, typically takes place within the oxidizing environment of the SR/ER lumen, not in the reducing environment of the cytosol. Only when Cys residues reside within special microenvironments will protein thiol moieties be reactive enough to actively take part in physiologic redox reactions. Examples come from studies of enzyme active sites such as glyceraldehyde-3-phosphate dehydrogenase (41), glutamine-dependent amidotransferases (42), and glutathione reductases (43).

The assay used to probe for hyperreactive thiols within the RyR1 complex utilized the nonfluorescent maleimide, 7-diethyl amino-3-(4'-maleimidylphenyl)-4-methylcoumarin (CPM), which undergoes Michael addition with protein thiols to produce a thioether adduct with high fluorescent yield. Utilizing CPM at very low concentrations (1-50 nM, *i.e.*, 0.02-1.0 pmol/ $\mu\text{g}$  SR protein) the kinetics of labeling junctional and longitudinal sarcoplasmic reticulum protein from rabbit skeletal and rat cardiac muscle was examined in the presence of physiologically and pharmacologically relevant channel activators or inhibitors. Under these

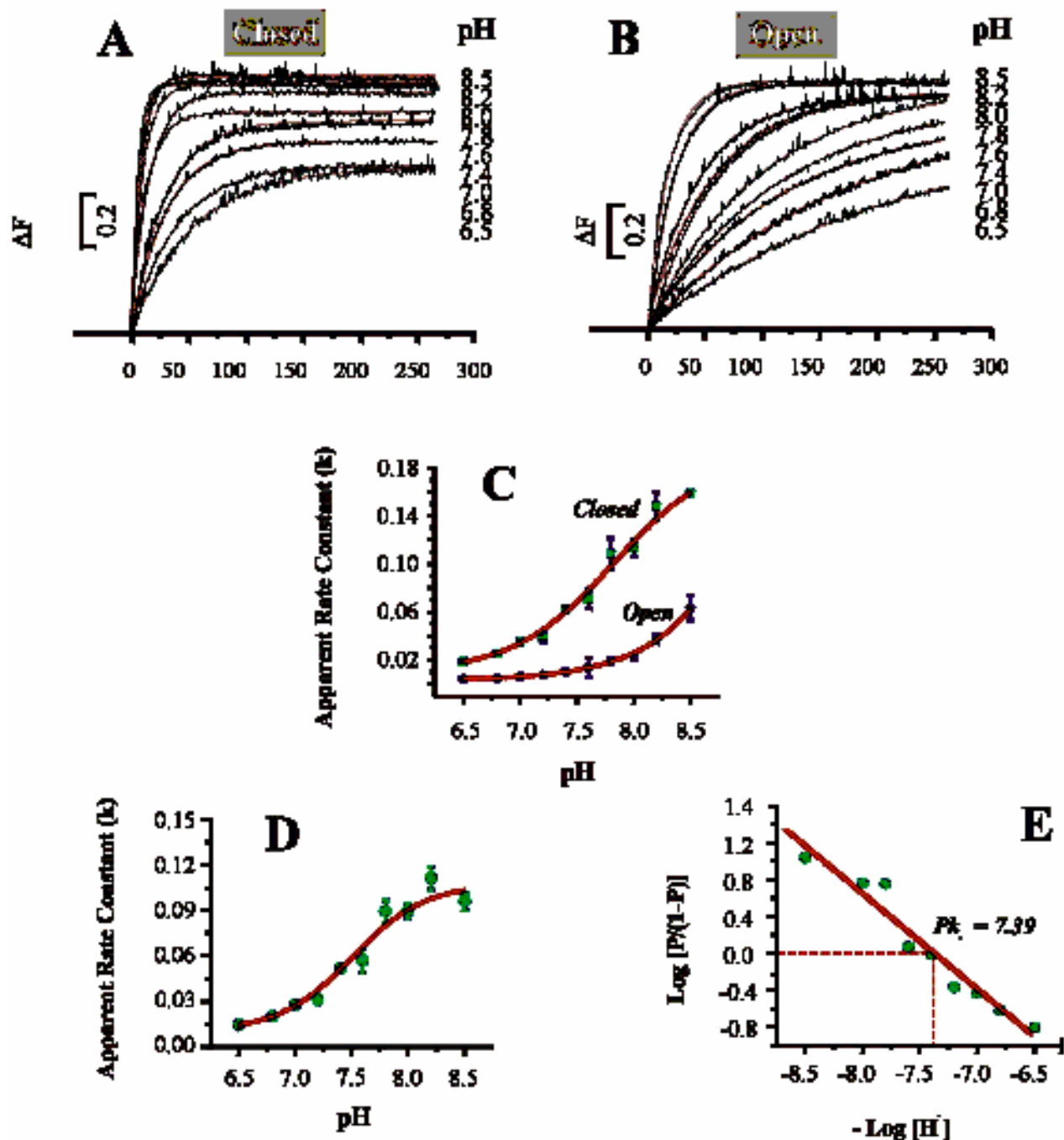


Figure 4. The rate of forming CPM-thioether adducts with junctional SR is highly dependent of pH and the constituents in the buffer that influence conformational state of the RyR1 complex: (A) closed conformation achieved with 10 mM Mg<sup>2+</sup>; (B) open conformation achieved with 100  $\mu$ M Ca<sup>2+</sup> and 10 mM caffeine.

conditions, where SR protein thiols greatly exceed the maleimide, the hypothesis that the RyR channel complex possesses a very small number of highly reactive (hyperreactive) thiol groups was tested. If this hypothesis proved incorrect, the anticipated (yet trivial) result would have been relatively slow formation of thioether adducts with the most abundant SERCA pump thiols, since SERCA pump protein accounts for 60-70% of the total SR protein.

However a very different result was observed. The CPM assay quantitatively revealed the existence of a very small number ( $\leq 1$  pmol/ $\mu$ g SR) of highly reactive cysteine residues within junctional SR (JSR) membranes enriched in RyR1, traidin and calsequestrin. Formation of CPM thioether adducts proceeded  $>6$ -fold faster in the presence of physiologic (e.g., Mg<sup>2+</sup>) or pharmacologic channel inhibitors when compared to rates in the presence of

channel activators (e.g. optimal  $\text{Ca}^{2+}$ ). Furthermore longitudinal SR membranes (LSR) lacking the channel complex only displayed slow labeling kinetics regardless of which channel modulator was present. Fluorograms of JSR protein labeled for 45 sec with 10 nM CPM and then size separated by SDS-PAGE revealed that in the presence channel inhibitors CPM formed thioether adducts selectively with the RyR protomer and triadin, whereas CPM labeling in the presence of channel activators form adducts with the abundant SERCA thiols. These results were intriguing because channel associated proteins account for <5% of the total protein of junctional SR preparations and attests to the hyperreactive nature of these thiol groups.

### Direct Measurement of pKa of Hyperreactive Thiols of RyR1 Complex

Underlying the hypothesis that hyperreactive thiols exist within the RyR1 complex and are an essential component of the redox sensor, it is reasonable to predict that a fraction of these thiols may exist in the deprotonated state at physiological pH. In this section we present new data that directly measure the pKa of hyperreactive thiols of the RyR1 complex.

### Experimental Procedures

#### Preparation of SR membranes.

Sarcoplasmic reticulum membrane vesicles enriched in biochemical markers of the terminal cisternae were prepared from back and hind limb skeletal muscles of New Zealand White rabbits according to the method of Saito (44). The preparations were stored in 10% sucrose, 5 mM imidazole, pH 7.4 at  $-80^\circ\text{C}$  until needed.

#### Kinetic fluorescence measurement of CPM-thioether adducts.

Junctional SR (50  $\mu\text{g}/\text{ml}$ ) was equilibrated in a solution containing 100 mM KCl and an appropriate buffer to obtain pH ranging from 6.5 to 8.5 at  $37^\circ\text{C}$ . CPM (7-diethylamino-3-(4'-maleimidylphenyl)-4-methylcoumarin; Molecular Probes, OR) was added at a final concentration of 10 nM to initiate the formation of fluorescent thioether adduct as previously described (36). The kinetics of forming CPM-thioether adducts were continuously measured fluorometrically (SLM 8000, SML Instruments Inc., Urbana, IL). Excitation and emission were set at 397 nm and 465 nm (width of slit = 4 nm), respectively. The buffers used were: 20 mM Mops for pH 6.5- 7.8; 20 mM Tris for pH 8.0 to 8.5; The kinetics of the reaction was measured at each experimental pH under two conditions; one aimed at activating (100  $\mu\text{M}$   $\text{Ca}^{2+}$  + 10 mM caffeine) RyR1; the other aimed at inhibiting channel activity (10 mM  $\text{Mg}^{2+}$ ). The rates of increasing fluorescence were sampled at 1 Hz and analyzed by nonlinear regression analysis with Origin<sup>®</sup> software. The measurements were replicated 4 times and the mean rate plotted as a function of pH. Rates measured in channel-activating buffer were subtracted from the corresponding rates measured in

channel-inhibiting buffer. The difference was analyzed by logit-log analysis to calculate the pKa of hyperreactive thiols in the junctional SR preparation.

### Results

Figure 4 shows the rate curves obtained from reacting 10 nM CPM with 50  $\mu\text{g}$  junctional SR under buffer conditions that either promoted the closed state of the channel (Fig.4A:  $\text{Mg}^{2+}=10$  mM  $\text{Ca}^{2+}= 40$  nM) or promoted channel opening (Fig. 4B:  $\text{Mg}^{2+} = 0$  mM  $\text{Ca}^{2+} = 100$   $\mu\text{M}$ ). Formation of CPM-thioether adducts in buffer promoting channel closure proceeded  $\geq 6$ -fold faster than in buffer promoting channel opening  $0.0645 \text{ sec}^{-1}$  vs.  $0.0103 \text{ sec}^{-1}$  at pH 7.4). The rate of the reaction was highly dependent on the pH, increasing with pH regardless of the constituents of the buffer. Kinetic analysis revealed that rates were significantly greater in buffer containing channel inhibitor compared to those measured in the presence of channel activators at all pH values examined (Fig. 4C). The *Open* curve titrated CPM with SR thiols that in general appeared to exhibit low reactivity toward arylation at physiological pH, but became more reactive at basic pH. The heightened reactivity observed with basic pH was likely the consequence of deprotonation of protein thiols. Interestingly under the *Closed* buffer condition, appreciable reaction rates were measured below pH 7 and the rate increased linearly above pH 8. The *Open* curve was subtracted from the *Closed* curve to yield a sigmoidal relationship which discriminated the protonation state of the most reactive thiols (hyperreactive thiols) within the junctional SR preparation (Fig. 4D). Logit-log analysis of the hyperreactive thiols revealed a pKa value of 7.39 (Fig. 4E). These results reveal that junctional SR contains a unique class of Cys residues, of which half exist in the deprotonated state at physiological intracellular pH (pH = 7.4). Moreover very small changes in cellular pH would be expected to have a pronounced influence of the fraction of hyperreactive Cys in the deprotonated state.

### Discussion

The pKa of hyperreactive Cys moieties was determined using a fluorometric assay that measures the rate of forming CPM-thioether adducts as a function of pH. Under conditions in the assay buffer that favor the open state of the RyR1 channel complex, the calculated pKa was  $>8$ . This was not surprising since protein thiols are generally protonated at physiological pH with the typical Cys thiol exhibiting a pKa of  $>8$  (39). A combination of highly reducing environment, low  $\text{pO}_2$ , and a pH that favors protonation that are normally found in cell cytosol under physiological conditions, assure low chemical reactivity toward protein thiols. An interesting observation was that the measured pKa of hyperreactive protein thiols associated with RyR1 complexes in buffer conditions promoting channel closure, possessed a pKa of 7.4. Therefore within the intracellular milieu of a typical muscle cell half of these Cys moieties will exist as a highly reactive deprotonated species (Figure 5).

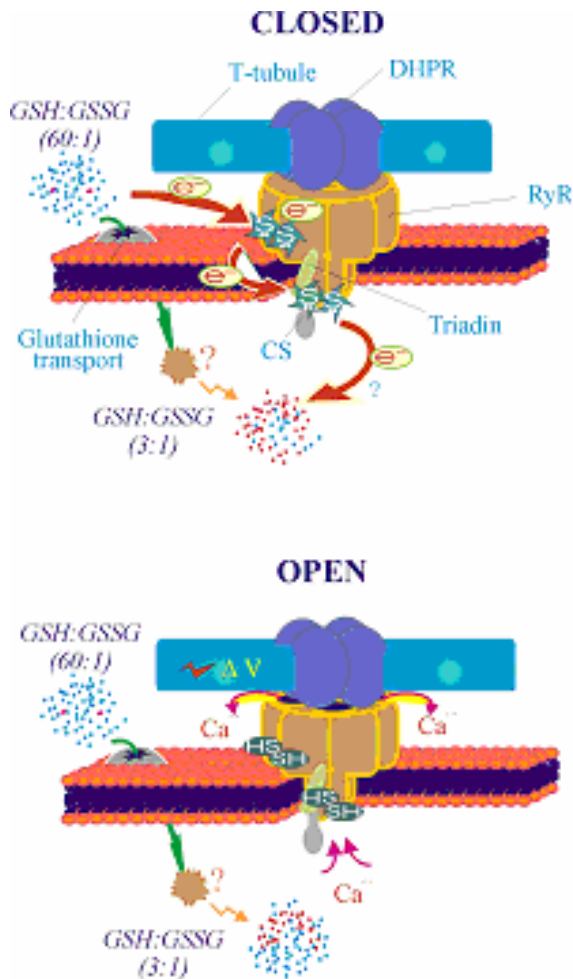


Figure 5. Possible mechanism by which the RyR1 complex senses changes to localized redox environment. In the closed channel conformation, Cys within a nucleophilic domain possesses deprotonated thio-anions that are hyperreactive and have mobile electrons ( $e^-$ ) that can delocalize. The local redox potential can donate electrons to this "redox sensing" domain. Conformational transitions that coincide with channel opening rearranges the redox sensing domain which loses its nucleophilicity and the critical Cys revert to typical reactivity of other protein thiols.

Taken together the findings indicated that RyR1 channel gating transitions between open and closed conformations were accompanied with changes in the microenvironment of hyperreactive Cys residues. One possible mechanism would invoke the formation of a highly nucleophilic domain that would promote the deprotonation of critical Cys and possible delocalization of their unpaired electrons. In such a scheme, the localized redox potential immediately adjacent to the redox sensing domain would have a dramatic influence on the electron distribution within the redox sensing domain which might in turn influence the stability of the closed state. This mechanism would predict that the closed conformation of the RyR1 complex is the redox sensing conformation, whereas the open conformation would reduce the nucleophilicity of the domain and the reactivity of critical Cys residues would revert to those more typically seen for protein thiols. Thus

rapid gating transitions would not coincide with oxidation and reduction of disulfide bonds, but rather the associated conformational transitions would create a reactive domain highly sensitive to local redox environment. Since one state of the channel, the closed state, appears to preferentially assemble the reactive domain with its integral hyperreactive Cys, local redox environment could influence the overall sensitivity of the channel (and SR  $Ca^{2+}$  release) to allosteric modulators of physiological and toxicological importance.

## Conclusions

Functional modification of enzymes, receptors, and ion channels with reagents that modify protein sulfhydryl groups has been extensively documented. Likewise the RyR complex can be subject to functional modification by sulfhydryl reagents in a complex manner depending on the nature of the chemical reaction taking place and the exact cysteines or disulfides modified. In this respect, both the length of time and conditions of exposing RyR to a given reagent will influence the functional outcome. However, RyR complexes appear to possess a class of highly reactive cysteine moieties whose pKa is near the physiological pH of the typical cytoplasm. The functional role of these hyperreactive cysteines does not mediate channel-gating transitions between open and closed states. Rather, hyperreactive Cys moieties are an essential component of an integral redox sensing mechanism within the RyR complex. The redox sensor does not appear to directly undergo oxidation-reduction cycles with channel gating transitions as previously suggested. It is also unlikely that the redox sensor contributes an obligatory mechanistic step in either e-c coupling (skeletal muscle) or CICR (other tissues). Rather the redox sensing properties of RyR complexes are likely to convey important information about localized changes in redox potential that are likely to occur across the SR/ER membrane in physiological and pathophysiological states. One possible molecular mechanism underlying redox sensing may involve delocalization of mobile electrons within the RyR complex and the local cellular redox buffer (scheme in Fig 5).

## References

1. Abramson J. J., J. L. Trimm, L. Weden, & G. Salama: Heavy metals induce rapid calcium release from sarcoplasmic reticulum vesicles isolated from skeletal muscle. *Proc Nat Acad Sci USA* 80, 1526-1530 (1983)
2. Trimm J. L., G. Salama, & J. J. Abramson: Sulfhydryl oxidation induces rapid calcium release from sarcoplasmic reticulum vesicles. *J Biol Chem* 261,16092-16098. (1986)
3. Pessah I. N., & W. Feng: Functional role of hyperreactive sulfhydryl moieties within the ryanodine receptor complex. *Antioxidants & Redox Signaling* 2, 17-25 (2000)
4. Pessah, I. N: Ryanodine receptor acts as a sensor for redox stress. *Pest Manag Sci* 57, 941-945. (2001)
5. Abramson J. J., & G. Salama: Critical sulfhydryls regulate calcium release from sarcoplasmic reticulum. *J Bioenerg Biomembr* 21, 283-294 (1989)
6. Abramson J. J., E. Buck,, G. Salama, , J. E. Casida, & I. N. Pessah: Mechanism of anthraquinone-induced calcium release from skeletal muscle sarcoplasmic reticulum. *J Biol Chem* 263, 18750-58 (1988)

7. Pessah I. N, E. Durie, M. J. Schiedt, & I. Zimanyi: Anthraquinone-sensitized Ca<sup>2+</sup> release channel from rat cardiac sarcoplasmic reticulum: possible receptor-mediated mechanism of doxorubicin cardiomyopathy. *Molec. Pharmacol.* **37**, 503-514 (1990)
8. Pessah I. N, R. A. Stambuk, & J. E. Casida: Ca<sup>2+</sup>-activated ryanodine binding: Mechanism of sensitivity and intensity modulation by Mg<sup>2+</sup>, caffeine, and adenine nucleotides. *Molec Pharmacol* **31**, 232-238 (1987)
9. Zaidi N. F, C. F. Langenaur, J. J. Abramson, I. N. Pessah, & G. Salama: Reactive disulfides trigger calcium release from sarcoplasmic reticulum via an oxidation reaction. *J Biol Chem* **264**, 21725-36 (1989)
10. Chen L, T. F. Molinski, & I. N. Pessah: Bastadin 10 stabilizes the open conformation of ryanodine-sensitive Ca<sup>2+</sup> release channel in an FKBP12-dependent manner. *J Biol Chem* **274**, 32603-12 (1999)
11. Feng W, G. Liu, R. Xia, J. J. Abramson & I. N. Pessah: Site-selective modification of hyperreactive cysteines of ryanodine receptor complex by quinones. *Molec Pharmacol* **55**, 821-831 (1999)
12. Pessah I. N, C. Beltzner, S. Burchiel, G. Sridhar, T. Penning, & W. Feng: A bioactive metabolite of benzo[a]pyrene, benzo[a]pyrene-7,8-dione, selectively alters microsomal Ca<sup>2+</sup> transport and ryanodine receptor function. *Molec Pharmacol* **59**, 506-513 (2001)
13. Aghdasi B, J. Z. Zhang, Y. Wu, M. B. Reid, & S. L. Hamilton: Multiple classes of sulfhydryls modulate the skeletal muscle Ca<sup>2+</sup> release channel. *J Biol Chem* **272**, 3739-3748 (1997a)
14. Cherednichenko G, W. Feng, & S. Schaefer, I. N. & Pessah: Endogenous 23kDa NADH oxidase activity maintains ryanodine receptor type 2 in reduced state. (submitted)
15. Meissner G, F. A. Lai, K. Anderson, L. Xu, Q. Y. Liu, Herrmann- A. Frank, E. Rousseau, R. V. Jones, & H. B. Lee: Purification and reconstitution of the ryanodine- and caffeine-sensitive Ca<sup>2+</sup> release channel complex from muscle sarcoplasmic reticulum. *Adv Exp Med Biol*, **304**, 241-256 (1991)
16. Zhang J, Z. Y. Wu, B. Y. Williams, G. Rodney, F. Mandel, G. M. Strasburg, & S. L. Hamilton: Oxidation of the skeletal muscle Ca<sup>2+</sup> release channel alters calmodulin binding. *Amer J Physiol* **276**, C46-53 (1999)
17. Rodney G. G, C. P. Moore, B. Y. Williams, J. G. Zhang, J. Krol, S. E. Pedersen, & S. L. Hamilton: Calcium binding to calmodulin leads to an N-terminal shift in its binding site on the ryanodine Receptor. *J Biol Chem* **276**, 2069-2074 (2001)
18. Sun J. H, C. L. Xin, J. P. Eu, J. S. Stamler, & G. Meissner: Cysteine-3635 is responsible for skeletal muscle ryanodine receptor modulation by NO. *Proc Natl Acad Sci USA* **98**, 11158-11162 (2001)
19. Hwang C, A. J. Sinskey, & H. F. Lodish: Oxidized redox state of glutathione in the endoplasmic reticulum. *Science* **257**, 1496-1502 (1992)
20. Sen, C. K: Redox signaling and the emerging therapeutic potential of thiol antioxidants. *Biochem. Pharmacol.* **55**, 1747-1758. (1998)
21. Sies, H: Glutathione and its role in cellular functions. *Free. Radic. Biol. Med.* **27**, 916-921 (1999)
22. Ba'nhgyi G, L. Lusini, F. Puska's, R. Rossi, R. Fulceri, L. Braun, V. Mile, P. di Simplicio, J. Mandl, & A. Benedetti: Preferential transport of glutathione versus glutathione disulfide in rat liver microsomal vesicles. *J Biol Chem* **274**, 12213-12216 (1999)
23. Ba'nhgyi G, P. Marcolongo, F. Puska's, R. Fulceri, J. Mandl, & A. Benedetti: Dehydroascorbate and ascorbate transport in rat liver microsomal vesicles. *J Biol Chem* **273**, 2758-2762 (1998).
24. Feng W, G. Liu, P. D. Allen, & I. N. Pessah: Transmembrane Redox Sensor of ryanodine receptor. *J Biol Chem* **275**, 35902-35907 (2000)
25. Csala M, R. Fulceri, J. Mandl, A. Benedetti, G. Banhegyi: Ryanodine receptor channel-dependent glutathione transport in the sarcoplasmic reticulum of skeletal muscle. *Biochem Biophys Res Com* **287**, 696-700 (2001)
26. Senft A. P, T. P. Dalton, & H. G. Shertzer: Determining glutathione and glutathione disulfide using the fluorescence probe o-phthalaldehyde. *Anal Biochem* **280**, 80-86 (2000)
27. Ba'nhgyi G, P. Marcolongo, R. Fulceri, C. Hinds, A. Burchell, & A. Benedetti: Demonstration of a metabolically active glucose-6-phosphate pool in the lumen of liver microsomal vesicles. *J Biol Chem* **272**, 13584-13590 (1997)
28. Wells W. W, D. P. Xu, Y. F. Yang, & P. A. Rocque: Mammalian thioltransferase (glutaredoxin) and protein disulfide isomerase have dehydroascorbate reductase activity. *J Biol Chem* **265**, 15361-15364 (1990)
29. Koshita M, K. Miwa, and T. Oba: Sulfhydryl oxidation induces calcium release from fragmented sarcoplasmic reticulum even in the presence of glutathione. *Experientia* **49**, 282-284 (1993)
30. Zable A.C, T. G. Favero, & J. J. Abramson: Glutathione modulates ryanodine receptor from skeletal muscle sarcoplasmic reticulum. Evidence for redox regulation of the Ca<sup>2+</sup> release mechanism. *J Biol Chem* **272**, 7069-7077 (1997)
31. Marengo J.J, C. Hidalgo, & R. Bull: Sulfhydryl oxidation modifies the calcium dependence of ryanodine-sensitive calcium channels of excitable cells. *Biophys J* **74**, 1263-1277 (1998)
32. Zahradníková A, I. Minarovic, R. C. Venema, L. G. & Mészáros: Inactivation of the cardiac ryanodine receptor calcium release channel by nitric oxide. *Cell Calcium* **22**, 447-454 (1997)
33. Aghdasi B, M. B. Reid, & S. L. Hamilton: Nitric oxide protects the skeletal muscle Ca<sup>2+</sup> release channel from oxidation induced activation. *J Biol Chem* **272**, 25462-25467 (1997)
34. Xu L, J. P. Eu, G. Meissner, J. S. Stamler: Activation of the cardiac calcium release channel (ryanodine receptor) by poly-S-nitrosylation. *Science* **279**, 234-237 (1998)
35. Feng W, & I. N. Pessah: Detection of redox sensor of ryanodine receptor complexes. *Meth Enz* (in press)
36. Liu G, J. J. Abramson, A. C. Zable, & I. N. Pessah: Direct evidence for existence and functional role of hyperreactive sulfhydryls on ryanodine receptor-triadin complex selectively labeled by the coumarin maleimide 7-dimethylamino-3-(4'-maleimidylphenyl)-4-methylcoumarin. *Molec Pharmacol* **45**, 189-200 (1994)
37. Liu G, & I. N. Pessah: Molecular interaction between ryanodine receptor and glycoprotein triadin involves redox cycling of functionally important hyperreactive sulfhydryls. *J Biol Chem* **269**, 33028-33034 (1994)
38. Xia R, T. Stangler, J. J. Abramson: Skeletal muscle ryanodine receptor is a redox sensor with a well defined redox potential that is sensitive to channel modulators. *J Biol Chem* **275**, 36556-36561 (2001)
39. Jocelyn, P.C: Biochemistry of the SH Group. *Academic Press, New York, NY*, 404pp. (1972)
40. Schöneich, C: Kinetics of thiol reactions. *Meth Enzy* **251**, 45-55 (1995)
41. Habenicht, A: The non-phosphorylating glyceraldehyde-3-phosphate dehydrogenase: biochemistry, structure, occurrence and evolution. *Biol Chem* **378**, 1413-1419 (1997)
42. Massière F, & M. A. Badet-Denisot: The mechanism of glutamine-dependent amidotransferases. *Cell Molec Life Sci* **54**, 205-222. (1998)
43. Washburn M. P, & W. W. Wells: The catalytic mechanism of the glutathione-dependent dehydroascorbate reductase activity of thioltransferase (glutaredoxin). *Biochem* **38**, 268-274 (1999)
44. Saito A, S. Seiler, A. Chu, & S. Fleischer: Preparation and morphology of sarcoplasmic reticulum terminal cisternae from rabbit skeletal muscle. *J Cell Biol* **99**, 875-885 (1984)

**Correspondence:**

Isaac N. Pessah  
Department of Molecular Biosciences  
School of Veterinary Medicine  
One Shields Avenue  
Davis CA.  
Voice: (530) 752-6696  
FAX: (530) 752-4698  
email: [inpessah@ucdavis.edu](mailto:inpessah@ucdavis.edu)

**Abbreviations:** BLM, bilayer lipid membrane; CPM, 7-diethylamino-3-(4'-maleimidylphenyl)-4-methylcoumarin; DTDP, 2,2'-dithiodipyridine; DTNB, 5,5'-dithiobis(2-nitro)benzoate; RyR, ryanodine receptor; SR, sarcoplasmic reticulum.

**Key words:** Ryanodine receptor complex; Redox sensing; Hyperreactive sulfhydryls.

**Running title:** RyR redox sensing properties

# Structural Interaction Between RYRs and DHPRs in Calcium Release Units of Cardiac and Skeletal Muscle Cells

Feliciano Protasi

Department of Anesthesia Research, Brigham and Women's Hospital, Harvard Medical School, Boston MA 02115 E-mail: [protasi@zeus.bwh.harvard.edu](mailto:protasi@zeus.bwh.harvard.edu)

**ABSTRACT** Excitation-contraction (e-c) coupling in muscle cells is a mechanism that allows transduction of exterior-membrane depolarization in  $\text{Ca}^{2+}$  release from the Sarcoplasmic Reticulum (SR). The communication between external and internal membranes is possible thanks to the interaction between Dihydropyridine Receptors (DHPRs), voltage-gated  $\text{Ca}^{2+}$  channels located in exterior membranes, and Ryanodine Receptors (RyRs), the  $\text{Ca}^{2+}$  release channels of the SR. In both skeletal and cardiac muscle cells the key structural element that allows DHPRs and RyRs to interact with each other is their vicinity. However, the signal that the two molecules use to communicate is not the same in the two muscle types. In the heart, the inward flux of  $\text{Ca}^{2+}$  through DHPRs, that follows depolarization, triggers the opening of RyRs (calcium induced calcium release). In skeletal muscle, on the other hand,  $\text{Ca}^{2+}$  is not needed for RyRs activation; instead the coupling between the two molecules involves a direct link between them (mechanical coupling). Ultrastructural studies show that functional differences can be explained by differences in the DHPR/RyR reciprocal association: whereas the two proteins are very close to each other in both muscles, DHPRs form tetrads only in skeletal fibers. Tetrads represent the structural DHPR/RyR link that allows  $\text{Ca}^{2+}$  independent coupling in skeletal muscle.

## INTRODUCTION

Muscle fibers are able to finely control cytoplasmic  $[\text{Ca}^{2+}]$  thanks to an extremely well organized system of tubules and vesicles that are collectively named Sarcoplasmic Reticulum (SR). The SR is a highly specialized version of the endoplasmic reticulum that closely surrounds myofibrils and that sequesters and releases  $\text{Ca}^{2+}$  in and out of the cytoplasm very efficiently (1). The signal that activates muscle contraction is the sudden increase in intracellular  $[\text{Ca}^{2+}]$  that follows the depolarization of exterior membranes (sarcolemma/T-tubules). This mechanism is named excitation-contraction (e-c) coupling and takes place at calcium release units (CRUs) or junctions, structures in which the SR and exterior membranes are closely associated with one another (2). CRUs are found in both cardiac and skeletal cells and, while they are structurally quite similar in the two muscle types, they use two different mechanisms to accomplish the same goal: the translation of an electrical signal carried by exterior membranes into  $\text{Ca}^{2+}$  release from the SR. In the heart, e-c coupling depends on the inward flux of  $\text{Ca}^{2+}$  through DHPRs, which triggers  $\text{Ca}^{2+}$  release from the SR stores. This mechanism is better known as calcium induced calcium release or CICR (3). Conversely, skeletal fibers do not need extracellular  $\text{Ca}^{2+}$  and the signal transduction relies on a mechanical interaction between the two membranes (4-5).

The differences between skeletal and cardiac e-c coupling have inspired a series of morphological studies on CRUs to test whether or not there are structural diversities that may explain how and why junctions use different mechanisms in the two muscle types.

## CALCIUM RELEASE UNITS MORPHOLOGY: DHPR/RYR VICINITY REPRESENTS THE STRUCTURAL BASE OF E-C COUPLING

### Different types of junctions: which and where?

Junctions between the SR and the sarcolemma/T-tubules are formed by specialized domains of the SR terminal cisternae (junctional SR) closely associated to junctional domains of exterior membranes. Junctions have different names (triads, dyads, and peripheral couplings) depending on the number of elements and the nature of the membranes that constitute them. Triads are formed by three elements, two SR terminal cisternae and one T-tubule (**figure 1 A**), while dyads and peripheral couplings are formed by only two elements, one junctional SR and respectively a T-tubule or the surface membrane itself (**figure 1, B and C**) (2). Whereas the different kinds of CRUs carry out the same function, it is possible to make a distinction on where and when they can be found. Triads are practically the only kind of junction present in adult skeletal muscle fibers, whereas dyads and peripheral couplings are the predominant type of CRUs in developing muscle and in the heart (6-7). Striated muscles of invertebrates have all three types of junctions, but not necessarily in the same fibers. A different type of CRU has been also described in literature: the extended junctional SR or Corbular SR, found in the interior of cardiac cells, and free of any association with external membranes (8). Corbular SR contains RyRs but not DHPRs and, therefore, will not be further discussed in this review.

### RyRs and DHPRs: the two major players of e-c coupling

One of the first structures described as an integral component of triads are the feet, large

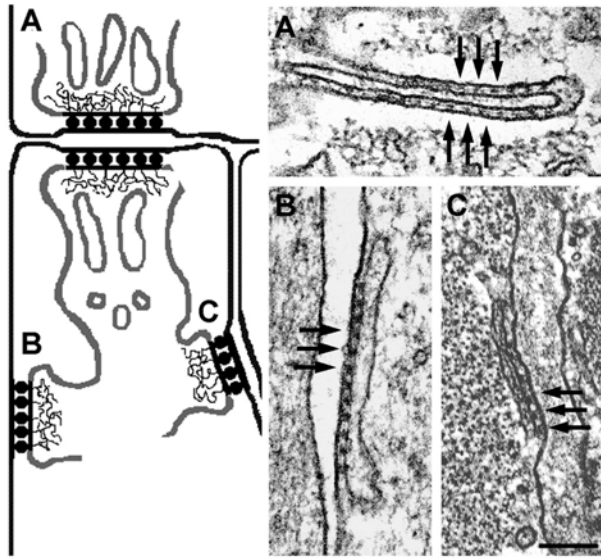


**Figure 1. Different types of Calcium Release Units in muscle cells.** CRUs, or junctions, are formed by the close apposition of SR terminal cisternae and exterior membranes. They are called triads, dyads, and peripheral couplings depending on the number and nature of the elements that constitutes them. A) Triads are formed by one T-tubule flanked by two SR cisternae (from adult toadfish swimbladder muscle). B and C) Peripheral couplings and dyads are formed by only two elements: one SR vesicle and respectively the surface membrane or a T-tubule (B, peripheral coupling in a BC3H1 cell; C, dyad in canine heart). The evenly spaced densities pointed by arrows in the junctional gap between the two membranes have been named feet by Clara Franzini-Armstrong and have been identified with the cytoplasmic domain of RyRs, the  $\text{Ca}^{2+}$  release channel of the SR. Bar, 0.1  $\mu\text{m}$  (EM courtesy of Clara Franzini-Armstrong).

electron-dense structures that bridge the narrow gap (about 12nm) separating the SR from the T-tubule/sarcolemma (**figure 1**, arrows) (9). Feet were later identified as the cytoplasmic domains of RyRs and RyRs in turn were identified as the  $\text{Ca}^{2+}$  release channels of the SR (10). The hydrophobic domain of RyRs (channel region) is inserted in the SR membrane, leaving the large hydrophilic portion (foot region) in the cytoplasm. In electron micrographs (EM) feet appear as evenly spaced densities in both skeletal and cardiac fibers (**figures 1 to 3**). Formation of ordered arrays seems to be an intrinsic property of RyRs since arrays are also formed when the protein is expressed in non-muscle cells and under in vitro conditions (11). Another extremely important component of CRUs is the dihydropyridine receptors (DHPRs), an L-type  $\text{Ca}^{2+}$  channel that plays a central role in triggering SR  $\text{Ca}^{2+}$  release (12). DHPRs are specifically localized in areas of exterior membranes that face junctional arrays of feet in both skeletal and cardiac muscle fibers (13, 14). DHPRs are not as visible as RyRs in thin sections because they have smaller hydrophilic domains. However DHPRs can be visualized in freeze-fracture replicas, a technique that allows separation of the two membrane leaflets, exposing intra-membrane domains of proteins. DHPRs appear as large particles

clustered in correspondence of CRUs when visualized by freeze-fracture (**figures 2 to 5**).

Despite the fact that many other proteins are involved structurally and functionally in e-c coupling (i.e. calsequestrin, triadin, junctin, FKBP12, mitsugumin, junctophilin, etc.), RyRs and DHPRs are still recognized as the two key elements of the mechanism. In both cardiac and skeletal cells the key feature that allows the two proteins to interact with each efficiently is their relative vicinity. DHPRs are always located in areas of exterior membranes that face RyR arrays of the SR, ideally placed to finely and promptly control the activation of  $\text{Ca}^{2+}$  release and start muscle contraction (**figure 2, 3, and 5**).

## DIFFERENCES IN DHPR/RYR STRUCTURAL ASSEMBLY BETWEEN SKELETAL AND CARDIAC FIBERS

### Different isoforms of DHPR and RyR are expressed in the two muscle types

We have seen in the previous section how RyRs and DHPRs are localized in the CRUs in both skeletal and cardiac muscle. However, a distinction needs to be made: the two muscle types express different isoforms of the two proteins (**figures 2, 3, and 5**). In skeletal muscle fibers two different RyR isoforms have been found: type 1 and type 3, or their non-mammalian muscle equivalent  $\alpha$  and  $\beta$ . Skeletal muscle contains either RyR1 only, approximately equal amounts of RyR1 and RyR3, or predominantly RyR1 co-expressed with low levels of RyR3 (15). On the other hand, in the heart practically the only isoform expressed is RyR type 2 (16). The COOH-terminal region is the most highly conserved and it is predicted to form the intramembrane  $\text{Ca}^{2+}$  release channel, while the amino-terminal region constitutes the large cytoplasmic domain known as the foot. Three-dimensional reconstruction of RyRs has shown minor but probably significant differences among the three isoforms (17-19); see section 6 for more details. DHPRs also have different isoforms in cardiac and skeletal fibers, however, the situation for this protein is far more complicated than for RyRs because DHPRs consist of five different subunits ( $\alpha_1$ ,  $\alpha_2$ ,  $\beta$ ,  $\gamma$ , and  $\delta$ ). The  $\alpha_1$  subunit forms the channel and structurally is very similar to the  $\text{Na}^+$  channel (20): it is constituted by four domains (I-IV) and contains the segment that has been identified as the voltage sensor of the molecule (21).  $\alpha_{1S}$ - and  $\alpha_{1C}$ -DHPR, the two isoforms expressed in skeletal muscle and heart respectively, share ~66% homology, mostly confined to the transmembrane regions, while higher divergence is found in the cytoplasmic domains and the loops that are thought to interact with RyRs. The other four subunits are regulatory components of the channel and will not be discussed in detail in this review.

### DHPR and RyR interact differently in skeletal and cardiac muscle

RyRs are closely associated with each other forming ordered arrays in both skeletal and cardiac muscles. In fact the feet appear as evenly spaced

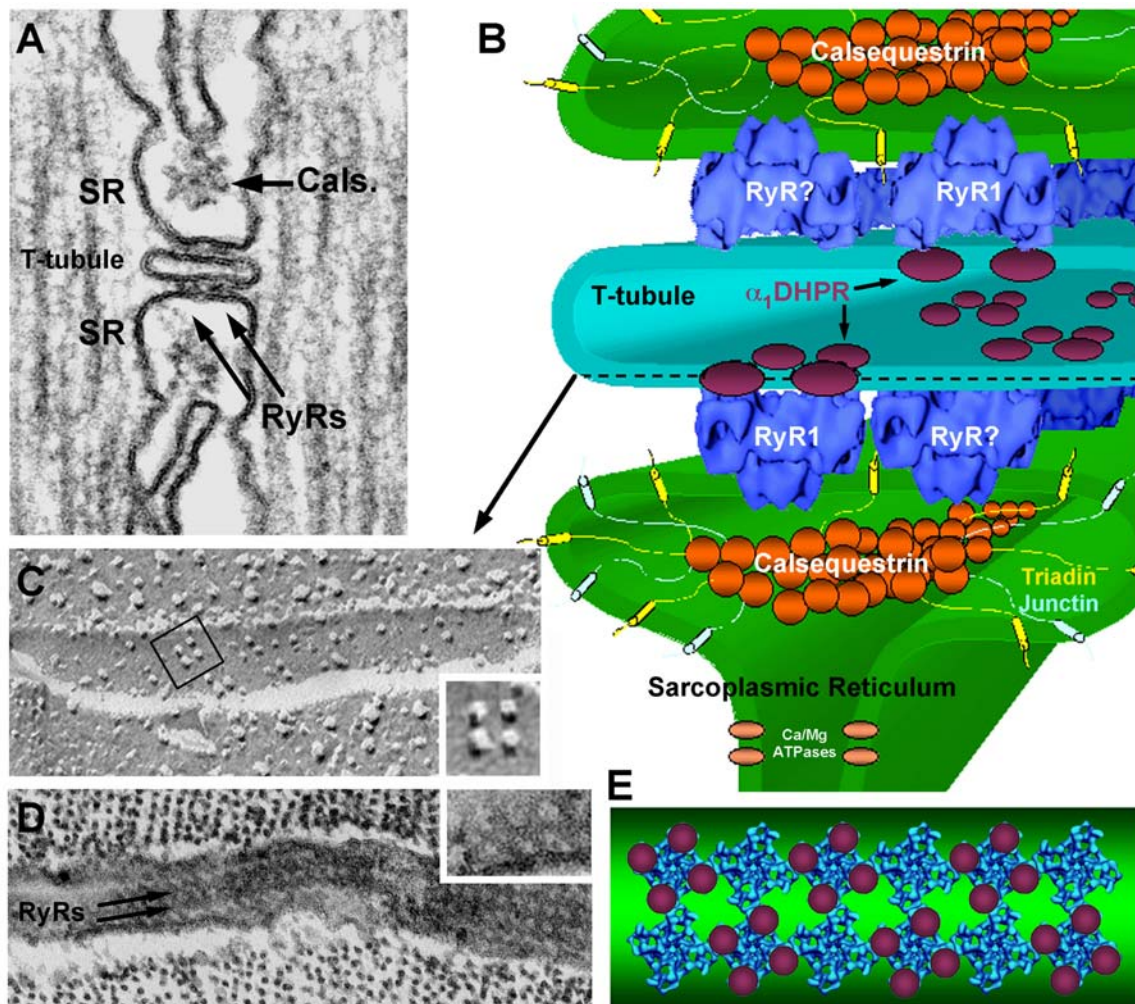


Figure 2. Structure of Calcium Release Units in adult skeletal muscle fibers. In adult skeletal muscle, junctions are mostly triads: two SR elements coupled to a central T-tubule. A) A triad from the toadfish swimbladder muscle in thin section EM: the cytoplasmic domains of RyRs, or feet, and calsequestrin are well visible. B) A tri-dimensional reconstruction of a skeletal muscle triad showing the ultrastructural localization of RyRs, DHPRs, Calsequestrin, Triadin, Junctin, and  $\text{Ca}^{2+}/\text{Mg}^{2+}$  ATPases. Note the localization of DHPRs in the T-tubule membrane: DHPRs are intramembrane proteins that are not visible in thin section EM but can be visualized by freeze fracture replicas of T tubules (see panel C). C) DHPRs in skeletal muscle DHPRs form tetrads, group of four receptors (see enlarged detail), that are linked to subunit of alternate RyRs (see models in B and E). D) In sections parallel to the junctional plane, feet arrays are clearly visible (toadfish swimbladder muscle): feet touch each other close to the corner of the molecule (see enlarged detail). E) Model that summarizes finding of panels C and D: RyRs form two (rarely three) rows and DHPRs form tetrads that are associated with alternate RyRs (RyRs in blue; DHPRs in purple; T-tubule in green). (EM courtesy of Clara Franzini-Armstrong; 3D reconstruction of RyRs courtesy of T. Wagenknecht).

densities in junctions seen in thin section electron microscopy (EM) (**figure 1 to 3**). While these images suggest that skeletal and cardiac arrays are identical, this interpretation is not conclusive since views of junctions such as the ones in **figure 1** and **figure 3 B** do not identify all the parameters that define an RyR array. Images parallel to the plane of the junction (such as the one in **figure 2 D**) have allowed definition of the subtle differences between RyR arrays in skeletal muscle and in body muscles of some invertebrates (22). Unfortunately no such images are available at this point for cardiac junctions.

While arrays of RyR1 and RyR2 are similar and possibly identical, major divergences exist between DHPRs arrangements. In skeletal muscle DHPRs are grouped into tetrads, groups of four

receptors located at the corner of small squares (detail in **figure 2 C**). Tetrads are superimposed on the feet so that each DHPR is located immediately above one of the RyR subunits and in a specific position relative to it. This spatial tetrad/RyR arrangement generates tetrad arrays that are related to the feet arrays (**figures 2, 4, and 5**). Tetrads are specifically and only formed by association of  $\alpha_1\text{sDHPRs}$  and RyR type 1 (see section 5 for more details). Surprisingly, tetrads are not associated with every foot but only with alternate ones (23, 24). This disposition was found in several different types of fibers regardless of the muscle containing only one (RyR1) or two (RyR1 and RyR3) isoforms, so that uncoupled feet could be either RyR1 or RyR3 (see

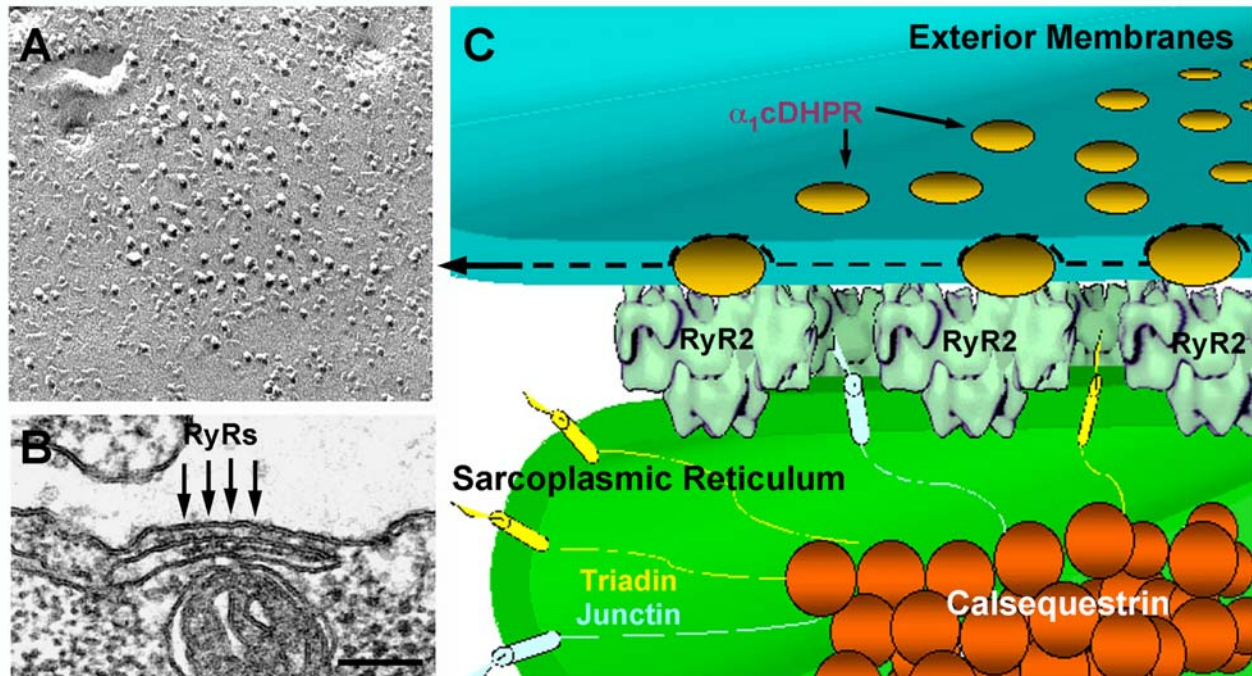


Figure 3. Structure of calcium release units in cardiac myocytes. Junctions in cardiac muscle cells are usually in the form of dyads or peripheral coupling formed by SR and either a T-tubule or the sarcolemma. A) DHPRs in cardiac junctions do not form tetrads, but they are randomly arranged in exterior membrane domains that face arrays of feet. This observation implicates that DHPRs are not directly linked to RyRs in the heart. B) RyRs, pointed by the arrow, usually form large clusters instead of the two rows described for skeletal muscle junctions. C) Tri-dimensional reconstruction of a cardiac muscle dyad/peripheral coupling showing the ultrastructural localization of RyRs, DHPRs, Calsequestrin, Triadin, and Junctin. Bar, 0.1  $\mu\text{m}$  (3D reconstruction of RyRs courtesy of T. Wagenknecht).

**figures 2 B and 5 C).** The possible reason for this alternate tetrad/RyR1 association will be further discussed in section 6. In cardiac muscle, immunohistochemistry experiments and morphological studies have shown that DHPRs are also clustered in close correspondence with RyR domains (7, 14). Indeed, studies in chicken developing peripheral couplings have shown that there is a very close relationship between the size of arrays of feet in the SR and the area covered by DHPR in the junctional portion of the sarcolemma (25). While DHPRs are clearly clustered closely to RyRs, freeze-fracture studies have shown no evidence of organization of DHPRs into tetrads (7-25). DHPRs are randomly clustered in junctional domains of exterior membranes and no spatial relationship with feet was detected (**figures 3, A and C and figure 5 D**). The lack of tetrads indicates a lack of a direct specific association between  $\alpha_1\text{cDHPR}$  and RyR2 and correlates well with the lack of direct functional interaction between the two (see section 6 for further discussion).

#### **DYSGENIC AND DYSPEDIC MICE CONTRIBUTION TO THE UNDERSTANDING OF DHPR/RyR INTERACTION**

Molecular biology and gene handling techniques in the last years have revolutionized research approaches in many fields and, among them, also in the study of e-c coupling. Knockouts have become very valuable tools to study protein function

and protein/protein interactions. Dysgenic and dyspedic mice, two animal models carrying null mutations for  $\alpha_1\text{sDHPR}$  and RyR1, have been crucial to the study of structural and functional roles of those two proteins in e-c coupling. Muscular dysgenesis is a spontaneous single nucleotide deletion in the gene encoding for the  $\alpha_1\text{s}$  subunit of the DHPR that causes a shift of the translational reading frame (26), while dyspedic mice were created by targeted disruption of the gene encoding for RyR type 1 (27). Initial functional studies have confirmed the central role of the two proteins in e-c coupling. Depolarization of the sarcolemma fails to elicit  $\text{Ca}^{2+}$  release from internal stores in both mutants (27, 28) while in both e-c coupling can be restored by transfection with cDNA encoding the missing element (12, 29). From the structural point of view, the two models have allowed a direct demonstration that tetrads and feet are indeed respectively DHPRs and RyRs. In fact the two structures are missing respectively in dysgenic and dyspedic mice and reappear after transfection with cDNA encoding the missing protein (30-32).

Surprisingly, absence of either  $\alpha_1\text{sDHPR}$  or RyR1 does not affect either formation of junctions or targeting of the second protein to junctional domains. In dysgenic muscle, triads containing organized arrays of feet are formed even if DHPRs are missing (33), and in dyspedic mice both triads and peripheral couplings are formed in the absence of RyRs (34). In regards to the targeting of DHPRs to junctions lacking RyRs, there have been some controversial results.

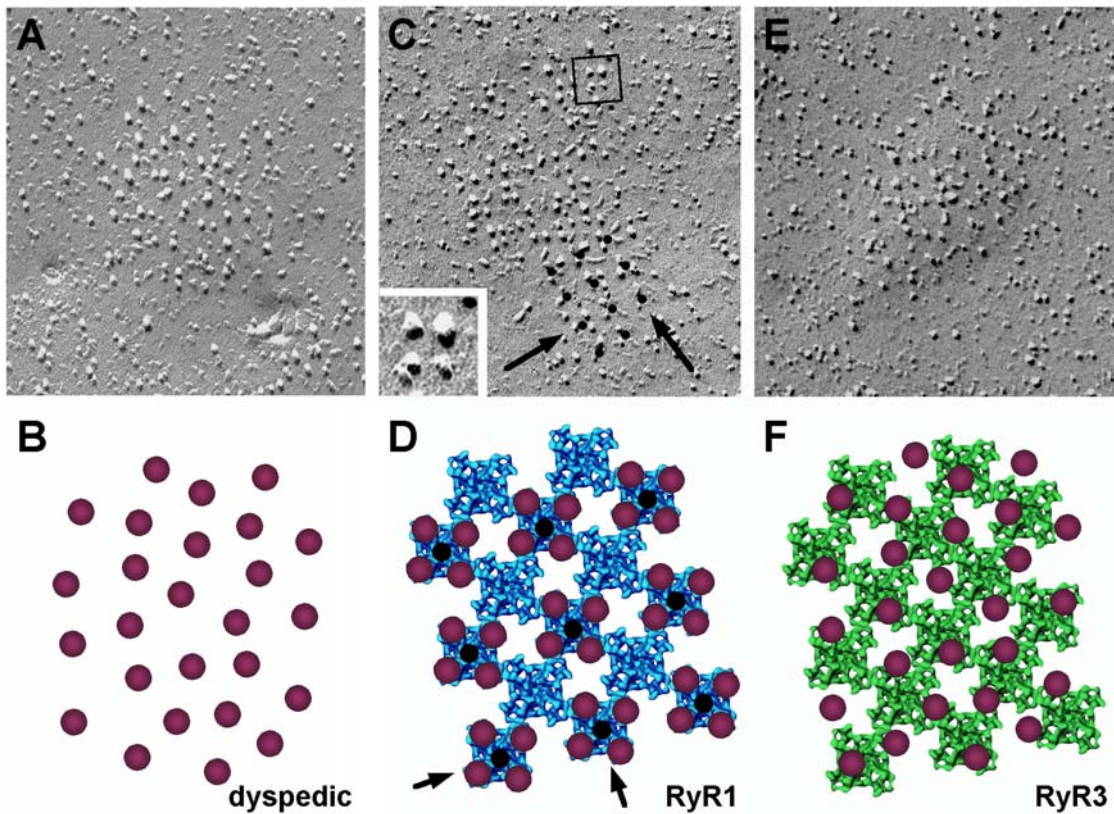


Figure 4. Interaction of RyR1 and RyR3 with skeletal DHPRs. A and B) In dyspedic 1B5 cells (RyR1  $-/-$ ), DHPRs are clustered in correspondence of CRUs, but they are not grouped in tetrads as in normal skeletal muscle cells because of lack of RyR type 1 in the SR junctional domains. C and D) DHPR tetrad arrangement is restored by transfection with cDNA encoding for RyR1. Dotting the center of tetrads in the array (C, bottom) results in an ordered pattern that is related to the arrays of feet in the SR. E and F) RyR3 expression does not restore DHPR tetrad arrays suggesting that RyR3 in skeletal muscle cells does not interact directly with DHPRs as RyR1 does. Bar, 0.1  $\mu\text{m}$  (3D reconstruction of RyRs courtesy of T. Wagenknecht).

Initially *in vivo* studies seemed to indicate that DHPRs did not cluster in the absence of RyRs (34), whereas more recently DHPRs were found clustered in correspondence to junctions lacking feet in a cell line of muscle origin carrying a null mutation for RyR1 (31). The reason for this discrepancy is still not clear, but it could be due to reduced amounts of  $\alpha_1\text{sDHPR}$  expressed in the *in vivo* model versus the higher level expressed in 1B5 myotubes.

DHPRs and RyRs are not involved in formation of junctions and in targeting of each other to the junctions. However, while RyRs do not need DHPRs to organize themselves into arrays, DHPRs depend on RyRs for their organizations into tetrads in skeletal muscle CRUs. In fact, skeletal DHPRs clustered at the junctions of dyspedic 1B5 myotubes are not organized into tetrads and resemble DHPR clusters in cardiac myocytes (figure 4, A and B). The key role of RyR1 in arranging DHPRs in groups of four was directly proven by the restoration of tetrads induced with cDNA encoding for RyR type 1 and interestingly, the alternate RyR/DHPR association was also restored in these cells (figure 4, C and D) (32). 1B5 myotubes were also used to test functional and structural roles of RyR type 3, the second RyR isoform expressed in skeletal muscle cells. While RyR1 could

restore both  $\text{K}^+$ -induced depolarization and DHPR tetrads, RyR3 failed to do so (figure 4, E and F) (32, 35). These results will be further discussed in section 6.

#### PERSPECTIVES: HOW THE STRUCTURE MAY EXPLAIN THE FUNCTION

The structural studies described in the previous sections have shown that, while RyRs and DHPRs are located in close proximity of each other in both cardiac and skeletal muscles, supra-molecular complexes are not assembled in the same way. RyRs are organized in arrays in both muscle types, while DHPRs form tetrad arrays only in skeletal fibers. This finding is extremely important because of its functional implications (figure 5). In cardiac myocytes the signal that triggers the opening of RyRs is the inward flux of  $\text{Ca}^{2+}$  through DHPRs that follows depolarization (CICR) (3), while in skeletal muscle,  $\text{Ca}^{2+}$  is not needed for RyR activation as the coupling between the two molecules seems to involve a direct protein-protein interaction (mechanical coupling) (4-5). The functional characteristics of the DHPR and RyR isoforms expressed in the two muscle types are in line with the mechanism they are part of:  $\alpha_1\text{sDHPR}$  has a higher open probability than  $\alpha_1\text{sDHPR}$ , and RyR2 is

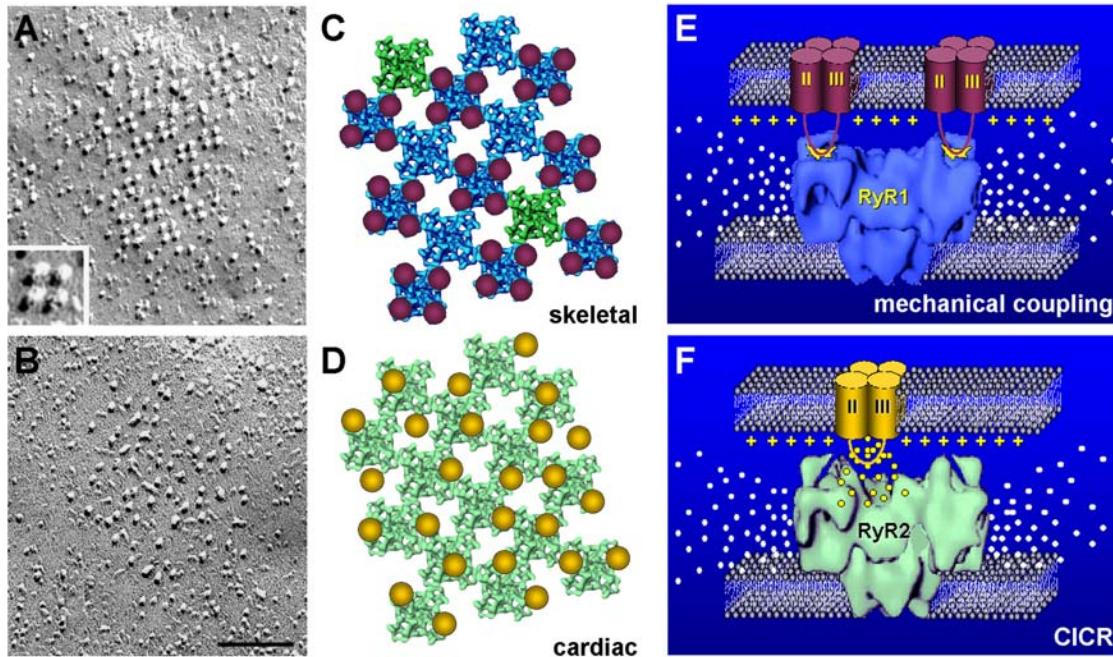


Figure 5. Structure/function correlation: lack of tetrads in cardiac cells explains the need of Ca<sup>2+</sup> in DHPR/RyR communication. A and B) DHPRs clustered respectively in peripheral coupling of BC3H1 cells (A) and in chicken ventricle (B). DHPRs form tetrads in the first, while in the second are randomly disposed in the junctional domain. C and D) both RyR1 (blue, C) and RyR2 (pale green, D) form ordered arrays. However, the specific link that allows associations of tetrads to alternate RyR1s in skeletal muscle cells is missing in the heart. The role and intracellular localization of RyR3 in skeletal muscle fibers is still not completely clear: RyR3 (green, C) may occupy some of the uncoupled positions of the RyR arrays. E and F) Cartoons illustrating the two different mechanisms that allow DHPR and RyR to communicate in e-c coupling: mechanical coupling in skeletal fibers and CICR in cardiac myocytes. Need of external Ca<sup>2+</sup> in heart (Φ) is the result of lack of a direct link between the two molecules, link that probably involves the II-III loop of the DHPR in skeletal fibers (E). Bar, 0.1 μm (3D reconstruction of RyRs courtesy of T. Wagenknecht).

indeed more sensitive to Ca<sup>2+</sup> than RyR1. Skeletal muscle has evolved a novel mechanism of e-c coupling that does not rely on Ca<sup>2+</sup> influx and the proteins involved in the process have evolved accordingly. The link that allows α<sub>1</sub>sDHPRs and RyR1 to form tetrads represents the structural basis for mechanical and Ca<sup>2+</sup> independent e-c coupling of skeletal muscle fibers. Lack of this link in cardiac cells results in need of a diffusible messenger for the transmission of the signal: extracellular Ca<sup>2+</sup> (**figure 5**).

Because skeletal e-c coupling does not depend on extracellular Ca<sup>2+</sup> the primary role of α<sub>1</sub>sDHPR cannot be to function as a Ca<sup>2+</sup> channel. It has been suggested that a positively charged intramembrane segment (S4 in each of the four DHPR domains) is responsible for providing the triggering signal that activates RyRs. In this way the α<sub>1</sub>sDHPR would act as a voltage sensor in the mechanism (37). However, while it is clear that α<sub>1</sub>sDHPR and RyR1 are specifically linked, the nature of the bond is still unknown. In fact, attempts to detect a direct binding between RyRs and DHPRs were unsuccessful, and the possibility of a third protein being interposed among them cannot yet be completely discarded.

Studies performed in knockout mice have allowed identification of DHPR and RyR domains that are critical for the mechanical communication between them. An extremely elegant work by Tanabe

et al. (1990)(37) showed that the expression of a α<sub>1</sub>DHPR chimera, containing only the cytoplasmic loop between the II and III domain from the skeletal isoform, was able to restore skeletal type e-c coupling in cultured dysgenic myotubes. Recently even a shorter domain of the II-III loop (46 amino acids) was found to be sufficient to restore skeletal type e-c coupling (38) and not even drastic alteration of the sequence surrounding those 46 amino acid could abolish its function (39). It has been proposed that also the β subunit of the DHPR plays an important role in e-c coupling. The β-DHPR is localized on the cytoplasmic side of the protein and interacts with the I-II loop of the α<sub>1</sub>DHPR. Studies in β-null mice (β-DHPR -/-) suggest that the carboxy-terminus region of this subunit is important for communicating with RyRs (40). Skeletal/cardiac chimeric RyR receptors expressed in dyspedic myotubes were used to determine which region of RyR1 receives the signal from the DHPR (41) and recent unpublished observations are leading to the conclusion that RyR1 interacts with DHPRs in multiple regions (unpublished data). One more piece was added to the puzzle by the fact that the signaling between the two molecules turned out to be bi-directional (29) and far more complex than expected. An orthograde signal allows triggering of RyR Ca<sup>2+</sup> release and a retrograde signal allows DHPRs to function as a channel. Existence of this two-way interaction is strong proof that an

intermolecular route indeed functionally links RyRs and DHPRs. However, while it is clear that the orthograde signal is essential to skeletal type e-c coupling, it is not clear whether the retrograde signaling that is necessary for calcium permeation through the DHPR plays any role in e-c coupling events. A correlation between the structural DHPR-RyR link that results in tetrad formation and the functional link that underlies orthograde and retrograde signaling has not yet been established and requires further investigation.

Tetrads are composed of four DHPRs associated with the corners of the four subunits of RyR1, as shown by a combination of thin sectioning and freeze-fracture techniques (**figure 2 E**). Interestingly, three-dimensional reconstruction of RyR1 (skeletal) and RyR2 (cardiac) have shown that one of the major structural differences between the two isoforms is localized in the corner of the cytoplasmic domain (clamp region). The region that bridges domains 5 and 6 of RyR1 is probably missing in RyR2 and differences in this region may definitely contribute to the differences in e-c coupling and DHPR/RyR association (18). DHPR tetrads are not associated with every foot but only and specifically with alternate feet even in muscles that express only RyR type 1. In this configuration only one of every two RyRs has the possibility of interacting directly with DHPRs since the remaining feet are not directly coupled (**figures 2 E, 4 D, and 5 B**). The reason for the alternate tetrad/RyR1 structural association is still unclear. It has been speculated that tetrads being bigger than feet, there is no space for tetrads on each RyR (24). However, studies of developing junctions in BC3H1 cells have shown that DHPRs are targeted specifically to alternate RyRs even when the tetrad arrays are incomplete. This study ruled out the possibility of simple steric hindrance as the only reason for alternate RyR/tetrad association and suggested that other molecular components of skeletal junctions could be involved in the formation of this pattern (42). It is also still unclear how uncoupled RyRs are activated. Hypothesis in which alternate RyRs are activated directly by DHPRs whereas the others are activated by CICR have been proposed (4-5). Marx et al. (1998) (43) suggested a different model: according to their results RyR1s are functionally associated in pairs through FKBP12 (coupled gating).

RyR3 is co-expressed with RyR1 in many muscle types and in some cases it constitutes about 50% or more of the RyRs. Because RyR3 is never expressed alone in skeletal muscle, it was initially difficult to test how this isoform is activated and what its contribution to CRU structure is under normal conditions. The first evidence has come from an animal model carrying a spontaneous null mutation of RyR1 (cn/cn chicks, crooked neck dwarf phenotype). The muscle fibers in the cn/cn chicks develop poorly and show no e-c coupling *in vivo* even when RyR3 is expressed (44). Cultured myotubes do show Ca<sup>2+</sup> transients, but these are dependent on the presence of external Ca<sup>2+</sup>. Lack of interaction between RyR3 and skeletal  $\alpha_1$ SDHPR is confirmed by failure of RyR3

to restore skeletal type e-c coupling and DHPR junctional tetrads in dyspedic 1B5 myotubes (32, 35). The relative position of  $\alpha_1$ SDHPRs and RyR3 is similar to that of  $\alpha_1$ CDHPRs and RyR2 in cardiac myocytes (**figure 4, E and F**), that is the two molecules are near each other but not apparently linked. These results taken together suggest that RyR3 does not participate directly in the interaction with  $\alpha_1$ SDHPRs and support once again the need of tetrads for mechanical coupling.

## ACKNOWLEDGEMENTS

This work was supported by MDA 2688 to Paul D. Allen and F. Protasi. I thank C. Franzini-Armstrong for the electron microscopy micrographs and T. Wagenknecht and M. Samsco for the RyR cryo-microscopy reconstruction images. Thanks also go to C. Franzini-Armstrong and Diane E. Sagnella and for their critical reading of this review.

## References

- Porter, K. R. The sarcoplasmic reticulum in muscle cells of *Amblystoma* larvae. *J. Biophys. Biochem. Cytol.* 2, 163-170 (1956)
- Franzini-Armstrong, C., and A. O. Jorgensen. Structure and development of e-c coupling units in skeletal muscle. *Annu. Rev. Physiol.* 56, 509-534 (1994)
- Fabiato, A. Calcium-induced release of calcium from cardiac sarcoplasmic reticulum. *Am. J. Physiol.* 245, C1-C14 (1983)
- Rios, E., J. Ma, and A. Gonzales. The mechanical hypothesis of excitation contraction coupling. *J. Muscle Res. Cell Motil.* 12, 127-135 (1991)
- Schneider, M. F. Control of calcium release in functioning skeletal muscle fibers. *Annu. Rev. Physiol.* 56, 463-84 (1994)
- Flucher, B. E., H. Takekura, and C. Franzini-Armstrong. Development of the excitation-contraction coupling apparatus in skeletal muscle: association of sarcoplasmic reticulum and transverse tubules with myofibrils. *Dev. Biol.* 160, 135-147 (1993)
- Sun, X-H., F. Protasi, M. Takahashi, H. Takeshima, D. G. Ferguson, and C. Franzini-Armstrong. Molecular architecture of membranes involved in excitation-contraction coupling of cardiac muscle. *J. Cell Biol.* 129, 659-671 (1995)
- Sommer, J. R. Comparative Anatomy: in praise of a powerful approach to elucidate mechanisms translating cardiac excitation into purposeful contraction. *J. Mol. Cell Cardiol.* 27, 19-35 (1995)
- Franzini-Armstrong, C. Studies of the triad. *J. Cell Biol.* 47, 488-499 (1970)
- Lai, F. A., H. P. Erickson, E. Rousseau, Q. Y. Liu, and G. Meissner. Purification and reconstitution of the calcium release channel from skeletal muscle. *Nature (Lond.)* 331, 315-319 (1988)
- Takekura, H., H. Takeshima, S. Nishimura, M. Takahashi, T. Tanabe, V. Flockerzi, F. Hoffman, and C. Franzini-Armstrong. Co-expression in CHO cells of two muscle proteins involved in e-c coupling. *J. Muscle Res. Cell Motil.* 16, 465-480 (1995)
- Tanabe, T., K. G. Beam, J. A. Powell, and S. Numa. Restoration of excitation-contraction coupling and slow calcium current in dysgenic muscle by dihydropyridine receptor complementary DNA. *Nature (Lond.)* 336, 134-139 (1988)
- Jorgensen, A. O., A. C-Y. Shen, W. Arnold, A. T. Leung, and K. P. Campbell. Subcellular distribution of the 1,4-Dihydropyridine receptor in rabbit skeletal muscle *in situ*: an immunofluorescence and immunocolloidal gold-labeling study. *J. Cell Biol.* 109, 135-147 (1989)
- Carl, S. L., K. Felix, A. H. Caswell, N. R. Brandt, W. J. Ball, P. L. Vaghy, G. Meissner and D. G. Ferguson.

- Immunolocalization of sarcolemmal dihydropyridine receptor and sarcoplasmic reticular triadin and ryanodine receptor in rabbit ventricle and atrium. *J. Cell Biol.* 129, 672-682 (1995)
15. Sorrentino, V. The ryanodine receptor family of intracellular calcium release channels. *Adv. Pharmacol.* 33, 67-90 (1995)
  16. Otsu, K., H. F. Willard, V. K. Khanna, F. Zorzato, N. M. Green, and D. H. MacLennan. Molecular cloning of cDNA encoding the Ca<sup>2+</sup> release channel (ryanodine receptor) of rabbit cardiac muscle sarcoplasmic reticulum. *J. Biol. Chem.* 265, 13472-13483 (1990)
  17. Radermacher, M., V. Rao, R. Grassucci, J. Frank, A. P. Timerman, S. Fleisher, and T. Wagenknecht. Cryo-electron microscopy and three-dimensional reconstruction of the calcium release channel/ryanodine receptor from skeletal muscle. *J. Cell Biol.* 127, 411-423 (1994)
  18. Sharma, M. R., P. Penczek, R. Grassucci, H. B. Hin, S. Fleischer, and T. Wagenknecht. Cryoelectron microscopy and image analysis of the cardiac ryanodine receptor. *J. Biol. Chem.* 273, 18429-18434 (1998)
  19. Sharma, M. R., L. H. Jeyakumar, S. Fleischer, and T. Wagenknecht. Three-dimensional structure of ryanodine receptor isoform three in two conformational states as visualized by cryo-electron microscopy. *J. Biol. Chem.* 275, 9485-9491 (2000)
  20. Catterall, W. A. Functional subunit structure of voltage-gated calcium channels. *Science* 253, 1499-1500 (1991)
  21. Adams, B. A., T. Tanabe, A. Mikami, S. Numa, and K. G. Beam. Intramembrane charge movement restored in dysgenic skeletal muscle by injection of dihydropyridine receptor cDNAs. *Nature (Lond.)* 346, 569-572 (1990)
  22. Loesser, K. E., L. Castellani, and C. Franzini-Armstrong. Dispositions of junctional feet in muscles of invertebrates. *J. Muscle Res. Cell. Motil.* 13, 161-173 (1992)
  23. Block, B. A., T. Imagawa, K. P. Campbell, and C. Franzini-Armstrong. 1988. Structural evidence for direct interaction between the molecular components of the transverse tubule/sarcoplasmic reticulum junction in skeletal muscle. *J. Cell Biol.* 107, 2587-2600 (1988)
  24. Franzini-Armstrong, C., and J. W. Kish. Alternate disposition of tetrads in peripheral couplings of skeletal muscle. *J. Muscle Res. Cell Motil.* 16, 319-324 (1995)
  25. Protasi, F., X-H. Sun, and C. Franzini-Armstrong. 1996. Formation and maturation of calcium release apparatus in developing and adult avian myocardium. *Develop. Biol.* 173, 265-278 (1996)
  26. Chaudhari, N. A single nucleotide deletion in the skeletal muscle-specific calcium channel transcript of muscular dysgenesis (mdg) mice. *J. Biol. Chem.* 267, 25636-25639
  27. Takeshima, H., M. Iino, H. Takekura, M. Nishi, J. Kuno, O. Minowa, H. Takano, and T. Noda. Excitation-contraction uncoupling and muscular degeneration in mice lacking functional skeletal muscle ryanodine-receptor gene. *Nature (Lond.)*. 369, 556-559 (1994)
  28. Rieger, F., M. Pincon-Raymond, A. M. Tassin, L. Garcia, G. Romey, M. Fosset, and M. Lazdunski. Excitation-contraction uncoupling in the developing skeletal muscle of the muscular dysgenesis mouse embryo. *Biochimie* 69, 411-417 (1987)
  29. Nakai, J., R. T. Dirksen, H. T. Nguyen, I. N. Pessah, K. G. Beam, and P. D. Allen. Enhanced dihydropyridine receptor channel activity in the presence of ryanodine receptor. *Nature (Lond.)*. 380, 72-75 (1996)
  30. Takekura, H., L. Bennet, T. Tanabe, K. G. Beam, and C. Franzini-Armstrong. Restoration of junctional tetrads in dysgenic myotubes by dihydropyridine receptor cDNA. *Biophys. J.* 67, 793-804 (1994)
  31. Protasi, F., C. Franzini-Armstrong, and P. D. Allen. Role of the ryanodine receptors in the assembly of calcium release units in skeletal muscle. *J. Cell Biol.* 140, 831-842 (1998)
  32. Protasi, F., H. Takekura, Y. Wang, S. R. Chen, G. Meissner, P. D. Allen, and C. Franzini-Armstrong. RYR1 and RYR3 have different roles in the assembly of calcium release units of skeletal muscle. *Biophys. J.* 79, 2494-2508 (2000)
  33. Franzini-Armstrong, C., M. Pincon-Raymond, and F. Rieger. Muscle fibers from dysgenic mouse *in vivo* lack a surface component of peripheral couplings. *Dev. Biol.* 146, 364-376 (1991)
  34. Takekura, H., M. Nishi, T. Noda, H. Takeshima, and C. Franzini-Armstrong. Abnormal junctions between surface membrane and sarcoplasmic reticulum in skeletal muscle with a mutation targeted to the ryanodine receptor. *Proc. Natl. Acad. Sci. USA.* 92, 3381-3385 (1995)
  35. Fessenden, J. D., Y. Wang, R. A. Moore, S. R. Chen, P. D. Allen, and I. N. Pessah. Divergent functional properties of ryanodine receptor types 1 and 3 expressed in a myogenic cell line. *Biophys. J.* 79:2509-2525 (2000)
  36. Schneider, M. F., and W. K. Chandler. Voltage dependence charge movement in skeletal muscle: a possible step in excitation contraction coupling. *Nature (Lond.)*. 242, 244-246 (1973)
  37. Tanabe, T., K. G. Beam, B. A. Adams, T. Niidome, and S. Numa. Regions of the skeletal muscle Dihydropyridine receptor critical for excitation-contraction coupling. *Nature* 344, 451-453 (1990)
  38. Grabner, M., R. T. Dirksen, N. Suda, and K. G. Beam. The II-III loop of the skeletal muscle dihydropyridine receptor is responsible for the Bi-directional coupling with the ryanodine receptor. *J. Biol. Chem.* 274, 21913-21919 (1999)
  39. Wilkens, C. M., N. Kasielke, B. E. Flucher, K. G. Beam, and M. Grabner. Excitation-contraction coupling is unaffected by drastic alteration of the sequence surrounding residues L720-L764 of the alpha 1S II-III loop. *Proc. Natl. Acad. Sci. U S A* 98, 5892-5897 (2001)
  40. Beurg, M., C. A. Ahern, P. Vallejo, M. W. Conklin, P. A. Powers PA, R. G. Gregg, R. Coronado. Involvement of the carboxy-terminus region of the dihydropyridine receptor beta1a subunit in excitation-contraction coupling of skeletal muscle. *Biophys. J.* 77, 2953-2967 (1999)
  41. Nakai, J., N. Sekiguchi, T. A. Rando, P. D. Allen, and K. G. Beam. Two regions of the ryanodine receptor involved in coupling with L-type Ca<sup>2+</sup> channels. *J. Biol. Chem.* 273, 13403-13406 (1998)
  42. Protasi, F., C. Franzini-Armstrong, and B. E. Flucher. Coordinated incorporation of skeletal muscle dihydropyridine receptors and ryanodine receptors in peripheral couplings of BC<sub>3</sub>H1 cells *J. Cell Biol.* 137, 859-870 (1997)
  43. Marx, S. O., K. Ondrias K, and A. R. Marks. Coupled gating between individual skeletal muscle Ca<sup>2+</sup> release channels (ryanodine receptors). *Science* 281, 818-821 (1998)
  44. Airey, J. A., M. D. Baring, C. F. Beck, Y. Chelliah, T. J. Deerinck, M. H. Ellisman, L. J. Houenou, D. D. McKemy, J. L. Sutko, and J. Talvenheimo. Failure to make normal alpha ryanodine receptor is an early event associated with the crooked neck dwarf (cn) mutation in chicken. *Dev. Dyn.* 197, 169-188 (1993)

**Abbreviations used in this paper:** CICR, calcium-induced calcium-release; CRU, calcium release unit; DHPR, dihydropyridine receptor; e-c, excitation contraction; EM, electron microscopy/micrographs; RyR, ryanodine receptor; RyR1, RyR2, and RyR3, skeletal isoform of ryanodine receptor, cardiac isoform of ryanodine receptor, and brain isoform of ryanodine receptor; SR, sarcoplasmic reticulum; T-tubule, transverse tubule.

**Running Title:** DHPR/RyR interaction in muscle cells:  
when structure explains function.

**Key words:** excitation-contraction coupling; skeletal  
and cardiac muscle; Dihydropyridine receptors,  
Ryanodine receptors; electron microscopy.

**Corresponding Author:**

Dr. Feliciano Protasi  
Dept. of Anesthesia Research  
Brigham and Women's Hospital  
Harvard Medical School  
75 Francis Street  
Boston, MA 02115  
Tel.: (617) 732 6881  
FAX: (617) 732 6927  
E-mail: [protasi@zeus.bwh.harvard.edu](mailto:protasi@zeus.bwh.harvard.edu)

# Ca<sup>2+</sup> release flux underlying Ca<sup>2+</sup> transients and Ca<sup>2+</sup> sparks in skeletal muscle.

Eduardo Ríos and <sup>‡</sup>Gustavo Brum.

Department of Molecular Biophysics and Physiology, Rush University, 1750 W. Harrison Street, Chicago, IL 60612.

<sup>‡</sup>Departamento de Biofísica, Facultad de Medicina, Universidad de la República, G. Flores 2125, Montevideo, Uruguay. Email: [erios@rush.edu](mailto:erios@rush.edu)

**ABSTRACT** Three main paths to derive the Ca<sup>2+</sup> release flux underlying Ca<sup>2+</sup> sparks are reviewed here. Some properties of release flux can be inferred from an examination of spark morphology. Others from model simulations, which generate sparks assuming an ion source within a cytoplasm-like medium. Finally, the release flux can be derived from the fluorescence transient by generalizing an algorithm developed earlier for global or whole cell signals. The transient and spatially limited nature of sparks adds many uncertainties to the process. These methods yield estimates between 1.4 and 30 pA, not clearly greater in skeletal than in cardiac muscle. At their low end, the estimates are consistent with generation of sparks by one or two ryanodine receptor channels, but the results are easier to explain if several channels, from as little as four to as many as 60, cooperate in their generation. How release flux determines spark shape and time course has been understood largely through simulations. The rise time of sparks corresponds to active release time. Both release flux and release time may vary among individual sparks, leading to their varied size and shape. Release flux turns off abruptly, therefore the decay of sparks is determined by Ca<sup>2+</sup> removal and diffusion. Spatial width increases with release time (rise time). That its experimentally determined value is too large compared with simulations, remains the single most important question in the interpretation of shape. Sparks are not the sole form of local fluorescence transients. When channel opening drugs are present, or sometimes spontaneously, sparks may be prolonged by embers. If the release flux calculated during an ember corresponds to a single open channel, then the release underlying a spark must require many open channels. The continued examination of Ca<sup>2+</sup> release flux appears to be an essential requisite for the interpretation of sparks and their place in calcium signaling.

## INTRODUCTION

Ca<sup>2+</sup> sparks (1) are regarded as  $\Delta$ the elementary events $\Delta$  of Ca<sup>2+</sup> release in skeletal and cardiac muscle. This concept has four components. One is semantic: Ca<sup>2+</sup> sparks are really fluorescence events, reflecting a transient increase in the concentration of a Ca<sup>2+</sup>-bound dye. Hence they are primarily related to and driven by an increase in [Ca<sup>2+</sup>]<sub>i</sub>. In that sense they are the local equivalent -- the elementary unit-- of the  $\Delta$ Ca<sup>2+</sup> transient $\Delta$  that takes place in the whole cell. Therefore, a more punctilious enunciation of the first concept is that the Ca<sup>2+</sup> release underlying a spark constitutes the elementary unit of cellular Ca<sup>2+</sup> release. A main topic of this article is how to derive from the (fluorescence) spark the underlying Ca<sup>2+</sup> release.

The second element in the idea of  $\Delta$ elementary event $\Delta$  is that they enter the whole additively, superimposed, much as bricks pile up in a wall. While there are some evidences that such is the case, there are ways other than addition to compose whole cell release. Say that sparks are generated by single channels or pairs of channels gating in unison. Then assume that one channel, or one pair, can gate another (channel or pair) if both are close to each other. This would imply that the spark generators interact, no longer constituting real units of release generation. In other words, the mathematics would in this case become more complex than addition, and the concept of sparks as units would lose much validity.

Another ingredient of the  $\Delta$ elementary event $\Delta$  concept, is that it is indivisible, atomic. Of course, this would be a property of sparks produced by single openings of single channels. Whether or not this is the case constitutes one of the main questions posed by the existence of sparks, and the answer has powerful consequences for mechanism. Any discussion of flux under a spark is basically an argument about composition of the spark generator  $\Delta$ whether it is composed of many channels, or a single one $\Delta$ .

Our opening statement contains yet a fourth idea, that sparks constitute the sole components of whole cell release. The question is whether in addition to bricks there is some sand or gravel in the release construction.

The above considerations should stress that sparks are studied to understand a cellular process, Ca<sup>2+</sup> release, and its control. It should also be a reminder that our only experimental approach to these processes is to measure a transient in the concentration of the Ca<sup>2+</sup>-bound form of a fluorescent dye. Everything else: the Ca<sup>2+</sup> transient, the release flux, and its mechanisms, are inferred from that single measurement.

## FROM GLOBAL Ca<sup>2+</sup> SIGNAL TO Ca<sup>2+</sup> RELEASE FLUX.

Current calculations of release under Ca<sup>2+</sup> sparks draw heavily from earlier work on whole cell Ca<sup>2+</sup> transients. Consequently, before examining the issue at the spark (or local) level, it is instructive to

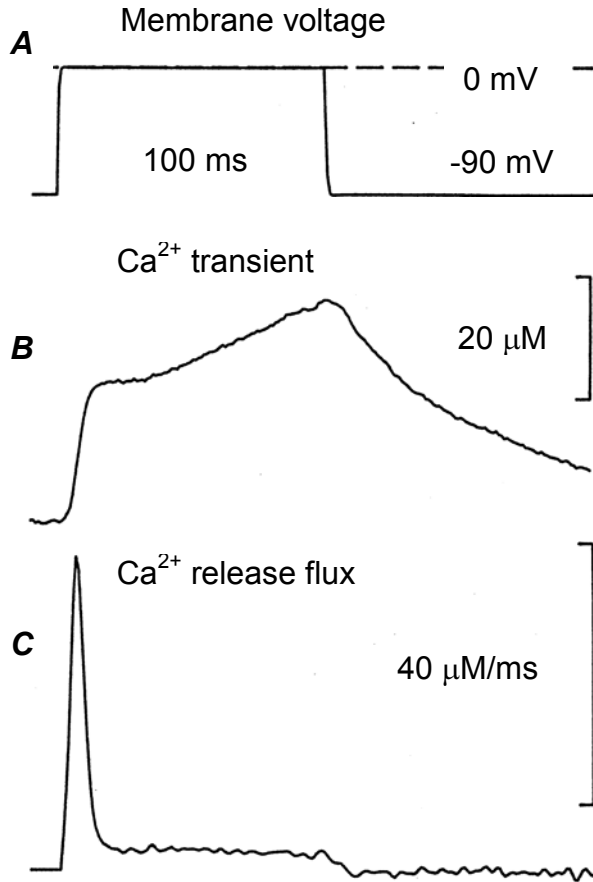


Fig. 1. The analysis of global signals. The pulse at top was applied to a frog fiber under voltage clamp. The  $\text{Ca}^{2+}$  transient was derived from the absorption change of the dye ApIII according to eqn. 1. The release flux record was derived from the  $\text{Ca}^{2+}$  transient using text eqn. 2. Removal flux was derived applying the method of Melzer et al. (3,4) to the  $\text{Ca}^{2+}$  transient shown and other transients not shown. Modified from Ríos and Pizarro (5).

consider the question of release flux at the macroscopic or global level.

The measurement of global  $\text{Ca}^{2+}$  transients may be carried out using any fluorescent  $\text{Ca}^{2+}$  indicator (though it was initially done with absorption dyes, mainly the fast-equilibrating Antipyrylazo III). In cells stimulated by action potential or voltage clamp, the signal  $S(t)$  (an absorption or a fluorescence) is a linear function of the bound dye, its change over time trailing the  $\text{Ca}^{2+}$  transient by an interval determined by the kinetic constants of the dye- $\text{Ca}^{2+}$  reaction, most importantly the off rate constant,  $k^-$ . The derivation of  $[\text{Ca}^{2+}](t)$  from  $S$  involves solving a first order differential equation (see for instance ref. 2), the solution of which has the following form:

$$[\text{Ca}^{2+}](t) = \frac{\frac{dS}{dt} + k^-(S - S_{\min})}{k^+(S_{\max} - S)} \quad (1)$$

Note the presence of a term proportional to the derivative of the signal (the weight of which decreases if

$k^-$  is high). This differentiation step increases the weight of the high frequency component of the signal. Thus the high frequency terms of the noise (which tends to have a flat spectrum) become more significant. The next step is to derive the flux of  $\text{Ca}^{2+}$  release from the  $\text{Ca}^{2+}$  transient. This question was solved in two different ways (3,4,6). A  $\text{Ca}^{2+}$  transient elicited by a voltage pulse, and the calculated release flux (3,4) are in fig. 1. Both approaches are based on an equation for release flux,  $R(t)$ ,

$$R = d[\text{Ca}^{2+}] / dt + d \text{rem} / dt \quad (2)$$

whereby release flux is equated to the sum of the rate of change of free  $[\text{Ca}^{2+}]_i$  plus a rate of  $\text{Ca}^{2+}$  removal by binding sites and other processes. Baylor et al. (6) calculated the net flux of  $\text{Ca}^{2+}$  exiting the SR as the sum of the rate of change of  $[\text{Ca}^{2+}]_i(t)$  plus the rate of binding of  $\text{Ca}^{2+}$  to the known cytoplasmic binding sites. The latter was calculated as the binding flux driven by the measured  $[\text{Ca}^{2+}]_i(t)$ , using literature values of ligand concentrations and their kinetic constants. Instead of using  $[\text{Ca}^{2+}]_i(t)$  to drive reactions with assumed kinetics, Melzer et al. (3,4) fitted (concentrations and binding constants of) a removal model, so that its  $[\text{Ca}^{2+}]_i$  would evolve in the same way as the measured one when the flux stopped after the pulse (curves in red in fig. 2A)<sup>1</sup>.

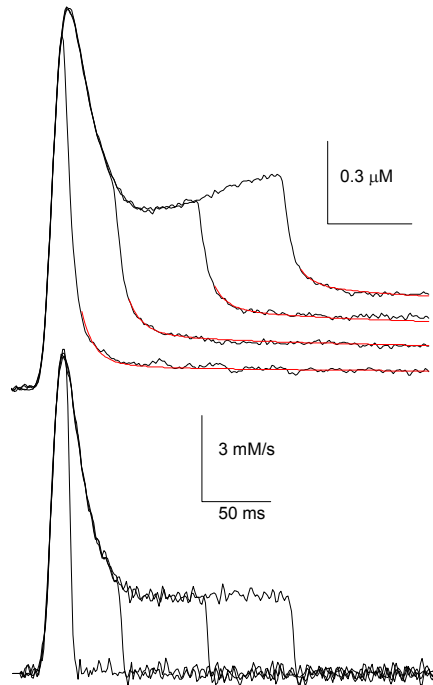


Fig. 2.  $\text{Ca}^{2+}$  transients and flux in the presence of a slow buffer. A,  $\text{Ca}^{2+}$  transients (determined in a frog fiber with ApIII), in response to pulses of various durations to  $-40$  mV. Lines in red represent  $\Delta[\text{Ca}^{2+}](t)$  predicted by the removal model during determination of release flux. B, the corresponding release flux records. Note how the presence of EGTA in the internal solution (12 mM) modified the  $\text{Ca}^{2+}$  transients (compared with those of fig. 1) bringing their time course closer to that of the release flux. Modified from Shirokova et al. (2).

In both cases, the contribution by the removal terms was much more important than the rate of change of the free  $[Ca^{2+}]_i$  as most calcium in the cytoplasm is bound. For both methods, the calculation involved differentiation of  $[Ca^{2+}]_i(t)$ , so that second derivatives of the measured signal entered the final flux. The drawbacks of the calculation therefore included a sharp enhancement of noise in the measurement, and the uncertainties involved in assignment of values to the removal model, which as stated makes a crucial contribution to the total flux. The increase in noise is improved by low-pass filtering, which blunts the prominent peak present in the  $Ca^{2+}$  release waveforms (figs 1 and 2B). These drawbacks would only become worse when these procedures were generalized to  $Ca^{2+}$  sparks.

Ways were concocted to improve the determination, all of which removed the uncertainty regarding the sequestering molecules by adding one to great excess over the others. For example, it was shown that a large concentration of the slow high affinity chelator EGTA would not only eliminate much of the uncertainty regarding removal parameters (simply because EGTA would reduce  $[Ca^{2+}]_i$  making the other components of removal less relevant) but would also render the temporal waveform  $[Ca^{2+}]_i(t)$  similar to that of release flux (7, 8,9). This is illustrated in fig. 2, showing  $Ca^{2+}$  transients elicited in a frog fiber by pulses of various durations to the same low voltage (A). In contrast with fig.1, and due to the inclusion of 10 mM EGTA in the internal solution, the transients in this case have many of the kinetic properties of the release waveforms, plotted in B. On the other extreme, a fast  $Ca^{2+}$  buffer, like arsenazo III (10), antipyrilazo III or furaptra, at high concentrations, also reduces the magnitude of the change in  $[Ca^{2+}]_i$ , but alters its course to bring it close to the time integral of the release flux. Of course these added buffers, which change the  $Ca^{2+}$  transient directly, might alter  $Ca^{2+}$  release if  $Ca^{2+}$  affected gating of the release channels. It is remarkable, however, that the waveform of release flux during a voltage clamp pulse (fig. 1) is only slightly altered by EGTA at 20 mM (11,8,9).

The flux of  $Ca^{2+}$  release thus calculated, reaches maxima of about 180 mM/s during a large voltage clamp pulse in frog muscle, and in one action potential add up to 0.5 mM, or 15% of the total releasable SR calcium (9,2,12).

### **Ca<sup>2+</sup> SPARKS.**

Using conventional confocal microscopy, sparks can be observed either in x-y scans or in line scans. Release flux with reasonable temporal resolution can only be derived from line scans. A new difficulty, not confronted at the whole cell level, is that  $\Delta$ object space, where sparks reside as local fluorescent packets of high  $[dye:Ca^{2+}]$ , must be translated to image space by the imaging system (microscope). That operation has two consequences: the image is rendered 2-dimensional (one dimensional in the case of line scans), and is also blurred in the x-y plane, becoming wider and flatter than the corresponding object. Hence the quantitative representation of spark morphology must be preceded by a correction, or deblurring. Because blurring is

mathematically a convolution (an average or integral weighted by the PSF of the microscope), its correction consists of a deconvolution, which selectively enhances the weight of high spatial frequency components. This operation therefore increases noise of high spatial frequency, while the next step, derivation of the local  $Ca^{2+}$  transient, adds noise in both space and time.

After reconstruction of the  $Ca^{2+}$  transient, the process follows similar steps as the derivation of release flux from whole cell signals, and is described in section 5. Before attempting such calculation, we will simply describe  $Ca^{2+}$  sparks as functions of time and space. The events= size and shape should be clues to the underlying release flux.

### **Morphology of Ca<sup>2+</sup> Sparks**

The  $\Delta$ amorphometric parameters usually defined include amplitude (strictly, peak amplitude), spatial width, duration and rise time. Additionally, a better indication of size is given by the spark= signal mass. Some published parameter values are collected in Table 1.

### **Amplitude**

Measured spark amplitude varies widely from the lower limits of detection, (defined by noise, usually around 0.3 units of  $F_0$ ) to high values of 14 in skeletal muscle (18) or 9 in ventricular myocytes (25). Fig 3 shows examples of sparks of high amplitude under two experimental conditions: (A) cut skeletal muscle fiber under voltage clamp, (B) a fiber permeabilized by saponin.

Amplitudes are usually much lower in permeabilized fibers (table 1). The reason may be quite simple:  $\Delta F/F_0$  is approximately proportional to the relative increase in local  $[Ca^{2+}]$ . In the voltage clamp experiments the cell may be able to maintain a  $[Ca^{2+}]_i$  substantially lower than in the solution at the cut ends, while in permeabilized fiber segments the free  $[Ca^{2+}]$  will equilibrate rapidly within the cell at the solution value of 100 nM. The relative increase in  $[Ca^{2+}]$  may therefore be lower in the latter case, simply because the initial value is higher (18).

Recently, we have been able to study a large number of sparks in adult rat EDL muscle (permeabilized by saponin). The amplitude of 2900 events was approximately 35% less than in frog fibers similarly prepared (26).

The distribution of spark amplitudes was subject to much scrutiny. Obviously, amplitude was taken as an indication of the magnitude of the underlying release, and the fact that several groups initially reported a modal distribution appeared to be consistent with the idea that sparks were generated by single channels. These observations were in error, as we now know. Indeed, all spark parameters, but most notably amplitude, are affected by a  $\Delta$ focusing error, due to the variable distance between the scanned line and the actual position of the source originating the spark. This error not only reduces the amplitude of detected sparks, but crucially alters the distribution of amplitudes, forcing it to be monotonous, without a mode (27, 28).

Izu et al. (29) and Cheng et al. (28) found that the distribution density of detected amplitudes of

	Preparation	Amplitude	FWHM $\mu\text{m}$	FDHM ms	Rise timems	Reference
FROG SKELETAL	Voltage clamp	2.93	1.46	10.4	4.56	13
	Permeabilized	1.92	1.31	11.0	5.6	14
	Notched fibers	0.75	1.7	10	5.5	15
	Intact fibers	3.7-4.6	0.97-1.02	5.5-6.2	3.7- 4.6 *	16
MAMMALIAN SKELETAL	Rat permeabilized	0.42	1.95	84	11.2	26
	Rat and mouse permeabilized Skinned	1.80	2.0	48.1 15.1 †	49.3 17.5 †	17
	Devel. mouse myotubes voltage clamp	1.27	1.4	25.3		18
	RyR3 knockout mouse voltage clamp	1.30	1.63	43.6		18
VENTRICULAR MYOCYTES	Rat intact cells	1.55	-	12.8‡	9.5	19
	Rat intact cells	1.85	1.98	23.7‡	-	58
	Rat cells: intact	1.67	1.75	27.7		20
	Permeabilized	1.72	1.85	26.1		
	Rat intact cells	2.0	1.7-2.2	20§	-	21
	Mouse voltage clamp	1.65	-	23.7§	-	22
	Rat trabecula intact cells	1.9-2.8	-	40	5	23

\* measured from 0-100 % amplitude; † mechanically skinned; ‡ half time of decay; §  $\mathcal{G}_{\text{decay}}$

Table 1. Morphology of  $\text{Ca}^{2+}$  sparks.

Gaussian sparks of constant size is inversely proportional to amplitude. Ríos et al. (30) used the result to devise a method of correction of the focusing error, which produced a true distribution of amplitudes that had a large spread. In other words, sparks as *objects* have widely variable amplitudes. Additionally, in many cases a mode was present in the corrected distribution. The mode was more marked in the presence of caffeine, a well known promoter of the activation of release channels by  $\text{Ca}^{2+}$ . To interpret this result it must first

be understood that a mode in spark amplitude does not necessarily imply a mode in  $\text{Ca}^{2+}$  release flux. It could, instead, correspond to a mode in the distribution of open times of the source. The implications of these alternatives will be clarified in section 5.1.

#### Spatial Width

Is usually measured by the FWHM (full width at half magnitude) at the time of peak signal. In voltage-clamped frog cut skeletal muscle fibers in Cs glutamate-

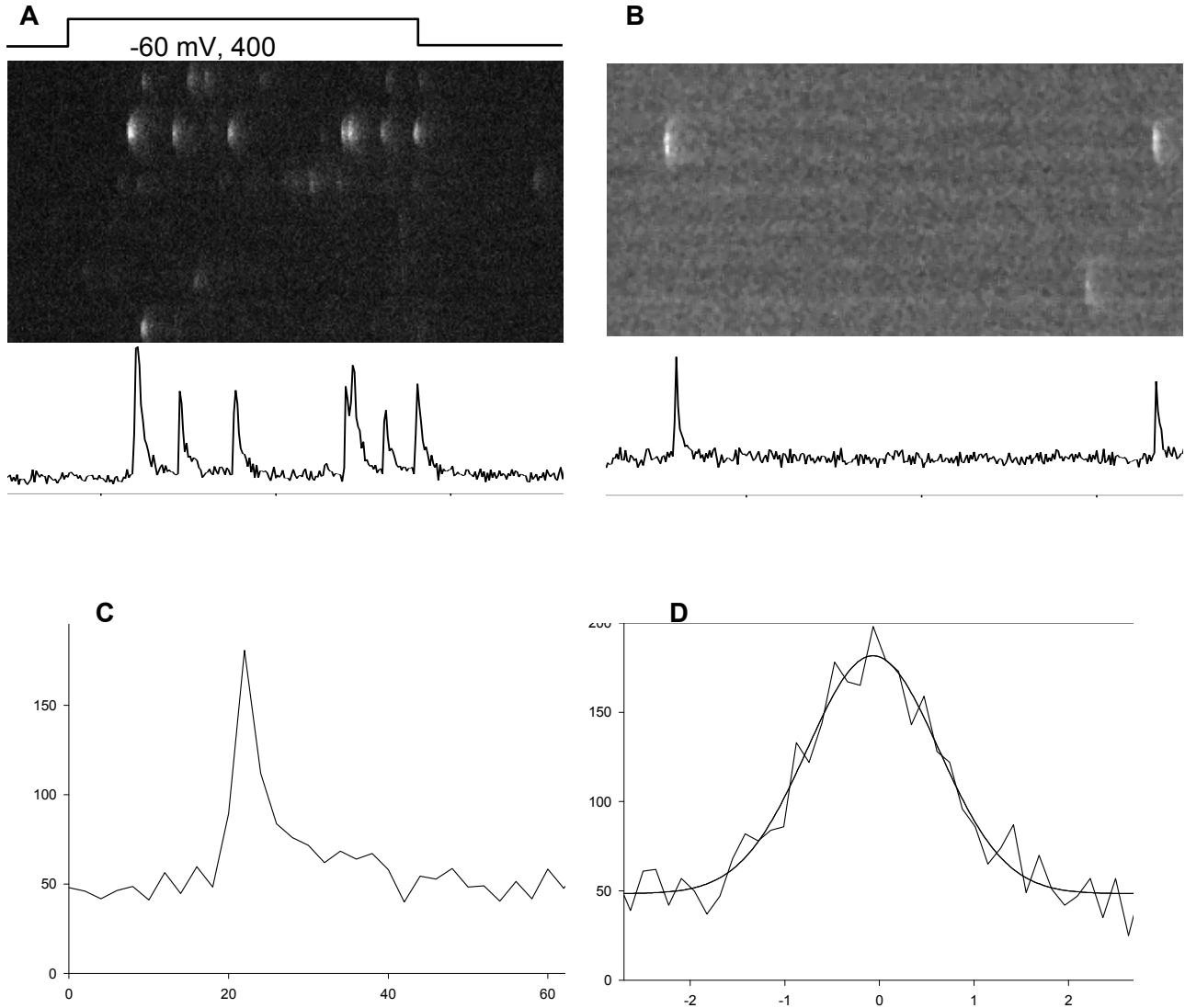


Fig. 3. Morphology of large sparks. A, part of line scan image of a voltage clamped frog fiber, held at  $-90$  mV and pulsed as shown. B, part of line scan image of a frog fiber permeabilized by saponin and immersed in a fluo 3-containing internal solution. In A and B the trace depicts fluorescence, averaged over three pixels centered at the arrow. Bar:  $10\mu\text{m}$ . C, temporal profile of large spark in B. D, spatial profile at the maximum and best fit gaussian (of standard deviation  $0.696\mu\text{m}$ , corresponding to a FWHM of  $1.64\mu\text{m}$ ). Methods and solutions used in A given by Shirokova *et al.* 1997. In B total fluo 3 was  $200\mu\text{M}$ . The images in panels A and B were obtained with similar settings, but the excitation light in A was 3 fold more intense. In B a myoplasmic dye concentration of  $369\mu\text{M}$  was estimated as that needed to produce the resting  $[\text{dye}:\text{Ca}^{2+}]$  ( $35.9\mu\text{M}$ , derived from  $F_0$  and calibrations in solution), assuming  $[\text{Ca}^{2+}] = 100\text{ nM}$  and  $K_D = 1.03\mu\text{M}$  for the dye reaction (24). This large spark requires a  $\text{Ca}^{2+}$  release current of about  $8\text{ pA}$  to account just for the  $\text{Ca}^{2+}$  bound to the dye.

based internal solutions, the average value over events elicited by mild depolarization was  $1.11\mu\text{m}$  (14). The value was greater (about  $1.5\mu\text{m}$ ) in fibers permeabilized with saponin or with notches (table 1). By contrast, in intact frog fibers the half width values (for spontaneous sparks, or those induced by increase in  $[\text{K}^+]$ ), was close to  $1\mu\text{m}$  (16). For mammalian  $\text{Ca}^{2+}$  sparks the width was approximately 20 % greater than in the similarly prepared frog muscles (26). In cardiac muscle, the values cover a range higher than that in skeletal muscle (table 1).

Width could be changed under some conditions: caffeine ( $1\text{ mM}$ ) increased it in voltage-elicited sparks to  $1.42\mu\text{m}$  (14; a smaller change in the same direction, was reported in intact fibers by 16). While reduction in

$[\text{Mg}^{2+}]$  did not change width of sparks detected by Lacampagne *et al.* (32), increase in  $[\text{Mg}^{2+}]$  to  $7\text{ mM}$  (from a reference value of  $0.6\text{ mM}$ ) reduced the width of voltage-elicited sparks to  $0.84\mu\text{m}$  (14). The implications of these numbers will best be considered in section 5, by contrasting them with simulations of sparks.

#### Rise Time

Defined as the interval between 10% and either 90% or 100% of the initial rise, it appears to be the parameter least sensitive to the focusing error (21, 33). Its average in frog cut fibers is about  $4.8\text{ ms}$  (14, 15, 32) and in intact fibers about  $4\text{ ms}$  (16). In mammalian skeletal muscle, the rise time was

approximately 20% greater than in the comparable group of amphibian cells (26). Both rise time and duration of sparks appear to be longer in cardiac myocytes.

González et al. (14) and Lacampagne et al. (15) found no correlation among spark parameters, other than a weak positive correlation between rise time and width (14). This correlation is present in most simulations of sparks (see below). It may explain why the spatial width of sparks in both cardiac myocytes and mammalian skeletal muscle is increased relative to the amphibian counterpart; their rise times are also greater.

It might also explain the widening effect of caffeine. However, when spatial widths were compared for groups of sparks of equal rise time in caffeine and reference, a significant difference was still found. Hence spark-widening by caffeine is a primary effect, which cannot be explained as consequential to a prolongation of rise time.

### Signal Mass

Is a function defined in line scans for every point in time as the integral of the signal intensity over three-dimensional space (34). The determination of signal mass is difficult because volume integration multiplies the intensity by the square of the distance to the spark center, implying a large amplification of the noise at long distances. For this reason, Shirokova et al. (18) suggested that it be approximated as the product of the amplitude by the volume of a sphere with diameter equal to FWHM. Although this turns out to be an underestimate<sup>2</sup>, the valid concept is that signal mass will be proportional to the third power of any measure of spatial width. This is important because signal mass is related more closely to release flux than any other parameter, which suggests that the release flux underlying a spark should also depend on the third power of spatial width.

### APPROACHES TO RELEASE FLUX.

Researchers have used two methods to advance from simple description of spark morphology to the underlying release flux. In a constructive, inductive, or *forward* calculation, sparks i.e. the fluorescence image associated to the local distribution of dye:Ca<sup>2+</sup> were generated in simulations that started with a source of given current in a medium of set properties (27, 21, 13, 33, 25). The converse, deductive, or *backward* calculation was also attempted: to start from the measured dye:Ca<sup>2+</sup> (in this case a function of  $t$  and spatial coordinates  $x$ ), then derive the corresponding  $[Ca^{2+}]_i(x, t)$  and deduce the release flux (35, 36, 13), much in the way it had been done earlier from the global Ca<sup>2+</sup> transients.

### Simulations.

The first effort in this direction was carried out by Pratusевич and Balke (27). Theirs and all other models of individual sparks assume release to be a simple function of time, usually a pulse, originating at a point or a small (sub-resolution) sphere. The medium on which released Ca<sup>2+</sup> impinges is geometrically elaborate in the case of Pratusевич and Balke and later simulations of Jiang et al. (33), as they try to reproduce the structural layout of fixed binding and removal sites.

Other simulations, instead, assume an aqueous medium with uniform properties, with binding sites that may be fixed, but are always at homogeneous density.

In the simulations of Pratusевич and Balke (27), assuming that release current was 1.4 pA, the sparks originating exactly in focus had an amplitude of 1.7. In the more detailed simulations of Jiang et al. (33), with parameters specifically copying skeletal muscle, the spark derived from a 1.4 pA source, open for 8 ms, had amplitude 1.1 and half width 1  $\mu$ m.

Assuming a homogeneous cytoplasm, Smith et al. (21) obtained sparks of up to 3.5  $F_0$  for a source of 2 pA. Again, the simulated sparks were much narrower than most experimental ones (FWHM  $\sim$  1  $\mu$ m), and could only be widened, albeit slightly, by either eliminating the buffers, or spreading the source to a 0.6  $\mu$ m diameter. This study also noted a proportionality between peak amplitude of the signal and source current, a somewhat paradoxical observation given the fact that local  $[Ca^{2+}]$  reached values much greater than the  $K_D$  of the indicator (fluo-3). While this convenient result was explained as a consequence of the lack of equilibrium between dye and Ca<sup>2+</sup> at short distances from the source (basically driving an irreversible transport of Ca<sup>2+</sup> away from the source, on the dye), there was also a bad consequence, that the spatial properties of the Ca<sup>2+</sup> transient were very poorly monitored. In other words, the lag with which the dye:Ca<sup>2+</sup> signal follows the global Ca<sup>2+</sup> transient is worsened in the case of the spatially resolved images, which both lag temporally and spatially dampen the Ca<sup>2+</sup> transient.

The overall impression gathered from the simulations of Pratusевич and Balke (27), Smith et al., (21) and Jiang et al. (33), is that the sparks simulated for sources of intensity comparable to that of single RyRs in bilayers, have brightness (amplitude) and time course similar to those measured experimentally. These simulated sparks, however, have consistently a 0.8 to 1  $\mu$ m spatial width, while those measured experimentally range between 1.0 and 3  $\mu$ m. The large width of experimental sparks suggests that the release flux corresponds to much more than the 1 or 2 pA assumed in the simulations. Release flux should account, at the very least, for the signal mass, which is proportional to the total amount of Ca<sup>2+</sup>:dye present. Other parameters being equal, sparks differing by a factor of 2 in spatial width will differ in signal mass by a factor of 8. Therefore, release currents of 1.4 to 2 pA are too small to account for the larger sparks observed in cut or permeabilized fibers, and in cardiac myocytes. Such currents, however, may be sufficient to simulate events recorded in intact skeletal muscle fibers (16).

The discrepancy in spatial width is troubling from the standpoint of mechanism, because there is no clear way in which to modify the simulation models in order to increase spatial width to this extent. An interesting suggestion of Izu et al. (25) is that sparks of large width could be *platykurtic* (flat-topped), reflecting local saturation of the dye. Few truly flat-topped sparks have been reported, and they were elongated, rather than circular, suggesting cotemporal opening of many channels (37). Local saturation of the dye requires (in simulations) currents of the order of 20 pA. Platykurtic sparks therefore add to the evidence for involvement of

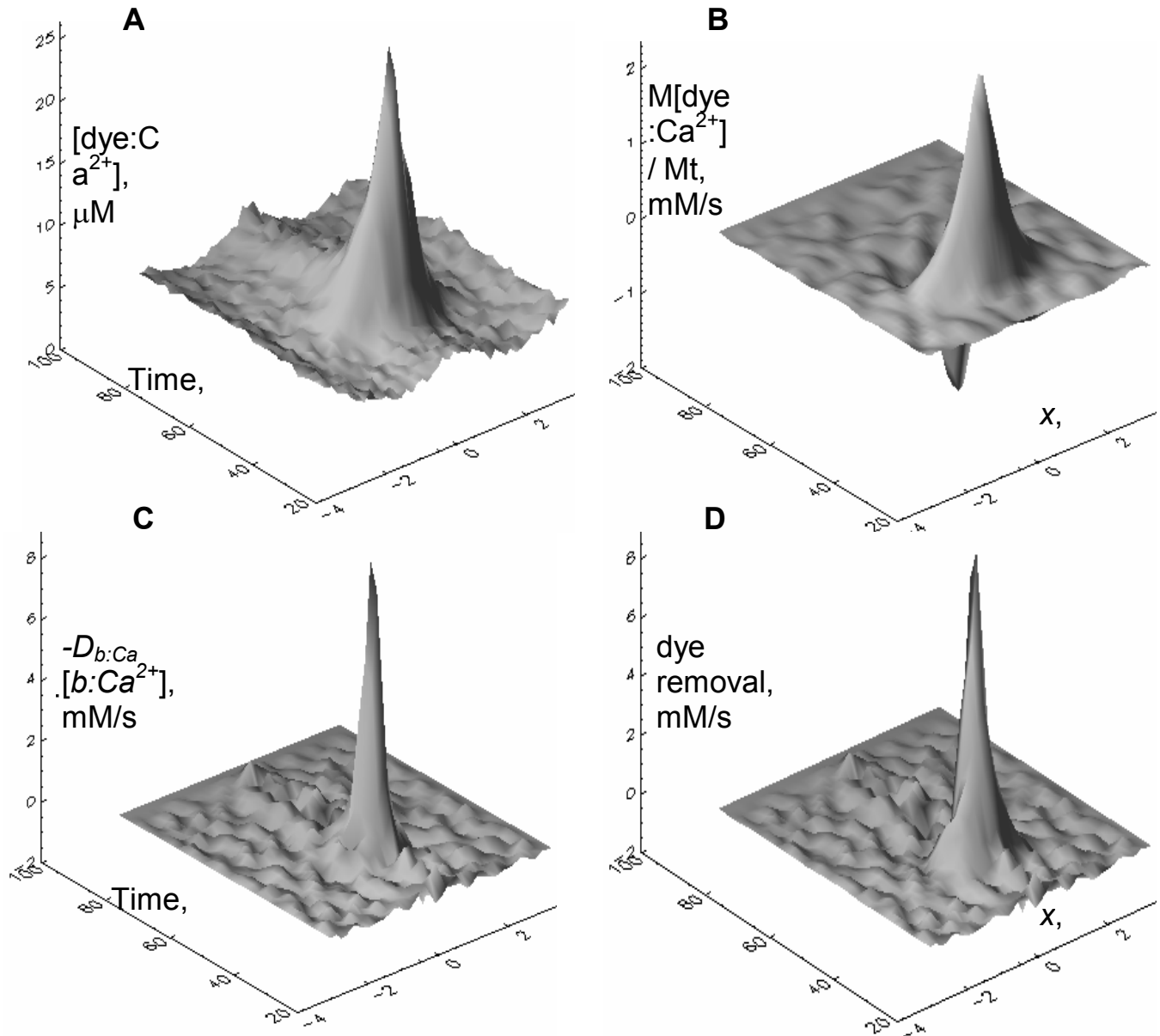


Fig. 4. Dye-related removal flux. A, local distribution of  $[dye:Ca^{2+}]$ , derived using eqn. 2b from the fluorescence average of 67 sparks elicited by depolarization (to -50 mV) in a frog fiber. The sparks were further selected for having rise times between 5 and 7 ms, and averaged by placing them centered at their peak amplitude. B, time derivative of  $[dye:Ca^{2+}]$ . According to eqn. 3 this rate of change results from reaction (with  $Ca^{2+}$ ) and diffusion. C, the diffusion term  $-D_{b:Ca} \Delta [dye:Ca^{2+}]$ . D, total removal flux into the dye (sum of B and C, eqn. 6). The calculations in figs. 4 through 8 used parameter values listed in table 2. (Fiber prepared as described in ref. 14, in an internal reference solution containing 50  $\mu M$  fluo-3 and 5 mM ATP and 1 mM EGTA as main  $Ca^{2+}$  ligands).

multiple channels in spark generation.

#### Calculations of release flux.

An algorithm that starts from the measured fluorescence to first calculate the  $Ca^{2+}$  transient and then derive release flux was introduced by Blatter et al. (35), then developed further by Lukyanenko et al. (36) and Ríos et al. (13). A simplified account is given here, following largely the latest of these references.

The first step in the procedure is deblurring. This procedure, which is quite standard, should take into account the characteristics of the specific setup, contained in its point spread function. In all confocal

microscopes the z or vertical spread is greater (its measure  $\sigma_z$  varying between 0.7 and 1.4  $\mu m$ ), while the spread in the image plane (x-y) is isotropic, of the order of the wavelength of emitted light. Deblurring results in substantial sharpening of the signal, and a large increase in relative amplitude (a factor of  $\sim 2$ ; ref 13).

Starting from the deblurred line scan signal  $F(x,t)$ ,  $[dye:Ca^{2+}](x,t)$  is derived as  $[dye:Ca^{2+}](x,t) = dye_r(x)(F(x,t) - F_{min}(x)) / (F_{max}(x) - F_{min}(x))$ . (2b)

Then  $[Ca^{2+}](x,t)$  is obtained numerically, solving the diffusion-reaction equation that governs the evolution of  $[dye:Ca^{2+}]$  in time and space:

$$\frac{\partial [\text{dye} : \text{Ca}^{2+}](x,t)}{\partial t} = [\text{dye}](x,t) [\text{Ca}^{2+}](x,t) k^+ - [\text{dye} : \text{Ca}^{2+}](x,t) k^- + D_{\text{dyeCa}} \Delta [\text{dye} : \text{Ca}^{2+}](x,t) \quad (3)$$

where  $k^+$  and  $k^-$  are the rate constants of the fluo-3:Ca<sup>2+</sup> reaction,  $D_{\text{dyeCa}}$  is the diffusion coefficient and  $\Delta$  is the laplacian operator ( $M^2/Mx^2 + M^2/My^2 + M^2/Mz^2$ ), which for all Ca<sup>2+</sup> complexes is less than zero near a Ca<sup>2+</sup> source. The line scan only provides the partial derivative in the  $x$  direction. M. Cannell (Univ. New Zealand) suggested assuming that the fluorescence increase is spherically symmetric, a function of time and the distance ( $\rho$ ) to its center. In that case the dependence of  $F$  with  $x$  gives all the information needed to calculate the laplacian correctly, as  $M^2/Mx^2 + 2(M/Mx)/x$ . Once the laplacian is substituted, eqn. 3 can be solved for  $[\text{Ca}^{2+}]$ , which turns out to be a sum of terms in  $[\text{dye}:\text{Ca}^{2+}]$  and its partial derivatives. Of course, this approach will give wrong results when the source (or the spark evolution) is not spherically symmetric.

Release flux is calculated from  $[\text{Ca}^{2+}](x,t)$  using a generalization of eqn. 2. The starting point is an equation, analogous to (3), that describes the evolution of free  $[\text{Ca}^{2+}]$

$$M[\text{Ca}^{2+}](x,t)/Mt = D_{\text{Ca}} \Delta [\text{Ca}^{2+}](x,t) + Y - Mrem/Mt \quad (4)$$

$D_{\text{Ca}}$  is the diffusion coefficient of Ca<sup>2+</sup>. The equation recognizes the existence of a source, of flux  $Y$ , a function of time and the spatial coordinate, and a removal system. Hence

$$Y = M[\text{Ca}^{2+}]/Mt - D_{\text{Ca}} \Delta [\text{Ca}^{2+}] + Mrem/Mt \quad (5)$$

$Mrem/Mt$  is the sum of the removal terms.

This is similar to the global eqn. 2. It includes all its terms plus the diffusion term  $-D_{\text{Ca}} \Delta [\text{Ca}^{2+}]$ . Even the dimensions, concentration over time, are the same as in the global equation<sup>3</sup>.

### The Removal Terms.

$Mrem/Mt$  is a sum of contributions for each buffer in the cell (the dye, parvalbumin, ATP, and sites in troponin and SR pump). An equation of the same form as 3 applied to each buffer  $b$ , yields the respective contribution as

$$M[b:\text{Ca}^{2+}]/Mt - D_{b:\text{Ca}} \Delta [b:\text{Ca}^{2+}] \quad (6)$$

An additional term (a positive function of time, constant in space) represents SR transport.

Because the medium is assumed spatially homogeneous, the sole difference with the global eqn. 2 is the appearance of diffusion terms, one for Ca<sup>2+</sup>, and one for each of the Ca<sup>2+</sup> complexes with diffusible buffers. Because the sign of the laplacian corresponds to the curvature of the local concentration, the diffusion terms will be positive near the source (where the distribution of the Ca<sup>2+</sup>-bound species can be viewed as convex) and become negative at a certain distance. All contributions of course cancel, except at the source. Ideally, the calculation should give an isolated peak in a very restricted region of space<sup>4</sup>.

Fig. 4A shows the local concentration of the dye:Ca<sup>2+</sup> complex, which in the case of fluo-3 is essentially proportional to the fluorescence. Panel B is its derivative with respect to time, which plays an important role in the calculation, not just because it participates in the calculation of free  $[\text{Ca}^{2+}]$  (eqn. 3), but also because it constitutes directly a component of

removal of Ca<sup>2+</sup>, in fact the only one that can be calculated with little error, giving rise to a lower bound to release flux that will be discussed later.

Parameter	Value	Reference
<b>Fluo-3:Ca ON-rate</b>	$3.2 \cdot 10^7 \text{ M}^{-1}\text{s}^{-1}$	(24)
<b>Fluo-3 dissociation const.</b>	1.03 $\mu\text{M}$	(24)
<b>EGTA:Ca ON-rate</b>	$0.2 \cdot 10^7 \text{ M}^{-1}\text{s}^{-1}$	(39)
<b>EGTA dissociation const.</b>	1 $\mu\text{M}$	(39)
<b>Trop:Ca ON-rate</b>	$5.7 \cdot 10^6 \text{ M}^{-1}\text{s}^{-1}$	(6)
<b>Trop:Ca OFF-rate</b>	11.4 $\text{s}^{-1}$	(6)
<b>ATP:Ca ON-rate</b>	$1.5 \cdot 10^8 \text{ M}^{-1}\text{s}^{-1}$	(40)
<b>ATP:Ca OFF-rate</b>	$3 \cdot 10^4 \text{ s}^{-1}$	(40)
<b>ATP:Mg ON-rate</b>	$1.5 \cdot 10^6 \text{ M}^{-1}\text{s}^{-1}$	(40)
<b>ATP:Mg OFF-rate</b>	195 $\text{s}^{-1}$	(40)
<b>Parv:Ca ON-rate</b>	$1.25 \cdot 10^8 \text{ M}^{-1}\text{s}^{-1}$	(6)
<b>Parv:Ca OFF-rate</b>	0.5 $\text{s}^{-1}$	(6)
<b>Parv:Mg ON-rate</b>	$3.3 \cdot 10^4 \text{ M}^{-1}\text{s}^{-1}$	(6)
<b>Parv:Mg OFF-rate</b>	3 $\text{s}^{-1}$	(6)
<b>Maximum pump rate [Parvalbumin]</b>	9.8 $\text{mM s}^{-1}$	†
<b>[Pump sites]</b>	1 $\text{mM}$	(6)
<b>[EGTA]</b>	0.2 $\text{mM}$	(6)
<b>[ATP]</b>	1 $\text{mM}$	*
<b>D<sub>Ca</sub></b>	5 $\text{mM}$	*
<b>D<sub>dye</sub></b>	$3.5 \cdot 10^{-6} \text{ cm}^2\text{s}^{-1}$	(41)
<b>D<sub>ATP</sub></b>	$2 \cdot 10^{-7} \text{ cm}^2\text{s}^{-1}$	(24)
<b>D<sub>parv</sub></b>	$1.4 \cdot 10^{-6} \text{ cm}^2\text{s}^{-1}$	(40)
<b>D<sub>EGTA</sub></b>	$2.6 \cdot 10^{-7} \text{ cm}^2\text{s}^{-1}$	(42)
	$3.6 \cdot 10^{-7} \text{ cm}^2\text{s}^{-1}$	(43)

Table 2. Values of parameters used by the release flux algorithm. Parv, parvalbumin. Trop, troponin.  $[\text{Ca}^{2+}]$  was 0.1  $\mu\text{M}$ .  $[\text{Mg}^{2+}]$  was 0.61  $\text{mM}$ . \* value in solution, † a value that fits global Ca<sup>2+</sup> transients when other parameters of removal had the values listed.

The dye provides an example of the contributions to  $\text{Ca}^{2+}$  removal made by all other diffusible buffers. As seen in the general equation 6 for every buffer the

contribution to removal may be viewed as sum of a local rate of change, represented for the dye in panel 4B, and the diffusional term, represented in panel 4C. Like other diffusional terms, it is much narrower and large at its center than the other component. 4D shows the sum of both components of removal by the dye.

Fig. 4A shows the local concentration of the dye: $\text{Ca}^{2+}$  complex, which in the case of fluo-3 is essentially proportional to the fluorescence. Panel B is its derivative with respect to time, which plays an important role in the calculation, not just because it participates in the calculation of free  $[\text{Ca}^{2+}]$  (eqn. 3), but also because it constitutes directly a component of removal of  $\text{Ca}^{2+}$ , in fact the only one that can be calculated with little error, giving rise to a lower bound to release flux that will be discussed later.

The dye provides an example of the contributions to  $\text{Ca}^{2+}$  removal made by all other diffusible buffers. As seen in the general equation 6 for every buffer the contribution to removal may be viewed as sum of a local rate of change, represented for the dye in panel 4B, and the diffusional term, represented in panel 4C. Like other diffusional terms, it is much narrower and large at its center than the other component. 4D shows the sum of both components of removal by the dye.

From the  $[\text{dye}:\text{Ca}^{2+}](x,t)$ , the  $\text{Ca}^{2+}$  transient is calculated by eqn. 3. It is shown in fig. 5. It is surprising that  $[\text{Ca}^{2+}]$  only reaches values of  $7 \mu\text{M}$  (up to  $25 \mu\text{M}$  for the largest sparks). In simulations, the concentration near the channel mouth may reach hundreds of  $\mu\text{M}$ . Comparable values are not reached here largely because of the coarse  $\Delta\text{grain}$ ,  $145 \text{ nm}$  per pixel in the present calculation. In trials with greater spatial resolution much greater central values were found. The values of release flux density also increased, but only in a small volume, and the calculated current did not change significantly.

The rest is a repeated calculation of removal terms, given by eqn. 6. These are formally similar to the

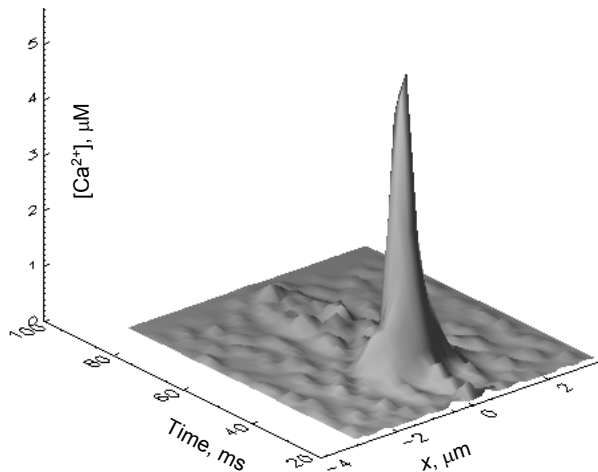


Fig. 5. The  $\text{Ca}^{2+}$  transient associated to a spark.  $[\text{Ca}^{2+}](x,t)$  derived from the  $[\text{dye}:\text{Ca}^{2+}](x,t)$  of the previous figure solving eqn. 3.

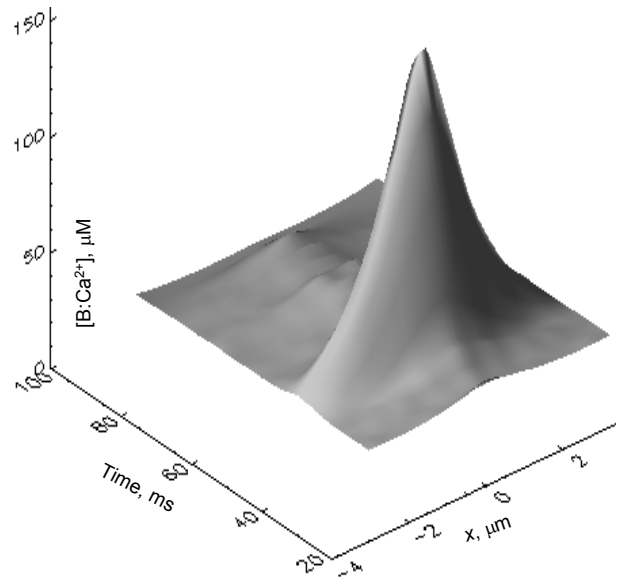


Fig. 6.  $\text{Ca}^{2+}$  bound to fixed buffers. Distribution of  $\text{Ca}^{2+}$  bound to sites on troponin C and the SR pump. The calculation used the  $\text{Ca}^{2+}$  transient of fig. 5 to drive binding reactions to the sites, assumed to be homogeneously distributed, with concentrations and reaction rate constants given in table 2.

ones shown for the dye. Fig. 6 illustrates the sum of the concentrations of  $\text{Ca}^{2+}$  bound to fixed removal molecules, in this case, sites of the SR pump and troponin C. Removal by these elements is simply the rate of change of the concentration shown.

In fig. 7 are the evolutions in space and time of  $[\text{Parvalbumin}:\text{Ca}^{2+}]$  and  $[\text{ATP}:\text{Ca}^{2+}]$ . In both cases  $\text{Mg}^{2+}$  competes for the binding sites. The corresponding  $\text{Mg}^{2+}$  complexes are also shown. The local parvalbumin contribution to removal is small, in part because of the occupancy by  $\text{Mg}^{2+}$ . ATP instead makes a sizable local contribution, due to its high reaction speed and concentration. The experimental sparks in these calculations were obtained at a relatively low  $[\text{Mg}^{2+}]$  ( $610 \mu\text{M}$ ). At higher, presumably more physiological  $[\text{Mg}^{2+}]$ , the attenuating effect of this ion on removal will be greater.

Fig. 8 compares three main terms of release flux. The first term in eqn. 5, rate of change in  $[\text{Ca}^{2+}]$ , is negligible. In A is the diffusional free  $\text{Ca}^{2+}$  term, which is relatively large due to the very sharp local  $[\text{Ca}^{2+}]$  gradient. In B is the removal flux by ligands other than the dye. The dominant component of this term in the example is removal by ATP. In C is the flux of transport by the SR pump, calculated as proportional to the square of the occupancy of its binding sites. It is comparatively very small, which explains why simulations assuming a homogeneous cytoplasm yield results very similar to those (27,33) that try to reproduce the spatial location of troponin and the SR pump. In Fig. 9A is total release flux, from which the release  $\text{Ca}^{2+}$  current, plotted in B, is calculated by integration over the volume of the source.

As shown in 9 B, the release current reached  $\sim 14 \text{ pA}$  in the example. In calculations using large

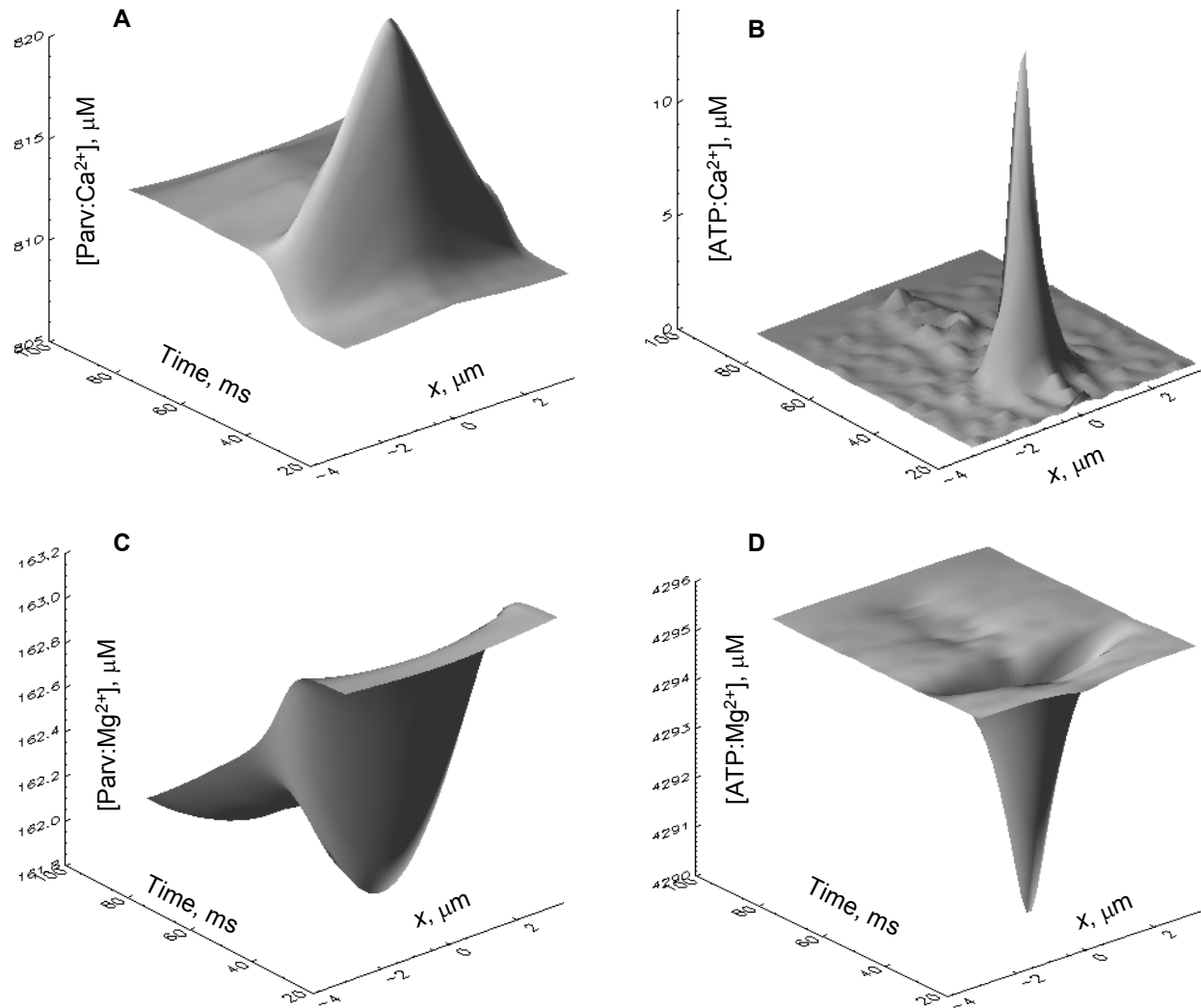


Fig. 7. Removal sites shared with  $Mg^{2+}$ . A, B, distribution of  $Ca^{2+}$  bound to sites on parvalbumin and ATP. C, D, distribution of the  $Mg^{2+}$ -bound forms of the same ligands. Note that in the present example, with  $Mg^{2+}$  present at a low concentration of 0.61 mM, over 80% of ATP and ~16% of parvalbumin are bound to  $Mg^{2+}$ . At greater, presumably more physiological  $[Mg^{2+}]$ , the attenuating effect of this ion on  $Ca^{2+}$  removal

sparks we have found values close to 20 pA (13).

#### A Lower Bound.

As discussed above, the calculation involves terms corresponding to different ligands, of which one must assume concentration, diffusion coefficient (of both free and  $Ca^{2+}$ -bound forms) and reaction rate constants. The exception is the dye, for which the total concentration may be measured, and the concentration of the  $Ca^{2+}$ -bound form directly derived from the fluorescence. Thus the dye removal contribution, illustrated in fig. 4D, is the only one that can be calculated with reasonable certainty, and constitutes a robust lower bound in the calculation of release flux. The current of removal by the dye (plotted in red in fig. 9B) is calculated as volume integral of the flux. In the example, where the total dye concentration was 50  $\mu M$ , it constitutes a minor component. When the dye concentration is greater, the contribution grows accordingly. In conditions of high [dye], Ríos et al. (13)

calculated a value of 8 pA for this lower bound, using large sparks in experiments on permeabilized fibers (see example in fig. 3).

#### Other estimates of release current.

Other estimates have been reported, but for sparks of cardiac muscle. Using essentially the same analysis described above, Blatter et al. (35) found a value of 3 pA for cat atrial cells. The reason for the lower value is that the amplitude of the sparks was lower, and also the removal model used to describe the atrial cytoplasm implied a lower buffer/removal capacity than in the skeletal muscle study. Lukyanenko et al. (36), who applied a similar technique to rat ventricular myocytes, did not report integrated release current but obtained values of release flux 2 to 10 times lower than Blatter et al. (35). Again, the explanation for the difference resides mainly in the smaller size of the sparks studied.

It is possible that the underlying release in

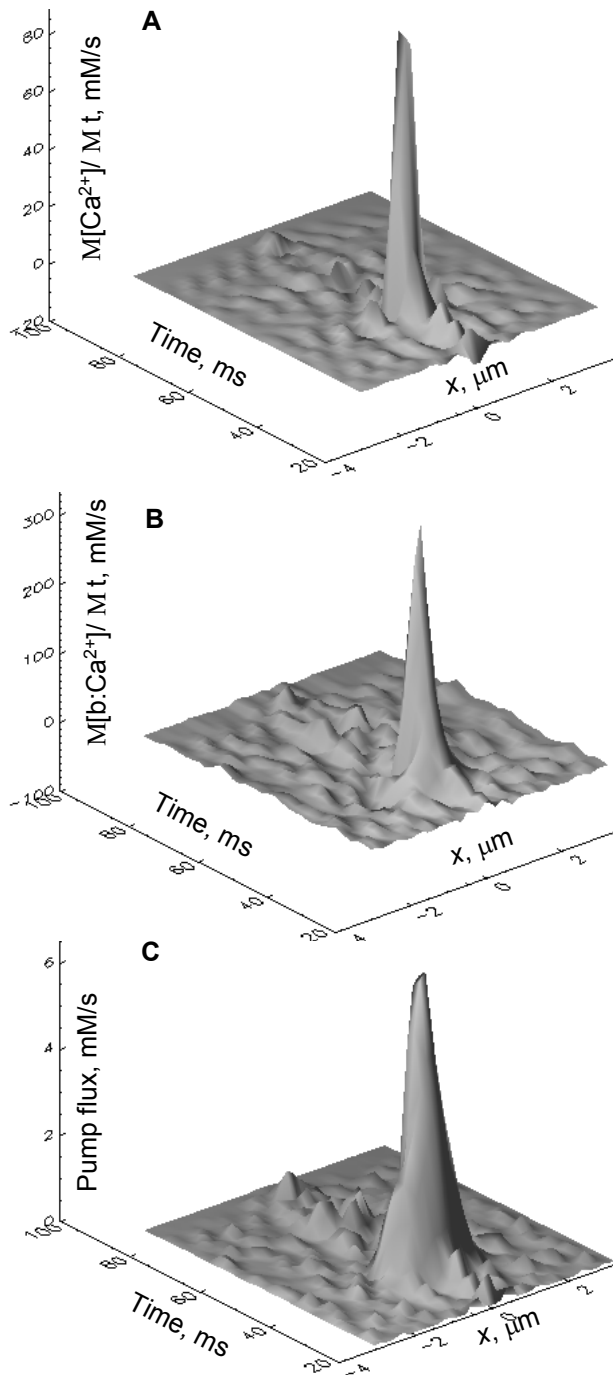


Fig. 8. Three main terms of release flux. A, diffusional free  $\text{Ca}^{2+}$  term:  $-D_{\text{Ca}} \Delta[\text{Ca}^{2+}]$ . B, removal flux by ligands other than the dye. C, flux of transport by the SR pump, calculated as proportional to the square of the occupancy of its binding sites.

cardiac sparks is smaller than in skeletal muscle: Wang et al. (44) recorded simultaneously sparks and sparklets due to opening of single L-type  $\text{Ca}^{2+}$  channels in the same dyadic unit of ventricular myocytes. The separate measurement of current underlying sparklets provided an accurate calibration of the optical signals, yielding a current of 2.1 pA for the spark. Again, sparks were of small size, hence the result is not in conflict with any of the other estimates.

Izu and colleagues (25) took an approach similar to the lower bound above that is, no buffers, other than 50  $\mu\text{M}$  dye. They calculated a minimum current needed to account for a spark of given amplitude and width, assumed to be a Gaussian function in space. Their results are represented in fig.10, as a function of spark amplitude, for three different assumptions regarding spatial width. In agreement with our example above, their minimum current for a spark of amplitude 2 and width 1.5  $\mu\text{m}$  would be nearly 2 pA. These authors also presented sparks of much greater amplitude and width, and concluded that a current of  $\sim 20$  pA underlies sparks. The events studied by Izu et al. (25) were greater than in the previous studies with cardiac muscle. They were similar to those studied by Ríos et al. (13) in skeletal muscle, and so were their estimates of current.

There is therefore general agreement regarding the derivation of release current. The disagreements that remain refer more to actual spark size. Because sparks as objects have variable amplitude, the release current will surely be variable. It is also worth recalling the 3<sup>rd</sup> order relationship between spatial width and signal mass. Thus the narrow events reported by Baylor et al. (16) in intact frog fibers should result from a much lower release current than the examples given above.

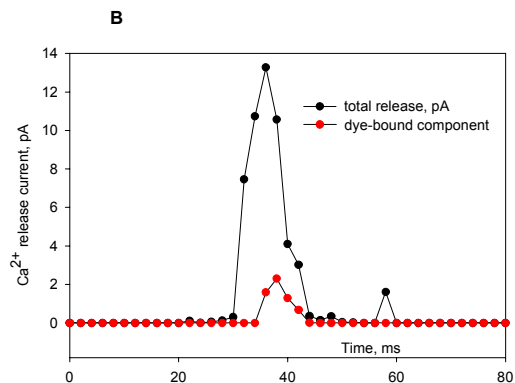
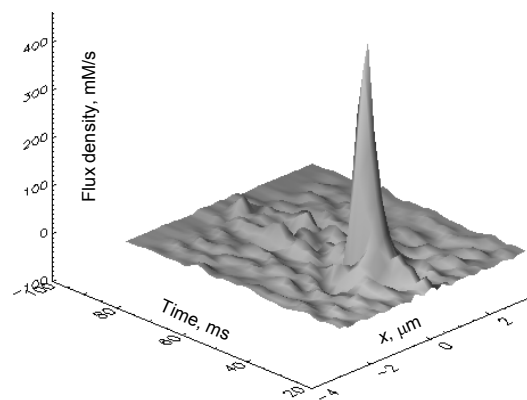


Fig.9.  $\text{Ca}^{2+}$  release flux. A, release flux calculated as sum of all terms in fig. 8 plus the dye removal term in fig. 4D. B, the  $\text{Ca}^{2+}$  release current, calculated from the volume integral of the flux in A. The current in red is calculated from the integral of the dye removal term.

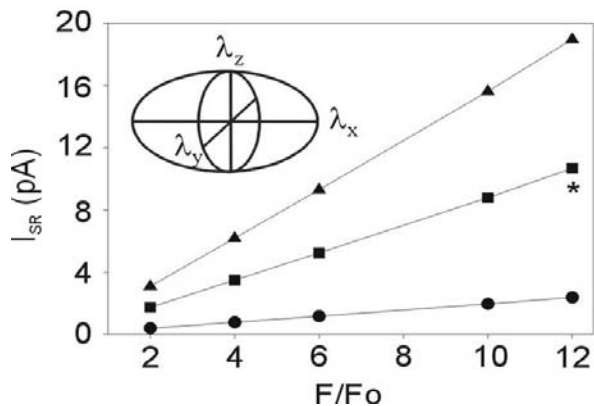


Fig.10. Lower bounds of  $\text{Ca}^{2+}$  release current. For these calculations, the fluorescent indicator is the only buffer. Spark dimensions are given by the FWHM (in  $\mu\text{m}$ ) along the x, y, and z axes, ( $\lambda_x$ ,  $\lambda_y$ ,  $\lambda_z$ ). The inset shows a schematic of an ellipsoidal spark. For a spherical spark  $\lambda_x = \lambda_y = \lambda_z$ . Circles show the current required to produce a spherical spark whose FWHM is 1  $\mu\text{m}$ ; squares are for an elliptical spark (of dimensions 2, 1.5, 1.5) and triangles are for a spherical spark (2, 2, 2). The current varies linearly with the spark amplitude  $F/F_0$ , and the slopes are proportional to the spark volume. Note that this lower estimate is consistent with that represented by the red trace in fig. 9B, considering that the spark analyzed in that figure had a FWHM of 1.5  $\mu\text{m}$  and amplitude  $\sim 2$ . Reproduced from Izu et al. (25).

#### Artificially induced events.

Finally, we will show how the calculations of release flux can be applied to events other than sparks. In the example shown in fig.11 (31), events were induced by application of imperatoxin A, extracted from scorpion venom. The drug induces the long-lasting events of low amplitude marked by arrows in panel A. These events (described in detail in ref. 45) correspond to long lasting open states of reduced conductance, induced by the drug in bilayer experiments (46,47). As shown, they usually start with a spark-like event of greater underlying current. In B and C are temporal and spatial profiles of the event indicated with a white arrow in A. In D is its signal mass, which decays from an early peak to a sustained level, about 8-fold lower. To evaluate the underlying current, the release calculation algorithm described above was applied to an average of 9 such events, represented in E. The resulting release current (panel F) peaks at 11.3 pA and then decays to a steady value averaging 0.68 pA. The peak/steady ratio is 16.6.

A recent report (17), shows that sparks of mammalian skeletal muscle often end with a prolonged *tail* of lower intensity. By analogy with an earlier observation of González et al. (14) on averages of sparks from amphibian muscle under voltage clamp, they termed these prolongations *embers*. The analogy with the events induced by imperatoxin A indicates that the release flux associated with embers is much lower than that during the initial spark.

#### Non-events.

A final question, indicated in the Introduction, is whether sparks constitute all of  $\text{Ca}^{2+}$  release, or there is

a different form. Shirokova and Rios (48) showed that the presence of the local anesthetic tetracaine results in a release without sparks in cells that normally have them. In these experiments, a faint *non-event* increase in fluorescence appeared upon very low depolarization in the absence of the drug, suggesting that this form of release exists normally, being uncovered rather than induced by the drug. Release flux in such cases should be extremely low, and clearly different in temporal and spatial properties from that in sparks. This release has been compared with the so-called *calcium quarks*, postulated to be manifestations of single channel activity (Egger and Niggli, this volume). One possibility is that courses through channels directly controlled by the *t* membrane voltage sensors. Such activity might produce the embers that follow or sometimes precede sparks (section 5.4), or diffuse release in conditions that inhibit spark production.

## CONSEQUENCES AND CONCLUSIONS.

### Single channels and sparks.

The current underlying a spark, 1.5 to 20 pA, should be compared with the physiological unitary current. Mejía-Alvarez et al. (49) reported a unitary current of 0.35 to 0.5 pA through dog cardiac channels in bilayers, carrying  $\text{Ca}^{2+}$  under  $[\text{Ca}^{2+}]$  gradients of physiological magnitude and direction. Kettlun et al. (50) reported a unitary current of  $\sim 0.7$  pA in  $\text{Ca}^{2+}$  release channels from frog skeletal muscle. The reason for the greater current was in part that the channels were kept open by 10 mM caffeine (to avoid underestimates due to flickering). Under the same conditions the cardiac channels carried a current of  $\sim 0.5$  pA. Hence a current of 2.1 pA, as reported by Wang et al. (44), would require 4 simultaneously open channels. A much greater number of open channels would be required with the estimates of spark current of Izu et al. (25). For skeletal muscle sparks, the number of open channels would have to be 10 to 30. A somewhat lower number is obtained from the analysis of release current associated to the events induced by imperatoxin A.

The idea that sparks are produced by several channels is consistent with evidence of multifocal origin of sparks in cardiac muscle (51, 35), and with the demonstration (37) of sources of spatially resolved size, extending along the Z lines in skeletal muscle. It is quite inconsistent with the demonstration (32) that the rising phase of sparks both starts and ends abruptly, as if a single channel gated open and close. If many channels contributed, they should open and close in unison.

### Single channels and global release flux.

These estimates of current per channel or per spark are roughly consistent with whole cell estimates of release flux. We update here a calculation of Shirokova et al. (18). The maxima of flux density under voltage clamp is  $\sim 180$  mM/s in the frog (2,52). The density of release channels can be calculated from morphometry or from ryanodine binding measurements. The ratio of *t* tubule length to fiber volume is  $0.82 \mu\text{m}^{-2}$  in frog twitch muscle(53).

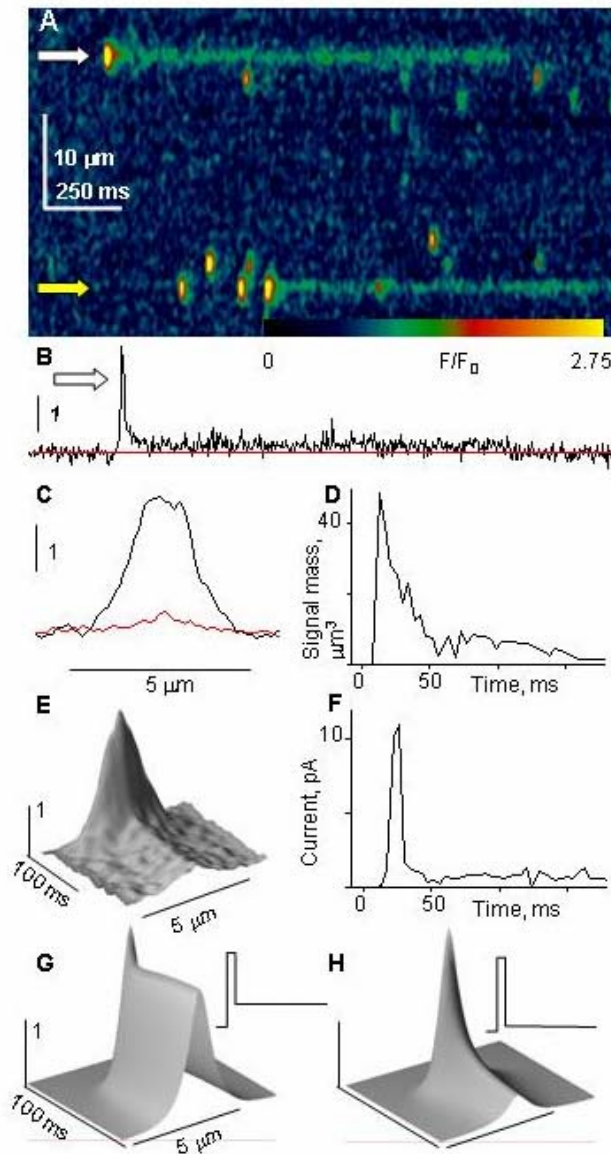


Fig.11. Release flux in drug-induced channel openings. A, image of a permeabilized cell, immersed in solution with 100 nM imperatoxin A. B, temporal profile of  $F/F_0$  at white arrow. C, spatial profile of  $F/F_0$  at the peak of the starter event and its average (red) during the long event that follows. D, time course of signal mass. E,  $F/F_0$  in an average of 9 long events selected by their large amplitude. F, release current, calculated from the average event. G, simulated fluorescence event for a  $\text{Ca}^{2+}$  source of initial current 10 pA, lasting 6 ms, followed by a steady current of 3.3 pA (inset). H, simulation where the opening at 10 pA is followed by a steady 0.5 pA current. The source diameter was 0,05  $\mu\text{m}$ . Details and parameter values of the simulation described in Ríos *et al.* (13). Figure reprinted from González *et al.* (31).

Assuming that 70% of this length is junctional and contains a double row of release channels at 30 nm spacing on each side, the number of channels per liter is  $0.7 \text{ H}33 \text{ channels/row}/\mu\text{m} \times \text{H}2 \text{ rows/junction} \times \text{H}2 \text{ junctions/triad} \times 0.82 \mu\text{m}^{-2}$ , or  $1.08 \times 10^{17}$  channels per liter of the aqueous myoplasmic volume. At 100% activation, such channels passing 0.7 pA would generate

a flux density of 360 mM/s. The unitary current figure of Kettlun *et al.* (50) is consistent with the largest release if channels reach 50% activation.

It is relevant in this regard that the ratio of ryanodine to dihydropyridine sites expected from the structural alignment model of Block *et al.* (54) is 0.5, a value that is found approximately in isolated membrane fractions of rabbit or human muscle (55, 56, 57). In frog muscle the value is instead about 1.5 (56,57), which would suggest an excess of release channels, probably outside the double row. This would predict an even larger maximum release in the morphometric-based calculation above, again indicating that the estimates of release per channel and release per spark are consistent with global release, even at values of open probability well under unity.

In summary, estimates of  $\text{Ca}^{2+}$  release current underlying sparks range between 1.4 and 30 pA, not clearly greater in skeletal than in cardiac muscle. At their low end, the estimates are consistent with generation of sparks by one or two channels, but the results are easier to explain if several channels, from as little as four to as many as 60, cooperate in their generation. Both the release flux and the open time may vary among individual sparks, leading to their varied size and shape. In sparks that end with an ember, release flux must fall from an early level consistent with many open channels, to a level requiring the current of one or two channels. The continued examination of  $\text{Ca}^{2+}$  release flux appears to be an essential requisite for the interpretation of sparks and their place in calcium signaling.

#### Acknowledgments.

We are grateful to all the colleagues and collaborators who allowed us to reprint figures from their work. We were supported by the National Institutes of Health (NIH) and Conicyt, Uruguay.

#### References

1. Cheng, H., W.J. Lederer, and M.B. Cannell. 1993. Calcium sparks: elementary events underlying excitation-contraction coupling in heart muscle. *Science* 262:740-744.
2. Shirokova, N., J. García, G. Pizarro, and E. Ríos.  $\text{Ca}^{2+}$  release from the sarcoplasmic reticulum compared in amphibian and mammalian skeletal muscle. *Journal of General Physiology* 107: 1-18 (1996).
3. Melzer, W., E. Ríos, and M.F. Schneider. Time course of calcium release and removal in skeletal muscle fibers. *Biophys.J.* 45:637-641 (1984).
4. Melzer, W., E. Ríos, and M.F. Schneider. A general procedure for determining the rate of calcium release from the sarcoplasmic reticulum in skeletal muscle fibers. *Biophys.J.* 51:849-863 (1987).
5. Ríos, E. and G. Pizarro. Voltage sensors and channels of excitation-contraction coupling. *News Physiol. Sci.* 3, 223-227.(1988)
6. Baylor, S.M., W.K. Chandler, and M.W. Marshall. Sarcoplasmic reticulum calcium release in frog skeletal muscle fibres estimated from Arsenazo III calcium transients. *J.Physiol.(Lond.)* 344: 625-666 (1983).
7. Ríos E. and G. Pizarro, Voltage sensor of excitation-contraction coupling in skeletal muscle. *Physiol Rev.* 71(3):849-908 (1991)
8. González A. and E. Ríos. Perchlorate enhances transmission in skeletal muscle excitation-contraction coupling. *J Gen Physiol.* 102(3):373-421 (1993).
9. Pape, P.C., D.S. Jong, and W.K. Chandler. Calcium release and its voltage dependence in frog cut muscle fibers

- equilibrated with 20 mM EGTA. *J.Gen.Physiol.* 106: 259-336 (1995).
10. Rakowski R.F., P.M. Best, M.R. James-Kracke. Voltage dependence of membrane charge movement and calcium release in frog skeletal muscle fibres. *J Muscle Res Cell Motil.* 6(4): 403-33 (1985)
  11. García J, G. Pizarro, E. Ríos, E. Stefani Effect of the calcium buffer EGTA on the "hump" component of charge movement in skeletal muscle. *J Gen Physiol.* 97(5):885-96 (1991).
  12. Baylor, S.M. and S. Hollingworth. Measurement and Interpretation of Cytoplasmic [Ca<sup>2+</sup>]. *News Physiol Sci.* 2000 Feb;15:19-26 (2000).
  13. Ríos E., M.D. Stern, A. González, G. Pizarro, N. Shirokova. Calcium release flux underlying Ca<sup>2+</sup> sparks of frog skeletal muscle. *J Gen Physiol.* 114(1):31-48 (1999).
  14. González, A., W.G. Kirsch, N. Shirokova, G. Pizarro, M.D. Stern, and E. Ríos. The spark and its ember: separately gated local components of Ca(2+) release in skeletal muscle. *J Gen Physiol.* 115(2):139-58 (2000a).
  15. Lacampagne, A., M.G. Klein, and M.F. Schneider. Modulation of the frequency of spontaneous sarcoplasmic reticulum Ca<sup>2+</sup> release events (Ca<sup>2+</sup> sparks) by myoplasmic [Mg<sup>2+</sup>] in frog skeletal muscle. *J.Gen.Physiol.* 111:207-224 (1998).
  16. Baylor, S.M., J. Peet, W.K. Chandler and S. Hollingworth Comparison of resting and voltage activated calcium sparks in intact skeletal muscle fibers of R. Temporaria and R. Pipiens. *Biophys J.* 80:66a (2001)
  17. Kirsch, W., D. Uttenweiler and R.H.A. Fink. Spark- and ember-like elementary Ca<sup>2+</sup> release events in skinned fibres of adult mammalian skeletal muscle. *J.Physiol* ((2001, in press)
  18. Shirokova N, A. Gonzalez, W.G. Kirsch, E. Rios, G. Pizarro, M.D. Stern, H. Cheng. Calcium sparks: release packets of uncertain origin and fundamental role. *J Gen Physiol.* 113:377-84 (1999).
  19. Tanaka, H., K. Nishimaru, T. Sekine, T. Kawanishi, R. Nakamura, K. Yamagaki and K. Shigenobu. Two-dimensional millisecond analysis of intracellular Ca<sup>2+</sup> sparks in cardiac myocytes by rapid scanning confocal microscopy: increase in amplitude by isoproterenol. *Biochem. Biophys. Res. Commun.* 233:413-418 (1997).
  20. Lukyanenko, V., and S. Gyöke. (1999) Ca<sup>2+</sup> sparks and Ca<sup>2+</sup> waves in saponin-permeabilized rat ventricular myocytes. *J Physiol* 521: 575-585 (1999).
  21. Smith, G.D., J.E. Keizer, J.D. Stern, W.J. Lederer, and H. Cheng. A simple numerical model of calcium spark formation and detection in cardiac myocytes. *Biophys. J.* 75:15-32 (1998).
  22. Santana, L.F., E.G. Kranias, and W.J. Lederer. Calcium sparks and excitation-contraction coupling in phospholamban-deficient mouse ventricular myocytes. *J. Physiol.* 503: 21-29 (1997).
  23. Wier W.G., H.E. ter Keurs, E. Marban, W.D. Gao, C.W. Balke. Ca<sup>2+</sup> 'sparks' and waves in intact ventricular muscle resolved by confocal imaging. *Circ Res.* 81:462-9 (1997).
  24. Harkins, A.B., N. Kurebayashi, and S.M. Baylor. Resting myoplasmic free calcium in frog skeletal muscle fibers estimated with fluo-3. *Biophys.J.* 65: 865-881 (1993).
  25. Izu, L.T., J.R. Mauban, C.W. Balke, W.G. Wier. Large currents generate cardiac Ca<sup>2+</sup> sparks. *Biophys J.* 80(1): 88-102 (2001).
  26. González, A., J. Zhou, W.G. Kirsch, D. Uttenweiler, R.A. Fink, E. Ríos and G. Brum. Morphology of Ca<sup>2+</sup> sparks of mammalian muscle. *Biophys. J. Abst.* (2002, in Press).
  27. Pratusевич, V.R., and C.W. Balke. Factors shaping the confocal image of the calcium spark in cardiac muscle cells. *Biophys.J.* 71: 2942-2957 (1996).
  28. Cheng, H., L.S. Song, N. Shirokova, A. González, E.G. Lakatta, E. Ríos, and M.D. Stern. Amplitude distribution of calcium sparks in confocal Images. Theory and studies with an automatic detection method. *Biophys.J.* 76:606-617 (1999).
  29. Izu, L.T., W.G. Wier, and C.W. Balke. Theoretical analysis of the Ca<sup>2+</sup> spark amplitude distribution. *Biophys.J.* 75: 1144-1162 (1998).
  30. Ríos E., N. Shirokova, W. Kirsch, G. Pizarro, M.D. Stern, H. Cheng and A. González. A preferred amplitude of calcium sparks in skeletal muscle. *Biophys J.* 80(1):169-83 (2001).
  31. González, A., W.G. Kirsch, N. Shirokova, G. Pizarro, G. Brum, I.N. Pessah, M.D. Stern, H. Cheng and E. Ríos. Involvement of multiple intracellular release channels in calcium sparks of skeletal muscle. *Proc Natl Acad Sci* 97(8):4380-5 (2000b).
  32. Lacampagne, A., C.W. Ward, M.G. Klein, and M.F. Schneider. Time course of individual voltage-activated Ca<sup>2+</sup> sparks recorded at ultra-high time resolution in frog skeletal muscle. *J. Gen. Physiol.* 113:187-198.
  33. Jiang, Y.H, Klein, M.G., Schneider, M.F. 1999 Numerical simulation of Ca<sup>2+</sup> "sparks" in skeletal muscle. *Biophys J.* 77(5): 2333-57 (1999).
  34. Sun, X. P., N. Callamaras, J.S. Marchant and I. Parker. A continuum of InsP<sub>3</sub>-mediated elementary Ca<sup>2+</sup> signalling events in *Xenopus* oocytes. *J. Physiol.* 509, 67-80 (1998).
  35. Blatter, L.A., J. Hüser, and E. Ríos. Sarcoplasmic reticulum Ca<sup>2+</sup> release flux underlying Ca<sup>2+</sup> sparks in cardiac muscle. *Proc.Natl.Acad.Sci.U.S.A* 94:4176-4181 (1997).
  36. Lukyanenko, V., T.F. Wiesner, and S. Gyöke. Termination of Ca<sup>2+</sup> release during Ca<sup>2+</sup> sparks in rat ventricular myocytes. *J. Physiol.* 507:667-677 (1998).
  37. Brum G, A. González, J. Rengifo, N. Shirokova and E. Ríos. Fast imaging in two dimensions resolves extensive sources of Ca<sup>2+</sup> sparks in frog skeletal muscle. *J. Physiol.* 528:419-33 (2000).
  38. Ríos, E., and M.D. Stern. Calcium in close quarters: microdomain feedback in excitation-contraction coupling and other cell biological phenomena. *Annu.Rev.Biophys.Biomol.Struct.* 26:47-82 (1997).
  39. Smith P.D., G.W. Liesegang, R.L. Berger, G. Czerlinski, R.J. Podolsky. A stopped-flow investigation of calcium ion binding by ethylene glycol bis(beta-aminoethyl ether)-N,N'-tetraacetic acid. *Anal Biochem.* 143:188-95 (1984).
  40. Baylor, S.M. and S. Hollingworth. The transient binding of calcium to ATP and diffusion of Ca-ATP help shape the amplitude and time course of the myoplasmic free Ca transients. *Biophys. J.* 74:A235 (1998).
  41. Kushmerick, M.J. and R.J. Podolsky. Ionic mobility in muscle cells. *Science.* 166(910):1297-8 (1969).
  42. Pechère, J.F., J.P. Capony and J. Demaille. Evolutionary aspects of the structure of muscular parvalbumins. *Syst. Zool.* 22:533-548 (1973).
  43. Pizarro G, L. Csernoch, I. Uribe, M. Rodriguez and E. Ríos. The relationship between Q gamma and Ca release from the sarcoplasmic reticulum in skeletal muscle. *J Gen Physiol.* 97:913-47 (1991)
  44. Wang S.Q., L.S. Song, E.G. Lakatta and H. Cheng. Ca<sup>2+</sup> signalling between single L-type Ca<sup>2+</sup> channels and ryanodine receptors in heart cells. *Nature.* 410(6828): 592-6 (2001).
  45. Shtifman A., C.W. Ward, J. Wang, H.H. Valdivia and M.F. Schneider. Effects of imperatoxin A on local sarcoplasmic reticulum Ca(2+) release in frog skeletal muscle. *Biophys J.* 79(2): 814-27 (2000).
  46. Tripathy, A., W. Resch, L. Xu, H. H. Valdivia, and G. Meissner. 1998 Imperatoxin A induces subconductance states in Ca<sup>2+</sup> release channels (ryanodine receptors) of cardiac and skeletal muscle. *J. Gen. Physiol.* 111:679-690 (1998).
  47. Gurrola, G. B., Arevalo, C., Sreekumar, R., Lokuta, A.J., Walker, J. W. and Valdivia, H. H. Activation or ryanodine receptors by imperatoxin A and a peptide segment of the II-III loop of the dihydropyridine receptor. *J. Biol. Chem.* 274:7879-7886 (1999).
  48. Shirokova N. and E. Ríos. Small event Ca<sup>2+</sup> release: a probable precursor of Ca<sup>2+</sup> sparks in frog skeletal muscle. *J Physiol.* 502:3-11 (1997).
  49. Mejía-Alvarez, R., C. Kettlun, E. Ríos, M.D. Stern, and M. Fill. Unitary Ca<sup>2+</sup> current trough cardiac ryanodine receptor channels under quasi-physiological ionic conditions. *J.Gen.Physiol.* 113:177-186 (1999).

50. Kettlun, C., A. González, W. Nonner, E. Ríos and M. Fill. Ryanodine receptor unitary Ca<sup>2+</sup> current is greater in frog skeletal muscle than in mammalian heart. *Biophys. J.* 78:2576 (2000).
51. Parker, I., W.J. Zang, and W.G. Wier. Ca<sup>2+</sup> sparks: involving multiple Ca<sup>2+</sup> release sites along Z-lines in rat heart cells. *J. Physiol.* 497:31-38 (1996).
52. Mobley B.A and B.R. Eisenberg. Sizes of components in frog skeletal muscle measured by methods of stereology. *J Gen Physiol.* 66(1):31-45 (1975).
53. Block, B.A., T. Imagawa, K.P. Campbell, and C. Franzini-Armstrong. Structural evidence for direct interaction between the molecular components of the transverse tubule/sarcoplasmic reticulum junction in skeletal muscle. *J. Cell Biology* 107: 2587-2600 (1988).
54. Bers, D.M., and V.M. Stiffel. Ratio of ryanodine to dihydropyridine receptors in cardiac and skeletal muscle and implications for E-C coupling. *Am.J.Physiol.* 264: C1587-C1593 (1993).
55. Margreth, A., E. Damiani, and G. Tobaldin. Ratio of dihydropyridine to ryanodine receptors in mammalian and frog twitch muscles in relation to the mechanical hypothesis of excitation-contraction coupling. *Biochem Biophys Res Commun* 197:1303-1311 (1993).
56. Anderson, K., A.H. Cohn and G. Meissner. High-affinity [3H]PN200-110 and [3H]ryanodine binding to rabbit and frog skeletal muscle. *Am J Physiol* 266:C462-6 (1994)
57. Cheng, H., M.R. Lederer, W.J. Lederer and M.B. Cannell. Calcium sparks and [Ca<sup>2+</sup>]<sub>i</sub> waves in cardiac myocytes. *Am. J. Physiol. Cell.* 270: C148-C159 (1996).

## Endnotes

<sup>1</sup>Unlike Baylor et al. (1983), Melzer and coworkers included transport by the SR pump in their removal model, hence their *R* is release proper, rather than the net balance of SR fluxes yielded by the other method.

<sup>2</sup>In a Gaussian approximation of sparks, the volume integral of a spherically symmetric Gaussian function of standard deviation  $\sigma$  and central value 1 is  $(2\pi)^{3/2}\sigma^3 = B$ . Then the signal mass of a spark of amplitude *A* should be *AB*. For Gaussian sparks,  $\text{FWHM} = 2(2 \ln 2)^{1/2} \sigma$ ; then signal mass =  $A(\pi/4 \ln 2)^{3/2} (\text{FWHM})^3$ . This is greater than the approximation of Shirokova et al. by a factor of 2.304.

<sup>3</sup>In general, flux is defined as a rate of movement of matter across the unit area of a defined surface, and it has vectorial properties. In the present analysis, there is no specified surface, hence the flux is defined as a scalar, and is distributed in the volume, thereby losing one spatial dimension.

<sup>4</sup>CALCULATION DETAILS. The terms  $[b:Ca^{2+}]$  are calculated from the function  $[Ca^{2+}](x,t)$  solving for  $[b:Ca^{2+}]$  the diffusion-reaction equation of form 3 for the corresponding buffer. In general this requires simultaneously solving an equation for the free buffer (see for instance eqns. 1-4 in ref 38). This is avoided assuming that the free buffer and its Ca<sup>2+</sup>-complex have the same diffusion coefficient, or equivalently that total buffer concentration is constant everywhere. In the case of parvalbumin and ATP, buffers that react with both Ca<sup>2+</sup> and Mg<sup>2+</sup>, diffusion reaction equations of the form 3 still apply, but  $[b:Ca^{2+}]$  is in both cases equal to  $[b]_T - [b] - [b:Mg^{2+}]$  (where  $[b]_T$  is the total concentration of buffer), and  $[b:Mg^{2+}]$ , a function of space and time, is calculated from its own

diffusion-reaction equation,

$$\frac{\partial [b : Mg^{2+}](x,t)}{\partial t} = [b](x,t) [Mg^{2+}] k_{ON} - [b : Mg^{2+}](x,t) k_{OFF} + D_b \Delta [b : Mg^{2+}](x,t) \quad (7)$$

assuming  $[Mg^{2+}]$  to be constant.

## Running title:

*Ca<sup>2+</sup> release in sparks.*

## Keywords:

*Skeletal muscle, cardiac muscle, ion channels, sarcoplasmic reticulum, calcium signaling.*

## Correspondence:

E. Ríos

Phone: (312)-942-2081.

Fax: (312)-942-8711.

erios@rush.edu

# Initiation and Termination of Calcium Sparks in Skeletal Muscle

Martin F. Schneider and Christopher W. Ward

Department of Biochemistry and Molecular Biology, University of Maryland School of Medicine 108 N. Greene St, Baltimore, MD 21201 Email: [mschneid@umaryland.edu](mailto:mschneid@umaryland.edu)

**ABSTRACT** Depolarization of the transverse tubules of a skeletal muscle fiber initiates release of  $\text{Ca}^{2+}$  ions via ryanodine receptor (RyR)  $\text{Ca}^{2+}$  release channels in the adjacent junctional sarcoplasmic reticulum (SR) membrane at triad junctions. Discrete localized  $\text{Ca}^{2+}$  release events ( $\text{Ca}^{2+}$  "sparks") detected by confocal imaging of  $\text{Ca}^{2+}$  indicator-containing muscle fibers may arise from the coordinated opening of a small group of RyR  $\text{Ca}^{2+}$  release channels, or possibly even from the opening of a single channel. These discrete  $\text{Ca}^{2+}$  release events originate at triad junctions and can be gated by fiber depolarization or by physiological cytosolic ligands in functioning muscle fibers. The global increase in myoplasmic  $\text{Ca}^{2+}$  during fiber depolarization appears to consist of the summation of huge numbers of  $\text{Ca}^{2+}$  sparks initiated during a brief time interval. Study of  $\text{Ca}^{2+}$  sparks thus offers a unique window into the operation of groups of SR  $\text{Ca}^{2+}$  release channels or individual channels within the normal structural and molecular environment of a functioning fiber. The  $\text{Ca}^{2+}$  release underlying a spark appears to turn on and off abruptly respectively at the start and at the peak of a spark. Under many stimuli, the frequency and/or pattern of occurrence of the  $\text{Ca}^{2+}$  sparks is altered, indicating changes in the closed time (or opening rate) of the channels that initiate the sparks. In contrast, the average values of the spatio-temporal properties of the individual events generally remain unchanged, indicating constancy of channel open time and constancy of total  $\text{Ca}^{2+}$  efflux via the channels generating a spark. The few conditions that alter the average properties of  $\text{Ca}^{2+}$  sparks provide rare insights regarding the open-time of the  $\text{Ca}^{2+}$  channels generating the  $\text{Ca}^{2+}$  spark.

## GENERAL BACKGROUND AND EARLY OBSERVATIONS OF $\text{Ca}^{2+}$ SPARKS

### Excitation-contraction coupling

Activation of skeletal muscle occurs over a time scale of ms or at most a few tens of msec. Special systems have evolved for achieving relatively large and fast release of calcium ions from the calcium-sequestering internal membrane system (SR) in skeletal muscle. Ryanodine receptor (RyR)  $\text{Ca}^{2+}$  release channels in the SR terminal cisternae membrane have a large cytosolic domain, the junctional foot, that spans the gap between the junctional SR and the adjacent transverse tubule (TT) and thus provides a structural basis for rapid direct or indirect molecular interaction between an RYR and a dihydropyridine receptor (DHPR) voltage sensor in the TT membrane. The voltage sensor responds to the change in TT membrane potential and directly initiates physiological  $\text{Ca}^{2+}$  release from the apposed RyR  $\text{Ca}^{2+}$  release channel without the need for entry of  $\text{Ca}^{2+}$  ions from the extracellular solution, the hallmark of "skeletal-type" EC coupling.

### "Macroscopic" and "Microscopic" SR $\text{Ca}^{2+}$ release in muscle fibers

Average cytosolic  $[\text{Ca}^{2+}]$  transients due to the combined activity of large numbers of calcium release channels in a single muscle fiber have been monitored by many laboratories in functionally intact skeletal muscle fibers. Such global or "macroscopic"  $\text{Ca}^{2+}$  transients have been analyzed to calculate the time course of the overall rate of release of calcium

from the SR in our own (1, 2) and other (3) laboratories. The resulting release wave form, which exhibits an early peak followed by a decline to a more maintained steady level during a voltage clamp depolarization (1), corresponds to the "macroscopic" calcium efflux through the population of SR calcium release channels throughout the muscle fiber, equivalent to a macroscopic calcium current across the SR membrane. In 1995 "microscopic" calcium release events ( $\text{Ca}^{2+}$  "sparks"), which may underlie the macroscopic calcium release waveform, were detected in skeletal muscle (4, 5) after having been first identified in cardiac myocytes (6). The  $\text{Ca}^{2+}$  sparks presumably occur in such high frequency and large numbers during depolarization of a muscle fiber that the individual events become indistinguishable during the macroscopic  $[\text{Ca}^{2+}]$  transient (7). The development of experimental conditions under which  $\text{Ca}^{2+}$  sparks could be observed and characterized constituted a major advance in the study of SR  $\text{Ca}^{2+}$  release in skeletal muscle. The ability to monitor  $\text{Ca}^{2+}$  sparks has revolutionized the study of SR channel behavior in functioning muscle fibers (eg, 8, 9, 10). Because of their robust properties and ease of experimental manipulation, single frog twitch skeletal muscle fibers have been utilized for the studies reviewed here unless otherwise indicated.

### Initial observations of $\text{Ca}^{2+}$ sparks in skeletal muscle

Our early work on  $\text{Ca}^{2+}$  sparks, as well as work at the same time in the Rios laboratory, developed procedures for studying both voltage activated and "spontaneous" (ie, ligand-activated)  $\text{Ca}^{2+}$  sparks in

skeletal muscle fibers. By using an extracellular dye that enters the transverse tubules and thus marks their location (11), we were able to identify the TT location in our fibers and to establish that voltage activated  $\text{Ca}^{2+}$  sparks were centered at the triads (7), as were the spontaneous release events. This is as expected since the calcium release channels are localized in the junctional SR membrane at the triad.

Our initial results showed that calcium sparks occurred during small depolarizations of fully polarized skeletal muscle fibers and also occurred "spontaneously" in fully polarized or fully depolarized fibers (5, 7). As in cardiac myocytes (6), these events were thought to correspond to the opening of functionally linked groups of a few SR calcium release channels or even of individual SR channels.

In fully polarized fibers, discrete  $\text{Ca}^{2+}$  sparks could be resolved only during relatively small depolarizations because during larger depolarizations the individual events were obscured by the large overall rise in fluorescence. However, over the limited range of depolarizations during which discrete events could be discerned, the event frequency increased steeply with increasing depolarization (e-fold in about 3 to 4 mV; (7)). We thus hypothesize that the macroscopic calcium transient generated during full activation of a fiber is due to the combined result of large numbers of discrete release events occurring at a frequency that is too high to allow resolution of individual events. The ability to detect and characterize these discrete release events provides an exciting and novel approach to gaining new understanding of SR channel activity in functioning muscle fibers.

## Considerations in imaging $\text{Ca}^{2+}$ sparks

### Generation of a $\text{Ca}^{2+}$ spark

Following the initiation of a  $\text{Ca}^{2+}$  spark there is a rise in local fluorescence (Fig. 1) that is comprised of an increase in the concentration of  $\text{Ca}^{2+}$ -fluo-3 within the confocal volume. This implies that  $\text{Ca}^{2+}$  entry into the confocal volume must exceed the net effect of  $\text{Ca}^{2+}$  "removal" by binding and diffusion out of the confocal volume. Thus, during the rising phase of a spark,  $\text{Ca}^{2+}$  ions are being released from the channel or channels responsible for generating the spark. In contrast, during the falling phase of fluorescence in a spark, there is a net reduction of  $\text{Ca}^{2+}$ -fluo-3 in the confocal volume, indicating that  $\text{Ca}^{2+}$  binding and  $\text{Ca}^{2+}$  diffusion out of the confocal volume exceed  $\text{Ca}^{2+}$  entry. Since the diffusion and  $\text{Ca}^{2+}$  binding properties of the myofibril are unlikely to change significantly during the spark, the declining phase of a spark must correspond to a period during which  $\text{Ca}^{2+}$  release occurs at a much lower rate than during the rising phase. In the extreme case, following spark activation  $\text{Ca}^{2+}$  release could occur at an approximately constant rate during the rising phase of the spark, and then stop completely during the falling phase. The duration of the rising phase of a  $\text{Ca}^{2+}$  spark thus provides a lower bound estimation of the time of  $\text{Ca}^{2+}$  release from the channel or channels generating the spark. Furthermore, the time course of the rising phase of a

spark may provide important information concerning the degree of synchrony of possible multiple channels generating the spark. In contrast, the spark amplitude provides a measure of the total amount of  $\text{Ca}^{2+}$  released in the event.

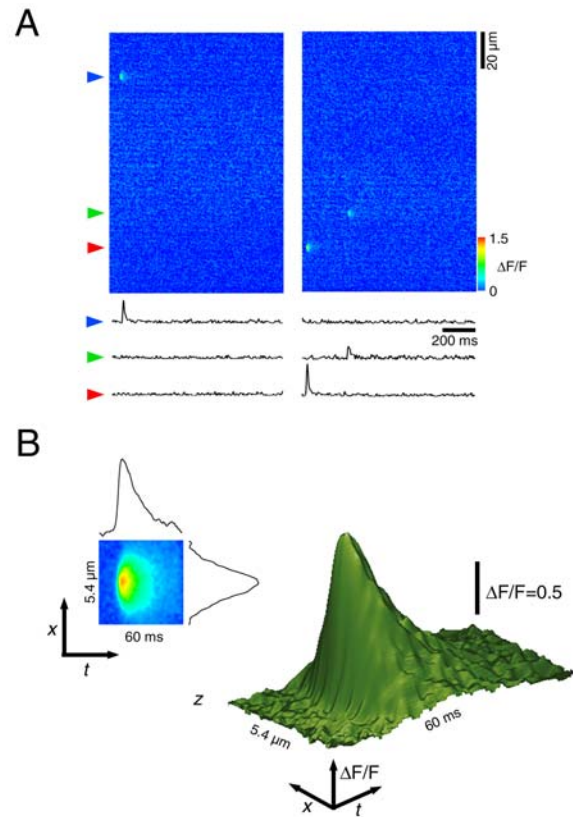


Figure 1.  $\text{Ca}^{2+}$  sparks in frog skeletal muscle A. Two successive line scan images (2 ms/line, 1 sec total time/image, pseudo-color  $\Delta\text{F}/\text{F}$  presentation) of a permeabilized frog skeletal muscle fiber equilibrated with Fluo-3 containing internal solution ( $[\text{Mg}^{2+}]_{\text{free}}=0.65$ ) are presented. Three  $\text{Ca}^{2+}$  sparks are apparent as discrete localized increases in fluorescence. Temporal  $\Delta\text{F}/\text{F}$  fluorescence profiles of select spatial locations (arrowheads) are presented below. B. 93  $\text{Ca}^{2+}$  sparks were spatially centered and temporally shifted to the 50% rise-time to construct a signal averaged event. The pseudo-color xt plot (left) is presented with spatial and temporal fluorescence profiles extracted through the peak of the fluorescence. A surface plot representation (right) provides a view of the temporal and spatial characteristics of the averaged  $\text{Ca}^{2+}$  spark.

### Out of focus events: effects on rise-time and amplitude

One technique used to image spatially localized, subcellular fluorescent transients (e.g.,  $\text{Ca}^{2+}$  sparks) is the use of a laser scanning confocal microscope (LSCM) in conjunction with  $\text{Ca}^{2+}$  indicator dyes. The LSCM limits the spatial sampling of fluorescence based on its ability to physically limit the detection of emission photons which are out of the focus volume of the microscope objective. This spatially restricted sampling volume can be estimated

by examining the point spread function of the LSCM, which for our consideration, can be roughly approximated as a spherical volume of approximately 1 $\mu$ m diameter. While confocal imaging provides restricted spatial sampling ability, the interpretation of the fluorescence signal (i.e., the shape of the Ca<sup>2+</sup> spark) can be affected by Ca<sup>2+</sup> diffusing out of the plane of focus as well as by events occurring some distance from the scanned line. Numerical simulation of the Ca<sup>2+</sup> spark morphology as a function of the distance of Ca<sup>2+</sup> spark generation from the sampling volume results in significant decrease in amplitude of the spark with increasing distance from the sampled volume, but much less alteration in the rise-time (12, 13)

#### **Rep-mode events exhibit constancy of released Ca<sup>2+</sup>**

Under conditions of very low activation, voltage activated and ligand activated Ca<sup>2+</sup> sparks appear in a stochastic manner and on average occur very rarely at any given triad. As an exception to this, a second mode of Ca<sup>2+</sup> spark activation (*rep-mode*) was identified in which, at low levels of overall activation, Ca<sup>2+</sup> release events occurred repetitively in a single triad at rates >100 fold the rate in the remaining triads (14). The events within a given *rep-mode* train were of similar amplitude and spatio-temporal extent, suggesting that each of these events arose from release of the same amount of Ca<sup>2+</sup> from a given group of channels within the same triad. Analysis of the inter-spark intervals revealed a lack of repetitive events occurring at very short intervals which is consistent with the need for the underlying channel unit to recover from inactivation prior to subsequent reactivation in the train. Additionally, the population of sparks within the *rep-mode* trains were similar in spatio-temporal characteristics to a population of singly occurring sparks in the same fibers consistent with a common mode of inactivation for both groups. Since the events in a *rep-mode* train arise from a given triad, all are the same distance from the scan line and thus are all recorded with the same relative distortion of amplitude and rise-time.

#### **Number of channels in the confocal volume at a triad**

It is important to take into account the structural composition of the skeletal muscle triad when interpreting the confocal imaging of Ca<sup>2+</sup> release. A detailed consideration of the shape, size and distribution of calcium release units and the functional coupling of these units to voltage sensors (i.e., couplons) has recently been published (15) Due to the limited scope of this review, we limit our consideration to an estimate of the number of Ca<sup>2+</sup> release channels sampled at each triad during confocal line scan imaging. In frog twitch fibers, a 1 $\mu$ m diameter sphere, which very roughly approximates the sampled confocal volume, includes about 50-100 RyR Ca<sup>2+</sup> release channels at each triad.

## **VOLTAGE-ACTIVATED Ca<sup>2+</sup> SPARKS**

### **Repriming protocol for studying voltage-activated events**

In fully polarized fibers, voltage elicited Ca<sup>2+</sup> sparks can only be clearly discerned during small depolarizations, which severely limits the study of voltage dependence of these events. In order to study voltage activated Ca<sup>2+</sup> sparks over the entire range of membrane potentials, we exploited a "repriming" protocol (16, 17) to avoid the large [Ca<sup>2+</sup>] transients which would otherwise obscure any discrete events during large depolarizations of fully polarized fibers. Starting with a chronically depolarized muscle fiber, we restore only a small fraction of the TT DHPR voltage sensors from the inactivated ("immobilized") state by brief repolarization (18, 19) and then activate the restored voltage sensors by depolarization (Fig. 2). We found that when a small group of reprimed voltage sensors is driven to their activating conformation by a large depolarization after brief repriming, calcium sparks similar to those activated by small depolarization of the same fully polarized fiber were observed (17). Ca<sup>2+</sup> released from RyRs coupled to and directly opened by activated voltage sensors may secondarily activate neighboring RyRs (Fig. 2) by calcium induced calcium release (CICR). Although it is impossible to resolve individual events during large depolarizations in a fully primed fiber, our results to date with partially reprimed fibers appear to be consistent with the hypothesis that large macroscopic releases are composed of the summation of a large number of individual calcium sparks occurring at a high frequency. Thus, knowledge of the properties of the underlying release events provides crucial information for understanding of the macroscopic voltage activated calcium release in a fully primed Fiber.

### **Initiation of Ca<sup>2+</sup> sparks during step depolarization**

Following brief repriming of a chronically depolarized fiber, step depolarizations reveal discrete Ca<sup>2+</sup> sparks occurring at individual triads. Analysis of the frequency of event occurrence relative to the start of a depolarization (i.e., latency histogram) provides an indication of the voltage dependent gating pattern of the available Ca<sup>2+</sup> channels at the triad. Our results show that during a large depolarization, which should rapidly and maximally activate all reprimed voltage sensors, the event latency histogram exhibits a marked early peak, corresponding to a burst of sparks within the first few ms of the pulse, followed by a much lower maintained steady rate of sparks (10). By using a moderate repriming time, the full voltage dependence of the frequency of events both during the peak rate at the start of a pulse, and during the steady level later in the pulse was determined (10). With increasing voltage, the total event frequency as well as an increase in the clustering of events near the initiation time of the voltage pulse was evident. In addition, analysis determined no differences in spatio-temporal properties of the Ca<sup>2+</sup> sparks based

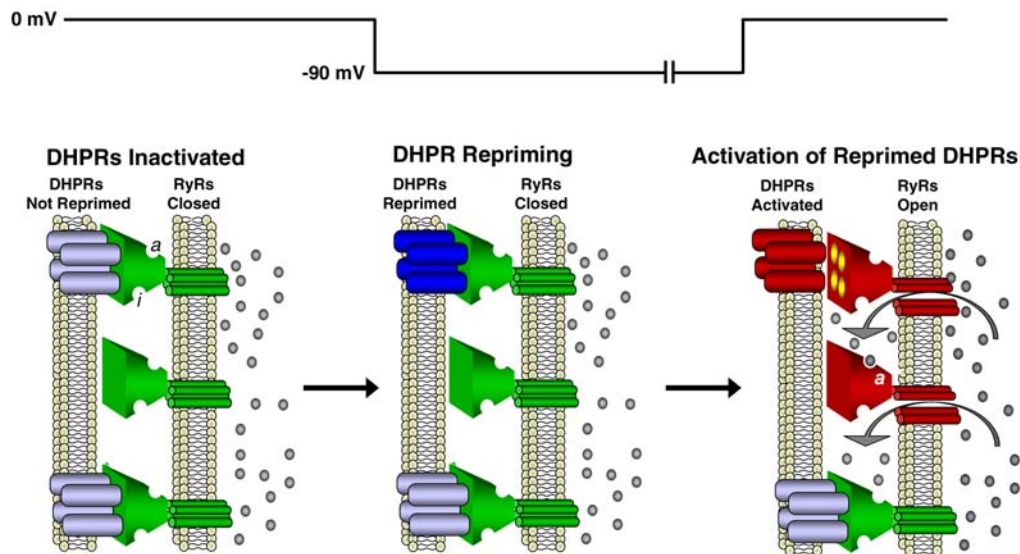


Figure 2. Cartoon depiction of the proposed states of the DHPR and RyR following brief repriming and subsequent depolarization in a chronically depolarized frog skeletal muscle fiber. DHPR voltage sensors are depicted as coupling with alternating RyRs. Ligand ( $\text{Ca}^{2+}/\text{Mg}^{2+}$ ) binding sites for activation by  $\text{Ca}^{2+}$  (a) and inactivation (i) by  $\text{Ca}^{2+}$  of  $\text{Mg}^{2+}$  are represented on each RyR  $\text{Ca}^{2+}$  release channel. Chronic fiber depolarization to 0 mV leads to inactivation of DHPR voltage sensors. In this condition the DHPRs coupled to RyRs are unable to initiate RyR opening. During a brief repriming period to  $-90$  mV, a small fraction of the DHPRs are reprimed for activation (blue DHPR, top) and subsequent depolarizations activate the reprimed DHPRs (red) and initiate RyR (red)  $\text{Ca}^{2+}$  release from RyRs coupled to the activated DHPR voltage sensor.  $\text{Ca}^{2+}$  release from the voltage coupled RyR channel can also activate neighboring RyRs to open by CICR due to the locally elevated  $[\text{Ca}^{2+}]_i$ .

on position of occurrence relative to the pulse suggesting that the underlying channel behavior and conductance was voltage independent.

### Pattern of occurrence of $\text{Ca}^{2+}$ sparks determines release wave form

Since the properties of  $\text{Ca}^{2+}$  sparks were voltage independent, we could assume that the rate of  $\text{Ca}^{2+}$  efflux via the open channel(s) underlying a spark to be on average the same for all events. We then could use the latency histogram together with the mean spark rise time (which provides a measure of the overall time for  $\text{Ca}^{2+}$  efflux during each event) to construct a time course of  $\text{Ca}^{2+}$  release from the SR due to the identified sparks (10). For large depolarizing test pulses we obtained a peaked release wave form, generally similar to the macroscopic rate of release wave forms calculated previously from average global  $[\text{Ca}^{2+}]_i$  transients in fully polarized fibers (1, 3), but possibly showing a somewhat more pronounced peak. Based on these findings, we were able to conclude that the voltage dependence in the  $\text{Ca}^{2+}$  release flux waveform is due to the temporal occurrence of individual  $\text{Ca}^{2+}$  sparks whose individual properties are independent of voltage.

### RyR isoforms and voltage sensor coupling to RyRs

RyRs coupled to TT voltage sensors (DHPRs) alternate with non-coupled RyRs along a "checkerboard" double row in toadfish swim bladder

muscle (20), and the same arrangement may occur in frog muscle. Two RyR isoforms, 1 and 3 or their homologues (alpha and beta in amphibian muscle) are expressed in skeletal muscle. RyR1 but not 3 organizes DHPRs (21, 22) and supports skeletal EC coupling (23). Thus, the coupled RyRs (Fig 1) must be RyR1. Toadfish swim bladder expresses only RyR1, so by inference the intervening non-coupled RyRs in frog muscle could also be RyR1. In that case, RyR3, which is expressed at the same level as RyR1 in frog muscle, would be located in the recently described row of non-coupled parajunctional RyR's (24) that runs on either side of the double row of alternating coupled and non coupled RyRs (above). The functional significance for  $\text{Ca}^{2+}$  sparks of such a possible isoform arrangement remains to be determined. However, in the dyspedic myotube cell system, exclusive expression of RyR3 causes the appearance of both isolated and *rep-mode*  $\text{Ca}^{2+}$  sparks having properties very similar to  $\text{Ca}^{2+}$  sparks in frog skeletal muscle fibers (25). Furthermore, myotubes from both RyR1 (26) and RyR3 (27, 28) KO mice exhibit  $\text{Ca}^{2+}$  sparks, as do dyspedic myotubes expressing RyR1 (29) and adult mammalian muscle fibers expressing exclusively RyR1 (30). Thus either isoform seems capable of generating a  $\text{Ca}^{2+}$  spark.

## TIME COURSE OF $\text{Ca}^{2+}$ RELEASE DURING AN INDIVIDUAL SPARK

### Abrupt turn-on and turn-off of $\text{Ca}^{2+}$ release in a spark

Studies of  $\text{Ca}^{2+}$  sparks in both skeletal and cardiac muscle have used laser scanning confocal microscope systems with galvanometer mirrors which scan the sample at rates of 1.5-2 ms per line. Since the rising phase of a typical  $\text{Ca}^{2+}$  spark is on the order of 4-6 ms, these systems provide only 2-3 time points, which is clearly insufficient to resolve details of the kinetics of the rising phase of the spark. In order to investigate the kinetic detail of  $\text{Ca}^{2+}$  sparks we have used a confocal system based on a resonant galvanometer for increased speed of scanning. This system, developed by Dr. Roger Tsien (31) and subsequently developed commercially by Nikon (RCM 8000) is used to image  $\text{Ca}^{2+}$  spark events at the standard video rate of 63  $\mu\text{s}$  per scan line, about 30 times faster than conventional confocal systems.

Figure 3 displays a representative image strip of a  $\text{Ca}^{2+}$  spark as well as corresponding  $\Delta\text{F}/\text{F}$  fluorescence transient monitored at the spatial center of the spark. The  $\Delta\text{F}/\text{F}$  time course of each individual  $\text{Ca}^{2+}$  spark imaged was characterized by fitting each record to a function that empirically reproduced the main features of these observed time courses (32). This function (i.e., sequence of 2 exponentials), which provides a discontinuous rate of change at start and peak of the spark, was able to accurately reproduce most aspects of the  $\text{Ca}^{2+}$  spark time course. Results from two studies (32, 33) demonstrate a very abrupt initiation of fluorescence beginning at a maximal mono-exponential rate and continuing through the rising phase of the spark. The rising phase was followed by an abrupt transition from rising to falling fluorescence at the peak of the spark. The falling phase then followed a mono-exponential decaying timecourse. These findings are consistent with a large, rapid and relatively constant  $\text{Ca}^{2+}$  release during the rising phase followed by abrupt decrease in the rate of  $\text{Ca}^{2+}$  release rate at the peak of the spark.

### Voltage sensor restoration can prematurely terminate $\text{Ca}^{2+}$ release in voltage-activated sparks

In recent studies of  $\text{Ca}^{2+}$  sparks using the high speed confocal system, we have investigated the question of whether sparks which are initiated by the voltage sensors during fiber depolarization remain under voltage sensor control after their initiation. To investigate this question we compared  $\text{Ca}^{2+}$  sparks produced by depolarizing test pulses which were relatively long (15-60 ms) relative to the spark rise time (about 4 ms) with  $\text{Ca}^{2+}$  sparks produced by pulses which were short (3-6 ms) relative to the spark rise time. The rationale behind this comparison was that during the short pulses, the voltage sensors could deactivate at the end of the pulse during the rising phase of a spark when the  $\text{Ca}^{2+}$  release in the spark was still occurring (Fig. 4). If the voltage

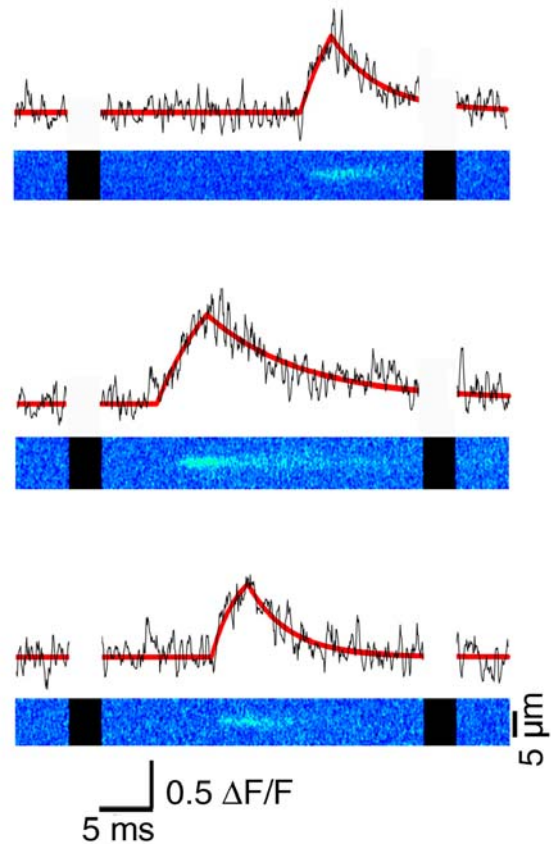


Figure 3. Representative  $\text{Ca}^{2+}$  sparks imaged at a substantially higher time resolution (63  $\mu\text{s}/\text{line}$ ) than in standard imaging methods (2 ms/line).  $\Delta\text{F}/\text{F}$  image strips of individual  $\text{Ca}^{2+}$  sparks as well as the corresponding  $\Delta\text{F}/\text{F}$  fluorescent transient monitored at the spatial center of the spark are shown. Black gaps in the image represent time gaps between successive images. The time course of each  $\text{Ca}^{2+}$  spark is fit to a function that empirically reproduced the main features of the observed time courses (see text).

sensor were required for continued activity of the SR  $\text{Ca}^{2+}$  release channels generating the spark, then the channels would be prematurely closed after the short pulse. In this case the rising phase of the spark would consequently be briefer than that of a spark during a long depolarization. Our results in fact showed that the mean duration of the rising phase of sparks elicited by 3 ms pulses was significantly shorter than the mean duration of the rising phase of sparks elicited by longer duration pulses (33). This result indicates that deactivation of voltage sensors provides one mechanism for terminating the SR  $\text{Ca}^{2+}$  release channel activity underlying a  $\text{Ca}^{2+}$  spark. The distance along the TT-SR junction over which the DHPR coupled RyR exerts an influence on neighboring RyRs, and the possible role of molecular coupling of adjacent RyRs (34) in this voltage sensor control remain to be determined. During longer duration depolarizing pulses, when the voltage sensor is continuously active, the rising phase of a spark is

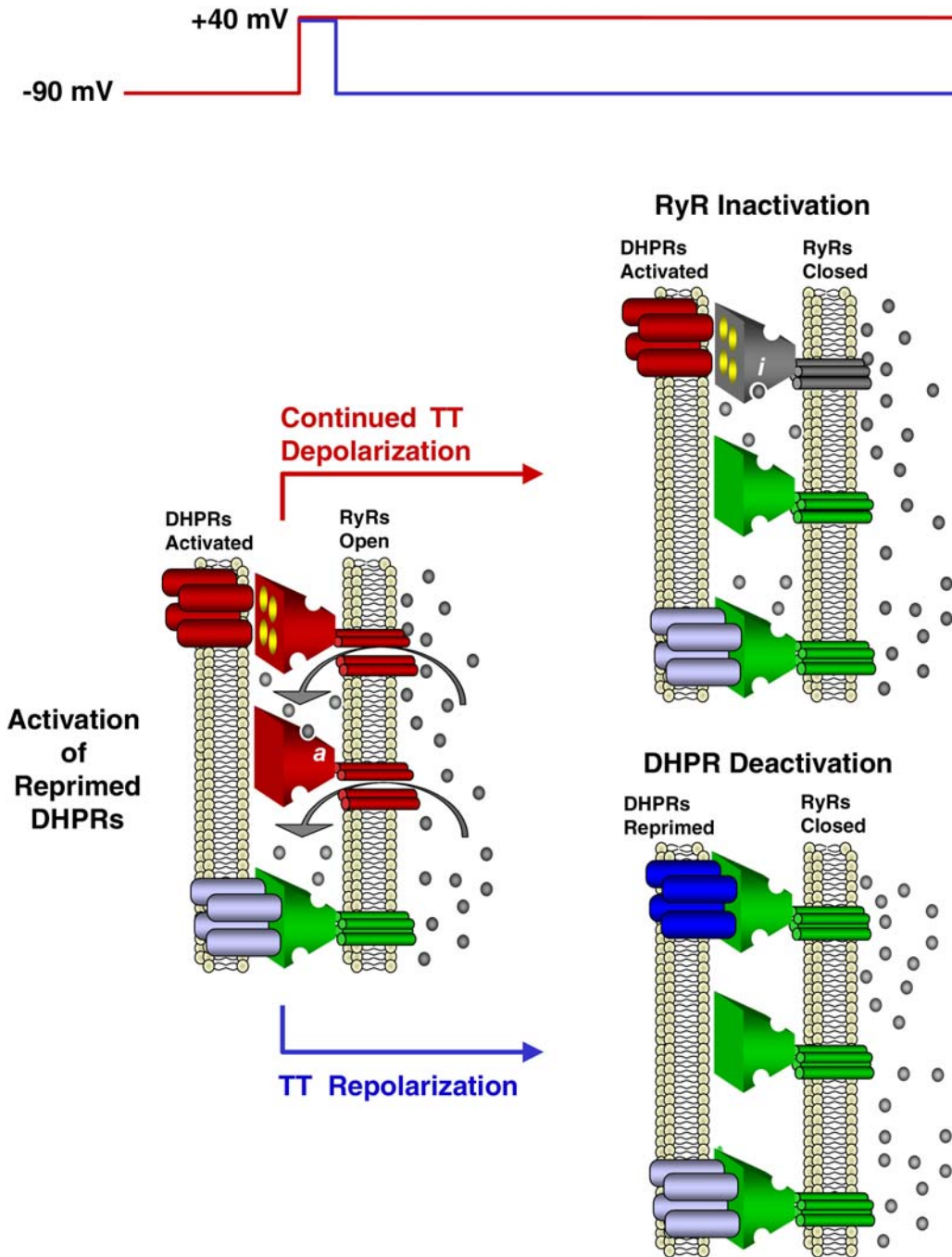


Figure 4. Cartoon interpretation of the two mechanisms of termination of  $\text{Ca}^{2+}$  sparks. Following the activation of RyR  $\text{Ca}^{2+}$  release channels by reprimed and subsequently depolarized voltage sensors (red), continued depolarization (top) results in inactivation of the RyRs (gray). Inactivation occurs most likely through ligand induced  $\text{Ca}^{2+}$  inactivation mechanism at both the voltage sensor coupled RyR (occupied i site) and the uncoupled RyR (inactivation not shown). Alternatively, during brief depolarization (bottom) reprimed DHPRs are deactivated (blue) causing premature closing of the coupled RyR.

also terminated (above). Therefore there must also be an inactivation mechanism that terminates the SR  $\text{Ca}^{2+}$  release channel activity underlying a spark even during the continued activation signal from the voltage sensor. Thus, the SR  $\text{Ca}^{2+}$  release channel

openings underlying a spark can be terminated by either of two alternative mechanisms (Fig. 2): either by voltage sensor deactivation, as occurs after short depolarizations, or by SR channel inactivation during more prolonged depolarizations. Spontaneous  $\text{Ca}^{2+}$

sparks, which appear to be initiated independent of voltage sensors, are activated by ligand interaction with the RyR and would be terminated by inactivation, also independently of the voltage sensor.

### **Ca<sup>2+</sup> release channel activity underlying a spark**

From our results presented above, it does not seem implausible that Ca<sup>2+</sup> release underlying a spark could be initiated at its maximal rate and then could turn off abruptly and completely at the peak of a spark. In this case the rise time of the spark would correspond to the total time that the channel or group of channels generating the spark were open, and the declining phase would be a time during which the release rate were zero. As discussed previously, (35) this interpretation could correspond to a single channel open for the entire rising phase of the spark. Alternatively, multiple channels, each of which remain open throughout the rising phase of the spark, or multiple channels that open and close asynchronously and repeatedly during the rising phase of the spark but which all close within a short interval at the time of peak of the spark would also be consistent with our observations.

Recent work by the Rios laboratory (36) has provided new data regarding channel activity underlying voltage activated Ca<sup>2+</sup> sparks. Under conditions in which the CICR potential was low (high [Mg<sup>2+</sup>] in the internal solution), voltage elicited Ca<sup>2+</sup> sparks were spatially narrowed and exhibited a low amplitude, prolongation (ember; <100ms) of fluorescence not seen in the control condition. In the presence of caffeine (high CICR potential), voltage elicited Ca<sup>2+</sup> sparks were spatially more extensive than in the control condition and did not present with ember fluorescence. These authors postulate that the low CICR potential reduced the recruitment of channels contributing to the Ca<sup>2+</sup> spark, thereby revealing an 'ember' fluorescence. This sustained low amplitude fluorescence was attributed to a single channel which is controlled by voltage sensor activation and remains open at low CICR potential despite the suppression of Ca<sup>2+</sup> release by RyRs activated secondarily via CICR. In this case the channel closing scheme for long depolarizations in Fig. 4 would have to be modified to show RyRs activated by CICR closing before the voltage activated channel at low CICR potential, but not at high CICR potential. In this model it is postulated that a "master" channel, activated by the TT voltage sensor, synchronizes the opening of neighboring Ca<sup>2+</sup> release channels during voltage activated Ca<sup>2+</sup> sparks at high, but not at low CICR potential.

In the most general interpretation, the rise time of a spark provides a lower limit for the open time of channels responsible for generating the spark. Some channel(s) might open or remain open during the declining phase, even though the rate of release must have been markedly less than during the rising phase (preceding paragraph). These types of interpretation can be made quantitative through the use of detailed modeling of Ca<sup>2+</sup> binding and diffusion in a fiber after Ca<sup>2+</sup> release from a channel or group of channels. (eg, 12, 13). Unfortunately detailed

discussion of these models is beyond the scope of this brief review; however, these quantitative models (12, 13) indicate that release could abruptly turn on and off at the start and peak of the observed sparks.

### **LIGAND ACTIVATED Ca<sup>2+</sup> SPARKS**

#### **Permeabilized fibers for the manipulation of cytosolic ligands**

Spontaneous Ca<sup>2+</sup> sparks have been visualized in fully polarized as well as in chronically depolarized fiber preparations (5, 7). These events are thought to be initiated by ligand activation, most likely through calcium-induced-calcium-release (CICR) mechanisms. Several techniques have been used to investigate ligand activated Ca<sup>2+</sup> sparks in depolarized fiber preparations, the purpose of all such techniques being to introduce Ca<sup>2+</sup> indicator dye and possible modulators (e.g., ions, small peptides) into the cytosol. Techniques such as mechanical disruption (e.g., notched, peeled fiber preparations) or chemical permeabilization (e.g., saponin, ionophore) are effective tools for this approach in skeletal and cardiac cells. In recent investigations we have used brief saponin permeabilization which provides a rapid equilibration of experimental solutions, including large molecules (i.e., peptides (IPTX<sub>a</sub>) and small proteins (Homer)), into and out of skeletal fibers (37). The permeabilized fibers exhibit spontaneous Ca<sup>2+</sup> sparks which have properties quantitatively similar to spontaneous Ca<sup>2+</sup> sparks imaged in mechanically notched fibers (38) as well as voltage activated sparks.

#### **Activation of Ca<sup>2+</sup> sparks by physiological ligands**

Cytosolic Ca<sup>2+</sup> and Mg<sup>2+</sup> ions are known physiologic modulators of SR Ca<sup>2+</sup> release. Based on a model adapted from Laver et al. (39) we know that as [Mg<sup>2+</sup>] is lowered, Mg<sup>2+</sup> first dissociates from a low affinity inactivation site ("i" site) at which binding of either Ca<sup>2+</sup> or Mg<sup>2+</sup> inhibits channel opening. Mg<sup>2+</sup> then dissociates from the high affinity Ca<sup>2+</sup> activation site ("a" site) at which either Ca<sup>2+</sup> or Mg<sup>2+</sup> can bind, but at which only Ca<sup>2+</sup> activates the channel. Thus, Mg<sup>2+</sup> binding at this site competitively inhibits Ca<sup>2+</sup> activation of the channel. After Mg<sup>2+</sup> dissociates from the site, Ca<sup>2+</sup> can bind to the ion-free site in a subsequent step in which the channel actually opens via a CICR dependent mechanism.

We have examined the effect of myoplasmic free [Mg<sup>2+</sup>] on the frequency and properties of spontaneous Ca<sup>2+</sup> sparks. Initial studies were carried out using "notched" (and consequently depolarized) segments challenged with various concentrations of free [Mg<sup>2+</sup>] and ~100nM [Ca<sup>2+</sup>]<sub>free</sub> (38). As myoplasmic [Mg<sup>2+</sup>] was lowered, the frequency of Ca<sup>2+</sup> sparks increased, indicating a pronounced increase in the activation rate of the channel or channels responsible for initiation the [Ca<sup>2+</sup>] sparks. Over the [Mg<sup>2+</sup>] range of about 0.1 to 2 mM, the event frequency increased in inverse proportion to the 1.6 power of [Mg<sup>2+</sup>], consistent with at least 2 Mg<sup>2+</sup> ions being involved in binding at an inhibitory site for channel opening, which

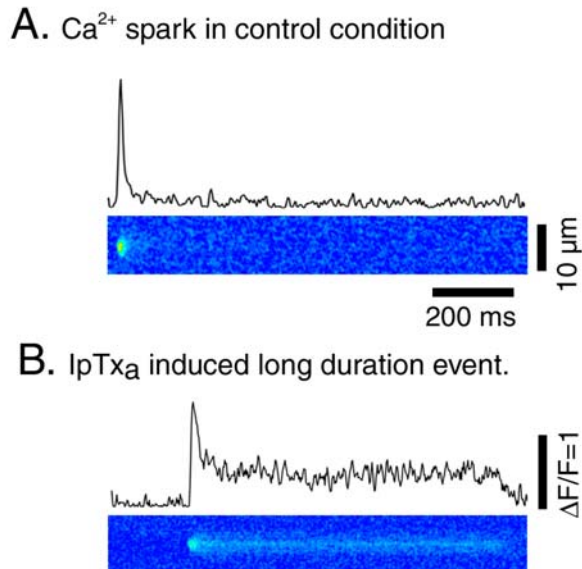


Figure 5. A. 1024 ms  $\Delta F/F$  image strip containing a single  $\text{Ca}^{2+}$  spark. The temporal fluorescent transient is presented above. The spark appears as a discrete, transient fluorescent increase within this image strip. B. Image strip and corresponding  $\Delta F/F$  time-course of long duration  $\text{Ca}^{2+}$  release event induced by application of 5 nM  $\text{IpTx}_\alpha$ . The sustained low amplitude fluorescence is apparent throughout the majority of the image strip and can be present with (this figure) or without (not shown) the presence of a discrete  $\text{Ca}^{2+}$  spark.

is consistent with the model put forward by Laver (39). In recent studies we have confirmed this [ $\text{Mg}^{2+}$ ] dependence using saponin permeabilized fibers, in which equilibration of cytosolic solutions is more rapid and is uniform along the length of the fiber (40).

Despite the steep rise in spark activation with decreasing cytosolic [ $\text{Mg}^{2+}$ ], the mean amplitude, amplitude distribution, mean rise time, rise time distribution, and the spatial spread of the sparks were all the same at each [ $\text{Mg}^{2+}$ ] level tested (38). These observations indicate that while the rate of  $\text{Ca}^{2+}$  spark activation was dramatically effected by [ $\text{Mg}^{2+}$ ], the inactivation kinetics of the  $\text{Ca}^{2+}$  spark was independent of [ $\text{Mg}^{2+}$ ]. Consequently, the average open time of the channel or channels underlying a spark was also presumably independent of [ $\text{Mg}^{2+}$ ], since it is unlikely that the SR  $\text{Ca}^{2+}$  content was changed during the experiment. Since raising [ $\text{Mg}^{2+}$ ] does not appear to speed the inactivation process, we conclude that the channels that opened following  $\text{Mg}^{2+}$  dissociation from the inhibitory site must close by some process independent of the rebinding of  $\text{Mg}^{2+}$  to the inhibitory site. Channel closing independent of  $\text{Mg}^{2+}$  could be achieved by  $\text{Ca}^{2+}$  binding to the inactivation site due to locally high  $\text{Ca}^{2+}$  in the immediate vicinity of the open channel.

According to the above scheme,  $\text{Ca}^{2+}$  is the activator of the channel in "spontaneous" (i.e., ligand activated) events, which are thus initiated by calcium-

induced calcium release (CICR). Increasing the frequency of occurrence of  $\text{Ca}^{2+}$  sparks can be demonstrated by increasing [ $\text{Ca}^{2+}$ ] in internal solutions exposed to notched (7) or permeabilized fibers. However, the increased indicator fluorescence accompanying the elevated [ $\text{Ca}^{2+}$ ], as well as the possibility of increased SR  $\text{Ca}^{2+}$  loading, make cytosolic  $\text{Ca}^{2+}$  a less convenient tool for manipulating spark frequency than cytosolic  $\text{Mg}^{2+}$ .

## MODULATION OF $\text{Ca}^{2+}$ SPARKS BY EXOGENOUS PEPTIDES IN PERMEABILIZED FIBERS

### Prolonged $\text{Ca}^{2+}$ channel opening by imperatoxin: long duration $\text{Ca}^{2+}$ sparks

Imperatoxin ( $\text{IpTx}_\alpha$ ) is a 33 amino acid peptide that structurally resembles the Thr<sup>671</sup>-Leu<sup>690</sup> portion of the dihydropyridine receptor II-II loop. In the planar lipid bilayer, this peptide interacts with single frog RyR's and induces long-lasting substates of ~30% of full current amplitude. In saponin permeabilized frog skeletal muscle fibers, 5nM  $\text{IpTx}_\alpha$  induced long duration (mean = 1.8 sec), relatively small (~30% of control spark peak amplitude) release events which occurred either with or without sparks superimposed on the fluorescence substate (37). The fluorescence waveforms were consistent with the "long openings" to subconductance state, often superimposed with full conductance openings, induced by  $\text{IpTx}_\alpha$  in lipid bilayers (41). In the presence of low [ $\text{IpTx}_\alpha$ ] there was no change in the frequency of the spontaneous short duration  $\text{Ca}^{2+}$  sparks also identified in the absence of  $\text{IpTx}_\alpha$ . The frequency of occurrence of long duration  $\text{IpTx}_\alpha$ -induced events increased in proportion to [ $\text{IpTx}_\alpha$ ] in a manner consistent with results from single channel recordings of RyRs in bilayers. The mean duration of the peptide-induced long duration events were independent of toxin concentration and agreed closely with the mean duration of subconductance states seen in the bilayer where  $\text{IpTx}_\alpha$  induced opening of single frog RyR channels to a subconductance state. These results that suggest involvement of a single molecule of  $\text{IpTx}_\alpha$  in the activation of a single RyR channel to produce the long duration event. Thus binding of a single  $\text{IpTx}_\alpha$  molecule to an RyR overrides the inactivation mechanism which would normally close the channel and terminate the spark. In this respect,  $\text{IpTx}_\alpha$  is unique as the only compound we have observed to alter closing properties of the channels underlying a  $\text{Ca}^{2+}$  spark.

### RyR domain peptide DP4 increases $\text{Ca}^{2+}$ spark frequency but does not alter spark properties

DP4 is a 36-residue synthetic peptide, which corresponds to the Leu<sup>2442</sup>-Pro<sup>2477</sup> region of RyR1. Based on single channel studies, it has been proposed that DP4 disrupts the normal interdomain interactions that stabilize the closed state of the  $\text{Ca}^{2+}$  release channel ((42); and review in this issue) thereby promoting  $\text{Ca}^{2+}$  channel activation. We investigated the effects of DP4 on  $\text{Ca}^{2+}$  sparks in saponin-permeabilized frog skeletal muscle fibers (40). DP4 caused a significant concentration dependent increase

in Ca<sup>2+</sup> spark frequency. However, the mean values of the amplitude, rise time, spatial half width and temporal half duration of the Ca<sup>2+</sup> sparks, as well as the distribution of these parameters, remained essentially unchanged in the presence of DP4. Thus, DP4 increased the rate of activation of the RyR Ca<sup>2+</sup> release channels initiating the Ca<sup>2+</sup> sparks but, unlike IpTx<sub>a</sub>, had no effect on the inactivation kinetics. The same peptide with an Arg<sup>17</sup> to Cys<sup>17</sup> replacement (DP4mut), which corresponds to the Arg<sup>2458</sup>-to-Cys<sup>2458</sup> mutation in malignant hyperthermia, did not produce a significant effect on RyR activation in muscle fibers, bilayers, or SR vesicles. Mg<sup>2+</sup>-dependence experiments conducted with permeabilized muscle fibers indicate that DP4 preferentially binds to partially Mg<sup>2+</sup>-free RyR(s), thus promoting channel opening and Ca<sup>2+</sup> spark activation (40).

## CONCLUSIONS

At the global level, the increase in myoplasmic Ca<sup>2+</sup> during fiber depolarization appears to consist of the summation of huge numbers of Ca<sup>2+</sup> sparks during a brief time interval. Therefore, insights into the processes by which Ca<sup>2+</sup> sparks are modulated could offer insight into the functioning of SR Ca<sup>2+</sup> release channel(s). At the local level, Ca<sup>2+</sup> spark activation can be initiated by either voltage or ligand dependent mechanisms. The frequency of occurrence of these events provides information concerning the rate of opening of RyR channels initiating Ca<sup>2+</sup> sparks, whereas the amplitude and rise-time provide indication of the amount of Ca<sup>2+</sup> release and the effective open time of the RyR channels generating a Ca<sup>2+</sup> spark.

## ACKNOWLEDGEMENTS

We gratefully acknowledge the many contributions of present and former members of this laboratory, as well as our outside collaborators, Drs. H. Valdivia, P.D. Allen, N. Ikemoto and their laboratories, to our work presented here. Our work was supported by NIH grants R01-NS23346 to M.F.S., K01-AR02177 to C.W.W and the Interdisciplinary Training Program in Muscle Biology (NIH T32-AR07592), and by a research grant from the National Science Foundation (MCB-9724045 to M.F.S.)

## References

- Melzer W, Rios E, Schneider MF: Time course of calcium release and removal in skeletal muscle fibres. *Biophys.J.* 45:637-641 (1984)
- Melzer W, Rios E, Schneider MF: A general procedure for determining calcium release from the sarcoplasmic reticulum in skeletal muscle fibers. *Biophys.J.* 51:849-863 (1987)
- Baylor SM, Chandler WK, Marshall MW: Sarcoplasmic reticulum calcium release in frog skeletal muscle fibres estimated from Arsenazo III calcium transients. *J Physiol* 344:625-666 (1983)
- Tsugorka A, Rios E, Blatter LA: Imaging elementary events of calcium release in skeletal muscle cells. *Science* 269:1723-1726 (1995)
- Klein MG, Cheng H, Santana LF, Lederer WJ, Schneider MF: Stochastic calcium release events activated by dual mechanisms at triad junctions in skeletal muscle. *J.Gen.Physiol.* 106(6):44A.(1995)
- Cheng H, Lederer WJ, Cannell MB: Calcium sparks: elementary events underlying excitation-contraction coupling in heart muscle. *Science* 262:740-744 (1993)
- Klein MG, Cheng H, Santana LF, Jiang Y-H, Lederer WJ, Schneider MF: Two mechanisms of quantized calcium release in skeletal muscle. *Nature* 379:455-458 (1996)
- Shirokova N, Rios E: Small events Ca<sup>2+</sup> release: a probable precursor of Ca<sup>2+</sup> sparks in frog skeletal muscle. *J.Physiol.* 502(1):3-11 (1997)
- Stern MD, Pizarro G, Rios E: Local control model of excitation-contraction coupling in skeletal muscle. *J Gen Physiol* 110:415-440 (1997)
- Klein MG, Lacampagne A, Schneider MF: Voltage dependence of the pattern and frequency of discrete Ca<sup>2+</sup> release events after brief repriming in frog skeletal muscle. *Proc.Natl.Acad.Sci.U.S.A.* 94:11061-11066 (1997)
- Endo M. Entry of fluorescent dyes into the sarcotubular system of the frog muscle. *J.Physiol.* 185:224-238 (1966)
- Pratusevich VR, Balke CW: Factors shaping the confocal image of the calcium spark in cardiac muscle cells. *Biophys.J.* 71:2942-2957 (1996)
- Jiang YH, Klein MG, Schneider MF: Numerical simulation of Ca(2+) "Sparks" in skeletal muscle. *Biophys.J.* 77:2333-2357 (1999)
- Klein MG, Lacampagne A, Schneider MF: A repetitive mode of activation of discrete Ca<sup>2+</sup> release events (Ca<sup>2+</sup> sparks) in frog skeletal muscle fibres. *J Physiol* 515 ( Pt 2):391-411 (1999)
- Franzini-Armstrong C, Protasi F, Ramesh V: Shape, size, and distribution of Ca(2+) release units and couplons in skeletal and cardiac muscles. *Biophys J* 77:1528-1539 (1999)
- Hodgkin AL, Horowitz P: Potassium contractures in single muscle fibres. *J.Physiol.* 153:386-403 (1960)
- Lacampagne A, Lederer WJ, Schneider MF, Klein MG: Repriming and activation alter the frequency of stereotyped discrete Ca<sup>2+</sup> release events in frog skeletal muscle. *J.Physiol.(Lond.)* 497:581-588 (1996)
- Chandler WK, Rakowski RF, Schneider MF: Effects of glycerol treatment and maintained depolarization on charge movement in skeletal muscle. *J Physiol* 254:285-316 (1976)
- Adrian RH, Chandler WK, Rakowski RF: Charge movement and mechanical repriming in skeletal muscle. *J Physiol* 254:361-388 (1976)
- Block BA, Franzini-Armstrong C: The structure of the membrane systems in a novel muscle cell modified for heat production. *J.Cell Biol.* 107:1099-1112 (1988)
- Protasi F. Role of ryanodine receptors in the assembly of calcium release units in skeletal muscle. *J.Cell Biol.* 140:831-842 (1998)
- Protasi F, Takekura H, Wang Y, Chen SR, Meissner G, Allen PD, Franzini-Armstrong C: RYR1 and RYR3 have different roles in the assembly of calcium release units of skeletal muscle. *Biophys J* 79:2494-2508 (2000)
- Fessenden JD, Wang Y, Moore RA, Chen SR, Allen PD, Pessah IN: Divergent functional properties of ryanodine receptor types 1 and 3 expressed in a myogenic cell line. *Biophys J* 79:2509-2525 (2000)
- Felder E, Franzini-Armstrong C: Possible parajunctional location of ryR3 in skeletal muscle *Biophys J* 80: 382a (2001)
- Ward CW, Schneider MF, Castillo D, Protasi F, Wang Y, Chen SR, Allen PD: Expression of ryanodine receptor RyR3 produces Ca<sup>2+</sup> sparks in dyspedic myotubes. *J Physiol* 525 Pt 1:91-103 (2000)
- Shirokova N, Garcia J, Rios E: Local calcium release in mammalian skeletal muscle. *J Physiol* 512 ( Pt 2):377-384 (1998)
- Shirokova N, Shirokov R, Rossi D, Gonzalez A, Kirsch WG, Garcia J, Sorrentino V, Rios E: Spatially segregated control of Ca<sup>2+</sup> release in developing skeletal muscle of mice. *J.Physiol.(Lond.)* 521 Pt 2:483-495 (1999)

28. Conklin MW, Ahern CA, Vallejo P, Sorrentino V, Takeshima H, Coronado R: Comparison of Ca<sup>2+</sup> sparks produced independently by two ryanodine receptor isoforms (type 1 or type 3). *Biophys J* 78:1777-1785 (2000)
29. Ward CW, Protasi F, Castillo D, Wang Y, Chen SR, Pessah IN, Allen PD, Schneider MF: Type 1 and Type 3 ryanodine receptors generate different Ca<sup>2+</sup> release event activity in both intact and permeabilized myotubes. *Biophys. J* 81: (2001) *in press*
30. Kirsch W.G., Uttenweiler D., Fink R.H.A., Spark- and ember-like elementary Ca<sup>2+</sup> release in skinned fibres of adult mammalian skeletal muscle, *J. Physiol* (2001) *in press*
31. Tsien RY, Bacskai BJ. Video-rate confocal microscopy. In: Pawley JB, ed. *Handbook of Biological Confocal Microscopy*. New York: Plenum Press, 1995:459-477.
32. Lacampagne A, Ward CW, Klein MG, Schneider MF: Time course of individual Ca<sup>2+</sup> sparks in frog skeletal muscle recorded at high time resolution. *J.Gen.Physiol.* 113:187-198 (1999)
33. Lacampagne A, Klein MG, Ward CW, Schneider MF: Two mechanisms for termination of individual Ca<sup>2+</sup> sparks in skeletal muscle. *Proc Natl Acad Sci U S A* 97:7823-7828 (2000)
34. Marx,S.O. Ondrias,K. Marks,A.R: Coupled gating between individual skeletal muscle Ca<sup>2+</sup> release channels (Ryanodine receptors). *Science* 281, 818-821. 1998.
35. Schneider MF. Ca<sup>2+</sup> sparks in frog skeletal muscle: generation by one, some, or many SR Ca<sup>2+</sup> release channels? *J.Gen.Physiol.* 113:365-372 (1999)
36. Gonzalez A, Kirsch WG, Shirokova N, Pizarro G, Stern MD, Rios E: The spark and its ember: separately gated local components of Ca(2+) release in skeletal muscle. *J.Gen.Physiol.* 115:139-158 (2000)
37. Shtifman A, Ward CW, Wang J, Valdivia HH, Schneider MF: Effects of imperatoxin A on local sarcoplasmic reticulum Ca(2+) release in frog skeletal muscle. *Biophys J* 79:814-827 (2000)
38. Lacampagne A, Klein MG, Schneider MF: Modulation of the frequency of spontaneous sarcoplasmic reticulum Ca<sup>2+</sup> release events (Ca<sup>2+</sup> sparks) by myoplasmic [Mg<sup>2+</sup>] in frog skeletal muscle. *J.Gen.Physiol.* 111:207-224 (1998)
39. Laver DR, Baynes TM, Dulhunty AF: Magnesium inhibition of ryanodine receptor calcium channels: evidence for two independent mechanisms. *J.Membrane Biol.* 156:213-229 (1997)
40. Shtifman AS, Ward CW, Yamamoto T, Wang J, Olbinski B, Valdivia HH, Ikemoto N, Schneider MFS: Interdomain Interactions within Ryanodine Receptors Regulate Ca<sup>2+</sup> Spark Frequency in Skeletal Muscle. *J Gen Physiol* (2002) *in press*
41. Tripathy A, Resch W, Xu L, Valdivia HH, Meissner G: Imperatoxin A induces subconductance states in Ca<sup>2+</sup> release channels (ryanodine receptors) of cardiac and skeletal muscle. *J Gen Physiol* 111:679-690 (1998)
42. Ikemoto N, Yamamoto T: Postulated role of inter-domain interaction within the ryanodine receptor in Ca<sup>2+</sup> channel regulation. *Trends Cardiovasc Med* 10:310-316 (2000)

**Key words:** ryanodine receptor, calcium spark, dihydropyridine receptor, calcium channel, voltage sensor.

**Send correspondence to:**

Martin Schneider, Ph.D., Dept. of Biochemistry and Molecular Biology, University of Maryland School of Medicine, 108 N. Greene St, Baltimore MD, 21201 Tel: (410)706-7812, Fax: (410)706-8297, Email: [mschneid@umaryland.edu](mailto:mschneid@umaryland.edu)

**Running title:** Initiation And Termination Of Calcium Sparks

# Ryanodine Receptor Type 3: Why Another Ryanodine Receptor Isoform?

Vincenzo Sorrentino

Molecular Medicine Section, Department of Neuroscience, University of Siena, via Aldo Moro 5, 53100, Italy. E-mail: [v.sorrentino@unisi.it](mailto:v.sorrentino@unisi.it)

**ABSTRACT** The family of ryanodine receptor (RyR) genes encodes three highly related  $\text{Ca}^{2+}$  release channels: RyR1, RyR2 and RyR3. Until about 10 years ago, RyRs were essentially known only for being the  $\text{Ca}^{2+}$  release channels of the sarcoplasmic reticulum of striated muscles, because of the high levels of expression of the RyR1 and RyR2 isoforms in skeletal and cardiac muscles, respectively. In contrast with the above picture, the RyR3 gene has been found not to be preferentially expressed in one specific tissue, but rather to be widely expressed in various cells. This wide expression pattern has been subsequently observed also for the RyR1 and RyR2 genes, which in addition to their preferential expression in striated muscles, have been found expressed also in several other cell types, although at lower levels than in striated muscles. Thus a closer look reveals that in several cells of vertebrates two or even three RyR isoforms can be co-expressed.

In this chapter we will review published work on the RyR3 gene and discuss a model where co-expression of different RyR channel isoforms is interpreted as an evolutionary solution to provide, by functional interactions of distinct isoforms of  $\text{Ca}^{2+}$  release channels, the several types of vertebrate cells with the cell-specific  $\text{Ca}^{2+}$  release machinery required for generating the sophisticated intracellular  $\text{Ca}^{2+}$  signals needed for optimal regulation of their functions.

## INTRODUCTION

### The ryanodine receptor gene family of $\text{Ca}^{2+}$ release channels and their pattern of expression

The family of ryanodine receptor (RyR) genes encodes three highly related  $\text{Ca}^{2+}$  release channels (1-3). The three RyR genes, named RyR1, RyR2 and RyR3 are located in humans on chromosomes 19q12-13.2, 1q42.1-43, 15q13-14 (1-3). Until about 10 years ago RyRs were only known as the  $\text{Ca}^{2+}$  release channels of the sarcoplasmic reticulum of striated muscles, as RyR1 and RyR2 were known to be expressed at high levels in skeletal and cardiac muscles, where they play a central role in skeletal and cardiac excitation-contraction (e-c) coupling, respectively (4). The preferential expression of RyRs in muscle tissues can be traced back to *Caenorhabditis elegans*, whose genome contains only one RyR gene (5). In *Caenorhabditis elegans*, that is the most primitive organism where a RyR gene has been studied, we can already observe a preferential expression and a functional role of the RyR gene in muscle contraction. This is at variance with the  $\text{InsP}_3\text{R}$  gene that in *Caenorhabditis elegans* is expressed in a more wide range of tissues (6). With the appearance of vertebrates, three RyR genes evolved. These genes present distinct tissue-specific patterns of expression and encode proteins that display distinctive regulatory properties. From this point of view, evolution and association of RyR1 and RyR2 with skeletal and cardiac tissue may reflect the increasing sophistication in the mechanisms of excitation-contraction coupling of these tissues in vertebrates. Through processes of gene duplication and diversification, the RyR1 and RyR2 isoforms emerged as the molecular tools necessary for the more sophisticated muscle tissues of vertebrate compared to the more primitive ones of invertebrates (7).

In contrast with the above picture of RyR1 and RyR2, which may suggest that these genes

were selected to encode specialized  $\text{Ca}^{2+}$  release channels for striated muscles, the RyR3 gene lacks specific localization and is found expressed in a wide variety of tissues (8). It should be noted however that, similar to RyR3, the RyR1 and RyR2 genes are also expressed in many other tissues and cells in addition to their preferential expression in striated muscles, although at lower levels (9,10). Actually, there are currently many examples of tissues or cells where two or three RyR isoforms are being co-expressed.

So the question could be presented in the following terms: if RyR3 is not preferentially associated with one tissue, what is its physiological role? And what is the functional significance of RyR1 and RyR2 gene expression outside of muscle cells? While at the moment little is known about tissues that express only RyR3, available evidence suggests that this isoform might contribute to form complex systems of  $\text{Ca}^{2+}$  release where more isoforms of RyR are required. Therefore, in addition to tissue-specific isoforms, co-expression of different RyR genes in a tissue may represent a developmentally regulated mechanism evolved to meet the signaling requirements of highly specialized cell types that are necessarily associated with the evolution of complex organisms (11). In the next paragraphs we shall review some examples in support of this hypothesis.

### RYR3 IS DEVELOPMENTALLY REGULATED IN SKELETAL MUSCLES OF MAMMALS.

Expression of RyR3 in mammalian skeletal muscle tissue is now well established. Initial studies performed shortly after the identification of the RyR3 gene revealed that mammalian skeletal muscles, in addition to expressing high levels of RyR1, also express detectable levels of RyR3. Studies *in vitro* using the C2C12 skeletal muscle cell line revealed that RyR3 channels were preferentially expressed in differentiated rather than in undifferentiated muscle cells and that RyR3

appeared simultaneously with RyR1 early during myotube differentiation (12). This was confirmed by the demonstration that RyR3 was expressed only in a few muscles of adult rodents (mainly diaphragm), but could not be detected in the majority of adult skeletal muscles (13). This picture has some analogies with what is known for skeletal muscles of non-mammalian vertebrates, where two RyR isoforms are often found at approximately equimolar ratio. These two isoforms (called  $\alpha$  and  $\beta$ ) have been demonstrated to be homologous to mammalian RyR1 and RyR3 respectively (14). The pattern of expression of RyR3 in mammals became clearer when a thorough analysis of RyR3 expression established that RyR3 was developmentally regulated in embryonic and neonatal skeletal muscles of mice (15,16). Accordingly, skeletal muscles of embryo contain the RyR3 isoform in all muscles in addition to RyR1. RyR3 expression increases after birth with a peak around 15 days after birth and a gradual decline after peak so that in adult musculature the RyR3 isoform is almost exclusively confined to the diaphragm and few other muscles. In general, however, RyR3 appears to contribute no more than 2-5 % of total ryanodine receptors of mammalian skeletal muscles (17,18).

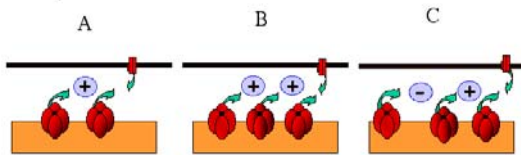


Fig.1: This figure presents three simple schemes on possible modalities of functional interactions that could form when more isoforms of RyR /  $\text{Ca}^{2+}$  release channels are co-expressed. Positive co-operation among two or three co-expressed channels are presented in Fig.1A and Fig.1B. The example in Fig.1C, on the other hand, indicates a different possibility where one isoform has an inhibitory effect on the activity of the other two.

### MUSCLE CONTRACTION AND $\text{Ca}^{2+}$ SIGNALING IS ALTERED IN SKELETAL MUSCLE OF NEONATAL RYR3 KO MICE.

In order to identify a functional correlate of RyR3 expression in neonatal skeletal muscle, contraction analysis was performed in skeletal muscle of normal and RyR3 KO mice (15). These experiments revealed an impairment of muscle contraction in skeletal muscles of RyR3 KO mice only when skeletal muscles preparations were isolated from mice in the first weeks after birth. Under these conditions, tension developed following electrical stimulation was significantly lower in RyR3 KO than in control mice, and an even stronger difference was observed when neonatal muscles of RyR3 KO mice were exposed to high caffeine concentration. No significant difference between normal and RyR3 KO mice was observed when the analysis was extended to preparation of skeletal muscles of adult mice. The reduced contractility observed following electrical and caffeine stimulation in RyR3 KO mice is suggestive of a qualitative contribution of RyR3-mediated  $\text{Ca}^{2+}$

release to regulation of contraction in neonatal skeletal muscles (19) (Fig. 1A).

In RyR1 KO myotubes in culture,  $\text{Ca}^{2+}$  release from the sarcoplasmic reticulum in response to increases in cytosolic  $\text{Ca}^{2+}$  concentration or caffeine was strongly reduced (20). A similar decrease in caffeine sensitivity was also observed in RyR3-null neonatal myocytes, suggesting a possible co-contribution of each RyR subtype to  $\text{Ca}^{2+}$  signaling, at least at embryonic / neonatal stages of myogenesis (21). In contrast, experiments on the rate of  $\text{Ca}^{2+}$  release in normal and RyR3 KO mice skeletal myotubes did not indicate a modulatory effect of RyR3 on  $\text{Ca}^{2+}$  release following electrical stimulation (22). Both the voltage dependence of the  $\text{Ca}^{2+}$  release process and the time course of the release rate during strong depolarization were identical, indicating that if RyR3 were contributing to this process the contribution would be small and definitely not a decisive factor for E-C coupling in cultured myotubes. Investigation of localized spontaneous  $\text{Ca}^{2+}$  release events in muscle cells lacking the RyR3 gene indicated however that RyR3 channels contributed to generate localized spontaneous  $\text{Ca}^{2+}$  release events in normal skeletal neonatal muscle cells (23,24). Further investigation in skeletal muscle fibers from neonatal mice KO for either RyR1 or RyR3 genes revealed that  $\text{Ca}^{2+}$  sparks produced independently by either RyR1 or RyR3 channels had similar spatio-temporal parameters (25). However, since sparks observed in RyR1 or RyR3 KO mice were smaller than those of wild type muscles, these data indicated that co-expression of the RyR1 and RyR3 isoforms is required to generate the localized  $\text{Ca}^{2+}$  release events that are observed in embryonal and neonatal wild type cells that express both isoforms. Interestingly, sparks observed following addition of sub-optimal caffeine concentrations were larger in cells expressing RyR3 than in cells expressing only RyR1 (25).

Cheng and colleagues have more recently contributed a significant advancement on the differential contribution of RyR1 and RyR3 to  $\text{Ca}^{2+}$  signaling in skeletal myotubes (26). The use of an imaging system able to obtain a high spatially and temporally resolved variation of  $\text{Ca}^{2+}$  levels enabled this group to observe different patterns of  $\text{Ca}^{2+}$  release in neonatal skeletal muscle cells lacking RyR3 compared with normal neonatal myotubes (i.e. expressing both RyR1 and RyR3). These results indicate the existence of a functional interplay between RyR1 and RyR3, which may serve important roles in the regulation of  $\text{Ca}^{2+}$  movements in neonatal muscle cells, where RyR3 channels appear to be capable of amplifying the  $\text{Ca}^{2+}$  induced  $\text{Ca}^{2+}$  release promoted by voltage activated RyR1 channels. The principal observation reported indicated that the time required for diffusion of a  $\text{Ca}^{2+}$  signal following depolarization from the membrane to the central region of a muscle fiber is higher in RyR3 KO mice, where speed of this signal in wild type cells is  $2200\mu\text{/sec}$  and in the RyR3 KO fibers is of  $190\mu\text{/sec}$ . These results indicate that co-expression of RyR3 with RyR1 contributes to build a system of amplification which results in a more uniform and synchronous activation of  $\text{Ca}^{2+}$  release across the whole cell body in neonatal skeletal

muscle, which is about 10 fold higher in wild type compared with RyR3 KO cells. Given the absence or poor development of T-tubules in embryonal and neonatal skeletal muscle fibers, co-expression of RyR3 may be important to facilitate  $Ca^{2+}$  signaling in muscle fibers at this stage of development. This elegant analysis thus provides a significant explanation at the level of  $Ca^{2+}$  signals for RyR1 and RyR3 co-expression in neonatal muscle cells that directly support the initial model proposed following the identification of defective contraction of neonatal skeletal muscles of RyR3 KO mice (15,19).

### **RYR3 EXPRESSION IN THE CENTRAL NERVOUS SYSTEM**

A considerable amount of evidence supports the notion that neuronal functions, like long-lasting changes of synaptic plasticity and long-term memory, require an initial elevation of the intracellular  $Ca^{2+}$  concentration (27). Such  $Ca^{2+}$  signals can result from an influx of  $Ca^{2+}$  via  $Ca^{2+}$  channels on the plasma membrane and/ or  $Ca^{2+}$  release from intracellular stores (28). All three isoforms of RyRs are expressed in the Central Nervous System (CNS) (8,9,10). In the brain the predominant isoform is RyR2; RyR1 and RyR3 contribute less than 5% of total RyR channels. Why multiple RyR isoforms exist in neurons and how these isoforms participate and interact in neuronal function is currently not understood. A role of RyRs in the induction of long-term potentiation (LTP) and/or depression (LTD) has been supported by a number of experiments based on the use of pharmacological agents (29); however these studies did not elucidate the functional contribution of each single isoform and the significance of the expression of multiple RyR isoforms within a single neuron.

On this basis, Balshun and colleagues adopted the RyR3 KO mice to study the eventual role of this RyR isoform in LTP, which is thought to mediate processes of learning and memory formation at the cellular level. RyR3 KO mice presented no obvious morphological alteration in the hippocampus, and LTP generated by strong tetanizations were not different between mutant and control animals. In contrast, LTP induced by a weak tetanization protocol and depotentiation was markedly changed by RyR3 deletion. In experiments performed with LTP generated by a weaker tetanization it was observed that RyR3 KO mice tended to have a lower initial amplitude of potentiation. In addition, LTP in RyR3 KO mice decayed within 30 min, whereas wild type mice still displayed a significant potentiation after 2 hours (30). Thus, RyR3 channels seem to play a distinct role in certain types of hippocampal synaptic plasticity.

A number of further behavioral tests were carried on RyR3 KO mice. Whereas the general behavior in the open field was not different between mutant and control mice, RyR3 KO mice displayed a higher speed of locomotion as also observed by Takeshima and co-workers (21). The RyR3 KO mice also presented a mild tendency to circular running. The caudate/putamen area represents one of the preferential expression sites of RyR3 in CNS but whether these motor alterations result from a dysfunction of this region is not known. The specific

effects of RyR3 gene deletion on synaptic plasticity agree with a role of these channels in hippocampus-dependent learning and behavior. Hippocampus-dependent spatial learning of RyR3 KO mice was examined in the Morris water maze test. In this type of experiments, during an acquisition phase the animals learn to use distant cues on the walls to locate an escape platform that is hidden at a constant location. In the acquisition phase and probe trial of the water maze task, RyR3 mutants were able to locate and to navigate to a hidden platform similarly to wild type mice. An interesting difference emerged after changing the platform position. Wild type animals learned the new position very rapidly, taking only 2-3 trials to reach the performance level they had shown at the end of acquisition. RyR3 KO mice, by contrast, needed the full 12 trials to learn the new position, apparently having no advantage with respect to the acquisition phase (30). An almost identical behavior in the water maze test has been reported by Futatsugi and colleagues (31). However these authors interpreted the persistent habit of the RyR3 KO mice in the reversal phase of the test as a sign of an increased capability to perform. By contrast, we think that RyR3 KO mice have a reduced flexibility to reuse and modify an acquired map once the goal position is changed in an otherwise unaltered environment. During the relearning part of the Morris test, in fact, the learning curve of RyR3 KO mice resembles that usually observed in a completely new setup indicating that hippocampal function may not be entirely normal in these mice. The response in the Morris test is generally considered as expression of the associative not-implicit learning which may find its cellular basis in hippocampal LTP, therefore the data discussed above indicate that RyR3 channels appear to participate of special forms of hippocampal synaptic plasticity, which might be required for the normal adaptation and modification of spatial maps. In a more general sense, RyR3 seems to be involved in a process that adapts the acquired memory flexibility to external /environmental changes or stimuli.

As of today, no evidence is available on defective  $Ca^{2+}$  release in neurons from RyR3 KO mice. Yet it is still reasonable to propose that, as in neonatal skeletal muscle cells, RyR3 channels may provide a qualitative contribution to  $Ca^{2+}$  release in neurons which if absent may result in altered regulation of neuronal activities.

### **RYR3 EXPRESSION AND FUNCTION IN SMOOTH MUSCLE CELLS**

In smooth muscle cells the generation of global or localized changes in intracellular  $Ca^{2+}$  levels has been associated with the specific control of opposite functions such as contraction and relaxation (28,32). Increased global intracellular  $Ca^{2+}$  levels, although reaching modestly high concentrations, spread throughout the entire cell and regulate contraction by activating myosin light chain kinase. By contrast,  $Ca^{2+}$  -dependent relaxation in smooth muscle cells is mediated by discretely localized  $Ca^{2+}$  release events resulting from the activation of RyRs located near the plasma membrane. These events provoke local increases in  $Ca^{2+}$  concentration that stimulate adjacent  $Ca^{2+}$  -

activated  $K^+$  channels (BK), causing BK-type currents named "spontaneous transient outward currents" or STOCs. STOCs inhibit voltage-dependent  $Ca^{2+}$  channel activity, decrease global  $Ca^{2+}$  and diminish arterial contraction leading to decreased blood pressure.

### **STUDIES ON RYR3 CHANNELS IN RAT PORTAL VEIN AND MOUSE MYOMETRIAL SMOOTH MUSCLE CELLS**

All smooth muscle cells tested so far have been proven to express RyR channels, although smooth muscle cells from different organs have been found to express different combinations of the three RyR isoforms. In rat portal vein myocytes, spatial and temporal recruitment of  $Ca^{2+}$  sparks result in propagating  $Ca^{2+}$  waves that trigger cell contraction. All three RyR isoforms are co-expressed in these cells, but the specific contribution of a given isoform has only recently been studied. Mironneau and colleagues determined the RyR subtypes responsible for  $Ca^{2+}$  sparks and global  $Ca^{2+}$  responses in rat portal vein myocytes by antisense oligo-nucleotides that specifically targeted each one of the RyR subtypes (33). They found that inhibition of either RyR1 or RyR2 by treatment with antisense oligonucleotides strongly reduced the number of vascular myocytes with spontaneous  $Ca^{2+}$  sparks, whereas inhibition of RyR3 was ineffective, indicating that both RyR1 and RyR2, but not RyR3, were required for  $Ca^{2+}$  release during  $Ca^{2+}$  sparks and  $Ca^{2+}$  waves induced by activation of L-type  $Ca^{2+}$  currents. In the same cells, activation of RyR3 channel activity was obtained under conditions of increased  $Ca^{2+}$  loading of the sarcoplasmic reticulum (34). A similar requirement for increased  $Ca^{2+}$  loading of the sarcoplasmic reticulum in order to sensitize RyR3 channels to stimulation by  $Ca^{2+}$  and caffeine has been reported by Mironneau and colleagues in mouse myometrial smooth muscle cells that only express RyR3 channels (35).

### **RYR3 DICTATES STOCs FREQUENCY IN BRAIN ARTERIAL SMOOTH MUSCLE CELLS: EFFECTS ON BLOOD PRESSURE**

Smooth muscle cells from cerebral arteries have been found to express the three RyR isoforms (36). To understand the contribution of the RyR3 isoforms to arterial contraction, Gollasch and colleagues tested the molecular role of RyR3 in  $Ca^{2+}$  spark regulation and STOCs generation in arterial smooth muscle cells of RyR3 KO mice (36). The spatial-temporal characteristics of individual  $Ca^{2+}$  sparks in arterial smooth muscle cells of RyR3 KO mice did not differ from those of control animals. Interestingly, analysis of BK current activation in arterial smooth muscle cells from RyR3 KO mice revealed a significant increase in the STOCs frequency compared to control mice. These results suggest that RyR3 channels specifically set the frequency of  $Ca^{2+}$  spark/STOCs in arterial smooth muscle cells. Thus, RyR3 channels seem to contribute to  $Ca^{2+}$  sparks by controlling the basal  $Ca^{2+}$  spark frequency while the remaining RyRs (i.e., RyR1 and RyR2) mainly contribute to the  $Ca^{2+}$  release underlying a single spark. To understand the physiological consequences of the increased  $Ca^{2+}$  sparks/STOCs frequency in arterial smooth muscle

cells, the effect of pressure on arterial diameter of intact, isolated cerebral arteries was tested. Arteries from RyR3 KO mice were less constricted at a given pressure than were control arteries, indicating that increased activity of BK channels in RyR3 KO arteries contributes to the regulation of arterial tone and that RyR3 limits arterial tone by an inhibition of basal BK channel/STOCs activity. On these bases Gollasch and colleagues proposed a model in which BK channels are activated by  $Ca^{2+}$  released from a compartment containing multiple RyR channels (36). In this model, activation of RyR1 and RyR2 channels results in  $Ca^{2+}$  sparks formation while RyR3 channels contributes an inhibitory component that sets the basal  $Ca^{2+}$  spark frequency (see Fig. 1C).

### **PERSPECTIVE**

Experiments in both neonatal skeletal muscle and hippocampal neurons of RyR3 KO mice have revealed that ablation of RyR3 results in alterations of cellular activities, in spite of the presence in both systems of robust levels of other RyR isoforms. This effect can be rationalized considering that in neonatal skeletal muscles and hippocampal neurons RyR1 and RyR2 constitute the main RyR-mediate  $Ca^{2+}$  release signal transduction pathway. In both cases RyR3 channels may provide a positive feedback, probably via a  $Ca^{2+}$  induced  $Ca^{2+}$  release mechanism, which can contribute to build specific aspects of  $Ca^{2+}$  signaling of these cells. In such a model, deletion of RyR3 channels would not block the main pathways for activation of RyR-mediated  $Ca^{2+}$  release in skeletal muscle cells and neurons, but would result in non-optimal signaling, as evidenced by the altered performance of these cells in RyR3 KO mice. It should be reminded here that several laboratories have reported that RyR3 channels have properties that make these channels more adaptive than other RyR isoforms to  $Ca^{2+}$  induced  $Ca^{2+}$  release (17,18,37,38,39). Such properties would make the RyR3 channels particularly flexible for providing a more sustained  $Ca^{2+}$  release efflux from the endoplasmic reticulum following an initial increase in the intracellular concentration of  $Ca^{2+}$  mediated by other  $Ca^{2+}$  release channels on the endoplasmic reticulum or by  $Ca^{2+}$  channels on the plasma membrane. Depending on the system these channels are working in, positive or negative effects may be generated (Fig. 1). Indeed, while in neonatal skeletal muscle cells (Fig 1A) and in neurons (Fig 1B) RyR3 channels appear to represent a positive contribution to the mechanism of  $Ca^{2+}$  release, work in smooth muscle cells from cerebral arteries suggests that RyR3 channels may have a negative role in regulating the frequency of  $Ca^{2+}$  sparks generated by RyR1 and RyR2 isoforms and hence STOCs frequency (Fig 1C).

An interesting and yet unanswered question is linked to the evidence reported by Mironneau and colleagues in smooth muscle cells from portal vein and mouse myometrium, where RyR3 channels do not seem to respond to activating stimuli unless the  $Ca^{2+}$  loading of the sarcoplasmic reticulum is increased (34,35). Why are not these channels activated by conditions that usually stimulate RyR1 and RyR2 isoforms? Interestingly, a similar finding

was observed in mink lung epithelial cells expressing RyR3 (8). Further studies are needed to answer this and other outstanding questions. Certainly, the idea of a cell-specific selective assembling of the molecular machinery that mediates Ca<sup>2+</sup> release from the endoplasmic reticulum represents only a basic scheme in the complex world of Ca<sup>2+</sup> signaling. However, it may provide a starting point to decipher the molecular players that generate the precise spatial and temporal aspects of the sophisticated Ca<sup>2+</sup> signals required for controlling cellular functions. Although we have reviewed here initial evidence in support of a model on the functional significance of co-expression of RyR channels that represent our working hypothesis, more work in the future is certainly required to further support and eventually extend it.

#### ACKNOWLEDGMENTS

I want to thank former and current members of my laboratory as well as colleagues from other laboratories who have collaborated in studies on RyR3, Carlo Reggiani for critical reading of this manuscript and stimulating discussions, and to acknowledge Telethon, MURST, ASI, EEC and PAR/University of Siena for supporting work in my laboratory.

#### References

1. Sorrentino V: The ryanodine receptor family of intracellular Ca<sup>2+</sup> release channels. *Advances in Pharmacology* 33, 67-90 (1995)
2. MacLennan DH, W. J. Rice & N. M. Green: The mechanism of Ca<sup>2+</sup> transport by sarco(endo)plasmic reticulum Ca<sup>2+</sup>-ATPases. *J Biol Chem* 272, 28815-28818 (1997)
3. Meissner G: Ryanodine receptor/ Ca<sup>2+</sup> release channels and their regulation by endogenous effectors. *Ann Rev Physiol*, 56, 485-508 (1994)
4. Franzini-Armstrong C, F. Protasi: Ryanodine receptors of striated muscles: a complex channel capable of multiple interactions. *Physiol Rev* 77, 699-729, (1997)
5. Maryon E B, R. Coronado & P. Anderson: unc-68 encodes a ryanodine receptor involved in regulating *C. elegans* body-wall muscle contraction. *J Cell Biol* 134, 885-893 (1996)
6. Dal Santo P, M.A. Logan, A.D. Chisholm & E.M. Jorgensen: The Inositol Trisphosphate Receptor Regulates a 50-Second Behavioral Rhythm in *C. elegans*. *Cell* 98, 757-767 (1999)
7. Sorrentino V, V. Barone & D. Rossi: Intracellular Ca<sup>2+</sup> release channels in evolution. *Curr Opin Gen Dev* 10, 662-667 (2000)
8. Giannini G, E. Clementi, R. Ceci, G. Marziali & V. Sorrentino: Expression of a novel Ryanodine-receptor/ Ca<sup>2+</sup> channel that is regulated by TGF $\beta$ . *Science* 257, 91-94 (1992)
9. Sorrentino V & P. Volpe: Ryanodine receptors: how many, where and why? *Trends in Pharmacol. Sciences* 14, 98-105 (1993)
10. Giannini G, A. Conti, S. Mammarella, M. Scrobogna & V. Sorrentino: The ryanodine receptor/ Ca<sup>2+</sup> channel genes are widely and differentially expressed in murine brain and peripheral tissues. *Journal of Cell Biology* 128, 893-904 (1995)
11. Sorrentino V & R. Rizzuto: Molecular genetics of Ca<sup>2+</sup> stores and intracellular Ca<sup>2+</sup> signalling *Trends in Pharmacol Sciences* 22, 459-464 (2001)
12. Tarroni P, D. Rossi, A. Conti & V. Sorrentino: Expression of the Ryanodine Receptor type 3 (RyR3) Ca<sup>2+</sup> release channel during development and differentiation of mammalian skeletal muscle cells. *Journal of Biological Chemistry* 272, 19808-19813 (1997)
13. Conti A, L. Gorza & V. Sorrentino: Differential content of ryanodine receptor type 3 (RyR3) in mammalian skeletal muscles. *Biochemical Journal* 316, 16-19 (1996)
14. Sutko JL & J. A. Airey: Ryanodine Receptor Ca<sup>2+</sup> Release Channels: Does Diversity in Form Equal Diversity in Function? *Pharmacol Rev* 76, 1027-1071 (1996)
15. Bertocchini F, C. Ovitt, A. Conti, V. Barone, H.R. Scholer, R. Bottinelli, C. Reggiani & V. Sorrentino: Requirement of the ryanodine receptor type 3 for efficient contraction in neonatal skeletal muscles, *The EMBO Journal* 16, 6956-6963 (1997)
16. Flucher BE, A. Conti, H. Takeshima & V. Sorrentino: Type 3 and Type 1 ryanodine receptors are colocalized in triads of developing skeletal muscle in mammals. *J Cell Biology* 146, 621-30 (1999)
17. Jeyakumar LH, J.A. Copello, A.M. O'Malley, G.M. Wu, R. Grassucci, T. Wagenknecht & S. Fleischer: Purification and characterization of ryanodine receptor type 3 from mammalian tissue. *J Biol Chem* 273, 26, 16011-16020 (1998)
18. Murayama T & Y. Ogawa: Characterization of Type 3 Ryanodine Receptor (RyR3) of Sarcoplasmic Reticulum from Rabbit Skeletal Muscles. *J Biol Chem* 272, 24030-24037 (1997)
19. Sorrentino V & C. Reggiani: Expression of Ryanodine receptor type 3 in skeletal muscle: a new partner in excitation-contraction coupling? *Trends in Cardiovascular Medicine* 9, 53-60 (1999)
20. Takeshima H, M. Iino, H. Takekura, M. Nishi, J. Kuno, O. Minowa, H. Takano & T. Noda: Excitation-contraction uncoupling and muscular degeneration in mice lacking functional skeletal muscle ryanodine-receptor gene. *Nature* 369, 556-559 (1994)
21. Takeshima H, T. Ikemoto, M. Nishi, N. Nishiyama, M. Shimuta, Y. Sugitani, J. Kuno, I. Saito, H. Saito, M. Endo, M. M. Iino & T. Noda: Generation and Characterization of Mutant Mice Lacking Ryanodine Receptor Type 3. *J Biol Chem*, 271, 19649-19652 (1996)
22. Dietsch B, F. Bertocchini, V. Barone, A. Struk, V. Sorrentino & W. Melzer: Voltage-controlled Ca<sup>2+</sup> release in normal and RyR3-deficient mouse myotubes. *J Physiology (Lond)* 513, 3-9 (1998)
23. Skirokova N, R. Shirokov, D. Rossi, J. Garcia, V. Sorrentino & E. Rios: Spatially segregated control of Ca<sup>2+</sup> release in developing skeletal muscle. *J Physiology (Lond)* 521, 483-495 (1999)
24. Conklin MW, V. Barone, V. Sorrentino & R. Coronado: Contribution of ryanodine receptor type 3 to calcium sparks in embryonic skeletal muscle. *Biophysical J* 77, 1394-1403. (1999)
25. Conklin MW, C.A. Ahern, P. Vallejo, V. Sorrentino, H. Takeshima & R. Coronado: Comparison of Ca(2+) Sparks Produced Independently by Two Ryanodine Receptor Isoforms (Type 1 or Type 3). *Biophys J* 78, 1777-1785 (2000)
26. Yang D, Z. Pan, H. Takeshima, C. Wu, R.Y. Nagaraj, J. Ma & H. Cheng: RyR3 amplifies RyR1-mediated Ca<sup>2+</sup>-induced Ca<sup>2+</sup> release in neonatal mammalian skeletal muscle. *J Biol Chem* 276, 40210-40214 (2001)
27. Bliss TVP & G.L. Collingridge: A synaptic model of memory: long-term potentiation in the hippocampus. *Nature* 361, 31-39 (1993)
28. Berridge MJ, P. Lipp & M.D. Bootman: The versatility and universality of calcium signalling. *Nat Rev Mol Cell Biol* 1, 11-21 (2000)
29. Wang Y, M.J. Rowan & R. Anwyl: Induction of LTD in the dentate gyrus in vitro is NMDA receptor independent, but dependent on Ca<sup>2+</sup> influx via low-voltage-activated Ca<sup>2+</sup> channels and release of Ca<sup>2+</sup> from intracellular stores. *J Neurophysiol* 77, 812-825 (1997)
30. Balschun D, D.P. Wolfer, F. Bertocchini, V. Barone, A. Conti, W. Zuschratter, L. Missiaen, H.P. Lipp, U. Frey & V. Sorrentino: Deletion of the ryanodine receptor Type 3 (RyR3) impairs forms of synaptic plasticity and spatial learning. *EMBO J* 18, 5264-5273 (1999)
31. Futatsugi A, K. Kato, H. Ogura, S.T. Li, E. Nagata, G. Kuwajuma, K. Tanaka, S. Itohara, K. Mikoshiba: Facilitation of NMDAR-independent LTP and spatial

- learning in mutant mice lacking ryanodine receptor type 3. *Neuron* 24, 701-713 (1999).
32. Nelson MT, H. Cheng, M. Rubart, L.F. Santana, A.D. Bonev, H.J. Knot & W.J. Lederer: Relaxation of arterial smooth muscle by calcium sparks. *Science* 270, 633-637 (1995)
  33. Coussin F, N. Macrez, J.L. Morel & J. Mironneau: Requirement of ryanodine receptor subtypes 1 and 2 for Ca(2+)-induced Ca(2+) release in vascular myocytes. *J Biol Chem* 275, 9596-603 (2000)
  34. Mironneau J, F. Coussin, L.H. Jeyakumar, S. Fleisher, C. Mironneau & N. Macrez: Contribution of ryanodine subtype 3 to calcium responses in Ca<sup>2+</sup>-overloaded cultured rat portal vein myocytes. *J Biol Chem* 276, 11257-11264 (2001)
  35. Mironneau M, N. Macrez, J. L. Morel, V. Sorrentino & C. Mironneau: Identification and function of ryanodine receptor subtype 3 in non-pregnant mouse myometrial cells. *J Physiology*, In press
  36. Löhn M, W. Jessner, M. Fürstenau, M. Wellner, V. Sorrentino, H. Haller, F. C. Luft & M. Gollasch: Regulation of Ca<sup>2+</sup> Sparks and Spontaneous Transient Outward Currents by RyR3 in Arterial Vascular Smooth Muscle Cells. *Circulation Research* 89, 1051 – 1057 (2001)
  37. Chen SRW, X. Li, K. Ebisawa & L. Zhang: Functional characterization of the recombinant type 3 Ca<sup>2+</sup> release channel (ryanodine receptor) expressed in HEK293 cells. *J Biol Chem* 272, 24234-46 (1997)
  38. Sonnleitner A, A. Conti, F. Bertocchini, H. Schindler & V. Sorrentino: Functional properties of the ryanodine receptor type 3 (RyR3) Ca<sup>2+</sup> release channel. *EMBO J* 17, 2790-2798 (1998)
  39. Simeoni I, D. Rossi, X. Zhu, J. García, H.H. Valdivia & V. Sorrentino: Imperatoxin A (IpTx) from *Pandinus imperator* stimulates [<sup>3</sup>H]ryanodine binding to RyR3 channels. *FEBS Letters* 508, 5-10 (2001)

**Corresponding author:**

Vincenzo Sorrentino  
Molecular Medicine Section,  
Department of Neuroscience,  
University of Siena,  
via Aldo Moro 5, 53100, Italy  
Phone 0039 0577 234 079; Fax 0039 0577 234 191  
e-mail: [v.sorrentino@unisi.it](mailto:v.sorrentino@unisi.it)

**key words:** ryanodine receptors isoforms, gene family, RyR3

**running title:** RyR3 isoform in Ca<sup>2+</sup> signalling

# Intracellular Ca<sup>2+</sup> Store in Embryonic Cardiac Myocytes

(Subtitle: RyR-2 and JP-2 in embryonic cardiac myocytes)

Hiroshi Takeshima

Department of Biochemistry, Tohoku University Graduate School of Medicine, Seiryō-machi, Aoba-ku, Miyagi 980-8575, Japan. E-mail: [takeshim@mail.cc.tohoku.ac.jp](mailto:takeshim@mail.cc.tohoku.ac.jp)

**ABSTRACT** In mature cardiac myocytes, Ca<sup>2+</sup> influx through the L-type Ca<sup>2+</sup> channel activates the ryanodine receptor and triggers Ca<sup>2+</sup> release from the sarcoplasmic reticulum (SR). This Ca<sup>2+</sup> signal amplification, termed Ca<sup>2+</sup>-induced Ca<sup>2+</sup> release (CICR), occurs within the junctional membrane complex between the plasma membrane and the SR, and is essential for cardiac excitation-contraction (E-C) coupling. On the other hand, Ca<sup>2+</sup> available during E-C coupling is predominantly derived from Ca<sup>2+</sup> influx in embryonic cardiac myocytes. To examine the role of the intracellular Ca<sup>2+</sup> store in immature cardiac myocytes, we have generated knockout mice lacking the cardiac type of the ryanodine receptor (RyR-2), or junctophilin (JP-2) contributing to formation of the junctional membrane complex. Both RyR-2- and JP-2-knockout mice show lethality at early embryonic stages immediately after beginning of heart beating. The loss of RyR-2 produced abnormal SR elements exhibiting vacuolated structures and Ca<sup>2+</sup>-overloading in embryonic cardiac myocytes. In JP-2-deficient cardiac myocytes, formation of junctional membrane complexes, called peripheral couplings, was disturbed, and abnormal Ca<sup>2+</sup> transients without spatial and temporal synchronization were observed. Therefore, the knockout mice have demonstrated that RyR-2-mediated Ca<sup>2+</sup> release at the junctional membrane complex is essential for cellular Ca<sup>2+</sup> homeostasis in immature cardiac myocytes.

## INTRODUCTION

The ryanodine receptor (RyR) constitutes a major class of intracellular Ca<sup>2+</sup> release channels that mediate Ca<sup>2+</sup>-induced Ca<sup>2+</sup> release (CICR), a mechanism that enhances cytoplasmic Ca<sup>2+</sup> concentrations during excitation-contraction (E-C) coupling (1). The RyR purified from skeletal muscle has been shown to form a homotetramer with the characteristic "foot" structure which spans the gap between the membranes of the sarcoplasmic reticulum (SR) and transverse tubule (2). The monomeric RyR is composed of ~5000 amino acid residues with the carboxyl-terminal channel region containing transmembrane segments and the remaining large cytoplasmic portion constituting the foot structure (3,4). A single gene encoding RyR is found in invertebrates, but mammalian genomes contain three genes for RyR subtypes, namely RyR-1, RyR-2 and RyR-3. The RyR subtypes are different not only in tissue distribution but also in physiological properties (for example, 5,6). During E-C coupling in skeletal muscle, opening of RyR-1 is directly controlled by the voltage-gated Ca<sup>2+</sup> channel/dihydropyridine receptor (DHPR), while in other cell types RyRs are thought to contribute to Ca<sup>2+</sup> signal amplification by the CICR mechanism.

The junctional membrane complex between the plasma membrane and the endoplasmic reticulum (ER) is common among excitable cells and is thought to provide a structural foundation for crosstalk between ionic channels (7,8). In skeletal muscle, the transverse (T-) tubule and the SR form a junctional complex, designated as the "triad junction" (9), where a proposed direct coupling between DHPR and RyR-1 converts the depolarization signal to Ca<sup>2+</sup> release

from the SR (10-12). Previous studies have demonstrated that the triad junctions are formed in mutant skeletal muscle cells lacking either DHPR or RyR (13,14), suggesting that the physiological coupling between DHPR and RyR requires the junctional membrane complex to be formed by as-yet-unidentified molecules. In our current experiments, junctophilin (JP) subtypes have been identified as major transmembrane proteins at junctional membrane complexes in excitable cells. JP subtypes are most likely to contribute to the stabilization of the junctional membrane complexes by anchoring the ER/SR and interacting with the plasma membrane to provide a structural framework for physical coupling between cell-surface and intracellular channels (15).

Heart muscle cells contain two types of junctional membrane complexes where DHPR (the L-type Ca<sup>2+</sup> channel) and RyR-2 (the channel responsible for CICR) are functionally coupled. The "diad" is formed by the T-tubular and SR membranes in mature myocytes, and the "peripheral coupling" is composed of the normal cell-surface membrane and SR in immature myocytes. During E-C coupling in mature cardiac myocytes, Ca<sup>2+</sup> flowing through DHPR binds to RyR and triggers a larger Ca<sup>2+</sup> release from the SR, generating a Ca<sup>2+</sup> signal that is essential for contraction (16,17). On the other hand, Ca<sup>2+</sup> available for E-C coupling in fetal cardiac myocytes is predominantly derived from Ca<sup>2+</sup> influx through DHPR (18), and therefore the function of the intracellular store in immature myocytes is not yet clear. In this review, we focus on the physiological role of Ca<sup>2+</sup> release from the developing SR in embryonic cardiac myocytes, with insights given by the observation of

RyR subtype	locus	tissue distribution	knockout phenotype
<b>mammalian</b>			
RyR-1	mouse 7A2-B3 human 19q13.1	skeletal muscle brain	neonatal lethality respiratory failure
RyR-2	mouse 13 human 1q42-43	cardiac & smooth muscles, brain	embryonic lethality heart failure
RyR-3	mouse 2E5-F3 human 15q14-15	skeletal & smooth muscles, brain	Impaired learning/memory hyperlocomotion
<b>invertebrate</b>			
nematodeRyR	chromosome V K11C4.5	muscle cells	hypolocomotion
fruit flyRyR	chromosome II position 44F	muscle cells	embryonic & larval lethality muscle dysfunction

Table I. Features of ryanodine receptor family members

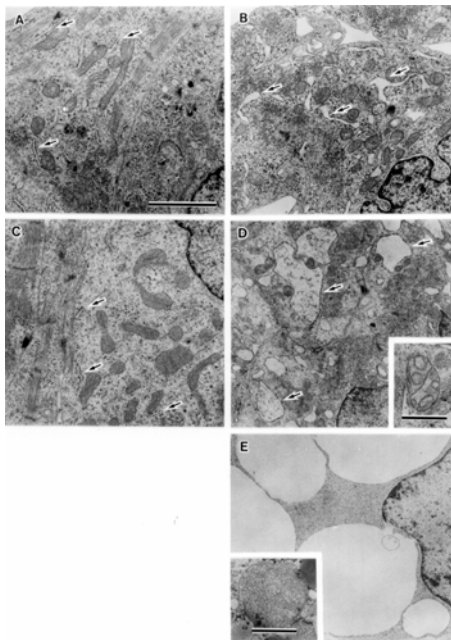


Fig. 1. Ultrastructural abnormalities in cardiac myocytes from the RyR-2-knockout embryonic mice. Electron micrographs were obtained from cardiac myocytes in (A) E8.5 wild-type, (B) E8.5 mutant, (C) E9.5 wild-type, (D) E9.5 mutant and (E) E10.5 mutant embryos. Abnormal vacuoles were detected in the mutant myocytes, and the growth of the vacuoles in size was observed during embryonic development. The normal rER (or developing SR) in wild-type myocytes and the rER carrying swelling parts and abnormal vacuoles in the mutant myocytes are indicated by arrows. The majority of mitochondria contained abnormal tubular cristae in the E9.5 mutant myocytes, and were further swelling in the E10.5 mutant myocytes (insets in D and E). Scale bars; 5  $\mu$ m in A-E, 1  $\mu$ m in insets of D and E. It has been demonstrated that the abnormal vacuoles of the mutant myocytes contain higher  $Ca^{2+}$  than the developing SR of wild-type myocytes in other experiments. The data suggest that  $Ca^{2+}$  overloading results in the formation of the vacuoles from the SR in the mutant myocytes.

heart failure in mutant mice (15,19),

## RESULTS AND DISCUSSION

### RYR-MUTANT ANIMALS

Cloning studies so far demonstrate that invertebrate and vertebrate genomes contain a single RyR gene and three RyR subtype genes, respectively, and that there is no RyR gene in yeast. In nematode and fruit fly, the RyR genes are predominantly activated in muscle cells. Voltage-dependent  $Ca^{2+}$  influx through the DHPR homologue seems to be essential in E-C coupling in invertebrate muscle cells (20). RyRs probably contribute to  $Ca^{2+}$  signal amplification as SR  $Ca^{2+}$  release channels in invertebrates, because the RyR-knockout nematode exhibits hypolocomotion due to weakened body-wall muscle cells (21), and the RyR-knockout fruit fly shows lethality at larval stages likely due to dysfunction of body-wall muscle (22).

Some general features of RyR subtypes are listed in Table I. RyR-1 is expressed predominantly in skeletal muscle and weakly in the brain. RyR-1-knockout mice die immediately after birth because E-C coupling is abolished in the mutant skeletal muscle (11,23). RyR-2 is predominantly expressed in cardiac muscle and is also distributed in smooth muscle and neurons. RyR-2-knockout mice exhibit embryonic lethality as described below. RyR-3 is detected in skeletal and smooth muscles, brain and certain non-excitable cells at low levels. RyR-3-knockout mice do not show lethality or obvious anatomical abnormalities (24), but bear impaired muscle and brain functions, weakened muscle contraction (25), hyperlocomotion (24) and insufficient learning and memory (26-28).

In human genetic diseases, several mutations have been determined in the RyR subtype genes. Genomic point mutations and resulting amino

acid substitutions in the RyR-1 primary structure are responsible for malignant hyperthermia and central core disease, and both diseases are caused by abnormalities in SR  $\text{Ca}^{2+}$  release in skeletal muscle (29). A recent study found that mutations in the RyR-2 gene underlie catecholaminergic polymorphic ventricular tachycardia (30).

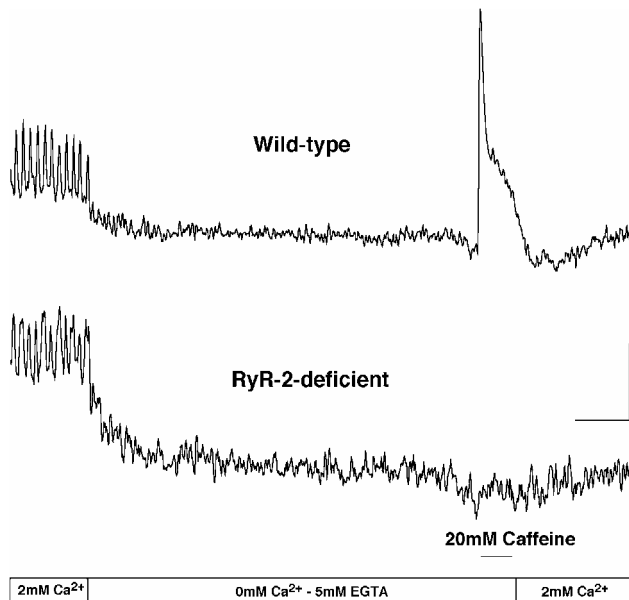


Fig. 2. Spontaneous  $\text{Ca}^{2+}$  oscillations and loss of caffeine-evoked  $\text{Ca}^{2+}$  transients in cardiac myocytes from E9.5 RyR-2-knockout mice. Intracellular  $\text{Ca}^{2+}$  concentrations of myocytes from wild-type (upper trace) and RyR-2-knockout (lower trace) embryos were measured with Fluo-3, and the time course of change in fluorescence intensity is shown.  $\text{Ca}^{2+}$  oscillations in both genotypes were abolished in a  $\text{Ca}^{2+}$ -free solution containing 5 mM EGTA. The application of 20 mM caffeine in the  $\text{Ca}^{2+}$ -free solution induced  $\text{Ca}^{2+}$  transients in wild-type myocytes, but not in the mutant myocytes. The horizontal scale indicates 20 s, and the vertical scale shows 10% change relative to the diastolic level in fluorescence intensity in upper trace and 5% in lower trace.

### Cardiac failure in RyR-2 knockout mice

To prepare RyR-2-knockout mice, a deletion mutation was introduced at the first exon of the RyR-2 gene in embryonic stem cells. The resulting knockout mice showed cardiac arrest and lethality at about embryonic day (E) 10.5. Histological analysis demonstrated that cardiac myocytes were irregularly arranged in the hearts (cardiac tubes) from the E9.5 RyR-2-knockout embryos. Ultrastructural analysis using an electron microscopy showed that the ER/SR elements were partly swollen in E8.5 mutant cardiac myocytes, and were further vacuolated at E9.5 and E10.5 (Fig. 1). In the analysis with calcium oxalate precipitates,  $\text{Ca}^{2+}$ -overloading was suggested in the vacuolated ER/SR from the RyR-2-knockout myocytes (data not shown). Moreover, mitochondria exhibited tubular cristae and were swollen in the mutant cardiac myocytes. The abnormal morphological features prior to cardiac arrest suggested that the RyR-2 deficiency primarily damages embryonic cardiac myocytes.

The hearts of both RyR-2-knockout and control embryos show beating at E9.5, and the

cardiac myocytes exhibited spontaneous  $\text{Ca}^{2+}$  oscillations that can be monitored with fluorometric  $\text{Ca}^{2+}$  indicators (Fig. 2). Application of caffeine, an activator of RyR subtypes, evoked  $\text{Ca}^{2+}$  transients in wild-type cardiac myocytes, but not in the RyR-2-knockout myocytes. Therefore, RyR-2 appears to be solely expressed in embryonic cardiac myocytes, although skeletal and smooth muscle cells contain at least two RyR subtypes. To determine the possible contribution of  $\text{Ca}^{2+}$  release via RyR-2 to E-C coupling in embryonic myocytes, control myocytes were examined under store-depleting conditions using caffeine and ryanodine (Fig. 3). Spontaneous contractions and  $\text{Ca}^{2+}$  oscillations were still retained after ryanodine treatment, even though depletion of stores was confirmed by the lack of response to subsequent application of caffeine. Therefore, the loss of CICR mediated by RyR-2 does not abolish E-C coupling in the hearts at the early embryonic stages.

On the basis of the above observations, it seems reasonable to conclude that RyR-2 does not play a significant role in  $\text{Ca}^{2+}$  signaling during E-C coupling in embryonic hearts; instead, it appears that it maintains the normal range of luminal  $\text{Ca}^{2+}$  levels in the developing SR (Fig. 7). Our proposal is that in the RyR-2-knockout cardiac myocytes, cytoplasmic  $\text{Ca}^{2+}$  derived from the extracellular fluid during E-C coupling may gradually accumulate in the developing SR; the cytoplasmic  $\text{Ca}^{2+}$  that cannot be sequestered by the overloaded SR may then flow into mitochondria, causing defective organelles and/or the abnormal  $\text{Ca}^{2+}$  homeostasis that leads to cellular dysfunction. Therefore, it is likely that RyR-2 can function as a safety valve for the intracellular  $\text{Ca}^{2+}$  store in embryonic cardiac myocytes. This conclusion is supported by the result that the vacuolated SR is shared by mutant skeletal muscle from double-knockout mice lacking both RyR-1 and RyR-3 (14). Skeletal muscle contains RyR-1 and RyR-3 as the major and minor components, respectively, but mutant muscle cells lacking either RyR-1 or RyR-3 do not exhibit such severe ultrastructural defects

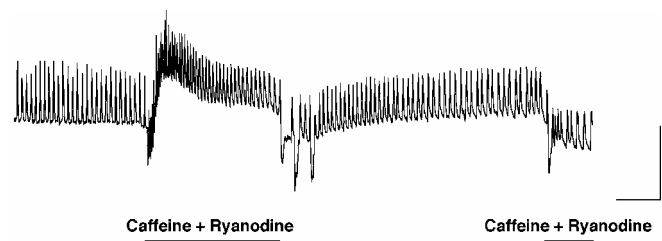


Fig. 3. Effects of ryanodine on spontaneous  $\text{Ca}^{2+}$  oscillations in embryonic cardiac myocytes. The time course of change in fluorescence intensity of Fluo-3 is shown, and representative responses are shown from experiments using E9.5, E10.5 and E11.5 wild-type cardiac myocytes. Ryanodine (100  $\mu\text{M}$ ) was applied with caffeine (20 mM) to deplete intracellular  $\text{Ca}^{2+}$  stores (the binding of ryanodine to RyR is enhanced when the RyR channel is opened by caffeine). Depletion of the stores was confirmed by no response to the secondary application of caffeine. The horizontal scale indicates 20 s, and the vertical scale represents 10% change in fluorescence intensity relative to the diastolic level. Downward deflections were due to movement artifacts of the specimen by solution exchanges.

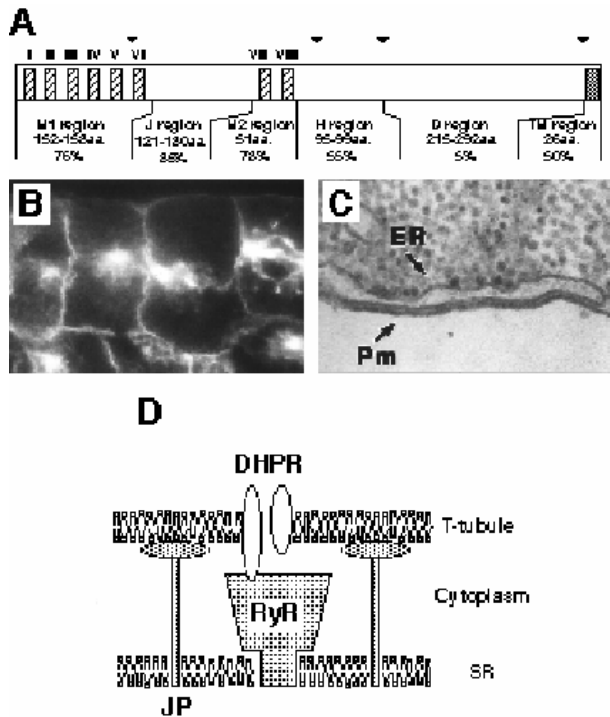


Fig. 4. Structure and proposed function of JP. Structural features of the JP subtypes (A). Several observations predict six intramolecular domains in JP; M1 region, MORN motif region 1; J region, joining region; M2, MORN motif region 2; H region, putative  $\alpha$ -helical region; D region, divergent region; TM region, membrane-spanning region (for details see ref. 32). Amino acid residue number and sequence identity among the JP subtypes are shown in each proposed domain. The locations of introns interrupting the JP subtype-coding sequences in human genome are indicated by arrows; the genomic organization is conserved among the JP subtypes. Analysis of amphibian embryonic cells expressing JP-1 (B,C). An immunofluorescence image of the cells expressing full-length JP-1 is shown in B. Specific staining with monoclonal antibody against JP-1 was observed on the plasma membrane of the embryonic cells. An electron micrograph of JP-1-expressing cells is shown in C. Junctional complexes between the plasma membrane (Pm) and the endoplasmic reticulum (ER) were formed in cells injected with JP-1 mRNA. No such ultrastructures were detected in control cells. Proposed role of JP at the triad junction in skeletal muscle (D). The subcellular localization and biochemical features suggest that JP contributes to formation of the triad junction, where proposed direct coupling between DHPR and RyR converts the depolarization signal into the cytoplasmic  $Ca^{2+}$  signal. As described in the text, skeletal muscle triad junctions contain both JP-1 and JP-2, and they may have different physiological roles.

(11,24). In striated muscle cells, the complete loss of  $Ca^{2+}$  release channels may produce such abnormalities in SR structure. The molecular mechanism for the vacuolated SR is unclear, because  $Ca^{2+}$  is not a major ion in comparison with  $K^+$ ,  $Na^+$  or  $Cl^-$ , and  $Ca^{2+}$ -overloading alone can not produce obvious osmotic changes between the SR lumen and the cytoplasm. One possibility is that luminal  $Ca^{2+}$ -sensitive  $K^+$  or  $Cl^-$  channels may be involved in formation of the vacuolated SR. The predicted channel might be probably shared by skeletal and

cardiac myocytes and could have an important physiological role in SR  $Ca^{2+}$  handling.

### Identification of JP as component of junctional membrane complex

To search for proteins supporting the structure of the triad junction, we prepared monoclonal antibody (mAb) libraries from mice immunized with membrane vesicles from rabbit skeletal muscle (31). Of the antibodies screened, mAb2510 labeled intracellular rows oriented transversely in the longitudinal skeletal muscle cryosections, and the location of the rows was assigned to interfaces between the A and I-bands, where triad junctions are localized. In the ultrastructural analysis of sections labeled with the immunocolloidal gold, specific labeling was detected near the triad junction and frequently located in the junctional gap between the T-tubule and SR. We named the antigen protein of  $\sim 72$  kilodaltons (kda) mitsugumin72 or junctophilin type 1 (JP-1). cDNA cloning demonstrated that rabbit JP-1 is composed of 662 amino acid residues and contains a single transmembrane segment at its carboxyl-terminal end. Therefore, the bulk of JP-1 is located in the cytoplasmic region of the junctional gap between the SR and T-tubular membranes. In the cytoplasmic region of JP-1, motif sequences of 14 residues, called "MORN motif" sequences, were found repeated eight times (Fig. 4A). The putative consensus sequence for this motif is "Tyr-Gln/Glu-Gly-Glu/Gln-Trp-x-Asn-Gly-Lys-x-His-Gly-Tyr-Gly".

To examine functional aspects, JP-1 mRNA was generated in vitro and was injected into amphibian embryos (15). Immunofluorescence observation indicated that expressed JP-1 was localized on the plasma membrane in the embryonic cells (Fig. 4B). Electron microscopy revealed junctional complexes between the ER and plasma membrane in the JP-1-expressing cells (fig. 4C); these ultrastructures could not be detected in control cells. Thus, it is likely that the junctional membrane complexes correspond to the immunoreactive plasma membrane observed histochemically. Furthermore, when the soluble form of JP-1 lacking the carboxyl-terminal transmembrane segment was expressed, immunolabeling was detected specifically on the plasma membrane, but no junctional membrane complexes were formed (data not shown). The subcellular distribution of the truncated JP-1 demonstrates the specific binding affinity of the cytoplasmic domain for the plasma membrane, and the membrane-spanning segment is essential for the generation of the junctional membrane structures. Successive expression experiments of deletion-bearing JP proteins indicated that MORN motifs contribute to specific binding with the plasma membrane in the cytoplasmic region (data not shown). Therefore, it is proposed that JP-1 is involved in the formation of the skeletal muscle triad junction by interacting with the T-tubule and spanning the junctional SR membrane as shown in Fig. 4D.

In an attempt to search for JP family members (15,22), we used the cross-hybridization

JP subtype	locus	tissue distribution	knockout phenotype
<b>mammalian</b>			
JP-1	mouse 1A2-5 human 8q21	skeletal muscle	perinatal lethality suckling failure
JP-2	mouse 2H1-3 human 20q12	skeletal, cardiac smooth muscles	embryonic lethality heart failure
JP-3	mouse 8E human 16q23-24	brain	motor discoordination
<b>invertebrate</b>			
nematode JP	chromosome I T22C1.7	muscle cells	hypolocomotion
fruit fly JP	chromosome II region 30B	?	?

Table II. Features of junctophilin family members

technique and isolated cDNAs encoding JP-2 and JP-3 from libraries derived from heart and brain, respectively. The defined mouse JP subtypes, composed of 660-744 amino acid residues, show homology in sequence (overall ~40% identity among them) and share structural features with rabbit JP-1. The regions containing the MORN motif sequences (~80% identity) and carboxyl-terminal hydrophobic segment spanning the ER/SR membrane (~50% identity) are conserved well among the JP subtypes, whereas the regions of 211-286 residues immediately preceding the transmembrane segment are highly divergent (~6% identity). Based on the regional sequence identities among the subtypes, structural features and genomic organization, six intermolecular domains are proposed in JP (Fig. 4A).

### JP-knockout animals

As in the case of the RyR gene, invertebrate genomes contain a single JP gene, mammalian genomes carry three JP subtype genes, and no JP gene is found in yeast. The nematode JP gene is predominantly activated in muscle cells. Nematodes, in which expression of JP was inhibited by RNA-mediated interference (RNAi), showed hypolocomotion. Taking into account data in RyR-knockout animals, the hypolocomotion is likely due to the deficiency of junctional membrane structures and the resulting reduction of  $Ca^{2+}$  signaling during E-C coupling in muscle cells (33). Mutant phenotype on the JP gene has not yet been reported in fruit fly.

Some general features of JP subtypes are listed in Table II. Northern and Western blot experiments in mouse and human tissues indicated that JP-1 is predominantly expressed in skeletal muscle, JP-2 is detected in skeletal, cardiac and smooth muscles, and JP-3 is abundantly expressed in the brain (15,32). Therefore, the JP subtypes seem to be distributed throughout excitable tissues and may take part in junctional membrane complexes

including the subsurface cisternae. JP-1-knockout mice die within a day after birth and show no milk suckling. In the mutant skeletal muscle containing JP-2 at normal levels, formation of triad junctions is impaired and contraction responses to low-frequency stimuli are reduced. These results suggest that JP-1 and JP-2 are functionally different in skeletal muscle, and that JP-1-mediated formation of triad junctions is required for efficient E-C coupling in newborn mice (34). JP-2-knockout mice exhibit embryonic lethality as described below. JP-3-knockout mice do not show lethality or obvious morphological abnormalities, but bear impaired motor coordination in different tasks (35). The brain-specific expression of JP-3 suggests that irregular functions of certain neurons induce motor uncoordination in the mutant mice. On the other hand, no human diseases caused by abnormalities of JP subtypes are known, although some genetic diseases are linked with the regions mapped to the JP subtype loci.

### Cardiac failure in JP-2 knockout mice

In the adult mouse heart, an antibody against JP-2 mainly recognized cytoplasmic rows along the Z-lines within myocytes. In fetal mice on E9.5, the looped cardiac tube of the immature heart was immunofluorescence-positive, and the labeled region was in the periphery of cardiac myocytes. These observations suggest that JP-2 is localized on the junctional SR in diads and peripheral couplings. The targeted disruption of the mouse JP-2 gene induced embryonic lethality in the homozygous state. In the E9.5 knockout embryos the hearts showed spontaneous contractions, but the heartbeats were often weak and irregular. More than half of the E10.5 mutants exhibited cardiac arrest and congested peripheral tissues, and the E11.5 mutants showed autolysis after death. Although JP-2 expression is observed throughout muscle cell types in adult mice, neither skeletal nor smooth muscle cells appear to be

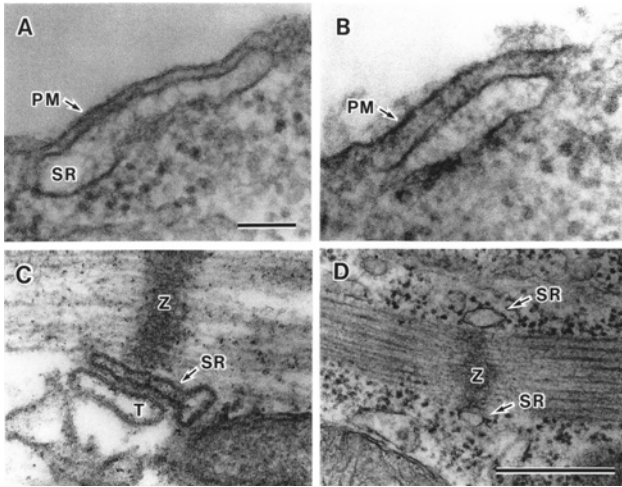


Fig. 5. Junctional membrane structures in embryonic cardiac myocytes. Cardiac myocytes from wild-type E9.5 embryos contained two types of junctional complexes between the cell-surface membrane and the SR with gap sizes of  $\sim 12$  (A) and  $\sim 30$  nm (B). In the diad observed in mature cardiac myocytes from adult mice, the gap size between the T-tubule and SR membranes was  $\sim 12$  nm (C). Therefore, the junctional membrane complex bearing the 12 nm gap is likely to correspond to the functional peripheral coupling as the structural foundation for the physiological crosstalk between the DHPR and RyR in the embryonic myocytes. The connection between the SR and Z-line is common to striated muscles, and the structures are also found in immature cardiac myocytes from E9.5 embryos (D). PM, plasma membrane; SR, sarcoplasmic reticulum; T, transverse tubule; Z, Z-line. Scale bars, 0.1  $\mu\text{m}$  in A-C and 0.5  $\mu\text{m}$  in D.

functionally developed in the early embryonic stages. Therefore, the loss of JP-2 in the mutant embryos affects mainly cardiac myocytes.

Cardiac myocytes from wild-type E9.5 embryos contained two types of junctional membrane complexes with gap sizes of  $\sim 12$  and  $\sim 30$  nm (Fig. 5A and B). According to previous reports, the gap size in the diad from mature cardiac myocytes is predominantly  $\sim 12$ -nm (Fig. 5C), suggesting that the 12-nm junctions correspond to functional peripheral couplings in embryonic myocytes. Statistical analysis demonstrated that in the JP-2-knockout myocytes the appearance of the 12-nm junction was reduced to only  $\sim 10\%$  of the control value; numbers of the junctions per 100  $\mu\text{m}$  plasma membrane in wild-type and mutant myocytes are  $12.4 \pm 0.2$  and  $15 \pm 0.7$ , respectively. Furthermore, the average length of the 12-nm junctional membrane complex in the mutant myocytes was significantly shorter than that in controls;  $0.17 \pm 0.06$   $\mu\text{m}$  in mutant myocytes and  $0.37 \pm 0.16$   $\mu\text{m}$  in controls. Also, there were no differences between the genotypes in control SR structures, the 30-nm junction and the close association between the SR and Z-line, namely "Z tubule" (36). The deficiency of the peripheral coupling, demonstrated in the mutant myocytes prior to cardiac arrest, clearly supports the hypothesis that JP subtypes contribute to the formation of the junctional membrane complexes in various cell types.

Functional abnormalities of the JP-2-knockout hearts from the E9.5 mutants were

examined in  $\text{Ca}^{2+}$ -imaging analysis. Because cardiac E-C coupling requires  $\text{Ca}^{2+}$  influx via DHPR, heart beats are abolished under  $\text{Ca}^{2+}$ -free conditions. In wild-type hearts, all myocytes showed synchronized  $\text{Ca}^{2+}$  transients, and the transients disappeared in a  $\text{Ca}^{2+}$ -free bathing solution (Fig. 6). However, in mutant hearts from the JP-2-knockout embryos, a large number of myocytes showed irregular  $\text{Ca}^{2+}$  transients that were not synchronized with the heartbeats and occurred randomly in space. Although the random transients were observed in all mutant hearts examined, the frequency of myocytes showing the abnormal transients was higher in the mutant hearts with infirm heart beatings. Moreover, the random transients were retained in the  $\text{Ca}^{2+}$ -free bathing solution, albeit the frequency was significantly reduced. Of the RyR subtypes only RyR-2 is expressed in the embryonic cardiac myocytes as described in the above section. The random transients in the JP-2-knockout myocytes were abolished by combined application of caffeine and ryanodine, and intracellular  $\text{Ca}^{2+}$  waves were observed during the random  $\text{Ca}^{2+}$  transients (data not shown). These results indicate that the abnormal transients in the JP-2-knockout hearts are evoked by  $\text{Ca}^{2+}$  release from the SR through RyR-2.

RyR-2 expressed in embryonic cardiac myocytes is prone to regenerative  $\text{Ca}^{2+}$  release responses even under resting  $\text{Ca}^{2+}$  levels because of its high  $\text{Ca}^{2+}$  sensitivity for channel activation. Thus, RyR-2 produces  $\text{Ca}^{2+}$  waves and oscillations independent of  $\text{Ca}^{2+}$  influx when expressed in cultured skeletal myocytes that have high SR  $\text{Ca}^{2+}$  contents (5). Moreover, abnormal intracellular  $\text{Ca}^{2+}$  waves have been observed in cardiac myocytes that have high SR  $\text{Ca}^{2+}$  loading and have been implicated in arrhythmia (37,38). As described above, the data from the RyR-2-knockout hearts suggest that SR  $\text{Ca}^{2+}$  levels can be increased by the reduction of RyR-2-mediated  $\text{Ca}^{2+}$  release in embryonic cardiac myocytes. It may be reasonable then that the loss of JP-2 disconnects the physiological coupling between cell-surface DHPR and SR RyR-2, because the deficiency of the functional peripheral coupling likely prevents close association of the channel molecules and interferes with effective activation of RyR-2 by DHPR-mediated  $\text{Ca}^{2+}$  influx. The resulting reduction of SR  $\text{Ca}^{2+}$  release may temporally produce the  $\text{Ca}^{2+}$ -overloaded SR in the mutant myocytes. The overloaded  $\text{Ca}^{2+}$  may be randomly released through RyR-2, and the generated  $\text{Ca}^{2+}$  rise in a microdomain may be expanded to neighboring SR regions by CICR to produce the intracellular  $\text{Ca}^{2+}$  waves (Fig. 7). The random  $\text{Ca}^{2+}$  transients in the mutant heart probably produce local extrasystoles and infirm heartbeats.

Mutant cardiac myocytes from both RyR-2-knockout and JP-2-knockout embryos contained mitochondria that have irregular internal structures. The abnormal  $\text{Ca}^{2+}$  homeostasis may produce mitochondria dysfunction and further toxic effects on the mutant myocytes. Stress and damage in mitochondria provokes permeability transition and triggers the cytochrome release as the cell-death signal (39). Cardiac failure in the mutant embryos

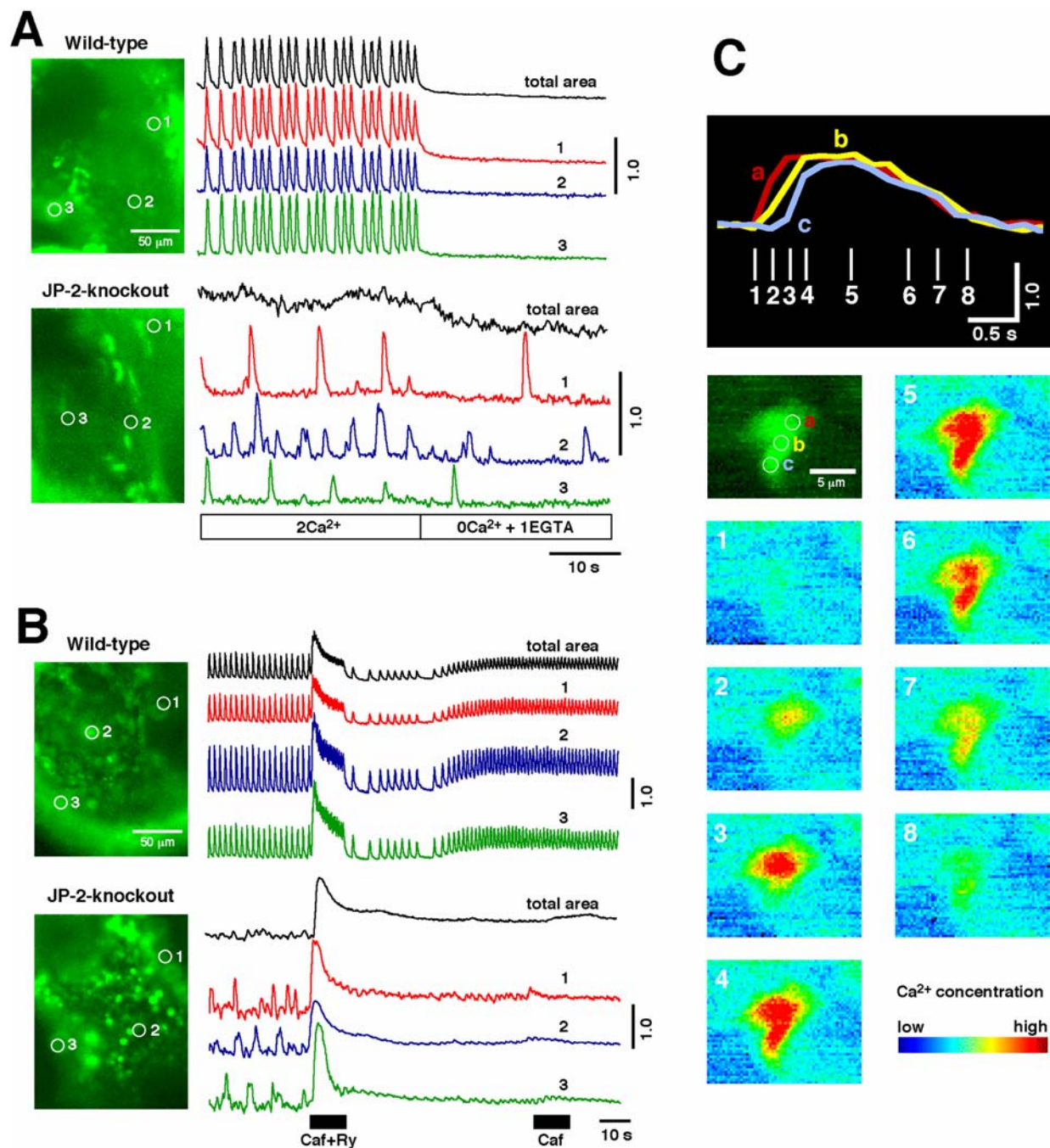
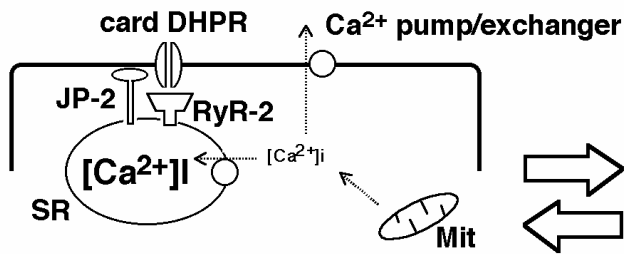
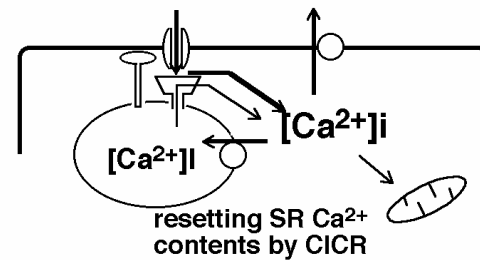


Fig. 6. Abnormal Ca<sup>2+</sup> transients in cardiac myocytes from the E9.5 JP-2-knockout embryos. Intracellular Ca<sup>2+</sup> changes during spontaneous oscillations in wild-type (upper traces) and JP-2-knockout (lower traces) cardiac myocytes from the cardiac tubes were measured in the normal bathing solution and the Ca<sup>2+</sup>-free solution containing 1 mM EGTA (A). The myocytes, examined for traces (1-3), are indicated by white circles in the fluorescence image of the embryonic heart. Abolishment of the random Ca<sup>2+</sup> transients in the mutant hearts under Ca<sup>2+</sup>-store-depleted conditions (B). The effects of the application of 20 mM caffeine (Caf) and 100  $\mu\text{M}$  ryanodine (Ry) on the Ca<sup>2+</sup> transients were examined in the normal bathing solution. In wild-type hearts, rhythm disturbances of heart beating were often observed after the caffeine applications with or without ryanodine. Spatial and temporal patterns of the random Ca<sup>2+</sup> transient in a single JP-2-knockout cardiac myocyte (C). The upper traces show the time-courses of changes in fluorescence intensity during a Ca<sup>2+</sup> transient; the intracellular regions examined are indicated in the fluorescence image of the myocyte (a-c). Intracellular Ca<sup>2+</sup> concentrations during the Ca<sup>2+</sup> transient are shown in pseudo-color images at the frames indicated in the upper panel (1-8). The vertical scales are indicated in  $\Delta F/F_0$ .

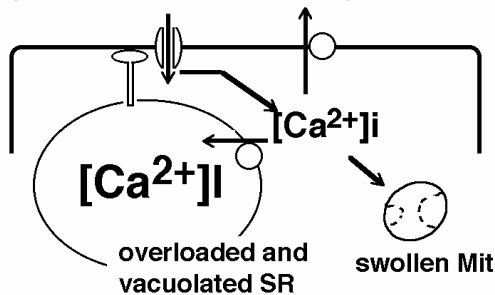
## Resting state



## Contraction state (CICR coupled with Ca<sup>2+</sup> influx)

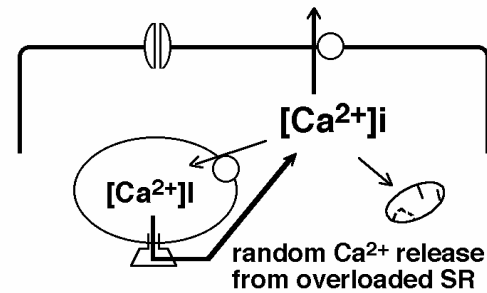


## RyR-2 knockout (CICR-defective mutation)



**Organelle defects probably induces myocyte dysfunction**

## JP-2-knockout (CICR-deficient mutation)



**Abnormal Ca<sup>2+</sup> transients in diastolic states probably produce local extrasystoles**

Fig. 7. Proposed roles of JP-2 and RyR-2 on the SR in embryonic cardiac myocytes. Based on the results of gene targeting studies, major intracellular Ca<sup>2+</sup> flows in embryonic cardiac myocytes are illustrated. Even though contributing slightly to Ca<sup>2+</sup> transients during E-C coupling, RyR-2-mediated Ca<sup>2+</sup> release coupled with Ca<sup>2+</sup> influx is essential for regulating Ca<sup>2+</sup> contents of the SR to maintain the cellular functions in embryonic cardiac myocytes. The loss of RyR-2 seems to induce Ca<sup>2+</sup>-overloading in the developing SR and produce SR vacuoles. JP-2-mediated formation of peripheral coupling appears to be essential for functional crosstalk between DHPR and RyR. Structural abnormalities of mitochondria are thought to be induced by irregular Ca<sup>2+</sup> homeostasis in RyR-2 and JP-2 knockout myocytes.

likely underlies the cell death triggered by mitochondria. Furthermore, possible crosstalk in Ca<sup>2+</sup> handling between the SR and mitochondria might be important to understand pathological defects in the failing hearts.

### PERSPECTIVE

In the embryonic heart, Ca<sup>2+</sup> release from the SR has no important role in Ca<sup>2+</sup> signaling during E-C coupling. However, our mutant mice lacking RyR-2 or JP-2 demonstrated that SR Ca<sup>2+</sup> release coupled with Ca<sup>2+</sup> influx is essential for cellular Ca<sup>2+</sup> homeostasis in embryonic cardiac myocytes, and further imply that reduction of Ca<sup>2+</sup> release and abnormalities in membrane structures may cause cardiac failure and heart arrest. Therefore, it is important to examine micro-structures at cellular and organelle levels for understanding RyR-mediated Ca<sup>2+</sup> release from intracellular stores. Current progress in the E-C coupling research field requires the combination of physiology with molecular biology. Further unification of molecular physiology with morphology and cell biology would be needed in future studies in this field.

### ACKNOWLEDGEMENTS

I thank many collaborators for their contributions in the studies. Our studies were supported in part by grants from the Ministry of Education, Science, Sports and Culture of Japan, the Ministry of Health and Welfare of Japan, the Japan Science and Technology Corporation (CREST), the Takeda Science Foundation, Mochida Memorial Foundation, Japan Heart Foundation, Japanese Foundation of Metabolism and Disease, Kimura Memorial Heart Foundation and Toray Science Foundation.

### References

1. M. Endo: Ca<sup>2+</sup> release from sarcoplasmic reticulum. *Curr. Topic. Membr. Transp.* 25, 181-230 (1985)
2. S. Fleisher & M. Inui: Biochemistry and biophysics of excitation-contraction coupling. *Annu. Rev. Biophys. Biophys. Chem.* 18, 333-364 (1989)
3. H. Takeshima, S. Nishimura, T. Matsumoto, H. Ishida, K. Kangawa, N. Minamino, H. Matsuo, M. Ueda, M. Hanaoka, T. Hirose & S. Numa: Primary structure and expression from complementary DNA of skeletal muscle ryanodine receptor. *Nature* 339, 439-445 (1989)
4. B. M. Bhat, J. Zhao, H. Takeshima & J. Ma: Functional calcium release channel formed by the carboxyl-terminal portion of ryanodine receptor. *Biophys. J.* 73, 1329-1336 (1997)
5. T. Yamazawa, H. Takeshima, T. Sakurai, M. Endo & M.

- Iino: Subtype specificity of the ryanodine receptor for Ca<sup>2+</sup> signal amplification in excitation-contraction coupling. *EMBO J.* 15, 6172-6177 (1996)
6. J. Nakai, T. Ogura, F. Protasi, C. Franzini-Armstrong, P. D. Allen & K. G. Beam: Functional nonequality of the cardiac and skeletal ryanodine receptors. *Proc. Natl. Acad. Sci. USA.* 94, 1019-1022 (1997)
  7. T. Pozzan, R. Rizzuto, P. Volpe & J. Meldolesi: Molecular and cellular physiology of intracellular calcium stores. *Physiol. Rev.* 74, 595-636 (1994)
  8. A. Verkhratsky & A. Shmigol: Calcium-induced calcium release in neurons. *Cell Calcium* 19, 1-14 (1996)
  9. B. E. Flucher: Structural analysis of muscle development: transverse tubules, sarcoplasmic reticulum, and the triad. *Dev. Biol.* 154, 245-260 (1992)
  10. T. Tanabe, K. G. Beam, J. A. Powell & S. Numa: Restoration of excitation-contraction coupling and slow calcium current in dysgenic muscle by dihydropyridine receptor complementary DNA. *Nature* 336, 134-139 (1988)
  11. H. Takeshima, M. Iino, H. Takekura, M. Nishi, J. Kuno, O. Minowa, H. Takano & T. Noda: Excitation-contraction uncoupling and muscular degeneration in mice lacking functional skeletal muscle ryanodine-receptor gene. *Nature* 369, 556-559 (1994)
  12. M. F. Schneider: Control of calcium release in functioning skeletal muscle fibers. *Annu. Rev. Physiol.* 56, 463-484 (1994)
  13. C. Franzini-Armstrong, M. Pincon-Raymond & F. Rieger: Muscle fibers from dysgenic mouse in vivo lack a surface component of peripheral couplings. *Dev. Biol.* 146, 364-376 (1991)
  14. T. Ikemoto, S. Komazaki, H. Takeshima, M. Nishi, T. Noda, M. Iino & E. Endo: Functional and morphological features of myocytes from mutant mice lacking both ryanodine receptors type 1 and type 3. *J. Physiol.* 501, 305-312 (1997)
  15. H. Takeshima, S. Komazaki, M. Nishi, M. Iino & K. Kangawa: Junctophilin: a novel family of junctional complex proteins. *Mol. Cell* 6, 11-22 (2000)
  16. A. Fabiato & F. Fabiato: Calcium triggered release of calcium from the sarcoplasmic reticulum of skinned cells of adult human, dog, cat, rabbit, rat and frog heart and fetal and newborn rat ventricles. *Ann. N. Y. Acad. Sci.* 307, 491-3522 (1978)
  17. M. Nabauer, G. Callewaert, L. Cleenman & M. Morad: Regulation of calcium release is gated by calcium current, not gating charge, in cardiac myocytes. *Science* 244, 800-803 (1989)
  18. T. Klitzner & W. F. Friedman: Excitation-contraction coupling in developing mammalian myocardium: evidence from voltage clamp studies. *Pediatr Res.* 23, 28-32 (1988)
  19. H. Takeshima, S. Komazaki, K. Hirose, M. Nishi, T. Noda & M. Iino: Embryonic lethality and abnormal cardiac myocytes in mice lacking ryanodine receptor type 2. *EMBO J.* 17, 3309-3316 (1998)
  20. R. Y. N. Lee, L. Lobel, M. Hnagartner, H. R. Horvitz & L. Avery: Mutations in the alpha1 subunit of an L-type voltage-activated Ca<sup>2+</sup> channel cause myotonia in *Caenorhabditis elegans*. *EMBO J.* 16, 6066-6076 (1997)
  21. Ed. B. Maryon, R. Coronado & P. Anderson: *unc-68* encodes a ryanodine receptor involved in regulating *C. elegans* body-wall muscle contraction. *J. Cell Biol.* 134, 885-893 (1996)
  22. K. M. C. Sullivan, K. Scott, C. S. Zuker & G. M. Rubin: The ryanodine receptor is essential for larval development in *Drosophila melanogaster*. *Proc. Natl. Acad. Sci. USA.* 97, 5942-5947 (2000)
  23. R. A. Moore, H. Nguyen, J. Galceran, I. N. Pessah & P. D. Allen: A transgenic myogenic cell line lacking ryanodine receptor protein for homologous expression studies: reconstitution of Ry1R protein and function. *J. Cell Biol.* 140, 843-851 (1998)
  24. H. Takeshima, T. Ikemoto, M. Nishi, N. Nishiyama, M. Shimuta, Y. Sugitani, J. Kuno, I. Saito, H. Saito, M. Endo, M. Iino & T. Noda: Generation and characterization of mutant mice lacking ryanodine receptor type 3. *J. Biol. Chem.* 271, 19649-19652 (1996)
  25. A. Sonnleitner, A. Conti, F. Bertocchini, H. Schindler & V. Sorrentino: Functional properties of the ryanodine receptor type 3 (RyR3) Ca<sup>2+</sup> release channel. *EMBO J.* 17, 2790-2798 (1998)
  26. D. Balschun, D. P. Wolfer, F. Bertocchini, V. Barone, A. Conti, W. Zuschratter, L. Missiaen, H. P. Lipp, J. U. Frey & V. Sorrentino: Deletion of the ryanodine receptor type 3 (RyR3) impairs forms of synaptic plasticity and spatial learning. *EMBO J.* 18, 5264-5273 (1999)
  27. Y. Kouzu, T. Moriya, H. Takeshima & S. Shibata: Mutant mice lacking ryanodine receptor type 3 exhibit deficits of contextual fear conditioning and activation of calcium/calmodulin-dependent protein kinase II in hippocampus. *Mol. Brain Res.* 76, 142-150 (2000)
  28. M. Shimuta, M. Yoshikawa, M. Fukaya, M. Watanabe, H. Takeshima & T. Manabe: Postsynaptic modulation of AMPA receptor-mediated synaptic responses and LTP by the type 3 ryanodine receptor. *Mol. Cell Neurosci.* 17, 921-930 (2001)
  29. J. R. Mickelson & C. F. Louis: Malignant hyperthermia: excitation-contraction coupling, Ca<sup>2+</sup> release channel, and cell Ca<sup>2+</sup> regulation defects. *Physiol. Rev.* 76, 537-592 (1996)
  30. S. G. Priori, C. Napolitano, N. Tiso, M. Memmi, G. Vignati, R. Bloise, V. Sorrentino & G. A. Danielli: Mutations in the cardiac ryanodine receptor gene (hRyR2) underlie catecholaminergic polymorphic ventricular tachycardia. *Circulation* 103, 196-200 (2001)
  31. H. Takeshima, M. Shimuta, S. Komazaki, K. Ohmi, M. Nishi, M. Iino, A. Miyata & K. Kangawa: Mitsugumin29, a novel synaptophysin family member from the triad junction in skeletal muscle. *Biochem. J.* 331, 317-322 (1998)
  32. M. Nishi, A. Mizushima, K. Nakagawara & H. Takeshima: Characterization of human junctophilin subtype genes. *Biochem. Biophys. Res. Commun.* 273, 920-927 (2000)
  33. M. Yoshida, A. Sugimoto, Y. Ohshima & H. Takeshima: Important role of junctophilin in nematode motor function. *Biochem. Biophys. Res. Commun.* in press (2001)
  34. K. Ito, S. Komazaki, K. Sasamoto, M. Yoshida, M. Nishi, K. Kitamura & H. Takeshima: Deficiency of triad junction and contraction in mutant skeletal muscle lacking junctophilin type 1. *J. Cell Biol.* 154, 1059-1068 (2001)
  35. M. Nishi, K. Kuriyama, S. Shibata & H. Takeshima: Motor discoordination in mutant mice lacking junctophilin type 3. submitted for publication.
  36. F. O. Simpson & D. G. Rayns: The relationship between the transverse tubular system and other tubules at the Z disc levels of myocardial cells in the ferret. *Am. J. Anat.* 122, 193-208 (1968)
  37. W. G. Wier, J. R. Cannell, J. R. Berlin, E. Marban & W. J. Lederer: Cellular and subcellular heterogeneity of [Ca<sup>2+</sup>]I in single heart cells revealed by fura-2. *Science* 235, 325-328 (1987)
  38. R. J. Berlin, B. M. Cannell & J. W. Lederer: Cellular origins of the transient inward current in cardiac myocytes. Role of fluctuations and waves of elevated intracellular calcium. *Circ. Res.* 65, 115-126 (1989)
  39. G. Kromer, B. Dallaporta & M. Resche-Rigon: The mitochondrial death/life regulation in apoptosis and necrosis. *Annu. Rev. Physiol.* 60, 619-642 (1998)

**Address all correspondence to:**

Hiroshi Takeshima

Department of Biochemistry, Tohoku University  
Graduate School of Medicine,  
Seiryomachi, Aoba-ku, Miyagi 980-8575, Japan.  
Tel: +81-22-717-8084

Fax: +81-22-717-8090

E-mail: takeshim@mail.cc.tohoku.ac.jp

# Three-Dimensional Reconstruction of Ryanodine Receptors

Terence Wagenknecht<sup>1,2</sup> and Montserrat Samsó<sup>1</sup>

<sup>1</sup>Biggs Laboratory, Wadsworth Center, New York State Department of Health, Albany, NY 12201.

E-mail: [tcw02@wcnotes.wadsworth.org](mailto:tcw02@wcnotes.wadsworth.org)

<sup>2</sup>Department of Biomedical Sciences School of Public Health, State University of New York at Albany, Albany, NY 12201

**ABSTRACT** early all available information on the three-dimensional structure of the ryanodine receptor (RyR) class of intracellular calcium release channels has come from electron microscopy. This review focuses on results that have been obtained by cryo-electron microscopy of purified, detergent-solubilized receptors in combination with single-particle image processing. This approach has led to the most detailed 3D models of RyRs, which are currently at resolutions of 20-30 Å. All three of the known genetic isoforms show essentially identical architectures at this resolution: a large, 4-fold symmetric, cytoplasmic assembly that accounts for greater than 80% of the receptor's mass and is composed of at least 10 discrete, loosely packed domains, and a transmembrane region whose dimensions lead us to conclude that very little of RyR's protein mass is present on the luminal side of the sarco/endoplasmic reticulum. Three-dimensional reconstructions determined for RyRs that have been exposed to conditions that promote either open or closed states show subtle differences, some of which are located in the cytoplasmic assembly, at sites more distant than 100 Å from the ion channel in the transmembrane region. Several of the ligands (FK506-binding protein, calmodulin, dihydropyridine receptor) that interact in vivo with the skeletal RyR have been, or are in the process of being, mapped to various locations on the cytoplasmic assembly.

## INTRODUCTION

Ryanodine receptors (RyRs), which comprise a class of intracellular calcium channels, are the largest ion channels known. In mammals, RyRs are homotetramers of net molecular mass 2.2-2.3 X 10<sup>6</sup> Daltons, the precise value depending on the particular genetic isoform, of which three have been characterized (1, 2). Isoform 1 (RyR1) is highly enriched in skeletal muscle, isoform 2 (RyR2) is enriched in cardiac muscle, and isoform 3 (RyR3), as well as RyR1 and RyR2, are found at lower levels in a variety of tissues.

Being both very large and integral membrane proteins, RyRs present special challenges to the determination of their three-dimensional structures. Probably the method of choice for detailed structural characterization of RyRs would be X-ray crystallography, but this technique requires highly ordered crystals, which are not easily obtained for membrane proteins or for large protein assemblies. Furthermore, in striated muscle, and possibly in other tissues as well, RyRs form specific interactions with other proteins to form gigantic signal-transducing assemblies of such complexity that there is little hope of isolating them, much less of determining their structure at the atomic level.

In the past decade, cryo-electron microscopy (cryo-EM) of isolated macromolecules, in conjunction with computerized single-particle image processing, has emerged as a powerful methodology for determining the three-dimensional structure of large, multi-component proteins and ribonucleoproteins (3-7). Cryo-EM has eliminated the artifacts associated with chemical fixation, dehydration, and contrast

enhancement by heavy metals that have plagued EM in the past, but it has necessitated averaging large numbers images to compensate for the low signal-to-noise ratio inherent in micrographs of native, ice-embedded proteins (8). Unlike other structural techniques where "smaller is better," this approach is best suited for large assemblies of macromolecules. Probably its most appreciated advantages are that crystals are unnecessary and that rather small quantities of specimen are required (e.g., less than a microgram of protein is required to make a single grid, which can provide sufficient data to determine a 3D structure to moderate resolution). The main limitation of the approach is that atomic resolution, although possible in principle, is difficult to attain, and for studies of RyR, the best resolution to date is 20 Å (9) and most published studies report resolutions about 30 Å.

In this review we summarize the major findings thus far in elucidating the 3D structure of RyRs by cryo-EM and single-particle image processing. For readers who desire more details on the methodology, as it pertains to RyRs, a recent review is recommended (10).

## BASIC FEATURES OF RYR ARCHITECTURE

The first 3D reconstructions from micrographs of frozen-hydrated, detergent-solubilized RyR1s were reported in the mid 1990s by our laboratory (11) and independently by another group at the Baylor College of Medicine (12). All subsequent studies to date that have applied 3D cryo-microscopy techniques to RyRs have been produced by these same two laboratories, which we will henceforth refer to as the Albany and

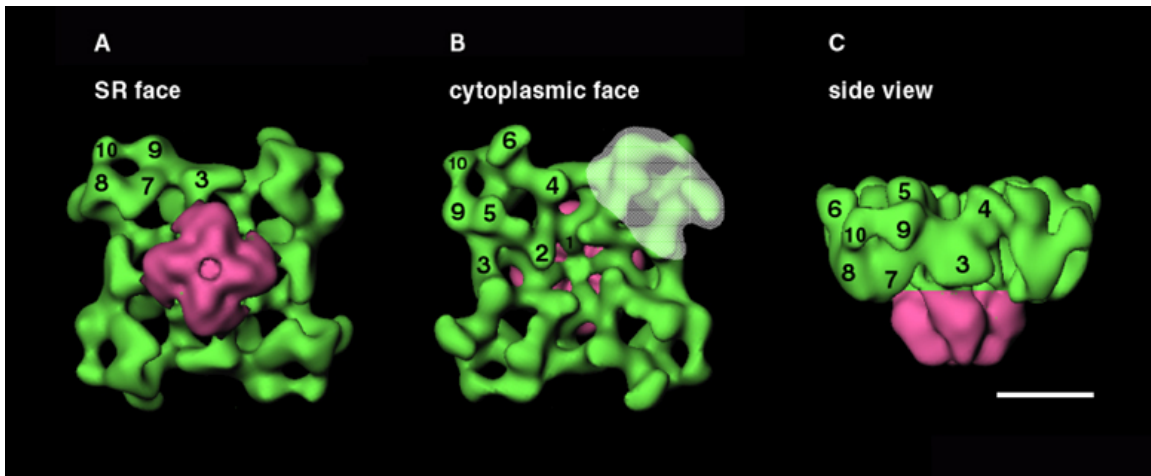


Figure 1. Three-dimensional architecture of RyR1. Solid body representations of RyR1 determined by cryo-electron microscopy and 3D reconstruction. The cytoplasmic assembly is shown in green and the transmembrane region is in pink. Numerals have been assigned to each of the domain-like structures that comprise the cytoplasmic assembly. Three orientations are shown. (A) View onto the SR face. This surface contains the transmembrane region. (B) View onto the opposite face from that in (A). This is the surface that would interact with the T-tubule in skeletal muscle. The white shadowing indicates one of the four equivalent areas with high probability of interaction with the DHPR. (C) A side view, obtained by rotating the views in (A), (B) by 90° about the horizontal. Scale bar, 100 Å. Adapted from (13).

Baylor groups when it is necessary to distinguish them. The initial reconstructions from the two groups, which were obtained by somewhat different methods (outlined in (13)), had an estimated resolution of  $\approx 30$  Å and, reassuringly, showed nearly identical structural features. A surface representation of the 3D model of Radermacher *et al.* (11) is illustrated in Figure 1 from which it is apparent that RyR has two main structural components: (a) a larger structure having a convoluted substructure and the overall shape of a square prism (280 X 280 X 120 Å), and (b) projecting from one of its faces, a smaller, 4-fold symmetric structure that appears more solid and less complex in appearance. The larger of these represents the cytoplasmic region of the receptor, whereas the smaller represents the transmembrane portion. The assignment of these cytoplasmic and transmembrane regions is based, in part, from the appearance of RyRs in electron micrographs of specimens in which the receptors remain integrated in their natural membrane environment (e.g. 14, 15). The clear fourfold symmetry is consistent with the receptor being a tetramer.

#### Cytoplasmic Assembly/Region.

The cytoplasmic assembly of RyR1 appears to consist of 10 or more discrete globular domains per subunit that are clearly resolvable due to their separation by solvent-accessible regions. Reassuringly, the arrangement of the various domains, as illustrated by Fig. 1, in which each domain has been assigned arbitrarily a numeral (Albany group), is essentially identical in all of the reconstructions that have been reported thus far. The four "3" domains, which form the sides of the square slab defined by the cytoplasmic assembly, are the largest of the domains, and the Baylor group has assigned to them a special name, the "handles". A cluster of domains (numbered 5-10) form each of the

corners of the cytoplasmic assembly, and the Baylor group has named these assemblages, the "clamps". The four "2" domains surround a central 40-50 Å diameter solvent-filled pocket that appears to extend to the proximal surface of the transmembrane region. Domain 1 appears to connect the cytoplasmic and transmembrane structures. Each clamp is connected to the remainder of the receptor via three interactions: (i) between domains 5/9 of the clamp and one of the handles, (ii) between clamp domain 6 and domain 4 which in turn attaches to the other handle, and (iii) between clamp domain 5 and domain 2.

We emphasize that the subunit boundaries cannot be discerned in the 3D reconstructions (i.e., it is not clear how to apportion the 4 sets of 10 domains to each of the four subunits). It is highly likely, however, that the entire cytoplasmic region is formed from amino acid residues beginning at the amino-terminus and extending to residues 4,000-4,500. The remainder of the 5,037 residues that comprise the RyR1 subunit form the transmembrane region.

#### Transmembrane assembly/region.

When viewed along the 4-fold symmetry axis and onto the face that contains it (Fig. 1A), the transmembrane region appears square in overall shape, but it is rotated by about 40 degrees from the square outlined by the cytoplasmic assembly. When RyR1 is viewed from the side (Fig. 1C), the transmembrane region frequently appears tapered, with the end that is connected to the cytoplasmic region having a larger diameter,  $\approx 120$  Å, than the other end. The transmembrane assembly's length is about 70 Å, more than sufficient to traverse a membrane bilayer. The shape of the transmembrane region varies between independently determined

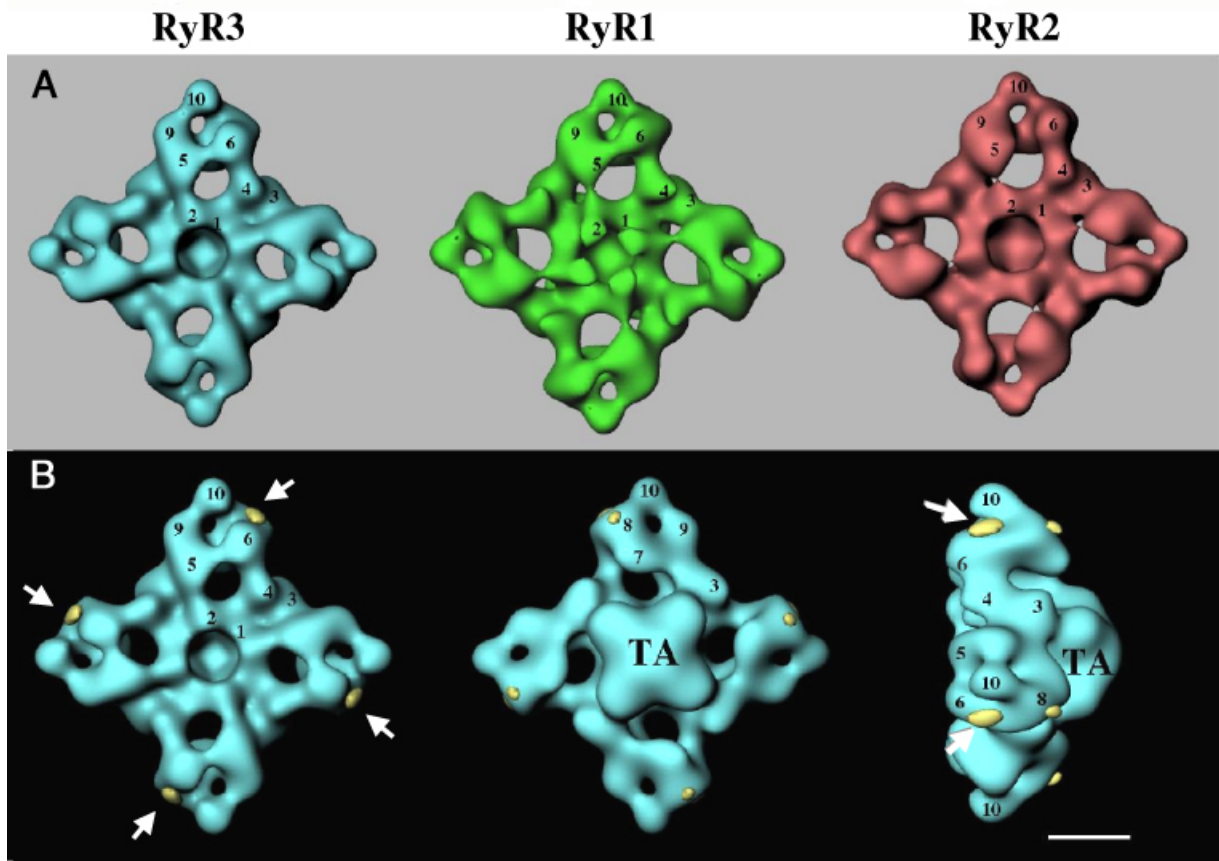


Figure 2. Comparison of 3D reconstructions of RyR1, RyR2, RyR3. (A) Shows solid body representations of RyR3 (blue), RyR1 (green), RyR2 (red) viewed onto the cytoplasmic surface. Note conservation of domain architecture. (B) RyR3 superimposed with the major differences (yellow) that are obtained when the 3D reconstruction of RyR3 is subtracted from that of RyR1. Arrows indicate the main difference which is tentatively attributed to the D2 region which is absent from RyR3 (see text for details). Adapted from (28).

reconstructions. As will be seen below, some of this variability is likely due to differing functional states of the receptor, but other uncharacterized factors are also involved. One possibility, for which there is some evidence (unpublished observations, Albany group), is that the transmembrane assembly's orientation with respect to the cytoplasmic assembly varies among the receptors that contribute to a reconstruction, resulting in this part of the reconstruction being less reliably resolved in some reconstructions.

In some 3D reconstructions of RyRs a 20-30 Å-diameter column of low density (indicating solvent accessibility) extends along the 4-fold symmetry axis of the transmembrane region (e.g., Radermacher et al. (11)). When treated with ryanodine, which according to functional analyses locks the receptor in an open or partially open state, this region becomes better defined, and it appears to form a channel across the transmembrane region (16). It has been argued that this channel corresponds to the wider regions of the ion-conducting pathway of RyR1. This argument is supported by analogy to the known structure of the potassium channel from *Streptomyces lividans* (17), which is also a tetramer and may be structurally homologous to RyR in the region of the transmembrane pore (18-20).

We suggest that the location of the ion-conducting pore or pores should be regarded as an open question, and that alternative "multi-barreled" models cannot be excluded at present (21). The single-pore model does not readily account for the four discrete, evenly spaced subconductance states that numerous laboratories have observed for RyR1 and RyR2 (22, 23). Possibly, four independent (but allosterically coupled) pores are present in the transmembrane region but are not resolvable at the resolutions attained in 3D reconstructions, and the centrally located low-density region is either not involved in ion conduction or represents only part of a pathway that branches to form four "subpores". It is worth remarking that the recently determined atomic models for aquaporin family members, also homotetramers, reveal functional transport pathways in each of the subunits, and a larger, centrally located gap between the four subunits that is not involved in transport (24-26). Finally, some recent reconstructions of RyR1 determined in our laboratory show low-density substructure in the transmembrane region that could be consistent with four pores per receptor (27).

## COMPARISON OF RYR ISOFORMS

Not surprisingly, given the >60% sequence identity among the three mammalian RyR isoforms, 3D reconstructions of RyR2 and RyR3 (Fig. 2A, left and right panels) are nearly identical to that of RyR1 (Fig. 2A, middle panel) in the 30-40 Å resolution range (28, 29). RyR3 differs significantly from RyR1 in a region at the distal edge of domain 6 (Fig. 2B) at each of the clamps. This difference corresponds to ≈10 kDa of protein mass that is present in RyR1 but absent in RyR3. Intriguingly, the sequence of RyR3 shows a deletion of 104 residues (1303-1406) relative to RyR's sequence. Thus, it seems likely that domain 6 bears this region of the sequence, which has been referred to as divergency region 2 (D2), one of three regions within RyR sequences that is highly variable among the three isoforms (30).

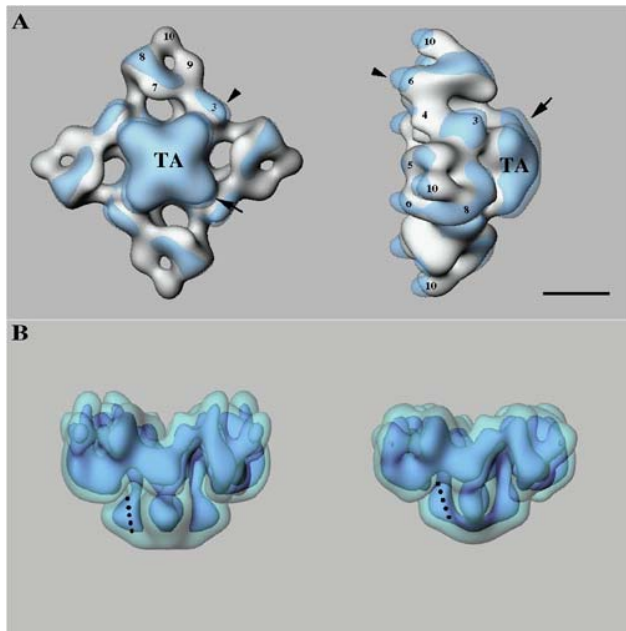


Figure 3. Comparison of putatively open and closed states of RyR3. (A) Solid body representation of closed RyR3 depicted in solid gray with open RyR3 superposed in transparent blue. Arrows denote regions where the surface of open RyR3 extends significantly beyond the surface of closed RyR3. (B) Open RyR3 (left) and Closed RyR3 (right) displayed at two density thresholds. The higher threshold (solid, darker blue) illustrates how the mass density shifts between the open and closed forms, particularly in the transmembrane region. Dotted line indicates an elongate region of density that splays outward in the open relative to the closed states. Scale bar, 100 Å. Adapted from (28).

### CONFORMATIONAL STATES OF RYR1 AND RYR3

Functional studies have established that open conformations of RyR1 are favored by the presence of  $\text{Ca}^{2+}$  (optimal at about 0.1 mM) and millimolar ATP. Channel closing is favored by the absence of nucleotide and submicromolar  $\text{Ca}^{2+}$ . The plant alkaloid ryanodine, binding to its high (nanomolar) affinity site, locks the receptor in an open state whose conductance is ≈40% that of the open state achieved with  $\text{Ca}^{2+}$  and nucleotide. The Baylor group compared a 3D reconstruction of RyR1 determined under conditions that favor the closed state with that

obtained in the presence of ryanodine (16). Subsequently, reconstructions of RyR1 in the presence of activating levels of  $\text{Ca}^{2+}$  and nucleotide were reported (31), and more recently the Albany group has determined 3D models of RyR3 under similar conditions (28). A caveat to all these studies is that they were performed on detergent-solubilized receptors, whereas functional gating analyses of the receptors are necessarily done on receptors in their native bilayer environment. Cryo-EM and 3D reconstruction of bilayer-associated RyRs have thus far not been feasible.

Reassuringly, the differences between the 3D reconstructions of the putatively open and closed states of the RyR1 (31) are remarkably similar to those reported for RyR3 (28). The results obtained for RyR3 are shown in figure 3. In figure 3A, the closed form is shown as a solid gray-colored body, and the open form is superimposed in transparent blue. Thus, wherever the receptor appears blue in color, the structure of the open form is outside of the envelope defined by the closed form; conversely where the receptor is gray, the envelope of the closed form is outside of that of the open form. In figure 3B, the open (left) and closed (right) structures are shown simultaneously at two density threshold levels: a semitransparent blue defines the molecular boundaries, and a higher threshold in a darker shade of blue is used to better reveal the nature of the structural differences between the two states, particularly in the transmembrane region.

The following are regarded as the most significant differences between open and closed RyR3 and RyR1:

1. The transmembrane assembly appears to rotate about the fourfold symmetry axis by a few degrees for RyR3 (Fig. 3A). This was seen for RyR1 in the ryanodine-induced open state, but it was not evident in the  $\text{Ca}^{2+}$  /nucleotide-induced open state.
2. Columnar regions of high density within the transmembrane region appear to splay apart in the open relative to the closed states (dotted lines in Fig. 3B), thereby creating a lower density running down the center of the transmembrane region. This effect was strongest for the ryanodine-modified RyR1. As discussed earlier, this region may or may not represent the pathway followed by ions when the receptor opens.
3. The transmembrane region is slightly taller when viewed from the side in the open vs. closed state (Fig 3A, rightmost arrow in right panel)
4. In the clamps, the height of domains 6 and 10 appear to increase in height by ≈15 Å.
5. A slight weakening of the density that connects domains 9 and 10 occurs in the open relative to the closed state. This effect is more apparent in the RyR1 reconstructions than in those of RyR3, and it is not clear in Fig. 3.

Most unexpected among the differences between open and closed RyRs were the changes in the clamps, which are separated by well over 100 Å from some of the changes that occur in the transmembrane region. As is discussed in more detail

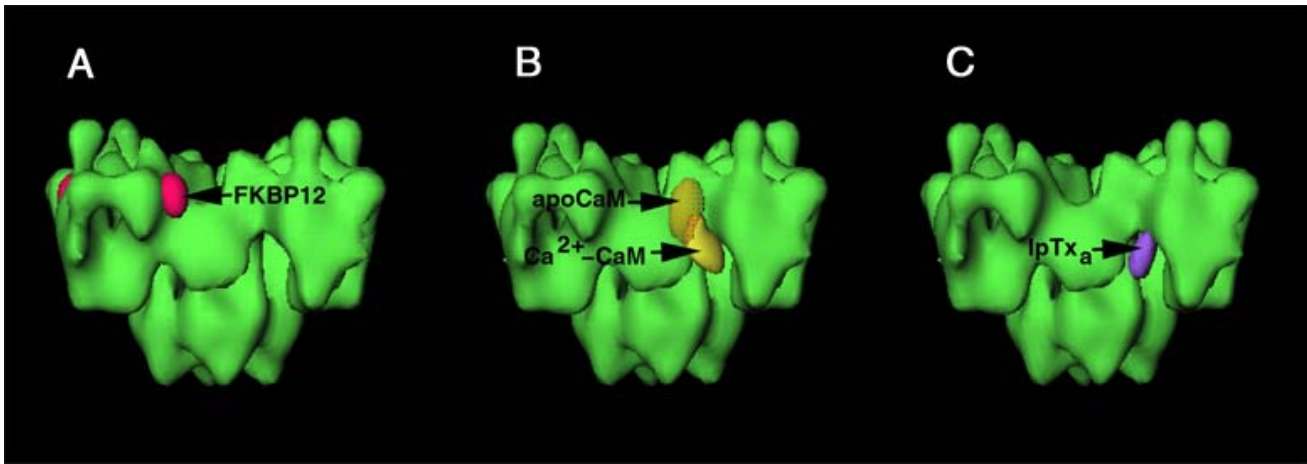


Figure 4. Ligand binding locations on RyR1. (A) Location of FKBP12 (fuchsia). (B) Location of both forms of CaM: apoCaM (transparent orange) and Ca<sup>2+</sup>-CaM (solid yellow) (C) Location of IpTx<sub>a</sub> (purple). The three 3D difference maps are superposed onto a common 3D reconstruction of RyR1 in absence of any ligand. bar, 100 Å. Adapted from (28).

below, the clamps are likely involved in interactions between the dihydropyridine receptor (DHPR) and RyR1 that appear to be essential for excitation-contraction (E-C) coupling in skeletal muscle (32). The changes in the clamp structure that accompany channel gating may be related to this communication between the two receptors.

#### INTERACTION SITES OF RYR MODULATORS

A major application of 3D cryo-EM is to characterize the modes of interaction between macromolecular assemblies and the proteins with which they functionally interact *in situ*. Among the ligands of RyR1 are the 12-kDa FK506-binding protein (FKBP12), calmodulin, the dihydropyridine receptor, calsequestrin, and the two integral membrane proteins of the sarcoplasmic reticulum (SR), triadin and junctin (33). The Albany group has investigated complexes of RyR1 with FKBP12, calmodulin, and an analog of the DHPR. The experiments are conceptually very simple: RyR and ligand are mixed *in vitro* under conditions favoring complex formation, the mixture is diluted if necessary, and then applied to specimen grids and frozen for EM in the usual way. If necessary, a control reconstruction is done of RyR lacking the ligand but otherwise identical. Finally, the reconstructions of the RyR with and without ligand are quantitatively compared by subtracting the corresponding voxels of the control from the experimental reconstruction to generate a 3D difference map.

#### FKBP12

FKBP12 is a *cis-trans* prolyl isomerase that binds with high affinity to RyR1 (34). Four copies of FKBP12 are bound per RyR1 tetramer and they can be induced to dissociate upon addition of either of the immuno-suppressant drugs, rapamycin or FK506 (35). Loss of FKBP12 appears to destabilize the closed state of RyR1(36, 37), but the role of FKBP12 *in vivo* is uncertain. Marks and co-workers found evidence that FKBP12 is involved in mediating

interactions between RyR1s, which form arrays in their native environment in muscle (38), and there is also evidence that FKBP12 plays a role in E-C coupling. RyR2 also binds FKBP12 or a close relative, FKBP12.6 (39), and RyR3 has been reported to bind FKBP12 (40, 41), although the functional effects, if any, on these isoforms are not clearly defined at present. A more detailed treatment of the FKBP:RyR2 interaction can be found elsewhere (A. Marks, 2002) in this volume.

Initial attempts to determine the FKBP12 binding site on RyR1 by our laboratory failed to detect any loss of protein mass from isolated RyR1 following treatment with the drug FK506. Apparently, the isolated RyR1 was deficient in bound FKBP12 because if FKBP12 was added exogenously to RyR1 in the presence and absence of FK506 (equivalent to FK506), then a highly significant difference was found that corresponded to excess mass in the non-drug-treated receptors (42, 43). The volume of the difference was consistent with that expected for a 12-kDa protein. Figure 4A shows that this density, which is attributed to FKBP12, is located adjacent to domain 9 where it joins to domain 3 (handle). Although no significant conformational changes in RyR1 were discernible at the rather limited resolution that was attained in this study, apparently such changes must not only occur, but they must be far-reaching. This is because the binding location of FKBP12 is about 120 Å from the center of the transmembrane region, which contains the ion-conducting pore (or pores) that is (are) modulated by FKBP12.

#### Calmodulin

As mentioned in Section 5, RyR is regulated by Ca<sup>2+</sup>. In addition, RyR is further modulated by CaM, another protein which is also regulated by Ca<sup>2+</sup>. CaM's structure and function depends on whether Ca<sup>2+</sup> is bound to each of its two modules (44, 45). These two forms of CaM exert opposite effects on the RyR. At submicromolar Ca<sup>2+</sup>, CaM (apoCaM) activates partially RyR1, whereas at millimolar Ca<sup>2+</sup>, Ca<sup>2+</sup>-CaM

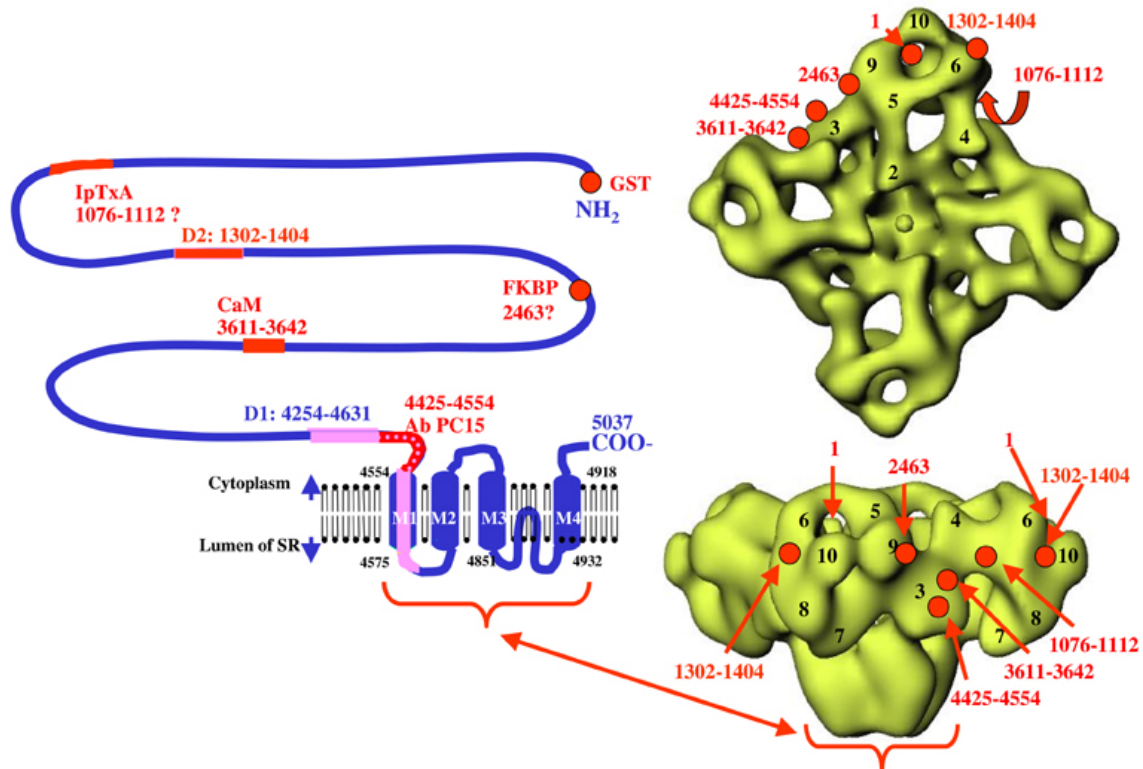


Figure 5. Sequence-structure correlation for RyR1 (tentative). Left side shows schematic representations of RyR1 sequence. Four transmembrane segments and a luminal loop between M3 and M4 that might form part of the ion pore are shown as proposed by Balshaw et al. (18), but the actual number of transmembrane segments may be greater than 4. Regions highlighted by red segments or dots are proposed to be involved in binding ligands that have been localized by 3D cryo-EM. The name of the ligand is also indicated in red, adjacent to the residue numbers. Question marks indicate assignments that are most speculative. Right side shows solid body representations of RyR1 in cytoplasmic and side views. The locations of the sequence-specific markers are indicated in red. The transmembrane region is bracketed and its relation to the sequence indicated by the double-headed red arrow. See text for references and details.

becomes a partial inhibitor (46-49). In the Albany laboratory we have localized this 16-kDa protein on the surface of RyR1, both at millimolar and submicromolar  $[Ca^{2+}]$ , by 3D difference mapping. Both types of CaM bind to the cytoplasmic assembly, with a stoichiometry of one CaM per RyR1 subunit, in agreement with current biochemical determinations (50). However, depending on the  $Ca^{2+}$  concentration, CaM localizes at slightly different sites.  $Ca^{2+}$ -CaM binds within the crevice formed by domains 3 and 5/6 (51, 52), and apoCaM binds to the external part of domain 3 (53) (Fig. 4B). The distance between the centers of the binding sites is  $33 \pm 5 \text{ \AA}$ , with a small area of overlap. This observed overlap is consistent with the protection found for two trypsin cleavage sites (after residues 3630 and 3637) by either form of CaM (50). In addition, recent results using synthetic peptides and single-point RyR1 mutants have shown that the two forms of CaM bind to very close, but distinct sites (54, 55). The separation between binding sites that we found is somewhat larger than one would expect from the separation in sequence (about 5 residues). This apparent discrepancy can be reconciled by taking into account the multiple binding possibilities of both CaM modules, e.g. as discussed in (53), by a RyR1 conformational change involving the CaM target sequence, or by a combination of both.

The proximity of both CaM binding sites might support switching of the CaM molecule between them under the successive  $Ca^{2+}$  cycles without necessity of complete dissociation from the RyR1, thus allowing a faster response.

### Dihydropyridine receptor

The interaction of RyR with the DHPR deserves special attention because of the key role it plays in E-C coupling in striated muscle. Within myofibers, specialized regions termed calcium release units (CRUs) occur where the terminal cisternae of the SR, which contains the RyRs, and tubular invaginations (T-tubules) of the plasma membrane, which contain the DHPRs, are close to each other (56); Protasi, 2002, in this volume. The close association of DHPRs and RyRs permits the activation of the latter by the former in a process known as E-C coupling. A similar functional coupling between RyR and DHPR has also been found in neurons (57, 58).

It is widely believed that in skeletal muscle E-C coupling occurs by a mechanical coupling mechanism (59, 60), whereby depolarization of the cell membrane/T-tubule induces a conformational change in the DHPR, which causes additional conformational changes in the RyR1 as a result of direct interactions between the two. Electron

microscopy of freeze fracture replicas revealed that calcium release units (CRUs) in skeletal muscle consist of ordered, complementary arrays of RyR1 and DHPR (14, 61, 62). Groups of four DHPRs (tetrads) appear to match alternate RyR1s. The relative geometry of the two proteins suggests that the clamps of RyR1 (see white shadowed area in Fig. 1B) are most likely to be involved in this interaction with DHPRs (13).

DHPR, an L-type  $\text{Ca}^{2+}$  channel, is a heteromer of 5 different subunits ( $\alpha 1$ ,  $\alpha 2$ ,  $\beta$ ,  $\delta$ ,  $\gamma$ ) (63). The ion-conducting pore and voltage sensor functions are supported mainly by the  $\alpha 1$  subunit, which contains 4 homologous repeats each with 6 predicted transmembrane domains. The three-dimensional structure of  $\alpha 1\beta$  complexes, as determined by EM and 3D reconstruction, is characterized by an elongate shape of 12 nm height and 9-10 nm width, with a central hole (64). Heart and skeletal muscle have distinct isoforms of  $\alpha 1$ , and the cytoplasmic loop between the second and third transmembrane repeats (II-III loop) is specially important in mediating the interaction between RyR and DHPR as well as in determining the type of E-C coupling (skeletal or cardiac) (65). Other cytoplasmic regions of the DHPR are probably also involved in the interaction with RyR1 (66, 67). The II-III loop contains functionally distinct subdomains, with activating and inhibiting activities (68, 69). Efforts to map more precisely the DHPR:RyR1 interaction have been hampered by the low affinity between these two proteins, and use of fixatives has found only moderate success (70).

The Albany group has used Imperatoxin a ( $\text{IpTx}_a$ ), a high affinity peptide mimetic of the activating region of DHPR's II-III loop (amino acid residues 666-791) (71), to begin mapping the RyR sites that interact with the DHPR (72).  $\text{IpTx}_a$  mimics a region near the N-terminus of the II-III loop that contains a cluster of basic residues. This 33-residue peptide toxin enhances binding of ryanodine to the receptors (73), and induces long-lived subconductance states (71, 74). Cryo-electron microscopy and image processing of streptavidin-labeled  $\text{IpTx}_a$  incubated with RyR1 showed that  $\text{IpTx}_a$  binds to the base of the crevice delimited by domains 3 and 7/8 of the cytoplasmic assembly (Fig. 4C). The relative large distance of the  $\text{IpTx}_a$  binding site from the putative ion channel ( $\sim 110 \text{ \AA}$ ) is indicative of an allosteric mechanism for activation of calcium release. The distance between the centers of mass of neighboring  $\text{IpTx}_a$ s is  $150 \text{ \AA}$ , a distance that is compatible with the distance between neighboring DHPRs of a tetrad in the triad junction (14). When RyR1 is viewed from the side (Fig. 4C),  $\text{IpTx}_a$  locates almost 5 nm from the T-tubule-face of RyR1. For the basic sequence of the II-III loop to reach this region would apparently require a fully extended conformation for the first 15 residues of the II-III loop that precede it (68).  $\text{IpTx}_a$  is discussed in more detail by Valdivia, et al (2002) in this volume.

An intriguing feature comes from the comparison of the  $\text{IpTx}_a$  binding site (Fig. 4C) with that of both CaM binding sites (Fig. 4B). In particular,

the binding site for  $\text{IpTx}_a$  is very close to that for  $\text{Ca}^{2+}$ -CaM. If indeed  $\text{IpTx}_a$  is a marker of the DHPR's II-III loop:RyR1 interaction, then CaM might play a direct role in the E-C coupling interaction.

Two additional results from 3D cryo-EM implicate RyR1's clamps as being involved in binding DHPR. Recall that the D2 region (RyR1 residues 1302-1404), which may be involved in the DHPR:RyR1 interaction (75), was assigned to domain 6, which is found in the clamps (section 5, Fig. 2B, Fig. 5). Finally, our laboratory has started to characterize the interaction of RyR1 with a cloned full-length II-III loop peptide (76), and preliminary results from cryo-EM are consistent with the II-III loop binding to a location near that assigned to the D2 region (77).

### **CORRELATION OF RYR1's AMINO ACID SEQUENCE WITH ITS 3D ARCHITECTURE**

An atomic structure for RyR seems not to be forthcoming, but even at the resolutions currently being attained by 3D cryo-EM it is feasible to determine the locations of surface-exposed amino acids if they can be appropriately labeled. With a sufficient number of amino-acid localizations it should be possible to largely define how the 5,037 amino acids that comprise the RyR1 subunit are apportioned among the various domains that are resolved in the 3D reconstructions. Even at this level of detail, it will in some cases be possible to evaluate the plausibility of hypothesized functions for particular amino acids from biochemistry experiments. For instance, amino acids of RyR1 that are proposed to interact directly with a ligand (e.g. calmodulin) should map to a spatially restricted region on the surface of the receptor that coincides with the location where the ligand itself is found to bind. If in the future high resolution structures are determined for cloned, expressed fragments of the RyR subunit, then having one or a few of a fragment's amino acid residues mapped on the receptor's surface by 3D cryo-EM will facilitate fitting the atomic model of the fragment into low-resolution density maps of the intact receptor.

An antibody of known specificity for a particular region of the RyR sequence would be a suitable probe for 3D cryo-microscopy. Although a number of sequence-specific antibodies have been described, our experience has been that many do not bind with sufficient affinity to detergent-solubilized RyRs for cryo-EM. A monoclonal antibody raised against an expressed fusion protein containing residues 4426-4621 of RyR1 (78) was found by 3D cryo-EM to bind on domain 3, near the transmembrane region (79). As indicated in figure 5 the antibody most likely recognizes an epitope contained within the amino-terminal half of the fusion protein.

For several of the ligands that were described in section 6, the amino acid residues of RyR that are involved in binding them are either known or plausible assignments have been made. Thus, these ligands can serve as sequence-specific probes. Calmodulin, for example, has been shown by two groups to bind at or very near to Cys-3635 of RyR1 (54,80). The

interaction site for FKBP12 has been mapped to amino acid residues in the immediate vicinity of Pro-2463, although another study implicated a site contained within residues 2756-2803 of RyR1 (41). More speculative is the site on RyR1 recognized by IpTx<sub>a</sub>. If IpTx<sub>a</sub> is indeed a mimic of the DHPR's II-III loop, then RyR1 residues 1076-1112 may be involved in the interaction (81). These localizations are summarized in figure 5.

The D2 region (RyR1 residues 1302-1404) is also tentatively indicated in figure 5. This assignment was made on the basis of the comparison of the RyR1 and RyR3 reconstructions discussed earlier (see also Fig 2). Recall that the D2 region is missing from the RyR3 sequence, and so we interpreted the excess mass that was present in the reconstruction of RyR1 relative to that of RyR3 as corresponding to this region of RyR1's sequence.

Finally, the location of the N-terminus of RyR1 was inferred to be near the center of the clamp (Fig. 5) from a 3D reconstruction of cloned, expressed RyR3 that contained glutathione transferase fused at the N-terminus (82). In the future, molecular cloning techniques that introduce modifications (e.g. insertions) at internal regions of the RyR sequence may result in an efficient, comprehensive protocol for determining the locations of surface-exposed segments of the receptor's sequence.

Most of the sequence assignments indicated in figure 5 should be regarded as tentative. As more sequence-specific probes are mapped, it will be possible to refine the assignments. Nevertheless, even with the limited data available, a self-consistent model is emerging. It appears that the amino terminal region of the RyR1 subunit, residues 1-1,400 at minimum, form each of the clamps (domains 5-10). The handle (domain 3) contains residues from the middle of the sequence (3,600- 4,400). Independent evidence from various sources has established that probably all of the transmembrane segments are contained within the 500-1000 carboxy-terminal amino acid residues (recently reviewed by Williams et al. (20).

## PERSPECTIVE

### High-resolution

The necessity of a high-resolution structure to gain a full understanding of how RyRs function cannot be understated. Efforts to obtain crystals of intact RyRs suitable for X-ray crystallography may require years before success is achieved. Electron crystallography, which requires two-dimensional crystals, could also yield a high-resolution structure for RyR, but the 2D crystals that have been obtained thus far show diffraction only to  $\approx 25$  Å resolution (83).

Whereas cryo-EM and single-particle image processing techniques can in principle achieve atomic resolution, this has not yet been achieved in practice. Currently, the highest resolution reported using these techniques for complexes that lack high symmetry is 7.5 Å, which was obtained for a 50S ribosomal subunit (84). Since the first 3D reconstructions of RyR1 were reported in 1994 (11), the resolution of

reported reconstructions has only improved from 30 Å to about 20 Å (Wah Chiu, Baylor School of Medicine, personal communication). It is not clear why the pace of progress has not been faster, but one possibility is that there is some intrinsic disorder in the RyR molecules which could be remedied by modifying the sample preparation techniques currently being used.

An alternative strategy to achieve atomic resolution is to crystallize and solve the atomic structures of cloned, expressed polypeptides corresponding in sequence to continuous segments of the RyR amino-acid sequence. Methods have been developed, and are continually improving, for fitting atomic models of component proteins into medium resolution maps obtained by 3D cryo-microscopy of the complexes containing them (85-87). If structures from a sufficient number of RyR-derived fragments could be obtained by X-ray crystallography or NMR techniques, and docked into RyR 3D maps, then a quasi-high resolution structure for the entire RyR could be determined in this piecemeal manner. Thus far crystallization of only one RyR1 fragment, corresponding to a portion of the D2 regions (see fig 5), has been reported (88).

### 3D localization of functional/structural sites.

The recent demonstration by Liu *et al.* (83) that structurally intact, genetically modified RyRs can be isolated from transfected cultured cells should greatly accelerate the rate of progress in determining the locations of functional/structural sites by 3D cryo-EM. Of the many possible modifications that might prove useful for this purpose, the one that we are currently testing involves introducing into the RyR sequence an insertion of amino acids that form an epitope for a commercially available monoclonal antibody. If the epitope is inserted into a surface-exposed region of RyR, then the addition of the antibody (or Fab fragment) to isolated receptors should result in the formation of immunocomplexes that can be solved by cryo-EM and 3D reconstruction. It should be appreciated that the precision with which labels (e.g. Fab fragments) can be positioned in the 3D density maps is several-fold greater than the resolution of the reconstruction itself; that is to say, epitope localizations with a precision approaching 10 Å should be achievable even at  $\approx 30$  Å resolution, which is routinely attained for RyRs.

### ACKNOWLEDGMENT

Supported by the National Institutes of Health R01AR40615, RR01219, and by the Muscular Dystrophy Association.

### References

1. Franzini-Armstrong, C. & Protasi, F. Ryanodine receptors of striated muscles: a complex channel capable of multiple interactions. *Physiol. Rev.* 77, 699-729 (1997).
2. Ogawa, Y., Kurebayashi, N. & Murayama, T. Ryanodine receptor isoforms in excitation-contraction coupling. *Advances In Biophysics* 36, 27-64 (1999).
3. Frank, J. Three-Dimensional Electron Microscopy of Macromolecular Assemblies. Academic Press, New York (1996).

4. Baumeister,W. & Steven,A.C. Macromolecular electron microscopy in the era of structural genomics . *Trends Biochem. Sci.* 25, 624-631 (2000).
5. Chiu,W., McGough,A., Sherman,M.B. & Schmid,M.F. High-resolution electron cryomicroscopy of macromolecular assemblies. *Trends in Cell Biology* 9, 154-159 (1999).
6. Frank,J. Cryo-electron microscopy as an investigative tool: the ribosome as an example . *BioEssays* 23, 725-732 (2001).
7. Nogales,E. & Grigorieff,N. Molecular machines: Putting the pieces together . *J. Cell Biol.* 152, F1-F10 (2001).
8. Dubochet,J., Adrian, M., Chang, J.-J., Homo, J.-C., Lepault, J., McDowell, A. W., & Schultz, P. Cryo-electron microscopy of vitrified specimens. *Quart. Rev. Biophys.* 21, 129-228 (1988).
9. Serysheva,I.I., Ludtke,S.J., Hamilton,S.L. & Chiu,W. Structure of skeletal muscle calcium release channel by electron cryomicroscopy: approaching high resolution. *Biophys. J.* 78, 485A (2000).
10. Orlova,E.V., Serysheva,I.I., Hamilton,S.L., Chiu,W. & van Heel,M. In: The structure and function of ryanodine receptors, 24-46. Eds: Sitsapesan,R. & Williams,A.J., Imperial College Press, London, UK (1998).
11. Radermacher,M., Rao, V., Grassucci, R., Frank, J., Timerman, A. P., Fleischer, S., & Wagenknecht, T. Cryo-electron microscopy and three-dimensional reconstruction of the calcium release channel ryanodine receptor from skeletal muscle. *J. Cell Biol.* 127, 411-423 (1994).
12. Serysheva,I.I., Orlova, E. V., Chiu, W., Sherman, M. B., Hamilton, S. L. & van Heel, M. Electron cryomicroscopy and angular reconstruction used to visualize the skeletal muscle calcium release channel. *Structural Biology* 2, 18-24 (1995).
13. Samsó, M. & Wagenknecht,T. Contributions of electron microscopy and single-particle techniques to the determination of the ryanodine receptor three-dimensional structure. *J. Struct. Biol.* 121, 172-180 (1998).
14. Block,B.A., Imagawa,T., Campbell,K.P. & Franzini-Armstrong,C. Structural evidence for direct interaction between the molecular components of the transverse tubule/sarcoplasmic reticulum junction in skeletal muscle. *J. Cell Biol.* 107, 2587-2600 (1988).
15. Saito,A., Inui,M., Radermacher,M., Frank,J. & Fleischer,S. Ultrastructure of the calcium release channel of sarcoplasmic reticulum. *J. Cell Biol.* 107, 211-219 (1988).
16. Orlova,E.V., Serysheva,I.I., van Heel,M., Hamilton,S.L. & Chiu,W. Two structural configurations of the skeletal muscle calcium release channel. *Nature Structural Biology* 3, 547-552 (1996).
17. Doyle,D.A. Cabral, J. M., Pfuetzner, R. A., Kuo, A., Gulbis, J. M., Cohen, S. L., Chait, B. T., MacKinnon, R. The structure of the potassium channel: molecular basis of K<sup>+</sup> conduction and selectivity. *Science* 280, 69-77 (1998).
18. Balshaw,D., Gao,L. & Meissner,G. Luminal loop of the ryanodine receptor: a pore-forming segment? *Proc. Natl. Acad. Sci. USA* 96, 3345-3347 (1999).
19. Zhao,M., Li, P., Li, X., Zhang, L., Winkfein, R. J. & Chen, S. R. W. Molecular identification of the ryanodine receptor pore-forming segment. *J. Biol. Chem.* 274, 25971-25974 (1999).
20. Williams,A.J., West,D.J. & Sitsapesan,R. Light at the end of the Ca<sup>2+</sup>-release channel tunnel: structures and mechanisms involved in ion translocation in ryanodine receptor channels. *Quart. Rev. Biophys.* 34, 61-104 (2001).
21. Marks,A.R. Cellular functions of immunophilins. *Physiol. Rev.* 76, 631-649 (1996).
22. Smith,J.S., Imagawa, T., Ma, J., Fill, M., Campbell, K. P., & Coronado, R. Purified ryanodine receptor from rabbit skeletal muscle is the calcium-release channel of sarcoplasmic reticulum. *J. Gen. Physiol.* 92, 1-26 (1988).
23. Williams,A.J. Ion Conduction and Discrimination in the Sarcoplasmic Reticulum Ryanodine Receptor/Calcium-Release Channel. *J. Muscle Res. Cell Motil.* 13, 7-26 (1992).
24. Ren,G., Reddy,V.S., Cheng,A., Melnyk,P. & Mitra,A.K. Visualization of a water-selective pore by electron crystallography in vitreous ice. *Proc. Natl. Acad. Sci. USA* 98, 1398-1403 (2001).
25. Fu,D.X., Libson, A., Miercke, L. J. W., Weitzman, C., Nollert, P., Krucinski, J. & Stroud, R. M. Structure of a glycerol-conducting channel and the basis for its selectivity. *Science* 290, 481-486 (2000).
26. Murata,K., Mitsuoka, K., Hirai, T., Walz, T., Agre, P., Heymann, J. B., Engel, A. & Fujiyoshi, Y. Structural determinants of water permeation through aquaporin-1. *Nature* 407, 599-605 (2000).
27. Samsó,M. & Wagenknecht,T. Cryo-electron microscopy of the ryanodine receptor transmembrane assembly. *Biophys. J.* 80, 330A (2001).
28. Sharma,M.R., Jeyakumar,L.H., Fleischer,S. & Wagenknecht,T. Three-dimensional structure of ryanodine receptor isoform three in two conformational states as visualized by cryo-electron microscopy. *J. Biol. Chem.* 275, 9485-9491 (2000).
29. Sharma,M.R., M. R., Penczek, P., Grassucci, R., Xin, H.-B., Fleischer, S., & Wagenknecht, T. Cryoelectron microscopy and image analysis of the cardiac ryanodine receptor. *J. Biol. Chem.* 273, 18429-18434 (1998).
30. Sorrentino,V. & Volpe,P. Ryanodine Receptors - How Many, Where and Why. *Trends Pharmacol. Sci.* 14, 98-103 (1993).
31. Serysheva,I.I., Schatz,M., van Heel,M., Chiu,W. & Hamilton,S.L. Structure of the skeletal muscle calcium release channel activated with Ca<sup>2+</sup> and AMP-PCP. *Biophys. J.* 77, 1936-1944 (1999).
32. Leong,P. & MacLennan,D.H. Complex interactions between skeletal muscle ryanodine receptor and dihydropyridine receptor proteins. *Biochemistry and Cell Biology* 76, 681-694 (1999).
33. Mackrill,J.J. Protein-protein interactions in intracellular Ca<sup>2+</sup>-release channel function. *Biochem. J.* 337, 345-361 (1999).
34. Jayaraman,T., Brillantes, A. M., Timerman, A. P., Fleischer, S., Erdjumentbromage, H., Tempst, P., & Marks, A. R. FK506 Binding Protein Associated with the Calcium Release Channel (Ryanodine Receptor). *J. Biol. Chem.* 267, 9474-9477 (1992).
35. Timerman,A.P., Ogunbumni, E., Freund, E., Wiederrecht, G., Marks, A. R., & Fleischer, S. The calcium release channel of sarcoplasmic reticulum is modulated by FK-506-binding protein. Dissociation and reconstitution of FKBP-12 to the calcium release channel of skeletal muscle sarcoplasmic reticulum. *J. Biol. Chem.* 268, 22992-22999 (1993).
36. Mayrleitner,M., Timerman,A.P., Wiederrecht,G. & Fleischer,S. The Calcium Release Channel of Sarcoplasmic Reticulum Is Modulated by FK-506 Binding Protein - Effect of FKBP-12 on Single Channel Activity of the Skeletal Muscle Ryanodine Receptor. *Cell Calcium* 15, 99-108 (1994).
37. Brillantes,A.B., Ondrias, K., Scott, A., Kobrinsky, E., Ondriasova, E., Moschella, M. C., Jayaraman, T., Landers, M., Ehrlich, B. E., & Marks, A. R. Stabilization of calcium release channel (ryanodine receptor) function by FK506-binding protein. *Cell* 77, 513-523 (1994).
38. Marx,S.O., Ondrias,K. & Marks,A.R. Coupled gating between individual skeletal muscle Ca<sup>2+</sup> release channels (ryanodine receptors). *Science* 281, 818-821 (1998).
39. Jeyakumar,L.H., Ballester, L., Cheng, D. S., McIntyre, J. O., Chang, P., Olivey, H. E., Rollins-Smith, L., Barnett, J. V., Murray, K., Xin, H. B., & Fleischer, S. FKBP binding characteristics of cardiac microsomes from diverse vertebrates. *Biochemical & Biophysical Research Communications* 281, 979-986 (2001).
40. Murayama,T., Oba, T., Katayama, E., Oyamada, H., Oguchi, K., Kobayashi, M., Otsuka, K., & Ogawa, Y. Further characterization of the type 3 ryanodine receptor (RyR3) purified from rabbit diaphragm. *J. Biol. Chem.* 274, 17297-17308 (1999).
41. Bultynck,G., De Smet, P., Rossi, D., Callewaert, G., Missiaen, L., Sorrentino, V., De Smedt, H., & Parys, J. B.

- Characterization and mapping of the 12 kDa FK506-binding protein (FKBP12)-binding site on different isoforms of the ryanodine receptor and of the inositol 1,4,5-trisphosphate receptor. *Biochem. J.* 354, 413-422 (2001).
42. Wagenknecht, T., Grassucci, R., Berkowitz, J., Wiederrecht, G. J., Xin, H.-B., & Fleischer, S. Cryoelectron microscopy resolves FK506-binding protein sites on the skeletal muscle ryanodine receptor. *Biophys. J.* 70, 1709-1715 (1996).
  43. Wagenknecht, T., Radermacher, M., Grassucci, R., Berkowitz, J., Xin, H.-B., & Fleischer, S. Locations of calmodulin and FK506-binding protein on the three-dimensional architecture of the skeletal muscle ryanodine receptor. *J. Biol. Chem.* 272, 32463-32471 (1997).
  44. Finn, B.E., Evenas, J., Drakenberg, T., Waltho, J. P., Thulin, E., & Forsen, S. Calcium-induced structural changes and domain autonomy in calmodulin. *Nat. Struct. Biol.* 2, 777-783 (1995).
  45. Zhang, M., Tanaka, T. & Ikura, M. Calcium-induced conformational transition revealed by the solution structure of apo calmodulin. *Nat. Struct. Biol.* 2, 758-767 (1995).
  46. Yang, H.C., Reedy, M.M., Burke, C.L. & Strasburg, G.M. Calmodulin Interaction with the Skeletal Muscle Sarcoplasmic Reticulum Calcium Channel Protein. *Biochemistry* 33, 518-525 (1994).
  47. Tripathy, A., Xu, L., Mann, G. & Meissner, G. Calmodulin activation and inhibition of skeletal muscle Ca<sup>2+</sup> release channel (ryanodine receptor). *Biophys. J.* 69, 106-119 (1995).
  48. Buratti, R., Prestipino, G., Menegazzi, P., Treves, S. & Zorzato, F. Calcium dependent activation of skeletal muscle Ca<sup>2+</sup> release channel (ryanodine receptor) by calmodulin. *Biochem. Biophys. Res. Commun.* 213, 1082-1090 (1995).
  49. Rodney, G.G., Williams, B.Y., Strasburg, G.M., Beckingham, K. & Hamilton, S.L. Regulation of RYR1 activity by Ca<sup>2+</sup> and calmodulin. *Biochemistry* 39, 7807-7812 (2000).
  50. Moore, C.P., Rodney, G., Zhang, J.-Z., Santacruz-Tolosa, L., Strasburg, G. M., & Hamilton, S. L. Apocalmodulin and Ca<sup>2+</sup> calmodulin bind to the same region on the skeletal muscle Ca<sup>2+</sup> release channel. *Biochemistry* 38, 8532-8537 (1999).
  51. Wagenknecht, T., Berkowitz, J., Grassucci, R., Timerman, A.P. & Fleischer, S. Localization of calmodulin binding sites on the ryanodine receptor from skeletal muscle by electron microscopy. *Biophys. J.* 67, 2286-2295 (1994).
  52. Wagenknecht, T., Radermacher, M., Grassucci, R., Berkowitz, J., Xin, H.-B., & Fleischer, S. Locations of calmodulin and FK506-binding protein on the three-dimensional architecture of the skeletal muscle ryanodine receptor. *J. Biol. Chem.* 272, 32463-32471 (1997).
  53. Samsó, M. & Wagenknecht, T. Apocalmodulin and Ca<sup>2+</sup>-calmodulin bind to neighboring locations on the Ryanodine Receptor. *J. Biol. Chem.*, in press (2002).
  54. Yamaguchi, N., Xin, C.L. & Meissner, G. Identification of apocalmodulin and Ca<sup>2+</sup>-calmodulin regulatory domain in skeletal muscle Ca<sup>2+</sup> release channel, ryanodine receptor. *J. Biol. Chem.* 276, 22579-22585 (2001).
  55. Rodney, G.G., Moore, C. P., Williams, B. Y., Zhang, J. Z., Krol, J., Pedersen, S. E., & Hamilton, S. L. Calcium binding to calmodulin leads to an N-terminal shift in its binding site on the ryanodine receptor. *J. Biol. Chem.* 276, 2069-2074 (2001).
  56. Franzini-Armstrong, C., Protasi, F. & Ramesh, V. Shape, size, and distribution of Ca<sup>2+</sup> release units and couplings in skeletal and cardiac muscles. *Biophys. J.* 77, 1528-1539 (1999).
  57. Chavis, P., Fagni, L., Lansman, J.B. & Bockaert, J. Functional coupling between ryanodine receptors and L-type calcium channels in neurons. *Nature* 382, 719-722 (1996).
  58. Fagni, L., Chavis, P., Ango, F. & Bockaert, J. Complex interactions between mGluRs, intracellular Ca<sup>2+</sup> stores and ion channels in neurons. *Trends in Neurosciences* 23, 80-88 (2000).
  59. Schneider, M.F. & Chandler, W.K. Voltage dependent charge movement of skeletal muscle: a possible step in excitation-contraction coupling. *Nature* 242, 244-246 (1973).
  60. Rios, E. & Pizarro, G. Voltage sensor of excitation-contraction coupling in skeletal muscle. *Physiol. Rev.* 71, 849-908 (1991).
  61. Franzini-Armstrong, C. & Kish, J.W. Alternate disposition of tetrads in peripheral couplings of skeletal muscle. *J. Muscle Res. Cell Motil.* 16, 319-324 (1995).
  62. Protasi, F., Franzini-Armstrong, C. & Flucher, B.E. Coordinated incorporation of skeletal muscle dihydropyridine receptors and ryanodine receptors in peripheral couplings of BC<sub>3</sub>H1 Cells. *J. Cell Biol.* 137, 859-870 (1997).
  63. Catterall, W.A. Structure and regulation of voltage-gated Ca<sup>2+</sup> channels. *Annual Review of Cell and Developmental Biology* 16, 521-555 (2000).
  64. Murata, K., Odahara, N., Kuniyasu, A., Sato, Y., Nakayama, H., & Nagayama, K. Asymmetric arrangement of auxiliary subunits of skeletal muscle voltage-gated L-type Ca<sup>2+</sup> channel. *Biochemical & Biophysical Research Communications* 282, 284-291 (2001).
  65. Tanabe, T., Beam, K.G., Adams, B.A., Nicodome, T. & Numa, S. Regions of the skeletal muscle dihydropyridine receptor critical for excitation-contraction coupling. *Nature* 346, 567-569 (1990).
  66. Leong, P. & MacLennan, D.H. The cytoplasmic loops between domains II and III and domains III and IV in the skeletal muscle dihydropyridine receptor bind to a contiguous site in the skeletal muscle ryanodine receptor. *J. Biol. Chem.* 273, 29958-29964 (1998).
  67. Sencer, S., Papineni, R. V., Halling, D. B., Pate, P., Krol, J., Zhang, J. Z., & Hamilton, S. L. Coupling of RYR1 and L-type calcium channels via calmodulin binding domains. *J Biol Chem* 276, 38237-38241 (2001).
  68. El-Hayek, R., Antoniu, B., Wang, J., Hamilton, S.L. & Ikemoto, N. Identification of calcium release-triggering and blocking regions of the II-III loop of the skeletal muscle dihydropyridine receptor. *J. Biol. Chem.* 270, 22116-22118 (1995).
  69. Casarotto, M.G., Green, D., Pace, S.M., Curtis, S.M. & Dulhunty, A.F. Structural determinants for activation or inhibition of ryanodine receptors by basic residues in the dihydropyridine receptor II-III loop. *Biophys. J.* 80, 2715-2726 (2001).
  70. Murray, B.E. & Ohlendieck, K. Cross-linking analysis of the ryanodine receptor and  $\text{Ca}_v1$ -dihydropyridine receptor in rabbit skeletal muscle triads. *Biochem. J.* 324, 689-696 (1997).
  71. Gurrola, G.B., Arevalo, C., Sreekkumar, R., Lokuta, A. J., Walker, J. W., Valdivia, H. H. Activation of ryanodine receptors by imperatoxin A and a peptide segment of the II-III loop of the dihydropyridine receptor. *J. Biol. Chem.* 274, 7879-7886 (1999).
  72. Samsó, M., Trujillo, R., Gurrola, G.B., Valdivia, H.H. & Wagenknecht, T. Three-dimensional location of the imperatoxin A binding site on the ryanodine receptor. *J. Cell Biol.* 146, 493-499 (1999).
  73. El-Hayek, R., Lokuta, A.J., Arevalo, C. & Valdivia, H.H. Peptide probe of ryanodine receptor function. Imperatoxin A, a peptide from the venom of the scorpion *Pandinus imperator*, selectively activates skeletal-type ryanodine receptor isoforms. *J. Biol. Chem.* 270, 28696-28704 (1995).
  74. Tripathy, A., Resch, W., Xu, L., Valdivia, H.H. & Meissner, G. Imperatoxin A induces subconductance states in Ca<sup>2+</sup> release channels (ryanodine receptors) of cardiac and skeletal muscle. *J. Gen. Physiol.* 111, 679-690 (1998).
  75. Yamazawa, T., Takeshima, H., Shimuta, M. & Iino, M. A region of the ryanodine receptor critical for excitation-contraction coupling in skeletal muscle. *J. Biol. Chem.* 272, 8161-8164 (1997).
  76. Lu, X., Xu, L. & Meissner, G. Activation of the skeletal muscle calcium release channel by a cytoplasmic loop of

- the dihydropyridine receptor. *J. Biol. Chem.* 269, 6511-6516 (1994).
77. Trujillo, R., Liu, Z., Samso, M., Pattanyak, V., Pasek, D. A., & Meissner, G. Localization of Dihydropyridine Receptor II-III Loop: Ryanodine Receptor Interaction by Cryo-Electron Microscopy. (abstract) *Biophys. J.*, in press (2002).
  78. Treves, S., Chiozzi, P. & Zorzato, F. Identification of the domain recognized by anti-(ryanodine receptor) antibodies which affect Ca<sup>2+</sup>-induced Ca<sup>2+</sup> release. *Biochem. J.* 291, 757-763 (1993).
  79. Benacquista, B.L., Sharma, M. R., Samso, M., Zorzato, F., Treves, S., & Wagenknecht, T. Amino acid residues 4425-4621 localized on the three-dimensional structure of the skeletal muscle ryanodine receptor. *Biophys. J.* 78, 1349-1358 (2000).
  80. Moore, C.P., Zhang, J.-Z. & Hamilton, S.L. A role for cysteine 3635 of RYR1 in redox modulation and calmodulin binding. *J. Biol. Chem.* 274, 36831-36834 (1999).
  81. Leong, P. & MacLennan, D.H. A 37-amino acid sequence in the skeletal muscle ryanodine receptor interacts with the cytoplasmic loop between domains II and III in the skeletal muscle dihydropyridine receptor. *J. Biol. Chem.* 273, 7791-7794 (1998).
  82. Liu, Z., Zhang, J., Sharma, M. R., Li, P., Chen, S. R. W., & Wagenknecht, T. Three-dimensional reconstruction of the recombinant type 3 ryanodine receptor and localization of its amino terminus. *Proc. Natl. Acad. Sci. USA* 98, 6104-6109 (2001).
  83. Yin, C.C. & Lai, F.A. Intrinsic lattice formation by the ryanodine receptor calcium-release channel. *Nature Cell Biology* 2, 669-671 (2000).
  84. Matadeen, R., Patwardhan, A., Gowen, B., Orlova, E. V., Pape, T., Cuff, M., Mueller, F., Brimacombe, R. & van Heel, M. The *Escherichia coli* large ribosomal subunit at 7.5 Å resolution. *Structure* 7, 1575-1583 (1999).
  85. Wriggers, W. & Birmanns, S. Using Situs for flexible and rigid-body fitting of multiresolution single-molecule data. *J. Struct. Biol.* 133, 193-202 (2001).
  86. Volkman, N. & Hanein, D. Quantitative fitting of atomic models into observed densities derived by electron microscopy. *J. Struct. Biol.* 125, 176-184 (1999).
  87. Jiang, W., Baker, M.L., Ludtke, S.J. & Chiu, W. Bridging the information gap: Computational tools for intermediate resolution structure interpretation. *J. Mol. Biol.* 308, 1033-1044 (2001).
  88. Kim, S., Shin, D.W., Kim, D.H. & Eom, S.H. Crystallization and preliminary X-ray crystallographic studies of the D2 region of the skeletal muscle ryanodine receptor. *Acta Crystallographica Section D-Biological Crystallography* 55, 1601-1603 (1999).

**Abbreviations:** 3D, three-dimensional, CaM, calmodulin; CRU, calcium release unit; DHPR, dihydropyridine receptor; E-C, excitation-contraction; EM, electron microscopy; FKBP, FK506-binding protein; IpTx<sub>a</sub>, imperatoxin A; RyR, ryanodine receptor; SR, sarcoplasmic reticulum; T-tubule, transverse tubule.

**Key words:** ryanodine receptor, dihydropyridine receptor, excitation-contraction coupling, FKBP, calmodulin, imperatoxin A, 3D reconstruction, cryo-electron microscopy, image processing

**Send correspondence to:** Dr. T. Wagenknecht.  
Tel: (518)-4742450; Fax: (518)-4747992;  
E-mail: tcw02@wcnotes.wadsworth.org.

**Running title:** 3D reconstruction of Ryanodine Receptors

# Quantitative Relationships between Ryanoids, Receptor Affinity and Channel Conductance.

William Welch

University of Nevada, Department of Biochemistry, Reno, Nevada 89557. E-mail: [jo@aol.com](mailto:jo@aol.com)  
([welch@unr.nevada.edu](mailto:welch@unr.nevada.edu))

**ABSTRACT** The review examines the relationship between the structure of several ryanodine analogs and (A) binding, (B) channel conductance, and (C) ligand binding kinetics. Comparative molecule field analysis (CoMFA) and comparative molecular similarity analysis (CoMSIA) are used to quantitatively assign structural correlations. Hydrogen bond donating (but not accepting) ability was found to be highly correlated with ligand affinity. Analysis of the correlation between hydrophobicity and ligand affinity indicates that, in general, deviation from the amphipathic nature of ryanodine weakens binding. Affinities and binding kinetics obtained *in vivo* are comparable to those obtained in the less-than-physiological *in vitro* conditions. Therefore, the structure-activity relationships surveyed are relevant to the living cell. The review presents arguments favoring the propositions that (A) the pyrrole is a major factor orienting the ligand in the receptor binding site and (B) that ryanoids alter ryanodine receptor function through allosteric mechanisms.

## INTRODUCTION

The ryanodine receptor (RyR or calcium induced calcium release channel) interacts with so many other cellular components it sometimes seems that with little exaggeration, one could teach an entire biochemistry course based on the ryanodine receptor. In delirious moments it seems as if the ryanodine receptor is the principal organizer of the eucaryotic cell. Fortunately, in this paper, the focus will be on only one class of the myriad of ryanodine receptor ligands, the ryanoids. Many have taken on the task of examining other aspects of the ryanodine receptor: a medline search lists more than 200 reviews dealing with one or more aspects of ryanodine receptor function. While only one of many modulators, ryanodine has served, and continues to serve, as an important tool in understanding the function of ryanodine receptors in the many cell types in which it is found.

## PREVIOUS QSAR

Ryanodine binds to the ryanodine receptor with remarkable affinity and specificity. Compared to the free receptor, the ryanodine complexes have radically altered conductance and gating kinetics. For that reason, the relationship between structure and function of the ryanoids has attracted the interest of researchers. Suitable ryanoids could serve as effective insect control agents, they could serve as useful therapeutic agents, and they could be extraordinarily useful research tools allowing pharmacological manipulation of calcium channel function in single cells, perfused tissues and intact organisms. The relationship between structure and ryanoid function has been reviewed previously. Sutko *et al.* (1) reviewed the

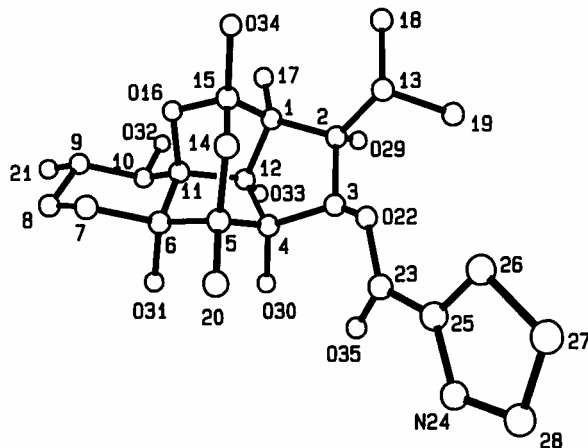


Figure 1. A perspective drawing to illustrate the numbering system used for the ryanodine and related compounds.

properties of the receptor and described several of the reactions leading to derivatives and analogs of ryanodine. Jefferies & Casida (2) provided an excellent overview of structure-activity relationships for vertebrate and non-vertebrate animals. In this review emphasis will be placed on some of the developments since the review by Welch (3). The focus will be on quantitative structure activity relationships (QSAR) at the high-affinity ryanodine binding site. The principal computational tool will be three-dimensional quantitative structure-activity relationships (3D-QSAR), in particular, comparative molecular field analysis (CoMFA, Reference 4) and comparative similarity index analysis (CoMSIA, Reference 5). Therefore, much

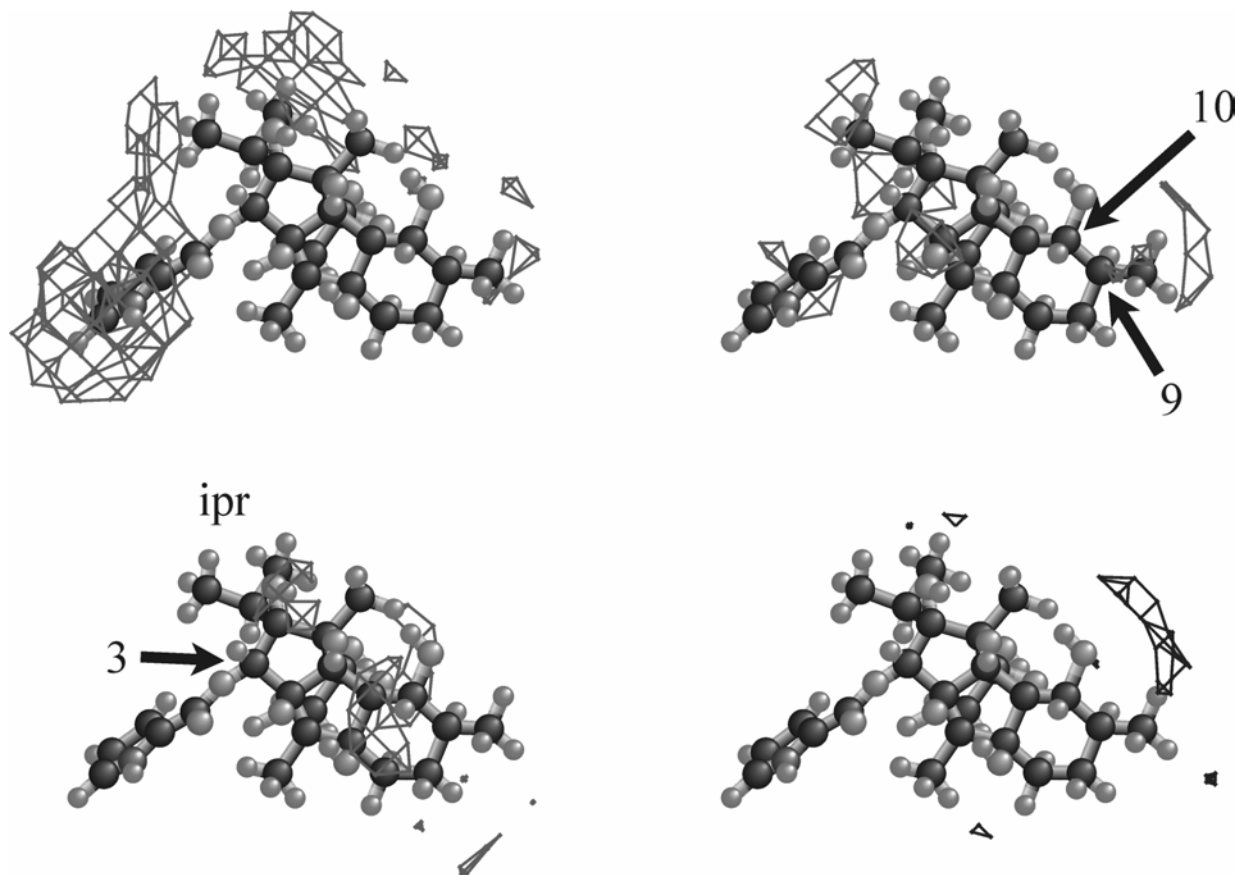


Figure 2. Structure activity relationship between rabbit skeletal ryanodine receptor (RyR1) dissociation constant and physical properties. The wireframes are contours at one-third of the absolute value of the maximum correlation between changes in physical property and dissociation constant. Numbered arrows locate specific atoms for orientation (See Fig 1 for numbering system; ipr = isopropyl). Ryanodine is used as a guide to the eye. Upper left: wire frames enclose volumes where increased steric bulk is strongly correlated with decreased dissociation constant. Upper right: wire frames enclose volumes where increased steric bulk is strongly correlated with increased dissociation constant. Lower left: wire frames enclose volumes where increased positive charge is highly correlated with decreased dissociation constant. Lower right: wire frames enclose volumes where increased negative charge is highly correlated with decreased dissociation constant.

elegant work measuring biological properties will not be mentioned. Much of that data should be mined in the future for QSAR studies.

In this review of ryanoid CoMFA, the desire is to focus on general trends between structure and function. Therefore, lists of compounds and structures will be absent. Please see Sutko *et al.* (1) and references therein for a comprehensive lists of structures. The figures summarize QSAR that includes some compounds added since the previous review (3) and may therefore be somewhat different, reflecting refinement of the model.

The ryanodine receptor is generally considered to bear one high affinity site and one or more low affinity sites per tetramer. Binding of ryanodine to the high affinity site is thought to cause the channel to enter a long-lived, partially-conducting state whereas binding to the low affinity site causes the channel to enter a long-lived, non-conducting state (see Reference 1 for a discussion of these points). Unless otherwise

indicated, the data refer to ryanoid interactions with the high affinity site.

Ryanodine is illustrated in Figure 1 along with the numbering system that will be used in this review. For convenience, the ryanodine structure will be divided into six areas: (I) pyrrole group or position 3, (II) isopropyl group or position 2, (III) polycyclic fused ring system or diterpene, (IV) 2-hydroxyl group, (V) 9-position, and (VI) 10-position.

#### COMFA MAP OF DISSOCIATION CONSTANTS

The relationship between structure and dissociation constant has been examined for many ryanodine analogs. The QSAR in this review is based on 38 compounds. The dissociation constants were determined by the ability of the test compounds to displace 7 nM radiolabeled ryanodine in a competitive binding assay. In all cases the competition follows a hyperbolic equation, completely displacing the ryanodine and giving no hint of multiple sites. At

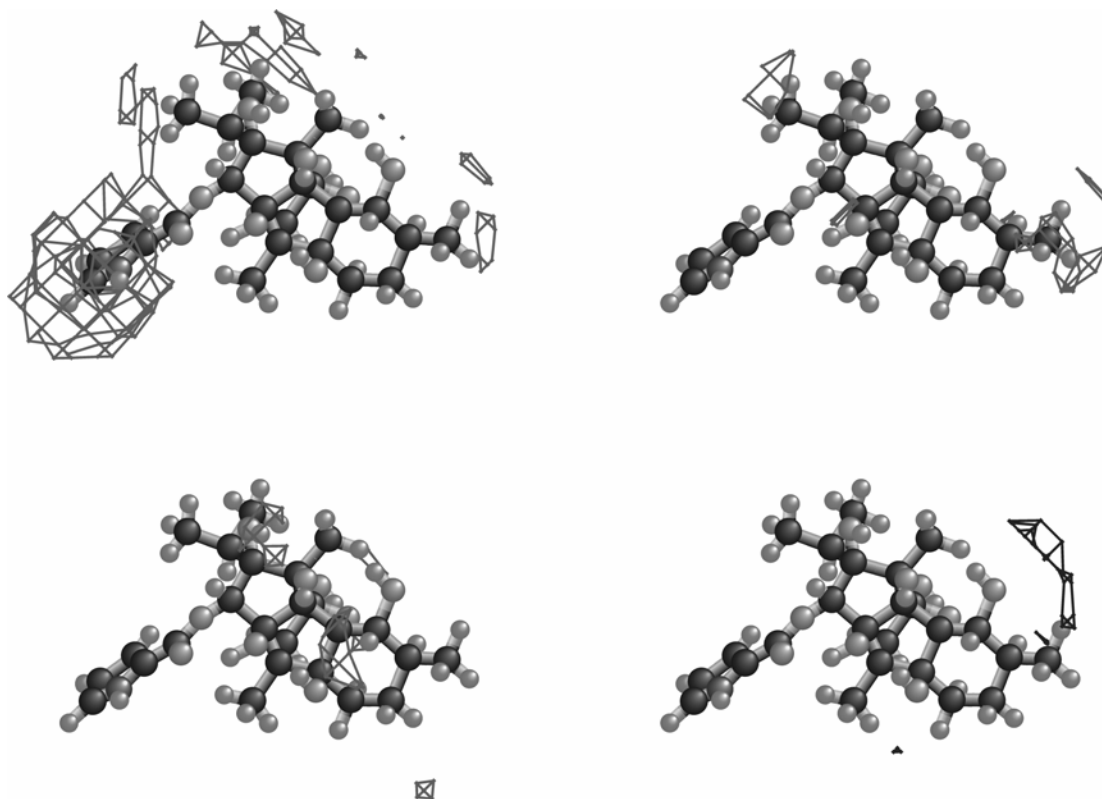


Figure 3. Structure activity relationship between rabbit cardiac ryanodine receptor (RyR2) dissociation constant and physical properties. The wireframes are contours at the same level as used in Figure 2. Ryanodine is used as a guide to the eye. Upper left: wire frames enclose volumes where increased steric bulk is strongly correlated with decreased dissociation constant. Upper right: wire frames enclose volumes where increased steric bulk is strongly correlated with increased dissociation constant. Lower left: wire frames enclose volumes where increased positive charge is highly correlated with decreased dissociation constant. Lower right: wire frames enclose volumes where increased negative charge is highly correlated with decreased dissociation constant.

7 nM ryanodine, the high affinity site is either -50% (rabbit skeletal) or -80% (rabbit cardiac) of saturation. These conditions were chosen to minimize contributions from the low affinity site. Therefore, all 3D-QSAR discussed here refer to characteristics of the high affinity site.

Figure 2 summarizes the correlation between changes in ryanoid structure and dissociation constant. The wire frames enclose those regions where the correlation is the strongest. These areas give clues about the nature of the interaction between ligand and receptor. Changes in steric bulk and electrostatic charge contribute about equally to the correlation between structure and dissociation constant (42% and 58% respectively). Interestingly, most of the steric correlation is located near the isopropyl and pyrrole groups (2- and 3-positions) in contrast to electrostatic contributions which are mostly located near the 9- and 10-positions. Steric (or van der Waals) interactions in CoMFA are approximated by the Lennard-Jones potential and, therefore, are most strongly responsive to local changes. Electrostatic changes are approximated by a modified Coulombs Law relationship. In practical terms this means that

addition of an amino group to the 21-position will produce only small changes in the steric field at the 8-position but will produce a large increase in the electrostatic potential at the 8-position. Therefore, correlations between electrostatic potential and dissociation constant may be the result of changes in charge at several remote locations. Changes in charge at the locus identified by the wire frame are important. There are just more ways of causing the change. Overall, Figure 2 is similar to, and a refinement of, previously reported QSAR.

Figure 3 summarizes the relationships between structure and function for the cardiac ryanodine receptor (RyR2). The contours are drawn at the same levels as Figure 2; therefore, the plots are directly comparable. There are numerous, but minor, differences between the 3D-QSAR of the two isoforms of the receptor. The largest differences are near the *iso*-propyl and pyrrole groups.

## COMSIA MAP OF DISSOCIATION CONSTANTS

### Hydrogen bonds

CoMSIA (comparative molecular similarity

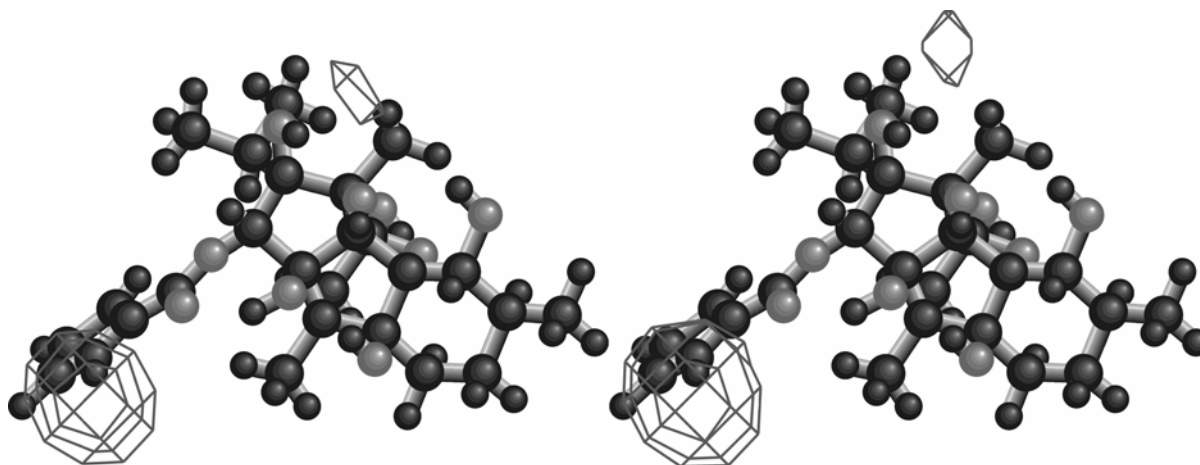


Figure 4. Structure activity relationship between rabbit skeletal (RyR1, left) and cardiac (RyR2, right) ryanodine receptor (RyR1 and 2) dissociation constants and the presence of hydrogen bond donors. The correlation between changes in hydrogen bond donor ability and dissociation constant are contoured at one-fourth of the maximum correlation. At this level the negative correlations are invisible. Therefore, the contours identify the regions where hydrogen bond donors strengthen binding. The contours are essentially identical for both RyR isoforms.

analysis) was conducted to find possible correlations between hydrogen bond acceptor sites on the ligand and binding. Only a random correlation between hydrogen bond accepting ability and binding was found. In contrast, changes in hydrogen bond donating ability are correlated with changes in dissociation constant. The positive correlations (the presence of hydrogen bonds is correlated with stronger binding) are focused at the pyrrole nitrogen and at the hydroxyl groups attached to the 2 and 12 positions on the fused ring system. Relative to the positive correlation, the negative correlation (the presence of hydrogen bond donors is correlated with weaker binding) are much more diffuse and all fall below one-fourth the maximum significance (Figure 4). The correlations are essentially identical for both the skeletal and cardiac isoforms.

### Hydrophobic interactions

Changes in hydrophobic interactions are highly correlated with changes in dissociation constant (Figure 5). As with the CoMFA maps (Figures 2 and 3), the hydrophobic CoMSIA contours are drawn at one third of the maximum correlation between changes in hydrophobic interaction and dissociation constant. In comparison to the correlation with hydrogen bond donating ability, which is confined to a small proportion of the molecular surface, the hydrophobic correlations cover a large portion of the surface of the molecule, indicating a more equitable participation in binding. The contour maps are almost identical for both cardiac (top) and skeletal (bottom) isoforms. The areas where increasing hydrophobicity is strongly correlated with decreasing dissociation constant are shown on the left; areas where increasing hydrophobicity is strongly correlated with increasing dissociation

constant are shown on the right. In Figure 5, the polar face of ryanodine (with most of the hydroxyl groups and the nitrogen edge of the pyrrole) is facing the viewer. The take-home message is that, from the point of view of hydrophobicity, the amphipathic distribution of ryanodine is well designed for tight binding. The contours on the left cover hydrophobic regions of ryanodine whereas the contours on the right cover hydrophilic areas of ryanodine. The amphipathic nature of the pyrrole group (the protrusion on the right) is reflected in the contour maps. The hydrophobic edge of the pyrrole (the side facing away from the viewer) is an area where increases in hydrophobicity are highly correlated with decreased dissociation constant (tighter binding). The hydrophilic edge of the pyrrole (the nitrogen, facing the viewer) is an area where increases in hydrophobicity are strongly correlated with increasing dissociation constant. In the fused ring system (a dipterpene), strong correlations between increasing a hydrophobicity and decreasing dissociation constant cover the 8-, 9- and 10-positions and extend toward the pyrrole carbonyl along the hydrophobic surface of ryanodine (away from the viewer). In contrast, the contours where increasing hydrophobicity is strongly correlated with decreased affinity, cover most of the hydroxyl groups (on the polar face which is toward the viewer). In general, anything that makes the hydrophobic surface of ryanodine less hydrophobic is correlated with decreased binding, and any changes that make the hydrophilic surfaces of ryanodine less hydrophilic are correlated with decreased binding. The notable exception is the isopropyl group. Steric factors (Figure 2) are highly correlated with binding but not with hydrophobicity (Figure 5). This is in keeping with the observation that adding a hydroxyl group to the isopropyl group

has little effect on dissociation constant (6; unpublished results, and see below).

## STRUCTURAL ANALYSIS

### Pyrrole group

The pyrrole carbonyl group (attached to the 3-position) is the single most important locus related to binding. This is most dramatically seen in the 800-fold increase in dissociation constant when the pyrrole carbonyl group is removed from ryanodine ( $K_D = 8$  nM) to form ryanodol ( $K_D = 6000$  nM). No other group is nearly as effective as the pyrrole. Slight changes in structure lead to large changes in affinity. Methylation of the pyrrole nitrogen produces an 8-fold increase in dissociation constant (7). Replacement of the pyrrole group with a pyridine, causes a 300-fold increase in dissociation constant (8). The complex nature of pyrrole interactions with the receptor is evident comparing Figures 2-5. The contours for antagonistic correlations of steric, electrostatic, and hydrophobic correlations surround the group. The presence of a hydrogen bond donor at the nitrogen edge of the pyrrole is highly correlated with binding to the high affinity site of both cardiac and skeletal RyR. Taken together, physical factors (steric, electrostatic, hydrogen bonding, and hydrophobicity) suggest a restrictive nature in the binding site in this region. Few pendant groups will have the necessary complementary interactions.

A SAR of other substituents is limited because of synthetic difficulties at the 3-position in the ryanodine stereochemistry. The 3-hydroxyl is sterically hindered; so researchers have been limited to what nature has chosen to offer. However, Ruest and his colleagues have synthesized 3-epiryanodol and a series of analogs have been synthesized and tested. The affinity of ryanodol and 3-epiryanodol for the RyR is roughly the same (6000 nM vs. 4000 nM, unpublished results). Addition of pyrrole carbonyl to the 3-epi position increases affinity 10-fold ( $K_D$  of 3-epiryanodine = 400 nM, see also Reference 9). Therefore, the effectiveness of the pyrrole carbonyl is greatly reduced by the isomerization. However, the comparison is complicated. The fact that the 3-epimer of ryanodine binds at all suggests that 3-epiryanodine binds to the RyR in an alternate orientation (see References 9 and 10). Seemingly isosteric changes, for example replacing the pyrrole ring with a furan ( $K_D = 3000$  nM) or a thiophene ( $K_D = 3000$  nM) failed to produce even modest enhancements compared to pyrrole (unpublished results). As stated previously, interactions between ligand and receptor are complex at this locus (Figures 2 and 3).

The most dramatic demonstration of the importance of the pyrrole comes from studies of 10-*O*-pyrrolecarbonyl ryanodol (9, 10). In this

compound ( $K_D = 200$  nM) the pyrrole carbonyl group has moved from the 3-hydroxyl group to the 10-hydroxyl group with only a small penalty (25-fold) in dissociation constant. Although the 40-fold increase in affinity relative to ryanodol might be due to interactions with parts of the binding site near the 10-position, all other substituents at that position on either ryanodine or ryanodol at best produce smaller enhancements in binding (for example, see below or Reference 1). At the 3-position, the pyridine-3-carbonyl (nicotiny) group enhances the binding of ryanodol 10-fold (compound named ryanodol nicotinate or 2-*O*-(pyridyl-3-carbonyl)ryanodol, References 8, 11); whereas this same group at the 10-position doubles the dissociation constant of ryanodol (unpublished results). In fact, the latter result was predicted by previous CoMFA and is consistent with the complex CoMFA at the 10-position (see Figures 2 and 3). Therefore, the effect is specific for the pyrrole. In addition the relationship between structure and fractional conductance (CoMFA) of the ryanoid-modified channel is markedly improved if the 10-*O*-pyrrolecarbonyl ryanodol and 3-epiryanodol are oriented so that the pyrrole carbonyl occupies the same subsite (10).

It has been argued that the pyrrole caused a reorientation of the ligand in the binding site in order to maximize the strong interactions between the receptor and the pyrrolecarbonyl group (9, 10). The most direct support for this hypothesis comes from the dissociation constant of 10-*O*-pyrrolecarbonylryanodine ( $K_D = 12$  nM) which is indistinguishable from that of ryanodine. Therefore, if the pyrrole is to interact with the receptor, the ligand must bind in an alternate orientation.

The importance of the pyrrole has been disputed by Bidasee & Besch (11). They ask why, if the pyrrole group is so important, pyrrole is not an effective competitive inhibitor of ryanodine binding. They claim that up to 1 mM pyrrole carbonate produces no detectable inhibition of ryanodine binding. Using their numbers (11), in the context of ryanodol the pyrrole carbonyl group provides 4.4 kcal/mol binding energy. Using this energy as an intrinsic energy of binding, one calculates a dissociation constant of ~1 mM for the binding of the pyrrole carbonyl fragment alone. The corresponding  $EC_{50}$  for the displacement of the radiolabeled ryanodine would be approximately 2 mM. However, the experimental value is expected to be considerably higher due the entropic effect of binding a ligated pyrrole vs. a free pyrrole. A back-of-the-envelope calculation of the estimated loss of translational and rotational entropy is 9 kcal/mol (see References 12-14 for a discussion on estimation of ligand receptor interactions). The loss of entropy will likely overwhelm the intrinsic interaction energy of the pyrrole carbonyl

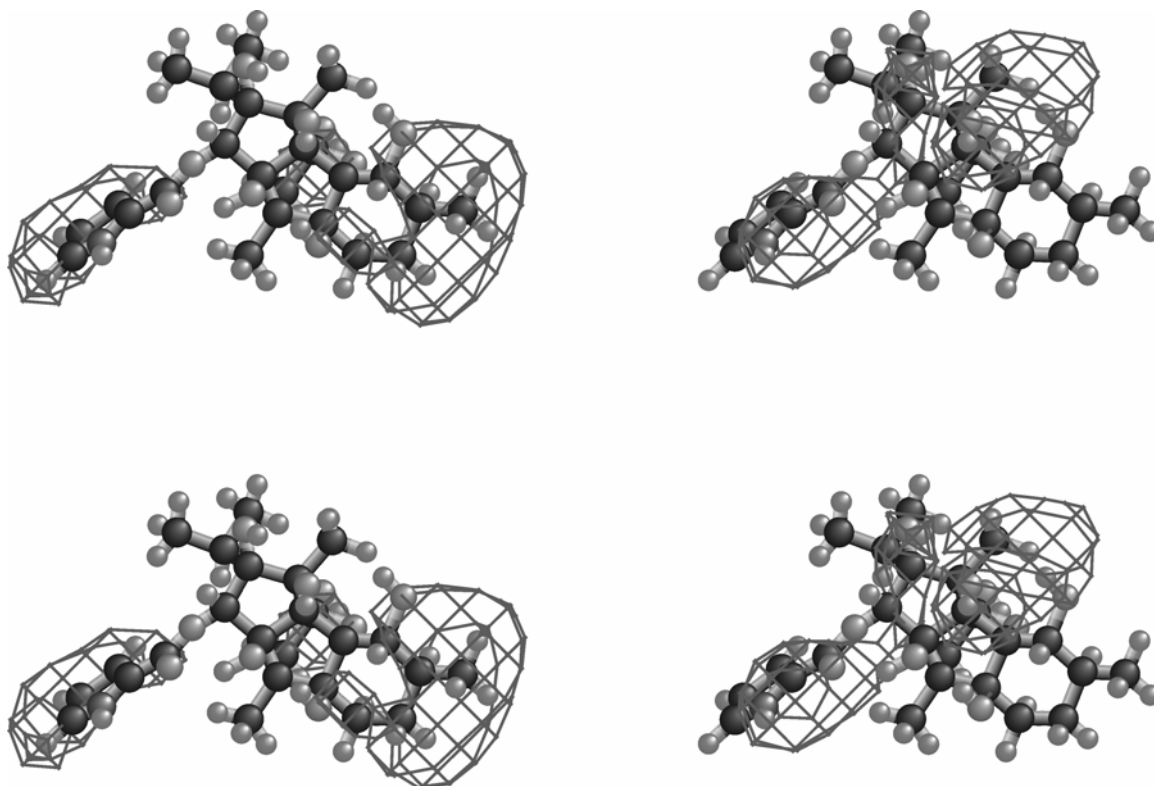


Figure 5. Structure activity relationship between rabbit cardiac (RyR2, top) and skeletal ryanodine receptor (RyR1, bottom) dissociation constant and hydrophobicity. The wireframes are contours at one-third of the absolute value of the maximum correlation between changes in hydrophobicity and dissociation constant. Ryanodine is used as a guide to the eye. Left side: wire frames enclose volumes where increased hydrophobicity is strongly correlated with decreased dissociation constant. Right side: wire frames enclose volumes where increased hydrophobicity is strongly correlated with increased dissociation constant.

fragment. In addition, the introduction of a negative charge (from the carboxyl in place of the carbonyl) is also likely to be deleterious to affinity (the ester or pyrrole itself would have been a better choice). In fact, the experimentally observed failure of 1 mM pyrrole to displace radiolabeled ryanodine is very much in keeping with the experimental binding data.

Referring to Figure 2, increasing steric bulk on the far edge (hydrophobic edge) of the pyrrole (upper right) increases the dissociation constant. In contrast, increasing steric bulk everywhere else around the pyrrole (including the bay between the pyrrole and the isopropyl group) enhances binding. Meanwhile, electronic changes at the 3-position are only weakly correlated with changes in affinity (Figure 2, bottom). This locus is the most highly correlated with hydrogen bond donating ability (Figure 4). While the presence of a hydrogen bond acceptor is not correlated with high affinity binding, the presence of a hydrogen bond donor is an important component of high affinity binding.

Compared to the skeletal isoform, increases in steric bulk around the pyrrole group are not as strongly correlated to increases in dissociation constant of the cardiac isoform (note the loss of contours comparing the upper right

panel of Figures 2 and 3).

Casida's laboratory has produced large numbers of structure-activity studies on both vertebrate and invertebrate RyR. Much of this data has not yet been incorporated into quantitative structure-activity analyses. Although the pyrrole is critical to the binding of ryanoids to the receptor, loss of the pyrrole has relatively little effect on toxicity to insects (2,6). In insect bioassays, ryanodol has one-fourth the potency of ryanodine. In vertebrate sarcoplasmic reticulum (SR) assays, the dissociation constant of ryanodol is 3000-fold larger than that of ryanodine. Gonzalez-Coloma *et al.* (15) made similar observation while investigating a number of alkaloid (ryanodine like) and non-alkaloid (ryanodol-like) compounds (15). The authors interpret their data as supporting a hypothesis of a ryanodol-specific mode of action in insects. Lehmberg & Casida (1994) made such a proposal based on the weak binding (relative to ryanodine) of ryanodol to insect RyR. Gonzalez-Coloma *et al.* (15) used compounds isolated from *Persea indica* (Lauraceae) and *Spigelia anthelmia* (Loganiaceae) rather than the more common source, *Ryania speciosa*. Other sources for ryanoids are welcome.

With successful isolation of insect RyR, a

SAR for binding affinity and channel conductance will be helpful. Scott-Ward *et al.* (16) found that the insect RyR binds ryanodine with a dissociation constant of 4 nM, similar to vertebrate RyR. This is consistent with the earlier report of ryanodine dissociation constants of ~5 nM in various insect tissues (17). Ryanodine modified insect RyR have a fractional conductance of 36% compared to 38% for rabbit cardiac RyR (16). The difference in fractional conductance between rabbit cardiac and sheep cardiac (57%; Reference 18) is the use of Ca<sup>2+</sup> as permeant ion in the former and K<sup>+</sup> in the latter case.

Ryanodine (at nanomolar levels), 9,21-didehydroryanodine and 9,21-didehydroryanodol can act on insect potassium channels (19, 20). The modification puts a double bond between the 9 and 21 carbons (see Figure 1) and causes little to no change in binding affinity. The channels are considerably less sensitive to the ryanodol than to the ryanodines. The results do not explain the similar toxicity of ryanodine and ryanodol on intact insects but does support multiple sites of ryanoid action.

### Isopropyl group

Compared to the pyrrole group, the *iso*-propyl group can tolerate quite large changes with little change in affinity. Steric interactions are as complex as those at the pyrrole locus. Some of these are indirect as the *iso*-propyl (unlike the pyrrole) group changes conformation in response to modifications at nearby locations. In general, increases in steric bulk on the far side of the *iso*-propyl group are correlated with increases in dissociation constant (upper left, Figure 2) whereas such increases on the near side of the *iso*-propyl group decrease the dissociation constant (upper right, Figure 2). Changes in charge at the *iso*-propyl group are strongly correlated with changes in binding (bottom, Figure 2). However, changes in hydrophobicity are only weakly correlated with changes in binding constants.

Changes in the isopropyl group lead to complex changes in binding. EsterC2 contains a double bond between the C1 and C2 atoms (positions 1 and 2), and contains a lactone ring (1). The double bond causes a reorientation of the *iso*-propyl group. These changes cause a 200-fold increase in dissociation constant of both the cardiac isoform (from 3 nM to 500 nM) and skeletal isoform (from 8 nM to 2000 nM). Addition of a double bond between the isopropyl group and the fused ring (as in 2-deoxy-2(13)dehydroryanodine) causes the group to become planar and non rotatable. This modification causes only a slight (2-fold, cardiac; 1.2-fold, skeletal) increase in dissociation constant. Apparently most of the loss of affinity of EsterC2 arises from changes in the fused ring

system. Addition of a hydroxyl group to the *iso*-propyl group causes a 9-fold increase in dissociation constant (inferred from Reference 6). We have observed a 20-fold (skeletal) to 30-fold increase (cardiac) in dissociation constant when hydroxyl groups are added to either the methyl groups of the isopropyl group (unpublished results).

Although not clear from Figures 2 and 3, the distribution of contours around the *iso*-propyl group is remarkable. In both figures the contours depict the strong correlation between increased steric bulk and decreased dissociation constant. For the skeletal isoform (RyR1, Figure 2, upper left) the contours are behind the isopropyl group. In contrast, for the cardiac isoform (RyR2, Figure 3, upper left) the contours are in front of the isopropyl group.

### Polycyclic fused ring system

Changes in the fused ring system (diterpene) are correlated with changes in binding albeit the contours of high electrostatic and steric correlations are less densely packed than on pendant groups. The CoMSIA contours show strong correlations between changes in hydrophobicity and binding. In general, these match the hydrophobic and polar surfaces of ryanodine. While some modifications produce dramatic changes in dissociation constant (for example see EsterC2 above), many changes in hydroxyl groups produce relatively little change in dissociation constant (7, 21, 22). No modifications that increase binding have been found. The CoMFA model above has successfully predicted all molecules tested from these references. The results are consistent with a model that allows the fused ring system to bind in more than one orientation. Additional alterations in the ring structure may reveal more detailed information.

A few examples of modification of the fused ring system are offered. A fairly minor modification, the oxidation of the hemiacetal ring to the corresponding lactone (esterC2, Reference 8) results in a 370-fold increase in dissociation constant. Introduction of a positive charge at the eight position strongly inhibits binding. An 8-equatorial amino group increases the dissociation constant 540-fold whereas the axial isomer increases dissociation constant 110-fold (8). These findings are noteworthy due to the different effects of introducing positive charge at the 9- and 10-positions (see above).

In summary, it appears that the fused ring system can bind to the receptor in at least two orientations (9, 10). One surmises that the requirement for tight binding does not require a large number of specific interactions with the fused ring system. Instead, a limited number of essential contacts are required and these interactions can be met in more than one way.

For example, of the six hydroxyl groups on ryanodine, only two (at the 2- and 12-positions) are strongly correlated with hydrogen bonding. The map is consistent with large variation of the impact of modifications on the diterpene.

### 2-hydroxyl group

As was noted previously (1) interactions between the hydroxyl group at the 2-position (the same attachment point as the *iso*-propyl group) is context dependant. The most prominent of these interactions are reflected in the upper right of Figure 2. Increases in steric bulk at the 2-hydroxyl position are strongly correlated to increases in dissociation constant. There are no strong correlations with electrostatic changes at the 2-hydroxyl group. However, there is a strong correlation between the presence of a hydrogen bond donor at the two position and decreased dissociation constant. No such correlation has been found for hydrogen bond acceptors.

Compared to the skeletal isoform, the cardiac isoform is much less sensitive to increases in steric bulk at the 2-hydroxyl position (compared upper right panels of Figures 2 and 3).

### 9-position

Because of its accessibility, this has been a site of many modifications. Fortunately, large groups can be introduced at this position with little loss of binding. Therefore, a number of experimentally useful groups can be introduced. Steric interactions with the receptor are complex at this locus with increased steric bulk both promoting and inhibiting binding (upper panels Figure 2). However, the introduction of large bulky groups such as BODIPY (8) indicates that the 9-position is not sterically restricted. In general (lower right Figure 2), introduction of ionic groups at this position decreases binding (For example, 21-amino-9- $\alpha$ -hydroxy ryanodine, 21-amino-9- $\beta$ -hydroxyryanodine).

### 10-position

Again, this is a position that has enjoyed much attention because of the relative accessibility of this group to modification. In general, addition of steric bulk at the 10-position enhances binding (upper left, Figure 2). Strong electrostatic correlations at this position are more complex. Positive charge generally favors binding (see the following paragraph). The tightest binding ryanoid has a positively charged pendant group attached to the 10-position (10-*O*-guanidinopropylryanodine, References 10, 11, 23, 24). Hydrophobic interactions are also complex (Figure 5). The 10-position is at the junction between contours showing strong positive and negative correlations between changes in hydrophobicity and dissociation constant.

The binding site at the 10-position, like the 9-position, must be extremely commodious.

The bulky 10-*O*-(NCBZ-aminoacyl)- and 10-*O*-(NCBZ-3-amino propanoyl)ryanodines bind with affinities equal to or better than ryanodine (9, 23, 25). We have modeled the ryanodine binding site as facing into the solvent (1, 9). This feature is preserved in the virtual site model of Schleifer (26) although no ryanoids with bulky substituents at either the 9- or 10-positions were used to build the model. A Glu and a Leu are the only residues near this region of the ryanoids. 10-*O*-guanidinoacetylryanodine and the slightly longer 10-*O*-guanidinopropanoylryanodine are one of the tightest binding ryanodine analogs discovered to date (9, 23, 25). The 10-*O*-guanidinopropanoyl group is particularly effective at promoting ryanoid binding in multiple contexts (10, 11, 23, 24). Using the data of Bidasee and Besch (11), one calculates that group enhances ryanodine binding by 1.1 kcal/mol, the binding of 3-*O*-nicotinyl ryanodol (Reference 27; also called pyridyl ryanodine, Reference 11) is enhanced by 2.2 kcal/mol, and the binding of ryanodol by 1.8 kcal/mol. In cardiac SR, the 10-*O*-guanidinopropanoyl group enhanced ryanodine binding 0.8 kcal/mol (10). These values are consistent with solvent-faced electrostatic (including hydrogen bonding) and hydrophobic interactions. The smaller, but cationic, 10-*O*- $\beta$ -alanyl group is also effective at reducing the dissociation constant of ryanodine (0.6 kcal/mol, skeletal SR, Reference 11; 0.8 kcal/mol, cardiac SR, Reference 10). As before, the cationic group is about twice as effective in the context of the weaker-binding ryanoids. 10-*O*- $\beta$ -alanyl group enhances binding of both 3-*O*-nicotinyl ryanodol and ryanodol by 1.8 kcal/mol (data from Reference 11). Ionic interactions are long range and it is difficult to assess what differences in binding might be sufficiently dramatic to account for the > 1 kcal/mol differences between compounds. Both the guanidino and  $\beta$ -alanyl groups are capable of forming hydrogen bonds where one of the partners will be charged. Hydrogen bonds are short-range interactions. Changes in ligand binding orientation or induced conformational changes in the RyR may be sufficient to form stronger ligand-receptor hydrogen bonds. The bulkier, but non-ionic, CBZ- $\beta$ -alanyl group also promotes binding (ryanodine, 0.03 kcal/mol; ryanodol, 0.4 kcal/mol; 3-*O*-nicotinyl 0.7 kcal/mol; data from Reference 11). At the 10-position the shorter CBZ-glycyl group actually inhibits ryanodine binding by 1.3 kcal/mol (10). In contrast, the same group in the same position slightly enhances binding of ryanodol to skeletal SR by 0.6 kcal/mol and to cardiac by 0.4 kcal/mol (unpublished results)

In contrast to the cationic pendant groups, the 10-*O*-succinyl group enhances the binding of ryanodol by 0.1 kcal/mol (unpublished results). The fact that the succinyl group did not antagonize ryanodol binding suggests that

enhanced binding of the cationic ryanoids is not due to formation of a salt link: the predominant interactions are more likely derived from steric and hydrogen bond interactions. Given the differential effects of other substituents at the 10-position, it is not surprising that anionic groups at the 10-position of ryanodine are reported to antagonize binding. In one report 10-*O*-succinyl ryanodine binding was so weak as to be unmeasurable (23) and in another report the anionic group raised the dissociation constant from 4 nM to 200 nM (24).

In passing, recall from the previous section that positive charge in this region of the molecule does not automatically enhance binding. For example, converting the methyl group at the 9-position to the amino methane group (21-amino-9- $\alpha$ -hydroxyryanodine, 21-amino-9- $\beta$ -hydroxyryanodine) increases the dissociation constant of ryanodine from 8.5 nM to 3700 nM ( $\alpha$ ) and 2000 nM ( $\beta$ ). This is a robust change (as much as 3.7 kcal/mol) for a site that can accommodate such large derivatives as BODIPY with little to no penalty. Based on molecular dynamics simulations the average distance between the amino groups of 21-amino-9- $\alpha$ -hydroxyryanodine and 10-*O*- $\beta$ -alanyl ryanodine is  $-5 \text{ \AA}$  (unpublished). All this indicates the complex relationship between receptor and ligand near the 9- and 10-positions.

In summary, the ability of the 10-position to accommodate large bulky substituents argues that this position is exposed to solvent in the receptor-ligand complex. The ability of the various substituents to differentially enhance ryanoid binding argues for receptor-ligand interactions at this site. The most likely analogy is to affinity chromatography. The linker used to anchor the affinity ligand while not part of the binding site *per se*, none-the-less has profound effects on solute binding.

#### MAP OF THE BINDING SITE

The CoMFA and CoMSIA contours provide a map of the ryanodine binding site. Regions of CoMFA and CoMSIA that have high correlation between structural changes and dissociation constant identify corresponding regions in the receptor. Therefore, areas where increased steric bulk enhance binding correspond to cavities in the receptor that provide a good fit with protrusions on the ligand. Likewise, regions where increased positive electrical potential are highly correlated with lower dissociation constant are regions of negative potential in the receptor. One can quantitate this relationship by investigating the effect of removing change or atoms (or both) on virtual molecules and examining the effect on predicted dissociation constant (or free energy of binding). The relationship can be visualized using the model by drawing contours that show the areas of a ligand that contribute to the

experimentally observed dissociation constant (e.g., Figure 25, Reference 1).

Schleifer (26) has carried mapping a step further by constructing a virtual ryanodine receptor binding site. Using the computer algorithm PrGen, amino acid residues were positioned around a collection of ryanodine analogs to obtain the strongest correlation between experimental and predicted free energies of binding. In the final pseudoreceptor model, six amino acid residues are positioned to make essential contacts with the bound ligands. It likely that the binding site of the ryanodine receptor includes more than six amino acids, the pseudoreceptor model provides a concrete representation of interactions sufficient to explain experimental binding data. Although different methods are used from those that generated Figures 2 and 3, the same important interactions are determined. These interactions are with the pyrrole carbonyl, the isopropyl group and the 9- and 10-positions. The pyrrole is surrounded by an asparagine (to provide polar contacts) and a combination of three hydrophobic residues (phenylalanine, tyrosine, isoleucine) to provide strong, but sterically restrictive, interactions with the pyrrole. The isopropyl group interacts with the phenylalanine and isoleucine residues. The other end of the binding site is defined by a leucine (to make steric and hydrophobic interactions) and a glutamate (to make polar and hydrogen bonds with the 9- and 10-positions). Schleifer (26) proposes that when ryanodine is bound to the receptor, the hydrophilic hemisphere of the diterpene fused ring system remains exposed to the solvent. This is consistent with the weak correlations between hydrogen bond acceptors or donors in this part of the molecule. The concentration of residues in the vicinity of the pyrrole is consistent with the experimentally observed strong binding energy and specificity associated with the 3-position. It is also consistent with the CoMFA presented in Figures 2 and 3 which show complicated steric interactions but relatively weak correlations with changes in charge. The CoMSIA of hydrogen bonding is consistent with the presence of asparagine and tyrosine acting as hydrogen bond partners. It differs in that it would suggest these residues optimally would act as hydrogen bond acceptors for the pyrrole nitrogen and hydroxyl groups at positions 2 or 12. The glutamate and leucine are consistent with the strong correlations between charge and steric bulk at the 9- and 10-positions while retaining the ability to attach large ligands at either of these positions.

#### RYANOID-INDUCED CONDUCTANCE STATES

Ryanodine is a complex modulator of RyR channel function producing changes in both channel gating kinetics and channel conductance. At nanomolar concentrations ryanodine causes

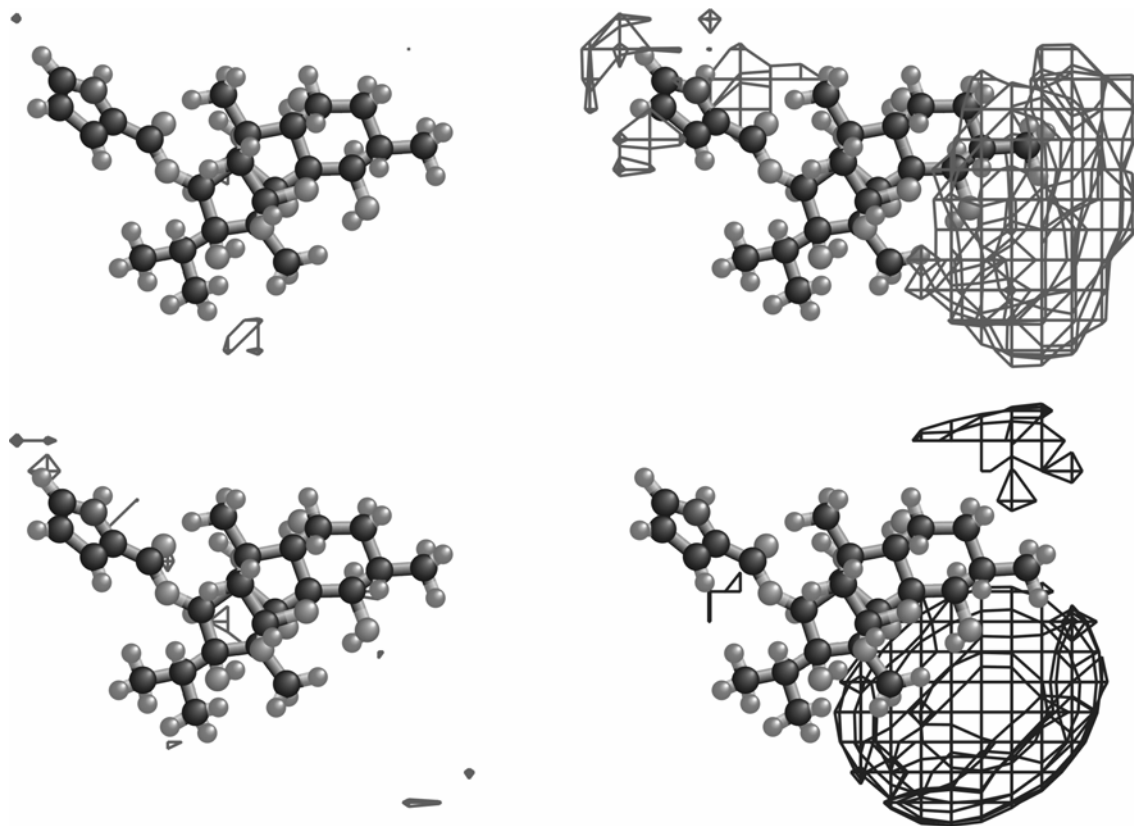


Figure 6. Relationship between structure and fractional conductance of the ryanoid-modified ovine cardiac RyR. To improve visibility of the contours, the ryanodine molecules as shown in Figure 2 have been rotated approximately 180° along the X-axis. In Figure 6 the pyrrole is at the upper left and the isopropyl group at the lower left of each molecule. The wire frames are contours at one third of the absolute value of the correlation between steric bulk (top panels) or electrostatic bulk (lower panels). Upper left: regions where increasing steric bulk are highly correlated with increased fractional conductance; upper right: regions where increasing steric bulk are highly correlated with decreasing fractional conductance; lower left: regions where increasing negative electrostatic charge are highly correlated with decreasing fractional conductance; lower right, regions where increasing positive charge are highly correlated with decreasing fractional conductance.

the channel to enter into a long-lived subconductance state. At micromolar concentrations ryanodine produces a long-lived, non-conducting state. These phenomena have been commonly observed in both calcium uptake and release studies and single channel recordings (28). Williams and his coworkers found that the magnitude of the subconductance state induced by binding to the high affinity site of sheep cardiac RyR was a function of the ryanoid structure. The structural determinants for channel modification map to loci different from the structural determinants of binding affinity (10).

#### CoMFA map of fractional conductance

Figure 6 is an update of earlier maps and includes compounds investigated since Tinker *et al.* (18) including 21-aminoryanodine, and 10-*O*-succinyl ryanodol. While ryanoids have been discovered that can almost completely block channel conductance while bound to the high affinity site, no ryanoids have been found that

induce a near maximal conductance of the ryanoid-modified state. Ryanodol, with a fractional conductance of 69% (18), is about the largest fractional conductance observed in the ryanoid modified channels. Changes in structure are highly correlated with fractional conductance. In Figures 2, 3, and 6 the wire frames are contours at one third of the maximum absolute value of the respective physical property. Therefore, these figures are comparable in terms of the level of correlation with specific regions in space. To improve the visibility of the wire frames in a two-dimensional drawing, the orientation of Figure 6 is approximately 180° relative to Figures 2 and 3. While high levels of correlation between increasing steric bulk (upper left; or increasing positive charge, lower left) and increasing fractional conductance are confined to small loci, high levels of correlation between steric bulk (upper right; or increasing positive electrostatic field, lower right) and decreasing fractional conductance extend over large region of space. Compared to binding, much more of the

relationship between physical properties and fractional conductance is located in the vicinity of the 9- and 10-positions. Attachment of groups of any kind to these positions results in lowered fractional conductance. Interestingly, no matter how large the group attached, the ryanoid-modified channel still has an appreciable conductance. This observation argues against ryanoid binding near the ion conductance pathway. Should the ryanoid bind at or near the conduction pathway, one would expect that eventually the ryanoid would become so large as to completely obstruct the channel. Even bulky biotinylated ryanoids, while binding with about the same affinity as ryanodine, have fractional conductances of 20% (Williams, personal communication). To achieve nearly zero conductance, a combination of positive charge and bulk is required (guanidinoryanodine has a fractional conductance of 6% whereas  $\beta$ -alanyl has 14%). The dramatic effect of positive charge is shown in the lower right panel of Figure 6 (the correlation between increasing negative charge and increasing fractional conductance or, in other words, increasing positive charge and decreasing fractional conductance).

#### **CoMSIA**

Unlike the correlations observed for dissociation constant, CoMSIA reveals a random relationship between changes in hydrogen bonds and hydrophobicity and the fractional conductance of the ryanoid-modified channel. It is important to interpret the CoMSIA properly. The CoMSIA does not say that these physicochemical factors are not important in determining fractional conductance. It does say that a model based on hydrogen bonds or hydrophobicity is insufficient to predict the fractional conductance of compounds, *i.e.*, one could do as well by random guesses. From another point of view, none of these factors, by themselves, are essential for setting the magnitude of the fractional conductance. As pointed out previously, there is no correlation between the strength of binding and the induced fractional conductance (3). Together, these data support the hypothesis that receptor-ligand interactions that promote strong binding are both qualitatively and quantitatively different from those that modify channel conductance. At least in principle it is possible to modulate affinity independently of conductance.

#### **Calcium release**

Immediately after finding a SAR for channel conductance one became curious about a potential SAR for the ryanoid-induced non-conducting state. One might ask the following questions. Is the ratio of EC<sub>50</sub> for the subconducting state to the EC<sub>50</sub> for the nonconducting state the same for all ryanoids or

does the ratio vary with structure? Can all ryanoids induce a non-conducting state or an alternate subconducting state? If a ryanoid fails to induce a non-conducting state, does the failure result from the inability to bind to a low affinity site? Can a ryanoid bind to a low affinity site, but lack the structural components required to induce a non-conducting state? These questions have not yet been answered satisfactorily. Bidasee and Besch (11) conducted a ryanoid SAR using calcium efflux as the probe. Their data show striking differences between the concentrations of ryanoid to half-activate and half-inhibit calcium efflux. However, the conditions of the experiment make it difficult to interpret the data. Calcium loading occurred at 1 mM Ca<sup>2+</sup> in the presence of the test ryanoid. Millimolar levels of calcium inhibit the open state of the channel and ryanoid binding (29, 30). The high levels of calcium ion may explain why (A) the EC<sub>50</sub> for stimulation of calcium efflux is orders of magnitude higher than the dissociation constant of the ryanoid and (B) the lack of correlation between dissociation constant and EC<sub>50</sub> for stimulation of calcium efflux. In addition, there is no correlation between the ryanoid-induced fractional conductance measured in single channels (18, 31, 32) and the EC<sub>50</sub> for stimulation of calcium efflux nor for the magnitude of the induced Ca<sup>2+</sup> efflux. 10-*O*-guanidinopropionyl ryanodine produced the largest calcium efflux (11) but has the lowest fractional conductance in single channel measurements (18). Only one subconductance state was observed in the 10-*O*-guanidinopropionyl ryanodine-modified channel. In related ryanoids with fast on/off rate constants, the dissociation constant inferred from the kinetics of modification is in agreement with the dissociation constant from equilibrium binding experiments. In addition, inhibition of Ca<sup>2+</sup> efflux by ryanodol or 10-*O*- $\beta$ -alanyl ryanodine was not observed (11) whereas high concentrations of both of these compounds (and 21-aminoryanodine) close the channel in single channel experiments (Williams, personal communication). Therefore, binding at the high affinity site appears sufficient to induce a long-lived, conducting state of the RyR. At this point, while the experiments are extremely interesting, it is not clear what is being measured in the calcium efflux experiments. Bidasee & Besch (11) suggest that vesicular calcium efflux is determined by the difference in affinity of a high affinity and low affinity site. Differential structural determinants appear to exist at two or more sites; however, additional mechanistic components are required to explain the dose-response curves and the magnitudes of the calcium efflux. More research on ryanoid-induced changes in calcium release is clearly warranted.

#### **Modulation of RyR channel function**

The binding of ryanoids to the receptor causes both a change in channel gating kinetics and channel conductance. These effects could result from the binding of the ryanodine at or near to the ion conduction path. The ligand would then be in a position to physically obscure both (A) the movement of amino acids that switch the channel from an open and a closed state and (B) the free flow of ions through the channel. However, the energetics of the relationship between structure and fractional conductance would appear to be at odds with this mechanism. The magnitude of the fractional conductance seems to bear no relationship between the size of the ryanoid. The effect of charge on anionic and cationic ryanoids appears to be too weak to have an intimate relationship between the ryanoid and the conduction pathway (see References 1 and 3 and the following section for more discussion).

Binding to allosteric sites could produce changes in fractional conductance and gating kinetics if one assumes that the ryanodine receptor exists in a number of rarely-populated conformations. The binding of ryanoid then stabilizes one or more of these conformations. Support for the allosteric mechanism comes from the work of Fessenden *et al.* (33) who find that ryanodine binding restores calcium sensitivity to a calcium insensitive mutant while failing to block conductance.

#### **APPLIED POTENTIAL VS. RYANOID BINDING (KINETICS OF RYANOID BINDING)**

Typically, ryanodine and related compounds were found to be slow binding ligands. The slow dissociation rates made measurement of the kinetics of single channel modification by ryanoids unattainable within the lifetime (up to 1 hr) of a single-channel experiment (18, 28, 34). Kinetics have been confined to ensemble experiments such as radioligand binding assays and vesicular calcium uptake and release assays. However, four derivatives (ryanodol, 9-hydroxy-21-azidoryanodine, 10-*O*-pyrrolocarbonyl ryanodine, 3-*epi*-ryanodine) have dwell times in the substate lasting tens of seconds to minutes (18). The effect caused by ryanodol is dependent on transmembrane voltage, with modification more likely to occur and lasting longer at +60 than at -60 mV holding potential (18). Tanna *et al.* (31, 32) have extended these observations using an uncharged ryanoid (ryanodol, Reference 32) a cationic ryanoid (21-amino-9 $\alpha$ -hydroxyryanodine, Reference 31), and an anionic ryanoid (10-*O*-succinyl ryanodine, Tanna *et al.*, unpublished results). All three show similar dependencies on applied potential: therefore, interactions between the applied field and the ligand are minor if they exist at all. It is clear that the RyR is sensing the applied electrostatic field by undergoing a

voltage-induced conformation change (31, 32). The isomerization of the RyR is not discerned by open probability of conductance but is detected by a change in the affinity of the RyR for ryanoids. This is manifested by voltage-induced changes in proportion of time the channel spends in the ryanoid-induced subconductance state, and in changes in the association and dissociation rate constants. Both the on and off rate constants are affected by applied potential. For the cationic, anionic and neutral ryanoid, increasing positive holding potential increases the association rate constant while the off rate constant decreases with increasing positive holding potential. At zero applied potential, the association and dissociation rate constants are ryanodol (0.035  $\mu\text{M}^{-1} \text{sec}^{-1}$ , 0.095  $\text{sec}^{-1}$ ), 21-amino-9 $\alpha$ -hydroxyryanodine (0.365  $\mu\text{M}^{-1} \text{sec}^{-1}$ , 0.99  $\text{sec}^{-1}$ ), and 10-*O*-succinyl ryanodol (0.0022  $\mu\text{M}^{-1} \text{sec}^{-1}$ , 0.085  $\text{sec}^{-1}$ ) Although it is dangerous to do so (because the binding and dissociation of a ryanoid is not an elementary process) one can estimate the dissociation constant from the ratio of the dissociation rate constant to the association rate constant. At zero applied potential the inferred dissociation constants for both ryanodol and 21-amino-9 $\alpha$ -hydroxyryanodine is 2.8  $\mu\text{M}$ , while that of 10-*O*-succinyl ryanodol is 36  $\mu\text{M}$ . The values obtained from binding isotherms to cardiac SR are 1.6 (ryanodol), 3.6  $\mu\text{M}$  (21-amino-9 $\alpha$ -hydroxyryanodine) and 4.8  $\mu\text{M}$  (10-*O*-succinyl ryanodol). The large discrepancy in the case of binding isotherms to cardiac SR are 1.6 (ryanodol), 3.6  $\mu\text{M}$  (21-amino-9 $\alpha$ -hydroxyryanodine) and 4.8  $\mu\text{M}$  (10-*O*-succinyl ryanodol). The large discrepancy in the case of the anionic derivative is unresolved. It may point to a difference in rate limiting step in the binding of the anionic ryanoid and the inadequacy of the calculation to account for the difference. Note that the order of magnitude difference between the on and off rate constants between the cationic ryanoid and the neutral and anionic ryanoids is not paralleled in binding isotherms in SR preparations of the RyR.

#### **CONFORMATION AND CONDUCTANCE**

That change in structure should lead to changes in ligand-receptor affinity is useful but not surprising. That change in structure should lead to changes in fractional conductance and gating kinetics of ryanodine receptors is less expected. The fact that affinity and modulation of channel properties map to different structural loci indicates the potential for design of the ligands with useful properties. What was surprising is that the ryanodine receptor can sense the conformation of the bound ligand. Both 21-*p*-nitrobenzoylamino-9 $\alpha$ -hydroxyryanodine (32) and succinyl ryanodol (Tanna *et al.* unpublished) induce multiple conformational states. Three distinct subconductance states are induced by 21-

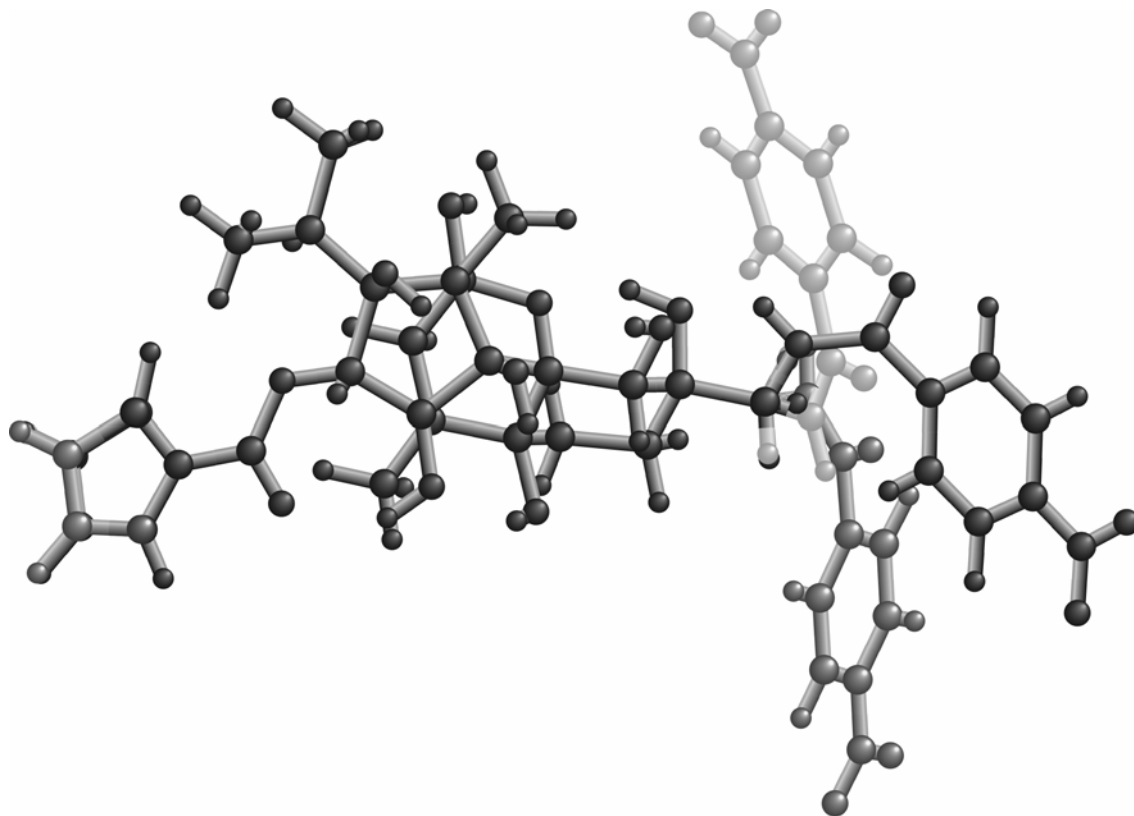


Figure 7. Three major conformational families of the 21-*p*-nitrobenzoylamino-9 $\alpha$ -hydroxylryanodine. The compound was run in molecular dynamics and therefore includes entropic contributions to conformation. The high energy barrier to rotation about the bond connecting the 9- and 21-carbons divides the molecule into distinct conformational families. After dividing the conformers into families, the average conformation was computed and then minimized by molecular mechanics. The three major conformations are superimposed with the *p*-nitrobenzoyl group to the right.

*p*-nitrobenzoylamino-9 $\alpha$ -hydroxylryanodine.

These subconductance states are correlated with three distinct conformations of the *p*-nitrobenzoyl group identified by extended, unrestrained molecular dynamics and family analysis. The fractional conductance states (and the percentage of total observations) are 0.27 (73%), 0.17 (20%) and 0.59 (7%). In Figure 7 the three major conformations are shown. They exist in the ratio of 73:24:1% the remaining 2% of the conformations correspond to several conformers that are rarely populated.

From examination of the single channel recordings, it appears that the receptor binds to one of the 21-*p*-nitrobenzoylamino-9 $\alpha$ -hydroxylryanodine conformers to enter the corresponding subconductance state. The ryanoid is released, and another or the same conformer is bound. There is no evidence for isomerization of the ligand within the binary receptor-ryanoid complex.

Succinyl ryanodol produces a large number of subconductance states. Molecular dynamics demonstrates that unlike the 21-*p*-nitrobenzoylamino-9 $\alpha$ -hydroxylryanodine, the succinyl group exists in a large number of distinct conformers. Because of the complexity of the

data, no analysis has been made. Conformational relationships of anionic ryanoids can be better addressed with pendant groups that are less conformationally mobile, for example a fumaric acid rather than a succinic acid.

#### **MODULATION BY BINDING IN THE CHANNEL OR BY ALLOSTERIC INTERACTIONS**

The location of the ryanodine binding site remains unknown. Covalent modification studies indicate that the ryanodine binding site includes, at the least, the carboxyl terminal part of the ryanodine receptor (which includes the transmembrane domain). In particular, a debate continues about how binding of ryanoids is translated into altered channel function. Any such model would have to explain both the altered channel gating kinetics and the altered conductance of the channel. In one model the ryanoids bind in the ion conduction pathway and partially block the ion conduction path. In this way ryanoids function in a manner analogous to a classical blocker. In another model, ryanoids bind at a site remote from the ion pore and alter channel function by stabilizing conformers rarely populated in unmodified RyR. The latter idea is attractive because of the many factors that

modulate channel conductance. Cryoelectron microscopy shows conformational changes remote from the transmembrane domain suggesting that ligands may stabilize functional conformers by binding to sites remote from the conduction path. The ability of ryanodine to enhance the RyR calcium sensitivity is also consistent with an allosteric model where two or more ligands act to stabilize a conformation of a protein (35).

The original argument for allosteric binding came from analysis of binding isotherms. Pessah and Zimanyi (36) had proposed the binding isotherm of ryanodine could be interpreted as strong negative cooperativity between binding sites. This review will not discuss the many excellent papers that analyze the complex binding isotherms. An insufficient number of ryanoids have been used to conduct a QSAR. Instead this review will recite the arguments for allosteric modulation of channel function based on QSAR of fractional conductance (9, 31, 32). First, there is little, if any, correlation between the steric bulk of ryanodine analogs and fractional conductance. Extremely bulky substituents at the 9- and 10-positions (some more than doubling the molecular volume of ryanodine) have relatively minor effects of fractional conductance. Second, introduction of charge at either the 9- or 10-position produces far less change in conductance than would be expected from an intimate relationship between the ryanodine binding site and the ion conduction path through the RyR. These points are discussed elsewhere in this review and in Reference 3.

Fessenden *et al.* (33) created a RyR1 mutant (E4032A) that is unresponsive to calcium, nucleotides or caffeine. High concentrations of ryanodine (200-500  $\mu$ M) convert the channel to a functioning state. Presumably this occurs by converting ryanodine binding energy to stabilization energy to compensate for protein interactions lost in the mutant. The authors provide a plausible mechanism to explain both the thermodynamics and kinetics of the observations. The fact that the restored channel activity will open to full conductance, strongly suggests that ryanodine binds remotely from the ion conduction path.

The E4032A mutant provides a potential opportunity for a SAR to answer some fundamental questions about the mechanism of ryanoid-induced changes in channel function (3). Does the channel exist in only two states, open and closed? Or does the channel exist as a manifold of conformers, many of which are rarely populated? Does the ryanoid alter channel function by binding at or near the cation conduction path, or does it alter channel function by binding to, and thereby stabilizing one or more of the rarely populated conformational states? Different ryanoids induce alternate fractional

conductances. The E4032A mutant stabilizes a conformer that lacks channel function. In the presence of ryanodine, an alternate, functional conformation is stabilized. Would all ryanoids stabilize this same functional conformer? In other words, is occupancy of the site by any ligand sufficient to promote the functional conformer? Or does the ryanoid contain information recognized by the receptor (and decoded by stabilization of alternative isomers of the receptor)? For example, the pyrrole carbonyl appears to be a critical determinant of ryanoid binding but it plays only a minor role in setting the conductance of the ryanoid-modified channel (57% ryanodine vs. 69% ryanodol, Reference 18). What is needed to restore function to the mutant? Does the pyrrole only provide interactions to increase the free energy of binding or does the pyrrole contain essential information required to induce a functional conformer of the mutant ryanodine receptor? In the absence of the pyrrole carbonyl, does the ryanoid bind differently or induce an alternate conformation of the RyR? Moving the pyrrole from the three position (ryanodine) to the 10-position alters the binding of ryanodol (see above). Would the positional isomer of ryanodine restore channel function? Would a ryanoid that induces a low conducting conformation (*e.g.*, the guanidyl ryanoids) induce the same functional state as ryanodine? The mutant may serve as a lens to magnify these structural differences.

### QSAR AND INTACT CELLS

A major purpose of 3D-QSAR is to develop useful probes of RyR function in cells, organs, and intact organisms. Proposed by John Sutko, fluorescent derivatives of ryanodine have been synthesized by conjugating BODIPY to ryanodine. Large fluorophores such as 4,4-difluoro-1,3,5,7-tetramethyl-4-bora-3,4-diazas-indacene-3-propionic acid succinimidyl ester (or6((4,4-difluoro-5,7-dimethyl-4-bora-3a,4a-diazas-indacene-3-propionyl)amino) hexanoic acid, BODIPY) can be incorporated at the 9- or 10-position with only minor effects on dissociation constant. Welch *et al.* (8) find a 2-fold increase (7 nM vs. 13 nM) in the dissociation constant when BODIPY is attached to the 21-position. Cifuentes *et al.* (37) report that BODIPY at the 10-position of ryanodine (B-FL-X ryanodine) increases the dissociation constant about 20-fold. From Figure 8 of Reference 38 we obtain the same result. These data are consistent with the steric and electrostatic contours in Figures 2 and 3 and the model of ryanodine binding site presented in Reference 3.

While the function of the RyR in striated muscle is at least partially understood, the function of RyR in neurons or non-excitabile tissues is far less clear. Localization of RyR in cells can provide insights into function. The BODIPY-

ryanodines have been used to localize ryanodine receptors in microsomes of rat parotid acinar cells (38), porcine endothelial cells (39), pancreatic  $\beta$ -cells (42) and vascular myocytes (40, 41). Cifuentes *et al.* (37) used the fluorescent BODIPY conjugated ryanodine to identify ryanodine receptors on the Golgi of rat sympathetic neurons. Holz *et al.* (Reference 42, Figure 2) using fixed tissue found 4 nM ryanodine inhibited the binding of 1 nM BODIPY-ryanodine binding 50%. This finding is consistent with the data in the paragraph above: addition of the BODIPY group causes little perturbation of binding. The Texas red conjugate of ryanodine was used to localize RyR in transgenic insect cells (43).

Cifuentes *et al.* (37) have pioneered details of ryanoid-receptor interactions in living cells. Using a fluorescent ryanodine (BODIPY attached to the 10-position) they measured ryanoid binding kinetics in a living cell (rat neuron). Binding is complete within 60 min. This is typical of time required for binding of ryanodine to SR *in vitro*. The apparent second order rate constant is  $9 \times 10^4 \text{ M}^{-1} \text{ min}^{-1}$  (pseudo first order rate constant =  $0.018 \text{ min}^{-1}$ ) compared to  $3 \times 10^6 \text{ M}^{-1} \text{ min}^{-1}$  (ryanodine, unpublished results) or  $5 \times 10^6 \text{ M}^{-1} \text{ min}^{-1}$  (44). As pointed out (37) the slower association rate constant may be due to the physical barriers not found in the SR binding assays. Dissociation of ryanoid from RyR in living cells consists of multiple kinetic components as seen by others *in vitro* (44; manuscript in preparation). The first order rate constants *in vivo* are  $0.16 \text{ min}^{-1}$  and  $0.017 \text{ min}^{-1}$ . In comparison, Wang *et al.* (44) observed three distinct dissociation rate constants under conditions of increasing concentrations of unlabeled ryanoid ( $k_{-1} = 0.0025 \text{ min}^{-1}$ ;  $k_{-2} = 0.00025 \text{ min}^{-1}$ ;  $k_{-3} = 0.012 \text{ min}^{-1}$ ). Privette *et al.* observed rate constants of  $0.025 \text{ min}^{-1}$  and  $0.001 \text{ min}^{-1}$  (manuscript in preparation). The slower of the *in vivo* dissociation rate constants is comparable to those observed in SR.

The Williams group found certain ryanoids have dissociation and association rates sufficiently fast to measure with the artificial bilayer/single channel technique (see above). At zero applied potential, the association and dissociation rate constants are ryanodol ( $2.1 \times 10^6 \text{ M}^{-1} \text{ min}^{-1}$ ,  $5.7 \text{ min}^{-1}$ ), 21-amino-9 $\alpha$ -hydroxyryanodine ( $2.19 \times 10^7 \text{ M}^{-1} \text{ min}^{-1}$ ,  $59.4 \text{ min}^{-1}$ ; Reference 32), and 10-O-succinyl ryanodol ( $1.32 \times 10^5 \text{ min}^{-1}$ ,  $5.1 \text{ min}^{-1}$ ; Tanna *et al.*, unpublished results). Although well below the diffusion-controlled limit, the association rate constants observed in the artificial bilayer are all faster than that estimated in the living cell. Again, this may be due to physical barriers in the cell not present in the artificial bilayer. Dissociation of weaker binding ryanoids in the bilayer experiments is faster than the BODIPY derivative *in vivo*, consistent with the

considerably tighter binding of the fluorescent ryanodine adduct. *In vivo* direct binding of B-FL-X Ry had an  $EC_{50}$  of 160 nM, (essentially the same as observed in isolated SR, see Reference 38) and close to the dissociation constant of 21-BODIPY ryanodine (8). As mentioned earlier, the relationship between kinetic rate constants and thermodynamic dissociation constants is true only for elementary processes. In spite of this important caveat, we have often found good agreement between rate constants and thermodynamic constants for both radioligand binding to SR and from rates of modification of single channels in artificial membranes. Using the rate constants from Reference 37, the derived dissociation constants are 2  $\mu\text{M}$  and 28 nM respectively. The relative magnitudes of the rate classes are consistent with the amount of binding to high and low affinity sites one would expect at a loading concentration of 200 nM BODIPY ryanodine. These values are in the range of the dissociation constant (160 nM) estimated in living neurons (37) and acinar cells (38). The differences may simply reflect the inaccuracies of using kinetics of multistep processes to infer binding constants. It is not the differences that are remarkable: it is the similarities. This data is wonderful support for the notion that the highly artificial binding conditions used in the SR experiments and artificial bilayers reflect ryanoid interactions in living cells.

At 1  $\mu\text{M}$ , ryanodine produces a use-dependent irreversible inhibition of caffeine response and on  $\text{Ca}^{2+}$  transients resulting from  $\text{Ca}^{2+}$  influx through voltage-gated channels. In comparison, application of 1  $\mu\text{M}$  of BODIPY ryanodine produced a small elevation of the resting  $\text{Ca}^{2+}$  levels and an attenuated response to potassium-induced membrane depolarization and caffeine (37). The authors suggested that ryanodine binding may block interactions between RyR,

The BODIPY derivatives have been useful because the conjugation of the fluorophore to ryanodine extracts only a small price in binding energy and retains high specificity and slow binding kinetics of ryanodine. These physical properties facilitate the localization of functional RyR in living cells. The CoMFA suggests the possibility of attaching other useful groups to the ryanodine structure. For example, one can conceive of attaching a sensor or reporter group to monitor the environment near the RyR. Cifuentes *et al.* (37) suggest that binding of ryanodine derivatives may block interactions between RyR: none-the-less such derivatives may provide insights into the compartments formed by RyR. One such molecule might sense calcium kinetics at the SR junction.

## CLOSING

Before ending one should note that two

isoflavones, tectoridin and 3'-hydroxy tectoridin, were found to bind to and modulate skeletal and cardiac RyR (45). While the affinity is about a thousandfold weaker than that of ryanodine, the isoflavones are able to fully displace ryanodine from the binding site. Removal of the sugar to form the aglycone tectorigenin resulted in a loss in affinity to RyR1 and could displace only 50% of the bound ryanodine. Remarkably, removal of the sugar apparently abolished binding to RyR2. While more experiments are required to prove that the isoflavones and ryanodine bind to the identical site on the RyR, these compounds are intriguing as they may provide clues into the synthesis of isoform-specific ryanomimetics.

While this brief review has mentioned only a few of the applications of ryanodine and related compounds, it is evident that ryanoids remain one of the most important tools in understanding ryanodine receptor function. The advantage of QSAR is one can make useful, quantitative predictions about ryanoid interactions without the necessity of synthesizing every possible variant. The application of three-dimensional QSAR to the ryanodine receptor is very much in the early stages. As computers and computational algorithms improve, three-dimensional structure-function relationships will be combined with experimental information and techniques to extend the insights provided by this important ligand and to guide synthesis of useful drugs and investigational tools.

#### ACKNOWLEDGEMENTS

Part of the work cited was supported by NSF grants MCB9317684 and 9817605

First, the author thanks Prof. Luc Ruest who synthesized many of the compounds discussed in this review. If it were not for his efforts, the ryanoid field would be much smaller. The author thanks Tracy Kipke, Tom Walkiewicz, Jennifer Herrick, Kathy Mitchell, Caran Mahaffy and Peter Thorkildson whose work was cited as unpublished results. The author also thanks Rebecca Sitsapesan and Alan Williams for being terrific collaborators. And a special thanks to Judith Airey and John Sutko who introduced the author to the fascinating realm of the ryanodine receptor and for their continued help and encouragement.

#### References

1. Sutko, J. L., J. A. Airey, W. Welch, & L. Ruest: The Pharmacology of Ryanodine and Related Compounds. *Pharmacol Reviews* 49, 53-98 (1997)
2. Jefferies, P. R., & J. E. Casida: Ryanoid Chemistry and Action. Chapter 9 In American Chemical Society Symposium Series 551, 130-144 (1994)
3. Welch, W: The Ryanodine Receptor: A Report from the Ryanoids. In: The

- Structure and Function of Ryanodine Receptors. Eds: Sitsapesan R, Williams, A J, Imperial College Press, London, 111-136 (1998)
4. Cramer, R. D., III; D. E. Patterson, & J. D. Bunce: Comparative Molecular Field Analysis (CoMFA). 1. Effect of Shape on Binding of Steroids to Carrier Proteins. *J Am Chem Soc* 110, 5959-5967 (1988)
  5. Klebe G, U. Abraham, T. Mietzner: Molecular similarity indices in a comparative analysis (CoMSIA) of drug molecules to correlate and predict their biological activity. *J Med Chem* 37, 4130-4146 (1994)
  6. Waterhouse AL, I. N. Pessah, A. O. Francini & J. E. Casida: Structural aspects of ryanodine action and selectivity. *J Med Chem* 30, 710-716 (1987)
  7. Jefferies PR, T. A. Blumenkopf, P. J. Gengo, L. C. Cole & J. E. Casida: Ryanodine action at calcium release channels. 1. importance of hydroxyl substituents. *J Med Chem* 39, 2331-2338 (1996)
  8. Welch, W., S. Ahmad, J. A. Airey, K. Gerzon, R. A. Humerickhouse, H. R. Besch, Jr., L. Ruest, P. Deslongchamps & J. L. Sutko: Structural Determinants of High-Affinity Binding of Ryanoids to the Vertebrate Skeletal Muscle Ryanodine Receptor: A Comparative Molecular Field Analysis. *Biochemistry* 33, 6074-6085 (1994)
  9. Welch W, J. L. Sutko, K. E. Mitchell, J. Airey & L. Ruest: The pyrrole locus is the major orienting factor in ryanodine binding. *Biochemistry* 35, 7165-7173 (1996)
  10. Welch, W., A. J. Williams, A. Tinker, K. E. Mitchell, P. Deslongchamps, J. Lamothe, K. Gerzon, K. R. Bidasee, H. R. Besch, Jr., J. A. Airey, J. L. Sutko & L. Ruest: Structural Components of Ryanodine Responsible for Modulation of Sarcoplasmic Reticulum Calcium Channel Function. *Biochemistry* 36, 2939-2950 (1997)
  11. Bidasee K. R. & H. R. Besch, Jr. Structure-Function Relationships among Ryanodine Derivatives: pyridyl ryanodine definitively separates activation potency from high affinity. *J Biol Chem* 273, 12176-12186 (1998)
  12. Novotny, J., R. E. Brucocoleri & F. A. Saul: On the Attribution of Binding Energy in Antigen-Antibody Complexes MCPC 603, D1.3 and HyHel-5. *Biochemistry* 28, 4735-4749 (1989)
  13. Krystek S., T. Stouch & J. Novotny: Affinity and specificity of serine

- endopeptidase-protein inhibitor interactions: empirical free energy calculations based on X-ray crystallographic structures. *J Mol Biol* 234, 661-679 (1993)
14. Tulip W. R., V. R. Harley, R. G. Webster & J. Novotny: N9 neuraminidase complexes with antibodies NC41 and NC10: empirical free energy calculations capture specificity trends observed with mutant binding data *Biochemistry* 33, 7986-7997.(1994)
  15. Gonzalez-Coloma A., C. Gutierrez, H. Hubner, H. Achenbach, D. Terrero & B. M. Fraga: Selective insect antifeedant and toxic action of ryanoid diterpenes. *J Agric Food Chem* 47, 4419-4424 (1999)
  16. Scott-Ward T. S., S J. Dunbar, J. D. Windass, A. J. Williams: Characterization of the ryanodine receptor-Ca<sup>2+</sup> release channel from the thoracic tissues of the lepidopteran insect *Heliothis virescens*. *J Membr Biol* 179,127-141 (2001)
  17. Lehmberg, E. & J. E. Casida: Similarity of insect and mammalian ryanodine binding sites. *Pest Biochem Physiol* 48, 145-152 (1994)
  18. Tinker A, J. L. Sutko, L. Ruest, P. Deslongchamps, W. Welch, J. A. Airey, K. Gerzon, K. R. Bidasee, H. R. Besch Jr & A. J. Williams: Electrophysiological effects of ryanodine derivatives on the sheep cardiac sarcoplasmic reticulum calcium-release channel. *Biophys J* 70, 2110-2119 (1996)
  19. Vais H. & P. N. Usherwood: Novel actions of ryanodine and analogues--perturbors of potassium channels. *Biosci Rep* 15, 515-530 (1995)
  20. Usherwood P. N. R. & H. Vais: Towards the development of ryanoid insecticides with low mammalian toxicity. *Toxicol Lett* 82-83, 247-54 (1995)
  21. Jefferies P.R., E. Lehmberg, W. W. Lam & J. E. Casida: Bioactive ryanoids from nucleophilic additions to 4,12-seco-4,12-dioxoryanodine. *J Med Chem* 36, 1128-1135 (1993)
  22. Jefferies P.R., P. J. Gengo, M. J. Watson & J. E. Casida: Ryanodine action at calcium release channels. 2. relation to substituents of the cyclohexane ring. *J Med Chem* 39, 2339-2346 (1996)
  23. Gerzon K., R. A. Humerickhouse, H. R. Besch Jr, K. R. Bidasee, J. T. Emmick, R. W. Roeske, Z. Tian, L. Ruest & J. L. Sutko: Amino- and guanidinoacylryanodines: basic ryanodine esters with enhanced affinity for the sarcoplasmic reticulum Ca(2+)-release channel. *J Med Chem* 36, 1319-1323 (1993)
  24. Humerickhouse RA, K. R. Bidasee, K. Gerzon, J. T. Emmick, S. Kwon, J. L. Sutko, L. Ruest, & H. R. Besch Jr: High affinity C10-Oeq ester derivatives of ryanodine. Activator-selective agonists of the sarcoplasmic reticulum calcium release channel. *J Biol Chem* 269, 30243-30253 1994
  25. Bidasee K. R., H. R. Besch Jr, K. Gerzon & R. A. Humerickhouse: Activation and deactivation of sarcoplasmic reticulum calcium release channels: molecular dissection of mechanisms via novel semi-synthetic ryanoids. *Mol Cell Biochem* 149/150, 145-160 (1995)
  26. Schleifer, K. J: Pseudoreceptor model for ryanodine derivatives at calcium release channels. *J Comput Aided Mol Des* 14, 467-475 (2000)
  27. Jefferies, P. R., R. F. Toia & J. E. Casida: Ryanodyl 3-(pyridine-3-carboxylate): a novel ryanoid from *Ryania* insecticide. *J Nat Prod* 54, 1147B1149 (1991)
  28. Rousseau E., J.S. Smith & G. Meissner: Ryanodine modifies conductance and gating behavior of single Ca<sup>2+</sup> release channel. *Am J Physiol* 253, C364-C368 (1987)
  29. Laver D. R: The power of single channel recording and analysis: its application to ryanodine receptors in lipid bilayers. *Clin Exp Pharmacol Physiol* 28, 675-686 (2001)
  30. Meissner G., E. Rios, A. Tripathy & D. A. Pasek: Regulation of Skeletal Muscle Ca<sup>2+</sup> Release Channel (Ryanodine Receptor) by Ca<sup>2+</sup> and Monovalent Cations and Anions. *J Biol Chem* 272, 1628-1638 (1997)
  31. Tanna B., W. Welch, L. Ruest, J. L. Sutko & A. J. Williams: Interactions of a reversible ryanoid (21-amino-9 $\alpha$ -hydroxy-ryanodine) with single sheep cardiac ryanodine receptor channels. *J Gen Physiol* 112, 55-69 (1998.)
  32. Tanna, B., W. Welch, L. Ruest, J. L. Sutko & A. J. Williams: The Interaction of a neutral Ryanoid with the Ryanodine Receptor Channel Provides Insights into the Mechanisms by which Ryanoid Binding Is Modulated by Voltage. *J Gen Physiol* 116, 1-10 (2000)
  33. Fessenden, J. D., L. Chen, Y. Wang, C. Paolini, C. Franzini-Armstrong, P. D. Allen & I. N. Pessah: Ryanodine receptor point mutant E4032A reveals an allosteric interaction with ryanodine. *Proc. Natl. Acad. Sci. USA* 98, 2856-2870 (2001)
  34. Lindsay A.R., A. Tinker. A. J. Williams: How does ryanodine modify ion handling in the sheep cardiac sarcoplasmic

- reticulum Ca(2+)-release channel? *J Gen Physiol* 104, 425-47 (1994)
35. Masumiya H, P. Li, L. Zhang & S. R. W. Chen: Ryanodine sensitizes the Ca<sup>2+</sup> release channel (ryanodine receptor) to Ca<sup>2+</sup> activation: *J Biol Chem* 276, 39727-39735 (2001)
  36. Pessah I. N & I. Zimanyi: Characterization of multiple [<sup>3</sup>H]ryanodine binding sites on the Ca<sup>2+</sup> release channel of sarcoplasmic reticulum from skeletal and cardiac muscle: Evidence for a sequential mechanism in ryanodine action. *Mol Pharmacol* 39, 679-689 (1991)
  37. Cifuentes, F., C. E. Gonzalez, T. Fiordeliso, G. Guerrero, F. A. Lai & A. Hernandez-Cruz: A ryanodine fluorescent derivative reveals the presence of high-affinity ryanodine binding site in the Golgi complex of rat sympathetic neurons, with possible functional roles in intracellular Ca<sup>2+</sup> signaling. *Cell Signalling* 13, 353-362 (2001)
  38. Zhang, X., J. Wen, K. R. Bidasee, H. R. Besch, Jr & R. P. Rubin: Ryanodine receptor expression is associated with intracellular Ca<sup>2+</sup> release in rat parotid acinar cells. *Am J Physiol* 273 (*Cell Physiol* 42), C1306-B1314 (1997)
  39. Graier W. F., J. Paltauf-Doburzynska, B. J. F. Hill, E. Fleischhacker, B. G. Hoebel, G. M. Kostner & M. Sturek: Submaximal stimulation of porcine endothelial cells causes focal Ca<sup>2+</sup> elevation beneath the cell membrane. *J Physiol* 506, 109-125.(1998)
  40. Coussin, F, N. Macrez, J.-L. Morel & J. Mironneau: Requirement of ryanodine receptor subtypes 1 and 2 for Ca(2+)-induced Ca(2+) release in vascular myocytes. *J Biol Chem* 275, 9596-9603 (2000)
  41. Gordienko, D. V., I. A. Greenwood & T. B. Bolton: Direct visualization of sarcoplasmic reticulum regions discharging Ca<sup>2+</sup> sparks in vascular myocytes. *Cell Calcium* 29, 13-28 (2001)
  42. Holz G. G., C. A. Leech, R. S. Heller, M. Castonguay & J. F. Habener: cAMP-dependent Mobilization of Intracellular Ca<sup>2+</sup> Stores by Activation of Ryanodine Receptors in Pancreatic [beta ] -Cells: A Ca<sup>2+</sup> signaling system stimulated by the insulinotropic hormone glucagon-like peptide-1-(7-37). *J Biol Chem* 274, 14147-14156 (1999)
  43. Antaramian A, A. Butanda-Ochoa, O. Vazquez-Martinez, M. Diaz-Munoz & L. Vaca: Functional expression of recombinant type 1 ryanodine receptor in insect cells. *Cell Calcium* 30, 9-17 (2001)
  44. Wang, J.P., D. H. Needleman & S. L. Hamilton: Relationship of Low affinity [<sup>3</sup>H]Ryanodine Binding Sites to High Affinity Sites on the Skeletal muscle Ca<sup>2+</sup> Release Channel. *J Biol Chem* 268, 20974-20982 (1993)
  45. Bidasee, K. R., A. Maxwell, W. F. Reynolds, V. Patel & H. R. Besch Jr: Tectoridins modulate skeletal and cardiac muscle sarcoplasmic reticulum calcium-release channels. *J Pharmacol Exp Ther* 293, 1074-1083 (2000)

**Send correspondence to :**

William Welch  
 Department of Biochemistry/330  
 University of Nevada  
 Reno, Nevada 89557  
 Tel: (312)-765-3232  
 Fax: (312)-765-3233  
 E-mail: [jo@aol.com](mailto:jo@aol.com) ([welch@unr.nevada.edu](mailto:welch@unr.nevada.edu))

**Running title:** 3D-QSAR of ryanoids

**Key words:** ryanodine receptor ryanoids CoMFA  
 CoMSIA QSAR subconductance kinetics

# Ion Conduction and Selectivity in the Ryanodine Receptor Channel

Williams, Alan J.

Cardiac Medicine, National Heart & Lung Institute, Faculty of Medicine, Imperial College of Science, Technology & Medicine, Dovehouse St., LONDON SW3 6LY, U.K. e-mail: [a.j.williams@ic.ac.uk](mailto:a.j.williams@ic.ac.uk)

**ABSTRACT** The ryanodine receptor channel is an intracellular membrane  $\text{Ca}^{2+}$ -release channel. The investigation of ion translocation and discrimination in individual channels under voltage-clamp conditions has revealed that the channel can sustain very high rates of cation translocation, has high affinity for divalent cations and displays relatively poor discrimination between physiologically relevant cations. In this article I will discuss the mechanisms underlying these characteristic properties, the regions of the channel molecule likely to be involved in ion handling and speculate on the structure of the conduction pathway of  $\text{Ca}^{2+}$ -release channels.

## INTRODUCTION

Ion channels are multimeric protein molecules that provide pathways for ion translocation through otherwise impermeable membranes. In all cases ions move through a membrane ion channel in response to an electrochemical driving force. A defining feature of channel mediated translocation is that rates of ion movement are very high and for the most part, very specific. The ability of channel proteins to distinguish between closely related ions is reflected in their generic classification as, for example,  $\text{K}^+$ ,  $\text{Na}^+$  and  $\text{Ca}^{2+}$  channels. Our understanding of the mechanisms that make it possible for ion channels to perform the intuitively contradictory tasks of maintaining very high rates of flux whilst discriminating between physically related ions has been greatly enhanced by the determination of the structure of a bacterial  $\text{K}^+$  channel at a resolution of 3.2 Å (1).

In this article I will review our current understanding of the structures and mechanisms involved in ion translocation and discrimination in a nominally  $\text{Ca}^{2+}$ -selective ion channel, the ryanodine receptor (RyR) and discuss how these might contribute to the function of this protein complex as a  $\text{Ca}^{2+}$ -release channel.

## THE PHYSIOLOGICAL ROLE OF THE RYANODINE RECEPTOR CHANNEL

Ryanodine receptor channels are expressed in intracellular membrane networks such as the sarcoplasmic reticulum of striated muscle cells and provide pathways for the regulated release of stored  $\text{Ca}^{2+}$  in response to appropriate stimuli. In striated muscle the ryanodine receptor plays a pivotal role in the initiation of cell contraction; RyR channel open probability increases in response to the depolarisation of the sarcolemma and  $\text{Ca}^{2+}$  ions flow from the sarcoplasmic reticulum down the concentration gradient, established by the ATP-driven  $\text{Ca}^{2+}$  pump, to initiate contraction (2).

RyR is clearly a very efficient  $\text{Ca}^{2+}$ -release channel. RyR gating responds to appropriate physiological stimuli and is modulated by a variety of physiologically relevant processes (3-5). Equally

important, when open, RyR provides a conduction pathway that allows for the release of enough  $\text{Ca}^{2+}$  from the sarcoplasmic reticulum to raise the free concentration of the highly buffered cytosol from its resting level of 100 nM to 1  $\mu\text{M}$  in a matter of milliseconds (2). It does this under prevailing conditions that include a relatively low concentration of the relevant cation (the concentration of free  $\text{Ca}^{2+}$  within the sarcoplasmic reticulum is likely to be in the region of 1 mM) and in the presence of a number of potentially competing ions such as  $\text{K}^+$  and  $\text{Mg}^{2+}$ . To achieve its physiological role it appears that RyR must have structural features and employ mechanisms that result in high rates of  $\text{Ca}^{2+}$  translocation, high affinity for  $\text{Ca}^{2+}$  and the ability to discriminate between  $\text{Ca}^{2+}$ ,  $\text{K}^+$  and  $\text{Mg}^{2+}$ .

## THE ION HANDLING PROPERTIES OF RyR

The sarcoplasmic reticulum membrane system contains a variety of ion transporting systems including ion channels permeable to monovalent cations (6) and anions (7;8). Detailed investigations of ion translocation and discrimination in RyR require the separation of this channel from the other cation transporting systems of the sarcoplasmic reticulum membrane network (9;10) and the incorporation of individual RyR channels into planar phospholipid bilayers. RyR channels incorporate into planar phospholipid bilayers in a fixed orientation so that the cytosolic and luminal faces of the channel protein can be defined (11). A rigorous investigation of ion translocation and discrimination can then be carried out under voltage clamp conditions. Using this approach we have characterised ion handling in the sheep cardiac isoform of the receptor channel (RyR2) by monitoring relative permeability, relative conductance and relative affinity of permeant ions and blocking parameters of impermeant ions. Details of these properties can be found in earlier publications (12;13) and I will summarise only the most important features here.

## Physiologically relevant cations

The first striking feature to emerge from these studies is that whilst within the cell  $\text{Ca}^{2+}$  is undoubtedly the physiological charge carrier in RyR,

the channel is in fact permeable to a very wide range of divalent and monovalent cations. Measurements of RyR channel activity in solutions of the group 1a monovalent cations in the absence of divalent cations demonstrate that  $K^+$ ,  $Na^+$ ,  $Cs^+$ ,  $Rb^+$  and  $Li^+$  are all translocated at very substantial rates through RyR. With symmetrical 210 mM solutions single channel current-voltage relationships are linear with single channel conductances ranging from approximately 210 pS in  $Li^+$  up to approximately 720 pS in  $K^+$ . However these rates of monovalent cation translocation can be increased by raising the activity of the permeant ion. Determinations of the dependence of single RyR channel conductance on group 1a monovalent cation activity indicate that in all cases conductance saturates, with values of maximal conductance ranging from approximately 250 pS with  $Li^+$  to 900 pS with  $K^+$ . Activities at which single channel conductance reach 50% of the maximal value range from 9.1 mM for  $Li^+$  to 34 mM for  $Cs^+$ . Despite the almost four fold range in maximal conductance, the permeability of the group 1a monovalent cations differs only slightly. Calculations of permeability relative to  $K^+$  from reversal potentials monitored with  $K^+$  at the cytosolic face of the channel and another group 1a monovalent cation at the luminal face of the channel indicate that, with the exception of  $Cs^+$  ( $pCs^+/pK^+ = 0.61$ ), this group of cations are essentially equally permeant in RyR.

Despite the high single channel conductance of the group 1a monovalent cations, RyR does show some discrimination between this class of cations and  $Ca^{2+}$ . Calculation of the relative permeability of  $Ca^{2+}$  to  $K^+$  from reversal potentials monitored with  $K^+$  at the cytosolic face of the channel and  $Ca^{2+}$  at the luminal face of the channel demonstrates that  $Ca^{2+}$  is 6.5 times more permeant in RyR than  $K^+$ . However, equivalent determinations of relative permeabilities of  $Ba^{2+}$ ,  $Sr^{2+}$  and  $Mg^{2+}$  relative to  $K^+$  indicate that these alkaline earth divalents are effectively as permeant as  $Ca^{2+}$  in RyR. These observations are confirmed by measurements of the relative permeability of  $Ca^{2+}$ ,  $Sr^{2+}$  and  $Mg^{2+}$  against  $Ba^{2+}$  which yield values in the range 1.0 to 1.1.

Single channel conductance with the alkaline earth divalents as charge carriers is very high, ranging from approximately 90 pS with 210 mM  $Mg^{2+}$  to approximately 200 pS with 210 mM  $Ba^{2+}$ . The observed unitary conductance of  $Ca^{2+}$  in RyR is approximately 10 fold higher than that monitored for the dihydropyridine-sensitive L-type  $Ca^{2+}$  channel under comparable ionic conditions (14). As is the case with monovalent inorganic cations, single RyR channel conductance increases and saturates as divalent cation activity is raised. The relationship between unitary conductance and  $Ba^{2+}$  activity demonstrates that 50% maximal conductance is seen at approximately 400  $\mu M$  suggesting that the affinity of RyR for divalent cations is very significantly higher than that for the monovalent inorganic cations.

The experiments summarised above demonstrate that the majority of the features of ion handling monitored in individual RyR channels are consistent with our expectations for an efficient  $Ca^{2+}$ -release channel. Under appropriate conditions rates of

translocation of  $Ca^{2+}$  through RyR can be extremely high. In addition, the conduction pathway of the RyR channel has a high affinity for divalent cations and is therefore likely to maintain near maximal rates of  $Ca^{2+}$  translocation at the relatively low  $Ca^{2+}$  activities found within the lumen of the sarcoplasmic reticulum. One feature of ion handling in RyR that appears to be at odds with our initial image of a  $Ca^{2+}$ -release channel is that RyR shows only limited powers of discrimination between physiologically relevant cations. As a result,  $Ca^{2+}$  flux through RyR is likely to be sensitive to variations in the intracellular activities of potentially competing cations such as  $Mg^{2+}$  that may occur in pathophysiological conditions including myocardial stunning (15).

### **Permeation and block by organic cations**

Physiologically relevant inorganic cations are not the only ionic species that interact with the conduction pathway of RyR. Organic monovalent cations have proved to be very useful tools in studying the mechanisms and structures underlying ion translocation and discrimination in many species of ion channel including RyR. We have investigated the relative permeability of a large number of monovalent organic cations in RyR by determining reversal potentials with the organic cation at the cytosolic face of the channel and  $K^+$  at the luminal face of the channel (16). These experiments have demonstrated that the relative permeability of this class of cations in RyR is related to the size of the cation; or more precisely to the minimum circular radius of the cation. Relative permeability of these ions appears to be dependent upon a simple sieving mechanism; permeability decreases as minimum circular radius is increased. This proposal is supported by the application of excluded area theory to the data in which the relative permeability of an ion is related to the squared difference between the radius of the narrowest region of the conduction pathway of the channel and the radius of the ion. These analyses indicate that the minimum radius of the RyR conduction pathway is likely to be in the region of 3.3 to 3.5 Å.

Impermeant organic cations are not without effect in RyR. Many are effective blockers of permeant ion translocation. Tetraalkylammonium (TAA) ions are well established blockers of permeant ion translocation in  $K^+$  channels (17). Short chain TAAs such as tetramethylammonium (TMA), tetraethylammonium (TEA) and tetrapropylammonium (TPra) block  $K^+$  flux in RyR. These cations are effective in millimolar concentrations acting as concentration- and voltage-dependent blockers when added to the cytosolic face of the RyR channel. Quantitative analysis of block of RyR by these small TAAs using the protocol devised by Woodhull for analysis of  $Na^+$  channel block by  $H^+$  (18) has revealed the presence of two sites of interaction for these cations within the conduction pathway of RyR. The smallest TAA, TMA, blocks by interacting with a site positioned approximately 50% into the voltage drop across the channel. Larger TAAs do not have access to this site. TEA, TPra and derivatives of TMA in which one methyl group is replaced by either an ethyl or propyl group are blockers with a greater

dependence on trans-membrane voltage than TMA. These cations (19;20), the local anaesthetics QX222 and procaine (21) and cocaine (22) interact with a site located approximately 90% into the voltage drop across the channel. The interaction of blocking cations with this site has proved to be very useful in the estimation of the physical distance over which the voltage drop across the RyR channel occurs. In this approach, which was originally used to monitor the length of the voltage drop in the sarcoplasmic reticulum  $K^+$  channel (23), blocking parameters of monovalent  $(CH_3-(CH_2)_{n-1}-N^+(CH_3)_3)$  and divalent  $((CH_3)_3N^+-(CH_2)_n-N^+(CH_3)_3)$  derivatives of trimethylammonium of varying chain length were determined. Both sets of cation were found to be voltage-dependent blockers of  $K^+$  flux when added to the cytosolic face of RyR (24). Analysis of the voltage dependence of block by the monovalent cations revealed that this parameter was unaffected by chain length; all produced values of effective valence of block of approximately 0.9, consistent with interaction of the cation with a site located 90% into the voltage drop across the channel from its cytosolic origin. This was not the case for the divalent cations; increasing chain length from  $n=2$  to  $n=7$  resulted in a linear decrease in the dependence of block on trans-membrane voltage. Effective valence decreased from 1.5 to a value approaching that obtained with the monovalent derivatives at  $n=7$ . Further increases in chain length ( $n=8$  or  $9$ ) produced no further alteration in effective valence. It is assumed that one cationic group of all the divalent derivatives interacts with the 90% site and that the high values of effective valence obtained with short chain derivatives reflects the presence of the second trimethylammonium cationic group within the voltage drop. The point at which the effective valence of the mono and divalent derivatives coincide indicates the point at which the second charged group of the divalent derivative "drops out" of the voltage drop. Knowing the  $N^+-N^+$  distance for the divalent derivatives it is possible to estimate the physical length of the voltage drop across RyR and this calculation yields a value of  $10.4 \text{ \AA}$  (24).

#### **SUMMARY OF THE PROPERTIES AND DIMENSIONS OF THE CONDUCTION PATHWAY IN RyR.**

Measurements of relative conductance, relative affinity, relative permeability and block obtained from a range of permeant and impermeant cations have provided useful information on the properties of RyR as a  $Ca^{2+}$ -release channel and estimates for the dimensions of the essential components of its conduction pathway. RyR is a high conductance, poorly selective, cation channel. The voltage drop across the channel occurs over a distance of approximately  $10 \text{ \AA}$  and the narrowest region of its conduction pathway has a radius of approximately  $3.4 \text{ \AA}$ . The observation that blocking cations such as TEA interact with a site located 90% into the voltage drop from its cytosolic origin indicates that the narrowest region of the conduction pathway must be located towards the luminal end of the voltage drop and that the constriction formed by this region is

unlikely to be more than  $1 \text{ \AA}$  in length (13). Does this information tell us anything about the mechanisms underlying ion translocation and discrimination in RyR? How do these features compare with those of other ion channels?

#### **MECHANISMS INVOLVED IN CATION TRANSLOCATION IN RyR**

Undoubtedly the most striking features of ion handling by RyR are the monumental values of single channel conductance obtained with both divalent and monovalent inorganic cations and the massive unitary currents seen at high holding potentials. Maximal conductance values in the range of  $1 \text{ nS}$  for  $K^+$  and  $200 \text{ pS}$  for  $Ba^{2+}$  far exceed those monitored in other native membrane channels and for that matter non-selective channels such as porin (13). We have monitored unitary current amplitudes of  $70 \text{ pA}$  at  $100 \text{ mV}$  with  $K^+$  (25) and  $20 \text{ pA}$  at  $100 \text{ mV}$  with  $Ba^{2+}$  (26). Under these conditions, current-voltage relationships are linear with no indication of saturation of single channel current amplitude. High unitary conductance and current amplitude are clearly advantageous for a  $Ca^{2+}$ -release channel but how are these rates of ion translocation achieved?

Information on the mechanisms responsible for high rates of ion translocation (although considerably lower than those observed in RyR) is available for  $K^+$  channels. A considerable body of experimental evidence indicates that high rates of ion flux in  $K^+$  channels are achieved as the result of electrostatic repulsion between cations in a multiply occupied selectivity filter. This proposal has been confirmed by the visualisation of this phenomenon in KcsA (1). The selectivity filter of the KcsA channel is a tunnel  $12 \text{ \AA}$  in length with a radius of  $1.5 \text{ \AA}$ . The structure is formed by the apposition of four identical loops (one from each monomer of a homotetramer) composed of residues (GYG) that are essential for  $K^+$  selectivity. At physiological  $K^+$  concentrations two cations are located within the selectivity filter separated by a distance of approximately  $7.5 \text{ \AA}$  (1). Under these conditions the electrostatic repulsion between the two cations is sufficient to overcome the interactions between the ions and the residues in the selectivity filter so that the affinity of the selectivity filter for  $K^+$  is reduced and rates of ion exit from the channel are maximised (27).

The suggestion that such a mechanism could underlie the phenomenal rates of cation translocation achieved by RyR is appealing; particularly as there are potential similarities between the  $K^+$  channel signature selectivity sequence and the putative selectivity sequence of RyR (see later). Unfortunately, investigations of ion occupancy in RyR, whilst not entirely excluding the possibility, are not consistent with multiple ion occupancy; RyR appears to be a single-ion channel. Briefly the evidence supporting this proposal is as follows (17): RyR shows simple saturation of conductance with increasing ion activity (19;26); bi-ionic reversal potentials are not dependent on concentration (16;26); we observe no anomalous mole-fraction effects (19;26); the effective valence of small monovalent cation blockers is less than 1.0 (19-

21) and ion handling can be described by a simple single occupancy rate theory model (28).

What mechanisms could produce extremely high rates of cation translocation in a single-ion channel? In such a system, conductance will be limited by the rate at which ions leave the channel and this will in turn depend upon the physical dimensions of the conduction pathway. Using a simple cylindrical pore as an analogous structure it can be shown that in a single-ion channel conductance will be maximised if the conduction pathway of the channel is short and wide (17;29). Is the conduction pathway of RyR short and wide? A radius of 3.3 – 3.5 Å is comparable with equivalent measurements made in relatively non-selective channels such as cGMP-activated channels (30) and nicotinic Ach receptors (31) and is more than twice the minimum pore radii estimated in K<sup>+</sup>-selective channels (17) and seen in KcsA (1). It is much more difficult to compare the relative lengths of channel pores. Different approaches provide information on different entities. The method described in an earlier section of this article yielded an estimate of the length of the voltage drop across the RyR channel; the selectivity filter visualised in KcsA is a physical

and divalent inorganic cations indicate that rates of ion entry into the channel are not limited by diffusion (13;28;32). As is the case with rates of ion exit from RyR, rates of ion entry into RyR could be optimised by specific structural characteristics of the channel. Adaptations that provide the channel with a large capture radius will aid rates of ion entry. The capture radius of a channel will be maximised by increasing the area via which ions can leave the bulk solution and enter the area of influence of the trans-membrane voltage. A large capture radius would be provided by a structure in which access to a short selectivity filter is via wide mouths or vestibules, with the voltage drop across the channel extending into the vestibules (13;29;33). The capture radius of a cation-selective single-ion channel could also be increased by the presence of fixed negative charge at the entrances of the channel (33;34). The possible involvement of such a mechanism in RyR is supported by experiments which demonstrate a reduction in channel conductance following chemical modification of luminal carboxyl groups (35) and by the observation that the rate of association of K<sup>+</sup> channel N-type inactivation peptides with sites at the cytosolic face of the RyR channel are increased approximately 500 fold when the net charge of the peptide is increased from +3 to +7 (36).

The picture that emerges for the region of RyR responsible for ion conduction and discrimination is of a structure comprising a short pore (or voltage drop) in which is located an even shorter, relatively wide, constriction or selectivity filter. The combination of these features is likely to maximise rates at which ions leave the channel and provide a large capture radius to maximise rates of ion entry (13).

#### IDENTIFICATION OF COMPONENTS OF THE RyR CONDUCTION PATHWAY

By analogy with other species of ion channel, the conduction pathway of RyR is expected to be formed by components of membrane spanning helices. Putative membrane spanning domains of the RyR monomer are located in the carboxyl-terminal region of the molecule although the identity and number of these regions is still an area of debate. Based on evidence from hydrophathy predictions Takeshima et al (37) proposed that RyR1 possessed four trans-membrane (T-M) helices. In contrast Zorzato et al (38) identified 12 hydrophobic sequences considered long enough to form T-M helices. T-M 5, 6, 8 and 10 of this model correspond to T-M 1, 2, 3 and 4 of the Takeshima model. A third model was proposed by Tunwell et al (39) in which the RyR monomer contains 6 T-M helices. Strong support for a carboxyl-terminal location of the RyR conduction pathway comes from experiments in which channel activity has been observed following the incorporation of trypsinised (40) or truncated (41;42) RyR channels into planar phospholipid bilayers.

The involvement of specific residues in the formation of the ion handling region of RyR was proposed by Balshaw et al (43) who noted a marked similarity between a sequence of residues present in

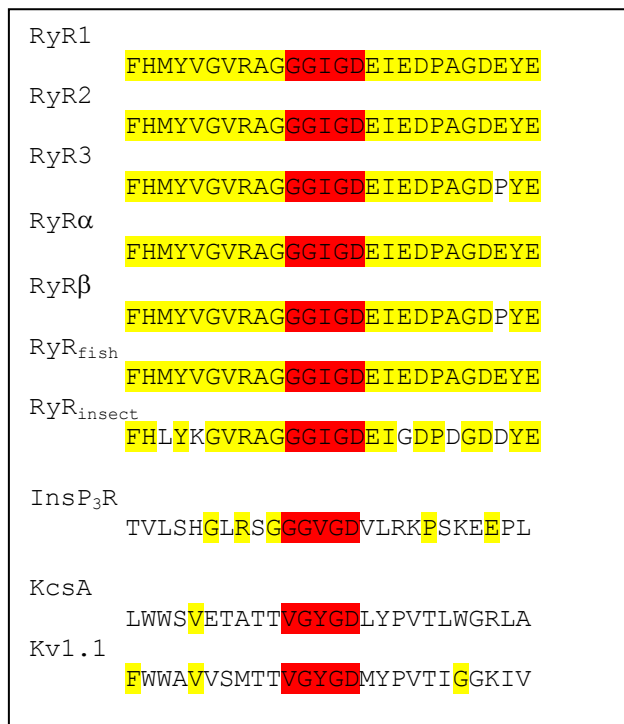


Figure 1. Sequence alignments for the putative pore-forming loops of RyR isoforms, InsP<sub>3</sub>R, a voltage-gated K<sup>+</sup> channel (Kv1.1) and KcsA. The residues essential for K<sup>+</sup> selectivity in K<sup>+</sup> channels and the proposed "selectivity filter" of the Ca<sup>2+</sup>-release channels are highlighted in red. Regions of identity are highlighted in yellow. Modified from Williams et al. Quarterly Reviews of Biophysics 34, 1 (2001), 61-104.

structure but the relationship between this and the voltage drop across the channel is not established.

The huge unitary current amplitudes seen at high holding potentials in RyR with both monovalent

luminal loops of both RyR and the related inositol 1,4,5-trisphosphate receptor (InsP<sub>3</sub>R) Ca<sup>2+</sup>-release channel (loop linking T-M 3 and T-M 4 in the RyR

significant changes in the unitary conductance of RyR channels under voltage clamp conditions. Altered conductance is seen with either K<sup>+</sup> or Ca<sup>2+</sup> as the

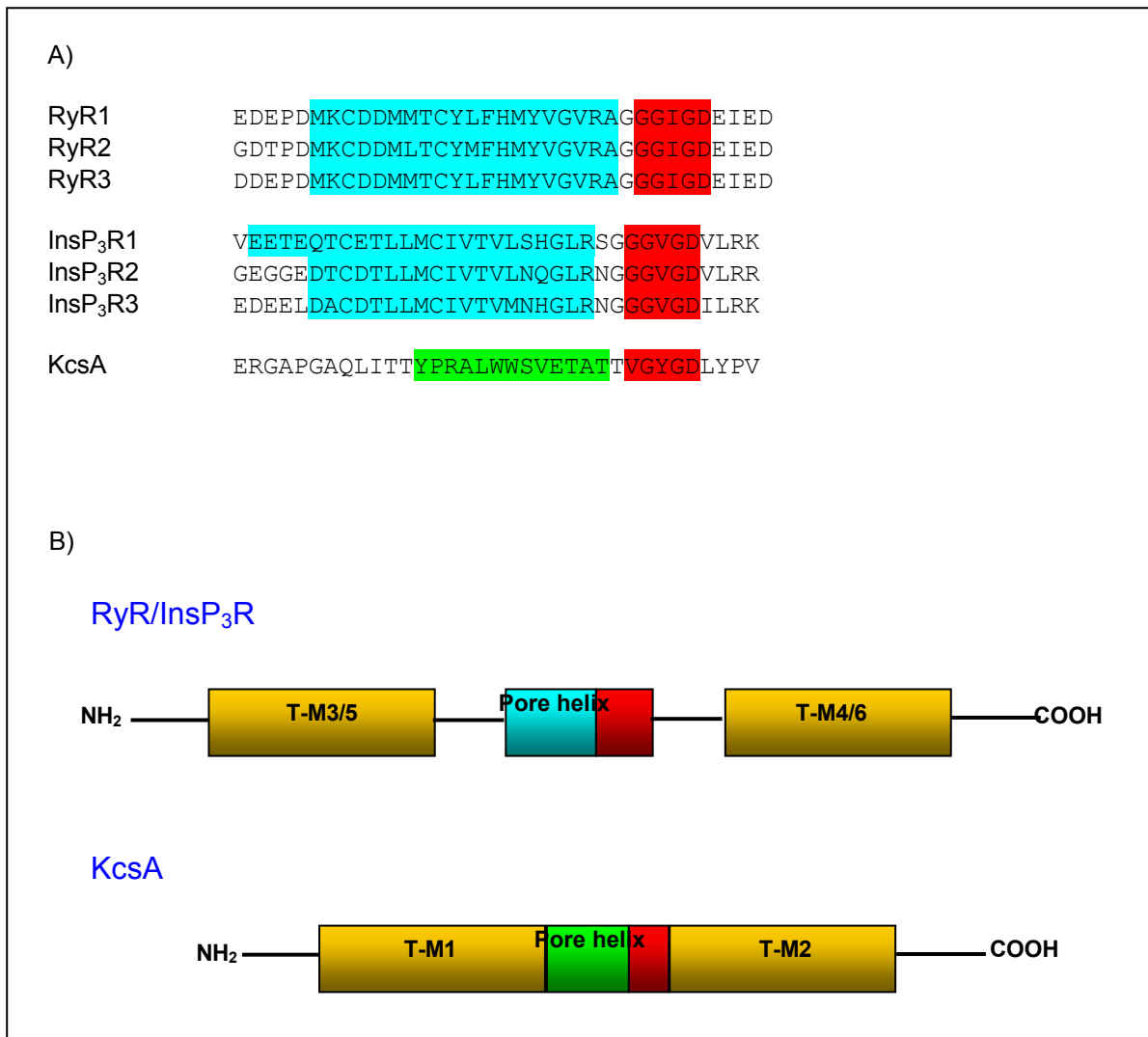


Figure 2. Secondary structure predictions of a putative pore helix in the pore-forming loops of isoforms of RyR and InsP<sub>3</sub>R. A) Sequence alignments for RyR and InsP<sub>3</sub>R (blue) together with KcsA (green). Selectivity sequences are shown in red. Secondary structure was predicted using PSIPred: <http://insulin.brunel.ac.uk/psipred>. B) Diagram showing the similarity in sequence of structural elements in the pore-forming loops of RyR, InsP<sub>3</sub>R and KcsA. Modified from Williams et al. Quarterly Reviews of Biophysics 34, 1 (2001), 61-104.

model of Takeshima et al (37); loop linking T-M8 and T-M10 in the Zorzato et al (38) model of RyR and loop linking T-M5 and T-M6 in InsP<sub>3</sub>R (44;45)) and the signature selectivity sequence in K<sup>+</sup> channels (46) (Figure 1). By analogy with known K<sup>+</sup> channel structure it was proposed that this loop, or more precisely one from each monomer of the homotetramer, might fold back into the membrane to form the selectivity filter or a component of the conduction pathway of the RyR channel.

Further support for this proposal comes from experiments in which residues in and around the RyR luminal loop have been mutated (13;47-49). Substitutions of amino acids in the GIGD sequence and contiguous regions of the luminal loop produce

charge carrying species. It should be noted that, in addition to ion translocation, mutations in this region of RyR modify properties such as the ability of the receptor to bind [<sup>3</sup>H]-ryanodine and its ability to release Ca<sup>2+</sup> when exposed, *in situ*, to caffeine (47-49).

#### CAN WE DRAW FURTHER ANALOGIES BETWEEN RYR AND K<sup>+</sup> CHANNELS?

It is established that the apparatus for pore formation, ion translocation and ion discrimination in both K<sup>+</sup> and RyR channels is located in a loop (extracellular in K<sup>+</sup> channels, luminal in RyR) that folds back into the membrane. In addition there is a similarity between the amino acid residues of the K<sup>+</sup>

channel selectivity filter and residues known to be involved in ion translocation in RyR. Do these observations suggest that the structures and mechanisms involved in ion handling in RyR might resemble those in  $K^+$  channels?

The determination of the three-dimensional structure of the KcsA bacterial  $K^+$  channel at a resolution of 3.2 Å (1) has led to a revolution in the understanding of the relationship between structure and function of membrane ion channels. On entering the KcsA channel from the intracellular solution, a permeant ion would encounter, in order, a water filled tunnel 18 Å in length, a water filled cavity approximately 10 Å in diameter and a selectivity filter 1.5 Å in radius and 12 Å in length. The functional channel is a homotetramer that spans the membrane with its pore formed by the apposition of the monomers. Each monomer consists of two trans-membrane helices linked by an extracellular loop that folds into the membrane to contribute to the pore. A portion of the loop forms a short helical region termed the pore helix (1). The four pore helices are positioned in such a way that their partial negative charge is orientated towards the 10 Å aqueous cavity and provide a mechanism for overcoming the dielectric barrier associated with the movement of an ion into the low dielectric environment of the membrane (50). The aqueous cavity is lined with hydrophobic residues of T-M2 (the inner helix) and the selectivity filter of KcsA is lined with oxygen atoms of the backbone carbonyls of residues of the signature selectivity sequence (GYG).

Given the superficial similarities between  $K^+$  channels and RyR set out above it is interesting to explore the possibility that KcsA might be used, at least qualitatively, as a structural template for the pore region of RyR. Towards this end we have made predictions of the secondary structure of the last two T-M regions of RyR and InsP<sub>3</sub>R (T-M3 and T-M4 in the model of Takeshima (37) and T-M5 and T-M6 in InsP<sub>3</sub>R (45)) together with their linking, pore-forming, loops and have compared these predictions with the known structure of KcsA (13). These predictions indicate a striking correspondence. Not only do the pore-forming loops of RyR and InsP<sub>3</sub>R contain sequences of amino acids that are predicted to form helices analogous to the pore helix of KcsA but the sequence of predicted structural elements in the loops is the same as that found in the bacterial  $K^+$  channel. That is trans-membrane helix (T-M3/ T-M5), pore helix, selectivity filter, trans-membrane helix (T-M4/ T-M6), carboxyl terminus (Figure 2).

If we were feeling particularly foolhardy we might suggest that in the light of these observations it would be possible to stretch the analogy and propose a completely hypothetical tertiary structure for the pore-forming region of the RyR and InsP<sub>3</sub>R monomers by folding the identified elements on the basis of the arrangement of the corresponding components in KcsA (13)(Figure 3). A hypothetical homotetramer formed from such monomers would provide the  $Ca^{2+}$ -release channels with the wherewithal to fulfil the basic requirements of an ion channel. As in KcsA, the homotetramer would contain a single conduction pathway. Helix dipoles arising from the putative pore helices and focused on a water-filled cavity opening to

the cytosol would provide a mechanism for surmounting the electrostatic barrier faced by a cation in the low dielectric environment of the membrane. A constricted region in the putative conduction pathway of the channel, formed by the apposition of loops containing the GIGD motif, could provide the short, wide, region of the channel over which trans-membrane voltage falls and limited discrimination between cations takes place.

The proposal that the pore-forming loops of the RyR and InsP<sub>3</sub>R  $Ca^{2+}$ -release channels might share a range of general structural traits with equivalent regions of other membrane ion channels does not require that the detailed architecture and hence the mechanisms governing ion translocation and discrimination in the  $Ca^{2+}$ -release channels be similar to those resolved in  $K^+$ -selective channels such as KcsA. RyR and InsP<sub>3</sub>R are not  $K^+$  channels and the relationship between the structure of the conduction pathways of these channels and their unusual ion handling properties remains an area of great interest and investigation.

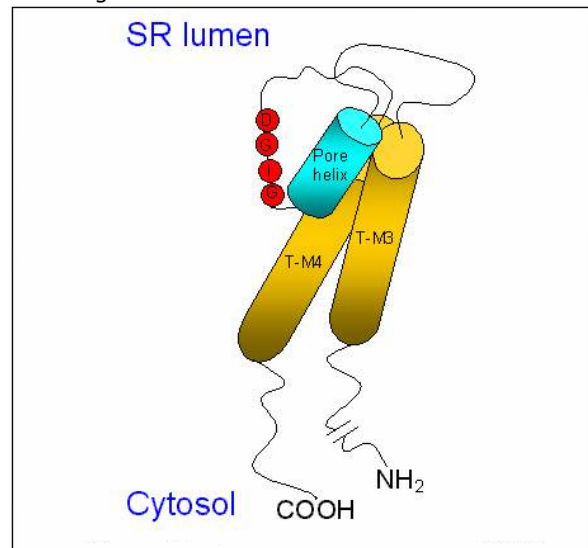


Figure 3. Cartoon depicting a hypothetical tertiary structure for the pore-forming loop of an RyR monomer. The relative location of the identified elements is based upon the established locations of corresponding elements in KcsA.

## ACKNOWLEDGEMENTS

I am grateful to the British Heart Foundation for continued financial support and to Dr Duncan West for many helpful discussions concerning the structures of the RyR and InsP<sub>3</sub>R pore-forming loops.

## References

1. Doyle D.A., J.M.Cabral, R.A. Pfuertner, A.L. Kuo, J.M. Gulbis, S.L. Cohen, B.T. Chait & R. MacKinnon: The structure of the potassium channel: Molecular basis of  $K^+$  conduction and selectivity. *Science* 280, 69-77 (1998) tractile force. Kluwer, Dordrecht, (2001)
2. Bers D.M.: Excitation-contraction coupling and cardiac contractile force. Kluwer, Dordrecht, (2001)
3. Zucchi R. & S. Ronca-Testoni: The sarcoplasmic reticulum  $Ca^{2+}$  channel/ryanodine receptor: Modulation by endogenous effectors, drugs and disease states. *Pharmacol. Rev.* 49, 1-51 (1997)

4. Shoshan-Barmatz V. & R.H. Ashley: The structure, function, and cellular regulation of ryanodine-sensitive Ca<sup>2+</sup> release channels. *Int. Rev. Cyto.* 183, 185-270 (1998)
5. Sitsapesan R. & A.J. Williams, Eds: *The Structure and Function of Ryanodine Receptors*. Imperial College Press, London, (1998)
6. Coronado R., R.L. Rosenberg & C. Miller: Ionic selectivity, saturation, and block in a K<sup>+</sup>-selective channel from sarcoplasmic reticulum. *J. Gen. Physiol.* 76, 425-446 (1980)
7. Rousseau E., M. Roberson & G. Meissner: Properties of single chloride selective channel from sarcoplasmic reticulum. *Eur. Biophys. J.* 16, 143-151 (1988)
8. Kourie J.I., D.R. Laver, P.R. Junankar, P.W. Gage & A.F. Dulhunty: Characteristics of two types of chloride channel in sarcoplasmic reticulum vesicles from rabbit skeletal muscle. *Biophys. J.* 70, 202-221 (1996)
9. Lai F.A., H.P. Erickson, E. Rousseau, Q-Y. Liu & G. Meissner: Purification and reconstitution of the Ca release channel from skeletal muscle. *Nature* 331, 315-319 (1988)
10. Lindsay A.R.G. & A.J. Williams: Functional characterisation of the ryanodine receptor purified from sheep cardiac muscle sarcoplasmic reticulum. *Biochim. Biophys. Acta*, 1064, 89-102 (1991)
11. Sitsapesan R. & A.J. Williams: Gating of the native and purified cardiac SR Ca<sup>2+</sup>-release channel with monovalent cations as permeant species. *Biophys. J.* 67, 1484-1494 (1994)
12. Williams A.J.: Ryanodine receptor ion conduction and selectivity. In: *The Structure and Function of Ryanodine Receptors*, Sitsapesan R. & Williams A.J. (eds.), Imperial College Press, London, (1998)
13. Williams A.J., D.J. West & R. Sitsapesan: Light at the end of the Ca<sup>2+</sup>-release channel tunnel: structures and mechanisms involved in ion translocation in ryanodine receptor channels. *Quart. Rev. Biophys.* 34, 61-104 (2001)
14. Hess P., J.B. Lansman & R.W. Tsien: Calcium channel selectivity for divalent and monovalent cations. Voltage and concentration dependence of single channel current in ventricular heart cells. *J. Gen. Physiol.* 88, 293-319 (1986)
15. Tinker A., A.R.G. Lindsay & A.J. Williams: Cation conduction in the cardiac sarcoplasmic reticulum calcium-release channel under physiological and pathophysiological conditions. *Cardiovas. Res.* 27, 1820-1825 (1993)
16. Tinker A. & A.J. Williams: Probing the structure of the conduction pathway of the sheep cardiac sarcoplasmic reticulum calcium-release channel with permeant and impermeant organic cations. *J. Gen. Physiol.* 102, 1107-1129 (1993)
17. Hille B.: *Ionic channels of excitable membranes*. Sinauer, Sunderland, Mass., (2001)
18. Woodhull A.M.: Ionic blockage of sodium channels in nerve. *J. Gen. Physiol.* 61, 687-708 (1973)
19. Lindsay A.R.G., S.D. Manning & A.J. Williams: Monovalent cation conductance in the ryanodine receptor-channel of sheep cardiac muscle sarcoplasmic reticulum. *J. Physiol.* 439, 463-480 (1991)
20. Tinker A., A.R.G. Lindsay & A.J. Williams: Block of the sheep cardiac sarcoplasmic reticulum Ca<sup>2+</sup>-release channel by tetraalkyl ammonium cations. *J. Membr. Biol.* 127, 149-159 (1992)
21. Tinker A. & A.J. Williams: Charged local anesthetics block ionic conduction in the sheep cardiac sarcoplasmic reticulum calcium-release channel. *Biophys. J.* 65, 852-864 (1993)
22. Tsushima R.G., J.E. Kelly & J.A. Wasserstrom: Characteristics of cocaine block of purified cardiac sarcoplasmic reticulum calcium release channels. *Biophys. J.* 70, 1263-1274 (1996)
23. Miller C.: Bis-Quaternary ammonium blockers as structural probes of the sarcoplasmic reticulum K<sup>+</sup> channel. *J. Gen. Physiol.* 79, 869-891 (1982)
24. Tinker A. & A.J. Williams: Measuring the length of the pore of the sheep cardiac sarcoplasmic reticulum calcium-release channel using trimethylammonium ions as molecular calipers. *Biophys. J.* 68, 111-120 (1995)
25. Lindsay A.R.G., A. Tinker & A.J. Williams: How does ryanodine modify ion-handling in the sheep cardiac sarcoplasmic reticulum Ca<sup>2+</sup>-release channel? *J. Gen. Physiol.* 104(3), 425-447 (1994)
26. Tinker A. & A.J. Williams: Divalent cation conduction in the ryanodine receptor-channel of sheep cardiac muscle sarcoplasmic reticulum. *J. Gen. Physiol.* 100, 479-493 (1992)
27. Miller C.: Ion channels: doing hard chemistry with hard ions. *Curr. Opin.Chem.Biol.* 4, 148-151 (2000)
28. Tinker A., A.R.G. Lindsay & A.J. Williams: A model for ionic conduction in the ryanodine receptor-channel of sheep cardiac muscle sarcoplasmic reticulum. *J. Gen. Physiol.* 100, 495-517 (1992)
29. Latorre R. & C. Miller: Conduction and selectivity in potassium channels. *J. Membr. Biol.* 71, 11-30 (1983)
30. Picco C. & A. Menini: The permeability of the cGMP-activated channel to organic cations in retinal rods of the tiger salamander. *J. Physiol.* 460, 741-758 (1993)
31. Dwyer T.M., D.J. Adams & B. Hille: The permeability of the endplate channel to organic cations in frog muscle. *J. Gen. Physiol.* 75, 469-492 (1980)
32. Mejía-Alvarez R., C. Kettlun, E. Ríos, M. Stern & M. Fill: Unitary Ca<sup>2+</sup> current through cardiac ryanodine receptor channels under quasi-physiological ionic conditions. *J. Gen. Physiol.* 113, 177-186 (1999)
33. Jordan P.C.: Ion channel electrostatics and the shapes of channel proteins. In: *Ion channel reconstitution*, Miller C. (ed.), Plenum Press, New York & London, pp. 37-55 (1986)
34. Green W.N. & O.S. Andersen: Surface charges and ion channel function. *Annu. Rev. Physiol.* 53, 341-359 (1991)
35. Tu Q., P. Velez, M. Cortes-Gutierrez & M. Fill: Surface charge potentiates conduction through the cardiac ryanodine receptor channel. *J. Gen. Physiol.* 103, 853-867 (1994)
36. Mead F.C., D. Sullivan & A.J. Williams: Evidence for negative charge in the conduction pathway of the cardiac ryanodine receptor channel provided by the interaction of K<sup>+</sup> channel N-type inactivation peptides. *J. Membr. Biol.* 163(3), 225-234 (1998)
37. Takeshima H., S. Nishimura, T. Matsumoto, H. Ishida, K. Kangawa, N. Minamino, H. Matsuo, M. Ueda, M. Hanaoka, T. Hirose & S. Numa: Primary structure and expression from complementary DNA of skeletal muscle ryanodine receptor. *Nature* 339, 439-445 (1989)
38. Zorzato F., J. Fujii, K. Otsu, N.M. Green, F.A. Lai, G. Meissner & D.H. MacLennan: Molecular cloning of cDNA encoding human and rabbit forms of the Ca<sup>2+</sup> release channel (ryanodine receptor) of skeletal muscle sarcoplasmic reticulum. *J. Biol. Chem.* 265, 2244-2256 (1990)
39. Tunwell R.E.A., C. Wickenden, B.M.A. Bertrand, V.I. Shevchenko, M.B. Walsh, P.D. Allen & F.A. Lai: The human cardiac muscle ryanodine receptor-calcium release channel: Identification, primary structure and topological analysis. *Biochem. J.* 318, 477-487 (1996)
40. Wang J.P., D.H. Needleman, A.B. Seryshev, B. Aghdasi, K.J. Slavik, S.Q. Liu, S.E. Pedersen & S.L. Hamilton: Interaction between ryanodine and neomycin binding sites on Ca<sup>2+</sup> release channel from skeletal muscle sarcoplasmic reticulum. *J. Biol. Chem.* 271, 8387-8393 (1996)
41. Bhat M.B., J.Y. Zhao, H. Takeshima & J.J. Ma: Functional calcium release channel formed by the carboxyl-terminal portion of ryanodine receptor. *Biophys. J.* 73, 1329-1336 (1997)
42. Xu X.H., M.B. Bhat, M. Nishi, H. Takeshima & J.J. Ma: Molecular cloning of cDNA encoding a Drosophila ryanodine receptor and functional studies of the carboxyl-terminal calcium release channel. *Biophys. J.* 78, 1270-1281 (2000)

43. Balshaw D., L. Gao & G. Meissner: Luminal loop of the ryanodine receptor: A pore-forming segment? *Proc. Natl. Acad. Sci. USA* 96, 3345-3347 (1999)
44. Yoshikawa S., T. Tanimura, A. Miyawaki, M. Nakamura, M. Yuzaki, T. Furuichi & K. Mikoshiba: Molecular cloning and characterization of the inositol 1, 4,5-trisphosphate receptor in *Drosophila melanogaster*. *J. Biol. Chem.* 267, 16613-16619 (1992)
45. Galvan D.L., E. Borrego-Diaz P.J. Perez & G.A. Mignery: Subunit oligomerization and topology of the inositol 1,4,5-trisphosphate receptor. *J. Biol. Chem.* 274, 29483-29492 (1999)
46. Kukuljan M., P. Labarca & R. Latorre: Molecular determinants of ion conduction and inactivation in K<sup>+</sup> channels. *Am. J. Physiol.* 268, C535-C556 (1995)
47. Zhao M.C., P. Li, X.L. Li, L. Zhang, R.J. Winkfein & S.R.W. Chen: Molecular identification of the ryanodine receptor pore-forming segment. *J. Biol. Chem.* 274, 25971-25974 (1999)
48. Gao L., D. Balshaw, L. Xu, A. Tripathy, C.L. Xin & G. Meissner: Evidence for a role of the luminal M3-M4 loop in skeletal muscle Ca<sup>2+</sup> release channel (ryanodine receptor) activity and conductance. *Biophys. J.* 79, 828-840 (2000)
49. Du G.G., X.H. Guo, V.K. Khanna & D.H. MacLennan: Functional characterization of mutants in the predicted pore region of the rabbit cardiac muscle Ca<sup>2+</sup> release channel (Ryanodine receptor isoform 2). *J. Biol. Chem.* 276, 31760-31771 (2001)
50. Roux B. & R. MacKinnon: The cavity and pore helices the KcsA K<sup>+</sup> channel: Electrostatic stabilization of monovalent cations. *Science* 285, 100-102 (1999)

**Key Words:** Ca<sup>2+</sup>-release channel, ryanodine receptor, conductance, permeability, selectivity, block

**Address for correspondence:** Professor Alan J. Williams, Cardiac Medicine, NHLI, Imperial College of Science, Technology & Medicine, Dovehouse St., LONDON SW3 6LY, U.K.  
 Telephone: +44 (0)20 7351 8137; Fax: +44 (0)20 7823 3392; e-mail: [a.j.williams@ic.ac.uk](mailto:a.j.williams@ic.ac.uk)